

Shaping the face

Cytoprotective mechanisms,
signaling pathways, and cleft repair

Christiaan Maarten Sutorp

Colofon

ISBN: 978-94-6421-536-6

The research described in this thesis was performed at the laboratory of the section Orthodontics and Craniofacial Biology, Department of Dentistry, Radboud university medical center, Radboud Institute for Molecular Life Sciences, Nijmegen, the Netherlands. The work was supported by the Radboud university medical center and the Radboud Institute for Molecular Life Sciences.

Printing: IPSKAMP printing

Cover Design: Christiaan Maarten Suttorp

Layout: IPSKAMP printing

Copyright ©: Christiaan Maarten Suttorp

All rights reserved. No parts of this publication may be reported or transmitted, in any form or by any means, without permission of the author.

Shaping the face

Cytoprotective mechanisms,
signaling pathways, and cleft repair

Proefschrift

ter verkrijging van de graad van doctor

aan de Radboud Universiteit Nijmegen

op gezag van de rector magnificus prof. dr. J.H.J.M. van Krieken,

volgens besluit van het college voor promoties

in het openbaar te verdedigen op donderdag 16 december 2021

om 10.30 uur precies

door

Christiaan Maarten Suttorp

Geboren op 13 november 1981

te Gouda

Promotor:

Prof. dr. A.M. Kuijpers-Jagtman

Copromotor:

Dr. F.A.D.T.G. Wagener

Manuscriptcommissie:

Prof. dr. G.J. Meijer

Prof. dr.Y. Ren (Universitair Medisch Centrum Groningen)

Dr. H. Zhou

Paranimfen:

Dr. Niels A.J. Cremers

Drs. Dries J.S. Desmedt

Shaping the face

Cytoprotective mechanisms,
signaling pathways, and cleft repair

Doctoral Thesis

to obtain the degree of doctor

from Radboud University Nijmegen

on the authority of the Rector Magnificus prof. dr. J.H.J.M. van Krieken,

according to the decision of the Council of Deans

to be defended in public on Thursday 16 December 2021

at 10.30 hours

by

Christiaan Maarten Suttorp

Born on November 13, 1981

in Gouda (the Netherlands)

Supervisor:

Prof. dr. A.M. Kuijpers-Jagtman

Co-supervisor:

Dr. F.A.D.T.G. Wagener

Doctoral Thesis Committee:

Prof. dr. G.J. Meijer

Prof. dr.Y. Ren (University Medical Center Groningen)

Dr. H. Zhou

Paranymphs:

Dr. Niels A.J. Cremers

Dries J.S. Desmedt, DDS

“Wat wij toeval noemen, is het toevluchtsoord der onwetendheid”

Nothing in Nature is random. A thing appears random only through the incompleteness of our knowledge.

Benedictus de Spinoza, Dutch philosopher, 1632-1677

To my beloved parents,

and in loving memory of my father in law and my grandparents

Printing of this thesis was financially supported by:

Radboud Universiteit



Radboudumc
university medical center

Institute for Molecular Life Sciences
Radboudumc

Contents

Chapter 1	General introduction	13
PART I:	Diminished cytoprotection in HO-2 deficient mice hampers fetal growth, without affecting chemokine signaling during palatal fusion or palatal osteogenesis	77
Chapter 2	Chemokine signaling during midline epithelial seam disintegration facilitates palatal fusion. <i>Front Cell Dev Biol, 2017 Oct 30;5:94.</i>	79
Chapter 3	CXCL12-CXCR4 interplay facilitates palatal osteogenesis in mice. <i>Front Cell Dev Biol. 2020 Aug 21;8:771.</i>	113
PART II:	Diminished cytoprotection by inhibition of HO-activity in mice promotes heme-induced placental inflammation and abortion	155
Chapter 4	Heme oxygenase protects against placental vascular inflammation and abortion by the alarmin heme in mice. <i>Int J Mol Sci. 2020 Jul 29;21(15):5385.</i>	157
PART III:	Mechanical stress, generated by orthodontic forces in rats or by splinting of excisional wounds in mice, induces the cytoprotective enzyme HO-1	185
Chapter 5	Orthodontic forces induce the cytoprotective enzyme heme oxygenase-1 in rats. <i>Front Physiol. 2016 Jul 19;7:283.</i>	187

Chapter 6	Mechanical stress changes the complex interplay between HO-1, inflammation and fibrosis, during excisional wound repair. <i>Front Med (Lausanne). 2015 Dec 15;2:86.</i>	209
PART IV:	Umbilical cord blood stem cells and molecular targets in tissue engineering may promote muscle and skin regeneration following surgical CLP repair	233
Chapter 7	Tissue engineering strategies combining molecular targets against inflammation and fibrosis, and umbilical cord blood stem cells to improve hampered muscle and skin regeneration following cleft repair. <i>Med Res Rev. 2020 Jan;40(1):9-26.</i>	235
PART V:	General discussion and Summary	261
Chapter 8	General discussion and future perspectives	263
Chapter 9	Summary	325
Chapter 10	Summary in Dutch	333
Acknowledgements		341
Curriculum Vitae		345
List of publications		347
PhD portfolio		349
Research data management		351

CHAPTER 1

General introduction

Overview

Preface

Personal introduction

Challenges in patients with CLP

Structure of the general introduction

Section 1. Craniofacial embryology and the etiology of CLP

1.1 Migration of cranial neural crest cells during embryonic craniofacial development

1.2 Palatogenesis and CLP development

1.3 Incidence and classification of CLP

1.4 Etiology of CLP

1.5 Oxidative and inflammatory stress in relation to CLP

Section 2. Surgical CLP repair, scarring and growth inhibition

2.1 Surgical CLP repair during childhood

2.2 A brief history of surgical CLP repair

2.3 Scarring following surgical cleft palate repair can hamper facial development

2.4 Wound healing and scar formation

2.5 Excessive scar formation following oxidative, inflammatory, and mechanical stress

Section 3. Cytoprotective mechanisms and signaling pathways in palatogenesis and wound healing

3.1 The cytoprotective enzyme system HO

3.2 The role of HO in embryonic development

3.3 The role of HO in wound healing

3.4.1 Common regenerative processes and signaling pathways in palatal fusion and wound healing

3.4.2 Mesenchymal cell recruitment and proliferation in palatal fusion and wound healing

3.4.3 Epithelium remodeling in palatal fusion and wound healing

3.5 The potential role of stem cells in wound healing

3.6 The complexity of chemokine-receptor signaling pathways

3.7 CXCL12-CXCR4 and CXCL11-CXCR3 signaling in relation to oxidative stress and HO-activity

3.8 The potential roles of CXCL12-CXCR4 and CXCL11-CXCR3 signaling in palatogenesis

Section 4. Aims of the thesis

4.1 Objectives and research questions

4.2 Outline of the thesis

Abbreviations

ADH1C	Alcohol dehydrogenase 1C
AP-2	Activating Protein 2
Ba	Branchial arch
BOR syndrome	Branchio-oto-renal syndrome
BVR	Biliverdin reductase
CCN1	Cysteine-rich protein 61
CCR2	C-C chemokine receptor type 2
CL	Cleft lip
CLP	Cleft lip and palate
CLPTM1	Cleft lip and palate transmembrane protein 1
CNCCs	Cranial neural crest cells
CO	Carbon monoxide
CP	Cleft palate
Crispld2	Cysteine-rich secretory protein LCCL domain-containing 2
CXCL10	Chemokine (C-X-C) ligand 10
CXCL11	Chemokine (C-X-C) ligand 11
CXCL12	Chemokine (C-X-C) ligand 12
CXCR3	Chemokine (C-X-C) receptor 3
CXCR4	Chemokine (C-X-C) receptor 4
CYP1A1	Cytochrome P450 family 1 subfamily A member 1
E0	Embryonic day 0
ECM	Extracellular matrix
EMT	Epithelial-to-mesenchymal transformation
Fgf10	Fibroblast growth factor 10
Fgfr2b	Fibroblast growth factor receptor 2b
G-CSF	Granulocyte colony-stimulating factor
GM-CSF	Granulocyte-macrophage colony-stimulating factor
GPCRs	G protein-coupled receptors
GSTM1	Glutathione S-transferase M1
Hb	Hemoglobin
HGF	Hepatocyte growth factor
HIF-1 α	hypoxia-inducible factor 1-alpha
HMEC-1	Human microvascular endothelial cells
HO	Heme oxygenase
HO-1	Heme oxygenase-1
HO-2	Heme oxygenase-2
H ₂ O ₂	Hydrogen peroxide
HUVECs	Human umbilical vein endothelial cells
IGFBPs	Insulin-like growth factor-binding proteins

IL-6	Interleukin-6
IL-8	Interleukin-8
IL-10	Interleukin-10
IL-1 β	Interleukine-1 beta
IL1-RA	Interleukin-1 receptor antagonist
IRF6	Interferon regulatory factor 6
KO	Knockout
LPS	Lipopolysaccharide
MCP-1	Monocyte Chemoattractant Protein-1
MEE	Medial edge epithelium
MES	Midline epithelial seam
MFPM	Mouse fetus's palatal mesenchymal cells
MMPs	Matrix metalloproteinases
MSCs	Mesenchymal stem cells
MSX1	Muscle segment homeobox 1
MTHFR	5,10-methylenetetrahydrofolate reductase
NADPH	Nicotinamide adenine dinucleotide phosphate
NAT2	<i>N</i> -Acetyltransferase 2
OFD1 syndrome	Oral-Facial-Digital Type 1 syndrome
P63	Translation related protein p63
PDGF-AA	Platelet-derived growth factor AA
PEDF	Pigment epithelium-derived factor
PP	Phosphatases
PVRL1	Poliovirus receptor-related 1
RARA	Retinoic acid receptor alpha
ROS	Reactive oxygen species
SnMP	Tin mesoporphyrin
SOD2	Superoxide dismutase 2
Sox9	SRY-Box Transcription Factor 9
TBX22	T-box transcription factor protein 22
TCS	Treacher Collins syndrome
TGF- α	Transforming growth factor-alpha
TGF- β 1	Transforming growth factor-beta 1
TGF- β 3	Transforming growth factor-beta 3
TNF- α	Tumor necrosis factor-alpha
VEGF	Vascular endothelial growth factor

Preface

Personal introduction

My first clinical experience with the treatment of patients with cleft lip and palate (CLP) was at the end of 2011, during my first year of the four-year postgraduate program in orthodontics at the Radboud university medical center in Nijmegen. Under supervision of Professor dr. Anne Marie Kuijpers-Jagtman and drs. Veronique Borstlap-Engels, I learned about the orthodontic treatment of patients with CLP. They also explained me about the different phases of CLP treatment, giving me insight into the long multidisciplinary treatment, from birth to adulthood, which most patients with CLP must undergo. Experience learned that orthodontic treatment of young patients and patients with syndromic forms of CLP is often challenging. Both technical and social skills are required for successfully running the cleft clinic. From my experiences at the cleft clinic, I developed enthusiasm for doing fundamental research in the field of CLP formation. Since 2018, I am a fulltime faculty member of the Department of Dentistry of the Radboud university medical center and frequently treat patients at the cleft clinic (Figure I).

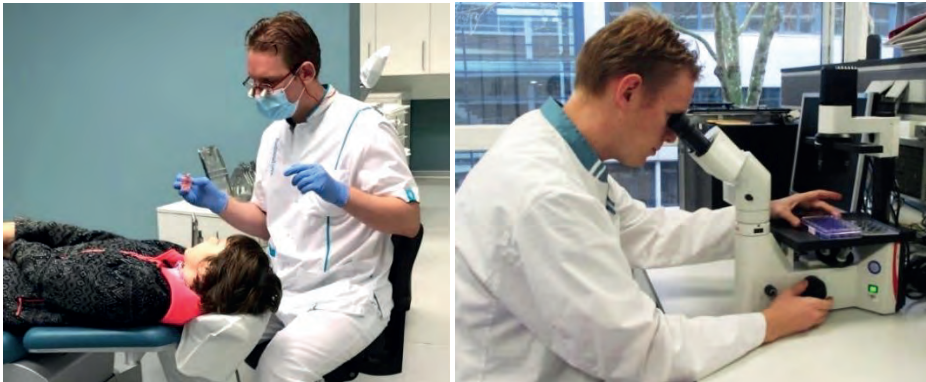


Figure I: The author of this thesis in action in the cleft clinic (**left**) and at the laboratory (**right**), connecting the “two worlds” within the section of Orthodontics and Craniofacial Biology.

With a background in biomedical sciences at the University of Amsterdam, prior to entering the dental school, I am also interested in the embryonic process of CLP formation. Therefore, my research supervisor Dr. Frank Wagener and I designed experimental studies in mice to investigate the process of palatogenesis in the absence or presence of the cytoprotective enzyme heme oxygenase (HO). Although we found interesting results, our study generated only more questions than answers regarding palatogenesis. My ultimate goal, the prevention of embryonic cleft formation, is still far away because of the inadequate knowledge in this field. Therefore, we expect that in the short term, science will mainly focus on postnatal interventions like improved

wound repair with less scar formation. Therefore, besides studying embryonic palatogenesis, we also experimentally studied the potential role of cytoprotective mechanisms and cellular signaling pathways in the wound repair process. Since our section within the Department of Dentistry is officially called “Orthodontics and Craniofacial Biology”, I hope my thesis will contribute to bridging the gap between these “two worlds”, the world of the cleft clinic, and our laboratory world.

Challenges in patients with CLP

CLP is an umbrella term given to congenital disorders in which the upper lip, and/or the alveolus, and/or the palate are affected by a cleft^{1,2,3}. CLP belongs to the most common congenital craniofacial anomalies (circa 1 in 700 newborns)⁴⁻⁸. Newborns with CLP demonstrate a large phenotypic heterogeneity⁹. In the past, CLP was diagnosed clinically immediately after birth¹⁰. Since the '90s, an increasing number of CLP cases could already be confirmed by routine prenatal ultrasound screening. Cleft lip (CL) can already be detected with ultrasound around the 13th week of pregnancy¹⁰. It was found worldwide that after prenatal counseling by the cleft team 85-93% of the parents felt well prepared psychologically for the birth of their child and considered prenatal diagnosis a benefit¹¹⁻¹³. However, it has recently been found that in Europe pregnancy termination is carried out in 13% of the cases after the parents received prenatally the solitary CLP diagnosis¹⁴.

The feeding of babies with CLP is more difficult because of the open connection between the mouth and nose¹⁵. The CLP anomaly can also affect the relationship between mother and child¹⁶. Parents are often concerned about the future of their child¹⁷, which impacts their quality of life¹⁸. Depending on the severity of the deformity patients with orofacial clefts need to undergo medical treatments from birth to adulthood, coordinated by a multidisciplinary cleft team consisting of diverse specialists⁵, including several surgical interventions, orthodontic treatment, and other non-surgical treatments, as speech therapy^{19,20}. This medical treatment process affects the psychological well-being of both the children and their family members^{19,20}. The malformation in newborns ranges from mild forms to complete bilateral clefts affecting the lip, alveolar process, and the palate²¹.

Different dental abnormalities are usually seen in patients with CLP, including collapsed maxillary dental arches, malformation of teeth, hypodontia in both the maxilla and the mandible, supernumerary teeth in the cleft region²², and midfacial deficiency²³.

Palatal clefting is often associated with Eustachian tube malfunction, which can result in conductive hearing loss, and subsequently, a delay in speech and language development^{18,24}. Moreover, patients with CLP often suffer from velopharyngeal insufficiency, a failure of the soft palate to close against the posterior pharyngeal wall causing hypernasal speech. Even 30% of the children with cleft palate demonstrate

velopharyngeal insufficiency, despite surgical palatal closure²⁴. It was found that patients with CLP experience hearing loss and hypernasality in 20% and 69%, respectively²⁵. Surgical velopharyngeal closure was found to correct hypernasality in only 50% of the patients²⁶. Notably, 60% of children with CLP report being bullied about their appearance and speech²⁷.

Surgical closure of the alveolus and palate, and pharyngeal flap surgery may result in hampered sagittal (anteroposterior), vertical, and transversal growth of the maxilla because of scarring²⁸. Scarring following surgical CL repair may also hamper dentoalveolar development^{29,30}. Scarring following cleft palate (CP) repair may inhibit sagittal growth of the maxilla, which can lead to midfacial deficiency³¹ (**Figure II**). Surgical maxillary advancement is often indicated to correct midfacial deficiency^{28,32}.

Residual scars are also often observed after cleft lip surgery³³. After CLP treatment, adult patients were found to rate their esthetic outcome worse than the experts of the cleft team³⁴. Especially female patients were dissatisfied with their esthetic outcomes, and 63% of them asked for additional upper lip and nose corrections³⁴. One study found that almost half of the patients with CLP were not satisfied with their facial appearance, although they seemed to be psychosocially well adjusted to their disability³⁵. Scarring of their lip can lead to serious psychological problems including low self-esteem and acceptance by peers^{34,36}. CLP patients were further found to score lower at social and emotional functioning³⁴.

To achieve healing with less scarring, fetal surgical repair of CLP has been proposed³⁷, and tested in mice^{38,39}, rabbits^{40,41}, goats⁴², and lambs⁴³. Unfortunately, fetal cleft surgery in a lamb model demonstrated a 25% risk of abortion⁴³. In utero surgical interventions for non-life-threatening diseases may only become feasible as fetal surgery becomes safer for both mother and fetus⁴⁴.

Both syndromic and non-syndromic CLP disorders have multifactorial causes that not only involve genetic predisposition, but also environmental influences³⁷. In the near future gene therapy or genetic engineering (e.g. using CRISPR-Cas9) becomes available to prevent embryonic CLP formation³⁷. However, those treatment options should first await a difficult ethical and moral debate³⁷. More research within the combined fields of CLP formation, wound healing and tissue engineering is warranted to develop preventive strategies and better clinical outcomes.

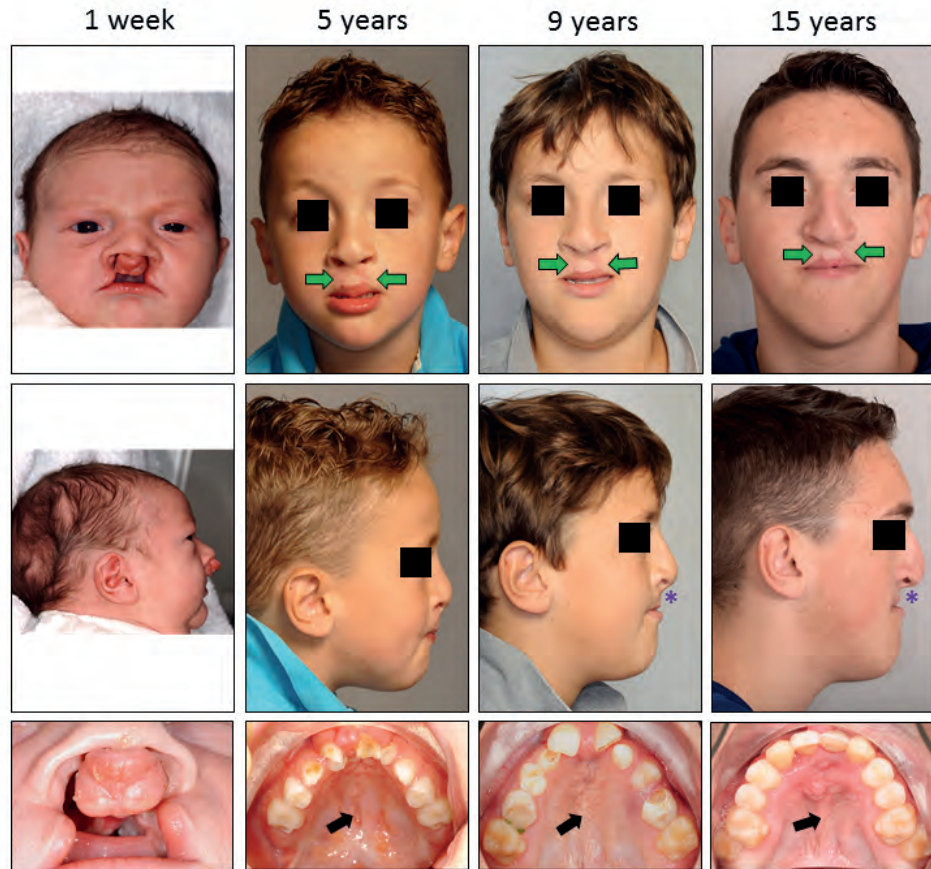


Figure II: Progressive midfacial deficiency in a patient with CLP. This patient was born with a complete bilateral CLP. Surgical CLP closure before the age of 9 months, and pharyngeal flap surgery at the age of 4 years were performed. Scarring of the upper lip (green arrow) and the palatal mucosa (black arrow) was already visible at 5 years of age. At 9 years of age, retro-inclined deciduous upper incisors were observed, together with collapse of the maxillary dental arch. Orthodontic expansion was performed to correct the collapsed maxillary dental arch. At 10 years of age, premaxilla repositioning with alveolar bone grafting was performed. At the age of 9 and 15 years, obvious midfacial deficiency is observed (purple asterisk), characterized by a retrusive maxilla, creating a negative lip step. This patient is unsatisfied with his facial appearance, and requests for esthetic improvement. An orthognathic surgical maxillary advancement, to correct the midfacial deficiency, is planned for the age of 18 years. Scarring of the upper lip and palatal mucosa with a retrusive maxilla are commonly found features in patients with CLP.

Structure of the general introduction

The general introduction is subdivided into 4 sections:

In *Section 1. Craniofacial embryology and the etiology of CLP*, the process of embryonic development of the orofacial region will be explored. Furthermore, the incidence and classification of CLP are addressed. The role of genetic and environmental factors in the etiology of CLP will also be discussed.

In *Section 2. Surgical CLP repair, scarring and growth inhibition*, scar formation following surgical CLP repair in relation to facial growth is debated. The influence of oxidative, inflammatory, and mechanical stress at wound healing and scar formation is covered.

In *Section 3. Cytoprotective mechanisms and cellular signaling pathways in palatogenesis and wound healing*, the role of the cytoprotective enzyme system heme oxygenase (HO) in embryonic development and wound healing is addressed. Furthermore, the common processes and signaling pathways in palatogenesis and wound healing are discussed. Finally, the potential roles of chemokine (C-X-C) ligand 11-chemokine (C-X-C) receptor 3 (CXCL11-CXCR3) and chemokine (C-X-C) ligand 12-chemokine (C-X-C) receptor 4 (CXCL12-CXCR4) chemokine-chemokine receptor signaling in palatogenesis are debated.

Lastly, in *Section 4. Aims of the thesis*, the research questions and aims are formulated and the outline of the thesis is presented.

Section 1. Craniofacial embryology and the etiology of CLP

1.1 Migration of cranial neural crest cells during embryonic craniofacial development

Craniofacial development is a complex process, and the mechanisms that regulate the formation of skeletal structures, sensory organs, the nervous system, and the orofacial region are still poorly understood⁴⁵. Cells of the facial compartment are derived from four main sources: 1). cranial neural crest cells (CNCCs), 2). the paraxial mesoderm, 3). the epidermis, and 4). the endoderm⁴⁶. The non-epithelial tissues in the facial region originate from migratory CNCCs and the paraxial mesoderm⁴⁶. Notably, the CNCCs act as stem cells and are the largest contributor to the developing face, responsible for e.g. the facial bone, cartilage and muscles, and are among the most motile cells in the embryo⁴⁷. Migration of the CNCCs starts at the neural crest and is directed, along well-defined routes, first as a continuous wave and quickly split into three discrete segregated streams, predominantly from rhombomeres (r) 2, 4 and 6 to populate the first, second and third branchial arches (ba)^{48,49} (**Figure 1; left panel**). The CNCCs of the first branchial arch form the different facial bones, muscles of mastication, and cranial nerves V2 and V3⁵⁰. The migration of CNCCs is directed by several signaling pathways. For short distances the migration of CNCCs starts by the process of polarization, which includes the formation of a “front end” and a “back end” of the cell by changing the shape of the cell, regulated by Wnt signaling⁵¹ (**Figure 1; right panel**). Wnt-signaling also regulates “contact inhibition by locomotion”, a process by which cells change their direction of migration upon cell-cell contact⁵¹⁻⁵³. Furthermore, both Ephrin-Ephrin ligand-receptor signaling^{54,55}, and complement factor component C3a ligand-C3a receptor-mediated chemotaxis⁵⁶ regulate the maintenance of the high density of the CNCCs stream during migration, termed “co-attraction”. For long distance migration, the chemokine CXCL12 directs the migration of CXCR4-positive CNCCs to the branchial arches ba1, ba2, and ba3^{47-49,57,58} (**Figure 1**).

In the mammalian fetus, CNCCs populating the pharyngeal arches are characterized by the expression of SRY-Box Transcription Factor 9 (Sox9)⁵⁹⁻⁶². After arrival of the multipotent CNCCs at the pharyngeal arches, the embryo is still very small and significant development and growth of the craniofacial structures must follow⁴⁵. In the process of craniofacial development, a controlled program, via signaling interactions between the migrating cells and their environment, determines the fate of the CNCCs⁶³. Next, the CNCCs migrate, proliferate and differentiate to form the orofacial region including the maxilla, mandible, dentin, pulp of the teeth, cartilage, connective tissues⁶⁴⁻⁶⁶, trigeminal nerve and mastication muscles^{59,67-69}. Since many complex gene regulatory networks and numerous cellular mechanisms are active in CNCCs during craniofacial development, the mechanisms that shape the face are still not fully elucidated⁷⁰.

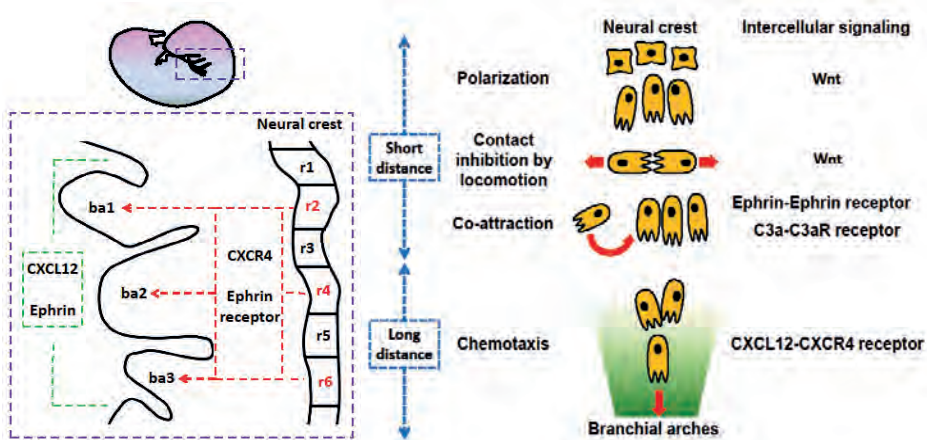


Figure 1: The migration of CNCCs from the neural crest to the branchial arches is directed by several signaling pathways. In the developing mammalian fetus, cranial neural crest cells (CNCCs) migrating from the neural crest split into three streams from the rhombomeres 2, 4 and 6 (r2, r4, r6) to the branchial arches 1, 2, and 3 (ba1, ba2, ba3) (left panel). Wnt, Ephrin-Ephrin receptor, and C3a-C3a receptor intercellular signaling pathways regulate the migration of CNCCs at short distances. CXCL12-CXCR4 signaling regulates the migration of CNCCs for long distances to the branchial arches (right panel). From the first branchial arch the different facial bones, including the maxilla, and muscles of mastication are finally formed. Only a selection is shown here, since various other signaling pathways and mechanisms contribute to the migration of CNCCs.

One-third of all congenital birth defects affect the head and face⁷¹. Numerous congenital craniofacial abnormalities affect the form and function of the face, including deformities, distractions, elongations, shortenings, asymmetries, and aberrant structures. Explanations for these malformations still await fundamental understanding of the underlying mechanistic failure of morphogenesis⁷². Most disorders of craniofacial development, such as CLP, Treacher Collins syndrome (TCS), Pierre Robin Sequence and craniosynostosis, are caused by defects in the formation, migration, proliferation, survival, or differentiation of CNCCs^{66,73,74}. Migration and survival of CNCCs can be disturbed by toxic drugs, and by disruption of expression of homeobox genes muscle segment homeobox (*Msx*) 1 and *Msx2*⁷⁵, transcription factor Activating Protein 2 (AP-2)^{76,77}, growth factor *Tgfb β 2*⁶⁸, and intercellular signaling pathways, such as Cysteine-rich secretory protein LCCL domain-containing 2 (*Crispld2*)⁷⁸. Interestingly, disrupted CXCL12-CXCR4 signaling in mice^{79,80}, chicken⁵⁷, and zebrafish⁸¹ impairs craniofacial development by misrouting the migration of CNCCs. Disturbance of these processes can lead to craniofacial malformations as CLP and TCS⁸. In this thesis we discuss craniofacial development especially in relation to CLP formation.

1.2 Palatogenesis and CLP development

In humans, the face starts to develop in the 4th week of embryogenesis from the facial primordia, originating from CNCCs, and development of the palate occurs between the 4th and 10th week post-conception⁸². Palatal development, named palatogenesis, is an

important part of craniofacial development in higher vertebrates⁸³. Most of our knowledge on palatogenesis has been obtained from mouse studies due to the similarity with human palatogenesis and the ethical limitations for research with human embryos⁸⁴. Since Sox9 expression was observed in the palatal shelves in mice, CNCCs are thought to contribute to the embryonic formation of the palate^{85,86}. In most mouse strains, palatal outgrowths are first detectable by embryonic day (E) 11.5, and palatal fusion is complete by E17⁸⁷. The facial primordia consist of the frontonasal prominence, the paired maxillary prominences and the paired mandibular prominences surrounding the oral cavity⁸⁸. Fusion of these prominences requires a precise spatiotemporal regulation, whilst disruption of this regulatory network can result in orofacial clefting⁸⁸. Partial or complete lack of fusion of the maxillary prominence with the medial nasal prominence on one or both sides can lead to a cleft of the lip, alveolus and primary palate. The secondary palate develops following ordered stages. First the paired palatal shelves grow vertically besides the developing tongue. As the mandible develops the tongue drops, allowing the paired palatal shelves to rise into a horizontally oriented position above the tongue. The two medial edge epithelium (MEE) layers covering the tips of the growing palatal shelves adhere to each other in the midline and form the midline epithelial seam (MES)⁸³ (**Figure 2**). Thereafter, the MES needs to disappear to allow mesenchymal confluence and fusion of the secondary palate⁸⁹. Failure of one of these events results in palatal clefting^{68,90}. Lack of fusion of the palatal shelves from the maxillary prominence results in palatal clefting posterior to the incisive foramen⁵.

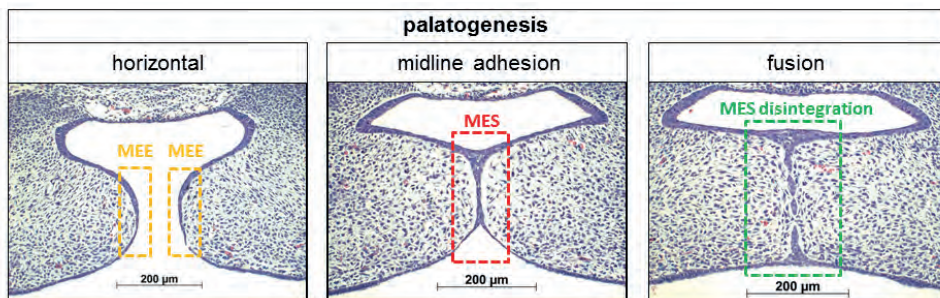


Figure 2: Formation and disintegration of the MES in the process of palatal fusion. Example of different stages of palatogenesis within the same fetus in HE stained coronal palatal sections (magnification: x100) in heme oxygenase-2 knockout (HO-2 KO) mice of a mixed 129Sv × C57BL/6 background at E15. Horizontal orientation of the palatal shelves with both tips covered by the medial edge epithelium (MEE) (**yellow boxes, left panel**), midline adhesion including the formation of the midline epithelial seam (MES) (**red box, middle panel**), and eventually disintegration of the MES (**green box**) to allow palatal fusion and mesenchymal confluence. The MES changed from a multi-cell-layer (**middle panel**) into a continuous one-single-cell-layer, to a disintegrating MES, during which islands of epithelium in the midline can be observed (**right panel**). This example demonstrates that MES formation and MES disintegration in mice occurs fairly quickly, within one day.

The secondary palate fuses anteriorly to the primary palate and anterodorsally to the nasal septum. Finally, the closed palate separates the oral cavity from the nasal cavity⁹⁰. Within the palatal mesenchyme intramembranous ossification in the anterior

part forms the hard palate, and myogenesis in the posterior part results in the soft palate⁸⁶.

Multiple mechanisms have been proposed to explain the disappearance of the MES. The main hypotheses underlying MES disintegration involve epithelial cell migration to the oral^{91,92}, or nasal epithelium^{92,93}, epithelial-to-mesenchymal transformation (EMT)⁹⁰, epithelial cell apoptosis⁹⁴, or a combination of these events⁹⁵. Cranial neural crest-derived mesenchymal cells must undergo osteogenic differentiation to form the hard palate⁹⁶. In mice, CNCCs form aggregated cell masses to initiate palatal bone formation in the palatal mesenchyme in mice between E14.5 and E16.5^{68,97}.

1.3 Incidence and classification of CLP

It is estimated that the prevalence rates of birth defects in total are with 6.4% the highest in the low-income countries, 5.6% in the middle-income countries, and with 4.7% the lowest in the developed countries^{98,99}. To put the numbers in perspective, the incidence of CLP (1 in 700)⁴⁻⁸ is higher compared to Down syndrome (1 in 1000)¹⁰⁰, and spina bifida (1 in 2.000)¹⁰¹, but lower compared to the incidence of congenital heart disease (1 in 167)^{102,103}. The incidence of isolated cleft palate is much lower, namely about 1 in 2.200 live births¹⁰⁴. Isolated cleft lip occurs in 1 in 1.700 live births¹⁰⁵. The CLP incidence depends on ethnic and geographical variation⁴⁻⁸. In addition, the incidence of CLP is highest among Asians, followed by Caucasians, and lowest in people of African descent¹⁰⁶⁻¹⁰⁸.

CLP shows a very heterogeneous anatomy. Accurate classification and subphenotyping of the cleft in the lip, and/or alveolus and/or palate is important to come to a correct diagnosis. CLP can be divided into isolated cleft lip and/or alveolar process, isolated cleft palate, and combined cleft lip, alveolus, and palate. CLP can be limited to one side (unilateral) or can be a double-sided (bilateral) cleft of the lip, with or without a cleft of the alveolus^{9,109}. Approximately 75% of clefts involving the lip are unilateral, and the left side is affected twice as often as the right-side⁴. The cleft can be subdivided into complete or incomplete¹¹⁰⁻¹¹². Considering its wide spectrum CLP can range from a mild condition to a severe craniofacial anomaly. For example, it can extend from only an incomplete cleft of the lip, with or without a cleft in the alveolar process, to a complete bilateral cleft of the lip and alveolus with a cleft running through the palate and anterior displacement of the premaxilla with a collapse of the maxillary dental arch^{113,114}. Examples of patients with different CLP diagnoses treated within the craniofacial-cleft clinic of the Radboud university medical center, Nijmegen, The Netherlands, are presented below (**Figure 3**). The maxilla is frequently deficient in the sagittal, vertical and transversal dimension, often accompanied by constriction of the maxillary dental arch¹¹⁵. The severity of maxillary hypoplasia is related to the cleft type¹¹⁶.

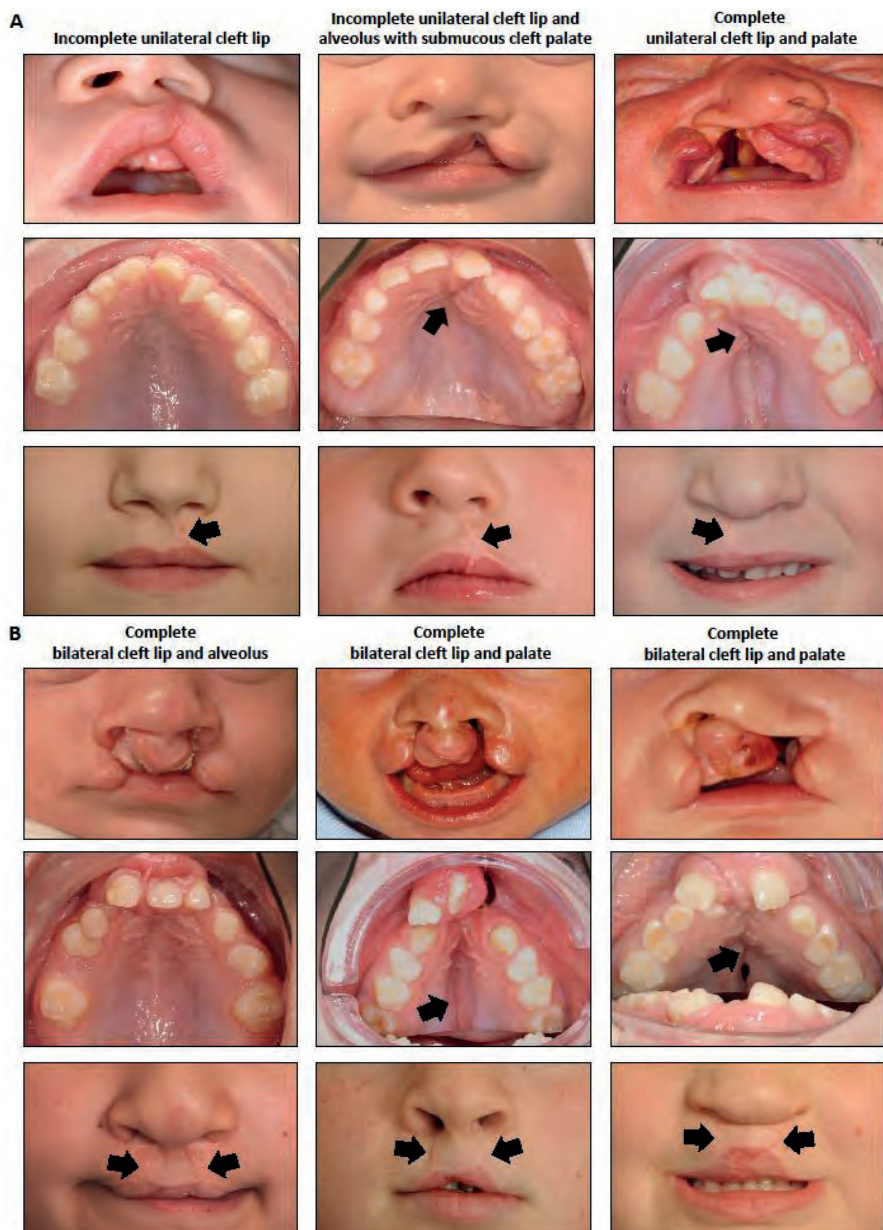


Figure 3: Patients with CLP demonstrate a heterogeneous anatomy both before and after surgical cleft repair. The features of patients with CLP can range from a mild condition to a severe type of cleft. **(A)** Unilateral and **(B)** bilateral clefts are shown, before and after surgical closure of the lip and/or palate. In the top row, extra-oral pictures at the age of 2-4 weeks, before surgical closure of the cleft lip. The photos in the middle row represent the intra-oral pictures of the mixed dentition of the same persons above after closure of the cleft of the lip and/or palate, taken between 5-9 years of age. The extra-oral pictures in the bottom row are of the same persons above, taken between 5-9 years of age. Scar formation of the lip and/or palate is observed (depicted by black arrow).

In unilateral cases, the premaxilla is commonly hypoplastic and deviates from the facial midline. Bilateral cleft cases show a wide variety in the shape and position of the premaxilla and tend to present a narrow maxilla as the result of the collapse of the lateral maxillary segments¹¹⁷.

The heterogeneity of clefts of the primary or secondary palate can be explained by differences in embryonic origin and underlying fusion or differentiation defects. Fusion defects of the primary palate lead to complete clefting of the lip (CL) either or not combined with a complete or incomplete cleft of the alveolus. Differentiation defects of the primary palate give rise to incomplete, submucous or hypoplastic cleft lip and/or alveolus. Fusion defects of the secondary palate lead to complete or incomplete hard-palate clefts) that may be combined with a cleft in the soft palate and/or uvula. Differentiation defects of the secondary palate give rise to a combination of submucous, hypoplastic hard and soft palate defects¹¹⁰⁻¹¹².

1.4 Etiology of CLP

Birth defects are the main cause of spontaneous abortion, stillbirth, perinatal death, infant death, and congenital disorders⁹⁹. The causes of birth defects are complex and include genetic and environmental factors and/or their interactions⁹⁹. Although the mechanisms are not fully elucidated, it is thought that in the etiology of CLP formation genetic predisposition and environmental factors both play a role¹¹⁸. CLP is typically classified into syndromic and non-syndromic, and both forms are characterized by a strong genetic component¹¹⁹.

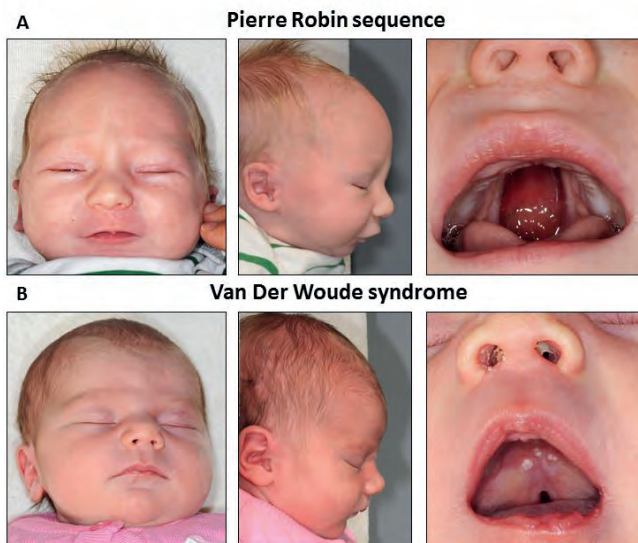


Figure 4: Genetic factors are responsible for syndromic CLP. Cleft palate found as a component of (A), the Pierre Robin sequence caused by chromosomal abnormalities near the SOX9 gene and (B), Van der Woude syndrome caused by mutations in the Interferon regulatory factor 6 (IRF6) gene.

In about 38% of the cases, CLP is diagnosed with additional congenital anomalies¹²⁰, due to chromosomal aberrations or monogenic diseases¹¹⁹, caused by a mutation of a single genetic locus^{120,121}, and are regarded as syndromic CLP. Syndromic forms of CLP consist of over 300 different conditions^{5,122}. The most common form of syndromic CLP are the Pierre Robin sequence (**Figure 4A**) and the Van der Woude syndrome (**Figure 4B**)^{3,123,124}. The Pierre Robin sequence is a rare disease with an incidence ranging from 1 to 8.500-30.000 newborns¹²⁵. It is characterized by the clinical features: micrognathia, glossoptosis, and compromised airway with variable extent of a cleft palate¹²⁶. Chromosomal abnormalities near the SOX9 gene, that is crucial for the function of CNCCs, were found to disrupt its regulation, leading to the condition¹²⁷. The incidence of Van der Woude syndrome has been reported as 1 in 75.000–100.000 live births¹²⁸. The Van der Woude syndrome is an autosomal dominant condition with high penetrance and variable expression. Clinical manifestation of this clefting syndrome includes bilateral midline lower lip pits, cleft lip, and cleft palate along with hypodontia¹²⁹. Van der Woude syndrome accounts for approximately 2% of all CLP cases^{130,131}. Mutations in the Interferon regulatory factor 6 (IRF6) gene were identified as driving factor for the etiology^{120,132}.

Some clefting syndromes are rare, affecting only 1 in 10.000-100.000 live births¹²¹. Examples of patients of our clinic with rare syndromic CLP include for example Greig syndrome¹³³, Branchio-oto-renal (BOR) syndrome¹³⁴, Oral-Facial-Digital Type I (OFD1) syndrome¹³⁵, Adrenogenital syndrome¹³⁶, and Kabuki syndrome¹³⁷ (**Figure 5**).

CLP cases occurring in isolated condition, unassociated with any recognizable anomalies, are non-syndromic CLP cases¹³⁸. In about 62% of the cases CLP occurs in isolation^{3,123}, caused by a combination of genetic and environmental factors^{111,124,139,140}. Deletions and mutations in the genes observed in mice, such as transcription factor translation related protein p63 (P63)^{141,142}, poliovirus receptor-related 1 (PVRL1) encoding a cell-cell adhesion molecule^{141,143,144}, cleft lip and palate transmembrane protein 1 (CLPTM1)^{145,146}, and T-box transcription factor protein 22 (TBX22)^{141,147} are associated with the development of non-syndromic CLP in humans¹⁴¹.

Variants of several genes are associated with increased risk of non-syndromic CLP, namely growth factors as transforming growth factor- α (TGF- α), transforming growth factor- β 3 (TGF- β 3)^{148,149}, transcription factors MSX1, TBX22 and IRF6¹⁵⁰⁻¹⁵⁹. Genes related to the nutritional metabolism such as the genes 5,10-methylenetetrahydrofolate reductase (*MTHFR*) and retinoic acid receptor alpha (*RARA*)^{160,161}, and genes involved in the metabolism of toxic compounds generated by maternal smoking, such as cytochrome P450 family 1 subfamily A member 1 (*CYP1A1*), glutathione S-transferase M1, (*GSTM1*), *N*-Acetyltransferase 2 (*NAT2*)¹⁶²⁻¹⁶⁴ are linked to increased risk of CLP as well.

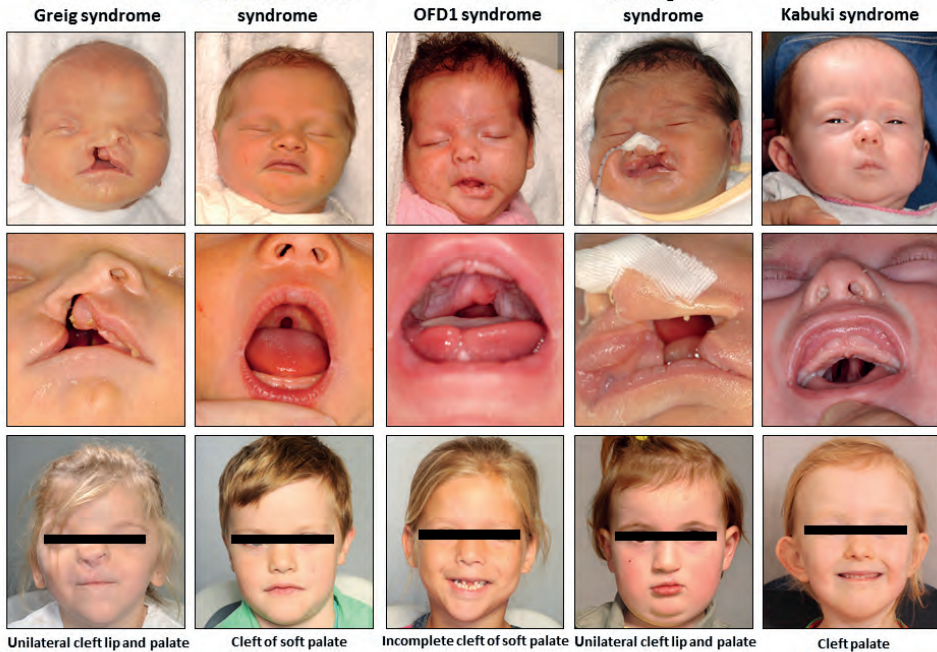


Figure 5: Examples of rare syndromic forms of CLP. On the top row, extra-oral pictures at the age of 2-4 weeks. The photos in the middle row represent the intra-oral pictures of the same persons above at the age of 2-4 weeks. The extra-oral pictures on the bottom row are of the same persons above, taken at 5 years of age.

Moreover, genes involved in immune response as *PVLR1*¹⁶⁵ are also related to increased risk of CLP. Examples of patients of our CLP clinic with *MSX1* and *IRF6* genetic variants are presented in **Figure 6**.

Environmental factors as smoking¹⁶⁶, alcohol consumption¹⁶⁷, anti-epileptic drugs phenytoin¹⁶⁸ and valproic acid¹⁶⁹, maternal corticosteroid use¹⁷⁰, diabetes¹⁷¹, maternal¹⁷² and paternal age¹⁷³, infections^{170,174}, folate deficiency, zinc deficiency, contact to teratogens such as chemical solvents, and both high- and low-dose vitamin A/retinoic acid intake are associated with increased risk for CLP^{169,175}. Nutrition guidelines for pregnant women and women planning to have a baby as prevention for getting babies with CLP recommend sufficient intake of folic acid, zinc, and multivitamin supplementation (containing vitamin A, B6 and C), and advise to keep a healthy lifestyle shortly before and during pregnancy^{114,176}. Despite these guidelines, the interplay between genetic predisposition and environmental factors cannot be prevented completely. The molecular mechanisms involved in CLP formation need to be better understood.

Since CLP has been observed in both members in 60% of monozygotic twins¹⁷⁷, but only in 3–10% of dizygotic twins^{121,177}, it is likely that both genetic and environmental factors are involved in the etiology of CLP. Namely, specific gene variants

are thought to correlate with specific environmental risk factors for CLP¹¹⁹. The combination of genetic variants of the genes TGF- α , TGF- β 3, MSX1 with maternal smoking¹⁷⁸⁻¹⁸¹, and the combination of genetic variants of TGF- β 3, MSX1, alcohol dehydrogenase 1C (ADH1C) with maternal alcohol consumption^{180,182,183} has been found to increase the risk of CLP. Furthermore, the combination of genetic variants of the gene RARA with high vitamin A intake before the seventh week of gestation was found to increase the risk of CLP¹⁸⁴. In addition, poor maternal vitamin B6 status was associated with an increased risk of CLP¹⁸⁵. The zebrafish ethmoid plate forms a good model to study the contribution of genetic and environmental interactions to palatal clefting. In the coming years, this model might deliver more insights in the complex etiology of CLP¹⁸⁶.

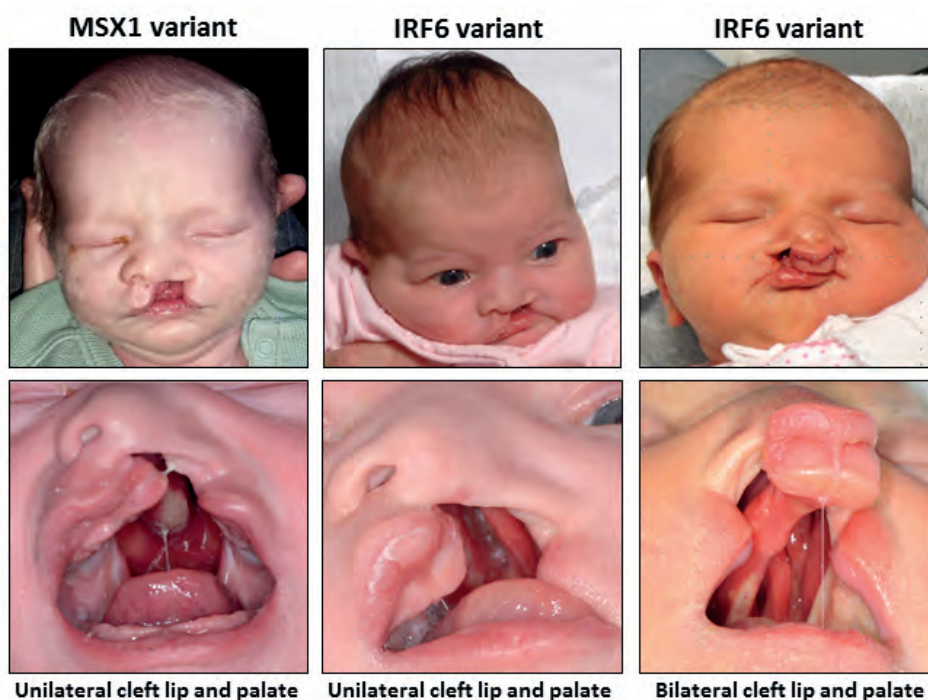


Figure 6: Genetic variants of the MSX1 and IRF6 genes in non-syndromic CLP patients. MSX1 and IRF6 genetic variants are related to increased risk of CLP. The photos in the lower row represent the intra-oral pictures of the same persons above. Note: the presented patients with CLP associated with variants of the IRF6 gene are sisters.

1.5 Oxidative and inflammatory stress in relation to CLP

Reactive oxygen species (ROS) are strong oxidants, and may interact cellular biomolecules, such as DNA, leading to modification and potentially serious consequences for the cell^{71,187}. ROS can contribute to the etiology of congenital malformations by disrupting migration of CNCCs to the orofacial region⁷¹. Exposure to ROS, generated by maternal smoking, was found to harm fetal growth and

development in humans¹⁸⁸⁻¹⁹¹. In rats, maternal diabetes was found to cause growth retardation and congenital anomalies in the offspring¹⁹². The relation between exposure to anti-epileptic drugs and the occurrence of CLP, and congenital heart disease was found¹⁹³⁻¹⁹⁵. Maternal smoking¹⁶⁶, alcohol consumption¹⁶⁷, infections^{170,174}, diabetes¹⁷¹, bleeding episodes during pregnancy¹⁹⁶, associated with increased oxidative and inflammatory stress¹⁹⁷⁻¹⁹⁹, were found to increase the incidence of babies with CLP. These findings strongly suggest that oxidative and inflammatory stress are involved in the etiology of CLP (**Figure 7**).

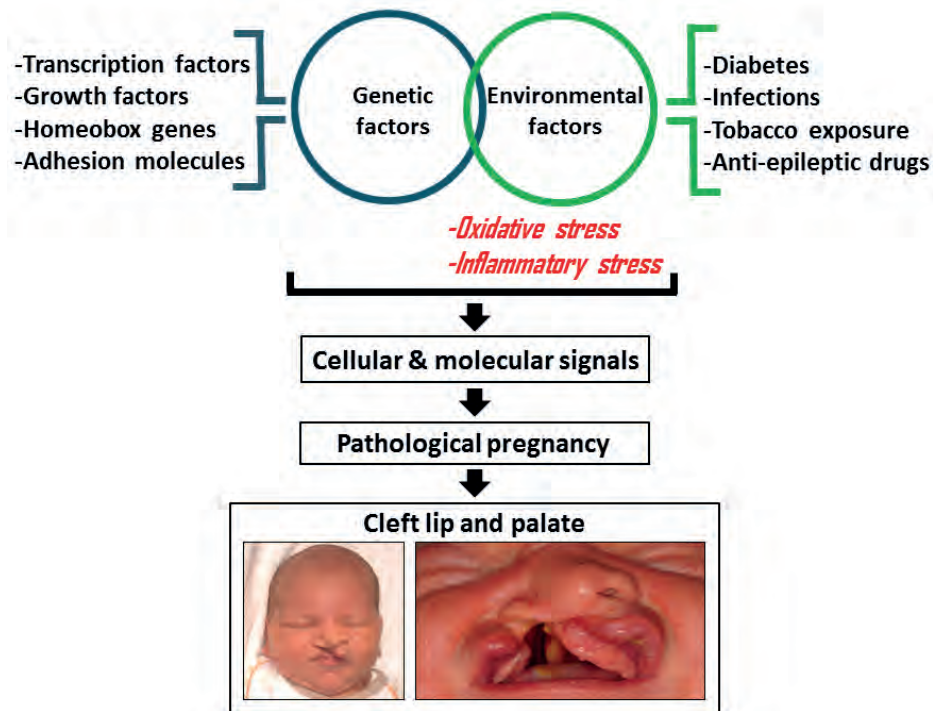


Figure 7: The etiology of cleft lip and palate. CLP can occur as syndromic and non-syndromic form. Syndromic CLP is characterized as CLP with additional congenital anomalies. Non-syndromic CLP is defined as CLP occurring in isolation. Syndromic CLP is caused by chromosomal aberrations and/or specific gene mutations. Non-syndromic CLP is caused by genetic factors, environmental factors, and the combination of both. Environmental factors can cause oxidative and inflammatory stress during pregnancy, promoting pathological pregnancy and increasing the risk of CLP formation.

Section 2. Surgical CLP repair, scarring and growth inhibition

2.1 Surgical CLP repair during childhood

Patients with CLP receive multidisciplinary treatment from early childhood until adulthood, including several surgeries by specialists. The treatment of CLP is complex, and many variables influence the outcome, e.g. the severity and extent of the malformation, the surgical strategy, the surgeon's experience, and the timing with respect to the patients age²⁰⁰. These multidisciplinary teams of specialists include a plastic and reconstructive surgeon, maxillofacial surgeon, orthodontist, otolaryngologist, speech therapist, pediatrician, geneticist, a nurse practitioner or social worker, and sometimes a psychologist^{201,202}. Notably, in 201 multidisciplinary cleft centers in Europe, 194 different protocols were applied for the treatment of CLP²⁰³, and not one protocol is generally accepted. If the cleft is not surgically corrected, patients are prone to functional problems, as hearing problems due to otitis media, speech and feeding difficulties, and abnormal dental development due to loss of lip pressure²⁰⁴. Surgical interventions are necessary to reconstruct the anatomy of the affected craniofacial structures. CLP can affect patient's feeding, hearing speaking and swallowing²⁰⁵. Surgical CLP treatment enhances facial esthetics, which is important to achieve improved psychosocial well-being²⁰⁵. However, dependent on its severity, CLP patients may face a life-long care plan, which can have an impact on their quality of life²⁰⁵⁻²⁰⁸.

2.2 A brief history of surgical CLP repair

Evidence of the first attempts of surgical closure of a cleft lip are found in ancient Chinese scriptures. In a scripture from the Chin Dynasty (ca 229-317 A.D.) surgery of "harelips", as the cleft lip anomaly was called, has been described²⁰⁹⁻²¹². Furthermore, in the Tang dynasty (618-901 A.D.) a surgeon named Fang Kan was titled as "the doctor of lips' repair"²¹². Hundreds of years later, the first person in Europe who described the procedure of cleft lip repair was the Flemish surgeon Jehan Yperman (1295-1351), from the city Ieper²¹². In 1556, the French surgeon Pierre Franco defined an operation for closure of a cleft lip after removing a piece of epithelium, skin or mucosa on both sides of the cleft²¹³. The Dutch surgeon Hendrik van Roonhuyze (1622-1672) from Amsterdam recommended early surgical cleft lip closure, at the age of 3 or 4 months²¹⁴. It is important to realize that before the 19th century operations were performed without anesthesia, and therefore surgical lip closure had to be performed fast. The English physician John Snow was in 1847 the first one who administered chloroform as anesthesia for a surgical cleft lip repair²¹⁵. To improve nasal form following unilateral cleft lip repair, the American plastic surgeon Millard published in 1968 the "rotation advancement principle" using an exchange flap in the region of the anterior nostrils²¹⁶. This method has subsequently been modified by others. The operative techniques for

unilateral clefts of the lip are now regarded as satisfying, but the surgical closure of bilateral clefts still remains a challenge because of the often severely malpositioned premaxilla²¹¹. Although many surgeons have tried to translate the successful surgical techniques for unilateral clefts to bilateral clefts, this remains still unsatisfactory²¹⁷.

The first experiences with surgical cleft palate closure date from the 18th century. In 1764, Le Monnier, a French dentist, performed the first surgical closure of the soft palate, and introduced several sutures for this procedure²¹⁸. At that time there was still not the benefit of general anesthesia, and without general anesthesia surgical closure of the hard palate was not possible. Not until 1861, the surgical palatal closure with the use of anesthesia was described by the German surgeon Von Langenbeck, who also applied antiseptics for this procedure²¹⁹. The Irish surgeon Maurice Collis performed surgical closure of the hard palate in Dublin in 1867 using chloroform for general anesthesia²²⁰. Staged palatal closure was introduced by the German surgeon Herman Schwegkandiek in Marburg in 1951, including early soft palate closure, but hard palate closure until approximately 8 years old in order to avoid growth impairment²²¹. However, this staged closure was found to show good results as far as maxillary growth is concerned, but the disadvantage is the late development of proper speech. Despite great advances, not one method of treatment of CLP has yet been universally accepted^{222,223}. As mentioned before, for CLP patients many treatment protocols are propagated, indicating a lack of agreement regarding their outcome²²². The Dutch Practice Guideline for treatment of Patients with Cleft lip and Palate, published in 2018, also states that there is no evidence for better treatment outcomes regarding specific CLP treatment protocols or a particular treatment timing. Despite 250 years of experience with surgical palate closure, significant improvements in treatment outcome are still needed.

2.3 Scarring following surgical cleft palate repair can hamper facial development

The consequences of surgical CLP repair on the craniofacial development remain controversial. An important factor for craniofacial growth is the iatrogenic effect of surgical interventions²²⁴. Structural distortions of the face can develop gradually over time and can be regarded as the price that has inevitably to be paid for the advantages that early surgical closure of the lip and palate brings²²⁵. Notably, individuals with a cleft that never had cleft surgery, such as in low-income countries and isolated habitats, demonstrated midfacial growth within quite normal limits^{226,227}, suggesting that the impaired growth is related to the scar formation following surgical CLP repair. Others found that the intrinsic hampering of maxillary development in unoperated bilateral cleft and alveolus patients was limited²²⁸. There remains an unresolved discussion on the effect of congenital maxillary growth deficiency vs. the effect of surgical intervention on the outcome of CLP treatment²²⁹. Intrinsic growth impairment in subjects with orofacial clefts can be studied by comparing facial morphology of subjects

with untreated cleft and unaffected individuals of the same ethnic background²²⁹. Interestingly, facial variation in subjects with unrepaired complete bilateral clefts²²⁹ and in subjects with unilateral cleft lip and alveolus/palate²³⁰ occurred in the anteroposterior direction. But, in controls the facial variation was mostly found in the vertical direction^{229,230}. These finding suggests that individuals with unilateral or bilateral clefts can have an intrinsic horizontal midfacial growth impairment affecting facial morphology^{229,230}.

Hypertrophic scar formation following primary cleft lip repair varies widely, from 8% to 47%^{29,231,232}. Cleft lip repair in unilateral CLP patients causes transverse narrowing of the maxilla²³³, resulting in a posterior cross bite, accompanied by crowding and retro-inclined upper incisors²²⁵. Scarring following cleft lip repair can lead to the creation of secondary deformities, such as deformed philtrum, Cupid's bow asymmetry, tight upper lip, whistle deformity, and irregularities in the functioning of orbicularis oris muscle^{30,234,235} (**Figure 8**). Notably, surgical cleft lip repair in unilateral CLP patients was found to cause transverse narrowing of the maxilla without sagittal growth restriction²³³. The normal elongation of the maxilla is thus usually not affected by lip surgery²³⁶.

Palatal surgery seems mainly responsible for sagittal growth inhibition of the maxilla³¹. However, surgical closure of the cleft palate by the vomerine flap repair was found not to affect maxillary growth at 10 years of age in UCLP patients, but at this age, the growth is not yet complete²³⁷. The displacement of the upper jaw in relation to the vomer is recognized, and surgical cleft palate repair can affect the growth of the vomero-(pre)maxillary suture²³⁶. Furthermore, growth of the periosteum, a dense fibrous membrane covering the surface of bones, necessary for the development of dentoalveolar structures, might be affected by scar tissue after surgical cleft palate repair²³⁶. The distribution of scar tissue on palates is related to the severity of the maxillary dental arch constriction²³⁸ (**Figure 9**). The scar tissue on the palate may thus not only impair dento-alveolar development but can also restrict normal midfacial growth²³⁹ (**Figure 9**).

In the literature there is still no consensus about the ideal timing for surgical palatal closure in patients with unilateral CLP in terms of facial growth²⁴⁰. To reduce the risk of growth interference, centers have experimented with 2-stage palate repairs with delayed hard palate closure. The 2-stage procedure was thought to narrow the palate, allowing the use of smaller flaps at the time of the hard palate repair²⁴¹⁻²⁴³. Indeed, several studies have observed that the 2-stage procedure facilitates normal midfacial growth^{31,244-246}. Because of the low level of evidence and high risk of bias in most studies, it is not possible to prove or rebut that postponing surgery of the hard palate will bring benefits in terms of maxillary growth²⁴⁰.

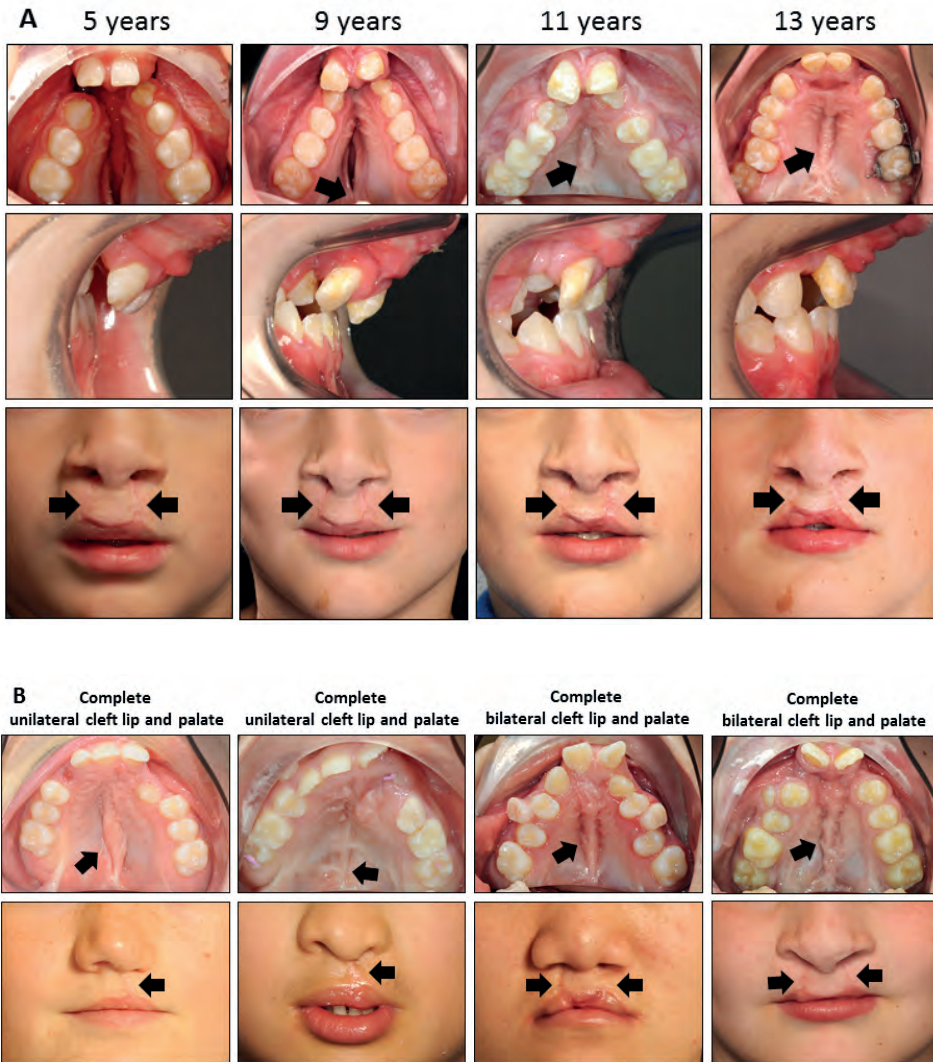


Figure 8: Scarring of the lip and palatal mucosa following surgical CLP repair. (A) This case demonstrates scarring (black arrow) of the upper lip and palatal mucosa following surgical CLP repair. Surgical lip closure, at 6 months of age, soft palate closure, at one year of age, and pharyngeal flap surgery was performed at 4 years of age. At 9 years of age a bilateral cleft of the alveolus together with displacement of the pre-maxilla, and a palatal cleft is present. Retro-inclined maxillary incisors are observed, together with a collapse of the lateral maxillary segments. At the age of 10 years alveolar bone grafting was performed combined with surgical hard palate closure. At 11 years of age the palatal mucosa demonstrated scar formation (black arrow) after surgical cleft palate closure. Orthodontic expansion was performed to correct the collapsed dental arch at the age of 13 years. Scarring of the palatal mucosa and upper lip is still obvious. **(B)** Scarring (black arrow) of the upper lip and palatal mucosa following CLP surgery in 2 patients with a unilateral and 2 patients with a bilateral cleft lip and palate. The top row shows intra-oral pictures at the age of 11 years, after surgical palatal closure. The extra-oral photos in the bottom row show scarring of the lip, because of the repaired cleft lip, and a residual deformation of the nose.

Furthermore, there is still a controversy between maxillofacial growth and speech. Children with CLP show delayed speech development²⁴⁷. Children who underwent early palate repair, before 12 months of age, exhibited better speech compared to those with palate repair between 12 and 27 months²⁴⁸, or between 24 and 36 months²⁴⁹. The downside of delayed hard palate closure is the higher incidence of velopharyngeal insufficiency and compensatory misarticulations^{245,250}. Velopharyngeal dysfunction, a failure of the soft palate to close against the posterior pharyngeal wall, leading to air leakage into the nasal passages during speech, causing hypernasal speech, can be reduced by performing pharyngeal flap surgery²⁵¹. Velopharyngeal dysfunction persists in 7 to 30% of the surgically-treated CLP patients^{252,253}. Pharyngeal flap surgery, between the ages of 5–7 years, was found to increase retro-inclination of the upper incisors²⁵⁴. Furthermore, 19% of CLP patients who underwent pharyngoplasty required a Le Fort I maxillary surgical advancement, against 8% of the CLP patients who did not undergo pharyngoplasty²⁵⁵, indicating that pharyngoplasty may impair maxillary growth from childhood to adulthood. In contrast, several other studies found no interference of pharyngoplasty with facial growth²⁵⁶⁻²⁵⁹.

In conclusion, scarring following cleft lip repair may affect facial esthetics and the dental arch form, but surgical lip closure seems not to restrict maxillary growth over time²³³. In contrast, surgical cleft palate closure is related to midfacial growth inhibition in the long term³¹. Interestingly, it is thought that in subjects with unoperated cleft lip and alveolus/palate a minor intrinsic growth deficiency may already be present^{229,230}. In addition, subjects with an unoperated complete-cleft lip, alveolus, and palate were found to develop a dental arch form with a significant smaller width and depth compared to subjects with unoperated cleft lip and alveolus without cleft palate²⁶⁰. Therefore, it is thought that the minor intrinsic growth deficiency may be further exaggerated by scar formation following surgical cleft palate repair.

Several animal studies have been performed to study the effects of CLP surgery on maxillary growth²⁶¹. Surgical closure of experimentally created CLP performed in 6-week-old rabbits and 8-week-old beagle dogs demonstrated impaired facial growth²⁶¹. Surgically-induced cleft lip, alveolus and palate cleft in 6-week-old rabbits resulted in impaired maxillary growth after surgical cleft closure²⁶². In beagle dogs, surgical repair of experimentally created cleft lip, alveolus and palate caused hampered craniofacial growth²⁶³. Surgical closure of experimentally created mucoperiosteal soft tissue defects, by elevating the palatal mucoperiosteum and leaving the bone adjacent to the dentition denuded, hampered transverse palatal growth in beagle dogs, but sagittal maxillary growth was affected to a minor degree²⁶⁴. However, in Old Spanish Pointer dogs with a 15-20% spontaneous congenital cleft palate rate, impaired sagittal and transversal growth of the maxilla was observed in the cleft palate dogs compared to the control dogs without congenital cleft palate²⁶⁵, indicating some intrinsic growth impairment in congenital cleft palate. Notably, several genes that are associated with

CLP development, as Wnt, TGF- β 3 and IRF6 are also involved in the process of wound repair²⁶⁶.

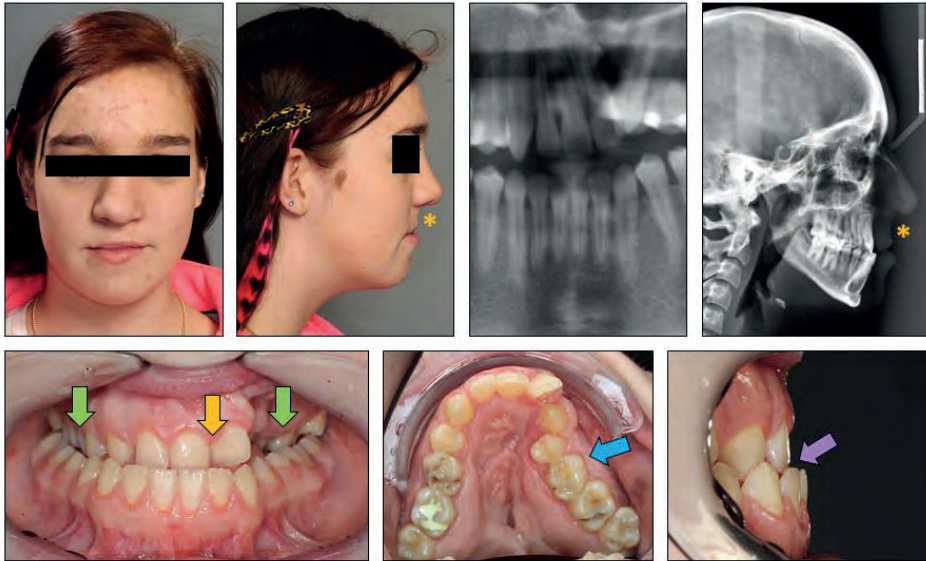


Figure 9: Disturbed development of maxillary skeletal and dento-alveolar structures following surgical CLP repair. Disturbed development of maxillary skeletal and dento-alveolar structures observed in a 15-year-old patient with unilateral CLP. The upper left lateral incisor was missing. A hampered midfacial sagittal growth (yellow asterisk), together with transversal maxillary dental arch collapse (blue arrow), leading to a bilateral posterior (green arrow) and frontal dental (purple arrow) crossbite. The upper incisors are retro-inclined, and the upper dental midline is severely deviated to the left side (yellow arrow).

2.4 Wound healing and scar formation

Wound healing is a precisely coordinated process of cellular, molecular, and biochemical events to restore the anatomy of the injured tissue²⁶⁷⁻²⁷⁰. Following hemostasis, the healing process occurs through a series of sequential overlapping phases: *inflammation*, *proliferation*, and *remodeling*^{268,271,272}.

During hemolysis, erythrocyte destruction leads to hemoglobin (Hb) release into the circulation. In the extracellular milieu, Hb undergoes different oxidation stages resulting in the release of free heme²⁷³. Upon hemolysis, release of free heme molecules in the circulation induce oxidative stress reactions by damaging endothelial cells and oxidizing lipoproteins, which can activate systemic inflammatory responses²⁷⁴. Local release of heme may be a physiologic trigger to start inflammatory processes in wound healing²³⁹.

The *Inflammation phase* is initiated to destroy possible invading bacteria and to eliminate damaged cells, preparing the wound bed for the growth of new tissue²⁷⁵. The fibrin aggregated platelets release growth factors and cytokines, attracting leukocytes, granulocytes, and macrophages to the site of injury^{272,276}. Transforming

growth factor beta 1 (TGF- β 1) is immediately released by platelets after injury, and recruits macrophages and fibroblasts to the wound site²⁷⁷. The granulocytes will clear the wound from invading pathogens and cellular debris²⁷⁸. Recruited monocytes differentiate into pro-inflammatory M1 macrophages and anti-inflammatory M2 macrophages²⁷⁹⁻²⁸¹. The M1 macrophages release pro-inflammatory cytokines and chemokines, such as Interleukin-8 (IL-8), Monocyte Chemoattractant Protein-1 (MCP-1), C-C chemokine receptor type 2 (CCR2), and CXCL10 to further attract additional leukocytes²⁸². The anti-inflammatory M2 macrophages clear the wound area from the apoptotic cells by phagocytosis, and cause resolution of inflammation by producing anti-inflammatory cytokines, such as IL-10 and vascular endothelial growth factor (VEGF)^{275,283}.

The *proliferation phase* is characterized by the replacement of the provisional extracellular matrix (ECM) with newly formed granulation tissue, contraction of the wound margins, and covering the wound by re-epithelialization²⁸⁴. The cellularity of the wound increases as fibroblasts, vascular endothelial cells and epithelial cells migrate to the site of injury and start to proliferate²⁸⁵. The newly formed capillaries grow into the wound site to deliver fluid, oxygen, nutrients, and leukocytes needed for the proliferating tissues^{286,287}. Fibroblasts then produce the ECM, which is a three-dimensional network of extracellular macromolecules containing collagen fibers, enzymes, and glycoproteins, that provide structural and biochemical support. In the wound healing process the ECM contains collagen type III fibers which are deposited in a disorganized manner²⁸⁷. Some fibroblasts then differentiate into myofibroblasts, and those myofibroblasts continue to deposit ECM of collagen type III fibers²⁸⁸. These myofibroblasts generate high contractile forces by using the α -smooth muscle type actin-myosin complex to close the wound through interactions with the ECM^{289,290}. The conversion of fibroblasts into contractile myofibroblasts, and their maintenance is driven by mechanical stress and the release of TGF- β 1²⁹⁰. Epithelialization is initiated during the response to injury and leads to keratinocyte proliferation and migration across the regenerating ECM²⁶⁶. Besides, TGF- β 1 signaling regulates keratinocyte proliferation and migration during epithelialization^{291,292}. Also, the release of chemokine CXCL11 by keratinocytes promotes the migration of undifferentiated keratinocytes into the wound to fulfil wound coverage by epithelialization²⁹³. After epithelialization is complete, wound contraction does not continue, and during normal wound healing most myofibroblasts undergo apoptosis^{294,295}, resulting in minimal scar tissue²⁸⁸.

The *remodeling phase* outlines tissue remodeling and maturation to gain greater tensile strength and flexibility. The remodeling of the ECM is mainly carried out by fibroblasts, degrading the collagen type III fibers, which are earlier produced mainly by myofibroblasts, by the release of matrix metalloproteinases (MMPs), and deposition of type I collagen fibers^{289,296}. This phase begins about a week after injury and may

continue for years^{297,298}. The collagen fibers get cross-linked, reducing the thickness of the scar tissue and making the skin area stronger²⁹⁹. Tensile strength can be restored to a maximum of 80% of its original strength in approximately one year^{267,300}. The majority of blood vessels finally disappear from the wound area²⁸⁷. Human wound healing normally ends up with some remaining non-functioning fibrotic tissue, known as a scar³⁰¹.

2.5 Excessive scar formation following oxidative, inflammatory, and mechanical stress

Although inflammation is a protective and necessary process, the inflammatory process needs to be tightly controlled to prevent chronic inflammation³⁰²⁻³⁰⁴. Inflammatory cells produce ROS, like H_2O_2 (hydrogen peroxide) via their plasma membrane nicotinamide adenine dinucleotide phosphate (NADPH) oxidase³⁰⁵. Prolonged inflammation and elevated levels of ROS can result in hampered wound repair and /or excessive scarring^{29,306}. Extended excessive oxidative and inflammatory stress may overwhelm adaptive protective mechanisms and aggravate tissue damage and can lead to pathological wound repair^{29,307,308}. Chronic inflammation can lead to deposition of excessive collagen type III fibers and ECM proteins within the wound area, fueling the process of hypertrophic scarring of the tissue, called fibrosis^{29,288,309,310}. Inflammation is crucial in the initiation, maintenance, and progression of hypertrophic scarring³¹¹. Enhanced TGF- β 1 levels are observed in the epidermis of human chronic wounds³¹². Elevated levels of TGF- β 1 is associated with hypertrophic scar formation³¹³, and decreasing TGF- β 1 signaling was found to improve the wound healing process with less scarring³¹⁴. Healing of the oral mucosa occurs normally quicker and form less scar tissue, because of rapid re-epithelization and collagen fibrils formation, compared with dermal wounds³¹⁵. In an experimental wound model study in mice a decreased TGF- β 1 production was found in oral mucosa compared to dermal wounds, underscoring that TGF- β 1 promotes scar formation³¹⁵. However, despite the reduction of TGF- β 1, scar tissue formation still occurs in oral mucosa following palatal surgery³¹⁵. Hypertrophic scar formation is a frequent postoperative complication that impairs soft tissue form, function, or movement²⁹. Studying the wound healing process in diabetic patients led to more insight into the relation between oxidative and inflammatory stress and impaired wound healing³¹⁶. In diabetic wounds, mitochondrial overproduction of ROS can lead to high oxidative stress levels³¹⁷, which was found to impair the wound healing process³¹⁸. Diabetes decreases angiogenesis in healing wounds³¹⁹, compromising the three phases of wound healing, and delaying the orderly progression of healing^{249,286,320}. Diabetic patients develop a chronic low-grade inflammation characterized by a chronic production of pro-inflammatory cytokines, such as TNF- α , IL-1 β and IL-6^{321,322}. Macrophages in diabetic wounds also exhibit reduced phagocytic capacity, which allows bacteria and debris to accumulate and decreases expression of growth factors, such as VEGF³²³⁻³²⁵. Results from wound healing assays suggest that oxidative stress can induce

apoptosis in fibroblasts that are stimulated to proliferate and migrate into the wound margins and could lead to disturbed wound healing^{326,327}. Furthermore, excess ROS can cause pathological changes in ECM structure and function³²⁰. ROS exposure also increases expression of cysteine-rich protein 61 (CCN1), a negative regulator of collagen I production, in human dermal fibroblasts³²⁸.

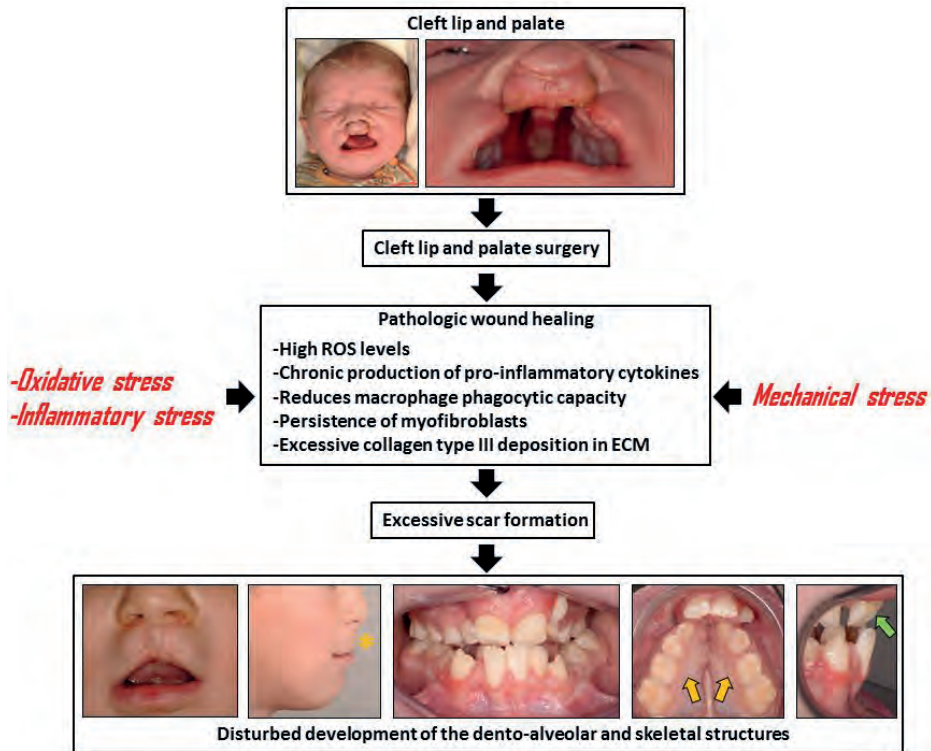


Figure 10: Etiology of excessive scar formation following cleft lip and palate surgery. Heme release, maternal diabetes and infections are associated with oxidative and inflammatory stress in the wound healing process. Prolonged wound contraction and skin stretching was found to generate mechanical stress during the wound healing process. During pathological wound healing the oxidative micro-environment, together with chronic production of pro-inflammatory cytokines and reduced macrophage phagocytic capacity, promotes the persistence of myofibroblasts, leading to excessive collagen type III deposition, generating excessive scar formation. These scars disturb the development of the skeletal and dento-alveolar structures, causing midfacial deficiency (yellow asterisk), transversal collapse of the upper dental arch (yellow arrow) with retro-inclined upper incisors (green arrow).

Prolonged tension by wound contraction, and mechanical stress caused by skin stretching is another causative factor for scar formation^{329,330}. Abnormal scars often occur at specific sites subjected to skin stretching, such as joints³⁰¹. Mechanical stress is crucial in the initiation, maintenance, and progression of hypertrophic scarring³¹¹. Activation of TGF- β 1 expression by mechanical stimuli has been demonstrated *in vitro* in rat lung tissue³³¹, in cultured human corneal epithelial cells³³², and human gingival

fibroblasts³³³. The myofibroblast phenotype is regulated by mechanical stresses to which they are subjected and thus by mechanical signaling²⁸⁹. Dysregulation of ECM reconstruction was found to result in high contractile forces, leading to development of fibrosis²⁹⁰. In conclusion, oxidative, inflammatory, and mechanical stress following surgical cleft repair can lead to pathological wound healing, resulting in excessive scar formation, hampering growth and development of the dento-alveolar and skeletal structures (**Figure 10**).

Section 3. Cytoprotective mechanisms and signaling pathways in palatogenesis and wound healing

3.1 The cytoprotective enzyme system HO

Free heme molecules in the circulation are able to provoke oxidative stress reactions and systemic inflammatory responses²⁷⁴. The heme oxygenase (HO) system belongs to the most important cytoprotective mechanisms³³⁴. Two distinct isoforms, namely HO-1 and HO-2, have been identified³³⁵. HO are the rate-limiting enzymes breaking down heme into biliverdin, free iron (Fe^{2+}) and carbon monoxide (CO). Biliverdin is next rapidly converted into the anti-oxidant bilirubin by biliverdin reductase (BVR)^{336,337}. Free iron is a potent pro-oxidant molecule, but the increase in intracellular iron promotes co-induction of the iron scavenger ferritin, leading to a net decrease in free iron and overall decrease in oxidant status^{338,339}. CO has anti-inflammatory and anti-apoptotic properties³⁴⁰ (**Figure 11**). HO-1 is the inducible isoform and can be induced by a variety of pathophysiological stimuli, including its substrate heme, cytokines, endotoxins, hypoxia and oxidative stress, while HO-2 is constitutively expressed³⁴¹.

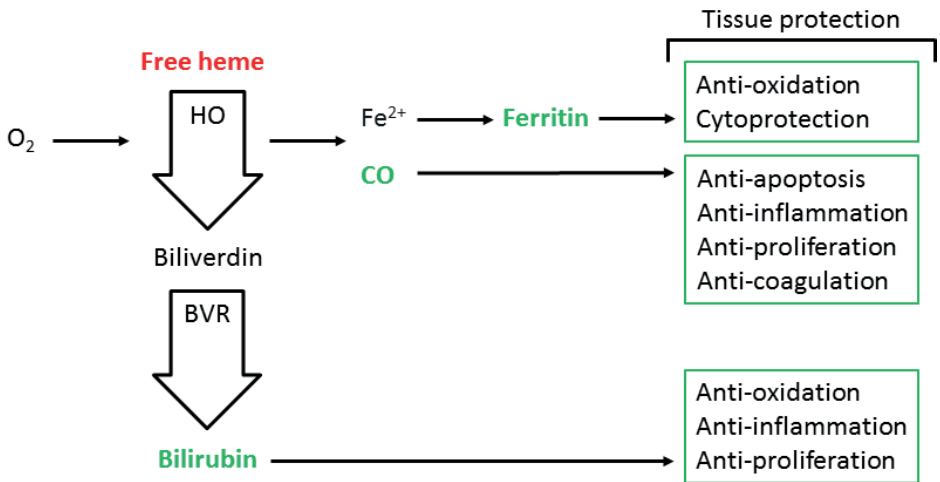


Figure 11: Free heme degradation by the cytoprotective enzyme systems HO and BVR. Circulating free heme molecules can generate oxidative and inflammatory stress (red). Degradation of free heme, via O_2 -dependent oxidation, by both isoforms heme oxygenase (HO)-1 and HO-2 enzyme systems produces biliverdin, free iron (Fe^{2+}), and carbon monoxide (CO). Biliverdin is converted into bilirubin by the enzyme biliverdin reductase (BVR). The HO end-products demonstrate diverse tissue protective effects (green). Free iron release following HO-activity triggers the production of ferritin, stimulating anti-oxidative and cytoprotective pathways. CO has been implicated in anti-apoptotic, anti-inflammatory, anti-proliferative, and anti-coagulative pathways. Bilirubin stimulates anti-oxidative, anti-inflammatory, and anti-proliferative pathways.

3.2 The role of HO in embryonic development

The HO system is a key regulator during embryological development. HO-1^{-/-} and HO-1^{+/-} mice exhibit a prolonged time for blastocyst attachment versus wild type mice³⁴². Both HO-1 and HO-2 enzymes are strongly expressed in the human placenta during embryonic development³⁴³. Maintenance of pregnancy is poor in HO-1^{-/-} mice, as extremely low birth rates are reported^{342,344}. In normal human third-trimester pregnancies, the placenta was found to express higher amounts of the HO-2 isoform than the HO-1 isoform³⁴⁵⁻³⁴⁷. In mice, HO-1 was found to promote intrauterine fetal survival³⁴², and showed critical in placentation, spiral artery remodeling, and blood pressure regulation during pregnancy³⁴⁸. Placental HO-1 activity modulates fetal growth in the rat³⁴⁹. HO-1³⁵⁰ and HO-2³⁴³ were downregulated in the placenta during human pathologic pregnancies. VEGF was shown to induce HO-1-dependent capillaries formation in cultured human microvascular endothelial cells (HMEC-1) and human umbilical vein endothelial cells (HUVECs) *in vitro*³⁵¹. In DBA/2-mated CBA/J females, used as an abortion-prone mouse model, a high rate of abortion was associated with decreased placental HO-1 expression³⁵². Placental HO protein expression is also decreased in preeclampsia patients³⁵³. HO-1 deficiency in both human and mice exhibits macromolecular oxidative damage, tissue injury and chronic inflammation^{354,355}. Pharmacological inhibition of HO-activity in pregnant rats resulted in a significant decrease in pup size, whereas transfection with adenoviral human HO-1 construct (hHO-1) resulted in increased pup size³⁴⁹.

3.3 The role of HO in wound healing

Following hemostasis after tissue injury Hb is endocytosed by macrophages and converted by the HO-1 pathway to release iron, CO and biliverdin in the wound area. Those three products of HO-1 activity can individually affect wound healing responses³⁵⁶. CO and bilirubin were found to exert anti-inflammatory properties to facilitate wound repair³⁵⁷. Induction of HO-1 mRNA and protein expression has been detected within three days after skin injury³⁵⁸. Interestingly, there is evidence that HO-1 expression in macrophages promotes formation of the anti-inflammatory M2-like phenotype²⁸¹. M1-like macrophages store the majority of the iron intracellularly in ferritin, whereas, M2-like macrophages release it to the extracellular environment via the transmembrane channel, ferroportin³⁵⁹. In a wound healing study in mice, the HO-1 pathway was found to promote angiogenesis and re-epithelialization³⁶⁰. HO-1 promotes wound closure by augmenting anti-inflammatory, antioxidant, and angiogenic activities in diabetic rats, suggesting an important role of heme breakdown in the wound healing process³⁶¹. Application of hydrogel incorporated with chestnut honey at full-thickness circular wounds in diabetic mice was found to promote early HO-1 expression, which accelerated the wound healing process³⁶². Excisional diabetic

wounds in rats showed faster wound closure following curcumin application, upregulating VEGF, TGF- β 1, CXCL12 and HO-1³⁶³. HO-1 induction following heme treatment increased cellular proliferation and collagen synthesis was observed, together with increased wound contraction in a full-thickness cutaneous wound model in rats³⁶⁴. Siam weed extract was found to increase HO-1 expression in Balb/c 3T3 fibroblast cell line, and promoted fibroblast migration in a cell migration assay *in vitro*³⁶⁵.

3.4.1 Common regenerative processes and signaling pathways in palatal fusion and wound healing

A paradigm within regenerative biology is that similar molecular and cellular signaling pathways controlling tissue generation during embryonic development often also control wound repair³⁶⁶. The process of palatogenesis shares many similarities with cutaneous wound healing²⁶⁶. The regenerative processes in palatal fusion and wound repair show familiar cellular signaling pathways and gene regulatory networks²⁶⁶. Especially proliferation and remodeling of mesenchymal and epithelial tissues in both processes will be discussed in relation to signaling via expression of transcription factors, growth factors and chemokines.

3.4.2 Mesenchymal cell recruitment and proliferation in palatal fusion and wound healing

The first similarity concerns recruitment of mesenchymal stem cells (MSCs) required for proliferation of the mesenchymal tissues for both growth of the palatal shelves, and regeneration of lost tissue during wound repair³⁶⁷. As discussed earlier, CNCCs migrate from the lateral ridges of the neural crest to the first branchial arch, to form the orofacial region, including the palatal structure of the maxilla^{59,67,68}. In particular, CXCL12-CXCR4 chemokine ligand-receptor-mediated chemotaxis was found to guide the migrating CNCCs over a long distance to their final destination^{47-49,57,58}. After the arrival of those CNCCs the face is still very small, and significant growth and expansion of the cranial structures will follow⁴⁵. In mice, the palatal shelf formation starts from the maxillary prominences at E11.5³⁶⁸. Each palatal shelf consists of a central core of neural-crest derived mesenchymal cells surrounded by an epithelium composed of cuboidal ectodermal cells⁹⁴. Proliferation of the mesenchyme alters the palate size and morphology of the palatal shelves³⁶⁹. Both palatal shelves first grow vertically besides the tongue, and thereafter, get elevated above the tongue⁸⁷. Sox9 expression was observed within the mesenchyme of the palatal shelves in mice during palatal shelf initiation at E12.5, vertical down-growth of palatal shelves at E13.5⁸⁵, and during palatal fusion at E15⁸⁶. It is therefore thought that Sox9-positive CNCCs contribute to the development of the palatal mesenchyme. Interestingly, CXCL12 expression in the medial and lateral part of the forming palate at E14.5 in mice has been observed³⁷⁰,

hypothesizing that CNCCs are actively recruited to the fusing palatal shelves. Repression of CNCC migration and proliferation by inhibiting the transcription factor family Zeb, was found to prevent fusion between cultured mice palatal shelves *in vitro*³⁶⁸. Furthermore, deletion of VEGFa reduced cell proliferation, and showed poor palatal shelf elongation, and variable palatal shelf elevation which led to cleft palate in mice *in vivo*³⁷¹. In the transgenic CL/Fr mouse 15% to 40% of newborns spontaneously develop CLP³⁷², and this finding was associated with a deficient cell proliferation of the secondary palatal mesenchyme³⁷³. Fgf10/Fgfr2b signaling was found to coordinate epithelial–mesenchymal interactions during palate formation in mice. *Fgf10* is expressed in the mesenchyme of developing palatal shelves, and its corresponding receptor, *Fgfr2b*, is expressed in the adjacent epithelium³⁷⁴.

Both *Fgfr2b*^{-/-} and *Fgf10*^{-/-} mouse mutants exhibit impaired shelf growth as the result of reduced palatal mesenchyme³⁷⁵. TGF-β1 drives palatal growth by promoting DNA synthesis and cell proliferation during early phases in mice³⁷⁶. TGF-β1 promotes also mesenchymal proliferation of the human palatal shelves³⁷⁷. Expression of TGF-β1 is found in the both palatal epithelial and mesenchymal cells between E12.0–E12.5 in mice³⁷⁸. Following suppression of expression levels of TGF-β1 receptor (TβR-I) by transfecting the siRNAs siTβR-I, murine cultured palatal shelves at E13 + 72 h were not fused which led to complete clefting in the anterior and posterior regions *in vitro*³⁷⁹. In A/J mice size reduction of the lateral nasal process was found following administration of phenytoin at E10, and led to orofacial clefting³⁸⁰. Administration of an overdose retinoic acid resulted in growth retardation of mouse fetus's palatal mesenchymal (MFPM) cells *in vitro*³⁸¹. Excessive retinoic acid administration permanently impeded palatal shelves growth *in vivo* in E13 in mice³⁸².

Proliferation of mesenchymal cells, including fibroblasts, endothelial cells, and inflammatory cells, is also essential for regeneration in cutaneous wound healing²⁶⁶. The importance of proliferation of mesenchymal tissue in wound healing has been demonstrated by several studies³⁸³. In murine full thickness ear wounds, increased CXCL12 expression was observed in the epithelium at day 3 and remained elevated through day 21. Thereby, CXCR4 was significantly elevated within 3 days of wounding in the epidermis³⁸⁴. CXCL12-delivering Lactobacilli, containing a plasmid encoding CXCL12, administrated topically to wounds in mice efficiently enhanced wound closure by increasing proliferation of dermal cells³⁸⁵. Impaired granulation tissue formation leads to delayed wound healing³⁸⁶. Treatment with MSCs significantly increased the proliferation of dermal fibroblasts and increased overall wound repair³⁸⁷. MSCs enhance angiogenesis by stimulating proliferation and recruitment of endothelial cells to facilitate new blood vessel formation³⁸⁸. MSCs were also found to enhance angiogenesis in chronic wounds by the secretion of VEGF³⁸⁹, and chemokine CXCL12³⁹⁰. CXCL12 is found to promote the recruitment of bone-marrow-derived MSCs which differentiate into endothelial cells and fibroblasts to form the granulation tissue^{272,391}.

3.4.3 Epithelium remodeling in palatal fusion and wound healing

The second similarity concerns epithelial cell migration during formation and remodeling of the epithelium involved in palatal fusion and wound closure²⁶⁶. In mice, a multi-layer epithelial seam is formed by the adhesion of the two MEE layers covering the tips of the palatal shelves at E14⁸³. Thereafter, the MEE seam thins to a single cell layer while at the same time MEE cells accumulate at the oral and nasal aspects to form epithelial triangle at E14,5 (**Figure 2**)³⁹². The epithelial seam eventually disappears so that only mesenchymal cells are observed in the midline of the palate, with islands of epithelial remnants by E15⁸³. One of the main hypotheses underlying MES disintegration is epithelial cell migration to either the oral^{91,92}, or nasal epithelium^{92,93}. Maintenance of the MES by repressing TGF- β signaling during the final stages of palatogenesis resulted in a failure of the palatal shelves to fuse³⁹³. However, expression of both TGF- β 1 and TGF- β 3 has been observed in the MEE³⁹⁴ and in the MES, and was associated with MES cell death³⁹⁵. Notably, loss of TGF- β signaling in the palatal epithelium leads to soft palate muscle cell proliferation and differentiation defects³⁹⁶. Live imaging analysis in unpaired murine palatal shelf culture, allowed observation of epithelial cell migration into the mesenchyme during the process of MEE removal *in vitro*⁹². Others found that MES cells migrated toward the oral side in *ex vivo* cultured mouse palatal shelves over 48 hours of tracking *in vitro*⁹¹. On the contrary, in another study migration of the MEE to the nasal side was observed in cultured mice palatal shelves, but not to the oral side *in vitro*⁹³. However, others found migration of the labeled MEE cells toward the oral and nasal ends³⁹⁷. Since these studies found no consensus of the direction of MEE migration, the process of MES disintegration during palatal fusion remains still not completely understood.

To close the defect in the epidermis following wound healing, keratinocytes have to get free from the basal lamina to migrate over the newly deposited ECM³⁹⁸. TGF- β 1 also promotes keratinocyte migration by stimulating MMPs³⁹⁹. After covering the wound bed keratinocytes start to proliferate to supply enough cells to form a multi-layered epithelium⁴⁰⁰. Once the wound is healed, defined as being fully epithelialized with no drainage, the proliferation signals cease and the stratification process begins³⁹⁸. Delayed wound closure is often due to reduced keratinocyte migration or proliferation⁴⁰¹. CXCR3, is expressed by maturing keratinocytes⁴⁰², and CXCL11-CXCR3 signaling increases keratinocyte migration²⁹³. Following CXCL11 exposure human keratinocytes demonstrated enhanced migration in a transmigration assay *in vitro*⁴⁰³, whereas CXCR3^{-/-} mice demonstrated a significant delay in re-epithelialization and deficient dermal maturation in excisional wounds⁴⁰⁴. Also in CXCL11^{-/-} mice delayed re-epithelialization in excisional wounds was found⁴⁰⁵.

In conclusion, mesenchymal cell proliferation is essential in both the developing palatal shelves and healing wounds, and inhibition was found to result in palatal clefting and delayed wound healing, respectively. Controlling the pro-oxidative

and pro-inflammatory stressors by induction of cytoprotective mechanisms that regulate inflammation and tissue repair may thus be necessary to promote tissue regeneration⁴⁰⁶. Formation and remodeling of the epithelium is needed in the process of palatal shelf adhesion and fusion and wound re-epithelialization.

3.5 The potential role of stem cells in wound healing

Stem cell therapy is clinically used in diverse pathologies, such as leukemia^{407,408}, and rheumatoid arthritis^{409,410}. Stem cell therapy has also potential for improving wound repair and promoting tissue regeneration⁴¹¹⁻⁴¹³. Administration of mesenchymal stem cells has been found to improve wound repair in rodents^{414,415}, minipigs⁴¹⁶, and humans⁴¹⁷. Stem cells are stored in niches, and are recruited to the site of injury, where they can differentiate into different cells necessary for wound repair, as keratinocytes, endothelial cells, pericytes, and monocytes⁴¹⁸. Wound repair can be improved by inducing re-epithelialization and angiogenesis⁴¹⁴. Unfortunately, stem cells die quickly after administration to an injured area^{419,420}. Seeding stem cells in collagen matrices has been found to enhance cell survival after delivery in non-healing wounds in humans⁴²¹, and diabetic rabbits⁴²². The lack of sufficient stem cell engraftment at sites of injury is a major limiting factor of stem cell-based therapies⁴²³. Interestingly, even when administered stem cells in the wound area do not differentiate, they still produce protective paracrine factors⁴²⁴. Cultured stem cells were found to produce diverse cytoprotective and anti-inflammatory proteins, including insulin-like growth factor-binding proteins (IGFBPs), granulocyte colony-stimulating factor (G-CSF), granulocyte-macrophage colony-stimulating factor (GM-CSF), platelet-derived growth factor AA (PDGF-AA), superoxide dismutase 2 (SOD2), pigment epithelium-derived factor (PEDF) and hepatocyte growth factor (HGF) *in vitro*⁴²⁵⁻⁴²⁷. The cytoprotective environment created by the stem cells inhibits the differentiation of fibroblasts into myofibroblasts, preventing the formation of hypertrophic scarring^{300,428}. However, the mechanisms of mesenchymal stem cell-mediated wound healing are still not completely understood⁴²⁹.

3.6 The complexity of chemokine-receptor signaling pathways

Chemokines are small proteins, usually 70–80 amino acid residues. The human genome and other mammalian genomes each encode approximately 50 different chemokines^{430,431}. Chemokines are classified into two major subfamilies (CC and CXC) and two minor subfamilies, CX3C and XC, based on the spacing of conserved cysteine (C) residues. Mammalian genomes each encode approximately 20 chemokine receptors. Chemokine receptors are classified according to the subfamily of chemokines to which most of their ligands belong. Receptors are named using the prefixes CCR, CXCR, CX3CR, and XCR followed by an identifying number^{430,431}. Chemokine receptors are integral membrane proteins composed of seven transmembrane helical segments. Activation occurs by binding of the chemokine to the

extracellular domain of the G protein-coupled receptor (GPCRs)⁴³². Notably, interaction between chemokines and their receptor can occur in a very complex manner. Different chemokines can interact with the same receptor, and different receptors can interact with the same chemokine⁴³³. Multiple chemokine ligands can also compete with each other and bind on different chemokine receptors⁴³¹. Chemokines can act as antagonists or synergize with other chemokines.

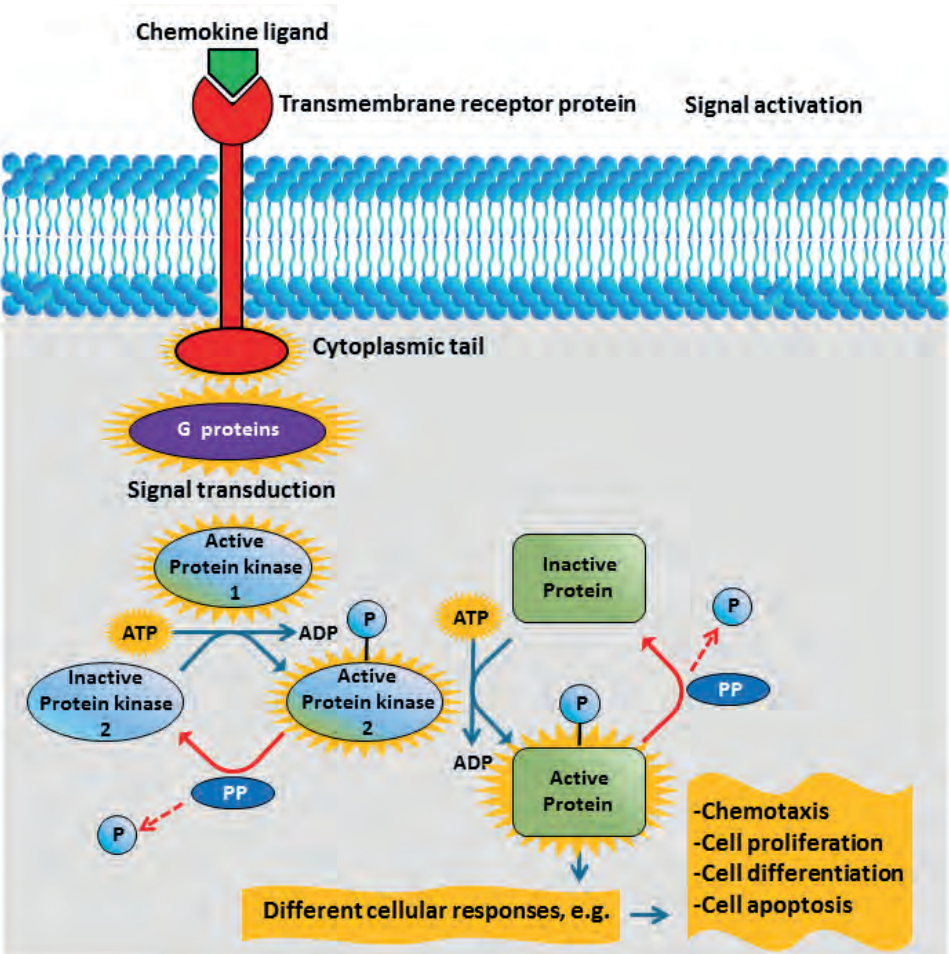


Figure 12: Schematic presentation of the mechanism of chemokine-chemokine receptor signaling pathways. Binding of the chemokine ligand to the chemokine transmembrane receptor changes its state and transduces a signal from its cytoplasmic tail inside the cell via G proteins or β -arrestins. Via phosphorylation of protein kinases a target protein gets phosphorylated, finally activating or inhibiting specific cellular responses. The phosphatases (PP) dephosphorylate the proteins bringing them to an inactive state.

Moreover, simultaneous or sequential triggering of two chemokine receptors can synergize its activation. Activation of one type of chemokine receptor can be synergized by chemokine heterocomplexes⁴³⁴. The available concentrations of other chemokines to which the receptor binds, and other receptors to which the chemokine binds influence their signaling⁴³⁰. However, there are also some chemokines that bind to receptors without inducing transmembrane signals⁴³⁰. The interplay between chemokine and receptor is even more complex than previously thought and still not entirely elucidated⁴³⁰.

Upon binding to their related chemokine ligands, the receptors undergo conformational changes and transduce a signal from their cytoplasmic tail inside the cell, activating intracellular effectors, as G proteins or β -arrestins, initiating signal transduction pathways^{430,435}. The signal transduction pathways run through a series of switch-like intermediates, going from inactivity to activity. In many cases the intermediates are protein kinases. Each phosphorylates the next kinase. These activated kinases are swiftly dephosphorylated by low-level phosphatases and return to inactivity. At the end of the pathway a particular cellular response gets inhibited or activated⁴³⁵ (**Figure 12**).

Signaling via chemokines is involved in a series of physiological and pathological events. Most chemokines are considered pro-inflammatory because their expression is induced in response to tissue damage⁴³⁰. Chemokine receptor activation leads to a variety of additional cellular and tissue responses, including chemotaxis, cellular proliferation, differentiation, apoptosis, angiogenesis, inflammation, hematopoiesis, and ECM remodelling⁴³⁶⁻⁴⁴². Chemokine signaling is also involved in a variety of processes like blastocyst implantation and placentation^{443,444}, recruitment of specific cells involved in wound healing⁴⁴⁵ and the immune system⁴⁴⁶, and in metastasis in cancer⁴⁴⁷⁻⁴⁴⁹.

3.7 CXCL12-CXCR4 and CXCL11-CXCR3 signaling in relation to oxidative stress and HO-activity

CXCL12 signaling is involved in processes that can reduce ROS levels. Administration of CXCL12 analog CTCE-0214D before LPS treatment in mice induced HO-activity and attenuated oxidative stress in liver and spleen tissue⁴⁵⁰. Cultured hematopoietic stem cells of CXCR4^{-/-} mice demonstrated increased endogenous production of ROS⁴⁵¹. Expression of CXCR4 in human cultured colorectal cancer cell lines was upregulated under hypoxia by hypoxia-inducible factor 1- α (HIF-1 α) activity⁴⁵².

In human cultured keratinocytes exposure to different concentrations of H₂O₂ promoted CXCL11 expression⁴⁵³. Low oxidative concentrations of H₂O₂ were found to impede CXCL11 mediated chemotaxis of activated human T cells *in vitro*⁴⁵⁴. Signaling via CXCR3-B was found to downregulate the expression of HO-1 in human breast cancer (MCF-7 and T47D) cell lines⁴⁵⁵.

Lastly, CXCL12-CXCR4 signaling was thus found to induce HO-1, reducing oxidative stress in human cell lines *in vitro*. By contrast, CXCR3 signaling was found to downregulate HO-1 and increase oxidative stress.

However, the complex relation between CXCL12-CXCR4 and CXCL11-CXCR3 signaling and HO-1 induction and oxidative stress has not been studied very extensively and needs further study.

3.8 The potential roles of CXCL12-CXCR4 and CXCL11-CXCR3 chemokine-receptor signaling in palatogenesis

We earlier described that CXCL12-CXCR4 chemokine-chemokine receptor signaling directs the migration of CNCCs to the branchial arches^{47-49,57,58}. CXCL12-CXCR4 signaling also plays a role in mechanisms as pregnancy, wound healing, immune system, cancer, and osteogenesis. CXCL12-CXCR4 signaling is involved in human blastocyst implantation⁴⁴⁴ by promoting cell survival and proliferation, and in inhibiting apoptosis of human trophoblasts⁴⁵⁶. Furthermore, CXCL12 and CXCR4 are diffusely expressed in human placenta⁴⁴³. In mice, CXCL12-CXCR4 signaling was found to recruit hematopoietic stem cells and mesenchymal stem cells to the wound area^{57,457}. CXCL12-CXCR4 signaling is associated with metastasis of rhabdomyosarcoma cells^{447,448}, breast cancer cells⁴⁵⁸, and colorectal cancer cells⁴⁵⁹. CXCL12-CXCR4 signaling also mediates osteogenic differentiation of cultured mesenchymal stem cells *in vitro*⁴⁶⁰.

We already discussed that in response to injury CXCL11-CXCR3 signaling promotes keratinocyte migration into the wound area²⁹³. Expression of CXCL11 was found to activate chemotaxis of CXCR3-positive T lymphocytes⁴⁶¹. CXCL11-CXCR3 signaling stimulated colon cancer metastasis to the draining lymph nodes⁴⁶². In zebrafish, CXCR3-CXCL11 signaling facilitated macrophage recruitment⁴⁶³.

Both CXCL12-CXCR4 and CXCL11-CXCR3 signaling pathways are thus involved in a wide variety of processes. Since its involvement in mesenchymal cell proliferation and migration, and osteogenesis, CXCL12-CXCR4 signaling may play an active role in palatogenesis. Since its regulatory role in keratinocyte migration and epithelial remodeling, CXCL11-CXCR3 signaling has a potential role in the coordination of MES disintegration to facilitate palatal fusion.

Section 4. Aims of the thesis

4.1 Objectives and research questions

In patients with CLP, the combined processes of palatogenesis, wound repair following surgical cleft repair, and orthodontic tooth movement all determine the resulting shape/morphology of the face. The purpose of this thesis is to explore the potential role of cytoprotective mechanisms in these processes.

We postulate that following oxidative and inflammatory stress during the process of palatal fusion, wound repair after surgical interventions, and orthodontic tooth movement the HO-system is induced to activate anti-oxidative and cytoprotective pathways. Furthermore, we hypothesize that decreased HO-activity during embryonic development, by either abrogation of HO-2 expression, or pharmacological inhibiting the activity of both HO isoforms, will lead to increased oxidative and inflammatory stress, leading to pathological pregnancy and increased risk of CLP formation (**Figure 13**). Moreover, we postulate for our experimental studies that mice fetuses exposed to oxidative and inflammatory stress following intraperitoneal administration of the alarmin heme in increasing doses at E12, will undergo pathological mechanisms, resulting in an increased risk of CLP formation.

The effects of palatogenesis in relation to HO-activity inhibition in combination with exposure to increasing heme levels will be studied as well. The effect of mechanical stress, generated by orthodontic forces in rats or by splinting of excisional wounds in mice, on the cytoprotective enzyme system HO will also be studied.

Proliferation and remodeling of the mesenchymal and epithelial tissues were essential in the process of both palatogenesis and wound healing. Since CXCL12-CXCR4 chemokine signaling is found to recruit CNCCs to form the craniofacial mesenchymal tissues, we postulate that chemokine receptor CXCR4 and its ligand CXCL12 are both expressed within the palatal shelves to facilitate palatal shelf growth, fusion and bone formation. Considering that CXCL11-CXCR3 chemokine signaling is important in the process of keratinocyte migration, epithelial remodeling and macrophage recruitment, we propose that chemokine receptor CXCR3 and its ligand CXCL11 will be expressed within the palatal shelves to promote MES disintegration and its clearance by macrophages.

Finally, we propose that stem cell administration may promote wound repair and reduce scar formation following cleft repair. Reduced scar formation possibly leads to minimized growth inhibition of the maxilla in surgically treated CLP patients, and may lead to less severe morphological features of CLP.

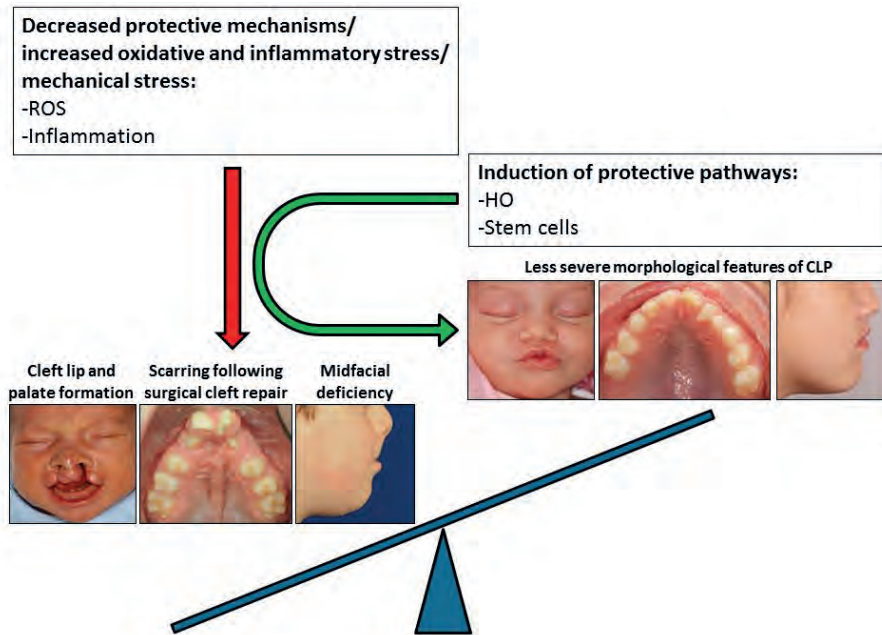


Figure 13: Cytoprotective mechanisms may harness against oxidative and inflammatory stress during palatogenesis and wound repair, and possibly reduce the risk of CLP formation or prevent excessive scarring following surgical cleft repair leading to less severe morphological features of CLP, respectively. Oxidative stress and inflammation are associated with a higher risk of CLP formation, and promote excessive scarring following injury. We postulate that decreased activity of the cytoprotective and anti-inflammatory enzyme system HO will cause increased ROS release and inflammation, leading to pathological pregnancy and increased risk of CLP formation. On the other hand, induction of HO-isoform HO-1 may neutralize ROS and inflammation, decreasing the risk of pregnancy pathology, including CLP formation. We postulate that inducing cytoprotective pathways, such as the HO system, prevent the development of pathological pregnancies, decreasing the risk of CLP formation. Furthermore, we suggest that HO-1 induction and stem cell administration may promote wound repair and reduce scar formation following surgical CLP repair. Reduction in scar formation possibly leads to less disturbed dento-alveolar structures and minimized growth inhibition of the maxilla in surgically treated CLP patients, and may lead to less severe morphological features of CLP. These processes will be investigated in animal models.

Research question 1: Do decreased cytoprotective mechanisms contribute to impaired embryonic development and palatogenesis?

Both genetic and environmental factors are involved in the etiology of CLP, and maternal risk factors as smoking, alcohol consumption, diabetes, infections, and anti-epileptic drugs were found to increase the risk of having a newborn with CLP. Oxidative and inflammatory signals contribute to the development of pathological pregnancies. A lack of protective signaling pathways may increase the risk of developing a pregnancy pathology, and possibly will increase the risk of CLP formation. In this thesis, we will investigate the effects of reduced cytoprotective mechanisms on embryonic growth and development, and palatogenesis in mice. Reduced cytoprotection was obtained by using a HO-2 KO mouse model, or by pharmacological inhibition of HO-activity using tin mesoporphyrin (SnMP) administration at E11.

Research question 2: Do decreased cytoprotective mechanisms in combination with exposure to increasing levels of oxidative and inflammatory stress impair embryonic development and palatogenesis in a dose-dependent manner?

To further clarify its role, the effects on embryonic growth and development, and palatogenesis will be studied in the presence and absence of protective pathways in combination with increasing oxidative and inflammatory stress levels. In mice, HO-activity was inhibited pharmacologically by SnMP administration and increasing oxidative and inflammatory stress levels were generated by administration of heme, an endogenous “alarmin” and the substrate of HO, in different dosage at E12. We postulate that administration of high doses of heme, in combination with HO-activity inhibition will lead to severe pathological pregnancy, resulting in disturbed embryonic development, with possibly increased risk of craniofacial anomalies, as CLP.

Research question 3: Does the CXCL11-CXCR3 chemokine-chemokine receptor signaling pathway facilitate MES disintegration during palatal fusion?

CXCL11-CXCR3 chemokine signaling has been found to regulate keratinocyte proliferation and migration during wound repair. We postulate that CXCL11-CXCR3 chemokine signaling is also important within the fusing palatal shelves to regulate MES disintegration during palatal fusion.

Research question 4: Does the CXCL12-CXCR4 chemokine-chemokine receptor signaling pathway facilitate palatal shelf development, and growth, and osteogenesis?

Chemokine-receptor signaling pathways regulate a wide variety of mechanisms during embryonic development. The CXCL12-CXCR4 chemokine-receptor signaling pathway is the main regulator of CNCCs recruitment to the first branchial arch, to form the mesenchymal tissues of the orofacial region. CXCL12-CXCR4 chemokine signaling also regulates osteogenesis. We therefore hypothesize that expression of CXCL12 and CXCR4 within the fusing palatal shelves in mice would regulate palatal shelf growth and palatal osteogenesis.

Research question 5: Does mechanical stress induce the cytoprotective enzyme HO-1 in the periodontal tissues following orthodontic force application, and in the regenerative wound area following excisional wound splinting?

Hampered facial growth often observed in CLP patients was associated with scar formation after surgical cleft palate repair. Surgical cleft palate closure can lead to impaired regeneration of muscle and skin, fibrosis, and scar formation. Resolution of acute inflammation is mediated and controlled by endogenous antioxidants and anti-inflammatory regulators and pathways. These protective factors are crucial for preventing excessive tissue damage. Oxidative stress and inflammation need to be

controlled to prevent excessive scar formation as the result of chronic inflammation. Recruited leukocytes into the wounded tissues may differentiate into anti-inflammatory M2 macrophages to form a regenerative environment. We further postulate that HO-1 is induced following mechanical stress during the process of orthodontic tooth movement and wound repair after surgical cleft repair. Upregulation of cytoprotective pathways must reduce the release of pro-inflammatory chemokines, cytokines and cell adhesion molecules to promote the proliferation and remodeling phases of wound repair, leading to less scar formation.

Research question 6: Do umbilical cord blood stem cells and molecular targets in tissue engineering promote muscle and skin repair following cleft surgery?

Surgical cleft palate closure can lead to impaired regeneration of muscle and skin, fibrosis, and scar formation resulting in hampered facial growth. Improved skin and muscle regeneration could possibly be obtained by targeting inflammatory pathways. Tissue engineering techniques using these cord blood stem cells and molecular targeting of inflammation and fibrosis during surgery may promote tissue regeneration.

4.2 Outline of the thesis

In **PART I**, we investigated the effect of diminished cytoprotective mechanisms on embryogenesis.

Using HO-2 deficient mice:

- In order to better understand the relation between embryonic development, MES disintegration at E15, and the absence of HO-2 expression. (**Chapter 2**),
- In order to better understand the process of MES disintegration at E15 in relation to CXCL11-CXCR3 signaling (**Chapter 2**),
- in order to better understand the process of palatal osteogenesis at E15 and E16 in relation to CXCL12-CXCR4 signaling (**Chapter 3**).

By pharmacological inhibition of HO-activity from E11:

- In order to understand the relation between palatal fusion at E16, and HO-activity (**Chapter 3**).

In **PART II**, we studied the effect of dose-dependent exposure to oxidative and inflammatory stress during embryogenesis in relation to diminished cytoprotective mechanisms:

- by inhibiting activity of both isozymes HO-1 and HO-2 from E11, and administration of heme at E12, an endogenous “alarmin” and the substrate of HO, in increasing concentrations, to better understand the process of embryonic development, placental development and palatal fusion at E16 (**Chapter 4**).

In **PART III**, we investigated the induction of cytoprotective mechanisms in relation to mechanical stress:

- within the cells of the PDL and osteoclasts, created by application of a constant orthodontic force, such as experienced in patients with CLP (**Chapter 5**).
- during excisional wound repair, such as experienced in growing patients with CLP after surgery, using a splinted excisional wound model; the natural physiological role of HO-1 during this process will be evaluated (**Chapter 6**).

In **PART IV**, we reviewed the role of molecular targets and umbilical cord blood stem cells in tissue engineering to improve hampered muscle and skin regeneration, as experienced in growing patients following surgical CLP repair (**Chapter 7**).

In **PART V**, we discuss our main findings and future perspectives are proposed (**Chapter 8**). This part concludes with summaries in English (**Chapter 9**) and Dutch (**Chapter 10**).

References

1. Carvajal Monroy PL, Grefte S, Kuijpers-Jagtman AM, Wagener FA, Von den Hoff JW. Strategies to improve regeneration of the soft palate muscles after cleft palate repair. *Tissue Eng Part B Rev.* 2012;18(6):468-477.
2. Bartzela TN, Carels CE, Bronkhorst EM, Ronning E, Rizell S, Kuijpers-Jagtman AM. Tooth agenesis patterns in bilateral cleft lip and palate. *Eur J Oral Sci.* 2010;118(1):47-52.
3. Worley ML, Patel KG, Kilpatrick LA. Cleft Lip and Palate. *Clin Perinatol.* 2018;45(4):661-678.
4. Gundlach KK, Maus C. Epidemiological studies on the frequency of clefts in Europe and world-wide. *J Craniomaxillofac Surg.* 2006;34 Suppl 2:1-2.
5. Mossey PA, Little J, Munger RG, Dixon MJ, Shaw WC. Cleft lip and palate. *Lancet.* 2009;374(9703):1773-1785.
6. Tanaka SA, Mahabir RC, Jupiter DC, Menezes JM. Updating the epidemiology of cleft lip with or without cleft palate. *Plast Reconstr Surg.* 2012;129(3):511e-518e.
7. Slavkin HC. Incidence of cleft lips, palates rising. *J Am Dent Assoc.* 1992;123(11):61-65.
8. Brown NL, Sandy JR. Tails of the unexpected: palatal medial edge epithelium is no more specialized than other embryonic epithelium. *Orthod Craniofac Res.* 2007;10(1):22-35.
9. Luijsterburg AJ, Rozendaal AM, Vermeij-Keers C. Classifying common oral clefts: a new approach after descriptive registration. *Cleft Palate Craniofac J.* 2014;51(4):381-391.
10. Lachmann R, Schilling U, Bruckmann D, Weichert A, Bruckmann A. Isolated Cleft Lip and Palate: Maxillary Gap Sign and Palatino-Maxillary Diameter at 11-13 Weeks. *Fetal Diagn Ther.* 2018;44(4):241-246.
11. James JN, Schlieder DW. Prenatal Counseling, Ultrasound Diagnosis, and the Role of Maternal-Fetal Medicine of the Cleft Lip and Palate Patient. *Oral Maxillofac Surg Clin North Am.* 2016;28(2):145-151.
12. Rey-Bellet C, Hohlfield J. Prenatal diagnosis of facial clefts: evaluation of a specialised counselling. *Swiss Med Wkly.* 2004;134(43-44):640-644.
13. Davalbhakta A, Hall PN. The impact of antenatal diagnosis on the effectiveness and timing of counselling for cleft lip and palate. *Br J Plast Surg.* 2000;53(4):298-301.
14. Clementi M, Tenconi R, Bianchi F, Stoll C. Evaluation of prenatal diagnosis of cleft lip with or without cleft palate and cleft palate by ultrasound: experience from 20 European registries. EUROSCAN study group. *Prenat Diagn.* 2000;20(11):870-875.
15. Johansson B, Ringsberg KC. Parents' experiences of having a child with cleft lip and palate. *J Adv Nurs.* 2004;47(2):165-173.
16. Tsuchiya S, Tsuchiya M, Momma H, et al. Association of cleft lip and palate on mother-to-infant bonding: a cross-sectional study in the Japan Environment and Children's Study (JECS). *BMC Pediatr.* 2019;19(1):505.
17. Hunfeld JA, Tempels A, Passchier J, Hazebroek FW, Tibboel D. Brief report: parental burden and grief one year after the birth of a child with a congenital anomaly. *J Pediatr Psychol.* 1999;24(6):515-520.
18. De Cuyper E, Dochy F, De Leenheer E, Van Hoecke H. The impact of cleft lip and/or palate on parental quality of life: A pilot study. *Int J Pediatr Otorhinolaryngol.* 2019;126:109598.
19. Al-Namankany A, Alhubaishi A. Effects of cleft lip and palate on children's psychological health: A systematic review. *J Taibah Univ Med Sci.* 2018;13(4):311-318.
20. Cobourne MT. Cleft Lip and Palate Epidemiology, Aetiology and Treatment Preface. *Front Oral Biol.* 2012;16:ix-ix.
21. Sivertsen A, Wilcox AJ, Skjaerven R, et al. Familial risk of oral clefts by morphological type and severity: population based cohort study of first degree relatives. *BMJ.* 2008;336(7641):432-434.
22. Germec Cakan D, Nur Yilmaz RB, Bulut FN, Aksoy A. Dental Anomalies in Different Types of Cleft Lip and Palate: Is There Any Relation? *J Craniofac Surg.* 2018;29(5):1316-1321.
23. De Clerck HJ, Cornelis MA, Cevdanes LH, Heymann GC, Tulloch CJ. Orthopedic traction of the maxilla with miniplates: a new perspective for treatment of midface deficiency. *J Oral Maxillofac Surg.* 2009;67(10):2123-2129.
24. Kummer AW. Communication disorders related to cleft palate, craniofacial anomalies, and velopharyngeal dysfunction. *Semin Speech Lang.* 2011;32(2):81-82.
25. Alfwaress FSD, Khwaileh FA, Rawashdeh MA, Alomari MA, Nazzal MS. Cleft Lip and Palate: Demographic Patterns and the Associated Communication Disorders. *J Craniofac Surg.* 2017;28(8):2117-2121.

26. Barbosa DA, Scarmagnani RH, Fukushima AP, Trindade IE, Yamashita RP. Surgical outcome of pharyngeal flap surgery and intravelar veloplasty on the velopharyngeal function. *Codas*. 2013;25(5):451-455.
27. Turner SR, Thomas PW, Dowell T, Rumsey N, Sandy JR. Psychological outcomes amongst cleft patients and their families. *Br J Plast Surg*. 1997;50(1):1-9.
28. Wolford LM, Stevao EL. Correction of jaw deformities in patients with cleft lip and palate. *Proc (Bayl Univ Med Cent)*. 2002;15(3):250-254.
29. Papathanasiou E, Trotman CA, Scott AR, Van Dyke TE. Current and Emerging Treatments for Postsurgical Cleft Lip Scarring: Effectiveness and Mechanisms. *J Dent Res*. 2017;96(12):1370-1377.
30. Bartkowska P, Komisarek O. Scar management in patients after cleft lip repair-Systematic review Cleft lip scar management. *J Cosmet Dermatol*. 2020;19(8):1866-1876.
31. Ross RB. Treatment variables affecting facial growth in complete unilateral cleft lip and palate. *Cleft Palate J*. 1987;24(1):5-77.
32. Leshem D, Tompson B, Phillips JH. Segmental LeFort I surgery: turning a predicted soft-tissue failure into a success. *Plast Reconstr Surg*. 2006;118(5):1213-1216.
33. Nocini PF, D'Agostino A, Trevisiol L, Bertossi D. Treatment of scars with Er:YAG laser in patients with cleft lip: a preliminary report. *Cleft Palate Craniofac J*. 2003;40(5):518-522.
34. Sinko K, Jagsch R, Precht V, Watzinger F, Hollmann K, Baumann A. Evaluation of esthetic, functional, and quality-of-life outcome in adult cleft lip and palate patients. *Cleft Palate Craniofac J*. 2005;42(4):355-361.
35. Marcusson A, Paulin G, Ostrup L. Facial appearance in adults who had cleft lip and palate treated in childhood. *Scand J Plast Reconstr Surg Hand Surg*. 2002;36(1):16-23.
36. Raud Westberg L, Hoglund Santamarta L, Karlsson J, Nyberg J, Neovius E, Lohmander A. Speech outcome in young children born with unilateral cleft lip and palate treated with one- or two-stage palatal repair and the impact of early intervention. *Logoped Phoniatr Vocol*. 2019;44(2):58-66.
37. Tollefson TT, Senders CW, Sykes JM. Changing perspectives in cleft lip and palate: from acrylic to allele. *Arch Facial Plast Surg*. 2008;10(6):395-400.
38. Hallock GG. In utero cleft lip repair in A/J mice. *Plast Reconstr Surg*. 1985;75(6):785-790.
39. Sullivan WG. In utero cleft lip repair in the mouse without an incision. *Plast Reconstr Surg*. 1989;84(5):723-730; discussion 731-722.
40. Longaker MT, Dodson TB, Kaban LB. A rabbit model for fetal cleft lip repair. *J Oral Maxillofac Surg*. 1990;48(7):714-719.
41. Kaban LB, Dodson TB, Longaker MT, Stern M, Umeda H, Adzick S. Fetal cleft lip repair in rabbits: long-term clinical and cephalometric results. *Cleft Palate Craniofac J*. 1993;30(1):13-21.
42. Peng Z, Yang K, Liu Y, Feng G. [An experimental study on chemically induced animal model of goat cleft palate in uterus]. *Zhongguo Xue Fu Chong Jian Wai Ke Za Zhi*. 2011;25(2):235-238.
43. Wenghoefer MH, Deprest J, Goetz W, Kuijpers-Jagtman AM, Berge S. Prenatal cleft lip and maxillary alveolar defect repair in a 2-step fetal lamb model. *J Oral Maxillofac Surg*. 2007;65(12):2479-2486.
44. Lorenz HP, Longaker MT. In utero surgery for cleft lip/palate: minimizing the "Ripple Effect" of scarring. *J Craniofac Surg*. 2003;14(4):504-511.
45. Kaucka M, Ivashkin E, Gyllborg D, et al. Analysis of neural crest-derived clones reveals novel aspects of facial development. *Sci Adv*. 2016;2(8):e1600060.
46. Trainor PA, Tam PP. Cranial paraxial mesoderm and neural crest cells of the mouse embryo: co-distribution in the craniofacial mesenchyme but distinct segregation in branchial arches. *Development*. 1995;121(8):2569-2582.
47. Theveneau E, Marchant L, Kuriyama S, et al. Collective chemotaxis requires contact-dependent cell polarity. *Dev Cell*. 2010;19(1):39-53.
48. Trainor PA. Specification and patterning of neural crest cells during craniofacial development. *Brain Behav Evol*. 2005;66(4):266-280.
49. Kulesa PM, Bailey CM, Kasemeier-Kulesa JC, McLennan R. Cranial neural crest migration: new rules for an old road. *Dev Biol*. 2010;344(2):543-554.
50. Casale J, Giwa AO. Embryology, Branchial Arches. In: *StatPearls*. Treasure Island (FL)2020.
51. Mayor R, Theveneau E. The role of the non-canonical Wnt-planar cell polarity pathway in neural crest migration. *Biochem J*. 2014;457(1):19-26.
52. Steventon B, Mayor R, Streit A. Neural crest and placode interaction during the development of the cranial sensory system. *Dev Biol*. 2014;389(1):28-38.

53. de Melker AA, Desban N, Duband JL. Cellular localization and signaling activity of beta-catenin in migrating neural crest cells. *Dev Dyn*. 2004;230(4):708-726.
54. Santiago A, Erickson CA. Ephrin-B ligands play a dual role in the control of neural crest cell migration. *Development*. 2002;129(15):3621-3632.
55. Smith A, Robinson V, Patel K, Wilkinson DG. The EphA4 and EphB1 receptor tyrosine kinases and ephrin-B2 ligand regulate targeted migration of branchial neural crest cells. *Curr Biol*. 1997;7(8):561-570.
56. Broders-Bondon F, Paul-Gilloteaux P, Gazquez E, et al. Control of the collective migration of enteric neural crest cells by the Complement anaphylatoxin C3a and N-cadherin. *Dev Biol*. 2016;414(1):85-99.
57. Rezzoug F, Seelan RS, Bhattacharjee V, Greene RM, Pisano MM. Chemokine-mediated migration of mesencephalic neural crest cells. *Cytokine*. 2011;56(3):760-768.
58. Guo Y, Hangoc G, Bian H, Pelus LM, Broxmeyer HE. SDF-1/CXCL12 enhances survival and chemotaxis of murine embryonic stem cells and production of primitive and definitive hematopoietic progenitor cells. *Stem Cells*. 2005;23(9):1324-1332.
59. Lee YH, Saint-Jeannet JP. Sox9 function in craniofacial development and disease. *Genesis*. 2011;49(4):200-208.
60. Hong CS, Saint-Jeannet JP. Sox proteins and neural crest development. *Semin Cell Dev Biol*. 2005;16(6):694-703.
61. Cheung M, Briscoe J. Neural crest development is regulated by the transcription factor Sox9. *Development*. 2003;130(23):5681-5693.
62. Li M, Zhao C, Wang Y, Zhao Z, Meng A. Zebrafish sox9b is an early neural crest marker. *Dev Genes Evol*. 2002;212(4):203-206.
63. Kessenbrock K, Wang CY, Werb Z. Matrix metalloproteinases in stem cell regulation and cancer. *Matrix Biol*. 2015;44-46:184-190.
64. Chai Y, Jiang X, Ito Y, et al. Fate of the mammalian cranial neural crest during tooth and mandibular morphogenesis. *Development*. 2000;127(8):1671-1679.
65. Achilleos A, Trainor PA. Neural crest stem cells: discovery, properties and potential for therapy. *Cell Res*. 2012;22(2):288-304.
66. Sakai D, Trainor PA. Treacher Collins syndrome: unmasking the role of Tcof1/treacle. *Int J Biochem Cell Biol*. 2009;41(6):1229-1232.
67. Birgfeld C, Heike C. Craniofacial Microsomia. *Clin Plast Surg*. 2019;46(2):207-221.
68. Ito Y, Yeo JY, Chytil A, et al. Conditional inactivation of Tgfb β 2 in cranial neural crest causes cleft palate and calvaria defects. *Development*. 2003;130(21):5269-5280.
69. Nie X. Sox9 mRNA expression in the developing palate and craniofacial muscles and skeletons. *Acta Odontol Scand*. 2006;64(2):97-103.
70. Gong SG. Cranial neural crest: migratory cell behavior and regulatory networks. *Exp Cell Res*. 2014;325(2):90-95.
71. Sakai D, Trainor PA. Face off against ROS: Tcof1/Treacle safeguards neuroepithelial cells and progenitor neural crest cells from oxidative stress during craniofacial development. *Dev Growth Differ*. 2016;58(7):577-585.
72. Buchanan EP, Xue AS, Hollier LH, Jr. Craniofacial syndromes. *Plast Reconstr Surg*. 2014;134(1):128e-153e.
73. Gebuijs IGE, Raterman ST, Metz JR, et al. Fgf8a mutation affects craniofacial development and skeletal gene expression in zebrafish larvae. *Biol Open*. 2019;8(9).
74. Siismets EM, Hatch NE. Cranial Neural Crest Cells and Their Role in the Pathogenesis of Craniofacial Anomalies and Coronal Craniosynostosis. *J Dev Biol*. 2020;8(3).
75. Ishii M, Han J, Yen HY, Sucov HM, Chai Y, Maxson RE, Jr. Combined deficiencies of Msx1 and Msx2 cause impaired patterning and survival of the cranial neural crest. *Development*. 2005;132(22):4937-4950.
76. Nottoli T, Hagopian-Donaldson S, Zhang J, Perkins A, Williams T. AP-2-null cells disrupt morphogenesis of the eye, face, and limbs in chimeric mice. *Proc Natl Acad Sci U S A*. 1998;95(23):13714-13719.
77. Brewer S, Feng W, Huang J, Sullivan S, Williams T. Wnt1-Cre-mediated deletion of AP-2alpha causes multiple neural crest-related defects. *Dev Biol*. 2004;267(1):135-152.

78. Swindell EC, Yuan Q, Maili LE, Tandon B, Wagner DS, Hecht JT. Crisp1d2 is required for neural crest cell migration and cell viability during zebrafish craniofacial development. *Genesis*. 2015;53(10):660-667.
79. Escot S, Blavet C, Faure E, Zaffran S, Duband JL, Fournier-Thibault C. Disruption of CXCR4 signaling in pharyngeal neural crest cells causes DiGeorge syndrome-like malformations. *Development*. 2016;143(4):582-588.
80. Duband JL, Escot S, Fournier-Thibault C. SDF1-CXCR4 signaling: A new player involved in DiGeorge/22q11-deletion syndrome. *Rare Dis*. 2016;4(1):e1195050.
81. Olesnicki Killian EC, Birkholz DA, Artinger KB. A role for chemokine signaling in neural crest cell migration and craniofacial development. *Dev Biol*. 2009;333(1):161-172.
82. Cox TC. Taking it to the max: the genetic and developmental mechanisms coordinating midfacial morphogenesis and dysmorphology. *Clin Genet*. 2004;65(3):163-176.
83. Ferguson MW. Palate development. *Development*. 1988;103 Suppl:41-60.
84. Hilliard SA, Yu L, Gu S, Zhang Z, Chen YP. Regional regulation of palatal growth and patterning along the anterior-posterior axis in mice. *J Anat*. 2005;207(5):655-667.
85. Watanabe M, Kawasaki K, Kawasaki M, et al. Spatio-temporal expression of Sox genes in murine palatogenesis. *Gene Expr Patterns*. 2016;21(2):111-118.
86. Xu J, Huang Z, Wang W, et al. FGF8 Signaling Alters the Osteogenic Cell Fate in the Hard Palate. *J Dent Res*. 2018;97(5):589-596.
87. Bush JO, Jiang R. Palatogenesis: morphogenetic and molecular mechanisms of secondary palate development. *Development*. 2012;139(2):231-243.
88. Helms JA, Cordero D, Tapadia MD. New insights into craniofacial morphogenesis. *Development*. 2005;132(5):851-861.
89. Dudas M, Li WY, Kim J, Yang A, Kaartinen V. Palatal fusion - where do the midline cells go? A review on cleft palate, a major human birth defect. *Acta Histochem*. 2007;109(1):1-14.
90. Nakajima A, C FS, Gulka AOD, Hanai JL. TGF-beta Signaling and the Epithelial-Mesenchymal Transition during Palatal Fusion. *Int J Mol Sci*. 2018;19(11).
91. Logan SM, Benson MD. Medial epithelial seam cell migration during palatal fusion. *J Cell Physiol*. 2020;235(2):1417-1424.
92. Aoyama G, Kurosaka H, Oka A, et al. Observation of Dynamic Cellular Migration of the Medial Edge Epithelium of the Palatal Shelf in vitro. *Front Physiol*. 2019;10:698.
93. Jin JZ, Ding J. Analysis of cell migration, transdifferentiation and apoptosis during mouse secondary palate fusion. *Development*. 2006;133(17):3341-3347.
94. Lan Y, Xu J, Jiang R. Cellular and Molecular Mechanisms of Palatogenesis. *Curr Top Dev Biol*. 2015;115:59-84.
95. Iseki S. Disintegration of the medial epithelial seam: is cell death important in palatogenesis? *Dev Growth Differ*. 2011;53(2):259-268.
96. Xu J, Wang L, Li H, et al. Shox2 regulates osteogenic differentiation and pattern formation during hard palate development in mice. *J Biol Chem*. 2019;294(48):18294-18305.
97. Oka K, Honda MJ, Tsuruga E, Hatakeyama Y, Isokawa K, Sawa Y. Roles of collagen and periostin expression by cranial neural crest cells during soft palate development. *J Histochem Cytochem*. 2012;60(1):57-68.
98. THE GLOBAL BURDEN OF DISEASE 2004 UPDATE Introduction. *Global Burden of Disease: 2004 Update*. 2008.
99. Chen J, Huang X, Wang B, et al. Epidemiology of birth defects based on surveillance data from 2011-2015 in Guangxi, China: comparison across five major ethnic groups. *BMC Public Health*. 2018;18(1):1008.
100. Hughes-McCormack LA, McGowan R, Pell JP, et al. Birth incidence, deaths and hospitalisations of children and young people with Down syndrome, 1990-2015: birth cohort study. *BMJ Open*. 2020;10(4):e033770.
101. Ryznychuk MO, Kryvchanska MI, Lastivka IV, Bulyk RY. Incidence and risk factors of spina bifida in children. *Wiad Lek*. 2018;71(2 pt 2):339-344.
102. Hoffman JJ, Kaplan S. The incidence of congenital heart disease. *J Am Coll Cardiol*. 2002;39(12):1890-1900.
103. Jesudason EC. The Epidemiology of Birth Defects. *Pediatric Surgery: Diagnosis and Management*. 2009:3-8.

104. Tanaka SA, Mahabir RC, Jupiter DC, Menezes JM. Updating the epidemiology of isolated cleft palate. *Plast Reconstr Surg.* 2013;131(4):650e-652e.
105. Harville EW, Wilcox AJ, Lie RT, Vindenes H, Abyholm F. Cleft lip and palate versus cleft lip only: are they distinct defects? *Am J Epidemiol.* 2005;162(5):448-453.
106. Mitchell LE. Genetic epidemiology of birth defects: nonsyndromic cleft lip and neural tube defects. *Epidemiol Rev.* 1997;19(1):61-68.
107. Derijcke A, Eerens A, Carels C. The incidence of oral clefts: a review. *Br J Oral Maxillofac Surg.* 1996;34(6):488-494.
108. Leck I. The geographical distribution of neural tube defects and oral clefts. *Br Med Bull.* 1984;40(4):390-395.
109. McBride WA, McIntyre GT, Carroll K, Mossey PA. Subphenotyping and Classification of Orofacial Clefts: Need for Orofacial Cleft Subphenotyping Calls for Revised Classification. *Cleft Palate Craniofac J.* 2016;53(5):539-549.
110. Vermeij-Keers C, Rozendaal AM, Luijsterburg AJM, et al. Subphenotyping and Classification of Cleft Lip and Alveolus in Adult Unoperated Patients: A New Embryological Approach. *Cleft Palate Craniofac J.* 2018;55(9):1267-1276.
111. Dixon MJ, Marazita ML, Beaty TH, Murray JC. Cleft lip and palate: understanding genetic and environmental influences. *Nat Rev Genet.* 2011;12(3):167-178.
112. Asllanaj B, Kragt L, Voshol I, et al. Dentition Patterns in Different Unilateral Cleft Lip Subphenotypes. *J Dent Res.* 2017;96(13):1482-1489.
113. Spauwen PH. [Fifty years of plastic surgery in the Netherlands. IV. Treatment of children with cleft lip and palate]. Vijftig jaar plastische chirurgie in Nederland. IV. De behandeling van het kind met schisis. *Ned Tijdschr Geneesk.* 2000;144(21):973-980.
114. Shkoukani MA, Chen M, Vong A. Cleft lip - a comprehensive review. *Front Pediatr.* 2013;1:53.
115. Susami T, Kuroda T, Amagasa T. Orthodontic treatment of a cleft palate patient with surgically assisted rapid maxillary expansion. *Cleft Palate Craniofac J.* 1996;33(5):445-449.
116. Good PM, Mulliken JB, Padwa BL. Frequency of Le Fort I osteotomy after repaired cleft lip and palate or cleft palate. *Cleft Palate Craniofac J.* 2007;44(4):396-401.
117. Posnick JC, Tompson B. Modification of the maxillary Le Fort I osteotomy in cleft-orthognathic surgery: the bilateral cleft lip and palate deformity. *J Oral Maxillofac Surg.* 1993;51(1):2-11.
118. Chung MK, Lao TT, Ting YH, Leung TY, Lau TK, Wong TW. Environmental Factors in the First Trimester and Risk of Oral-Facial Clefts in the Offspring. *Reprod Sci.* 2013;20(7):797-803.
119. Stuppia L, Capogreco M, Marzo G, et al. Genetics of syndromic and nonsyndromic cleft lip and palate. *J Craniofac Surg.* 2011;22(5):1722-1726.
120. Venkatesh R. Syndromes and anomalies associated with cleft. *Indian J Plast Surg.* 2009;42 Suppl:S51-55.
121. Leslie EJ, Marazita ML. Genetics of cleft lip and cleft palate. *Am J Med Genet C Semin Med Genet.* 2013;163C(4):246-258.
122. Cobourne MT. The complex genetics of cleft lip and palate. *Eur J Orthod.* 2004;26(1):7-16.
123. Tolarova MM, Cervenka J. Classification and birth prevalence of orofacial clefts. *Am J Med Genet.* 1998;75(2):126-137.
124. Levi B, Brugman S, Wong VW, Grova M, Longaker MT, Wan DC. Palatogenesis: engineering, pathways and pathologies. *Organogenesis.* 2011;7(4):242-254.
125. Giudice A, Barone S, Belhous K, et al. Pierre Robin sequence: A comprehensive narrative review of the literature over time. *J Stomatol Oral Maxillofac Surg.* 2018;119(5):419-428.
126. Hsieh ST, Woo AS. Pierre Robin Sequence. *Clin Plast Surg.* 2019;46(2):249-259.
127. R S, A MP. Role of SOX9 in the Etiology of Pierre-Robin Syndrome. *Iran J Basic Med Sci.* 2013;16(5):700-704.
128. Malik S, Kakar N, Hasnain S, Ahmad J, Wilcox ER, Naz S. Epidemiology of Van der Woude syndrome from mutational analyses in affected patients from Pakistan. *Clin Genet.* 2010;78(3):247-256.
129. Deshmukh PK, Deshmukh K, Mangalgi A, Patil S, Hugar D, Kodangal SF. Van der woude syndrome with short review of the literature. *Case Rep Dent.* 2014;2014:871460.
130. Burdick AB. Genetic epidemiology and control of genetic expression in van der Woude syndrome. *J Craniofac Genet Dev Biol Suppl.* 1986;2:99-105.
131. Schutte BC, Bjork BC, Coppage KB, et al. A preliminary gene map for the Van der Woude syndrome critical region derived from 900 kb of genomic sequence at 1q32-q41. *Genome Res.* 2000;10(1):81-94.

132. Kondo S, Schutte BC, Richardson RJ, et al. Mutations in IRF6 cause Van der Woude and popliteal pterygium syndromes. *Nat Genet.* 2002;32(2):285-289.
133. Balk K, Biesecker LG. The clinical atlas of Greig cephalopolysyndactyly syndrome. *Am J Med Genet A.* 2008;146A(5):548-557.
134. Lindau TA, Cardoso AC, Rossi NF, Giacheti CM. Anatomical Changes and Audiological Profile in Branchio-oto-renal Syndrome: A Literature Review. *Int Arch Otorhinolaryngol.* 2014;18(1):68-76.
135. Toriello HV, Franco B, Bruel AL, Thauvin-Robinet C. Oral-Facial-Digital Syndrome Type I. In: Adam MP, Ardinger HH, Pagon RA, et al., eds. *GeneReviews*((R)). Seattle (WA)1993.
136. Nimkarn S, New MI. Prenatal diagnosis and treatment of congenital adrenal hyperplasia. *Pediatr Endocrinol Rev.* 2006;4(2):99-105.
137. Adam MP, Hudgins L, Hannibal M. Kabuki Syndrome. In: Adam MP, Ardinger HH, Pagon RA, et al., eds. *GeneReviews*((R)). Seattle (WA)1993.
138. Murthy J, Bhaskar L. Current concepts in genetics of nonsyndromic clefts. *Indian J Plast Surg.* 2009;42(1):68-81.
139. Drew SJ. Clefting syndromes. *Atlas Oral Maxillofac Surg Clin North Am.* 2014;22(2):175-181.
140. Watkins SE, Meyer RE, Strauss RP, Aylsworth AS. Classification, epidemiology, and genetics of orofacial clefts. *Clin Plast Surg.* 2014;41(2):149-163.
141. Funato N, Nakamura M, Yanagisawa H. Molecular basis of cleft palates in mice. *World J Biol Chem.* 2015;6(3):121-138.
142. Rinne T, Clements SE, Lamme E, et al. A novel translation re-initiation mechanism for the p63 gene revealed by amino-terminal truncating mutations in Rapp-Hodgkin/Hay-Wells-like syndromes. *Hum Mol Genet.* 2008;17(13):1968-1977.
143. Cheng H-Q, Huang E-M, Xu M-Y, Shu S-Y, Tang S-J. PVRL1 as a candidate gene for nonsyndromic cleft lip with or without cleft palate: no evidence for the involvement of common or rare variants in southern Han Chinese patients. *DNA Cell Biol.* 2012;31(7):1321-1327.
144. Suzuki K, Hu D, Bustos T, et al. Mutations of PVRL1, encoding a cell-cell adhesion molecule/herpesvirus receptor, in cleft lip/palate-ectodermal dysplasia. *Nature genetics.* 2000;25(4):427-430.
145. Yoshiura K, Machida J, Daack-Hirsch S, et al. Characterization of a novel gene disrupted by a balanced chromosomal translocation t(2;19)(q11.2;q13.3) in a family with cleft lip and palate. *Genomics.* 1998;54(2):231-240.
146. Zang Y, Nie W, Fang Z, Li B. Cleft lip and palate transmembrane protein 1 rs31489 polymorphism is associated with lung cancer risk: a meta-analysis. *Tumour Biol.* 2014;35(6):5583-5588.
147. Dai J, Xu C, Wang G, et al. Novel TBX22 mutations in Chinese nonsyndromic cleft lip/palate families. *J Genet.* 2018;97(2):411-417.
148. Marazita ML, Murray JC, Lidral AC, et al. Meta-analysis of 13 genome scans reveals multiple cleft lip/palate genes with novel loci on 9q21 and 2q32-35. *Am J Hum Genet.* 2004;75(2):161-173.
149. Vieira AR. Association between the transforming growth factor alpha gene and nonsyndromic oral clefts: a HuGE review. *Am J Epidemiol.* 2006;163(9):790-810.
150. Suazo J, Santos JL, Carreno H, Jara L, Blanco R. Linkage disequilibrium between MSX1 and non-syndromic cleft lip/palate in the Chilean population. *J Dent Res.* 2004;83(10):782-785.
151. Marciano AC, Doudney K, Braybrook C, et al. TBX22 mutations are a frequent cause of cleft palate. *J Med Genet.* 2004;41(1):68-74.
152. Zuccherro TM, Cooper ME, Maher BS, et al. Interferon regulatory factor 6 (IRF6) gene variants and the risk of isolated cleft lip or palate. *N Engl J Med.* 2004;351(8):769-780.
153. Scapoli L, Palmieri A, Martinelli M, et al. Strong evidence of linkage disequilibrium between polymorphisms at the IRF6 locus and nonsyndromic cleft lip with or without cleft palate, in an Italian population. *Am J Hum Genet.* 2005;76(1):180-183.
154. Jugessur A, Rahimov F, Lie RT, et al. Genetic variants in IRF6 and the risk of facial clefts: single-marker and haplotype-based analyses in a population-based case-control study of facial clefts in Norway. *Genet Epidemiol.* 2008;32(5):413-424.
155. Birnbaum S, Ludwig KU, Reutter H, et al. IRF6 gene variants in Central European patients with non-syndromic cleft lip with or without cleft palate. *Eur J Oral Sci.* 2009;117(6):766-769.
156. Pan Y, Ma J, Zhang W, et al. IRF6 polymorphisms are associated with nonsyndromic orofacial clefts in a Chinese Han population. *Am J Med Genet A.* 2010;152A(10):2505-2511.

157. Wu T, Liang KY, Hetmanski JB, et al. Evidence of gene-environment interaction for the IRF6 gene and maternal multivitamin supplementation in controlling the risk of cleft lip with/without cleft palate. *Hum Genet.* 2010;128(4):401-410.
158. Rahimov F, Marazita ML, Visel A, et al. Disruption of an AP-2alpha binding site in an IRF6 enhancer is associated with cleft lip. *Nat Genet.* 2008;40(11):1341-1347.
159. Jehee FS, Burin BA, Rocha KM, et al. Novel mutations in IRF6 in nonsyndromic cleft lip with or without cleft palate: when should IRF6 mutational screening be done? *Am J Med Genet A.* 2009;149A(6):1319-1322.
160. Shaw D, Ray A, Marazita M, Field L. Further evidence of a relationship between the retinoic acid receptor alpha locus and nonsyndromic cleft lip with or without cleft palate (CL +/- P). *American journal of human genetics.* 1993;53(5):1156-1157.
161. Shotelersuk V, Ittiwut C, Siriwan P, Angspatt A. Maternal 677CT/1298AC genotype of the MTHFR gene as a risk factor for cleft lip. *J Med Genet.* 2003;40(5):e64.
162. Lammer EJ, Shaw GM, Iovannisci DM, Van Waes J, Finnell RH. Maternal smoking and the risk of orofacial clefts: Susceptibility with NAT1 and NAT2 polymorphisms. *Epidemiology.* 2004;15(2):150-156.
163. Lammer EJ, Shaw GM, Iovannisci DM, Finnell RH. Maternal smoking, genetic variation of glutathione s-transferases, and risk for orofacial clefts. *Epidemiology.* 2005;16(5):698-701.
164. Shi M, Christensen K, Weinberg CR, et al. Orofacial cleft risk is increased with maternal smoking and specific detoxification-gene variants. *Am J Hum Genet.* 2007;80(1):76-90.
165. Avila JR, Jezewski PA, Vieira AR, et al. PVRL1 variants contribute to non-syndromic cleft lip and palate in multiple populations. *Am J Med Genet A.* 2006;140(23):2562-2570.
166. Shi M, Wehby GL, Murray JC. Review on genetic variants and maternal smoking in the etiology of oral clefts and other birth defects. *Birth Defects Res C Embryo Today.* 2008;84(1):16-29.
167. DeRoo LA, Wilcox AJ, Drevon CA, Lie RT. First-trimester maternal alcohol consumption and the risk of infant oral clefts in Norway: a population-based case-control study. *Am J Epidemiol.* 2008;168(6):638-646.
168. Webster WS, Howe AM, Abela D, Oakes DJ. The relationship between cleft lip, maxillary hypoplasia, hypoxia and phenytoin. *Curr Pharm Des.* 2006;12(12):1431-1448.
169. Wyszynski DF, Beaty TH. Review of the role of potential teratogens in the origin of human nonsyndromic oral clefts. *Teratology.* 1996;53(5):309-317.
170. Carmichael SL, Shaw GM, Ma C, et al. Maternal corticosteroid use and orofacial clefts. *Am J Obstet Gynecol.* 2007;197(6):585 e581-587; discussion 683-584, e581-587.
171. Correa A, Gilboa SM, Besser LM, et al. Diabetes mellitus and birth defects. *Am J Obstet Gynecol.* 2008;199(3):237 e231-239.
172. Bille C, Skytthe A, Vach W, et al. Parent's age and the risk of oral clefts. *Epidemiology.* 2005;16(3):311-316.
173. Herkrath AP, Herkrath FJ, Rebelo MA, Vettore MV. Parental age as a risk factor for non-syndromic oral clefts: a meta-analysis. *J Dent.* 2012;40(1):3-14.
174. Acuna-Gonzalez G, Medina-Solis CE, Maupome G, et al. Family history and socioeconomic risk factors for non-syndromic cleft lip and palate: a matched case-control study in a less developed country. *Biomedica.* 2011;31(3):381-391.
175. Mitchell LE, Murray JC, O'Brien S, Christensen K. Retinoic acid receptor alpha gene variants, multivitamin use, and liver intake as risk factors for oral clefts: a population-based case-control study in Denmark, 1991-1994. *Am J Epidemiol.* 2003;158(1):69-76.
176. Oginni FO, Adenekan AT. Prevention of oro-facial clefts in developing world. *Ann Maxillofac Surg.* 2012;2(2):163-169.
177. Christensen K. The 20th century Danish facial cleft population--epidemiological and genetic-epidemiological studies. *The Cleft palate-craniofacial journal : official publication of the American Cleft Palate-Craniofacial Association.* 1999;36(2):96-104.
178. Shaw GM, Wasserman CR, Lammer EJ, et al. Orofacial clefts, parental cigarette smoking, and transforming growth factor-alpha gene variants. *Am J Hum Genet.* 1996;58(3):551-561.
179. Christensen K, Olsen J, Norgaard-Pedersen B, et al. Oral clefts, transforming growth factor alpha gene variants, and maternal smoking: a population-based case-control study in Denmark, 1991-1994. *Am J Epidemiol.* 1999;149(3):248-255.
180. Romitti PA, Lidral AC, Munger RG, Daack-Hirsch S, Burns TL, Murray JC. Candidate genes for nonsyndromic cleft lip and palate and maternal cigarette smoking and alcohol consumption:

- evaluation of genotype-environment interactions from a population-based case-control study of orofacial clefts. *Teratology*. 1999;59(1):39-50.
181. Lidral AC, Romitti PA, Basart AM, et al. Association of MSX1 and TGFβ3 with nonsyndromic clefting in humans. *American journal of human genetics*. 1998;63(2):557-568.
 182. Mitchell LE, Murray JC, O'Brien S, Christensen K. Evaluation of two putative susceptibility loci for oral clefts in the Danish population. *Am J Epidemiol*. 2001;153(10):1007-1015.
 183. Boyles AL, DeRoo LA, Lie RT, et al. Maternal alcohol consumption, alcohol metabolism genes, and the risk of oral clefts: a population-based case-control study in Norway, 1996-2001. *Am J Epidemiol*. 2010;172(8):924-931.
 184. Rothman KJ, Moore LL, Singer MR, Nguyen US, Mannino S, Milunsky A. Teratogenicity of high vitamin A intake. *N Engl J Med*. 1995;333(21):1369-1373.
 185. Munger RG, Sauberlich HE, Corcoran C, Nepomuceno B, Daack-Hirsch S, Solon FS. Maternal vitamin B-6 and folate status and risk of oral cleft birth defects in the Philippines. *Birth Defects Res A Clin Mol Teratol*. 2004;70(7):464-471.
 186. Raterman ST, Metz JR, Wagener F, Von den Hoff JW. Zebrafish Models of Craniofacial Malformations: Interactions of Environmental Factors. *Front Cell Dev Biol*. 2020;8:600926.
 187. Cooke MS, Evans MD, Dizdaroğlu M, Lunec J. Oxidative DNA damage: mechanisms, mutation, and disease. *FASEB J*. 2003;17(10):1195-1214.
 188. Simpson WJ. A preliminary report on cigarette smoking and the incidence of prematurity. *American journal of obstetrics and gynecology*. 1957;73(4):807-815.
 189. Andres RL. The association of cigarette smoking with placenta previa and abruptio placentae. *Semin Perinatol*. 1996;20(2):154-159.
 190. Shah NR, Bracken MB. A systematic review and meta-analysis of prospective studies on the association between maternal cigarette smoking and preterm delivery. *American journal of obstetrics and gynecology*. 2000;182(2):465-472.
 191. Ion R, Bernal AL. Smoking and Preterm Birth. *Reprod Sci*. 2015;22(8):918-926.
 192. Al Ghaffi MHM, Padmanabhan R, Kataya HH, Berg B. Effects of alpha-lipoic acid supplementation on maternal diabetes-induced growth retardation and congenital anomalies in rat fetuses. *Mol Cell Biochem*. 2004;261(1-2):123-135.
 193. Tomson T, Battino D, Bonizzoni E, et al. Comparative risk of major congenital malformations with eight different antiepileptic drugs: a prospective cohort study of the EURAP registry. *Lancet Neurol*. 2018;17(6):530-538.
 194. Hill DS, Włodarczyk BJ, Palacios AM, Finnell RH. Teratogenic effects of antiepileptic drugs. *Expert Rev Neurother*. 2010;10(6):943-959.
 195. Vajda FJ, O'Brien TJ, Graham J, Lander CM, Eadie MJ. Associations between particular types of fetal malformation and antiepileptic drug exposure in utero. *Acta Neurol Scand*. 2013;128(4):228-234.
 196. Silva H, Arruda TTS, Souza KSC, et al. Risk factors and comorbidities in Brazilian patients with orofacial clefts. *Braz Oral Res*. 2018;32:e24.
 197. Chen X, Scholl TO. Oxidative stress: changes in pregnancy and with gestational diabetes mellitus. *Curr Diab Rep*. 2005;5(4):282-288.
 198. Albano E. Alcohol, oxidative stress and free radical damage. *Proc Nutr Soc*. 2006;65(3):278-290.
 199. Kamceva G, Arsova-Sarafinovska Z, Ruskovska T, Zdravkovska M, Kamceva-Panova L, Stikova E. Cigarette Smoking and Oxidative Stress in Patients with Coronary Artery Disease. *Open Access Maced J Med Sci*. 2016;4(4):636-640.
 200. Sinko K, Cede J, Jagsch R, et al. Facial Aesthetics in Young Adults after Cleft Lip and Palate Treatment over Five Decades. *Sci Rep*. 2017;7(1):15864.
 201. Kosowski TR, Weathers WM, Wolfswinkel EM, Ridgway EB. Cleft palate. *Semin Plast Surg*. 2012;26(4):164-169.
 202. Kuijpers-Jagtman AM. The orthodontist, an essential partner in CLP treatment. *B-ENT*. 2006;2 Suppl 4:57-62.
 203. Shaw WC, Semb G, Nelson P, et al. The Eurocleft Project 1996-2000: overview. *J Cranio Maxill Surg*. 2001;29(3):131-140.
 204. Flynn T, Moller C, Jonsson R, Lohmander A. The high prevalence of otitis media with effusion in children with cleft lip and palate as compared to children without clefts. *Int J Pediatr Otorhinolaryngol*. 2009;73(10):1441-1446.
 205. Berkowitz S. *Cleft lip and palate : diagnosis and management*. Third Edition. ed. New York: Springer; 2013.

206. Bos A, Prah C. Oral health-related quality of life in Dutch children with cleft lip and/or palate. *Angle Orthod*. 2011;81(5):865-871.
207. Wehby GL, Cassell CH. The impact of orofacial clefts on quality of life and healthcare use and costs. *Oral Dis*. 2010;16(1):3-10.
208. Robin NH, Baty H, Franklin J, et al. The multidisciplinary evaluation and management of cleft lip and palate. *South Med J*. 2006;99(10):1111-1120.
209. Vrebos J. Harelip surgery in ancient China: further investigations. *Plast Reconstr Surg*. 1992;89(1):147-150.
210. Boo-Chai K. An ancient Chinese text on a cleft lip. *Plast Reconstr Surg*. 1966;38(2):89-91.
211. Perko M. The history of treatment of cleft lip and palate. *Prog Pediatr Surg*. 1986;20:238-251.
212. Rogers BO. Harelip Repair in Colonial America. A Review of 18th Century and Earlier Surgical Techniques. *Plast Reconstr Surg*. 1964;34:142-162.
213. Barsky AJ. Pierre Franco, Father of Cleft Lip Surgery: His Life and Times. *Br J Plast Surg*. 1964;17:335-350.
214. Grabb WC, Rosenstein SW, Bzoch KR. *Cleft lip and palate; surgical, dental, and speech aspects*. 1st ed. Boston,: Little; 1971.
215. Jones RG. A short history of anaesthesia for hare-lip and cleft palate repair. *Br J Anaesth*. 1971;43(8):796-802.
216. Millard DR. Extensions of the rotation-advancement principle for wide unilateral cleft lips. *Plast Reconstr Surg*. 1968;42(6):535-544.
217. Millard DR, Jr. Results of surgical lengthening of the short nose in the bilateral cleft lip patient. *Plast Reconstr Surg*. 1978;62(3):438-440.
218. Iyer VS. Isolated cleft palate. *Cleft Palate J*. 1967;4:124-128.
219. Murison MS, Pigott RW. Medial Langenbeck: experience of a modified Von Langenbeck repair of the cleft palate. A preliminary report. *British journal of plastic surgery*. 1992;45(6):454-459.
220. Dorrance GM, Shirazy E. *The operative story of cleft palate*. Philadelphia and London,: W. B. Saunders company; 1933.
221. Schweckendiek H. [The problem of early and late surgery in congenital fissure of the of the lips and palate]. Zur Frage der Fruh- und Spatoperationen der angeborenen Lippen-Kiefer-Gaumen-Spalten. *Z Laryngol Rhinol Otol*. 1951;30(2):51-56.
222. Fudalej P, Katsaros C, Bongaarts C, Dudkiewicz Z, Kuijpers-Jagtman AM. Nasolabial esthetics in children with complete unilateral cleft lip and palate after 1- versus 3-stage treatment protocols. *J Oral Maxillofac Surg*. 2009;67(8):1661-1666.
223. de Ladeira PRS, Alonso N. Protocols in cleft lip and palate treatment: systematic review. *Plast Surg Int*. 2012;2012:562892.
224. Meazzini MC, Donati V, Garattini G, Brusati R. Maxillary growth impairment in cleft lip and palate patients: a simplified approach in the search for a cause. *J Craniofac Surg*. 2008;19(5):1302-1307.
225. Segna E, Khonsari RH, Meazzini MC, Battista VMA, Picard A, Autelitano L. Maxillary shape at the end of puberty in operated unilateral cleft lip and palate: A geometric morphometric assessment using computer tomography. *J Stomatol Oral Maxillofac Surg*. 2020;121(1):9-13.
226. Chen ZQ, Wu J, Chen RJ. Sagittal maxillary growth pattern in unilateral cleft lip and palate patients with unrepaired cleft palate. *J Craniofac Surg*. 2012;23(2):491-493.
227. Sinno H, Tahiri Y, Thibaudeau S, et al. Cleft lip and palate: an objective measure outcome study. *Plast Reconstr Surg*. 2012;130(2):408-414.
228. Latief BS, Lekkas C, Kuijpers MA. Maxillary arch width in unoperated adult bilateral cleft lip and alveolus and complete bilateral cleft lip and palate. *Orthod Craniofac Res*. 2010;13(2):82-88.
229. Latif A, Kuijpers MAR, Rachwalski M, Latief BS, Kuijpers-Jagtman AM, Fudalej PS. Morphological variability in unrepaired bilateral clefts with and without cleft palate evaluated with geometric morphometrics. *J Anat*. 2020;236(3):425-433.
230. Latief BS, Kuijpers MAR, Stebel A, Kuijpers-Jagtman AM, Fudalej PS. Pattern of Morphological Variability in Unrepaired Unilateral Clefts With and Without Cleft Palate May Suggest Intrinsic Growth Deficiency. *Front Cell Dev Biol*. 2020;8:587859.
231. Soltani AM, Francis CS, Motamed A, et al. Hypertrophic scarring in cleft lip repair: a comparison of incidence among ethnic groups. *Clin Epidemiol*. 2012;4:187-191.
232. Wilson AD, Mercer N. Dermabond tissue adhesive versus Steri-Strips in unilateral cleft lip repair: an audit of infection and hypertrophic scar rates. *Cleft Palate Craniofac J*. 2008;45(6):614-619.

233. Rousseau P, Metzger M, Frucht S, Schupp W, Hempel M, Otten J-E. Effect of lip closure on early maxillary growth in patients with cleft lip and palate. *JAMA Facial Plast Surg.* 2013;15(5):369-373.
234. Cohen M. Residual deformities after repair of clefts of the lip and palate. *Clin Plast Surg.* 2004;31(2):331-345.
235. Stal S, Hollier L. Correction of secondary cleft lip deformities. *Plast Reconstr Surg.* 2002;109(5):1672-1681; quiz 1682.
236. Friede H. Growth sites and growth mechanisms at risk in cleft lip and palate. *Acta Odontol Scand.* 1998;56(6):346-351.
237. Hay N, Patel B, Haria P, Sommerlad B. Maxillary Growth in Cleft Lip and Palate Patients, With and Without Vomerine Flap Closure of the Hard Palate at the Time of Lip Repair: A Retrospective Analysis of Prospectively Collected Nonrandomized Data, With 10-Year Cephalometric Outcomes. *Cleft Palate Craniofac J.* 2018;55(9):1205-1210.
238. Ishikawa H, Nakamura S, Misaki K, Kudoh M, Fukuda H, Yoshida S. Scar tissue distribution on palates and its relation to maxillary dental arch form. *Cleft Palate Craniofac J.* 1998;35(4):313-319.
239. Wagener FA, van Beurden HE, von den Hoff JW, Adema GJ, Figdor CG. The heme-heme oxygenase system: a molecular switch in wound healing. *Blood.* 2003;102(2):521-528.
240. Salgado KR, Wendt AR, Fernandes Fagundes NC, Maia LC, Normando D, Leao PB. Early or delayed palatoplasty in complete unilateral cleft lip and palate patients? A systematic review of the effects on maxillary growth. *J Craniomaxillofac Surg.* 2019;47(11):1690-1698.
241. Lilja J, Mars M, Elander A, et al. Analysis of dental arch relationships in Swedish unilateral cleft lip and palate subjects: 20-year longitudinal consecutive series treated with delayed hard palate closure. *Cleft Palate Craniofac J.* 2006;43(5):606-611.
242. Molsted K, Brattstrom V, Prah-Andersen B, Shaw WC, Semb G. The Eurocleft study: intercenter study of treatment outcome in patients with complete cleft lip and palate. Part 3: dental arch relationships. *Cleft Palate Craniofac J.* 2005;42(1):78-82.
243. Markus AF, Delaire J, Smith WP. Facial balance in cleft lip and palate. II. Cleft lip and palate and secondary deformities. *Br J Oral Maxillofac Surg.* 1992;30(5):296-304.
244. Liao YF, Yang IY, Wang R, Yun C, Huang CS. Two-stage palate repair with delayed hard palate closure is related to favorable maxillary growth in unilateral cleft lip and palate. *Plast Reconstr Surg.* 2010;125(5):1503-1510.
245. Bardach J, Morris HL, Olin WH. Late results of primary veloplasty: the Marburg Project. *Plast Reconstr Surg.* 1984;73(2):207-218.
246. Schweckendiek W, Doz P. Primary veloplasty: long-term results without maxillary deformity. a twenty-five year report. *Cleft Palate J.* 1978;15(3):268-274.
247. Nagarajan R, Savitha VH, Subramanian B. Communication disorders in individuals with cleft lip and palate: An overview. *Indian J Plast Surg.* 2009;42 Suppl:S137-143.
248. Dorf DS, Curtin JW. Early cleft palate repair and speech outcome. *Plast Reconstr Surg.* 1982;70(1):74-81.
249. Pradel W, Senf D, Mai R, Ludicke G, Eckelt U, Lauer G. One-stage palate repair improves speech outcome and early maxillary growth in patients with cleft lip and palate. *J Physiol Pharmacol.* 2009;60 Suppl 8:37-41.
250. Shaye D, Liu CC, Tollefson TT. Cleft Lip and Palate: An Evidence-Based Review. *Facial Plast Surg Clin North Am.* 2015;23(3):357-372.
251. Woo AS. Velopharyngeal dysfunction. *Semin Plast Surg.* 2012;26(4):170-177.
252. Marrinan EM, LaBrie RA, Mulliken JB. Velopharyngeal function in nonsyndromic cleft palate: relevance of surgical technique, age at repair, and cleft type. *The Cleft palate-craniofacial journal : official publication of the American Cleft Palate-Craniofacial Association.* 1998;35(2):95-100.
253. Inman DS, Thomas P, Hodgkinson PD, Reid CA. Oro-nasal fistula development and velopharyngeal insufficiency following primary cleft palate surgery--an audit of 148 children born between 1985 and 1997. *Br J Plast Surg.* 2005;58(8):1051-1054.
254. Long RE, Jr., McNamara JA, Jr. Facial growth following pharyngeal flap surgery: skeletal assessment on serial lateral cephalometric radiographs. *Am J Orthod.* 1985;87(3):187-196.
255. Voshol IE, van Adrichem LN, van der Wal KG, Koudstaal MJ. Influence of pharyngeal flap surgery on maxillary outgrowth in cleft patients. *Int J Oral Maxillofac Surg.* 2013;42(2):192-197.
256. Semb G, Shaw WC. Pharyngeal flap and facial growth. *Cleft Palate J.* 1990;27(3):217-224.
257. Pearl RM, Kaplan EN. Cephalometric study of facial growth in children after combined pushback and pharyngeal flap operations. *Plast Reconstr Surg.* 1976;57(4):480-483.

258. Heliovaara A, Haapanen ML, Hukki J, Ranta R. Long-term effect of pharyngeal flap surgery on craniofacial and nasopharyngeal morphology in patients with cleft palate. *Acta Odontol Scand.* 2003;61(3):159-163.
259. Shi B, Losee JE. The impact of cleft lip and palate repair on maxillofacial growth. *Int J Oral Sci.* 2015;7(1):14-17.
260. Derijcke A, Kuipers-Jagtman AM, Lekkas C, Hardjowasito W, Latief B. Dental arch dimensions in unoperated adult cleft-palate patients: an analysis of 37 cases. *J Craniofac Genet Dev Biol.* 1994;14(1):69-74.
261. Bardach J, Kelly KM. Role of animal models in experimental studies of craniofacial growth following cleft lip and palate repair. *Cleft Palate J.* 1988;25(2):103-113.
262. Eisbach KJ, Bardach J. Effect of lip closure on facial growth in the surgically induced cleft rabbit. *Otolaryngology.* 1978;86(5):ORL-786-803.
263. Bardach J, Mooney MP. The relationship between lip pressure following lip repair and craniofacial growth: an experimental study in beagles. *Plast Reconstr Surg.* 1984;73(4):544-555.
264. Wijdeveld MG, Grunning EM, Kuipers-Jagtman AM, Maltha JC. Growth of the maxilla after soft tissue palatal surgery at different ages in beagle dogs: a longitudinal radiographic study. *J Oral Maxillofac Surg.* 1988;46(3):204-209.
265. Paradas-Lara I, Casado-Gomez I, Martin C, et al. Maxillary growth in a congenital cleft palate canine model for surgical research. *J Craniomaxillofac Surg.* 2014;42(1):13-21.
266. Biggs LC, Goudy SL, Dunnwald M. Palatogenesis and cutaneous repair: A two-headed coin. *Dev Dyn.* 2015;244(3):289-310.
267. Stechmiller JK. Understanding the role of nutrition and wound healing. *Nutr Clin Pract.* 2010;25(1):61-68.
268. Diegelmann RF, Evans MC. Wound healing: an overview of acute, fibrotic and delayed healing. *Front Biosci.* 2004;9:283-289.
269. Wild T, Rahbarnia A, Kellner M, Sobotka L, Eberlein T. Basics in nutrition and wound healing. *Nutrition.* 2010;26(9):862-866.
270. Singer AJ, Clark RA. Cutaneous wound healing. *N Engl J Med.* 1999;341(10):738-746.
271. Reinke JM, Sorg H. Wound repair and regeneration. *Eur Surg Res.* 2012;49(1):35-43.
272. Broughton G, 2nd, Janis JE, Attinger CE. The basic science of wound healing. *Plast Reconstr Surg.* 2006;117(7 Suppl):12S-34S.
273. Roumenina LT, Rayes J, Lacroix-Desmazes S, Dimitrov JD. Heme: Modulator of Plasma Systems in Hemolytic Diseases. *Trends Mol Med.* 2016;22(3):200-213.
274. Smith A, McCulloh RJ. Hemopexin and haptoglobin: allies against heme toxicity from hemoglobin not contenders. *Front Physiol.* 2015;6:187.
275. Koh TJ, DiPietro LA. Inflammation and wound healing: the role of the macrophage. *Expert Rev Mol Med.* 2011;13:e23.
276. Golebiewska EM, Poole AW. Platelet secretion: From haemostasis to wound healing and beyond. *Blood Rev.* 2015;29(3):153-162.
277. Lichtman MK, Otero-Vinas M, Falanga V. Transforming growth factor beta (TGF-beta) isoforms in wound healing and fibrosis. *Wound Repair Regen.* 2016;24(2):215-222.
278. Rodriguez PG, Felix FN, Woodley DT, Shim EK. The role of oxygen in wound healing: a review of the literature. *Dermatol Surg.* 2008;34(9):1159-1169.
279. Wynn TA, Vannella KM. Macrophages in Tissue Repair, Regeneration, and Fibrosis. *Immunity.* 2016;44(3):450-462.
280. Minutti CM, Knipper JA, Allen JE, Zaiss DM. Tissue-specific contribution of macrophages to wound healing. *Semin Cell Dev Biol.* 2017;61:3-11.
281. Naito Y, Takagi T, Higashimura Y. Heme oxygenase-1 and anti-inflammatory M2 macrophages. *Arch Biochem Biophys.* 2014;564:83-88.
282. Mahdavian Delavary B, van der Veer WM, van Egmond M, Niessen FB, Beelen RH. Macrophages in skin injury and repair. *Immunobiology.* 2011;216(7):753-762.
283. Sindrilaru A, Scharffetter-Kochanek K. Disclosure of the Culprits: Macrophages-Versatile Regulators of Wound Healing. *Adv Wound Care (New Rochelle).* 2013;2(7):357-368.
284. Landen NX, Li D, Stahle M. Transition from inflammation to proliferation: a critical step during wound healing. *Cell Mol Life Sci.* 2016;73(20):3861-3885.
285. Kasuya A, Tokura Y. Attempts to accelerate wound healing. *J Dermatol Sci.* 2014;76(3):169-172.
286. Okonkwo UA, DiPietro LA. Diabetes and Wound Angiogenesis. *Int J Mol Sci.* 2017;18(7).

287. Gonzalez AC, Costa TF, Andrade ZA, Medrado AR. Wound healing - A literature review. *An Bras Dermatol*. 2016;91(5):614-620.
288. Marshall CD, Hu MS, Leavitt T, Barnes LA, Lorenz HP, Longaker MT. Cutaneous Scarring: Basic Science, Current Treatments, and Future Directions. *Adv Wound Care (New Rochelle)*. 2018;7(2):29-45.
289. Darby IA, Laverdet B, Bonte F, Desmouliere A. Fibroblasts and myofibroblasts in wound healing. *Clin Cosmet Investig Dermatol*. 2014;7:301-311.
290. Wipff PJ, Hinz B. Myofibroblasts work best under stress. *J Bodyw Mov Ther*. 2009;13(2):121-127.
291. Ramirez H, Patel SB, Pastar I. The Role of TGFbeta Signaling in Wound Epithelialization. *Adv Wound Care (New Rochelle)*. 2014;3(7):482-491.
292. Tredget EB, Demare J, Chandran G, Tredget EE, Yang L, Ghahary A. Transforming growth factor-beta and its effect on reepithelialization of partial-thickness ear wounds in transgenic mice. *Wound Repair Regen*. 2005;13(1):61-67.
293. Satish L, Blair HC, Glading A, Wells A. Interferon-inducible protein 9 (CXCL11)-induced cell motility in keratinocytes requires calcium flux-dependent activation of mu-calpain. *Mol Cell Biol*. 2005;25(5):1922-1941.
294. Hinz B, Phan SH, Thannickal VJ, et al. Recent developments in myofibroblast biology: paradigms for connective tissue remodeling. *Am J Pathol*. 2012;180(4):1340-1355.
295. Desmouliere A, Chaponnier C, Gabbiani G. Tissue repair, contraction, and the myofibroblast. *Wound Repair Regen*. 2005;13(1):7-12.
296. Haukipuro K. Synthesis of collagen types I and III in re-incised wounds in humans. *Br J Surg*. 1991;78(6):708-712.
297. Gurtner GC, Werner S, Barrandon Y, Longaker MT. Wound repair and regeneration. *Nature*. 2008;453(7193):314-321.
298. Guo S, Dipietro LA. Factors affecting wound healing. *J Dent Res*. 2010;89(3):219-229.
299. Xue M, Jackson CJ. Extracellular Matrix Reorganization During Wound Healing and Its Impact on Abnormal Scarring. *Adv Wound Care (New Rochelle)*. 2015;4(3):119-136.
300. Jackson WM, Nesti LJ, Tuan RS. Mesenchymal stem cell therapy for attenuation of scar formation during wound healing. *Stem Cell Res Ther*. 2012;3(3):20.
301. Agha R, Ogawa R, Pietramaggiore G, Orgill DP. A review of the role of mechanical forces in cutaneous wound healing. *J Surg Res*. 2011;171(2):700-708.
302. Medzhitov R. Origin and physiological roles of inflammation. *Nature*. 2008;454(7203):428-435.
303. Wagener FA, Carels CE, Lundvig DM. Targeting the redox balance in inflammatory skin conditions. *Int J Mol Sci*. 2013;14(5):9126-9167.
304. Lundvig DM, Immenschuh S, Wagener FA. Heme oxygenase, inflammation, and fibrosis: the good, the bad, and the ugly? *Front Pharmacol*. 2012;3:81.
305. Rojkind M, Dominguez-Rosales JA, Nieto N, Greenwel P. Role of hydrogen peroxide and oxidative stress in healing responses. *Cell Mol Life Sci*. 2002;59(11):1872-1891.
306. van der Veer WM, Bloemen MC, Ulrich MM, et al. Potential cellular and molecular causes of hypertrophic scar formation. *Burns*. 2009;35(1):15-29.
307. Nathan C, Ding A. Nonresolving inflammation. *Cell*. 2010;140(6):871-882.
308. Wagener FA, Eggert A, Boerman OC, et al. Heme is a potent inducer of inflammation in mice and is counteracted by heme oxygenase. *Blood*. 2001;98(6):1802-1811.
309. Grieb G, Steffens G, Pallua N, Bernhagen J, Bucala R. Circulating fibrocytes--biology and mechanisms in wound healing and scar formation. *Int Rev Cell Mol Biol*. 2011;291:1-19.
310. Volk SW, Wang Y, Mauldin EA, Liechty KW, Adams SL. Diminished type III collagen promotes myofibroblast differentiation and increases scar deposition in cutaneous wound healing. *Cells Tissues Organs*. 2011;194(1):25-37.
311. Liu XJ, Xu MJ, Fan ST, et al. Xiamenmycin attenuates hypertrophic scars by suppressing local inflammation and the effects of mechanical stress. *J Invest Dermatol*. 2013;133(5):1351-1360.
312. Liarte S, Bernabe-Garcia A, Nicolas FJ. Role of TGF-beta in Skin Chronic Wounds: A Keratinocyte Perspective. *Cells*. 2020;9(2).
313. Kryger ZB, Sisco M, Roy NK, Lu L, Rosenberg D, Mustoe TA. Temporal expression of the transforming growth factor-Beta pathway in the rabbit ear model of wound healing and scarring. *J Am Coll Surg*. 2007;205(1):78-88.
314. Finnson KW, McLean S, Di Guglielmo GM, Philip A. Dynamics of Transforming Growth Factor Beta Signaling in Wound Healing and Scarring. *Adv Wound Care (New Rochelle)*. 2013;2(5):195-214.

315. Schrementi ME, Ferreira AM, Zender C, DiPietro LA. Site-specific production of TGF-beta in oral mucosal and cutaneous wounds. *Wound Repair Regen.* 2008;16(1):80-86.
316. Ramalho T, Filgueiras L, Silva-Jr IA, Pessoa AFM, Jancar S. Impaired wound healing in type 1 diabetes is dependent on 5-lipoxygenase products. *Sci Rep.* 2018;8(1):14164.
317. Brownlee M. The pathobiology of diabetic complications: a unifying mechanism. *Diabetes.* 2005;54(6):1615-1625.
318. Kavitha KV, Tiwari S, Purandare VB, Khedkar S, Bhosale SS, Unnikrishnan AG. Choice of wound care in diabetic foot ulcer: A practical approach. *World J Diabetes.* 2014;5(4):546-556.
319. Dinh T, Veves A. Microcirculation of the diabetic foot. *Curr Pharm Des.* 2005;11(18):2301-2309.
320. Kunkemoeller B, Kyriakides TR. Redox Signaling in Diabetic Wound Healing Regulates Extracellular Matrix Deposition. *Antioxid Redox Signal.* 2017;27(12):823-838.
321. Hink U, Tsilimingas N, Wendt M, Munzel T. Mechanisms underlying endothelial dysfunction in diabetes mellitus: therapeutic implications. *Treat Endocrinol.* 2003;2(5):293-304.
322. Kono H, Onda A, Yanagida T. Molecular determinants of sterile inflammation. *Curr Opin Immunol.* 2014;26:147-156.
323. Blakytyn R, Jude EB. Altered molecular mechanisms of diabetic foot ulcers. *Int J Low Extrem Wounds.* 2009;8(2):95-104.
324. Falanga V. Wound healing and its impairment in the diabetic foot. *Lancet.* 2005;366(9498):1736-1743.
325. Khanna S, Biswas S, Shang Y, et al. Macrophage dysfunction impairs resolution of inflammation in the wounds of diabetic mice. *PLoS One.* 2010;5(3):e9539.
326. Chowdhury AR, Ghosh I, Datta K. Excessive reactive oxygen species induces apoptosis in fibroblasts: role of mitochondrially accumulated hyaluronic acid binding protein 1 (HABP1/p32/gC1qR). *Experimental cell research.* 2008;314(3):651-667.
327. Takahashi A, Aoshiba K, Nagai A. Apoptosis of wound fibroblasts induced by oxidative stress. *Exp Lung Res.* 2002;28(4):275-284.
328. Qin Z, Robichaud P, He T, Fisher GJ, Voorhees JJ, Quan T. Oxidant exposure induces cysteine-rich protein 61 (CCN1) via c-Jun/AP-1 to reduce collagen expression in human dermal fibroblasts. *PLoS One.* 2014;9(12):e115402.
329. Son D, Harijan A. Overview of surgical scar prevention and management. *J Korean Med Sci.* 2014;29(6):751-757.
330. Brouwer KM, Lundvig DM, Middelkoop E, Wagener FA, Von den Hoff JW. Mechanical cues in orofacial tissue engineering and regenerative medicine. *Wound Repair Regen.* 2015;23(3):302-311.
331. Froese AR, Shimbori C, Bellaye PS, et al. Stretch-induced Activation of Transforming Growth Factor-beta1 in Pulmonary Fibrosis. *Am J Respir Crit Care Med.* 2016;194(1):84-96.
332. Utsunomiya T, Ishibazawa A, Nagaoka T, et al. Transforming Growth Factor-beta Signaling Cascade Induced by Mechanical Stimulation of Fluid Shear Stress in Cultured Corneal Epithelial Cells. *Invest Ophthalmol Vis Sci.* 2016;57(14):6382-6388.
333. Nan L, Zheng Y, Liao N, et al. Mechanical force promotes the proliferation and extracellular matrix synthesis of human gingival fibroblasts cultured on 3D PLGA scaffolds via TGFbeta expression. *Mol Med Rep.* 2019;19(3):2107-2114.
334. Morse D, Choi AM. Heme oxygenase-1: from bench to bedside. *Am J Respir Crit Care Med.* 2005;172(6):660-670.
335. Ewing JF, Maines MD. Regulation and expression of heme oxygenase enzymes in aged-rat brain: age related depression in HO-1 and HO-2 expression and altered stress-response. *J Neural Transm (Vienna).* 2006;113(4):439-454.
336. Gozzelino R, Jeney V, Soares MP. Mechanisms of cell protection by heme oxygenase-1. *Annu Rev Pharmacol Toxicol.* 2010;50:323-354.
337. Grochot-Przeczek A, Dulak J, Jozkowicz A. Haem oxygenase-1: non-canonical roles in physiology and pathology. *Clin Sci (Lond).* 2012;122(3):93-103.
338. Eisenstein RS, Garcia-Mayol D, Pettingell W, Munro HN. Regulation of ferritin and heme oxygenase synthesis in rat fibroblasts by different forms of iron. *Proc Natl Acad Sci U S A.* 1991;88(3):688-692.
339. George EM, Warrington JP, Spradley FT, Palei AC, Granger JP. The heme oxygenases: important regulators of pregnancy and preeclampsia. *Am J Physiol Regul Integr Comp Physiol.* 2014;307(7):R769-777.

340. Ryter SW, Choi AM. Heme oxygenase-1/carbon monoxide: from metabolism to molecular therapy. *Am J Respir Cell Mol Biol*. 2009;41(3):251-260.
341. Weng YH, Yang G, Weiss S, Dennerly PA. Interaction between heme oxygenase-1 and -2 proteins. *J Biol Chem*. 2003;278(51):50999-51005.
342. Zencussen ML, Casalis PA, El-Mouseleh T, et al. Haem oxygenase-1 dictates intrauterine fetal survival in mice via carbon monoxide. *J Pathol*. 2011;225(2):293-304.
343. Zencussen AC, Lim E, Knoeller S, et al. Heme oxygenases in pregnancy II: HO-2 is downregulated in human pathologic pregnancies. *Am J Reprod Immunol*. 2003;50(1):66-76.
344. Zhao H, Wong RJ, Kalish FS, Nayak NR, Stevenson DK. Effect of Heme Oxygenase-1 Deficiency on Placental Development. *Placenta*. 2009;30(10):861-868.
345. Barber A, Robson SC, Myatt L, Bulmer JN, Lyall F. Heme oxygenase expression in human placenta and placental bed: reduced expression of placenta endothelial HO-2 in preeclampsia and fetal growth restriction. *FASEB J*. 2001;15(7):1158-1168.
346. Lyall F, Barber A, Myatt L, Bulmer JN, Robson SC. Hemeoxygenase expression in human placenta and placental bed implies a role in regulation of trophoblast invasion and placental function. *FASEB J*. 2000;14(1):208-219.
347. Yoshiki N, Kubota T, Aso T. Expression and localization of heme oxygenase in human placental villi. *Biochem Biophys Res Commun*. 2000;276(3):1136-1142.
348. Zencussen ML, Linzke N, Schumacher A, et al. Heme oxygenase-1 is critically involved in placentation, spiral artery remodeling, and blood pressure regulation during murine pregnancy. *Front Pharmacol*. 2014;5:291.
349. Kreiser D, Nguyen X, Wong R, et al. Heme oxygenase-1 modulates fetal growth in the rat. *Lab Invest*. 2002;82(6):687-692.
350. Sollwedel A, Bertoja AZ, Zencussen ML, et al. Protection from abortion by heme oxygenase-1 up-regulation is associated with increased levels of Bag-1 and neuropilin-1 at the fetal-maternal interface. *J Immunol*. 2005;175(8):4875-4885.
351. Jozkowicz A, Huk I, Nigisch A, et al. Heme oxygenase and angiogenic activity of endothelial cells: stimulation by carbon monoxide and inhibition by tin protoporphyrin-IX. *Antioxid Redox Signal*. 2003;5(2):155-162.
352. Zencussen AC, Sollwedel A, Bertoja AZ, et al. Heme oxygenase as a therapeutic target in immunological pregnancy complications. *Int Immunopharmacol*. 2005;5(1):41-51.
353. Ahmed A, Rahman M, Zhang X, et al. Induction of placental heme oxygenase-1 is protective against TNF α -induced cytotoxicity and promotes vessel relaxation. *Mol Med*. 2000;6(5):391-409.
354. Poss KD, Tonegawa S. Heme oxygenase 1 is required for mammalian iron reutilization. *Proc Natl Acad Sci U S A*. 1997;94(20):10919-10924.
355. Yachie A, Niida Y, Wada T, et al. Oxidative stress causes enhanced endothelial cell injury in human heme oxygenase-1 deficiency. *J Clin Invest*. 1999;103(1):129-135.
356. Krzyszczyk P, Schloss R, Palmer A, Berthiaume F. The Role of Macrophages in Acute and Chronic Wound Healing and Interventions to Promote Pro-wound Healing Phenotypes. *Front Physiol*. 2018;9:419.
357. Kapitulnik J. Bilirubin: an endogenous product of heme degradation with both cytotoxic and cytoprotective properties. *Mol Pharmacol*. 2004;66(4):773-779.
358. Hanselmann C, Mauch C, Werner S. Haem oxygenase-1: a novel player in cutaneous wound repair and psoriasis? *Biochem J*. 2001;353(Pt 3):459-466.
359. Cairo G, Recalcati S, Mantovani A, Locati M. Iron trafficking and metabolism in macrophages: contribution to the polarized phenotype. *Trends Immunol*. 2011;32(6):241-247.
360. Grochot-Przeczek A, Lach R, Mis J, et al. Heme oxygenase-1 accelerates cutaneous wound healing in mice. *PLoS One*. 2009;4(6):e5803.
361. Chen QY, Wang GG, Li W, Jiang YX, Lu XH, Zhou PP. Heme Oxygenase-1 Promotes Delayed Wound Healing in Diabetic Rats. *J Diabetes Res*. 2016;2016:9726503.
362. Choi DS, Kim S, Lim YM, et al. Hydrogel Incorporated with Chestnut Honey Accelerates Wound Healing and Promotes Early HO-1 Protein Expression in Diabetic (db/db) Mice. *Tissue Eng Regen Med*. 2012;9(1):36-42.
363. Kant V, Gopal A, Kumar D, et al. Curcumin-induced angiogenesis hastens wound healing in diabetic rats. *J Surg Res*. 2015;193(2):978-988.
364. Ahanger AA, Prawez S, Leo MD, et al. Pro-healing potential of hemin: an inducer of heme oxygenase-1. *Eur J Pharmacol*. 2010;645(1-3):165-170.

365. Pandith H, Zhang X, Liggett J, Min KW, Gritsanapan W, Baek SJ. Hemostatic and Wound Healing Properties of Chromolaena odorata Leaf Extract. *ISRN Dermatol.* 2013;2013:168269.
366. Martin P, Parkhurst SM. Parallels between tissue repair and embryo morphogenesis. *Development.* 2004;131(13):3021-3034.
367. Hu MS, Borrelli MR, Lorenz HP, Longaker MT, Wan DC. Mesenchymal Stromal Cells and Cutaneous Wound Healing: A Comprehensive Review of the Background, Role, and Therapeutic Potential. *Stem Cells Int.* 2018;2018:6901983.
368. Shin JO, Lee JM, Bok J, Jung HS. Inhibition of the Zeb family prevents murine palatogenesis through regulation of apoptosis and the cell cycle. *Biochem Biophys Res Commun.* 2018;506(1):223-230.
369. Wu W, Gu S, Sun C, et al. Altered FGF Signaling Pathways Impair Cell Proliferation and Elevation of Palate Shelves. *PLoS One.* 2015;10(9):e0136951.
370. Potter AS, Potter SS. Molecular Anatomy of Palate Development. *PLoS One.* 2015;10(7):e0132662.
371. Hill C, Jacobs B, Kennedy L, et al. Cranial neural crest deletion of VEGFa causes cleft palate with aberrant vascular and bone development. *Cell Tissue Res.* 2015;361(3):711-722.
372. Millicovsky G, Ambrose LJ, Johnston MC. Developmental alterations associated with spontaneous cleft lip and palate in CL/Fr mice. *Am J Anat.* 1982;164(1):29-44.
373. Sasaki Y, Tanaka S, Hamachi T, Taya Y. Deficient cell proliferation in palatal shelf mesenchyme of CL/Fr mouse embryos. *J Dent Res.* 2004;83(10):797-801.
374. Rice R, Spencer-Dene B, Connor EC, et al. Disruption of Fgf10/Fgfr2b-coordinated epithelial-mesenchymal interactions causes cleft palate. *J Clin Invest.* 2004;113(12):1692-1700.
375. Okuhara S, Iseki S. Epithelial integrity in palatal shelf elevation. *Jpn Dent Sci Rev.* 2012;48(1):18-22.
376. Nawshad A, LaGamba D, Hay ED. Transforming growth factor beta (TGFbeta) signalling in palatal growth, apoptosis and epithelial mesenchymal transformation (EMT). *Arch Oral Biol.* 2004;49(9):675-689.
377. Lambert-Messerlian G, Eklund E, Pinar H, Tantravahi U, Schneyer AL. Activin subunit and receptor expression in normal and human fetal cleft palate tissues. *Pediatr Devel Pathol.* 2007;10(6):436-445.
378. Gehris AL, D'Angelo M, Greene RM. Immunodetection of the transforming growth factors beta 1 and beta 2 in the developing murine palate. *Int J Dev Biol.* 1991;35(1):17-24.
379. Nakajima A, Ito Y, Tanaka E, et al. Functional role of TGF-beta receptors during palatal fusion in vitro. *Arch Oral Biol.* 2014;59(11):1192-1204.
380. Sulik KK, Johnston MC, Ambrose LJ, Dorgan D. Phenytoin (dilantin)-induced cleft lip and palate in A/J mice: a scanning and transmission electron microscopic study. *Anat Rec.* 1979;195(2):243-255.
381. Yoshikawa H, Kukita T, Kurisu K, Tashiro H. Effect of retinoic acid on in vitro proliferation activity and glycosaminoglycan synthesis of mesenchymal cells from palatal shelves of mouse fetuses. *J Craniofac Genet Dev Biol.* 1987;7(1):45-51.
382. Zhang H, Liu X, Gao Z, et al. Excessive retinoic acid inhibit mouse embryonic palate mesenchymal cell growth through involvement of Smad signaling. *Anim Cells Syst (Seoul).* 2017;21(1):31-36.
383. Lee DE, Ayoub N, Agrawal DK. Mesenchymal stem cells and cutaneous wound healing: novel methods to increase cell delivery and therapeutic efficacy. *Stem Cell Res Ther.* 2016;7:37.
384. Yellowley CE, Toupadakis CA, Vapniarsky N, Wong A. Circulating progenitor cells and the expression of Cxcl12, Cxcr4 and angiopoietin-like 4 during wound healing in the murine ear. *PLoS One.* 2019;14(9):e0222462.
385. Vagesjo E, Ohnstedt E, Mortier A, et al. Accelerated wound healing in mice by on-site production and delivery of CXCL12 by transformed lactic acid bacteria. *Proc Natl Acad Sci U S A.* 2018;115(8):1895-1900.
386. Jiang D, Scharffetter-Kochanek K. Mesenchymal Stem Cells Adaptively Respond to Environmental Cues Thereby Improving Granulation Tissue Formation and Wound Healing. *Front Cell Dev Biol.* 2020;8:697.
387. Lee SH, Jin SY, Song JS, Seo KK, Cho KH. Paracrine effects of adipose-derived stem cells on keratinocytes and dermal fibroblasts. *Ann Dermatol.* 2012;24(2):136-143.
388. Chen L, Tredget EE, Wu PY, Wu Y. Paracrine factors of mesenchymal stem cells recruit macrophages and endothelial lineage cells and enhance wound healing. *PLoS One.* 2008;3(4):e1886.

389. Liu J, Hao H, Xia L, et al. Hypoxia pretreatment of bone marrow mesenchymal stem cells facilitates angiogenesis by improving the function of endothelial cells in diabetic rats with lower ischemia. *PLoS One*. 2015;10(5):e0126715.
390. Shen C, Lie P, Miao T, et al. Conditioned medium from umbilical cord mesenchymal stem cells induces migration and angiogenesis. *Mol Med Rep*. 2015;12(1):20-30.
391. Abkowitz JL, Robinson AE, Kale S, Long MW, Chen J. Mobilization of hematopoietic stem cells during homeostasis and after cytokine exposure. *Blood*. 2003;102(4):1249-1253.
392. Carette MJ, Ferguson MW. The fate of medial edge epithelial cells during palatal fusion in vitro: an analysis by Dil labelling and confocal microscopy. *Development*. 1992;114(2):379-388.
393. Shin JO, Lee JM, Cho KW, et al. MiR-200b is involved in Tgf-beta signaling to regulate mammalian palate development. *Histochem Cell Biol*. 2012;137(1):67-78.
394. Fitzpatrick DR, Denhez F, Kondaiah P, Akhurst RJ. Differential expression of TGF beta isoforms in murine palatogenesis. *Development*. 1990;109(3):585-595.
395. Murillo J, Maldonado E, Barrio MC, et al. Interactions between TGF-beta1 and TGF-beta3 and their role in medial edge epithelium cell death and palatal fusion in vitro. *Differentiation*. 2009;77(2):209-220.
396. Iwata J, Suzuki A, Yokota T, et al. TGFbeta regulates epithelial-mesenchymal interactions through WNT signaling activity to control muscle development in the soft palate. *Development*. 2014;141(4):909-917.
397. Soeno Y, Taya Y, Aoba T. Fate of Medial Edge Epithelium in Mouse Palatogenesis in vitro: Apoptosis, Migration, and Epithelial-mesenchymal Transformation. *J Oral Biosci*. 2006;48(4):286-296.
398. Pastar I, Stojadinovic O, Yin NC, et al. Epithelialization in Wound Healing: A Comprehensive Review. *Adv Wound Care (New Rochelle)*. 2014;3(7):445-464.
399. Zambruno G, Marchisio PC, Marconi A, et al. Transforming growth factor-beta 1 modulates beta 1 and beta 5 integrin receptors and induces the de novo expression of the alpha v beta 6 heterodimer in normal human keratinocytes: implications for wound healing. *J Cell Biol*. 1995;129(3):853-865.
400. Morasso MI, Tomic-Canic M. Epidermal stem cells: the cradle of epidermal determination, differentiation and wound healing. *Biol Cell*. 2005;97(3):173-183.
401. Werner S, Krieg T, Smola H. Keratinocyte-fibroblast interactions in wound healing. *J Invest Dermatol*. 2007;127(5):998-1008.
402. Tensen CP, Flier J, Van Der Raaij-Helmer EM, et al. Human IP-9: A keratinocyte-derived high affinity CXC-chemokine ligand for the IP-10/Mig receptor (CXCR3). *J Invest Dermatol*. 1999;112(5):716-722.
403. Tortelli F, Pisano M, Briquez PS, Martino MM, Hubbell JA. Fibronectin binding modulates CXCL11 activity and facilitates wound healing. *PLoS One*. 2013;8(10):e79610.
404. Yates CC, Whaley D, Hooda S, Hebda PA, Bodnar RJ, Wells A. Delayed reepithelialization and basement membrane regeneration after wounding in mice lacking CXCR3. *Wound Repair Regen*. 2009;17(1):34-41.
405. Yates CC, Whaley D, A YC, Kulesekanan P, Hebda PA, Wells A. ELR-negative CXC chemokine CXCL11 (IP-9/I-TAC) facilitates dermal and epidermal maturation during wound repair. *Am J Pathol*. 2008;173(3):643-652.
406. Nathan C. Points of control in inflammation. *Nature*. 2002;420(6917):846-852.
407. Sanchez-Aguilera A, Mendez-Ferrer S. The hematopoietic stem-cell niche in health and leukemia. *Cell Mol Life Sci*. 2017;74(4):579-590.
408. Pollyea DA, Jordan CT. Therapeutic targeting of acute myeloid leukemia stem cells. *Blood*. 2017;129(12):1627-1635.
409. Keerthi N, Chimutengwende-Gordon M, Sanghani A, Khan W. The potential of stem cell therapy for osteoarthritis and rheumatoid arthritis. *Curr Stem Cell Res Ther*. 2013;8(6):444-450.
410. Wang L, Huang S, Li S, et al. Efficacy and Safety of Umbilical Cord Mesenchymal Stem Cell Therapy for Rheumatoid Arthritis Patients: A Prospective Phase I/II Study. *Drug Des Devel Ther*. 2019;13:4331-4340.
411. Cerqueira MT, Pirraco RP, Marques AP. Stem Cells in Skin Wound Healing: Are We There Yet? *Adv Wound Care (New Rochelle)*. 2016;5(4):164-175.
412. Butler KL, Gorman J, Ma H, et al. Stem cells and burns: review and therapeutic implications. *J Burn Care Res*. 2010;31(6):874-881.

413. Teng S, Liu C, Krettek C, Jagodzinski M. The application of induced pluripotent stem cells for bone regeneration: current progress and prospects. *Tissue Eng Part B Rev.* 2014;20(4):328-339.
414. Wu Y, Chen L, Scott PG, Tredget EE. Mesenchymal stem cells enhance wound healing through differentiation and angiogenesis. *Stem Cells.* 2007;25(10):2648-2659.
415. Rustad KC, Wong VW, Sorkin M, et al. Enhancement of mesenchymal stem cell angiogenic capacity and stemness by a biomimetic hydrogel scaffold. *Biomaterials.* 2012;33(1):80-90.
416. Fu X, Fang L, Li X, Cheng B, Sheng Z. Enhanced wound-healing quality with bone marrow mesenchymal stem cells autografting after skin injury. *Wound Repair Regen.* 2006;14(3):325-335.
417. Dash NR, Dash SN, Routray P, Mohapatra S, Mohapatra PC. Targeting nonhealing ulcers of lower extremity in human through autologous bone marrow-derived mesenchymal stem cells. *Rejuvenation Res.* 2009;12(5):359-366.
418. Sasaki M, Abe R, Fujita Y, Ando S, Inokuma D, Shimizu H. Mesenchymal stem cells are recruited into wounded skin and contribute to wound repair by transdifferentiation into multiple skin cell type. *J Immunol.* 2008;180(4):2581-2587.
419. Wagner J, Kean T, Young R, Dennis JE, Caplan AI. Optimizing mesenchymal stem cell-based therapeutics. *Curr Opin Biotechnol.* 2009;20(5):531-536.
420. Nuschke A. Activity of mesenchymal stem cells in therapies for chronic skin wound healing. *Organogenesis.* 2014;10(1):29-37.
421. Lafosse A, Desmet C, Aouassar N, et al. Autologous Adipose Stromal Cells Seeded onto a Human Collagen Matrix for Dermal Regeneration in Chronic Wounds: Clinical Proof of Concept. *Plast Reconstr Surg.* 2015;136(2):279-295.
422. O'Loughlin A, Kulkarni M, Creane M, et al. Topical administration of allogeneic mesenchymal stromal cells seeded in a collagen scaffold augments wound healing and increases angiogenesis in the diabetic rabbit ulcer. *Diabetes.* 2013;62(7):2588-2594.
423. Chen JS, Wong VW, Gurtner GC. Therapeutic potential of bone marrow-derived mesenchymal stem cells for cutaneous wound healing. *Front Immunol.* 2012;3:192.
424. Shin L, Peterson DA. Human mesenchymal stem cell grafts enhance normal and impaired wound healing by recruiting existing endogenous tissue stem/progenitor cells. *Stem Cells Transl Med.* 2013;2(1):33-42.
425. Kim WS, Park BS, Kim HK, et al. Evidence supporting antioxidant action of adipose-derived stem cells: protection of human dermal fibroblasts from oxidative stress. *J Dermatol Sci.* 2008;49(2):133-142.
426. Kim WS, Park BS, Sung JH, et al. Wound healing effect of adipose-derived stem cells: a critical role of secretory factors on human dermal fibroblasts. *J Dermatol Sci.* 2007;48(1):15-24.
427. Park BS, Jang KA, Sung JH, et al. Adipose-derived stem cells and their secretory factors as a promising therapy for skin aging. *Dermatol Surg.* 2008;34(10):1323-1326.
428. Leung A, Crombleholme TM, Keswani SG. Fetal wound healing: implications for minimal scar formation. *Curr Opin Pediatr.* 2012;24(3):371-378.
429. Balaji S, Keswani SG, Crombleholme TM. The Role of Mesenchymal Stem Cells in the Regenerative Wound Healing Phenotype. *Adv Wound Care (New Rochelle).* 2012;1(4):159-165.
430. Stone MJ, Hayward JA, Huang C, Z EH, Sanchez J. Mechanisms of Regulation of the Chemokine-Receptor Network. *Int J Mol Sci.* 2017;18(2).
431. Thiele S, Rosenkilde MM. Interaction of chemokines with their receptors—from initial chemokine binding to receptor activating steps. *Curr Med Chem.* 2014;21(31):3594-3614.
432. Moser B, Wolf M, Walz A, Loetscher P. Chemokines: multiple levels of leukocyte migration control. *Trends Immunol.* 2004;25(2):75-84.
433. Rees PA, Greaves NS, Baguneid M, Bayat A. Chemokines in Wound Healing and as Potential Therapeutic Targets for Reducing Cutaneous Scarring. *Adv Wound Care (New Rochelle).* 2015;4(11):687-703.
434. Proudfoot AE, Uguccioni M. Modulation of Chemokine Responses: Synergy and Cooperativity. *Front Immunol.* 2016;7:183.
435. Gerhart J. 1998 Warkany lecture: signaling pathways in development. *Teratology.* 1999;60(4):226-239.
436. Yoshie O. Role of chemokines in trafficking of lymphocytes and dendritic cells. *Int J Hematol.* 2000;72(4):399-407.
437. Zlotnik A, Yoshie O. Chemokines: a new classification system and their role in immunity. *Immunity.* 2000;12(2):121-127.

438. Mackay CR. Chemokines: immunology's high impact factors. *Nat Immunol.* 2001;2(2):95-101.
439. Dimberg A. Chemokines in angiogenesis. *Curr Top Microbiol Immunol.* 2010;341:59-80.
440. Speyer CL, Ward PA. Role of endothelial chemokines and their receptors during inflammation. *J Invest Surg.* 2011;24(1):18-27.
441. Luther SA, Cyster JG. Chemokines as regulators of T cell differentiation. *Nat Immunol.* 2001;2(2):102-107.
442. Rossi D, Zlotnik A. The biology of chemokines and their receptors. *Annu Rev Immunol.* 2000;18:217-242.
443. Zhou WH, Du MR, Dong L, Yu J, Li DJ. Chemokine CXCL12 promotes the cross-talk between trophoblasts and decidual stromal cells in human first-trimester pregnancy. *Human reproduction.* 2008;23(12):2669-2679.
444. Wang L, Li X, Zhao Y, et al. Insights into the mechanism of CXCL12-mediated signaling in trophoblast functions and placental angiogenesis. *Acta biochimica et biophysica Sinica.* 2015;47(9):663-672.
445. Su Y, Richmond A. Chemokine Regulation of Neutrophil Infiltration of Skin Wounds. *Advances in wound care.* 2015;4(11):631-640.
446. Kaplan AP. Chemokines, chemokine receptors and allergy. *International archives of allergy and immunology.* 2001;124(4):423-431.
447. Grymula K, Tarnowski M, Wyszczynski M, et al. Overlapping and distinct role of CXCR7-SDF-1/ITAC and CXCR4-SDF-1 axes in regulating metastatic behavior of human rhabdomyosarcomas. *International journal of cancer.* 2010;127(11):2554-2568.
448. Libura J, Drukala J, Majka M, et al. CXCR4-SDF-1 signaling is active in rhabdomyosarcoma cells and regulates locomotion, chemotaxis, and adhesion. *Blood.* 2002;100(7):2597-2606.
449. Balkwill F. Cancer and the chemokine network. *Nature reviews Cancer.* 2004;4(7):540-550.
450. Seemann S, Lupp A. Administration of a CXCL12 Analog in Endotoxemia Is Associated with Anti-Inflammatory, Anti-Oxidative and Cytoprotective Effects In Vivo. *PLoS One.* 2015;10(9):e0138389.
451. Zhang Y, Depond M, He L, et al. CXCR4/CXCL12 axis counteracts hematopoietic stem cell exhaustion through selective protection against oxidative stress. *Sci Rep.* 2016;6:37827.
452. Romain B, Hachet-Haas M, Rohr S, et al. Hypoxia differentially regulated CXCR4 and CXCR7 signaling in colon cancer. *Mol Cancer.* 2014;13:58.
453. Li S, Zhu G, Yang Y, et al. Oxidative stress drives CD8(+) T-cell skin trafficking in patients with vitiligo through CXCL16 upregulation by activating the unfolded protein response in keratinocytes. *J Allergy Clin Immunol.* 2017;140(1):177-189 e179.
454. Ball JA, Vlisidou I, Blunt MD, Wood W, Ward SG. Hydrogen Peroxide Triggers a Dual Signaling Axis To Selectively Suppress Activated Human T Lymphocyte Migration. *J Immunol.* 2017;198(9):3679-3689.
455. Balan M, Pal S. A novel CXCR3-B chemokine receptor-induced growth-inhibitory signal in cancer cells is mediated through the regulation of Bach-1 protein and Nrf2 protein nuclear translocation. *J Biol Chem.* 2014;289(6):3126-3137.
456. Lu J, Zhou WH, Ren L, Zhang YZ. CXCR4, CXCR7, and CXCL12 are associated with trophoblastic cells apoptosis and linked to pathophysiology of severe preeclampsia. *Experimental and molecular pathology.* 2016;100(1):184-191.
457. Tang T, Jiang H, Yu Y, et al. A new method of wound treatment: targeted therapy of skin wounds with reactive oxygen species-responsive nanoparticles containing SDF-1alpha. *International journal of nanomedicine.* 2015;10:6571-6585.
458. Muller A, Homey B, Soto H, et al. Involvement of chemokine receptors in breast cancer metastasis. *Nature.* 2001;410(6824):50-56.
459. Itatani Y, Kawada K, Inamoto S, et al. The Role of Chemokines in Promoting Colorectal Cancer Invasion/Metastasis. *International journal of molecular sciences.* 2016;17(5).
460. Liu C, Weng Y, Yuan T, et al. CXCL12/CXCR4 signal axis plays an important role in mediating bone morphogenetic protein 9-induced osteogenic differentiation of mesenchymal stem cells. *Int J Med Sci.* 2013;10(9):1181-1192.
461. Cole KE, Strick CA, Paradis TJ, et al. Interferon-inducible T cell alpha chemoattractant (I-TAC): a novel non-ELR CXC chemokine with potent activity on activated T cells through selective high affinity binding to CXCR3. *The Journal of experimental medicine.* 1998;187(12):2009-2021.
462. Kawada K, Hosogi H, Sonoshita M, et al. Chemokine receptor CXCR3 promotes colon cancer metastasis to lymph nodes. *Oncogene.* 2007;26(32):4679-4688.

463. Torraca V, Cui C, Boland R, et al. The CXCR3-CXCL11 signaling axis mediates macrophage recruitment and dissemination of mycobacterial infection. *Dis Model Mech*. 2015;8(3):253-269.

Part I

Diminished cytoprotection in HO-2 deficient mice hampers fetal growth, without affecting chemokine signaling during palatal fusion or palatal osteogenesis

CHAPTER 2

Chemokine signaling during midline epithelial seam disintegration facilitates palatal fusion

Suttorp CM, Cremers NAJ, van Rheden REM, Regan RF, Helmich MPAC, van Kempen S, Kuijpers-Jagtman AM, Wagener FADTG.

Front Cell Dev Biol, 2017 Oct 30;5:94.

Abstract

Disintegration of the midline epithelial seam (MES) is crucial for palatal fusion, and failure results in cleft palate. Palatal fusion and wound repair share many common signaling pathways related to epithelial-mesenchymal cross-talk. We postulate that chemokine CXCL11, its receptor CXCR3, and the cytoprotective enzyme heme oxygenase (HO), which are crucial during wound repair, also play a decisive role in MES disintegration. Fetal growth restriction and craniofacial abnormalities were present in HO-2 knockout (KO) mice without effects on palatal fusion. CXCL11 and CXCR3 were highly expressed in the disintegrating MES in both wild-type (wt) and HO-2 KO animals. Multiple apoptotic DNA fragments were present within the disintegrating MES and phagocytized by recruited CXCR3-positive wt and HO-2 KO macrophages. Macrophages located near the MES were HO-1-positive, and more HO-1-positive cells were present in HO-2 KO mice compared to wild-type. This study of embryonic and palatal development provided evidence that supports the hypothesis that the MES itself plays a prominent role in palatal fusion by orchestrating epithelial apoptosis and macrophage recruitment via CXCL11-CXCR3 signaling.

Keywords: Embryology, cleft palate, chemokine, macrophage, heme oxygenase, apoptosis.

Abbreviations

ABC	Avidin-biotin peroxidase complex
ANOVA	Analysis of variance
AP	Alkaline phosphatase
BCIP	5-bromo-4-chloro-3'-indolylphosphate
CLP	Cleft lip and palate
CPO	Cleft palate only
CO	Carbon monoxide
CXCL11	Chemokine (C-X-C) ligand 11
CXCR3	Chemokine (C-X-C) receptor 3
DAB	Diaminobenzidine-peroxidase
E0	Embryonic day 0
EMT	Epithelial-to-mesenchymal transformation
FragEL	Fragment End Labeling
F4/80	EGF-like module-containing mucin-like hormone receptor-like 1
HE	Haematoxylin and eosin
HO	Heme oxygenase
KO	Knockout
KS-test	Kolmogorov-Smirnov test
MEE	Midline epithelial edge
MES	Midline epithelial seam
NBT	Nitro-blue tetrazolium
PBSG	Phosphate-buffered saline with glycine
ROS	Reactive oxygen species
TdT	Terminal deoxynucleotidyl Transferase
Wt	Wild-type

Introduction

Formation of the secondary palate requires adhesion by the midline epithelial edge (MEE) of both palatal shelves, formation of the transient midline epithelial seam (MES), disintegration of the MES, and fusion of the palatal shelves¹. Only after disintegration of the MES the mesenchyme of the palatal shelves can fuse to form the secondary palate. Failure of epithelial adhesion between both palatal shelves² or a lack of MES disintegration^{3,4} will result in cleft palate with (CLP) or without cleft lip (CPO). Multiple mechanisms have been proposed to explain the disappearance of the MES. The main hypotheses underlying MES disintegration involve epithelial cell migration to the oral or nasal epithelium⁵, epithelial-to-mesenchymal transformation (EMT)⁶, epithelial cell apoptosis⁷⁻¹⁰, or a combination of these events³.

CLP is the most common congenital facial malformation in humans and occurs in approximately 1/700 live births¹¹. However, CPO is the rarest form of oral clefting, with an incidence ranging from 1.3 to 25.3/10,000 live births¹². Although the exact biological mechanisms underlying orofacial clefting are not completely understood¹³, a combination of genetic and environmental factors is thought to play a role. Approximately 50% of children born with CPO have a genetic syndrome¹⁴, compared to 30% with CLP¹⁵. Notably, maternal smoking, diabetes, and infections have been shown to strongly increase the risk for babies with orofacial clefts^{13,16}, suggesting that control of oxidative and inflammatory stress is important.

Accumulating data suggest that the heme-degrading antioxidative enzyme heme oxygenase (HO) is a key regulator during embryological development¹⁷⁻¹⁹. HO facilitates placentation, fetal growth, and -development by restricting excessive free heme levels. Heme promotes oxidative and inflammatory stress^{20,21} and may lead to intrauterine fetal growth restriction and fetal loss¹⁷. HO protects against this inflammatory stress by degrading heme and generating free iron/ferritin, carbon monoxide (CO), and biliverdin/bilirubin²². These HO effector molecules regulate vasodilation and anti-apoptotic signaling, inhibit platelet aggregation, reduce leukocyte adhesion, and reduce pro-inflammatory cytokines^{22,23}. Two functional isoforms of HO have been described, HO-1 and HO-2. HO-1 has low basal levels but is strongly inducible, whereas HO-2 is largely constitutively expressed. HO-2 is highly expressed in the brain, testes, and blood vessels²⁴. Interestingly, the cytoprotective HO-1 and HO-2 enzymes are both strongly expressed in the placenta during embryonic development and in neural crest cells that form the craniofacial tissues in mice and humans^{18,25}. Elevated inflammatory, oxidative, and angiogenic factors have been demonstrated in the endothelial cells of HO-2 knockout (KO) mice²⁶. During pregnancy, down-regulation of both HO-1²⁷ and HO-2¹⁸ in the placenta is associated with pregnancy failure. Spontaneous abortion, pre-eclampsia, or fetal growth retardation are associated with lower HO-2 protein levels compared to healthy pregnant controls¹⁸.

Palatal fusion and wound repair are regenerative processes that share common signaling pathways and gene regulatory networks²⁸. Epithelial-mesenchymal cross-talk is essential in both processes. Decreased signaling between the versatile CXCL11 and its receptor CXCR3 on epithelial cells leads to delayed re-epithelialization and impaired epidermis maturation during wound repair²⁹. Moreover, CXCR3 KO mice present excessive scar formation following injury³⁰. Macrophages are important in regenerative and embryonic developmental processes³¹⁻³⁴, and blocking the CXCL11-CXCR3 axis suppresses macrophage infiltration^{35,36}. Recently, slower wound closure and delayed CXCL11 expression in wounds was observed in HO-2 KO mice³⁷. Interestingly, HO-2 deficiency was shown to result in impaired macrophage function³⁸. Although CXCL11-CXCR3 signaling regulates diverse cellular functions, including influx of immune cells during inflammation^{39,40} and wound repair^{29,41}, little is known about its role during palatal fusion.

We postulate that palatal fusion is hampered in HO-2 KO mice by disruption of epithelial cell and macrophage cross-talk in the MES due to hampered CXCL11-CXCR3 signaling. In the present study, MES disintegration is investigated in relation to chemokine signaling and the effects of HO-2 deficiency on embryonic development and palatal fusion.

Materials and Methods

Animals used for the study

To obtain fetuses for this study, 8-week-old female wild-type (wt) ($n=7$) and HO-2 KO ($n=8$) mice were mated with respectively wt and HO-2 KO male mice. Homozygote HO-2 KO mice generated by targeted disruption of the HO-2 gene^{26,42}, and wt mice, both of a mixed 129Sv x C57BL/6 background, were bred and maintained in our animal facility. The animals were housed under normal laboratory conditions with 12 h light/dark cycle and *ad libitum* access to water and powdered rodent chow (Sniff, Soest, The Netherlands) and were allowed to acclimatize for at least 1 week before the start of the experiment. Ethical permission for the study was obtained according to the guidelines of the Board for Animal Experiments of the Radboud University Nijmegen (RU-DEC 2012-166).

Hormone administration before mating

Preliminary experiments (RU-DEC 2009-160) demonstrated that young animals (8-10 weeks old), that were mated for the first time, often did not carry fetuses. This was demonstrated for both wt mice and HO-2 KO mice. The chance of pregnancy was therefore enhanced using the hormones Folligonan (Genadotropin serum, Intervet Nederland B.V., Boxmeer, The Netherlands) and Pregnyl (Human chorionic gonadotropin, N.V. Organon, Oss, The Netherlands). Because there is a lag time of

approximately 13 days between hormone application and palatal formation, we expected minor influence on the experimental outcome. At day -3 at 16.00 h Folligonan (6E in 30 μ l) and at day -1 at 16.00 h Pregnyl (6E in 30 μ l) was administered by intraperitoneal injection.

Plugging day and obtaining wt and HO-2 KO fetuses

The presence of a vaginal copulation plug, indicating that mating has occurred, was taken as day 0 of pregnancy (embryonic day 0; E0)⁴³. 1 wt mouse and 2 HO-2 KO mice demonstrated no plugged status. These animals were mated again 4 weeks later, and all demonstrated then a plugged status.

Since the palatal shelves fuse between embryonic day E14.5 and E15.5 in wt mice⁴⁴ we presumed that fetuses of E15 were suitable for our study. At embryonic day E15, 7 wt and 7 HO-2 KO animals were killed by CO₂/O₂ inhalation for 10 minutes. Only 3 out of 7 plugged wt mice, and 4 out of 7 plugged HO-2 KO mice carried fetuses. In total, 16 wt fetuses of E15 and 11 HO-2 KO fetuses of E15 were obtained.

In order to monitor the growth restriction found in HO-2 KO fetuses in more detail, we also analyzed the body size of E16 HO-2 KO fetuses. Therefore, 1 pregnant HO-2 KO mouse was killed at embryonic day 16, resulting in 12 HO-2 KO fetuses of E16.

Implantation rate

The uterus and fetuses were photographed (**Figure 1**). For the fetus carrying mice the mean implantation rate was analyzed by calculating the percentage of fetuses to the total number of embryonic implantations (fetuses+non-viable or hemorrhagic embryonic implantations).

The wt and HO-2 KO fetuses compared for weight, length, and body surface

The weight and size of wt fetuses (E15) and HO-2 KO fetuses (E15/E16) was measured. Severely malformed fetuses ($n=2$) were excluded for weight and size analysis. The body length, body surface and head surface of the fetuses were measured from photographs using ImageJ (1.48v) software (National institutes of health, Bethesda, MD, USA) and used for statistical analysis, for details see **Figure 1**.

Assessment of mRNA expression of HO-2, CXCL11, CXCR3 and HO-1 in fetus head samples by quantitative real-time PCR

To screen for differences in gene expression between HO-2 KO and wt fetuses, cDNAs were synthesized from samples from heads of wt (E15; $n=5$) and HO-2 KO (E15; $n=4$) fetuses. Fetuses were decapitated and total RNA was extracted using Trizol (Invitrogen, Carlsbad, CA, USA) and a RNeasy Mini kit (Qiagen, Hilden, Germany), and cDNA was produced using the iScript cDNA synthesis kit (Bio-Rad, Hercules, CA, USA). cDNAs were analyzed for gene expression of HO-1, HO-2, CXCL11 and CXCR3, using custom-designed

primers (**Table 1**) and iQ SYBR Green Supermix (Invitrogen, Carlsbad, CA, USA) in a CFX96 real-time PCR system (Bio-Rad, Hercules, CA, USA). Relative gene expression values were evaluated with the $2^{(-\Delta\Delta Ct)}$ method using GAPDH as housekeeping gene⁴⁵.

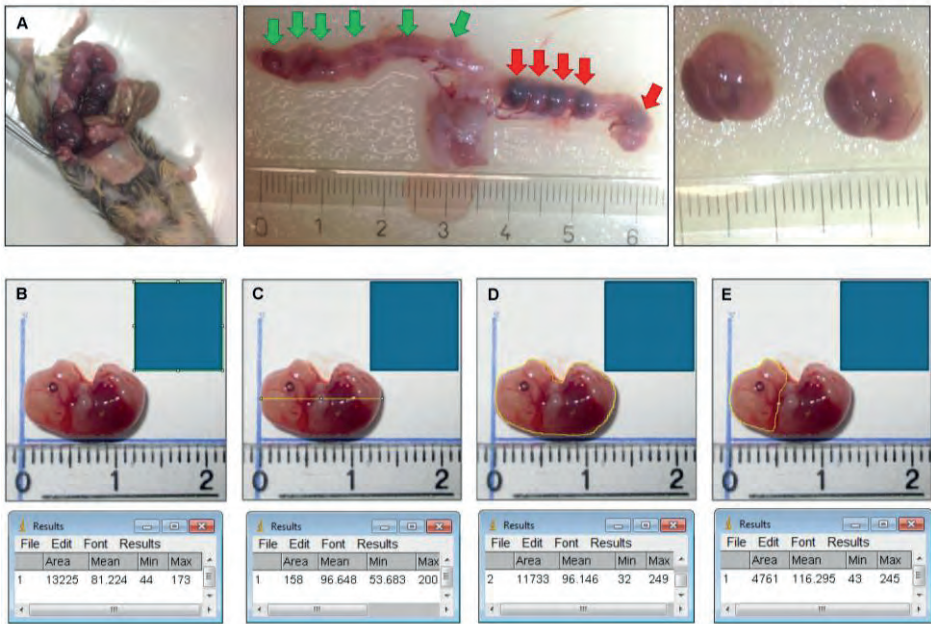


Figure 1: (A) Isolation of the fetuses and measurement of body length, body surface, head surface. Plugged mouse (e.g., HO-2 KO at E15) was sacrificed by CO₂/O₂ inhalation for 10 minutes, the uterus and organs were removed. Fetuses were isolated from the uterus. Location of the 6 fetuses in the uterus before they were removed (green arrows). Location of the 5 non-viable/hemorrhagic embryonic implantations (red arrows). **(B)** A square scale bar was drawn at the ruler in each photograph of 10 x 10 mm (1 cm²) and the total number of pixels within the square was determined (e.g., 13225 pixels). **(C)** A line in the length of the body of the fetus was drawn and the number of pixels was recorded (e.g., 158 pixels). The length was calculated (e.g., 158/√13225 = 13,7 mm). **(D)** The outline of the total body surface of the fetus was drawn and the number of pixels was recorded (e.g., 11733 pixels). The total body surface was calculated (e.g., 11733/13225 = 0,89 cm²). **(E)** The outline of the head surface was drawn, and the number of pixels was recorded (e.g., 4761 pixels). The head surface was calculated (e.g. 4761/13225 = 0,36 cm²).

Table 1: Custom-designed mouse primers used for assessment of mRNA expression of GAPDH, HO-1, HO-2, CXCL11 and CXCR3 in fetus head samples by quantitative real-time PCR.

Marker	Gene name	Forward primer (5'-3')	Reverse primer (5'-3')
Reference gene	<i>Gapdh</i>	GGCAAATTCACGGCACA	GTTAGTGGGGTCTCGTCTCTG
Cytoprotection	<i>Hmox1</i>	CAACATTGAGCTGTTTGAGG	TGGTCTTTGTGTTCTCTGTGTC
Cytoprotection	<i>Hmox2</i>	AAGGAAGGGACCAAGGAAG	AGTGGTGGCCAGCTTAAATAG
Chemokine	<i>Cxcl11</i>	CACGCTGCTCAAGGCTTCCTTATG	TGTCGCAGCCGTTACTCGGGT
Chemokine receptor	<i>Cxcr3</i>	CAGCCTGAACCTTTGACAGAACCT	GCAGCCCCAGCAAGAAGA

Haematoxylin-Eosin staining of transversal sections through the secondary palate

Mouse tissue samples were fixed for 24h in 4% paraformaldehyde and further processed for routine paraffin embedding. Paraffin sections were deparaffinized using Xylol, rehydrated using an alcohol range (100%-70%), and used for immunohistochemistry and FragEL™ analysis. Serial transversal sections through the secondary palate region of 5 µm thickness mounted on Superfrost Plus slides (Menzel-Gläser, Braunschweig, Germany) were routinely stained with Haematoxylin and Eosin (HE) for general tissue survey. The exact location of the fusing palatal shelves was determined per individual fetus. The HE stainings were subdivided into the four stages of palatogenesis based on the anatomy of the palatal shelves: elevation, horizontal, midline adhesion and fusion, according to Dudas et al.⁴⁴ and screened for anatomical abnormalities. These series were used as reference to obtain transversal sections containing palatal shelves in midline adhesion and fusion for immunohistochemical staining (**Figure 2**).

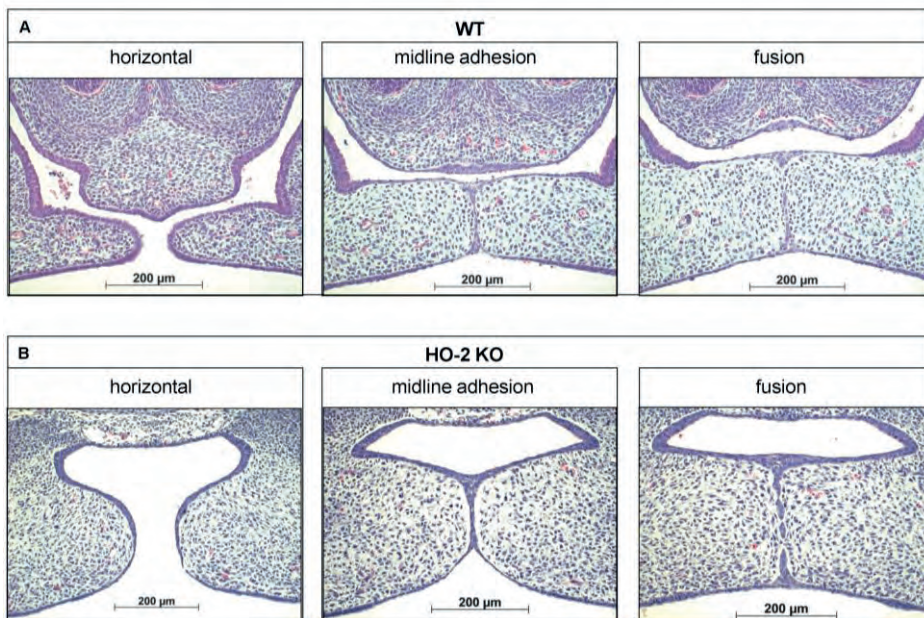


Figure 2: Palatal fusion observed in both wt and HO-2 KO fetuses at E15. HE stainings demonstrated horizontal orientation of the palatal shelves, midline adhesion and fusion within the same fetus. **(A)** Wt fetus at E15 (magnification: x100). Palatal shelves in a later stage of the palatal fusion increased in size. The MES changed from a multi-cell-layer into a continuous one-single-cell-layer, to a disintegrating MES, during which islands of epithelium in the midline were observed. **(B)** HO-2 KO fetus at E15 (magnification: x100). Palatal shelves in a later stage of the palatal fusion increased to some extent in size. Several islands of epithelium in the midline were observed.

Immunohistochemistry

Selected paraffin embedded sections were deparaffinized using Xylol and rehydrated using an alcohol range (100-70%). Endogenous peroxidase activity was quenched with 3% H₂O₂ in methanol for 20 min, and immunohistochemical stainings for HO-1, CXCL11, CXCR3 and macrophage marker F4/80 were performed as previously described⁴⁶. In brief, tissue sections were incubated for 60 min with a biotin-labeled secondary antibody (**Tables 2, 3**). Next, the sections washed with PBSG (phosphate-buffered saline with glycine) and treated with avidin-biotin peroxidase complex (ABC) for 45 min in the dark. After extensive washing with PBSG, diaminobenzidine-peroxidase (DAB) staining was performed for 10 min for the HO-1, CXCL11 and CXCR3 stainings.

Table 2: Antibodies and antigen retrievals used for immunohistochemical stainings for HO-1, CXCL11, CXCR3, and F4/80.

Antibody	Specificity	Dilution	Antigen retrieval	Source
SPA-895	HO-1	1:600	Combi: Citrate buffer 70°C for 10 min Trypsin digestion in PBS 0,015% 37°C for 5 min	Stressgen
Sc-34785	CXCL11	1:200	Citrate buffer 70°C for 2 hrs	Santa Cruz Biotechnology, Santa Cruz, CA, USA
NB100-56404	CXCR3	1:50	Citrate buffer 70°C for 2 hrs	Novus Biologicals, Littleton, USA
BM8	F4/80	1:400	Combi: Citrate buffer 70°C for 10 min Trypsin digestion in PBS 0,015% for 5 min	eBioscience

Analysis of apoptosis and recruited F4/80 positive macrophages in the palate

For studying apoptosis in the MES, transversal sections containing palatal shelves in midline contact and fusion stage of wt and HO-2 KO fetuses were selected. During apoptosis, cellular endonucleases cleave nuclear DNA between nucleosomes, producing specific DNA fragments with free 3'-OH groups at the end. These 3' OH group can be labeled using Fragment End Labeling (FragEL™, Calbiochem, San Diego, CA, USA) allowing detection of apoptotic DNA fragments at the individual cell level as previously described⁴⁷. The procedure was performed according to the protocol of the manufacturer (Calbiochem, San Diego, CA, USA). In brief, rehydrated paraffin sections were subjected to proteinase K digestion (0,5 µg/ml) for 10 min. Endogenous peroxidase activity was quenched with 3% H₂O₂ in methanol for 20 min. TdT (Terminal deoxynucleotidyl Transferase) added biotin labeled deoxynucleotides to the end of these DNA fragments. After addition of ABC, DAB was added and incubated at room temperature for 10 min. For the F4/80 staining + AP (alkaline phosphatase) + NBT (nitro-blue tetrazolium) + BCIP (5-bromo-4-chloro-3'-indolylphosphate) was used. For used

antibodies and antigen retrievals, see **Tables 2, 3**. Photographs were taken using a Carl Zeiss Imager Z.1 system (Carl Zeiss Microimaging GmbH, Jena, Germany) with AxioVision (4.8v) software (Zeiss, Göttingen, Germany).

Table 3: Secondary antibodies used for HO-1, CXCL11, CXCR3, apoptotic DNA fragments immunohistochemical staining, and F4/80 with apoptotic DNA fragments/CXCR3/HO-1 double stainings.

Secondary antibody	Specificity	Dilution	Color	Source
A11008	goat anti-rabbit AlexaFluor-488	1:500	Green	Invitrogen Thermofisher scientific
145-712-065-153 in combination with S-11226	donkey anti-rat Biotin	1:500	-	Jackson Immunoresearch Europe LTD
	Streptavidin	1:500	Red	Invitrogen Thermofisher scientific
715-065-151	donkey anti-rabbit Biotin +ABC+DAB	1:500	Brown	Jackson Immunoresearch Europe LTD
	donkey anti-rat Biotin+ABC+AP+ nbt/bcip	1:500	Blue	Calbiochem, San Diego, CA, USA

Antigen retrieval used for double stainings: Combi = Citrate buffer 70°C for 10 min + Trypsin digestion in PBS 0,075% 37°C for 5 min.

Quantification of CXCL11, CXCR3 and HO-1 immunoreactivity within the epithelium of the palatal shelves

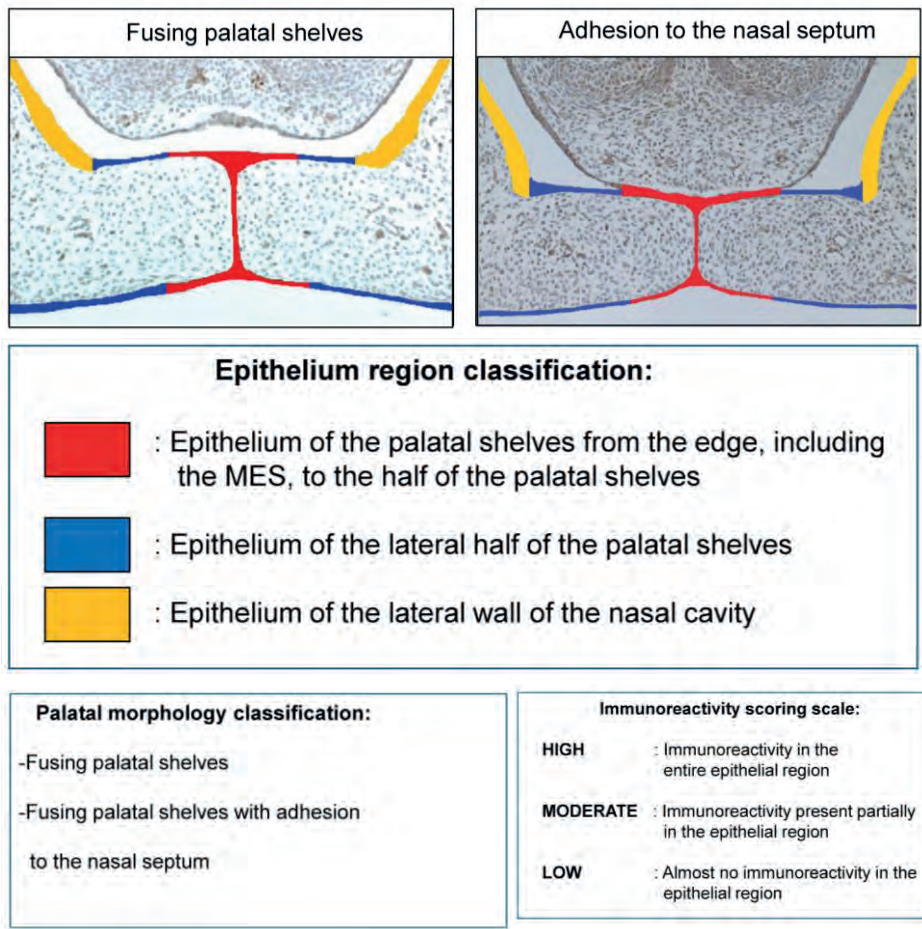
Transversal sections through the secondary palate of wt and HO-2 KO fetuses were screened. For quantification sections were selected following the inclusion criteria: transversal sections containing palatal shelves in midline adhesion and fusion with at least the presence of a part of the MES.

The immunostained sections were first categorized into two categories based on their palatal morphology (palatal morphology classification): fusing palatal shelves, and fusing palatal shelves with adhesion to the nasal septum, see **Figure 3**.

Within each section the epithelium of the palatal shelves was then subdivided into three separate regions (**Figure 3**) according to morphological characteristics (Epithelium region classification): epithelium of the palatal shelves from the edge, including the MES, to the half of the width of the shelves (in RED), epithelium of the lateral half of the palatal shelves (in BLUE), epithelium of the lateral wall of the nasal cavity, this region is positioned outside the palatal shelves and served as a control region (in YELLOW), see **Figure 3**.

CXCL11, CXCR3 and HO-1 immunoreactivity was evaluated by two observers, by blindly scoring, independently of each other. The epithelial regions per single section

were semi-quantitatively scored according to the immunoreactivity scoring scale in three categories (HIGH, MODERATE and LOW). For each individual fetus the modulus of the scoring per epithelial region was used for further statistical analysis. For details see **Figure 3**. To determine the inter-examiner reliability, 10 sections were measured by the two observers and acceptable coefficient of determination (R^2) scores > 0.80 were obtained for immunoreactivity scoring.



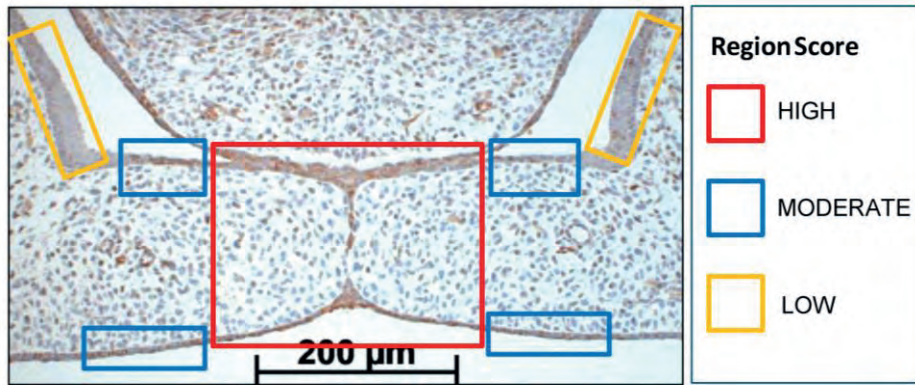


Figure 3: Palatal morphology classification: The CXCL11, CXCR3 and HO-1 immunostained sections were categorized in two stages according to their morphological characteristics: fusing palatal shelves, and fusing palatal shelves with adhesion to the nasal septum. **Epithelium region classification:** For each section epithelial layers were subdivided in 3 regions of interest according to morphological characteristics: epithelium of the palatal shelves from the edge, including the MES, to half of the width of the shelves (in RED), epithelium of the lateral half of the palatal shelves (in BLUE), epithelium of the lateral wall of the nasal cavity, this region is positioned outside the palatal shelves and served as a control region (in YELLOW). **Immunoreactivity scoring scale:** Semi-quantitative scoring of CXCL11, CXCR3 and HO-1 immunoreactivity in epithelium of the palatal shelves. Each epithelial region was semi-quantitatively scored according to the following scale: HIGH) Immunoreactivity present in the entire epithelial region; MODERATE) Immunoreactivity present only partially in the epithelial region; LOW) Almost no immunoreactivity present in the epithelial region. **Lower panel:** Immunoreactivity scored for the 3 epithelial locations in a CXCL11 immunostained section (e.g., wt fetus, E15, section with adhesion of the palatal shelves and adhesion to the nasal septum). RED region was scored as HIGH, BLUE region was scored as MODERATE, YELLOW region was scored as LOW for CXCL11 immunoreactivity.

Quantification of CXCL11, CXCR3 and HO-1 positive cells in the mesenchyme of the palatal shelves

The immunostained sections, wt and HO-2 KO, were first categorized based on their morphology (Palatal morphology classification, **Figure 3**). Since a significant variance in the size of the palatal shelves was present, expression was adjusted to surface area. The individual surface of each pair of shelves was measured using ImageJ (1.48v) software (Zeiss, Göttingen, Germany). Then, the number of CXCL11, CXCR3 and HO-1 positive cells within the outline of the mesenchyme of the palatal shelves was counted. For details see **Figure 4**. For each section the number of positive mesenchymal cells/mm² was calculated. Cell counting was performed twice, by two blinded observers independently of each other, and the mean value of positive cells/mm² per fetus was calculated and used for statistical analysis. To determine the inter-examiner reliability, 10 sections were measured by the two observers and acceptable coefficient of determination (R^2) scores > 0.80 were obtained for cell counting.

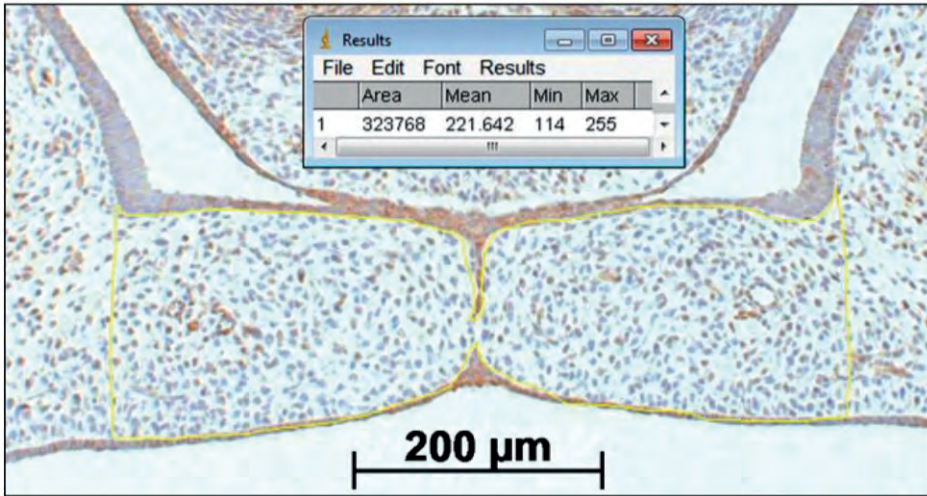


Figure 4: Palatal shelf surface measurement for determining the number of CXCL11, CXCR3 and HO-1 positive immunostained cells/mm² within the mesenchyme of the palatal shelves. A square scale bar was drawn in the microscopic picture (magnification: x100) of the section of 1000µm x 1000µm (1 mm²) and the total number of pixels within the square was determined (e.g., 1 mm² = 3442880 pixels). The contour of the mesenchyme of the shelves was drawn (yellow line). The number of pixels for this area was determined by the ImageJ (1.48v) software (323768 pixels). The number of positive immunostained cells within this mesenchymal area of the palatal shelves were counted by direct observation using the Zeiss microscope (e.g., 52 CXCL11 positive cells). The number of cells/mm² was calculated (3442880/323768) x 52 = 553 cells/mm².

Apoptotic DNA fragments in macrophages

Transversal sections containing palatal shelves in midline adhesion and fusion of wt and HO-2 KO fetuses were selected for the F4/80-immuno staining - FragEL™ DNA fragmentation kit combination. The F4/80 surface receptor is considered as one of the best markers for mature macrophages⁴⁸. The proximity of macrophages to apoptotic DNA fragments within the MES and the presence of apoptotic DNA fragments within the F4/80 positive macrophages were studied. For used antibodies and antigen retrievals, see **Tables 2, 3**.

CXCR3 and HO-1 expression in macrophages studied by immunofluorescence microscopy

Double staining for F4/80 with CXCR3/HO-1 were performed on paraffin sections of wt and HO-2 KO fetuses. Tissue samples were fixed for 24h in 4% paraformaldehyde and further processed for routine paraffin embedding. Sections were deparaffinized using Histosafe and rehydrated using an alcohol range (100%-70%). Fluorescent immunohistochemical double stainings for F4/80 with CXCR3, and F4/80 with HO-1 were performed. Nuclear staining was performed with DAPI. For antibodies used, see **Tables 2, 3**.

Statistical analysis

The data for the implantation rate, fetus weight, fetus length, fetus surface, fetus head surface and the PCR data for the mRNA expression of HO-1, HO-2, CXCL11, and CXCR3 showed a normal distribution as evaluated by the Kolmogorov-Smirnov test (KS-test).

To compare differences in implantation rate between the wt group and HO-2 KO group the Independent-Samples *T*-test was performed.

To analyze the fetus weight, fetus length, fetus surface, fetus head surface for the wt E15 group, the HO-2 KO E15 group and the HO-2 KO E16 group the ANOVA and Tukey's multiple comparison *post hoc* test were used.

The HO-1, CXCL11 and CXCR3 immunoreactivity in the epithelium regions was semi-quantitatively scored and analyzed using the non-parametric Kruskal-Wallis ANOVA on ranks test and Dunn's Multiple Comparison *post hoc* test to compare differences between the wt group and HO-2 KO group.

The data from quantification of the number of HO-1 positive cells in the mesenchyme showed a non-normal distribution as measured by the KS-test and the non-parametric Mann-Whitney test was used to compare differences between the wt group and HO-2 KO group.

Quantification data of the number of CXCL11 and CXCR3 positive cells in the mesenchyme showed a normal distribution as measured by the KS-test. Independent-Samples *T*-test was performed to compare differences between the wt group and HO-2 KO group.

To determine the inter-examiner reliability, the coefficient of determination (R^2) was calculated by the square of the Pearson correlation coefficient for the quantitative data, and calculated by the square of the Spearman correlation coefficient for the semi-quantitative data.

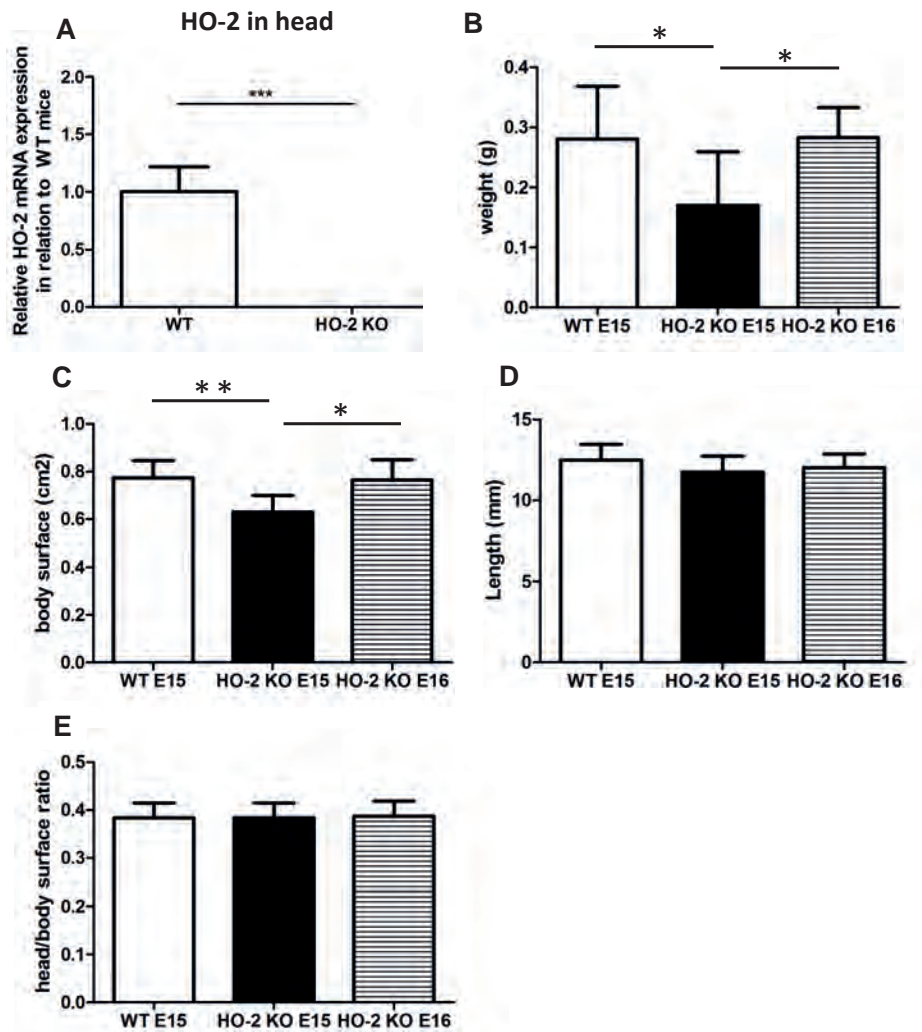
Differences were considered significant if $p < 0.05$. All statistical analyses were performed using Graphpad Prism 5.03 software (GraphPad Software, San Diego, CA, USA).

Results

Fetal growth restriction and malformations occur in the absence of HO-2 expression

Quantitative real-time PCR confirmed the genotypes of mice by showing that HO-2 mRNA was only present in samples from wild-type (wt) fetuses, and not in HO-2 KO fetuses ($p < 0.001$, **Figure 5A**). Hemorrhagic embryonic implantations were found in both wt and HO-2 KO animals (**Figure 1A**). No significant difference in the mean implantation rate was found between pregnant wt and HO-2 KO mice (46% versus 52%, $p = 0.79$). At E15, HO-2 KO fetuses weighed significantly less ($p < 0.05$, **Figure 5B**) with a significantly smaller body surface than wt fetuses ($p < 0.01$, **Figure 5C**). The differences fetus length ($p = 0.25$, **Figure 5D**) and in head/body surface ratio ($p = 0.97$, **Figure 5E**) for both genotypes were not significantly different at E15. To monitor the restriction of fetal

growth in HO-2 KO fetuses in more detail, we also analyzed the body size of E16 HO-2 KO fetuses. No significant difference was found between the E15 wt fetuses and E16 HO-2 KO fetuses in regard to weight (**Figure 5B**) and body surface (**Figure 5C**). No malformations or craniofacial anomalies were found in the wt fetuses (**Figure 5F**). Among the 15 HO-2 KO fetuses (E15 and E16), 1 E16 fetus had severe malformations (**Figure 5I**), 1 E16 fetus exhibited a craniofacial anomaly (**Figure 5J**), and 1 E15 fetus appeared to be the smallest fetus without anomalies (**Figure 5K**).



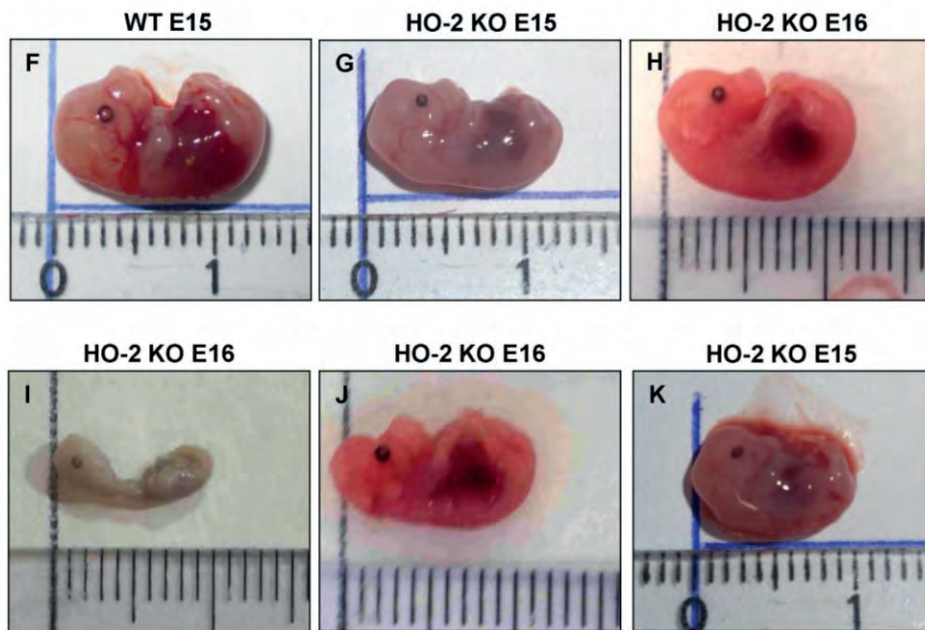


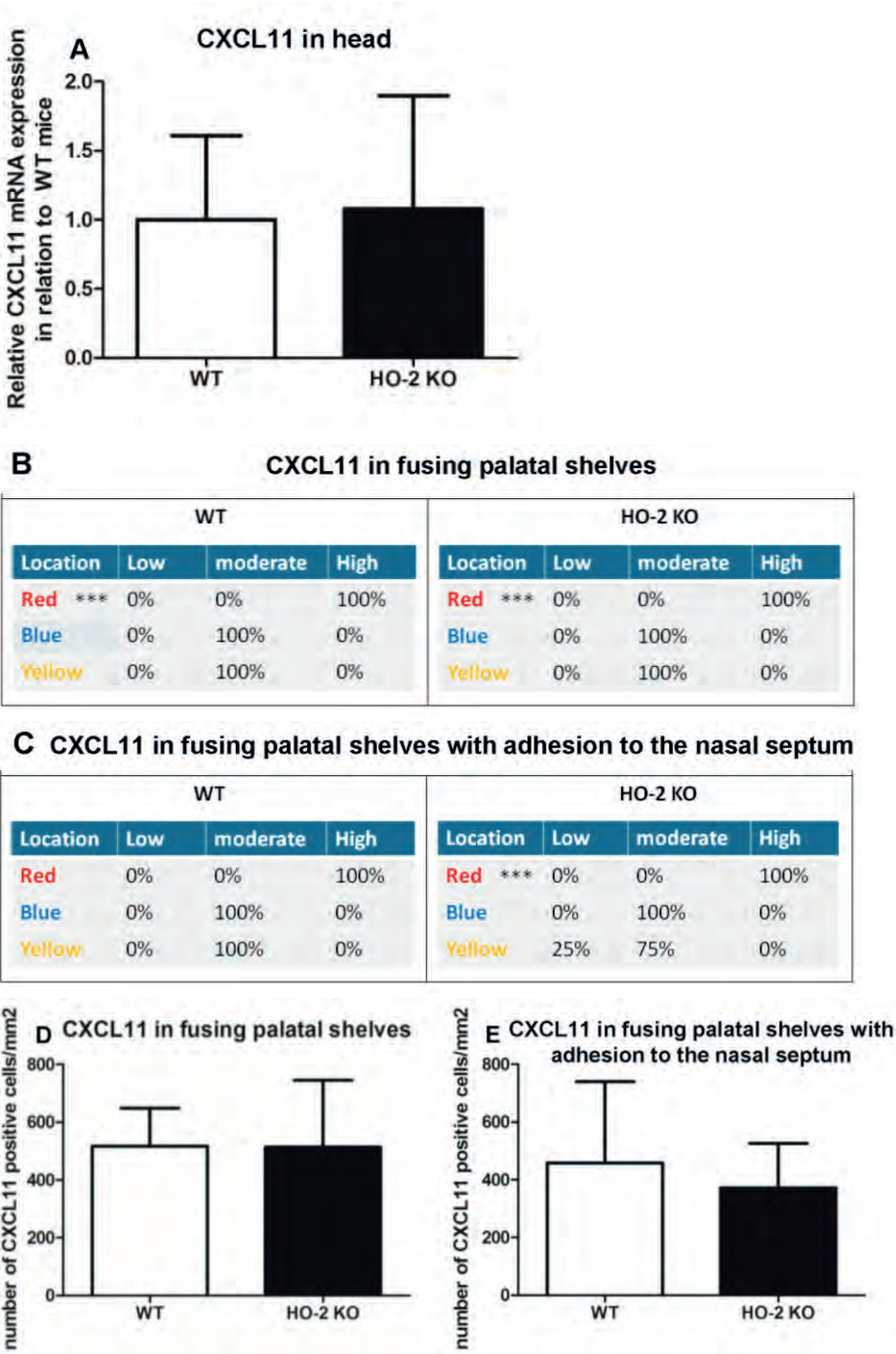
Figure 5: Fetal growth restriction and malformations occur in the absence of HO-2 expression. (A) HO-2 mRNA was not found in HO-2 KO fetuses. HO-2 mRNA was observed in wt fetuses E15 ($n=5$), but not in HO-2 KO fetuses E15 ($n=4$). Wt fetuses E15 ($n=15$), HO-2 KO fetuses E15 ($n=4$) and HO-2 KO fetuses E16 ($n=11$) were compared for (B) weight, (C) body surface and (D) length ($p=0.25$), (E) head/body surface ratio ($p=0.97$). Data present mean \pm SD. (*= $p<0.05$; **= $p<0.01$), (***)= $p<0.001$). (F) wt fetus at E15 (0,28g; 12,9mm). (G) HO-2 KO fetus at E15 (0,13g; 12,5mm). (H) HO-2 KO fetus at E16 (0,31g; 12,4mm). (I) HO-2 KO fetus at E16 demonstrating severe malformations (0,065g; 10mm). (J) HO-2 KO fetus at E16 demonstrating a craniofacial anomaly (0,20g, 12,2mm). (K) HO-2 KO fetus at E15 appeared to be the smallest fetus without anomalies (0,10g, 10,3mm).

Palatal fusion observed in both wt and HO-2 KO fetuses at E15

Though the HO-2 KO fetuses were smaller in size, no difference in the adhesion and fusion of the palatal shelves was observed between the sections from wt and HO-2 KO fetuses at E15. In 2 wt fetuses and 2 HO-2 KO fetuses at E15, the palatal shelves were not yet elevated. In both genotypes, different phases of palatogenesis were observed in histological sections from the same fetus. The MES changes from a multi-cell layer into a continuous single-cell layer, to a disintegrating MES, during which islands of epithelium are observed. For more details, see **Figure 2**.

CXCL11 expression in the MES and mesenchyme

Because CXCL11 plays an important role in wound repair, we investigated the mRNA expression of chemokine CXCL11 in fetal head samples. CXCL11 mRNA was observed in samples from both wt and HO-2 KO fetuses without reaching a significant difference between the two genotypes ($p=0.88$, **Figure 6**).



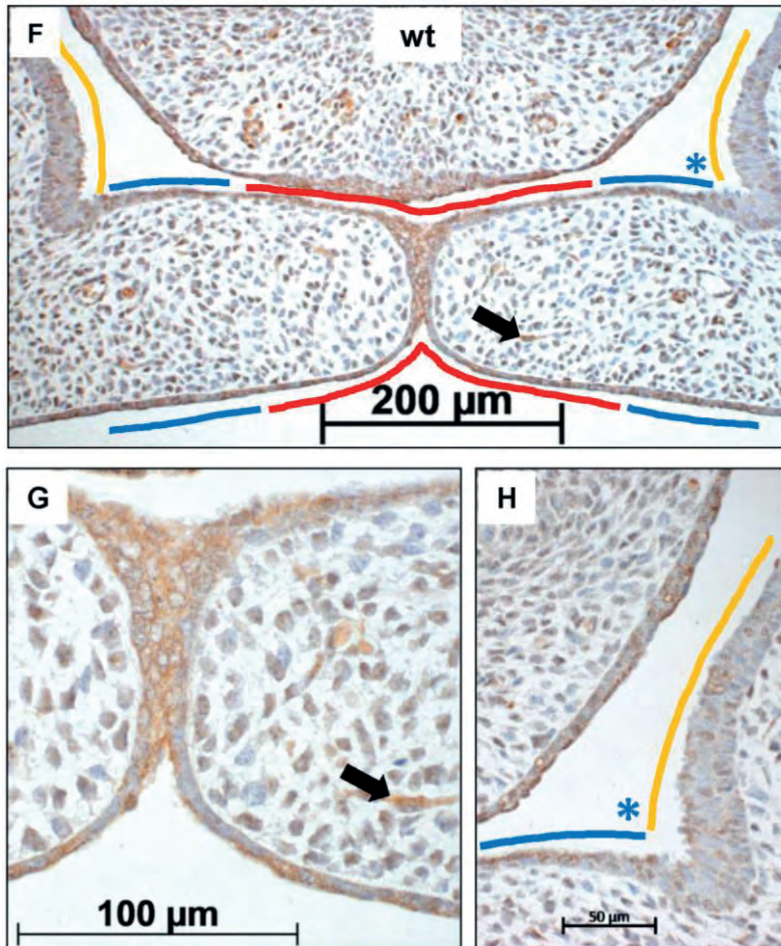


Figure 6: CXCL11 expression in the MES and mesenchyme in both wt and HO-2 KO fetuses. (A) CXCL11 mRNA expression was both present in wt ($n=5$) and in HO-2 KO E15 fetuses ($n=4$) ($p=0.88$). Data presented as mean \pm SD. CXCL11 overexpression in the MES in wt and HO-2 KO fetuses. Scoring was performed according to figure 3.3. (B) Significant higher CXCL11 expression was observed in the MES (in RED) (***) ($p<0.001$) compared to the other epithelial regions in the fusing palatal shelves (in BLUE) and the nasal cavity (in YELLOW) in the wt group and HO-2 KO group. (C) Significant higher CXCL11 expression was observed in the MES (in RED) (***) ($p<0.001$) compared to the BLUE region and YELLOW region in the HO-2 KO sections with fusing palatal shelves with adhesion to the nasal septum. (D) No significant difference in the number of CXCL11 positive cells/mm² in the mesenchyme of the fusing palatal shelves was found between the wt and HO-2 KO fetuses ($p=0.97$). Data presented as mean \pm SD. (E) No significant difference in the number of CXCL11 positive cells/mm² was found in the mesenchyme between the wt and HO-2 KO group in the sections with fusing palatal shelves with adhesion to the nasal septum ($p=0.97$). Data presented as mean \pm SD. (F) Representative CXCL11 immunostaining in fusing palatal shelves without adhesion to the nasal septum of a wt fetus (E15) (magnification: x100). The MES (in RED) was highly CXCL11 positive compared to the other epithelial regions; epithelium of the lateral half of the palatal shelves (in BLUE) and epithelium of the lateral wall of the nasal cavity (in YELLOW). (G) Several CXCL11 positive cells in the mesenchyme were observed (e.g., black arrow indicates a CXCL11 positive cell in the mesenchyme) (magnification: x400). This was found in both wt and HO-2 KO fetuses. (H) Moderate CXCL11 expression in the epithelium of the lateral half of the palatal shelf (in BLUE), and in the epithelium of the lateral wall of the nasal cavity (in YELLOW) (magnification: x400).

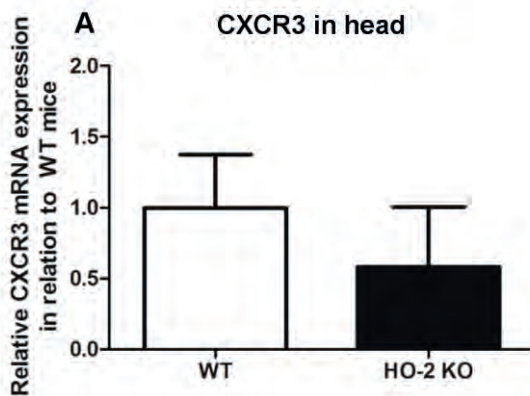
Next, we investigated the cellular expression of CXCL11 during palatal fusion. CXCL11 protein was significantly higher expressed in the epithelium of the MES compared to the other epithelial layers of the fusing palatal shelves and the epithelium of the nasal cavity in both wt ($p<0.001$) and HO-2 KO fetuses ($p<0.001$) (Figure 6B, C, F-H). No significant difference was found between the genotypes. High CXCL11 protein expression was also found within the epithelium of the tips of the palatal shelves lacking midline adhesion, in sections of both genotypes (data not shown). CXCL11-positive cells were also observed in the mesenchyme of the palatal shelves, but no significant difference in the number of CXCL11-positive cells/mm² was found between the wt and HO-2 KO groups ($p=0.97$, Figure 6D) or in the samples with fusing palatal shelves with adhesion to the nasal septum ($p=0.47$, Figure 6E).

CXCR3 expression in the MES and mesenchyme

Next, we investigated the expression of CXCL11 receptor CXCR3 at the mRNA level. In samples from heads of wt and HO-2 KO fetuses, CXCR3 mRNA expression was observed but with no significant difference between the groups ($p=0.16$, Figure 7).

CXCR3 protein expression was significantly higher in the epithelium of the MES than the other epithelial layers of the palatal shelves and the epithelium of the nasal cavity in the fusing palatal shelves of the wt fetuses ($p<0.05$, Figure 7B, F-H). Higher CXCR3 protein expression in the epithelium of the MES was also observed in the fusing palatal shelves with adhesion to the nasal septum from the HO-2 KO fetuses ($p<0.001$, Figure 7C).

Interestingly, CXCR3-positive cells were also observed in the mesenchyme of the palatal shelves. No significant difference in the number of CXCR3-positive cells/mm² was found between the wt and HO-2 KO groups in the fusing palatal shelves ($p=0.96$, Figure 7D) or the fusing palatal shelves with adhesion to the nasal septum ($p=0.20$, Figure 7E).



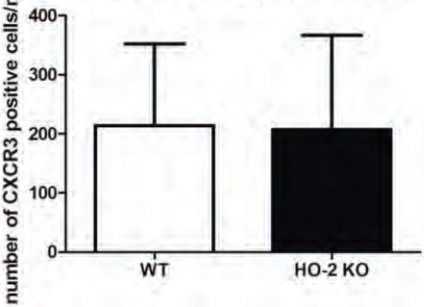
B CXCR3 in fusing palatal shelves

WT				HO-2 KO			
Location	Low	moderate	High	Location	Low	moderate	High
Red *	0%	0%	100%	Red	0%	0%	100%
Blue	0%	40%	60%	Blue	0%	100%	0%
Yellow	0%	100%	0%	Yellow	0%	100%	0%

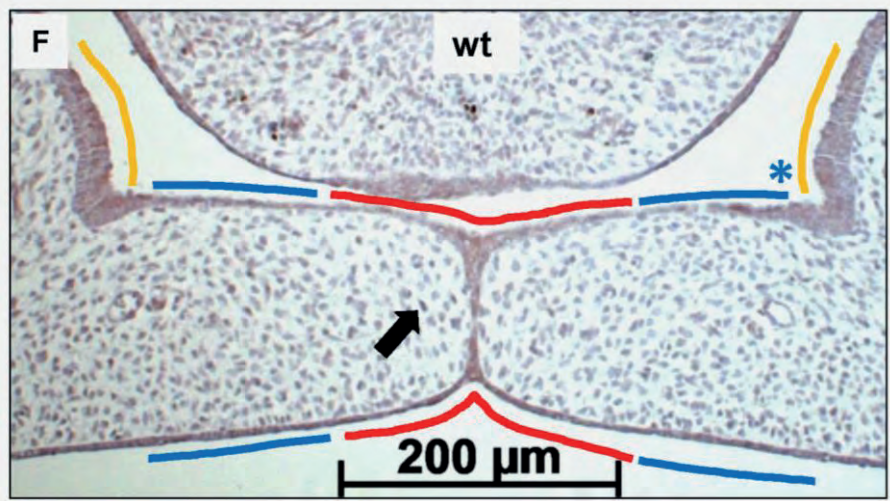
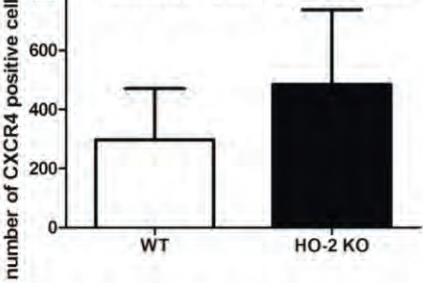
C CXCR3 in fusing palatal shelves with adhesion to the nasal septum

WT				HO-2 KO			
Location	Low	moderate	High	Location	Low	moderate	High
Red	0%	0%	100%	Red ***	0%	0%	100%
Blue	0%	75%	25%	Blue	0%	100%	0%
Yellow	0%	100%	0%	Yellow	0%	100%	0%

D CXCR3 in fusing palatal shelves



E CXCR3 in fusing palatal shelves with adhesion to the nasal septum



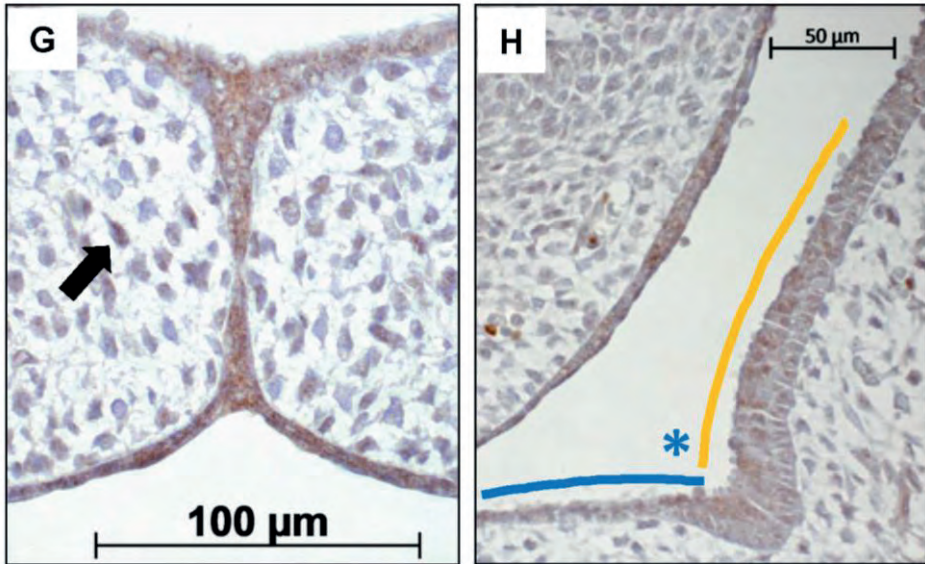


Figure 7: CXCR3 expression in the MES and mesenchyme in both wt and HO-2 KO fetuses. (A) CXCR3 mRNA expression was found in wt fetuses E15 ($n=5$) and in HO-2 KO fetuses E15 ($n=4$) ($p=0.16$). Data presented as mean \pm SD. (B) Statistically significant higher CXCR3 expression was observed in the wt group in the MES (in RED) ($*=p<0.05$) compared to the YELLOW region. (C) Significant higher CXCR3 expression was observed in the MES (in RED) ($***=p<0.001$) compared to the BLUE region and YELLOW region in the HO-2 KO sections with adhesion of the palatal shelves and adhesion to the nasal septum. (D) No significant difference in the number of CXCR3 positive cells/mm² in the mesenchyme of the fusing palatal shelves was found between the wt and HO-2 KO fetuses ($p=0.96$). Data presented as mean \pm SD. (E) No significant difference in the number of CXCR3 positive cells/mm² in the mesenchyme was found between the wt and HO-2 KO group of the sections with adhesion of the palatal shelves and adhesion to the nasal septum ($p=0.47$). Data presented as mean \pm SD. (F) Representative CXCR3 immunostaining of fusing palatal shelves without adhesion to the nasal septum of a wt fetus (E15) (magnification: $\times 100$). The MES (in RED) had higher CXCR3 expression compared to the other epithelial regions (in BLUE) and (in YELLOW). (G) Some CXCR3 positive cells in the mesenchyme were observed. This was found for the wt sections and HO-2 KO sections (black arrow indicates a CXCR3 positive cell in the mesenchyme) (magnification: $\times 400$). (H) Moderate CXCR3 expression in the epithelium of the lateral half of the palatal shelf (in BLUE), and in the epithelium of the lateral wall of the nasal cavity (in YELLOW) (magnification: $\times 400$).

CXCR3-positive macrophages were located near the MES and phagocytized apoptotic cell fragments of the MES

CXCR3-positive cells are suspected of being macrophages based on morphology and because macrophages have been shown to be positive for CXCR3^{35,36}. Therefore, we investigated whether CXCR3-positive macrophages are present within the fusing palate using immunofluorescence microscopy. F4/80-CXCR3 double-positive macrophages were observed in the fusing palatal shelves, with some located near the disintegrating MES, in both wt and HO-2 KO fetuses (Figure 8).

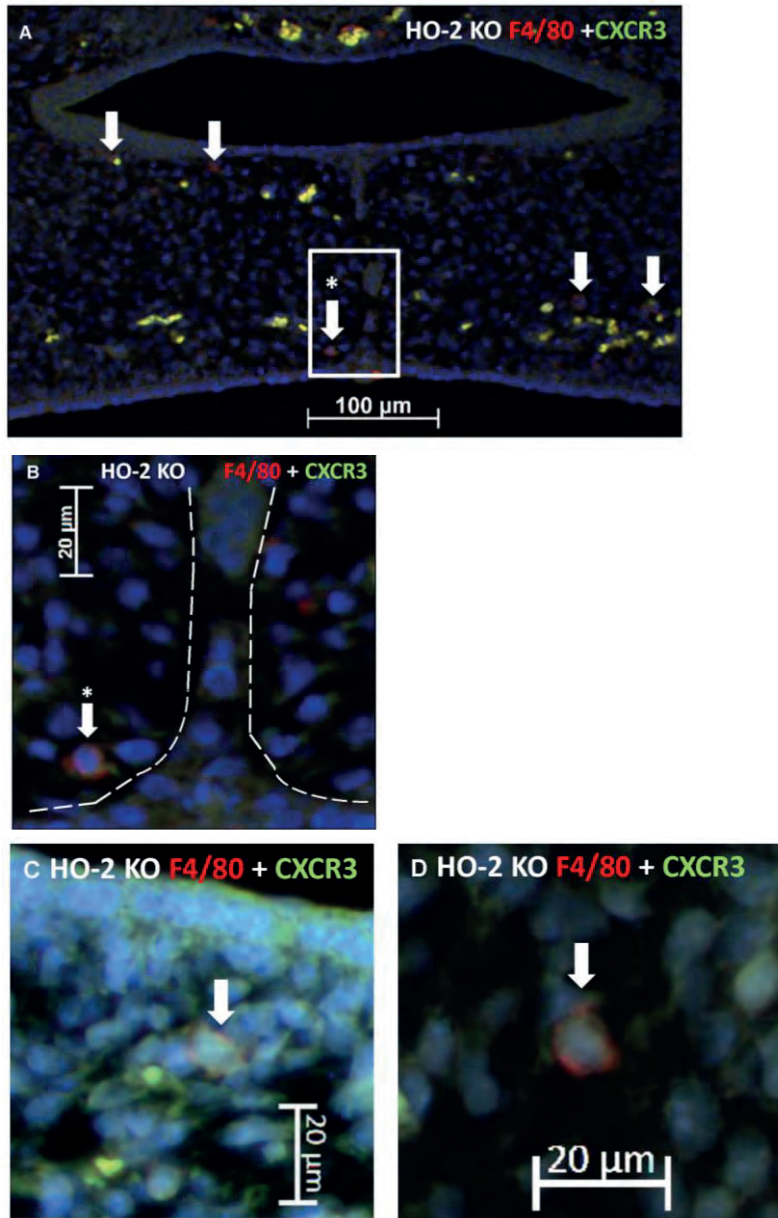
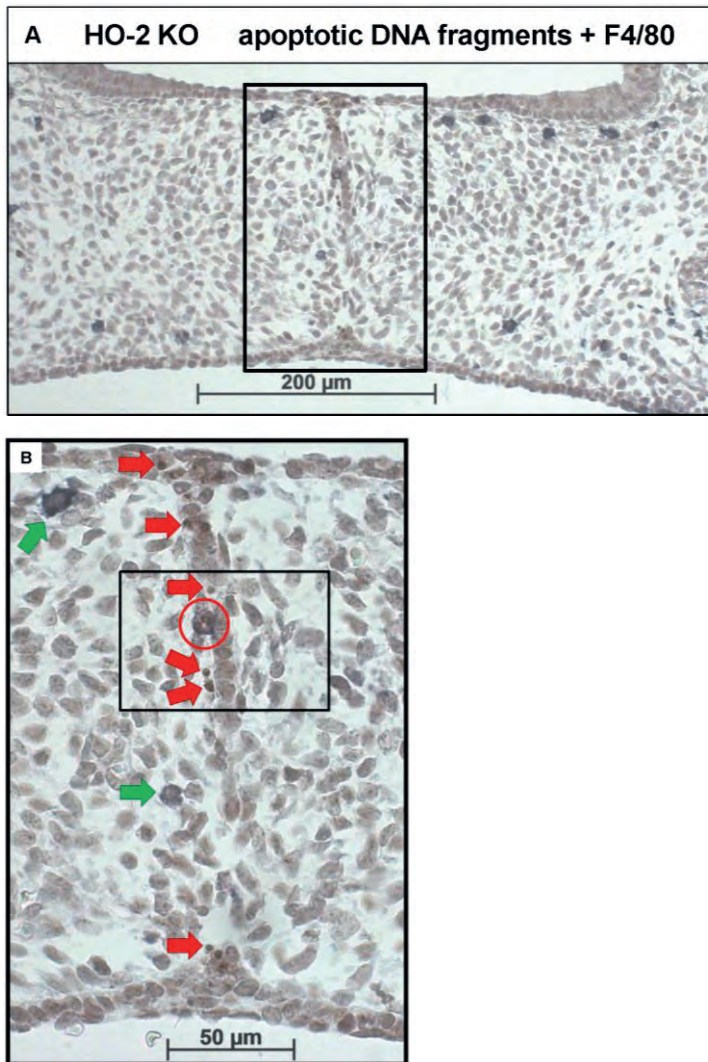


Figure 8: CXCR3-positive macrophages were located near the MES. (A) Representative immunofluorescent histochemical double staining for F4/80 (red) with CXCR3 (green) in HO-2 KO section (E16). Nuclear staining with DAPI (Blue). The mesenchyme demonstrates the presence of a F4/80-positive HO-2 KO macrophages, which also express CXCR3 (white arrows) (magnification: x200). One CXCR3 F4/80-positive HO-2 KO macrophage was located near the disintegrating MES (white arrow within the white square). (B) Magnification of a F4/80-positive HO-2 KO macrophage located near the MES (area between the dotted white lines) (magnification: x400). (C) Magnification of a F4/80-positive HO-2 KO macrophage located in the mesenchyme of the palate shelf (magnification: x400). (D) Magnification of a F4/80-positive HO-2 KO macrophage located outside the palatal shelf (magnification: x400).

In both wt and HO-2 KO fetuses, multiple apoptotic DNA fragments were present in the epithelial cells of the disintegrating MES. No apoptotic cell fragments were observed in the other epithelial regions. To assess whether the recruited macrophages phagocytose these apoptotic cell fragments, we stained for both apoptotic fragments and macrophages (FragEL™ DNA fragmentation assay in combination with F4/80). Macrophages located near the MES did phagocytose apoptotic DNA fragments (**Figure 9A-C**). Other macrophages were observed in the mesenchyme closely localized near the apoptotic DNA fragments within the disintegrating MES (**Figure 9B**).



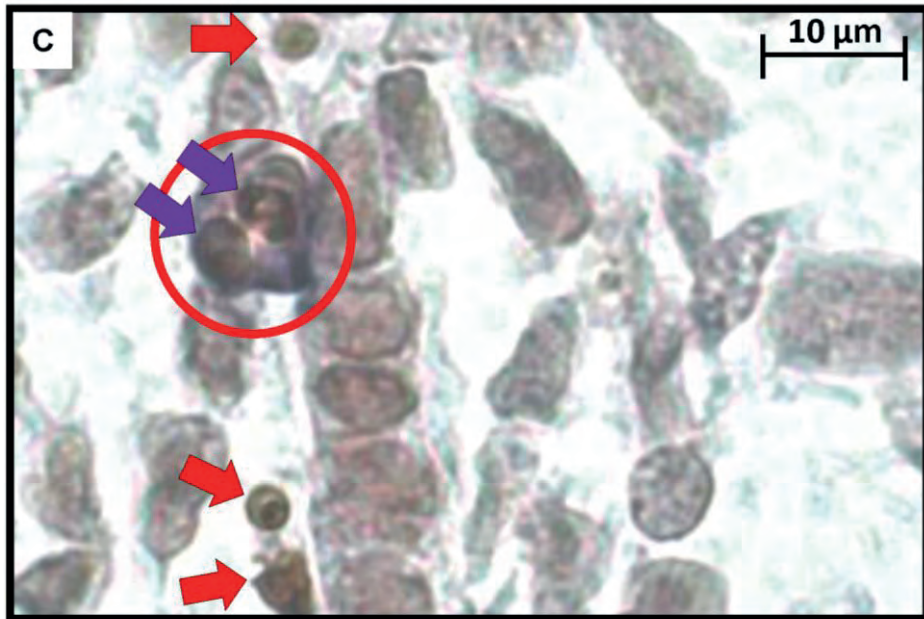
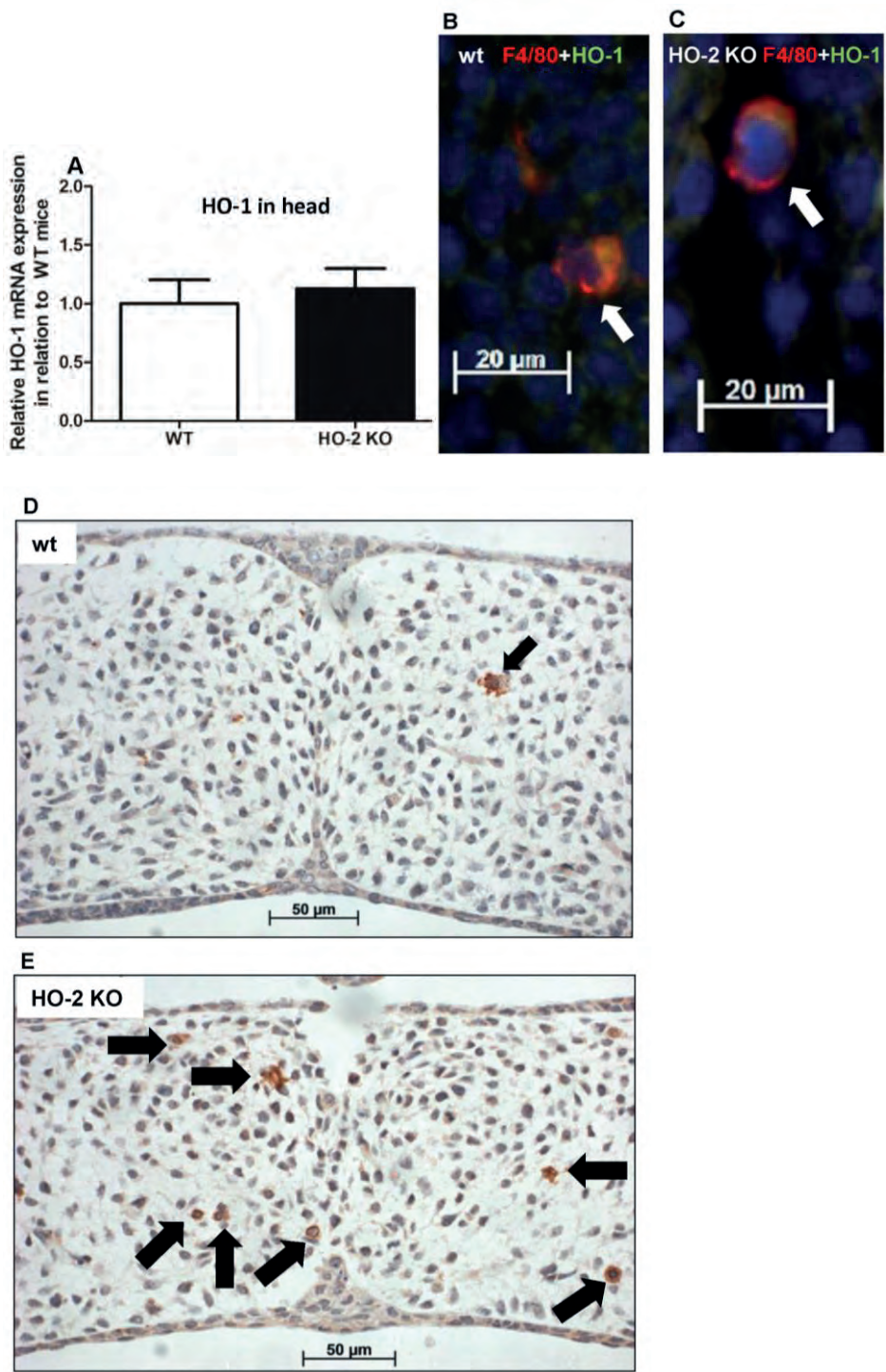


Figure 9: Macrophages located near the MES phagocytose apoptotic cell fragments. (A) Representative FragEL™ DNA fragmentation assay (brown) in combination with F4/80 (dark blue) macrophage staining. Fusing palatal shelves in a HO-2 KO fetus (E16) (magnification: x100). Multiple macrophages were observed in the mesenchyme of the palatal shelves. **(B)** Magnification of the disintegrating MES (magnification: x400, black square). Multiple apoptotic DNA fragments are observed within the MES (Red arrows). The only apoptotic DNA fragments in the palatum outside the MES are in macrophages that had taken up epithelial cells. Two macrophages were located near the MES (green arrows), one macrophage was in close contact with the MES (red circle). **(C)** Magnification of the macrophage in close contact with the MES (black square). In this macrophage (red circle), two apoptotic cell fragments within its cell body are present (purple arrows). Apoptotic DNA fragments near the macrophage were observed (red arrows). These findings were representative for both wt and HO-2 KO sections.

More HO-1-positive cells are found in palatal shelves from HO-2 KO fetuses

As macrophages can express the cytoprotective enzyme HO-1 during the digestion of cellular debris^{49,50}, we studied whether HO-1-positive macrophages are present within the fusing palate.

HO-1 mRNA was observed in samples from the heads of both wt and HO-2 KO fetuses without reaching a significant difference between the two genotypes ($p=0.35$, **Figure 10A**). Double immunostaining for macrophage marker F4/80 and HO-1 showed that many F4/80-positive macrophages were positive for HO-1. F4/80 and HO-1-positive cells were observed in the fusing palatal shelves and near the disintegrating MES in both wt and HO-2 KO fetuses (**Figure 10B, C**).



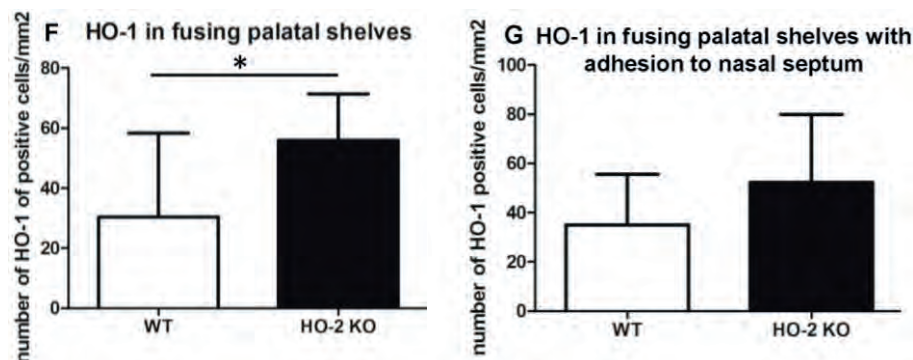


Figure 10: More HO-1-positive cells are found in palatal shelves from HO-2 KO fetuses. (A) HO-1 mRNA expression was similar in wt fetuses E15 ($n=5$) and in HO-2 KO fetuses E15 ($n=4$) ($p=0.35$). Data presented as mean \pm SD. (B) Representative fluorescent immunohistochemical double staining for F4/80 and HO-1 of fusing palatal shelves with adhesion to the nasal septum of a wt fetus (E15) (magnification: x400). A part of the mesenchyme around the MES, showing a F4/80-positive macrophage (red) expressing HO-1 (green) located near the MES (white arrow). Nuclear staining with DAPI (Blue). (C) Representative fluorescent immunohistochemical double staining for F4/80 with HO-1 of fusing palatal shelves with adhesion to the nasal septum of a HO-2 KO fetus (E16) (magnification: x400). A F4/80-positive HO-2 KO macrophage (red) expressing HO-1 (green) located near the MES (white arrow). Nuclear staining with DAPI (Blue). (D) Representative HO-1 immunostaining of palatal shelves of a wt fetus (E15) (magnification: x400). This part of the mesenchyme demonstrates the presence of one HO-1 positive cell (black arrow). (E) Representative HO-1 immunostaining of fusing palatal shelves of a HO-2 KO fetus (E16) (magnification: x400). This part of the mesenchyme demonstrates the presence of seven HO-1-positive cells (black arrows). (F) Significant higher numbers of HO-1-positive cells/mm² were observed in the HO-2 KO fetuses compared to the wt fetuses in the fusing palatal shelves ($p=0.02$). Data presented as mean \pm SD. (G) Numbers of HO-1-positive cells/mm² in the mesenchyme of wt and HO-2 KO fetuses in the fusing palatal shelves with adhesion to the nasal septum ($p=0.60$). Data presented as mean \pm SD.

The number of HO-1-positive cells in the mesenchyme of the fusing palatal shelves was significantly higher in the HO-2 KO group than in the wt group ($p=0.02$, **Figure 10D-G**). Almost no HO-1 expression was observed in the epithelium of the palatal shelves in the wt and HO-2 KO groups.

Discussion

Although deletion of HO-2 expression in mice leads to fetal growth restriction, severe malformations, and craniofacial anomalies, we found no evidence of disruption of palatal fusion in HO-2 KO fetuses. We showed that multiple apoptotic DNA fragments were exclusively present in the MES of both genotypes, supporting earlier findings that apoptosis of epithelial cells drives MES disintegration⁸. We demonstrated that both CXCR3 and its ligand, the chemokine CXCL11, were highly expressed by epithelial cells in the MES, suggesting that chemokine signaling acts via an autocrine loop to initiate processes involved in its own disintegration. Although, probably also other downstream mechanisms play a role in this process, such as enzymes, like caspases, and apoptotic DNA fragments. We demonstrated that apoptotic DNA fragments from the MES were phagocytized by both wt and HO-2 KO macrophages. It is likely that CXCR3-positive

macrophages were recruited via CXCL11 expression by the MES (**Figure 11**). However, we cannot exclude that additionally, other mechanisms can in a later phase facilitate macrophage recruitment. For example, apoptotic nucleotide fragments derived from the MES have been demonstrated to promote macrophage contributed to this recruitment⁵¹. Macrophages near the disintegrating MES were positive for HO-1 in both wt and HO-2 KO fetuses, but more HO-1-positive cells were found in the palatal mesenchyme from HO-2 KO fetuses. Although HO-2 KO macrophages have been shown to be dysfunctional in a mouse corneal epithelial debridement model³⁸, HO-2 KO macrophages phagocytosis of apoptotic DNA fragments still function, possibly with help of HO-1 overexpression.

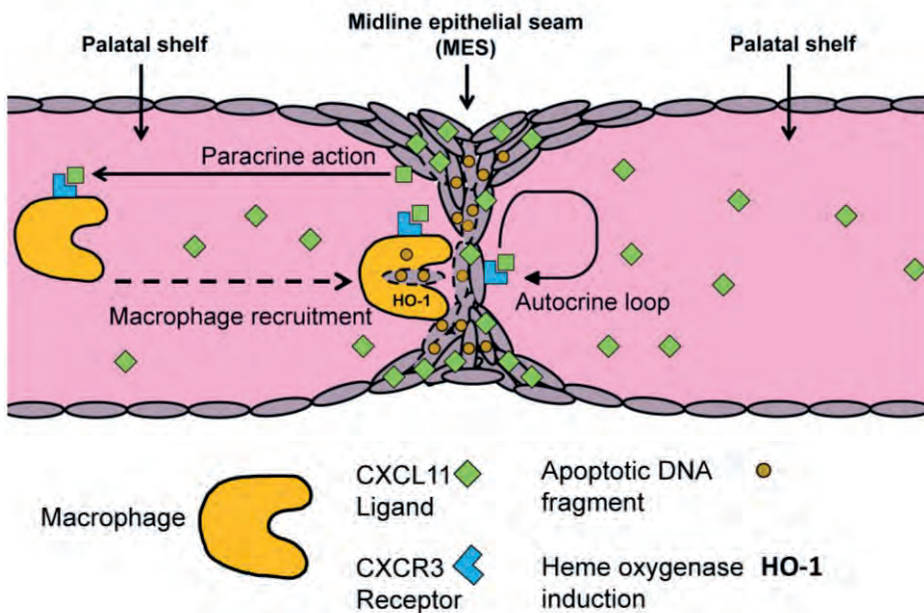


Figure 11: MES mediated chemokine signaling facilitates MES disintegration and palatal fusion.

Conceptual model: Autocrine and paracrine MES signaling facilitates palatal fusion. CXCL11/CXCR3 autocrine signaling controls migration and/or apoptosis of epithelial cells during disintegration of the MES. CXCL11-CXCR3 paracrine signaling recruits macrophages to clean up the MESs. HO-2 KO macrophages are still able to phagocytize apoptotic DNA fragments from the MES due to induction of HO-1.

Adult HO-2-deficient mice are morphologically indistinguishable from wt mice⁴², but only full-grown mice have been studied thus far. To the best of our knowledge, this is the first study of HO-2 KO embryonic development. Down-regulation of HO-2 is associated with spontaneous abortion in humans¹⁸. We did not find that the absence of HO-2 expression resulted in an increased fetal loss rate or decreased implantation rate in mice. However, non-viable and hemorrhagic embryonic implantations were frequently observed in both genotypes. Homozygote HO-2 KO mice were recently demonstrated to be viable³⁷, though they demonstrated delayed wound

repair^{37,52} and an exaggerated inflammatory response after corneal epithelial wounding⁵³. Fetal growth retardation is associated with down-regulation of HO-2 in human pathologic pregnancies¹⁸, which is in line with our findings that HO-2 deletion leads to a developmental growth delay at E15 of approximately 1 day. Among the HO-2 KO fetuses, one was severely malformed and another presented a head anomaly, but no anomalies or malformations were found in wt fetuses.

Environmental factors, such as maternal diabetes, oxidative stress, and infections can have a disturbing influence on palatal fusion and lead to clefting of the lip and palate¹⁶. HO-2 is essential for regulating physiological levels of reactive oxygen species (ROS)^{54,55}. Although we found growth restriction and morphological anomalies in HO-2 KO fetuses, proper fusion of the palatal shelves was observed. In the absence of additional stresses, HO-2 KO fetuses can thus develop into mice with a normal palate, possibly due to compensation by elevated HO-1 expression. Next, we studied palatogenesis in HO-2 KO mice in more detail.

We demonstrated increased expression of chemokine CXCL11 and its receptor CXCR3 within the disintegrating MES in both genotypes. CXCR3-CXCL11 signaling serves as a coordinator in wound repair^{56,57} and is involved in the process of re-epithelialization and epidermis maturation³⁷. In keratinocytes, CXCR3 signaling activated μ -calpain to loosen the adhesions for migration²⁹. Scars in CXCR3 KO mice exhibited hyperkeratosis and hypercellularity³⁰, features that are also observed in hypertrophic scar formation in humans⁵⁶. CXCR3 plays a key role in coordinating the switch from regeneration of the epithelial compartment towards maturation⁵⁸ and modulates cell proliferation and apoptosis^{59,60}. In the disintegrating MES CXCL11-CXCR3 signaling is therefore likely involved in controlling processes, such as migration and apoptosis of epithelial cells.

We found many apoptotic DNA fragments throughout the disintegrating MES, supporting apoptosis as a driving mechanism in MES disintegration⁷⁻¹⁰. No apoptotic DNA fragments were found in the other epithelial regions of the palatal shelves or the mesenchyme of the palatal shelves. Blocking cell death with z-VAD, an inhibitor of caspases, leads to persistence of the MES structure, which interferes with fusion of the palatal shelves *in vitro*⁶¹, suggesting that this could lead to cleft palate. However, a role of epithelial migration in MES disintegration cannot be excluded.

In addition to CXCR3 expression in the epithelial MES layer, we also demonstrated CXCR3 expression in the mesenchyme of the fusing palatal shelves. We found CXCR3-positive and phagocytosing macrophages near the disintegrating MES, suggesting that macrophages are actively recruited by CXCL11. This demonstrates that the MES actively participates in its disintegration via chemokine signaling. However, we cannot exclude that also other mechanisms play a role, such as caspases, other enzymes and enzyme inhibitors. Recruitment of CXCR3-positive macrophages by CXCL11 paracrine signaling was demonstrated previously also in other models^{35,36}.

Although HO-2 deletion impaired macrophage function in corneal epithelial wound repair³⁸, in our study both wt and HO-2 KO macrophages phagocytosed apoptotic DNA fragments and, thus, were still functional. Although impairment of macrophage function by HO-2 deletion was found in a wound repair study in adult mice³⁸, we studied macrophage function in a non-pathological environment during embryonic development. However, our findings contradict another wound healing study, demonstrating that HO-2 deletion was associated with impaired HO-1 induction⁵². Significantly more HO-1-positive cells were found in the palatal mesenchyme of HO-2 KO fetuses compared to wt fetuses, in which HO-1-positive cells were scarce. We suggest that the higher HO-1 expression during embryonic development is a compensating mechanism for HO-2 deletion in recruited macrophages in the fusing palatal shelves. An increased HO-1 induction could explain in part the discrepancy in function between HO-2 KO macrophages in adult and embryonic mice.

A limitation of the present study was the relatively small number of fetuses. However, among the 23 HO-2 KO fetuses, one demonstrated severe malformations and another viable fetus had a craniofacial anomaly, suggesting that HO-2 supports fetal growth and development.

In conclusion, we determined that HO-2 deletion leads to fetal growth restriction and craniofacial anomalies. In contrast to our hypothesis, no disturbance was observed in palatal fusion in HO-2 KO fetuses. However, CXCL11 and CXCR3 were highly expressed in the disintegrating MES in both wt and HO-2 KO animals. Both wt and HO-2 KO CXCR3-positive macrophages were functional since apoptotic cells from the disintegrating MES were phagocytosed. Increased numbers of HO-1-positive cells were found within the mesenchyme of the fusing palatal shelves of the HO-2 KO fetuses. It is tempting to speculate that HO-2 deletion leads to up-regulation of HO-1 expression in macrophages, protecting them from oxidative stress following ingestion of apoptotic epithelial fragments from the disintegrating MES. Our data supports the hypothesis that chemokine signaling by the MES orchestrates its disintegrating by epithelial apoptosis and macrophage recruitment via CXCL11-CXCR3 signaling. However, also alternative pathways may have contributed to these processes. Further research is needed to investigate whether hampered palatal fusion can be the result of disrupted chemokine signaling and whether reduced protection against oxidative and inflammatory stresses promote craniofacial malformations.

References

1. Ackermans MM, Zhou H, Carels CE, Wagener FA, Von den Hoff JW. Vitamin A and clefting: putative biological mechanisms. *Nutr Rev.* 2011;69(10):613-624.
2. Dudas M, Kim J, Li WY, et al. Epithelial and ectomesenchymal role of the type I TGF-beta receptor ALK5 during facial morphogenesis and palatal fusion. *Dev Biol.* 2006;296(2):298-314.
3. Iseki S. Disintegration of the medial epithelial seam: is cell death important in palatogenesis? *Dev Growth Differ.* 2011;53(2):259-268.
4. Gritli-Linde A. Molecular control of secondary palate development. *Dev Biol.* 2007;301(2):309-326.
5. Jin JZ, Ding J. Analysis of cell migration, transdifferentiation and apoptosis during mouse secondary palate fusion. *Development.* 2006;133(17):3341-3347.
6. Nawshad A. Palatal seam disintegration: to die or not to die? that is no longer the question. *Dev Dyn.* 2008;237(10):2643-2656.
7. Vukojevic K, Kero D, Novakovic J, Kalibovic Govorko D, Saraga-Babic M. Cell proliferation and apoptosis in the fusion of human primary and secondary palates. *Eur J Oral Sci.* 2012;120(4):283-291.
8. Lan Y, Xu J, Jiang R. Cellular and Molecular Mechanisms of Palatogenesis. *Curr Top Dev Biol.* 2015;115:59-84.
9. Xu X, Han J, Ito Y, Bringas P, Jr., Urata MM, Chai Y. Cell autonomous requirement for Tgfb2 in the disappearance of medial edge epithelium during palatal fusion. *Dev Biol.* 2006;297(1):238-248.
10. Vaziri Sani F, Hallberg K, Harfe BD, McMahon AP, Linde A, Gritli-Linde A. Fate-mapping of the epithelial seam during palatal fusion rules out epithelial-mesenchymal transformation. *Dev Biol.* 2005;285(2):490-495.
11. Brown NL, Sandy JR. Tails of the unexpected: palatal medial edge epithelium is no more specialized than other embryonic epithelium. *Orthod Craniofac Res.* 2007;10(1):22-35.
12. Burg ML, Chai Y, Yao CA, Magee W, 3rd, Figueiredo JC. Epidemiology, Etiology, and Treatment of Isolated Cleft Palate. *Front Physiol.* 2016;7:67.
13. Mossey PA, Little J, Munger RG, Dixon MJ, Shaw WC. Cleft lip and palate. *Lancet (London, England).* 2009;374(9703):1773-1785.
14. Watkins SE, Meyer RE, Strauss RP, Aylsworth AS. Classification, epidemiology, and genetics of orofacial clefts. *Clin Plast Surg.* 2014;41(2):149-163.
15. Drew SJ. Clefting syndromes. *Atlas Oral Maxillofac Surg Clin North Am.* 2014;22(2):175-181.
16. Brocardo PS, Gil-Mohapel J, Christie BR. The role of oxidative stress in fetal alcohol spectrum disorders. *Brain Res Rev.* 2011;67(1-2):209-225.
17. Zencclussen ML, Casalis PA, El-Mousleh T, et al. Haem oxygenase-1 dictates intrauterine fetal survival in mice via carbon monoxide. *J Pathol.* 2011;225(2):293-304.
18. Zencclussen AC, Lim E, Knoeller S, et al. Heme oxygenases in pregnancy II: HO-2 is downregulated in human pathologic pregnancies. *Am J Reprod Immunol.* 2003;50(1):66-76.
19. Zencclussen ML, Linzke N, Schumacher A, et al. Heme oxygenase-1 is critically involved in placentation, spiral artery remodeling, and blood pressure regulation during murine pregnancy. *Front Pharmacol.* 2014;5:291.
20. Wagener FA, Eggert A, Boerman OC, et al. Heme is a potent inducer of inflammation in mice and is counteracted by heme oxygenase. *Blood.* 2001;98(6):1802-1811.
21. Wagener FA, Abraham NG, van Kooyk Y, de Witte T, Figdor CG. Heme-induced cell adhesion in the pathogenesis of sickle-cell disease and inflammation. *Trends Pharmacol Sci.* 2001;22(2):52-54.
22. Wagener FA, Volk HD, Willis D, et al. Different faces of the heme-heme oxygenase system in inflammation. *Pharmacol Rev.* 2003;55(3):551-571.
23. Grochot-Przeczek A, Dulak J, Jozkowicz A. Haem oxygenase-1: non-canonical roles in physiology and pathology. *Clin Sci (Lond).* 2012;122(3):93-103.
24. Ewing JF, Maines MD. Regulation and expression of heme oxygenase enzymes in aged-rat brain: age related depression in HO-1 and HO-2 expression and altered stress-response. *J Neural Transm (Vienna).* 2006;113(4):439-454.
25. Shi J, Mei W, Yang J. Heme metabolism enzymes are dynamically expressed during *Xenopus* embryonic development. *Biozell.* 2008;32(3):259-263.
26. Bellner L, Martinelli L, Halilovic A, et al. Heme oxygenase-2 deletion causes endothelial cell activation marked by oxidative stress, inflammation, and angiogenesis. *J Pharmacol Exp Ther.* 2009;331(3):925-932.

27. Sollwedel A, Bertoja AZ, Zenclussen ML, et al. Protection from abortion by heme oxygenase-1 up-regulation is associated with increased levels of Bag-1 and neuropilin-1 at the fetal-maternal interface. *J Immunol.* 2005;175(8):4875-4885.
28. Biggs LC, Goudy SL, Dunnwald M. Palatogenesis and cutaneous repair: A two-headed coin. *Developmental dynamics : an official publication of the American Association of Anatomists.* 2015;244(3):289-310.
29. Satish L, Blair HC, Glading A, Wells A. Interferon-inducible protein 9 (CXCL11)-induced cell motility in keratinocytes requires calcium flux-dependent activation of mu-calpain. *Mol Cell Biol.* 2005;25(5):1922-1941.
30. Yates CC, Krishna P, Whaley D, Bodnar R, Turner T, Wells A. Lack of CXC chemokine receptor 3 signaling leads to hypertrophic and hypercellular scarring. *Am J Pathol.* 2010;176(4):1743-1755.
31. Epelman S, Lavine KJ, Randolph GJ. Origin and functions of tissue macrophages. *Immunity.* 2014;41(1):21-35.
32. Epelman S, Liu PP, Mann DL. Role of innate and adaptive immune mechanisms in cardiac injury and repair. *Nat Rev Immunol.* 2015;15(2):117-129.
33. Roszer T. Understanding the Mysterious M2 Macrophage through Activation Markers and Effector Mechanisms. *Mediators Inflamm.* 2015;2015:816460.
34. Mass E, Ballesteros I, Farlik M, et al. Specification of tissue-resident macrophages during organogenesis. *Science.* 2016;353(6304).
35. Kakuta Y, Okumi M, Miyagawa S, et al. Blocking of CCR5 and CXCR3 suppresses the infiltration of macrophages in acute renal allograft rejection. *Transplantation.* 2012;93(1):24-31.
36. Torraca V, Cui C, Boland R, et al. The CXCR3-CXCL11 signaling axis mediates macrophage recruitment and dissemination of mycobacterial infection. *Dis Model Mech.* 2015;8(3):253-269.
37. Lundvig DM, Scharstuhl A, Cremers NA, et al. Delayed cutaneous wound closure in HO-2 deficient mice despite normal HO-1 expression. *J Cell Mol Med.* 2014;18(12):2488-2498.
38. Bellner L, Marrazzo G, van Rooijen N, Dunn MW, Abraham NG, Schwartzman ML. Heme oxygenase-2 deletion impairs macrophage function: implication in wound healing. *FASEB J.* 2015;29(1):105-115.
39. Kaplan AP. Chemokines, chemokine receptors and allergy. *Int Arch Allergy Immunol.* 2001;124(4):423-431.
40. Van Raemdonck K, Van den Steen PE, Liekens S, Van Damme J, Struyf S. CXCR3 ligands in disease and therapy. *Cytokine Growth Factor Rev.* 2015;26(3):311-327.
41. Balaji S, Watson CL, Ranjan R, King A, Bollyky PL, Keswani SG. Chemokine Involvement in Fetal and Adult Wound Healing. *Advances in wound care.* 2015;4(11):660-672.
42. Poss KD, Thomas MJ, Ebralidze AK, O'Dell TJ, Tonegawa S. Hippocampal long-term potentiation is normal in heme oxygenase-2 mutant mice. *Neuron.* 1995;15(4):867-873.
43. Behringer R, Gertsenstein M, Nagy KV, Nagy A. Selecting Female Mice in Estrus and Checking Plugs. *Cold Spring Harb Protoc.* 2016;2016(8):pdb prot092387.
44. Dudas M, Li WY, Kim J, Yang A, Kaartinen V. Palatal fusion - where do the midline cells go? A review on cleft palate, a major human birth defect. *Acta Histochem.* 2007;109(1):1-14.
45. Livak KJ, Schmittgen TD. Analysis of relative gene expression data using real-time quantitative PCR and the 2(-Delta Delta C(T)) Method. *Methods.* 2001;25(4):402-408.
46. Tan SD, Xie R, Klein-Nulend J, et al. Orthodontic force stimulates eNOS and iNOS in rat osteocytes. *J Dent Res.* 2009;88(3):255-260.
47. Siemieniuch MJ. Apoptotic changes in the epithelium germinativum of the cat (*Felis catus* s. domestica, L. 1758) at different ages and breeding seasons. *Reprod Domest Anim.* 2008;43(4):473-476.
48. Lin HH, Faunce DE, Stacey M, et al. The macrophage F4/80 receptor is required for the induction of antigen-specific efferent regulatory T cells in peripheral tolerance. *J Exp Med.* 2005;201(10):1615-1625.
49. Shibahara S, Yoshida T, Kikuchi G. Mechanism of increase of heme oxygenase activity induced by hemin in cultured pig alveolar macrophages. *Arch Biochem Biophys.* 1979;197(2):607-617.
50. Okinaga S, Takahashi K, Takeda K, et al. Regulation of human heme oxygenase-1 gene expression under thermal stress. *Blood.* 1996;87(12):5074-5084.
51. Elliott MR, Chekeni FB, Trampont PC, et al. Nucleotides released by apoptotic cells act as a find-me signal to promote phagocytic clearance. *Nature.* 2009;461(7261):282-286.

52. Seta F, Bellner L, Rezzani R, et al. Heme oxygenase-2 is a critical determinant for execution of an acute inflammatory and reparative response. *Am J Pathol.* 2006;169(5):1612-1623.
53. Bellner L, Wolstein J, Patil KA, Dunn MW, Laniado-Schwartzman M. Biliverdin Rescues the HO-2 Null Mouse Phenotype of Unresolved Chronic Inflammation Following Corneal Epithelial Injury. *Invest Ophthalmol Vis Sci.* 2011;52(6):3246-3253.
54. Burgess AP, Vanella L, Bellner L, et al. Heme oxygenase (HO-1) rescue of adipocyte dysfunction in HO-2 deficient mice via recruitment of epoxyeicosatrienoic acids (EETs) and adiponectin. *Cell Physiol Biochem.* 2012;29(1-2):99-110.
55. He JZ, Ho JJ, Gingerich S, Courtman DW, Marsden PA, Ward ME. Enhanced translation of heme oxygenase-2 preserves human endothelial cell viability during hypoxia. *J Biol Chem.* 2010;285(13):9452-9461.
56. Huen AC, Wells A. The Beginning of the End: CXCR3 Signaling in Late-Stage Wound Healing. *Adv Wound Care (New Rochelle).* 2012;1(6):244-248.
57. Kroeze KL, Boink MA, Sampat-Sardjoepersad SC, Waaijman T, Scheper RJ, Gibbs S. Autocrine regulation of re-epithelialization after wounding by chemokine receptors CCR1, CCR10, CXCR1, CXCR2, and CXCR3. *J Invest Dermatol.* 2012;132(1):216-225.
58. Yates CC, Whaley D, A YC, Kulesekaran P, Hebda PA, Wells A. ELR-negative CXC chemokine CXCL11 (IP-9/I-TAC) facilitates dermal and epidermal maturation during wound repair. *Am J Pathol.* 2008;173(3):643-652.
59. Ma B, Khazali A, Wells A. CXCR3 in carcinoma progression. *Histol Histopathol.* 2015;30(7):781-792.
60. Fulton AM. The chemokine receptors CXCR4 and CXCR3 in cancer. *Curr Oncol Rep.* 2009;11(2):125-131.
61. Cuervo R, Covarrubias L. Death is the major fate of medial edge epithelial cells and the cause of basal lamina degradation during palatogenesis. *Development.* 2004;131(1):15-24.

Chemokine signaling during midline epithelial seam disintegration facilitates palatal fusion.

CHAPTER 3

CXCL12-CXCR4 interplay facilitates palatal osteogenesis in mice

Verheijen N, **Suttorp CM**, van Rheden REM, Regan RF, Helmich MPAC, Kuijpers-Jagtman AM, Wagener FADTG.

Front Cell Dev Biol. 2020 Aug 21;8:771.

Abstract

Cranial neural crest cells (CNCCs), identified by expression of transcription factor Sox9, migrate to the first branchial arch and undergo proliferation and differentiation to form the cartilage and bone structures of the orofacial region, including the palatal bone. Sox9 promotes osteogenic differentiation and stimulates CXCL12-CXCR4 chemokine-receptor signaling, which elevates alkaline phosphatase (ALP)-activity in osteoblasts to initiate bone mineralization. Disintegration of the midline epithelial seam (MES) is crucial for palatal fusion. Since we earlier demonstrated chemokine-receptor mediated signaling by the MES, we hypothesized that chemokine CXCL12 is expressed by the disintegrating MES to promote the formation of an osteogenic center by CXCR4-positive osteoblasts. Disturbed migration of CNCCs by excess oxidative and inflammatory stress is associated with increased risk of cleft lip and palate (CLP). The cytoprotective heme oxygenase (HO) enzymes are powerful guardians harnessing injurious oxidative and inflammatory stressors and enhances osteogenic ALP-activity. By contrast, abrogation of HO-1 or HO-2 expression promotes pregnancy pathologies. We postulate that Sox9, CXCR4, and HO-1 are expressed in the ALP-activity positive osteogenic regions within the CNCCs-derived palatal mesenchyme. To investigate these hypotheses, we studied expression of Sox9, CXCL12, CXCR4, and HO-1 in relation to palatal osteogenesis between E15 and E16 using (immuno)histochemical staining of coronal palatal sections in wild-type (wt) mice. In addition, the effects of abrogated HO-2 expression in HO-2 KO mice and inhibited HO-1 and HO-2 activity by administering HO-enzyme activity inhibitor SnMP at E11 in wt mice were investigated at E15 or E16 following palatal fusion. Overexpression of Sox9, CXCL12, CXCR4, and HO-1 was detected in the ALP-activity positive osteogenic regions within the palatal mesenchyme. Overexpression of Sox9 and CXCL12 by the disintegrating MES was detected. Neither palatal fusion nor MES disintegration seemed affected by either HO-2 abrogation or inhibition of HO-activity. Sox9 progenitors seem important to maintain the CXCR4-positive osteoblast pool to drive osteogenesis. Sox9 expression may facilitate MES disintegration and palatal fusion by promoting epithelial-to-mesenchymal transformation (EMT). CXCL12 expression by the MES and the palatal mesenchyme may promote osteogenic differentiation to create osteogenic centers. This study provides novel evidence that CXCL12-CXCR4 interplay facilitates palatal osteogenesis and palatal fusion in mice.

Keywords: embryology, cranial neural crest cells, Sox9, osteogenesis, palatogenesis, CXCL12-CXCR4, pathological pregnancy, heme oxygenase.

Abbreviations

ABC	Avidin-biotin peroxidase complex
ANOVA	Analysis of variance
AP-2a	Activating Protein 2a
BMP2	Bone morphogenetic protein 2
BMP6	Bone morphogenetic protein 6
ALP	Alkaline phosphatase
CLP	Cleft lip and palate
CO	Carbon monoxide
CNCCs	Cranial neural crest cells
CXCL12	Chemokine (C-X-C) ligand 12
CXCR4	Chemokine (C-X-C) receptor 4
DAB	Diaminobenzidine-peroxidase
DABCO	1, 4-Diazobicyclo-(2,2,2-octane
DPX	Distyrene plasticizer xylene
E0	Gestational/Embryonic day 0
EMT	Epithelial-to-mesenchymal transformation
HE	Haematoxylin and eosin
HO	Heme oxygenase
I.p.	Intraperitoneal
KO	Knockout
KS-test	Kolmogorov-Smirnov test
LPS	Lipopolysaccharide
MES	Midline epithelial seam
NDS	Normal donkey serum
PBSG	Phosphate-buffered saline with glycine
ROS	Reactive oxygen species
SD	Standard deviation
SnMP	Tin mesoporphyrin
Sox9	SRY-Box Transcription Factor 9
Wt	Wild-type

Introduction

In the process of craniofacial development, cranial neural crest cells (CNCCs) migrate from the lateral ridges of the neural plate to the first branchial arch to form the orofacial region, including the maxilla, mandible, zygoma, trigeminal nerve, and muscles of mastication¹⁻³. CNCCs have to migrate and undergo proliferation and differentiation to form the dentin and pulp of the teeth, connective tissues, cartilage, and bone of the head⁴⁻⁶. In animal studies, CNCCs populating the pharyngeal arches are characterized by expression of transcription factor Sox9^{2,7-10}. In addition, Sox9 acts as a key transcription factor that is required for both early and late stages of osteogenic¹¹⁻¹⁴ and chondrogenic differentiation¹⁴⁻²⁰. To initiate bone formation, CNCCs were found to form aggregated cell masses in the orofacial mesenchyme¹. In mice fetuses, Sox9 expression has been observed in the osteogenic cell compartments in the craniofacial bones between E12-E16¹¹. CXCL12-CXCR4 chemokine-receptor signaling drives both osteogenic and chondrogenic differentiation²¹. CXCL12-CXCR4 signaling mediates both immature and mature murine osteoblast development^{22,23}. Moreover, CXCL12-CXCR4 signaling promotes Sox9-mediated chondrogenesis in synovium derived stem cells²⁴, whilst blocking CXCL12-CXCR4 signaling inhibits chondrogenic differentiation *in vitro*¹⁸. However, Sox9 knockout (KO) mice show reduced CXCR4 expression in the kidney²⁵.

CXCL12-CXCR4 signaling regulates osteoblast formation by promoting alkaline phosphatase (ALP)-activity in human^{26,27}, and murine osteoblasts²⁸ *in vitro*. ALP-activity is often used as a marker of osteoblastic development²⁹, and ALP KO mice demonstrate defects in bone mineralization³⁰. Mesenchymal stem cells exposed to osteogenic medium with CXCL12 demonstrated higher ALP-activity, supporting a role for CXCL12 in osteogenic differentiation *in vitro*³¹.

Since Sox9 expression was observed in the palatal shelves in mice fetuses at E12.5, E13.5³², E14.5^{32,33}, and E15³⁴, migrating CNCCs are thought to contribute to the embryonic formation of the palate, named palatogenesis^{32,34}. Palatogenesis is an important event during craniofacial development of higher vertebrates³⁵. Our basic understanding of palatal morphogenesis comes principally from research conducted in mice. Palatogenesis occurs during the intrauterine weeks 8–12 in humans and during embryonic days E12–E15.5 in mice³⁶. Palatogenesis involves the vertically downward outgrowth of the paired palatal shelves from the maxillary region, elevation above the tongue (E14.5-E15), horizontal growth and adherence, formation of the midline epithelial seam (MES), and eventually disintegration of the MES, allowing complete palatal fusion (E15.5)³⁶⁻³⁸. Cranial neural crest-derived mesenchymal cells have to undergo osteogenic differentiation to form the hard palate³⁹. In mice, CNCCs form aggregated cell masses to initiate palatal bone formation in the palatal mesenchyme in mice between E14.5 and E16.5^{1,40}. In cultured mouse palatal shelves, inhibition of

osteoblast differentiation by treatment with 10 mM lithium chloride prevented palatal fusion⁴¹.

Since CXCL12-CXCR4 expression was found to promote bone formation^{22,23} and ALP-activity³¹, we postulate that both CXCL12 and CXCR4 are expressed within the palatal mesenchyme to facilitate palatal osteogenesis. Transcription factor Sox9 may promote CXCL12-CXCR4 signaling to initiate ALP-activity, facilitating osteoblast and chondrocyte formation within the CNCCs derived mesenchyme, starting osteogenesis in the developing orofacial region.

MES disintegration is crucial for palatal fusion⁴². The main hypotheses underlying MES disintegration during palatal fusion involve epithelial cell migration to the oral^{43,44} or nasal epithelium^{43,45} epithelial-to-mesenchymal transformation (EMT)⁴⁶⁻⁴⁸, epithelial cell apoptosis^{49,50}, or a combination of these events⁴². We previously demonstrated that the MES highly expresses chemokine CXCL11, suggesting its involvement in recruiting CXCR3-positive macrophages to facilitate phagocytosis of apoptotic cells of the disintegrating MES during palatal fusion⁵⁰. Notably, palatal bone formation in mice starts at E14.5^{1,40}, simultaneously with MES disintegration³⁶⁻³⁸. Therefore, we postulate that the MES might also express other chemokines involved in other pathways, such as CXCL12, to promote maturation of immature CXCR4-positive osteoblasts and ALP-activity to start palatal osteogenesis.

Disturbed migration of CNCCs to the orofacial region can lead to craniofacial abnormalities⁵¹. Exposure to reactive oxygen species (ROS), generated by diabetes, infections, or social poisons, including maternal smoking, alcohol consumption, and exposure to teratogens, was found to harm fetal growth and development and could even lead to craniofacial anomalies in rats⁵², zebrafish^{53,54}, and humans⁵⁵⁻⁶⁰. ROS can contribute to the etiology of congenital malformations by disrupting migration of CNCCs to the orofacial region⁶¹. In chick embryo, ROS production generated by caffeine exposure was found to disturb CNCC migration, leading to asymmetrical microphthalmia and abnormal orbital bone development⁶².

During palatogenesis, failure of elevation, horizontal growth, adherence of the palatal shelves, or disruption of MES formation and MES disintegration results in cleft palate⁴⁸. Palatal clefting can be caused by disturbed migration of CNCCs to the orofacial region⁵¹. In humans, disruption of CNCC migration to the oral region can lead to cleft lip and palate (CLP)¹ and Pierre Robin sequence, a congenital craniofacial anomaly characterized by mandibular micrognathia, glossoptosis, and cleft palate^{63,64}.

A combination of genetic and environmental factors is thought to play a role in the etiology of orofacial clefting⁶⁵⁻⁶⁷. Mice lacking transcription factor Activating Protein 2a (AP-2a) show hampered CNCC migration resulting in congenital anomalies, including cleft palate⁶⁸. Repression of CNCC proliferation by inhibiting the transcription factor family Zeb prevents fusion between cultured mice palatal shelves *in vitro*⁶⁹. Failure of palatal bone formation between E14.5 and E16.5 in mice is associated with

cleft palate⁴⁰. Maternal smoking⁷⁰, alcohol consumption⁷¹, and diabetes⁷², associated with oxidative and inflammatory stress⁷³⁻⁷⁵, were found to increase the risk at babies with CLP. Gestational treatment with nicotine inhibited palatal fusion by persistence of the MES in mice fetuses^{76,77}. In pregnant CL/Fr mice, having an incidence of spontaneous CLP of 35–40% in the offspring, exposure to hypoxia at E11 doubled the incidence of CLP at E18, indicating that a combination of genetic susceptibility and oxidative stress can result in CLP⁷⁸.

The heme oxygenase (HO) enzyme system protects against oxidative and inflammatory stress by degrading the prooxidant heme, thereby generating free iron/ferritin, carbon monoxide (CO), and the antioxidants biliverdin/bilirubin⁷⁹⁻⁸¹. These HO-effector molecules regulate vasodilation, inhibit platelet aggregation, suppress leukocyte adhesion, and reduce pro-inflammatory cytokine release⁸⁰. The HO-system consists of two functional isoforms; HO-1 has low basal levels but is strongly inducible, whereas HO-2 is constitutively expressed⁸². Downregulation of HO-1⁸³ and HO-2⁸⁴ in human placenta is associated with spontaneous abortion, pre-eclampsia, and fetal growth retardation. HO-2 KO mice demonstrated fetal growth restriction, severe malformations, craniofacial anomalies⁵⁰, and elevated endothelial inflammatory and angiogenic factors⁸⁵. HO-1 KO mice demonstrated a high prenatal mortality, with survivors showing growth retardation, organ fibrosis, and inflammatory tissue damage⁸⁶. Others found that HO-1 KO mice are highly susceptible to ischemia, reperfusion injury, and right ventricular infarction^{87,88}. Induction of HO-1 decreased ROS levels in obese diabetic mice⁸⁹. Interestingly, HO-1 expression promoted ALP-activity in the process of differentiation of osteoblast stem cells of human⁹⁰⁻⁹³, mouse⁹⁴, and rat into osteoblasts⁹⁵. In human periodontal ligament cells, induction of HO-1 leads to upregulation of osteogenic differentiation *in vitro*⁹⁶. However, blocking of HO-activity has therapeutically been used in preterm infants since administration of SnMP, a competitive inhibitor of HO-1 and HO-2, attenuates the development of hyperbilirubinemia⁹⁷.

We postulate that Sox9, CXCR4, and HO-1 are expressed in the ALP-activity positive osteogenic regions within the CNCCs derived mesenchyme during palatal fusion in mice. Furthermore, we hypothesize that chemokine CXCL12 is expressed by the disintegrating MES to promote the formation of an osteogenic center by CXCR4-positive osteoblasts. In addition, we expect that increased levels of oxidative and inflammatory stress in HO-2 KO mice, and further increase of these stress levels, obtained by administration of HO-1 and HO-2 activity inhibitor SnMP at E11 in wt mice disrupts the migration of CNCCs to the orofacial region, increasing the risk of cleft palate.

In the present study, expression of Sox9, CXCL12, CXCR4, and HO-1 was studied in relation to MES disintegration at E15 and palatal osteogenesis between E15 and E16 marked by ALP-activity, in wild-type (wt) mice using (immuno)histochemical staining of

coronal palatal sections. Additionally, the effects of absence of HO-2 in HO-2 KO mice, or inhibition of HO-1 and HO-2 activity using SnMP from E11 in wt mice on palatal bone formation at E15 and E16, was investigated.

Materials and Methods

Mice selection and mating

Because HO-1 KO mice demonstrated severe pregnancy complications with a fetal loss rate of more than 85%⁹⁸, and HO-2 mice demonstrated to be viable⁹⁹, the HO-2 mouse model was considered more suitable to collect fetuses for this study. Homozygote HO-2 KO mice were generated by targeted disruption of the HO-2 gene with mixed 129Sv x C57BL/6 background^{85,100}. By quantitative realtime PCR, we previously confirmed the genotypes of mice by showing that HO-2 mRNA was only present in samples from wt fetuses, and not in HO-2 KO fetuses⁵⁰. The wt mice strain with mixed 129Sv x C57BL/6 background were used to obtain fetuses for the control group. Both the wt (n = 7) and HO-2 KO mice (n = 7) of 8 weeks old were bred and maintained in our animal facility. Female wt mice were mated with wt males, and female HO-2 KO mice were mated with HO-2 KO males. The next morning the mice were checked for the presence of a vaginal copulation plug, taken as day 0 of pregnancy (gestational/embryonic day 0; E0)¹⁰¹. Preliminary experiments (Ethical permission # RU-DEC 2009-160) demonstrated that both wt and HO-2 KO animals with mixed 129Sv x C57BL/6 background often did not carry fetuses. The hormones Folligonon (Gonadotropin serum, Intervet Nederland BV, Boxmeer, Netherlands) and Pregnyl (Human chorionic gonadotropin, NV Organon, Oss, Netherlands) were used to enhance the chance of pregnancy. At day -3 at 16.00 h Folligonon (6E in 30 ml) and at day -1 at 16.00 h Pregnyl (6E in 30 ml) was administered by intraperitoneal (i.p.) injection. At first, 1 wt mouse and two HO-2 KO mice demonstrated no plugged status. These animals were mated again 4 weeks later, and all demonstrated a plugged status the next morning.

Female CD1 mice of 12–17 weeks old (n = 11) were mated with male mice from the same strain at the animal facility of the animal suppliers Envigo (Venray, Netherlands). The plugged CD1 mice were transported to our animal facility and could acclimatize for at least 1 week before the start of the experiment. Absence of HO expression (both isoforms HO-1 and HO-2) was found to severely affect embryonic implantation⁹⁸. SnMP can bind to the enzymes HO-1 and HO-2, but cannot be broken down by both isotypes, acting as a competitive inhibitor of the HO system¹⁰². Instead of heme (iron protoporphyrin IX dichloride), SnMP (Sn mesoporphyrin IX dichloride) consists of a protoporphyrin IX ring with tin in its center¹⁰³. SnMP was purchased from Frontier Scientific (Carnforth, United Kingdom). SnMP was freshly dissolved with Trizma base. The pH was adjusted to pH 7.6–8.0 with HCl, and further diluted till 10 mL with H₂O. The SnMP solution was filter sterilized before administration. To study palatal

fusion in the absence of HO-1 and HO-2 activity (later referred to as HO-activity), pharmacological blocking of HO-activity in CD1 wt mice was obtained by administration of SnMP at the start of palatogenesis at E11.

Sample size, housing, ethical permission

To detect an effect size of 0.40 (generalized estimation of the reduction in fetal body weight following HO-2 abrogation/HO-activity inhibition) with power of 0.80 and a significance level of 0.05 for the four groups (wt E15, HO-2 KO E15, wt CD1 E16, and wt CD1 SnMP E16) a total sample size of $n = 76$ fetuses for this study was calculated by the one-way ANOVA power analysis *a priori* (G*Power 3.1 software)¹⁰⁴. This indicated that the mean sample size per group should comprise approximately 19 fetuses. We estimated that the litter size could range from 8 to 18 fetuses, suggesting that each group should contain three pregnant mice. The chance of conception was assumed to be around 70%, indicating that for each group at least five mice should be mated.

The animals of both models were housed under specific pathogen-free housing conditions with 12 h light/dark cycle and ad libitum access to water and powdered rodent chow.

Ethical permission for the study was obtained according to the guidelines of the Board for Animal Experiments of the Radboud University Nijmegen (Ethical permission # RU-DEC 2012-166).

Studying chemokine expression by the MES in the presence or absence of HO-activity

To be able to study chemokine expression by the MES, fetuses should be studied before the palatal shelves are completely fused. In wt mice the palatal shelves fuse between E14.5 and E15.5. In this period, the MES disintegrates, allowing the formation of mesenchymal confluence³⁶. Therefore, fetuses of E15 were suitable to study chemokine expression by the disintegrating MES. In the absence of HO-2 expression chemokine expression by the MES was examined in HO-2 KO fetuses of E15 (later referred to as HO-2 KO E15). The E15 wt fetuses served as controls (later referred to as wt E15).

Studying palatal fusion in the presence or absence of HO-activity

To investigate palatal clefting, fetuses should be studied beyond the time point of palatal fusion. Since the epithelium of the palatal shelves loses its capacity to fuse at E16, the absence of palatal fusion at E16 is diagnosed as palatal clefting³⁶. Therefore, fetuses of E16 were suitable to study palatal fusion. In the absence of HO-activity, obtained by SnMP administration, palatal fusion was examined in wt CD1 fetuses of E16 (later referred to as wt CD1 SnMP E16). In the control group, no SnMP was administered (later referred to as wt CD1 E16). All CD1 mice were randomly assigned to the wt CD1 E16 or wt CD1 SnMP E16 group.

Isolation of mice fetuses

The plugged animals of both models were sacrificed by CO₂/O₂ inhalation for 10 min, and the uteri and fetuses were isolated and photographed (see **Figure 1**). The wt and HO-2 KO mice were sacrificed at E15. Only three out of seven plugged wt mice, and four out of seven plugged HO-2 KO mice carried fetuses. In total, 16 wt E15 fetuses and 11 HO-2 KO E15 fetuses were obtained. The CD1 wt mice, the controls, and SnMP administered mice, were sacrificed at E16. In total of six out of six plugged wt mice of the control group, and four out of five plugged wt mice of the SnMP group carried fetuses. In total, 91 wt CD1 E16 fetuses and 56 wt CD1 SnMP E16 fetuses were obtained.

Fetal loss rate calculation

For the fetus-carrying mice of both models, the fetal loss rate, the percentage of non-viable and hemorrhagic embryonic implantations to the total number of embryonic implantations (non-viable or hemorrhagic embryonic implantations+fetuses) was calculated.

Fetal body weight

To study the effects of the absence of HO-2 expression on fetal growth wt E15 fetuses ($n = 15$) and HO-2 KO E15 fetuses ($n = 4$) were weighed. Unfortunately, when the isolation of the uterus was performed for the first time, we weighed the fetuses in their amniotic sacs together with their placentas. During preparation we noticed that in some cases the amniotic fluid was partially leaked away caused by a perforation of the amniotic membrane, making this method unreliable. Subsequently, it was decided to perform the weighing of the fetuses separately from their amniotic sacs and placentas. Therefore, the weight of 1 wt E15 and 7 HO-2 KO E15 fetuses was not collected. To study the effects of HO-activity inhibition on fetal growth the wt CD1 E16 fetuses ($n = 91$) and wt CD1 SnMP E16 fetuses ($n = 56$) were weighed.

Paraffin embedding and section cutting of head samples

Fetuses were decapitated and the head samples were fixed for 24 h in 4% paraformaldehyde and further processed for routine paraffin embedding. Serial coronal sections through the secondary palate region of 5- μ m thickness were mounted on Superfrost Plus slides (Menzel-Gläser, Braunschweig, Germany). The paraffin sections were deparaffinized using Histosafe (Adamas Instrumenten B.V., Rhenen, Netherlands) and rehydrated using an alcohol range (100%–90%–80%–70%–35%–0%) for further (immuno)histochemistry.

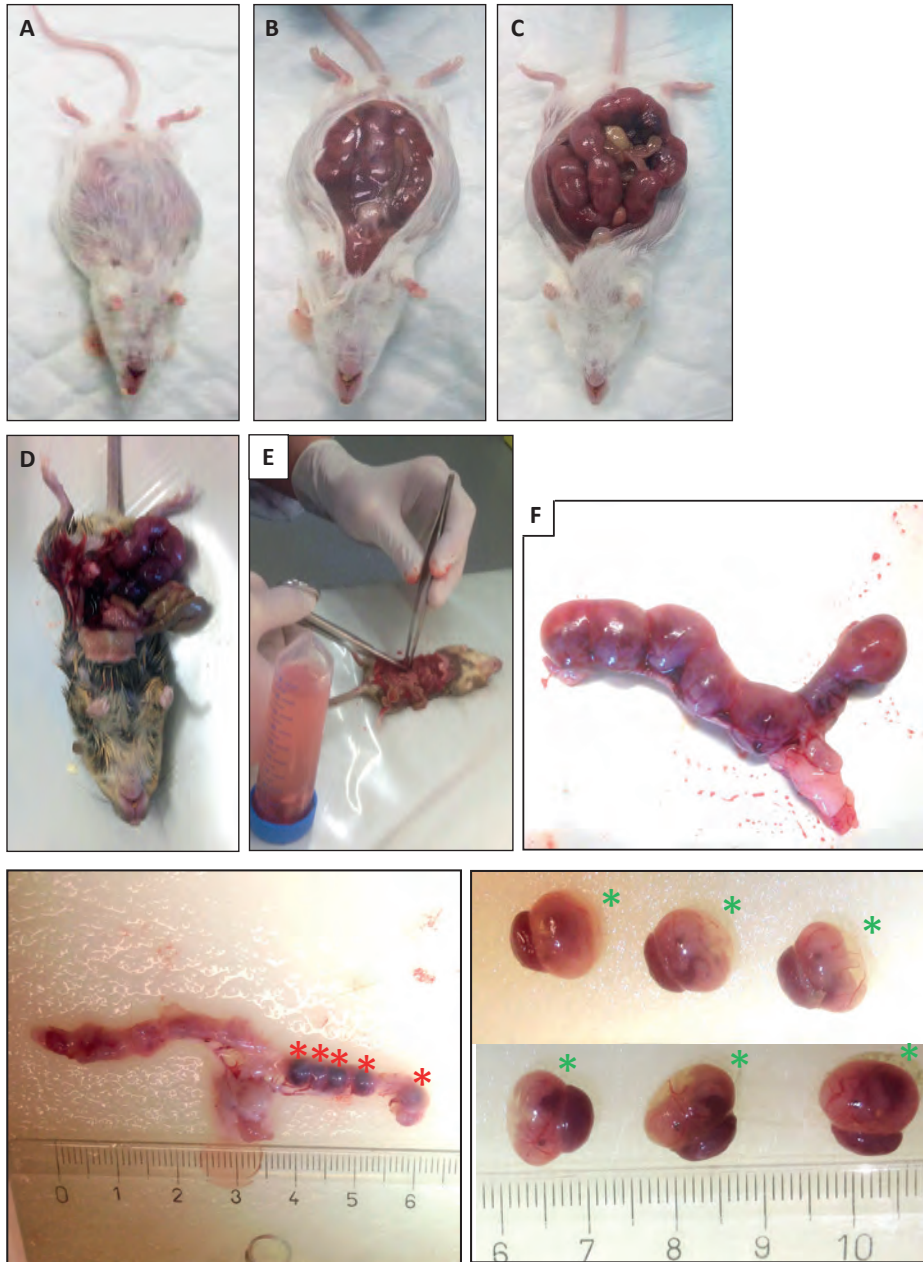


Figure 1: Isolation of the uteri and mice fetuses. After sacrifice of the plugged mice the uteri were isolated: (A) wt E15 mouse. (B) wt E15 mouse, (C) wt CD1 SnMP E16 mouse, (D,E) HO-2 KO E15 mouse. (F) Isolation of the fetuses from the uterus of a HO-2 KO E15 mouse. Uterus containing 6 fetuses (green asterisks) in total. **Lower left panel:** After removal of the fetuses five resorptions (red asterisks) were found (centimeter ruler). **Lower right panel:** Overview of the six isolated fetuses with placenta (green asterisks).

Palatogenesis classification of HE-stained palatal sections

Serial coronal palatal sections from the wt E15, HO-2 KO E15, wt CD1 E16 and wt CD1 SnMP E16 fetuses were routinely stained with hematoxylin and eosin (HE). Because the palate is not fused in once, the four stages according to Dudas et al. (2007)³⁶ and Suttorp et al. (2017)⁵⁰ can all be present on the same embryonic day. Therefore, the sections were classified into the four stages of palatogenesis based on the anatomy of the secondary palatal shelves: elevation, horizontal growth, midline adhesion, and fusion. Per individual fetus palatogenesis was studied on multiple sections. A minimum of five sections from five to seven head samples per group were assayed. Microscopic photographs were taken using a Carl Zeiss Imager Z.1 system (Carl Zeiss Microimaging GmbH, Jena, Germany) with AxioVision (4.8 v) software (Zeiss, Göttingen, Germany). HE series from the wt E15 and HO-2 KO fetuses were used as reference to obtain coronal palatal sections containing the MES for (immuno)histochemical staining. HE series from the wt CD1 E16 and wt CD1 SnMP E16 fetuses were used as reference to obtain coronal palatal sections containing the middle region of the fusing palatal shelves for (immuno)histochemistry.

Palatal osteogenesis identification by ALP-activity

ALP-activity is often used as a marker of osteoblastic development²⁹. In the coronal palatal sections, increased expression of ALP-activity was found to indicate enhanced differentiation of mesenchymal stem cells into osteoblasts^{105,106}. Therefore, in this study ALP-positive stained regions were judged sites of initiated osteogenic differentiation. Paraffin embedded sections were selected from the wt E15, HO-2 KO E15, wt CD1 E16, and wt CD1 SnMP E16 fetuses. The sections were rinsed in demineralized water. Then, the sections were incubated for 60 min with TRIS buffer at 37°C, followed by incubation with Medium Alkaline Phosphatase at 37°C for half an hour. After rinsing with demineralized water, the sections were counterstained by Na-acetate buffer 0.1M pH 5.1, continued with 0.1% Methyl green in Na-acetate buffer with pH 5.1. The sections were briefly rinsed before mounting in Kaiser's gelatin. Microscopic photographs of the ALP-stained palatal sections were taken.

Immunofluorescence staining for Sox9, CXCR4, and HO-1 expression in the palate

For the Sox9 immunofluorescence staining, paraffin-embedded coronal palatal sections from the wt E15 and HO-2 KO E15 fetuses containing a complete or partial MES were selected. For the CXCR4 and HO-1, and the double-staining Sox9-CXCR4 and Sox9-HO-1 paraffin embedded sections from the wt E15, HO-2 KO E15, wt CD1 E16, and wt CD1 SnMP E16 fetuses were selected. Antigens were retrieved with citrate buffer at 70°C for 10 min, following by incubation in 0.015% trypsin in PBS at 35°C for 5 min. Next, the sections were pre-incubated with 10% normal donkey serum (NDS) in phosphate-buffered saline with glycine (PBSG). First, antibodies were applied overnight, see **Table**

1, after rinsing, followed by the secondary antibodies, see **Table 1**, for 1 h. For the double-staining, the second first antibodies were also applied overnight. Nuclear staining was performed with DAPI. The sections were mounted with a glycerol based mounting medium containing 1, 4-Diazobicyclo-(2,2,2-octane (DABCO). Microscopic photographs of the immunofluorescence-stained sections were taken.

Table 1. First and secondary antibodies used for CXCL12, Sox9, CXCR4, and HO-1 immunohistochemical staining.

First Antibody	Specificity	Concentration (µg/mL)	Source	
14-7992-81	CXCL12	10	Affymetrix eBioscience, San Diego, CA, United States	
Sc 17340	Sox9	0,33	Santa Cruz via Bio-Connect, Santa Cruz, CA, United States	
PA3-305	CXCR4	3,33	Thermo Fisher Scientific, Waltham, MA, United States	
SPA 895	HO-1	2	Enzo Life Sciences BVBA, Bruxelles, Belgium	

Secondary Antibody	Specificity	Concentration (µg/mL)	color	Source
101909	Donkey anti Rabbit Biotine	3,4	-	Jackson ImmunoResearch Europe LTD, Ely, United Kingdom
714270	Donkey anti Goat Alexa Fluor 594	20	Red	Invitrogen Thermo Fisher Scientific, Waltham, MA, United States
A11008	Goat anti Rabbit Alexa Fluor 488	4	Green	Invitrogen Thermo Fisher Scientific, Waltham, MA, United States
1777945	Goat anti Rabbit Alexa Fluor 594	4	Red	Invitrogen Thermo Fisher Scientific, Waltham, MA, United States

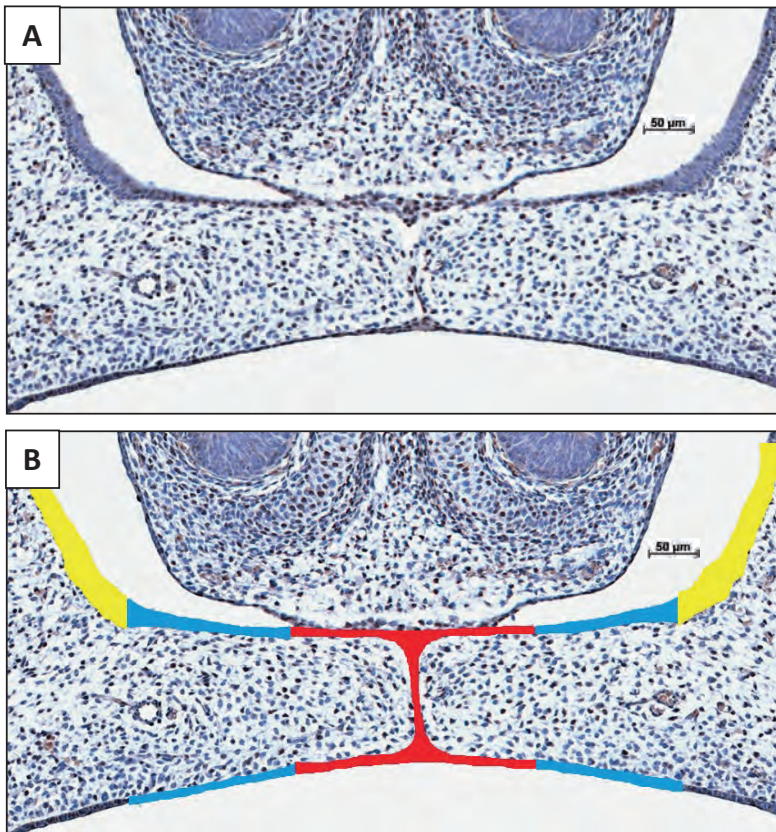
Immunohistochemical staining of palatal CXCL12 expression

Paraffin-embedded coronal palatal sections from the wt E15 and HO-2 KO E15 fetuses, containing a full or partial MES, were selected. Endogenous peroxidase activity was quenched with 3% H₂O₂ in methanol for 20 min. No antigen retrieval was used. Next, the sections were pre-incubated with 10% NDS in PBSG. First antibody for CXCL12, see **Table 1**, was diluted in 2% NDS in PBSG and incubated overnight at 4°C. After washing with PBSG, sections were incubated for 60 min with a biotin-labeled second antibody against host species, see **Table 1**, as previously described¹⁰⁷. Next, the sections were washed with PBSG and treated with avidin-biotin peroxidase complex (ABC) for 45 min

in the dark. After extensive washing with PBSG, diaminobenzidine-peroxidase (DAB) staining was performed for 10 min for the CXCL12 staining. Finally, the nuclei were stained with Hematoxylin for 10 s and sections were rinsed for 10 min in water, dehydrated, and embedded in distyrene plasticizer xylene (DPX). Microscopic photographs of the CXCL12 stained sections were taken.

Quantification of CXCL12 immunoreactivity in the palatal epithelium

The CXCL12 immunostained coronal palatal sections from the wt E15 and HO-2 KO E15 fetuses were examined. Within each section the epithelium of the palatal shelves was subdivided into three separate regions of interest (Inside, Outside, and Lateral nasal wall) according to morphological characteristics (epithelium region classification) as previously described⁵⁰. The epithelial regions per single section were semi-quantitatively scored according to the immunoreactivity scoring scale in three categories: HIGH, MODERATE and LOW, for details see **Figure 2**. CXCL12 immunoreactivity was evaluated by two observers, independently and blinded for the groups. The inter- and intra-examiner reliability was determined. For each individual fetus the modus of the scoring per epithelial region was calculated.



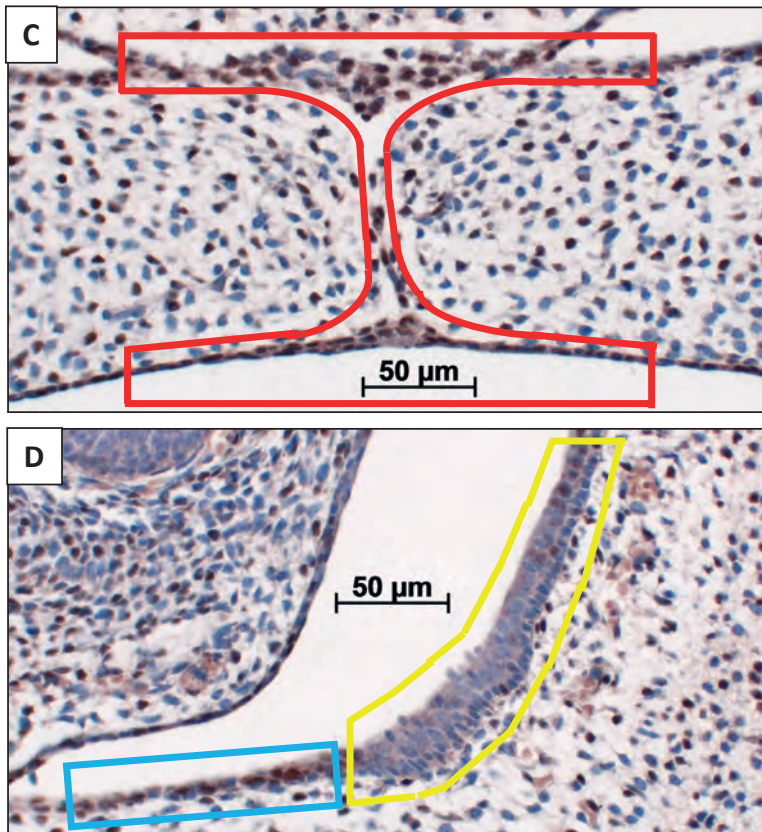


Figure 2: Palatal epithelium classification. (A) Coronal palatal section, e.g., HO-2 KO E15. (B) For each section the palatal epithelial layers were subdivided into three regions of interest according to morphological characteristics: (Inside) epithelium of the palatal shelves from the edge, including the MES, to half of the width of the shelves (in red); (Outside) epithelium of the lateral half of the palatal shelves (in blue); (Lateral nasal wall) epithelium of the lateral wall of the nasal cavity, this region is positioned outside the palatal shelves and served as a control region (in yellow). **Immunoreactivity scoring scale:** Semi-quantitative scoring of CXCL12 immunoreactivity within the epithelial regions according to the following scale: HIGH, immunoreactivity present in almost the entire epithelial region; MODERATE, immunoreactivity present only partially in the epithelial region; LOW, almost no immunoreactivity present in the epithelial region. Immunoreactivity scored for the three regions of interest in a CXCL12 immunostained section. (C) Inside region was scored as HIGH, in red. (D) Outside region was scored as MODERATE, in blue. Lateral nasal wall region was scored as LOW, in yellow.

Quantification of CXCL12-positive cells in the palatal mesenchyme

Because the coronal palatal sections showed a significant variance in size of the palatal shelves, CXCL12 staining was adjusted to the surface area. The individual cross-sectional surface of the inner and outer half of each pair of shelves was measured using Fiji Image J 1.51n software (Zeiss, Göttingen, Germany).

Then, the number of CXCL12-positive cells within the outline of the inner and outer half of the mesenchyme of the palatal shelves was counted, for details see **Figure 3**.

The number of mesenchymal CXCL12-positive cells/mm² per inner and outer half of the palatal mesenchyme per section was calculated. Cell counting was performed by two observers, independently and blinded for the groups. The inter- and intra-examiner reliability was determined. For each individual fetus the mean number of mesenchymal CXCL12-positive cells/mm² per inner and outer half of the mesenchyme of the palatal shelves was calculated.

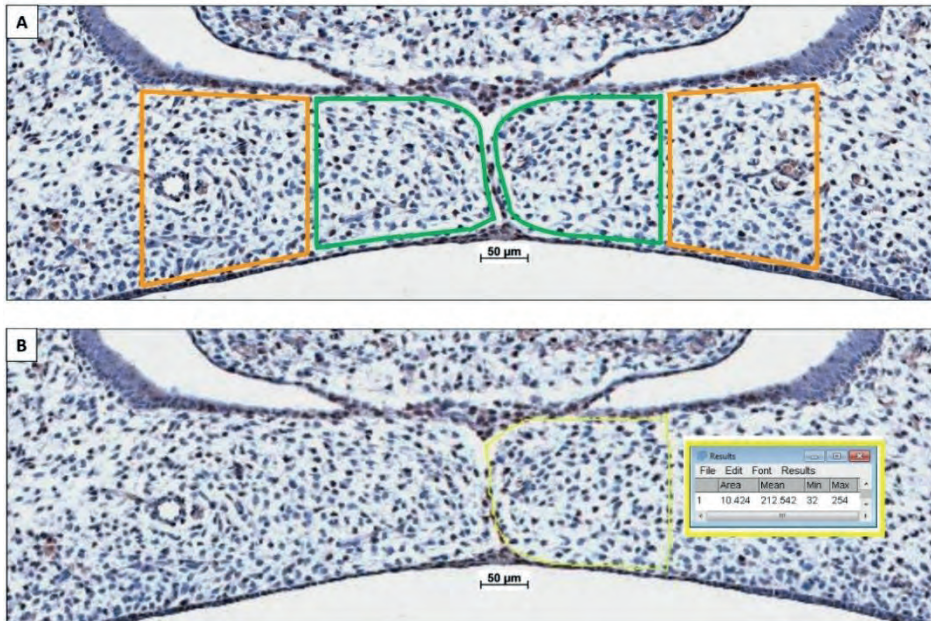


Figure 3: Palatal shelf cross-sectional surface measurement determining the number of CXCL12-positive immunostained cells/mm² within the mesenchyme. (A) The individual cross-sectional surface of the inner half (in green) and outer half (in orange) of each palatal shelf was measured. (B) A square scale bar was drawn in the microscopic picture of 1,000 x 1,000 mm (mm²) and the total number of pixels was determined (e.g., HO-2 KO E15: 1 mm² = 635,000 pixels), data not shown. The contour of the mesenchyme was drawn (yellow line). The number of pixels for this area was determined by the Fiji Image J 1.51n software (10,424 pixels). The number of CXCL12-positive stained cells within this mesenchymal area of the palatal shelves was counted (e.g., inner half contains 31 CXCL12-positive cells. The number of cells/mm² was calculated (635,000/10,424 x 31 = 1888 cells/mm²).

Statistical analysis

The fetal loss rate of the wt E15 and HO-2 KO E15 fetuses, and the wt CD1 E16 and wt CD1 SnMP E16 fetuses, showed a non-normal distribution as evaluated by the Kolmogorov-Smirnov test (KS-test). The differences in fetal loss rate between those

groups were compared using the non-parametric Kruskal- Wallis ANOVA on ranks test and Dunn's Multiple Comparison post hoc test.

The fetal body weight of the wt E15 and HO-2 KO E15 fetuses showed a normal distribution as evaluated by the KS-test. To compare differences between those groups the Independent-Samples *T*-test was performed. The fetal body weight of the wt CD1 E16 and wt CD1 SnMP E16 fetuses showed a non-normal distribution as evaluated by the KS-test. The nonparametric Mann-Whitney test was used to compare differences between both groups.

The CXCL12 immunoreactivity in the three regions of interest of the palatal epithelium of the wt E15 and HO-2 KO E15 fetuses was semi-quantitatively scored and analyzed using the nonparametric Kruskal-Wallis ANOVA on ranks test and Dunn's Multiple Comparison *post hoc* test to compare differences between both groups.

The number of CXCL12-positive cells/mm² within the outline of the inner and outer half of the palatal mesenchyme of the wt E15 and HO-2 KO E15 fetuses was quantitatively scored and showed a normal distribution as evaluated by the KS-test. The data was analyzed using the ANOVA and Tukey's multiple comparison *post hoc* test to compare differences between the inner and outer half of the palatal mesenchyme of both groups.

To determine the inter- and intra-examiner reliability for the semi-quantitative data of the CXCL12 immunoreactivity in the epithelium, the Cohen's kappa coefficient was calculated. Acceptable scores >0.80 were obtained for the semi-quantitatively scoring.

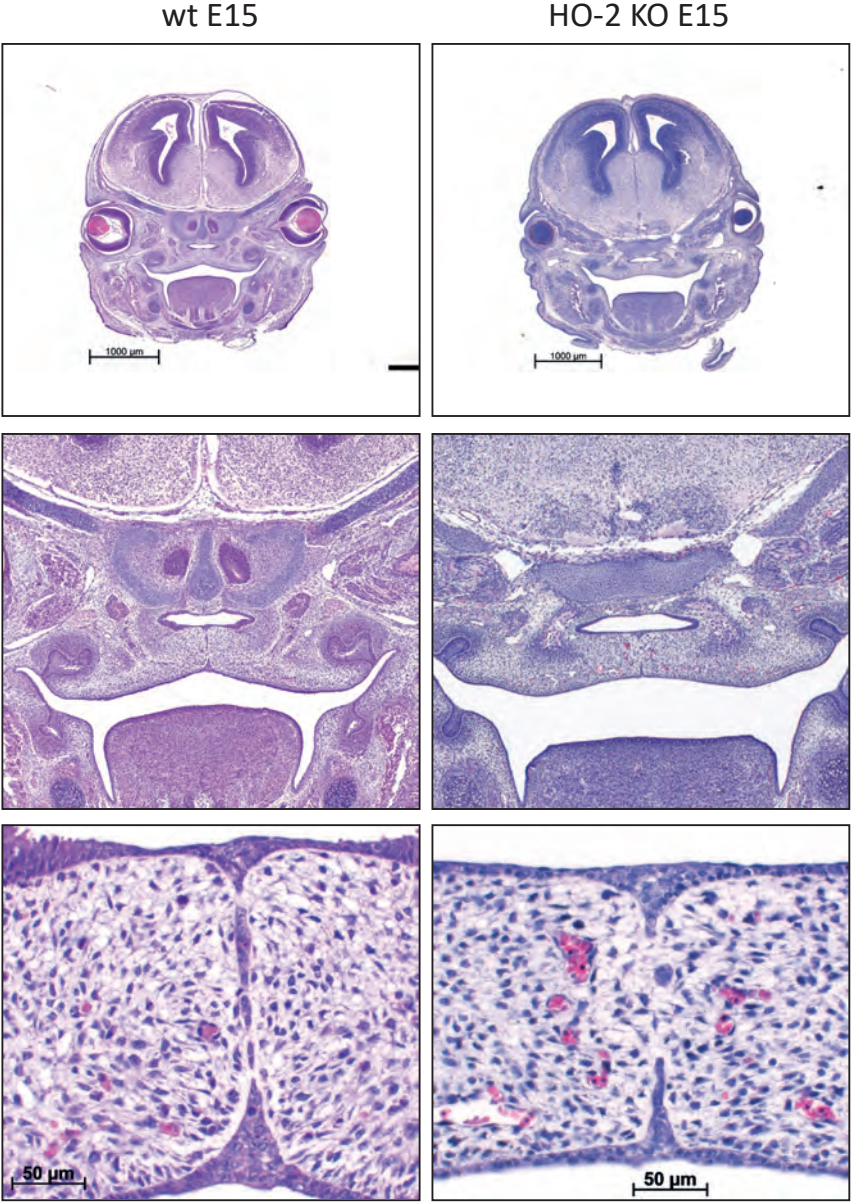
To determine the inter- and intra-examiner reliability, the coefficient of determination (R^2) was calculated by the square of the Pearson correlation coefficient for the quantitative data of the CXCL12-positive cells/mm² in the palatal mesenchyme. Acceptable scores > 0.80 were obtained for the counting.

Differences were considered significant if $p < 0.05$. All statistical analyses were performed using Graphpad Prism 5.03 software (GraphPad Software, San Diego, CA, United States).

Results

MES disintegration despite HO-2 abrogation and palatal fusion despite HO-activity inhibition from E11

In the HE-stained coronal palatal sections of the wt E15 and HO-2 KO E15 fetuses, the tips of the palatal shelves were attached and disintegration of the MES was found. In the HE-stained sections from the wt CD1 E16 and wt CD1 SnMP E16 fetuses, the palatal shelves were fused. Representative palatal section per group was shown in **Figure 4**.



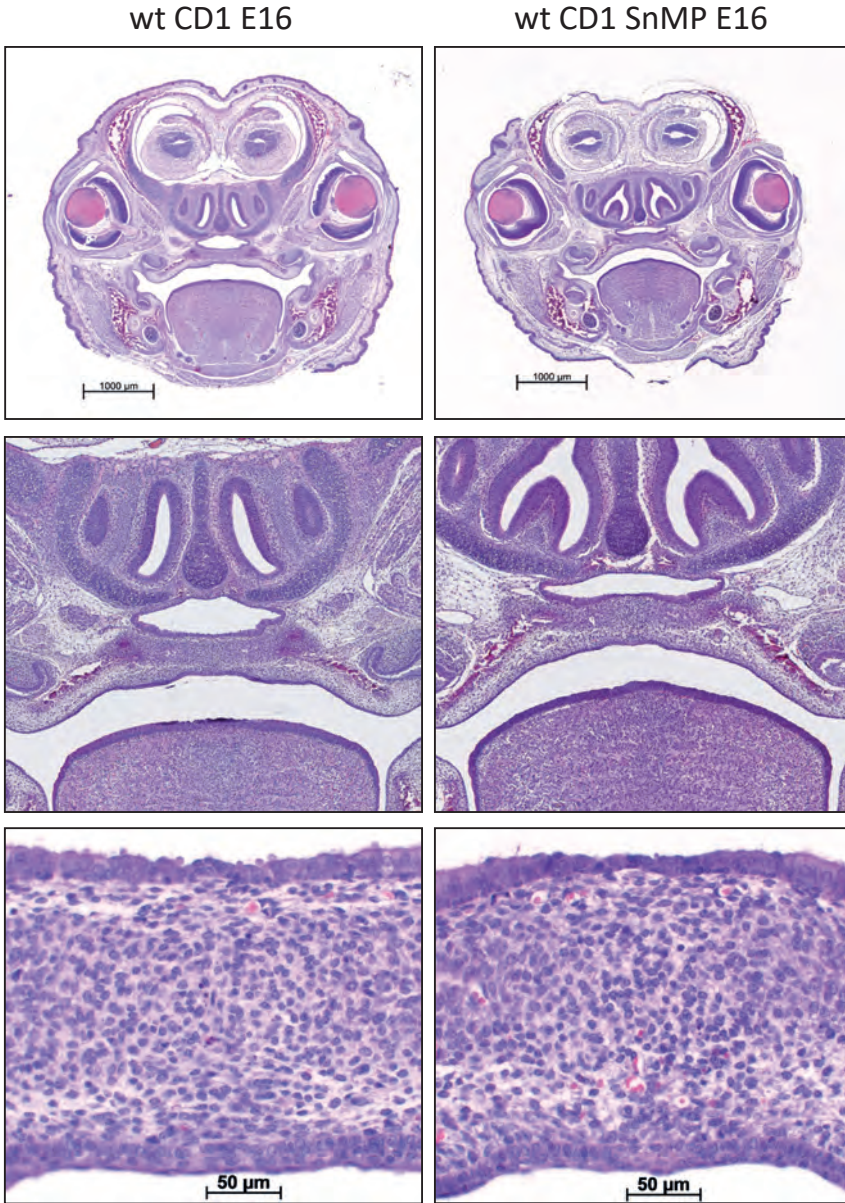


Figure 4: MES disintegration despite HO-2 abrogation and palatal fusion despite HO-activity inhibition from E11. In the HE-stained coronal palatal sections of the wt E15 and HO-2 KO E15 fetuses, the palatal shelves were attached and disintegration of the MES was found. In the HE-stained coronal palatal sections from wt CD1 E16 and wt CD1 SnMP E16 fetuses, the palatal shelves were fused. Representative palatal section per group was shown.

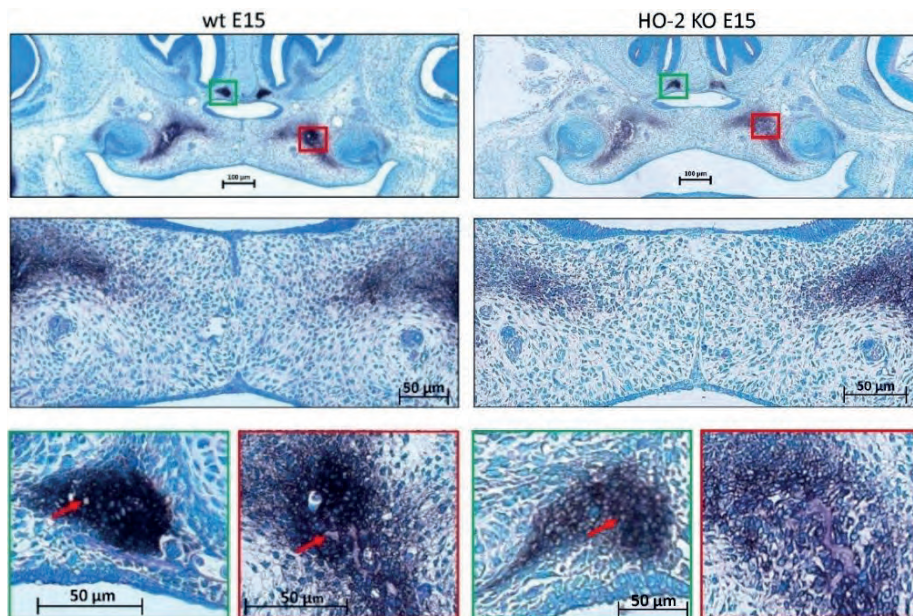
Palatal osteogenesis during MES disintegration is normal despite HO-activity inhibition

In the coronal palatal sections of the wt E15 and HO-2 KO E15 fetuses, clusters of ALP-positive-stained mesenchymal cells including small bone matrix depositions were found in the regions lateral of the fusing palatal shelves and lateral near the nasal septum. No disruption of ALP expression due to HO-2 abrogation was found. In the coronal palatal sections of the wt CD1 E16 and wt CD1 SnMP E16 fetuses, clusters of ALP-positive-stained mesenchymal cells surrounding large areas of bone depositions were found in both the center and lateral regions of the palatal shelves, and lateral near the nasal septum. Because of their ALP-activity, and their location around bone depositions, these ALP-positive clustered cells were regarded as osteoblast progenitors and osteoblasts.

No disruption of ALP-activity due to HO-activity inhibition was found. Representative sections per group are shown in **Figure 5**.

The clusters of ALP-positive-stained mesenchymal cells of the fusing palate were considered as palatal osteogenic centers and determined as region of interest for studying CXCL12, CXCR4, and Sox9 expression.

A



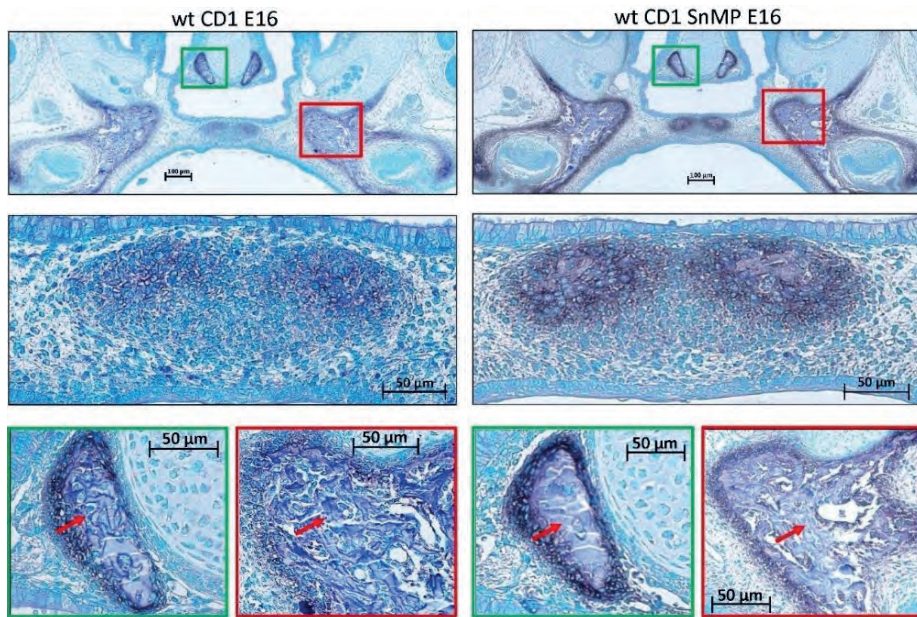
B

Figure 5: Palatal osteogenesis during MES disintegration: (A) Upper panel: Histochemical stained coronal palatal section for ALP-activity, representative for the wt E15 and HO-2 KO E15 fetuses. **Middle panel:** Magnification of the central part of the fusing palate including the MES. The palatal mesenchymal cells demonstrated positive staining for ALP-activity. **Green panel:** Magnification of the nasal septum. A cluster of ALP-activity positive-stained mesenchymal cells was found in the region lateral from the nasal septum including some small bone matrix depositions (red arrow). **Red panel:** Magnification of the lateral part of the palatal shelf. A cluster of ALP-positive stained mesenchymal cells was found including small bone matrix depositions (red arrow). **(B) Upper panel:** Histochemical stained sections through the maxilla for ALP-activity, representative for the wt CD1 E16 and wt CD1 SnMP E16 fetuses. **Middle panel:** Magnification of the central part of the fusing palate. A cluster of ALP-positive stained mesenchymal cells including bone matrix depositions was found at the former location of the MES and was regarded as an osteogenic center. **Green panel:** Magnification of the nasal septum. A cluster of ALP-positive-stained mesenchymal cells surrounding a large area of bone matrix deposition (red arrow) was found. **Red panel:** Magnification of the lateral part of the palatal shelf. A cluster of ALP-positive-stained mesenchymal cells in the lateral part of the fusing palate surrounding a large area of bone matrix deposition (red arrow) was found.

Sox9 expressing cells present in the MES and palatal osteogenic centers

In both wt E15 and HO-2 KO E15 fetuses, Sox9 high expressing cells were found in the disintegrating MES. Moreover, clusters of Sox9-positive mesenchymal cells were found in the osteogenic centers in the lateral parts of the fusing palate and at the oral side of the forming nasal septum. Regarding their clustered arrangement in the osteogenic centers, it was assumed that these Sox9-positive cells are predominantly osteoblast progenitors. Furthermore, Sox9 expressing mesenchymal cells were present in the cartilage of the nasal septum, and are likely chondroblasts because of their specific position, see **Figure 6**. The non-specific autofluorescence is shown in **Figure 7A**.

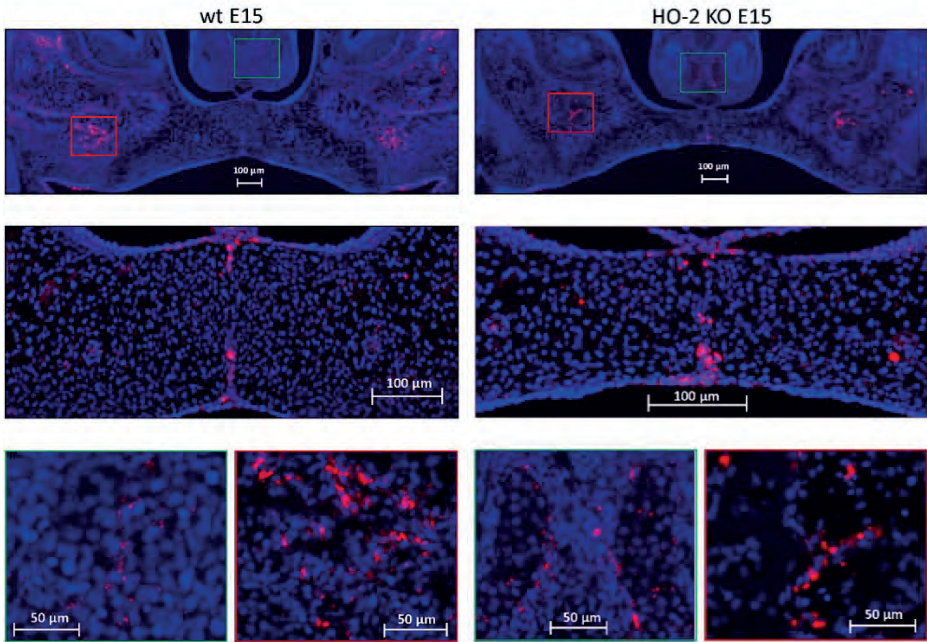


Figure 6: Sox9 expressing cells in the MES and the palatal osteogenic centers. Upper panels: Fluorescent immunohistochemical-stained coronal palatal sections for Sox9-activity (red), representative for the wt E15 fetuses and HO-2 KO E15 fetuses. Middle panels: Strong Sox9 expressing cells (red) were found in the remnants of the MES. Green panels: Sox9 expressing mesenchymal cells were present in the osteogenic centers at the oral side of the forming nasal septum, and in the cartilage of the nasal septum. Red panels: The osteogenic centers in the lateral parts of the fusing palate demonstrated clusters of strong Sox9 expressing cells.

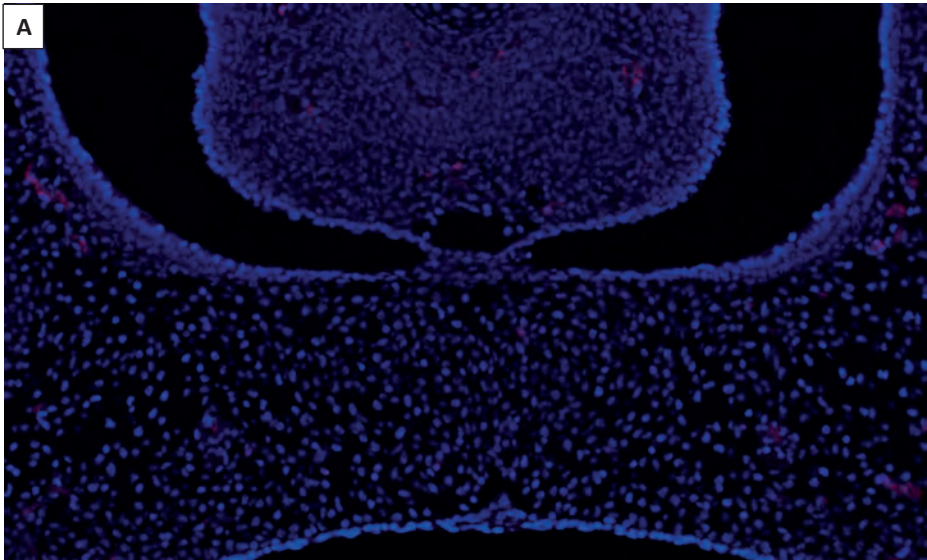




Figure 7: Immunofluorescence background staining for Sox9 (A) and CXCR4 (B). (A) This coronal palatal section of the HO-2 E15 fetus is not incubated with the first antibody for Sox9, but just 2% NDS in PBSG. Little nonspecific red staining is shown. (B) This coronal palatal section of the HO-2 KO E15 fetus is not incubated with the first antibody for CXCR4 but just 2% NDS in PBSG. Little nonspecific green staining is shown, predominantly erythrocytes demonstrated nonspecific staining.

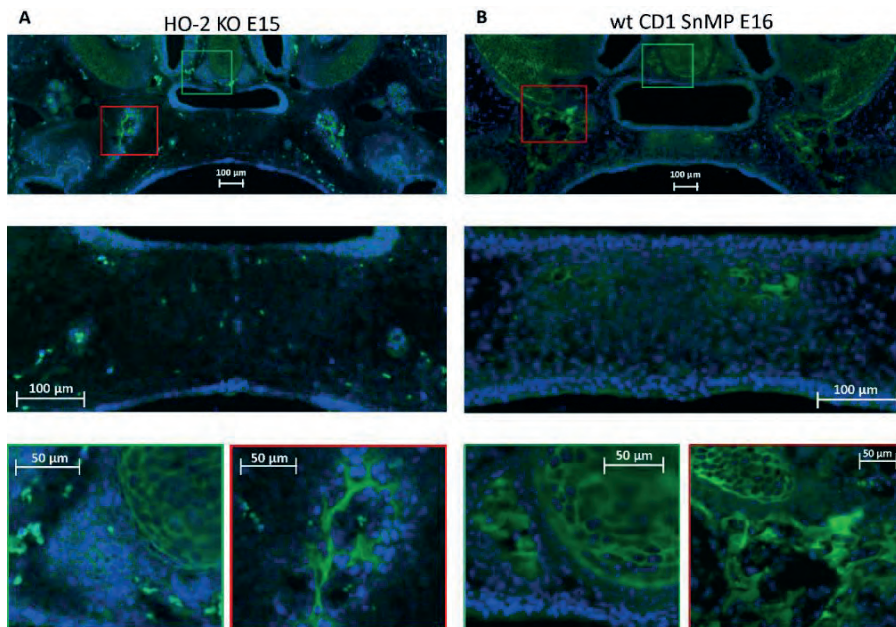


Figure 8: CXCR4 expressing cells in the palatal osteogenic centers. (A) **Upper panel:** Fluorescent immunohistochemical-stained coronal palatal section for CXCR4 expression (green), representative for the wt E15 and HO-2 KO E15, e.g., HO-2 KO. **Middle panel:** Within the disintegrating MES almost no CXCR4 expressing cells were found. **Green panel:** Near the forming nasal septum clusters of strong CXCR4 expressing cells were found. Also within the cartilage of the forming nasal septum CXCR4 expressing cells were present. **Red panel:** The osteogenic centers in the lateral parts of the fusing palate demonstrated clusters of strong CXCR4 expressing cells. (B) **Upper panel:** Fluorescent immunohistochemical stained coronal palatal section for CXCR4 expression (green), representative for the wt CD1 E16 and wt CD1 SnMP E16 fetuses, e.g., wt CD1 SnMP E16. **Middle panel:** in the osteogenic centers in the central part of the fusing palate clusters of CXCR4-positive-stained mesenchymal cells were found. **Green panel:** Near the forming nasal septum clusters of strong CXCR4 expressing cells were found. Also within the cartilage of the forming nasal septum CXCR4 expressing cells were present. **Red panel:** The osteogenic centers in the lateral parts of the fusing palate demonstrated clusters of strong CXCR4 expressing cells.

CXCR4 expressing cells in the palatal osteogenic centers

In both wt E15 and HO-2 KO E15 fetuses, clusters of CXCR4-positive mesenchymal cells were found in the osteogenic centers in the lateral parts of the fusing palate. No CXCR4 expression was found within the disintegrating MES. In the wt CD1 E16 and wt CD1 SnMP E16 fetuses, CXCR4- positive stained cells in the osteogenic centers in both the central and lateral parts of the forming palate were found.

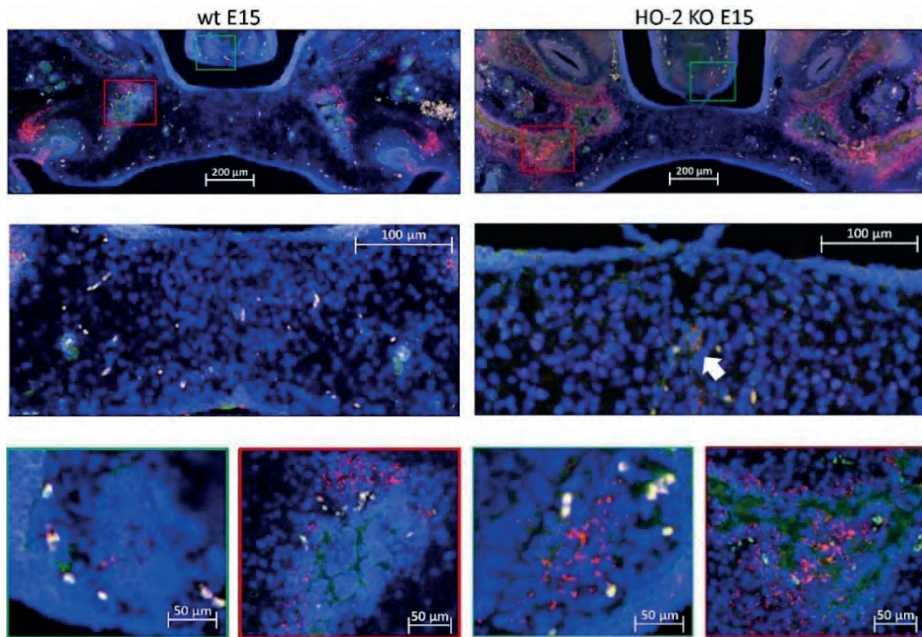
Furthermore, at the oral side of the forming nasal septum CXCR4 expressing cells were found at E15 and E16, see **Figure 8**. Regarding their clustered arrangement in the osteogenic centers, these CXCR4-positive mesenchymal cells were supposed to be primarily osteoblasts.

In the cartilage of the nasal septum, the observed CXCR4-positive cells were considered generally chondroblasts. The non-specific staining of the second antibody for CXCR4 is shown in **Figure 7B**.

Most CXCR4-positive cells in the palatal osteogenic centers are not positive for Sox9

In both wt and HO-2 KO E15 fetuses, clusters of Sox9 expressing cells surrounding CXCR4-positive cells in the osteogenic centers in the lateral parts of the forming palate were found, see **Figure 9**.

A



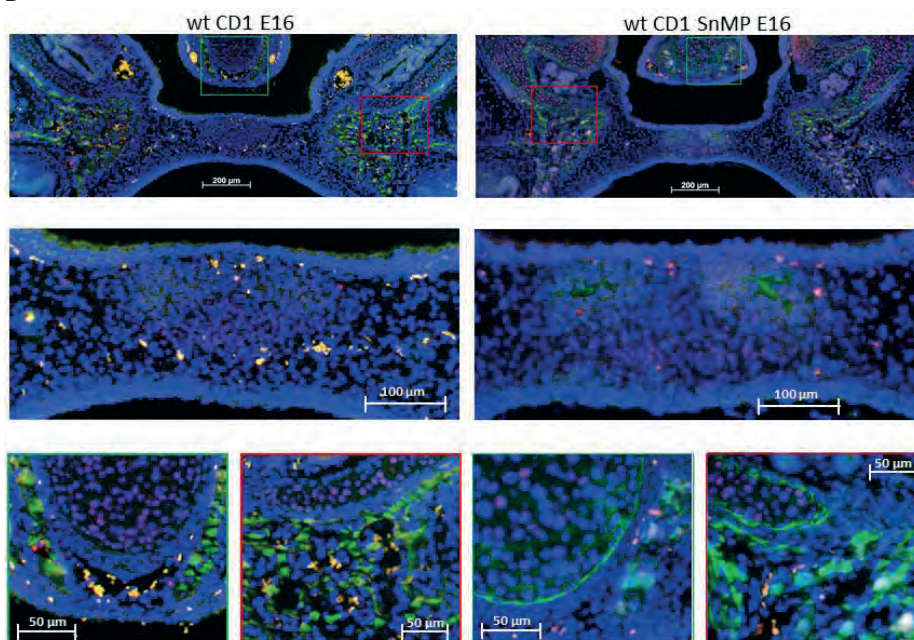
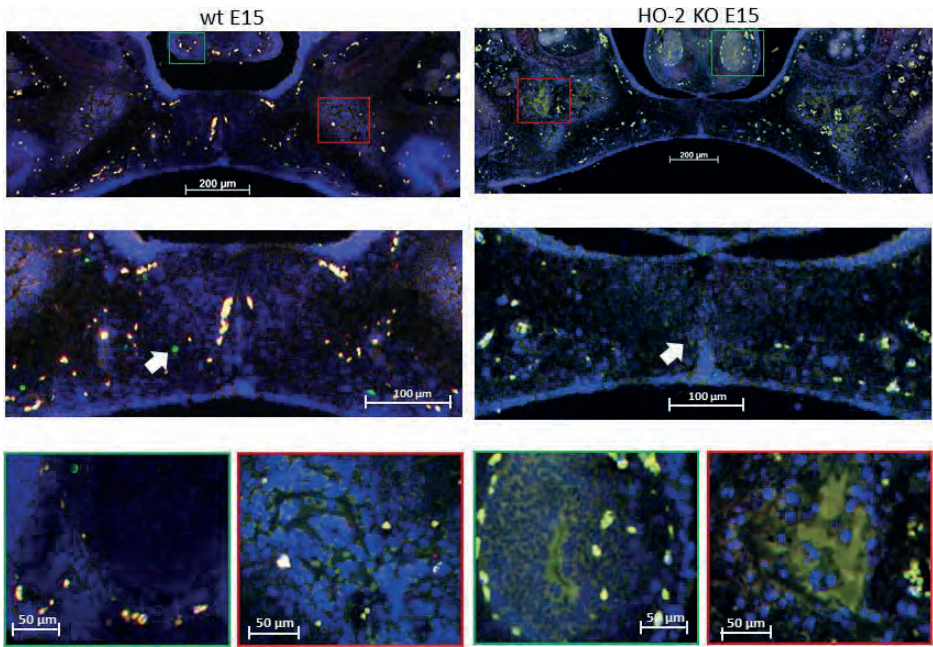
B

Figure 9: Most CXCR4-positive cells in the palatal osteogenic centers are not positive for Sox9. (A) Upper panel: Fluorescent immunohistochemical double-stained coronal palatal section for Sox9 (red) with CXCR4 (green), representative for the wt E15 and HO-2 KO E15 fetuses. **Middle panel:** Near the disintegrating MES only a few Sox9-CXCR4 double-positive stained cells (white arrow) were found. **Green panel:** In the osteogenic centers near the forming nasal septum clusters of Sox9 expressing cells together with CXCR4 expressing cells. **Red panel:** The osteogenic centers in the lateral parts of the fusing palate demonstrated clusters of Sox9 expressing cells near CXCR4 expressing cells. **(B) Upper panel:** Fluorescent histochemical double-stained coronal palatal section for Sox9 (red) with CXCR4 (green), representative for the wt CD1 E16 and wt CD1 SnMP E16 fetuses. **Middle panel:** In the osteogenic centers in the central part of the fusing palate, almost no Sox9-CXCR4 double-positive stained cells were found. **Green panel:** Near the forming nasal septum clusters of Sox9 expressing cells were found near CXCR4 positive cells. Also in the cartilage of the nasal septum CXCR4 positive cells were found close to Sox9 positive cells. **Red panel:** The osteogenic centers in the lateral parts of the fusing palate demonstrated clusters of Sox9 expressing cells near CXCR4 expressing cells.

Only a few Sox9-CXCR4 double-positive stained cells were found near the remnants of the MES. In the wt CD1 E16 and wt CD1 SnMP E16 fetuses, almost no Sox9-CXCR4 double-positive stained cells were found in the osteogenic centers in the central part of the forming palate. In general, less Sox9 expressing cells were found in the palatal mesenchyme in the wt CD1 E16 and wt CD1 SnMP E16 fetuses compared to the wt E15 and HO-2 KO E15 fetuses. In the osteogenic centers, Sox9 expressing cells were surrounding CXCR4-positive cells. At the oral side of the forming nasal septum CXCR4 expressing cells near Sox9 expressing cells were found at E15 and E16. The observation that Sox9-positive cells were located close to CXCR4-positive cells surrounding the osteogenic centers supports the suggestion that these Sox9-positive cells could be osteoblast progenitors to maintain the osteoblast pool to drive osteogenesis.

A



B

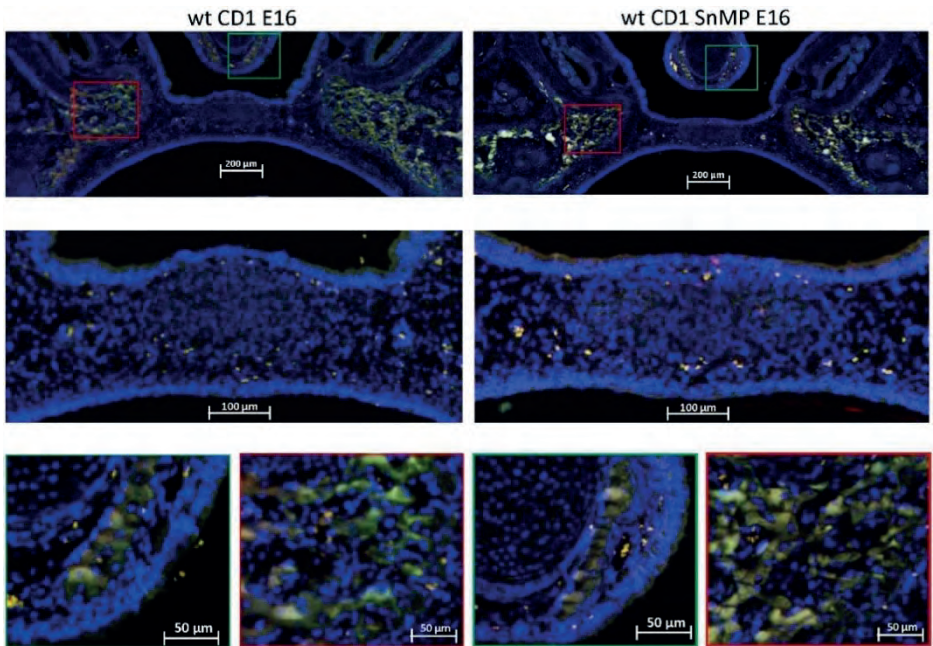


Figure 10: HO-1 expressing cells in the palatal osteogenic centers. (A) Upper panel: Fluorescent histochemical stained coronal palatal section for HO-1 expression (green), representative for the wt E15 and HO-2 KO E15 fetuses. **Middle panel:** In the mesenchyme near the disintegrating MES some HO-1 expressing cells (white arrow) were found. **Green panel:** Near the forming nasal septum clusters of strong HO-1 expressing cells were found. **Red panel:** The osteogenic centers in the lateral parts of the fusing palate

demonstrated clusters of strong HO-1 expressing cells. **(B) Upper panel:** Fluorescent histochemical-stained coronal palatal section for HO-1 expression (green), representative for the wt CD1 E16 and wt CD1 SnMP E16 fetuses. **Middle panel:** In the central part of the fusing palate some HO-1 expressing cells were found. **Green panel:** Near the forming nasal septum clusters of strong HO-1 expressing cells were found. **Red panel:** The osteogenic centers in the lateral parts of the fusing palate demonstrated clusters of strong HO-1 expressing cells.

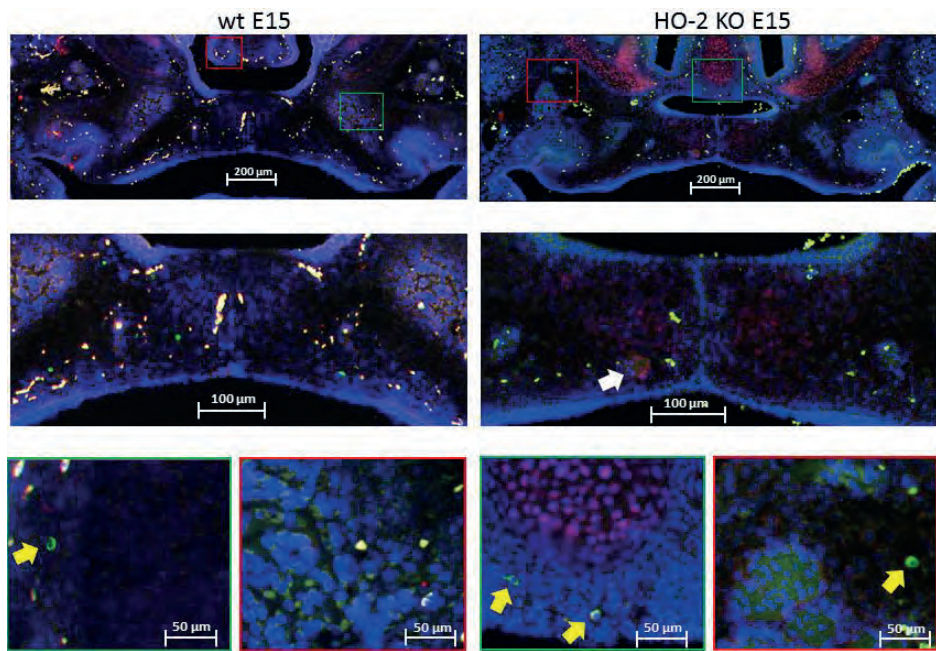
HO-1 expressing cells in the palatal osteogenic centers

In both wt E15 and HO-2 KO E15 fetuses, HO-1-positive-stained cells were found in the osteogenic centers in the central part but mainly in the osteogenic centers in the lateral parts of the forming palate. In the wt CD1 E16 and wt CD1 SnMP E16 fetuses, a few HO-1-positive stained cells were found in the osteogenic centers in the central part, but clusters of HO-1-positive stained cells were dominantly found in the osteogenic centers in the lateral parts of the forming palate. At the oral side of the forming nasal septum, HO-1 expressing cells were found at E15 and E16, see **Figure 10**. Since many HO-1-positive cells were found in the osteogenic centers, they were considered predominantly osteoblasts.

Most HO-1-positive cells in the palatal osteogenic centers are not positive for Sox9

In both wt and HO-2 KO E15 fetuses, only a few Sox9-HO-1 double-positive stained cells were found near the remnants of the MES, see **Figure 11**.

A



B

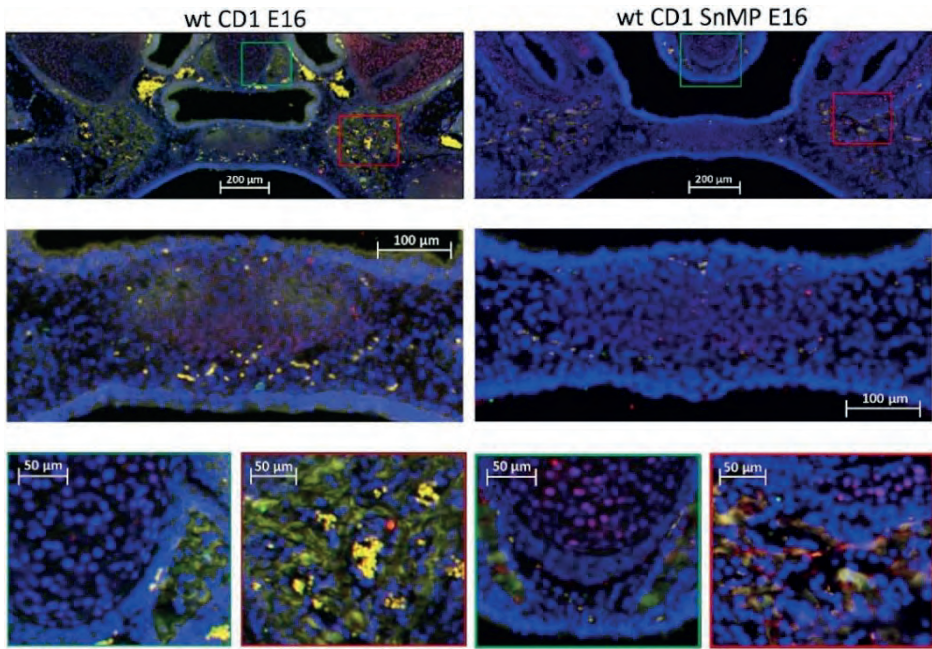


Figure 11: Most HO-1 positive cells in the palatal osteogenic centers are not positive for Sox9. (A) Upper panel: Fluorescent histochemical double-stained coronal palatal section for Sox9 (red) with HO-1 (green), representative for the wt E15 and HO-2 KO E15 fetuses. **Middle panel:** Near the disintegrating MES Sox9-HO-1 double-positive-stained cells (white arrow) were sporadically found. **Green panel:** In the osteogenic centers near the forming nasal septum clusters some HO-1 expressing cells were found. Furthermore, some solitary HO-1 expressing cells (yellow arrow) were found. In the cartilage of the nasal septum, multiple Sox9 expressing cells were found. **Red panel:** The osteogenic centers in the lateral parts of the fusing palate demonstrated clusters of HO-1 expressing cells, and solitary strong HO-1 expressing cells (yellow arrows) in the mesenchyme. **(B) Upper panel:** Fluorescent histochemical double-stained coronal palatal section for Sox9 (red) with HO-1 (green), representative for the wt CD1 E16 and wt CD1 SnMP E16 fetuses. **Middle panel:** In the fusing palate clusters of HO-1, expressing cells were found within the palatal osteogenic centers. **Green panel:** Near the forming nasal septum clusters of HO-1 expressing cells were found. In the cartilage of the nasal septum multiple Sox9 expressing cells were found. **Red panel:** The osteogenic centers in the lateral parts of the fusing palate demonstrated clusters of HO-1 expressing cells.

In the wt CD1 E16 and wt CD1 SnMP E16 fetuses, HO-1 expressing cells were found in the osteogenic centers in the central part of the forming palate, but almost no Sox9-HO-1 double-positive stained cells were found. At the oral side of the forming nasal septum, clusters of HO-1 expressing cells were present.

The examination that Sox9-positive cells surrounded the osteogenic centers containing multiple HO-1- positive cells possibly means that osteoblast progenitors are not HO-1 positive.

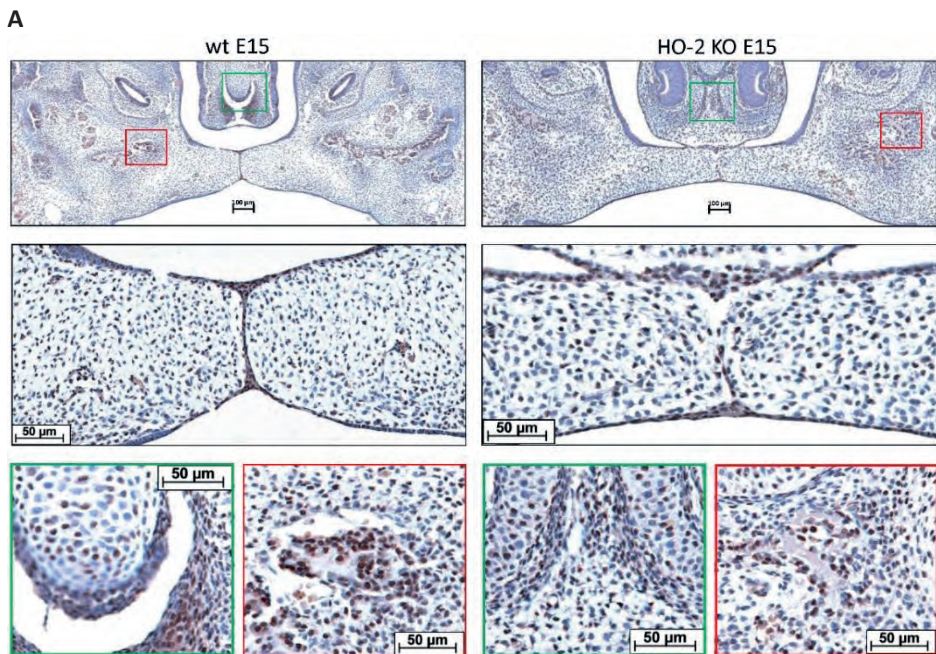
CXCL12 expression present in the MES and palatal osteogenic centers

Chemokine CXCL12 was significantly higher expressed in the inside epithelial region including the MES (Inside) of the wt E15 and HO-2 KO E15 fetuses compared to the other epithelial layers of the fusing palatal shelves (Outside), and the lateral epithelium of the nasal cavity (Lateral nasal wall) ($p < 0.001$), see **Figures 12A,B**.

CXCL12 expressing cells were also observed in the mesenchyme of the palatal shelves, but the number of CXCL12-positive cells/mm² in palatal section showed no significant difference between the wt E15 and HO-2 KO E15 fetuses, and between the inner half and outer half ($p = 0.85$), see **Figure 12C**. Based on their uniformly distribution, most of these CXCL12-positive cells in the palatal mesenchymal were considered to be fibroblasts.

Furthermore, the osteogenic centers in the lateral parts of the fusing palate demonstrated clusters of strong CXCL12 expressing cells. Considering their clustered arrangement in the osteogenic centers, these CXCL12-positive cells were thought to be osteoblast progenitors or osteoblasts.

Also within the cartilage of the forming nasal septum CXCL12 expressing cells were present, and these cells were regarded as chondroblast because of their specific location, see **Figure 12A**.



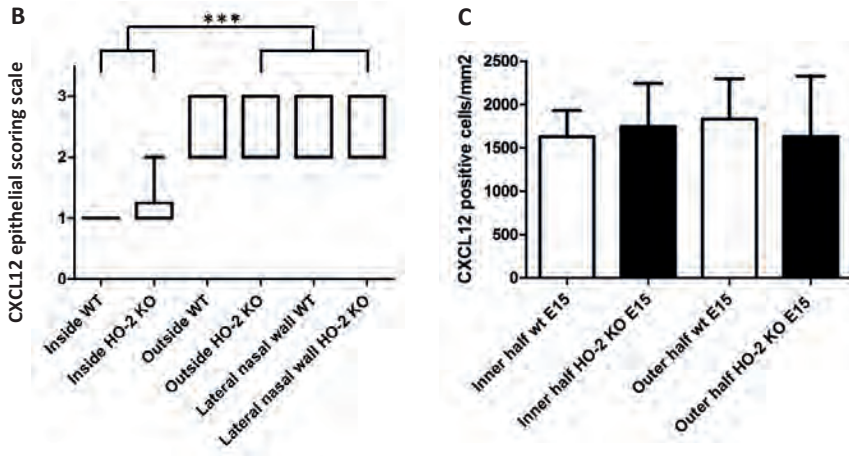
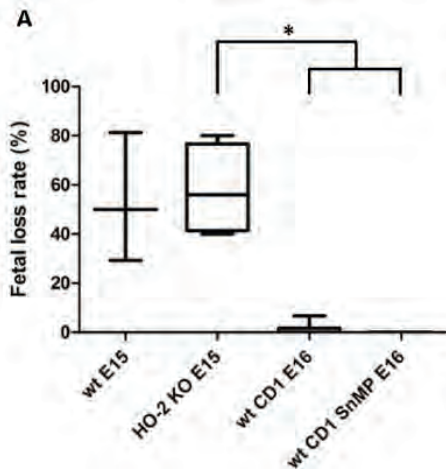


Figure 12: CXCL12 expression in the MES and palatal osteogenic centers. (A) **Upper panel:** Coronal palatal section stained for CXCL12 expression, representative for the wt and HO-2 KO fetuses. **Middle panel:** Magnification of the central part of the fusing palate including the MES. The MES demonstrated strong CXCL12 expression. CXCL12-positive cells were also found in the palatal mesenchyme. **Green panel:** The osteogenic centers at the lateral/oral side of the nasal septum demonstrated clusters of strong CXCL12 expressing cells. Also in the cartilage of the forming nasal septum CXCL12 expressing cells were present. **Red panel:** The osteogenic centers in the lateral parts of the fusing palate demonstrated clusters of strong CXCL12 expressing cells. (B) Box-and-whisker plot with 10–90 percentiles of semi-quantitative assessment of the CXCL12 expression in the palatal epithelial layers (scoring scale in three categories: 1 = HIGH, 2 = MODERATE and 3 = LOW) compared for the different regions in sections from wt E15 ($n = 7$) and HO-2 KO E15 fetuses ($n = 10$), *** = $p < 0.001$. (C) Bar chart of the number of mesenchymal CXCL12-positive cells cells/mm² compared for the wt E15 ($n = 7$) and HO-2 KO E15 fetuses ($n = 10$) between the outline of the inner and outer half of the mesenchyme. Data are shown as mean \pm SD. No statistically significant differences in CXCL12 expression were found ($p = 0.85$).

Fetal resorption independent of HO-2 expression and HO-activity

Approximately half of the wt E15 and HO-2 KO E15 fetuses were resorbed. Contrarily, in the wt CD1 E16 and wt CD1 SnMP E16 fetuses, the number of fetal resorptions was low (less than 7%).



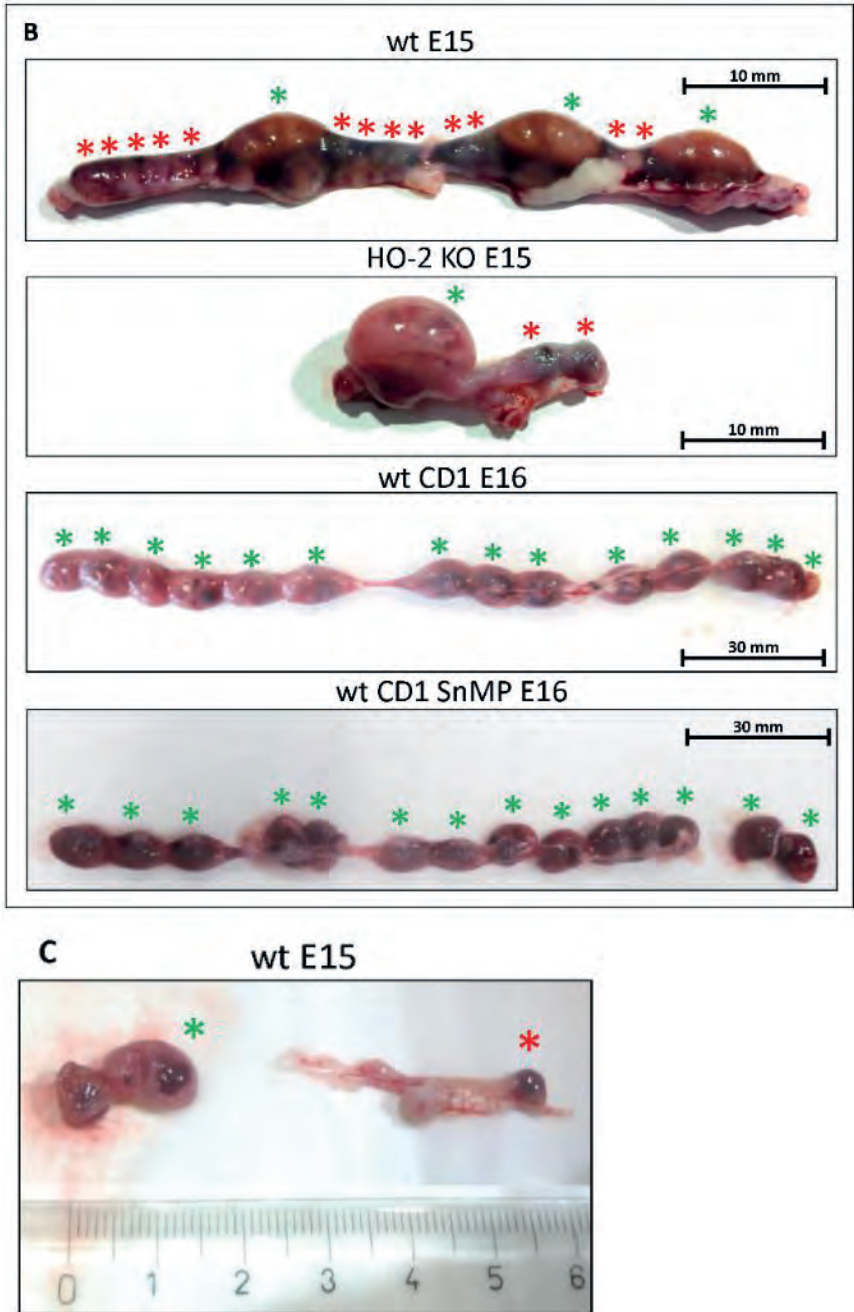
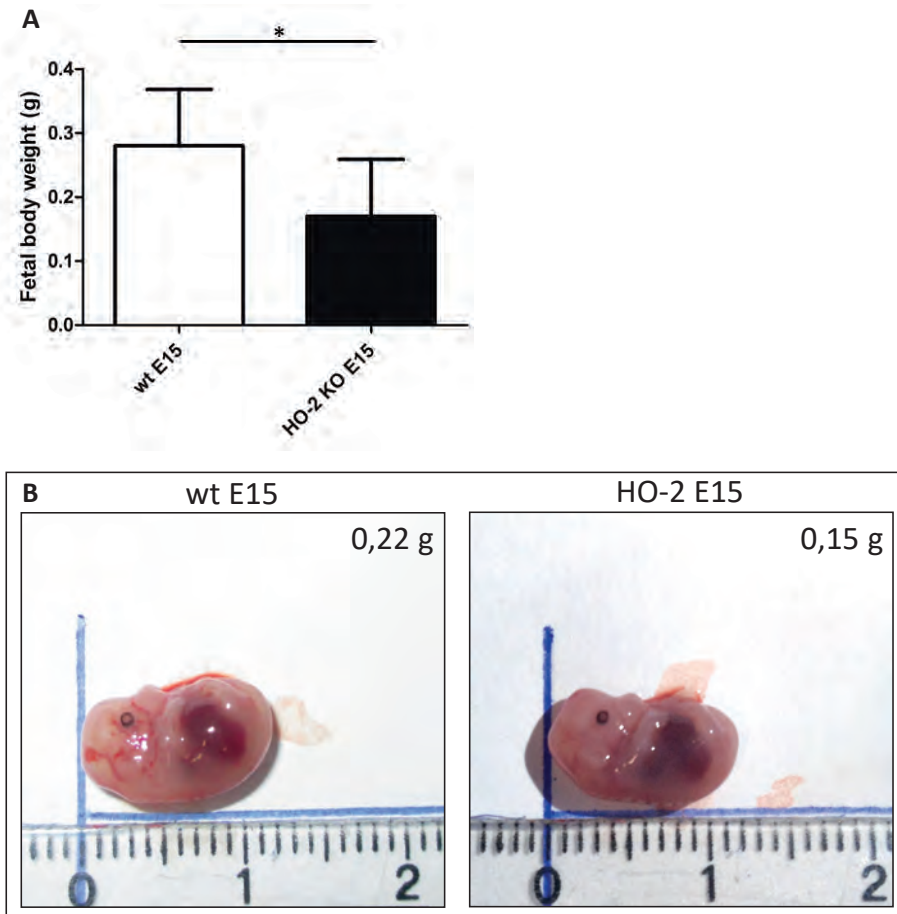


Figure 13: Fetal resorption independent of HO-2 KO expression and HO-activity. (A) Box-and-whisker plot with 10–90 percentiles of quantitative assessment of the fetal loss ratio in the wt ($n = 3$) and HO-2 KO pregnant mice ($n = 4$) at E15, and wt CD1 mice ($n = 6$) and wt CD1 SnMP mice ($n = 4$) at E16, $*p < 0.05$. (B) The uteri were photographed, the green asterisk indicated a fetus, the red asterisk indicated a fetal resorption. Representative uterus per group was shown. (C) Isolated fetus with placenta and isolated fetal resorption from the uterus.

Higher fetal loss rate was found in the HO-2 KO E15 group compared to both the wt CD1 E16 and wt CD1 SnMP groups ($p < 0.05$), see **Figure 13**. Disruption of HO-2 expression and HO-activity inhibition both did not result in increased fetal loss ($p > 0.05$).

Fetal body weight is decreased by absence of HO-2 expression but increased by HO-activity inhibition from E11

The HO-2 KO E15 fetuses demonstrated a reduced fetal body weight compared to the wt E15 fetuses ($p = 0.0416$), see **Figures 14A,B**. On the other hand, in CD1 fetuses of E16, inhibition of the HO-activity by SnMP from E11 increased the fetal body weight ($p < 0.0001$), see **Figures 14C,D**. A representative fetus per group is shown in **Figures 14B,D**.



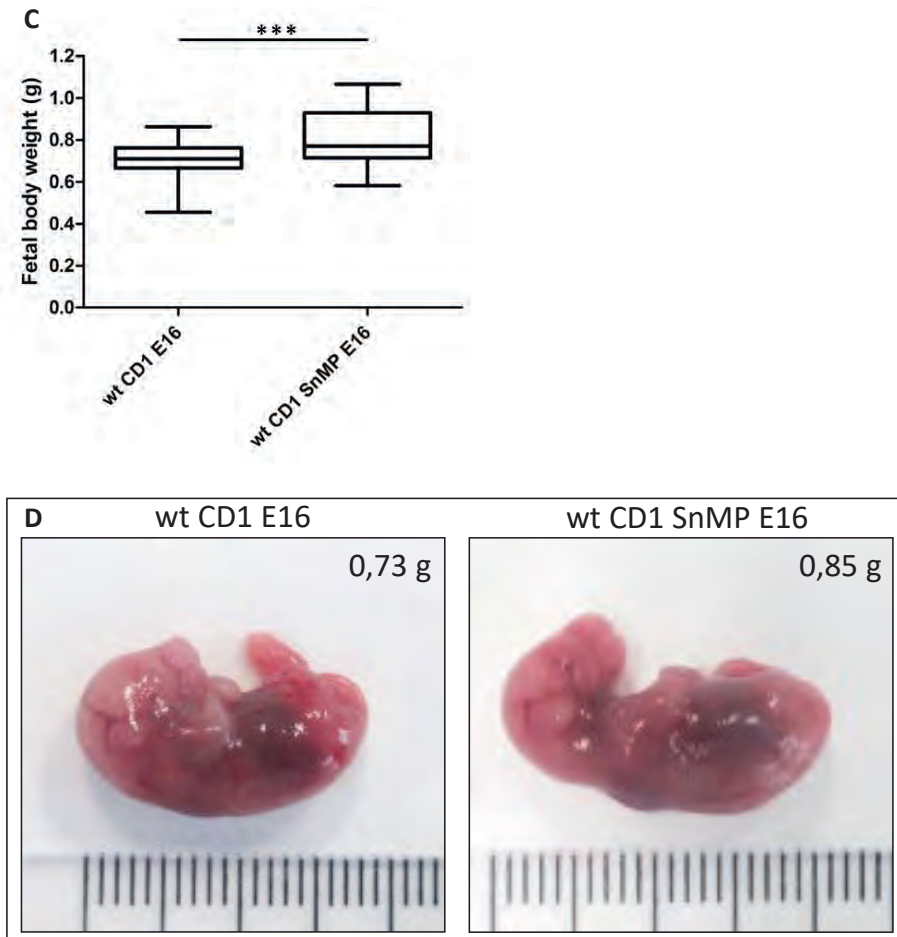


Figure 14: Fetal body weight decreases by disruption of HO-2, but increases by HO-activity inhibition from E11. (A) Bar chart of the fetal body weight of the wt E15 fetuses ($n = 15$) and HO-2 KO E15 fetuses ($n = 4$), $*p < 0.05$. Data are shown as mean \pm SD. (B) Representative fetus per group was shown (centimeter ruler). (C) Box-and-whisker plot with 10–90 percentiles of quantitative assessment of the body weight of the wt CD1 E16 fetuses ($n = 91$) and wt CD1 SnMP E16 fetuses ($n = 56$), $***p < 0.001$. (D) Representative fetus per group was shown (centimeter ruler).

Discussion

We found clusters of Sox9 expressing cells surrounding CXCR4-positive cells in the ALP-positive osteogenic centers of the palatal shelves at E15 and E16 in wt mice. However, most Sox9 positive cells in the palate were not positive for CXCR4 expression. Furthermore, we showed that chemokine CXCL12, the ligand of receptor CXCR4, was overexpressed within these palatal osteogenic centers. Sox9, CXCR4, and CXCL12 expressing cells were also observed within the cartilage of developing nasal septum, suggesting their involvement in chondrogenesis. Several *in vitro* and *in vivo* studies on the role of CXCL12-CXCR4 signaling in relation to bone formation have been

performed¹⁰⁸. CXCL12 expression in non-differentiated mesenchymal stem cells in bone was demonstrated, but toward the end of osteogenic differentiation CXCL12 was downregulated²¹. Deletion of CXCL12 in osteoprogenitor cells resulted in decreased bone mass in the femur bone in mice¹⁰⁹. CXCL12 antibody administration inhibited new bone formation during the repair of femoral bone graft in mice¹¹⁰. CXCR4 KO fetuses of E18.5 were smaller and showed deficient bone marrow development compared to the controls¹¹¹. CXCR4-deficient bone marrow-derived mesenchymal stromal stem cells from mice exhibited impaired osteogenic differentiation in response to BMP2 stimulation *in vitro*¹¹². Primary cultures for osteoblastic cells derived from CXCR4 KO mice showed decreased proliferation and impaired osteoblast differentiation in response to BMP2 or BMP6 stimulation *in vitro*²². Additionally, disruption of CXCR4 receptor in mouse hematopoietic stem cells led to increased endogenous ROS production¹¹³. Since our results showed that Sox9 and CXCR4 do not have overlapping expression, we suggest that Sox9-positive cells are osteoblast progenitors. maintaining the osteoblast pool to drive osteogenesis, and that both CXCL12 and CXCR4 are later expressed by the mature osteoblasts. Furthermore, we propose that Sox9 expression and CXCL12-CXCR4 signaling in the cartilage of the nasal septum develop chondroblast formation. Since CXCL12-CXCR4 signaling promotes osteoblast formation, it is suggesting that CXCL12 expression by the disintegrating MES is a major initiator of palatal osteogenesis.

Studies on CXCL12-CXCR4 signaling in the developing palate are scarce. We provided novel evidence that chemokine CXCL12, the ligand of receptor CXCR4, was overexpressed by the epithelial cells of the MES, possibly to activate osteoblasts progenitors to facilitate palatal bone formation. In human palatal sections, CXCR4 expression was observed within the MES¹¹⁴. On the contrary, in our study we did not observe CXCR4 overexpression within the disintegrating MES. We could not find other studies that demonstrated CXCR4 expression in the MES. It is suggesting that CXCL12 expression by the disintegrating MES is a major initiator of palatal osteogenesis. Besides chemokine CXCL12, the disintegrating MES demonstrated strong expression of Sox9. Although Sox9 expression is demonstrated in the developing palatal shelves in mice fetuses³²⁻³⁴, to our knowledge we are the first who demonstrated Sox9 expression specifically in the disintegrating MES. Sox9 signaling showed to be essential in the EMT mechanism in non-small-cell lung carcinoma cells^{115,116}, mouse embryonic mammary cells¹¹⁷, mouse gastric cancer cells¹¹⁸, human colorectal cancer cells¹¹⁹, human hepatocellular carcinoma cells¹²⁰, thyroid cancer cells¹²¹, and avian neural crest cells¹²² *in vitro*. Therefore, it's tempting to speculate that Sox9 expression near the MES is involved in EMT processes, turning the basal epithelial layer of the MES into mesenchyme during palatal fusion.

Our novel hypothetical model (**Figure 15**) proposes that CXCL12-CXCR4 signaling facilitates osteogenesis during palatal fusion in mice. Expression of Sox9 in

osteoblast progenitors was thought to initiate osteogenic differentiation by promoting CXCL12-CXCR4 signaling. CXCL12 expression by the MES and osteogenic centers in the fusing palatal shelves could promote maturation of immature CXCR4-positive osteoblasts. Sox9 progenitors thus seem important to maintain the CXCR4-positive osteoblast pool to drive osteogenesis. Furthermore, Sox9 expression found in the MES may in addition regulate MES disintegration by the process of EMT.

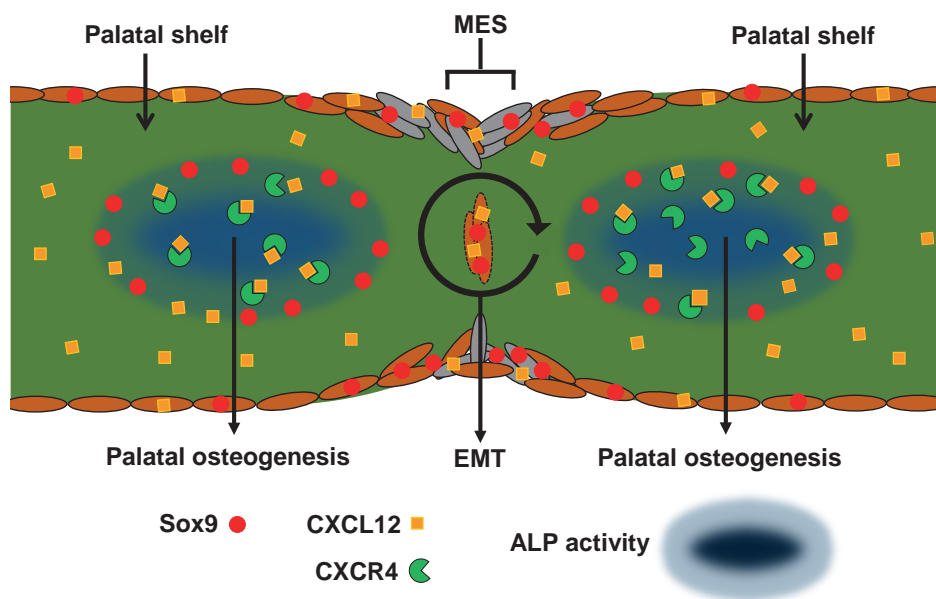


Figure 15: Hypothetical model: CXCL12-CXCR4 interplay facilitates palatal osteogenesis. We propose that the CXCL12-CXCR4 interplay facilitates osteogenesis during palatal fusion in mice. Expression of transcription factor Sox9 in osteoblast progenitors was thought to initiate differentiation into osteoblasts by promoting CXCL12-CXCR4 signaling. CXCL12 expression in the midline epithelial seam (MES) could promote maturation of immature CXCR4-positive osteoblast. Sox9 progenitors maintain the CXCR4-positive osteoblast pool to drive osteogenesis. Furthermore, Sox9 expression found in the MES, possibly regulates MES disintegration by the process of epithelial-to-mesenchymal transformation (EMT).

Only a few Sox9-positive cells in the palatal mesenchyme were also positive for HO-1. Studies on the role of HO-activity on embryonic craniofacial development in mice are limited⁵⁰. As far as we know, this is the first study on the effects of inhibition of HO-1 and HO-2 by SnMP administration during palatogenesis. Adult HO-1 KO mice demonstrate growth retardation¹²³, but HO-2 KO mice were found to be morphologically indistinguishable from wt mice¹⁰⁰. In rat, HO-1 inhibition by zinc deuteroporphyrin IX 2,4 bis glycol resulted in a significant decrease in pup size¹²⁴. This study showed that neither adhesion of the palatal shelves nor Sox9 and CXCL12

expression by the MES was affected by HO-2 KO disruption. We found that pharmacologically blocking of HO-activity by SnMP did not disturb palatal fusion or expression of Sox9, CXCR4, HO-1, and ALP-activity in the osteogenic regions.

Besides the absence of HO-activity, we did not further disturb the pregnancy by additional oxidative and inflammatory stress. Interestingly, HO-1 expression, but not HO-2, was found to rescue mesenchymal stem cells from H₂O₂-induced cell death *in vitro*¹²⁵. It is likely that the role of HO is underestimated when its function is studied only during normal physiological conditions. For future experiments we consider combining HO-activity inhibition with heme administration in different dose to study the effects of higher oxidative and inflammatory stress levels at palatal fusion. More research is needed to elucidate the relation between HO-activity and palatogenesis during stress-induced pathological pregnancy.

In our study, HO-2 abrogation demonstrated no increased fetal loss since both the HO-2 KO mice and wt mice showed a high fetal loss rate. Others found that HO-2 KO mice were fertile^{99,100}, although, no information was provided about the litter size. In another study, an increased abortion rate in mice was experimentally generated by lipopolysaccharide (LPS) injection at E18 in a dose-dependent fashion¹²⁶. A limitation of the present study was the relatively small number of wt E15 and HO-2 KO E15 fetuses. Although we tried to enhance the fertility by administration of the hormones Folligonan and Pregnyl before mating, only three out of seven plugged wt mice, and four out of seven plugged HO-2 KO mice carried fetuses. It is suggested that the low fertility and high fetal loss rate in our mice with mixed 129Sv x C57BL/6 background possibly have dominated the effects of HO-2 abrogation in this study. However, our data could not provide evidence for this statement. The low fertility could possibly be explained by the excessive inbreeding within the colony. For future studies this problem could be solved by breeding homozygous HO-2 knockouts with hybrid 129Sv x C57BL/6 wt mice. By breeding the resulting heterozygotes, wt and homozygous HO-2 KO mice would then be obtained. HO-activity inhibition from E11 was not found to increase the fetal loss rate compared to the controls. HO-activity inhibition by administration of zinc mesoporphyrin early in pregnancy in mice between E0-E6 was also found to increase the abortion rate^{84,127}. We demonstrated that HO-2 KO fetuses showed a reduced fetal body weight, but, interestingly, pharmacological blocking of HO-activity by SnMP administration at E11 resulted into a higher fetal body weight. This suggests that during implantation HO-activity promotes fetal growth, whereas HO-activity at later moments (E11-E16) inhibits embryonal growth. In fact, others showed that adult HO-2 KO mice were obese, induced by disrupted metabolic homeostasis, caused by insulin resistance and elevated blood pressure¹²⁸. It would then be interesting to investigate whether induction of HO-1 could indeed counteract this obesity. However, no difference in phenotype was found between HO-2 KO and wt mice by others¹²⁹. We hypothesize that

HO-activity is especially essential during implantation and early embryonic development, but stress-level-dependent in the later stages of fetal development.

In conclusion, our results support the hypothesis that CXCL12-CXCR4 interplay facilitates palatal osteogenesis during palatal fusion in mice. To the best of our knowledge, this is the first study demonstrating Sox9 and CXCL12 expression in the disintegrating MES and other palatal osteogenic centers. Neither CXCL12 expression during the MES disintegration nor palatal fusion was affected by HO-2 abrogation or inhibition of HO-activity. Further research is needed to unravel the role of cytoprotective HO-activity in the presence of additional oxidative and inflammatory stresses in relation to the development of craniofacial malformations, including palatal clefting.

References

1. Ito Y, Yeo JY, Chytil A, et al. Conditional inactivation of *Tgfb β 2* in cranial neural crest causes cleft palate and calvaria defects. *Development*. 2003;130(21):5269-5280.
2. Lee YH, Saint-Jeannet JP. Sox9 function in craniofacial development and disease. *Genesis*. 2011;49(4):200-208.
3. Birgfeld C, Heike C. Craniofacial Microsomia. *Clin Plast Surg*. 2019;46(2):207-221.
4. Chai Y, Jiang X, Ito Y, et al. Fate of the mammalian cranial neural crest during tooth and mandibular morphogenesis. *Development*. 2000;127(8):1671-1679.
5. Sakai D, Trainor PA. Treacher Collins syndrome: unmasking the role of *Tcof1*/treacle. *Int J Biochem Cell Biol*. 2009;41(6):1229-1232.
6. Achilleos A, Trainor PA. Neural crest stem cells: discovery, properties and potential for therapy. *Cell Res*. 2012;22(2):288-304.
7. Li M, Zhao C, Wang Y, Zhao Z, Meng A. Zebrafish *sox9b* is an early neural crest marker. *Dev Genes Evol*. 2002;212(4):203-206.
8. Cheung M, Briscoe J. Neural crest development is regulated by the transcription factor Sox9. *Development*. 2003;130(23):5681-5693.
9. Hong CS, Saint-Jeannet JP. Sox proteins and neural crest development. *Semin Cell Dev Biol*. 2005;16(6):694-703.
10. Wu T, Chen G, Tian F, Liu HX. Contribution of cranial neural crest cells to mouse skull development. *Int J Dev Biol*. 2017;61(8-9):495-503.
11. Yamashiro T, Wang XP, Li Z, et al. Possible roles of Runx1 and Sox9 in incipient intramembranous ossification. *J Bone Miner Res*. 2004;19(10):1671-1677.
12. Stockl S, Gottl C, Grifka J, Grassel S. Sox9 Modulates proliferation and expression of osteogenic markers of adipose-derived stem cells (ASC). *Cell Physiol Biochem*. 2013;31(4-5):703-717.
13. Loebel C, Czekanska EM, Bruderer M, Salzmann G, Alini M, Stoddart MJ. In vitro osteogenic potential of human mesenchymal stem cells is predicted by Runx2/Sox9 ratio. *Tissue Eng Part A*. 2015;21(1-2):115-123.
14. Rutkovskiy A, Stenslokken KO, Vaage IJ. Osteoblast Differentiation at a Glance. *Med Sci Monit Basic Res*. 2016;22:95-106.
15. Akiyama H, Chaboissier MC, Martin JF, Schedl A, de Crombrughe B. The transcription factor Sox9 has essential roles in successive steps of the chondrocyte differentiation pathway and is required for expression of Sox5 and Sox6. *Genes Dev*. 2002;16(21):2813-2828.
16. Akiyama H, Kim JE, Nakashima K, et al. Osteo-chondroprogenitor cells are derived from Sox9 expressing precursors. *P Natl Acad Sci USA*. 2005;102(41):14665-14670.
17. Hattori T, Muller C, Gebhard S, et al. SOX9 is a major negative regulator of cartilage vascularization, bone marrow formation and endochondral ossification. *Development*. 2010;137(6):901-911.
18. Guang LG, Boskey AL, Zhu W. Regulatory role of stromal cell-derived factor-1 in bone morphogenetic protein-2-induced chondrogenic differentiation in vitro. *Int J Biochem Cell Biol*. 2012;44(11):1825-1833.
19. Henry SP, Liang S, Akdemir KC, de Crombrughe B. The postnatal role of Sox9 in cartilage. *J Bone Miner Res*. 2012;27(12):2511-2525.
20. Jeon SY, Park JS, Yang HN, et al. Co-delivery of Cbfa-1-targeting siRNA and SOX9 protein using PLGA nanoparticles to induce chondrogenesis of human mesenchymal stem cells. *Biomaterials*. 2014;35(28):8236-8248.
21. Ito H. Chemokines in mesenchymal stem cell therapy for bone repair: a novel concept of recruiting mesenchymal stem cells and the possible cell sources. *Mod Rheumatol*. 2011;21(2):113-121.
22. Zhu W, Liang G, Huang Z, Doty SB, Boskey AL. Conditional inactivation of the CXCR4 receptor in osteoprecursors reduces postnatal bone formation due to impaired osteoblast development. *J Biol Chem*. 2011;286(30):26794-26805.
23. Shahnazari M, Chu V, Wronski TJ, Nissenson RA, Halloran BP. CXCL12/CXCR4 signaling in the osteoblast regulates the mesenchymal stem cell and osteoclast lineage populations. *FASEB J*. 2013;27(9):3505-3513.
24. Wang Y, Chen J, Fan W, et al. Stromal cell-derived factor-1 α and transforming growth factor- β 1 synergistically facilitate migration and chondrogenesis of synovium-derived stem cells through MAPK pathways. *Am J Transl Res*. 2017;9(5):2656-2667.
25. Reginensi A, Clarkson M, Neirijnck Y, et al. SOX9 controls epithelial branching by activating RET effector genes during kidney development. *Hum Mol Genet*. 2011;20(6):1143-1153.

26. Hosogane N, Huang Z, Rawlins BA, et al. Stromal derived factor-1 regulates bone morphogenetic protein 2-induced osteogenic differentiation of primary mesenchymal stem cells. *Int J Biochem Cell Biol.* 2010;42(7):1132-1141.
27. Li Z, Wang W, Xu H, et al. Effects of altered CXCL12/CXCR4 axis on BMP2/Smad/Runx2/Osterix axis and osteogenic gene expressions during osteogenic differentiation of MSCs. *Am J Transl Res.* 2017;9(4):1680-1693.
28. Liu C, Weng Y, Yuan T, et al. CXCL12/CXCR4 signal axis plays an important role in mediating bone morphogenetic protein 9-induced osteogenic differentiation of mesenchymal stem cells. *Int J Med Sci.* 2013;10(9):1181-1192.
29. Stein GS, Lian JB. Molecular mechanisms mediating proliferation/differentiation interrelationships during progressive development of the osteoblast phenotype. *Endocr Rev.* 1993;14(4):424-442.
30. Wennberg C, Hessel L, Lundberg P, et al. Functional characterization of osteoblasts and osteoclasts from alkaline phosphatase knockout mice. *J Bone Miner Res.* 2000;15(10):1879-1888.
31. Kortessidis A, Zannettino A, Isenmann S, Shi S, Lapidot T, Gronthos S. Stromal-derived factor-1 promotes the growth, survival, and development of human bone marrow stromal stem cells. *Blood.* 2005;105(10):3793-3801.
32. Watanabe M, Kawasaki K, Kawasaki M, et al. Spatio-temporal expression of Sox genes in murine palatogenesis. *Gene Expr Patterns.* 2016;21(2):111-118.
33. Potter AS, Potter SS. Molecular Anatomy of Palate Development. *PLoS One.* 2015;10(7):e0132662.
34. Xu J, Huang Z, Wang W, et al. FGF8 Signaling Alters the Osteogenic Cell Fate in the Hard Palate. *J Dent Res.* 2018;97(5):589-596.
35. Ferguson MWJ. Palate Development. *Development.* 1988;103:41-60.
36. Dudas M, Li WY, Kim J, Yang A, Kaartinen V. Palatal fusion - where do the midline cells go? A review on cleft palate, a major human birth defect. *Acta Histochem.* 2007;109(1):1-14.
37. Chai Y, Maxson RE, Jr. Recent advances in craniofacial morphogenesis. *Dev Dyn.* 2006;235(9):2353-2375.
38. Levi B, Brugman S, Wong VW, Grova M, Longaker MT, Wan DC. Palatogenesis: engineering, pathways and pathologies. *Organogenesis.* 2011;7(4):242-254.
39. Xu J, Wang L, Li H, et al. Shox2 regulates osteogenic differentiation and pattern formation during hard palate development in mice. *J Biol Chem.* 2019;294(48):18294-18305.
40. Oka K, Honda MJ, Tsuruga E, Hatakeyama Y, Isokawa K, Sawa Y. Roles of collagen and periostin expression by cranial neural crest cells during soft palate development. *J Histochem Cytochem.* 2012;60(1):57-68.
41. Meng L, Wang X, Torensma R, Von den Hoff JW, Bian Z. Lithium inhibits palatal fusion and osteogenic differentiation in palatal shelves in vitro. *Arch Oral Biol.* 2015;60(3):501-507.
42. Iseki S. Disintegration of the medial epithelial seam: is cell death important in palatogenesis? *Dev Growth Differ.* 2011;53(2):259-268.
43. Aoyama G, Kurosaka H, Oka A, et al. Observation of Dynamic Cellular Migration of the Medial Edge Epithelium of the Palatal Shelf in vitro. *Front Physiol.* 2019;10:698.
44. Logan SM, Benson MD. Medial epithelial seam cell migration during palatal fusion. *J Cell Physiol.* 2020;235(2):1417-1424.
45. Jin JZ, Ding J. Analysis of cell migration, transdifferentiation and apoptosis during mouse secondary palate fusion. *Development.* 2006;133(17):3341-3347.
46. Nawshad A. Palatal seam disintegration: to die or not to die? that is no longer the question. *Dev Dyn.* 2008;237(10):2643-2656.
47. Serrano MJ, Liu J, Svoboda KK, Nawshad A, Benson MD. Ephrin reverse signaling mediates palatal fusion and epithelial-to-mesenchymal transition independently of Tgfs3. *J Cell Physiol.* 2015;230(12):2961-2972.
48. Nakajima A, C FS, Gulka AOD, Hanai JI. TGF-beta Signaling and the Epithelial-Mesenchymal Transition during Palatal Fusion. *Int J Mol Sci.* 2018;19(11).
49. Lan Y, Xu J, Jiang R. Cellular and Molecular Mechanisms of Palatogenesis. *Curr Top Dev Biol.* 2015;115:59-84.
50. Suttrop CM, Cremers NA, van Rheden R, et al. Chemokine Signaling during Midline Epithelial Seam Disintegration Facilitates Palatal Fusion. *Front Cell Dev Biol.* 2017;5:94.
51. Wang Q, Kurosaka H, Kikuchi M, Nakaya A, Trainor PA, Yamashiro T. Perturbed development of cranial neural crest cells in association with reduced sonic hedgehog signaling underlies the pathogenesis of retinoic-acid-induced cleft palate. *Dis Model Mech.* 2019;12(10).

52. Al Ghafli MH, Padmanabhan R, Kataya HH, Berg B. Effects of alpha-lipoic acid supplementation on maternal diabetes-induced growth retardation and congenital anomalies in rat fetuses. *Mol Cell Biochem.* 2004;261(1-2):123-135.
53. Kim MS, Louis KM, Pedersen JA, Hamers RJ, Peterson RE, Heideman W. Using citrate-functionalized TiO₂ nanoparticles to study the effect of particle size on zebrafish embryo toxicity. *Analyst.* 2014;139(5):964-972.
54. de Peralta MS, Mouguelar VS, Sdrigotti MA, et al. Cnbp ameliorates Treacher Collins Syndrome craniofacial anomalies through a pathway that involves redox-responsive genes. *Cell Death Dis.* 2016;7(10):e2397.
55. Simpson WJ. A preliminary report on cigarette smoking and the incidence of prematurity. *Am J Obstet Gynecol.* 1957;73(4):807-815.
56. Andres RL. The association of cigarette smoking with placenta previa and abruptio placentae. *Semin Perinatol.* 1996;20(2):154-159.
57. Shah NR, Bracken MB. A systematic review and meta-analysis of prospective studies on the association between maternal cigarette smoking and preterm delivery. *Am J Obstet Gynecol.* 2000;182(2):465-472.
58. Ion R, Bernal AL. Smoking and Preterm Birth. *Reprod Sci.* 2015;22(8):918-926.
59. Parks WT. Placental hypoxia: the lesions of maternal malperfusion. *Semin Perinatol.* 2015;39(1):9-19.
60. Zadzinska E, Koziel S, Borowska-Struginska B, Rosset I, Sitek A, Lorkiewicz W. Parental smoking during pregnancy shortens offspring's legs. *Homo.* 2016;67(6):498-507.
61. Sakai D, Trainor PA. Face off against ROS: Tcof1/Treacle safeguards neuroepithelial cells and progenitor neural crest cells from oxidative stress during craniofacial development. *Dev Growth Differ.* 2016;58(7):577-585.
62. Ma ZL, Wang G, Cheng X, et al. Excess caffeine exposure impairs eye development during chick embryogenesis. *J Cell Mol Med.* 2014;18(6):1134-1143.
63. Jakobsen LP, Knudsen MA, Lespinasse J, et al. The genetic basis of the Pierre Robin Sequence. *Cleft Palate Craniofac J.* 2006;43(2):155-159.
64. Chen Y, Wang Z, Chen Y, Zhang Y. Conditional deletion of Bmp2 in cranial neural crest cells recapitulates Pierre Robin sequence in mice. *Cell Tissue Res.* 2019;376(2):199-210.
65. Spilson SV, Kim HJ, Chung KC. Association between maternal diabetes mellitus and newborn oral cleft. *Ann Plast Surg.* 2001;47(5):477-481.
66. Mossey PA, Little J, Munger RG, Dixon MJ, Shaw WC. Cleft lip and palate. *Lancet.* 2009;374(9703):1773-1785.
67. Brocardo PS, Gil-Mohapel J, Christie BR. The role of oxidative stress in fetal alcohol spectrum disorders. *Brain Res Rev.* 2011;67(1-2):209-225.
68. Nottoli T, Hagopian-Donaldson S, Zhang J, Perkins A, Williams T. AP-2-null cells disrupt morphogenesis of the eye, face, and limbs in chimeric mice. *Proc Natl Acad Sci U S A.* 1998;95(23):13714-13719.
69. Shin JO, Lee JM, Bok J, Jung HS. Inhibition of the Zeb family prevents murine palatogenesis through regulation of apoptosis and the cell cycle. *Biochem Biophys Res Commun.* 2018;506(1):223-230.
70. Shi M, Wehby GL, Murray JC. Review on genetic variants and maternal smoking in the etiology of oral clefts and other birth defects. *Birth Defects Res C Embryo Today.* 2008;84(1):16-29.
71. DeRoo LA, Wilcox AJ, Drevon CA, Lie RT. First-trimester maternal alcohol consumption and the risk of infant oral clefts in Norway: a population-based case-control study. *Am J Epidemiol.* 2008;168(6):638-646.
72. Correa A, Gilboa SM, Besser LM, et al. Diabetes mellitus and birth defects. *Am J Obstet Gynecol.* 2008;199(3):237 e231-239.
73. Chen X, Scholl TO. Oxidative stress: changes in pregnancy and with gestational diabetes mellitus. *Curr Diab Rep.* 2005;5(4):282-288.
74. Albano E. Alcohol, oxidative stress and free radical damage. *Proc Nutr Soc.* 2006;65(3):278-290.
75. Kamceva G, Arsova-Sarafinovska Z, Ruskovska T, Zdravkovska M, Kamceva-Panova L, Stikova E. Cigarette Smoking and Oxidative Stress in Patients with Coronary Artery Disease. *Open Access Maced J Med Sci.* 2016;4(4):636-640.
76. Kang P, Svoboda KK. Nicotine inhibits palatal fusion and modulates nicotinic receptors and the PI-3 kinase pathway in medial edge epithelia. *Orthod Craniofac Res.* 2003;6(3):129-142.

77. Ozturk F, Sheldon E, Sharma J, Canturk KM, Otu HH, Nawshad A. Nicotine Exposure During Pregnancy Results in Persistent Midline Epithelial Seam With Improper Palatal Fusion. *Nicotine Tob Res.* 2016;18(5):604-612.
78. Millicovsky G, Johnston MC. Hyperoxia and hypoxia in pregnancy: simple experimental manipulation alters the incidence of cleft lip and palate in CL/Fr mice. *Proc Natl Acad Sci U S A.* 1981;78(9):5722-5723.
79. Wagener FA, Volk HD, Willis D, et al. Different faces of the heme-heme oxygenase system in inflammation. *Pharmacol Rev.* 2003;55(3):551-571.
80. Grochot-Przeczek A, Dulak J, Jozkowicz A. Haem oxygenase-1: non-canonical roles in physiology and pathology. *Clin Sci (Lond).* 2012;122(3):93-103.
81. Gorlach A, Dimova EY, Petry A, et al. Reactive oxygen species, nutrition, hypoxia and diseases: Problems solved? *Redox Biol.* 2015;6:372-385.
82. Ewing JF, Maines MD. Regulation and expression of heme oxygenase enzymes in aged-rat brain: age related depression in HO-1 and HO-2 expression and altered stress-response. *J Neural Transm (Vienna).* 2006;113(4):439-454.
83. Zenclussen AC, Lim E, Knoeller S, et al. Heme oxygenases in pregnancy II: HO-2 is downregulated in human pathologic pregnancies. *Am J Reprod Immunol.* 2003;50(1):66-76.
84. Sollwedel A, Bertoja AZ, Zenclussen ML, et al. Protection from abortion by heme oxygenase-1 up-regulation is associated with increased levels of Bag-1 and neuropilin-1 at the fetal-maternal interface. *J Immunol.* 2005;175(8):4875-4885.
85. Bellner L, Martinelli L, Halilovic A, et al. Heme oxygenase-2 deletion causes endothelial cell activation marked by oxidative stress, inflammation, and angiogenesis. *J Pharmacol Exp Ther.* 2009;331(3):925-932.
86. Kapturczak MH, Wasserfall C, Brusko T, et al. Heme oxygenase-1 modulates early inflammatory responses: evidence from the heme oxygenase-1-deficient mouse. *Am J Pathol.* 2004;165(3):1045-1053.
87. Yoshida T, Maulik N, Ho YS, Alam J, Das DK. Hmox-1 constitutes an adaptive response to effect antioxidant cardioprotection - A study with transgenic mice heterozygous for targeted disruption of the heme oxygenase-1 gene. *Circulation.* 2001;103(12):1695-1701.
88. Liu X, Wei J, Peng DH, Layne MD, Yet SF. Absence of heme oxygenase-1 exacerbates myocardial ischemia/reperfusion injury in diabetic mice. *Diabetes.* 2005;54(3):778-784.
89. Li M, Kim DH, Tsenovoy PL, et al. Treatment of obese diabetic mice with a heme oxygenase inducer reduces visceral and subcutaneous adiposity, increases adiponectin levels, and improves insulin sensitivity and glucose tolerance. *Diabetes.* 2008;57(6):1526-1535.
90. Barbagallo I, Vanella A, Peterson SJ, et al. Overexpression of heme oxygenase-1 increases human osteoblast stem cell differentiation. *J Bone Miner Metab.* 2010;28(3):276-288.
91. Vanella L, Sanford C, Jr., Kim DH, Abraham NG, Ebraheim N. Oxidative stress and heme oxygenase-1 regulated human mesenchymal stem cells differentiation. *Int J Hypertens.* 2012;2012:890671.
92. Kim DH, Liu J, Bhat S, et al. Peroxisome proliferator-activated receptor delta agonist attenuates nicotine suppression effect on human mesenchymal stem cell-derived osteogenesis and involves increased expression of heme oxygenase-1. *J Bone Miner Metab.* 2013;31(1):44-52.
93. Guo S, Fei HD, Ji F, Chen FL, Xie Y, Wang SG. Activation of Nrf2 by MIND4-17 protects osteoblasts from hydrogen peroxide-induced oxidative stress. *Oncotarget.* 2017;8(62):105662-105672.
94. Cheng J, Wang H, Zhang Z, Liang K. Stilbene glycoside protects osteoblasts against oxidative damage via Nrf2/HO-1 and NF-kappaB signaling pathways. *Arch Med Sci.* 2019;15(1):196-203.
95. Gu Q, Cai Y, Huang C, Shi Q, Yang H. Curcumin increases rat mesenchymal stem cell osteoblast differentiation but inhibits adipocyte differentiation. *Pharmacogn Mag.* 2012;8(31):202-208.
96. Kook YA, Lee SK, Son DH, et al. Effects of substance P on osteoblastic differentiation and heme oxygenase-1 in human periodontal ligament cells. *Cell Biol Int.* 2009;33(3):424-428.
97. Valaes T, Petmezaki S, Henschke C, Drummond GS, Kappas A. Control of jaundice in preterm newborns by an inhibitor of bilirubin production: studies with tin-mesoporphyrin. *Pediatrics.* 1994;93(1):1-11.
98. Zenclussen ML, Casalis PA, El-Mouseh T, et al. Haem oxygenase-1 dictates intrauterine fetal survival in mice via carbon monoxide. *J Pathol.* 2011;225(2):293-304.
99. Lundvig DM, Scharstuhl A, Cremers NA, et al. Delayed cutaneous wound closure in HO-2 deficient mice despite normal HO-1 expression. *J Cell Mol Med.* 2014;18(12):2488-2498.

100. Poss KD, Thomas MJ, Ebralidze AK, O'Dell TJ, Tonegawa S. Hippocampal long-term potentiation is normal in heme oxygenase-2 mutant mice. *Neuron*. 1995;15(4):867-873.
101. Behringer R, Gertsenstein M, Nagy KV, Nagy A. Selecting Female Mice in Estrus and Checking Plugs. *Cold Spring Harb Protoc*. 2016;2016(8).
102. Stevenson DK, Rodgers PA, Vreman HJ. The use of metalloporphyrins for the chemoprevention of neonatal jaundice. *Am J Dis Child*. 1989;143(3):353-356.
103. Lutton JD, Jiang S, Drummond GS, Abraham NG, Kappas A. Comparative pharmacology of zinc mesoporphyrin and tin mesoporphyrin: toxic actions of zinc mesoporphyrin on hematopoiesis and progenitor cell mobilization. *Pharmacology*. 1999;58(1):44-50.
104. Faul F, Erdfelder E, Lang AG, Buchner A. G*Power 3: a flexible statistical power analysis program for the social, behavioral, and biomedical sciences. *Behav Res Methods*. 2007;39(2):175-191.
105. Rosa AL, Beloti MM, van Noort R. Osteoblastic differentiation of cultured rat bone marrow cells on hydroxyapatite with different surface topography. *Dent Mater*. 2003;19(8):768-772.
106. George J, Kuboki Y, Miyata T. Differentiation of mesenchymal stem cells into osteoblasts on honeycomb collagen scaffolds. *Biotechnol Bioeng*. 2006;95(3):404-411.
107. Tan SD, Xie R, Klein-Nulend J, et al. Orthodontic force stimulates eNOS and iNOS in rat osteocytes. *J Dent Res*. 2009;88(3):255-260.
108. Gilbert W, Bragg R, Elmansi AM, et al. Stromal cell-derived factor-1 (CXCL12) and its role in bone and muscle biology. *Cytokine*. 2019;123:154783.
109. Tzeng YS, Chung NC, Chen YR, Huang HY, Chuang WP, Lai DM. Imbalanced Osteogenesis and Adipogenesis in Mice Deficient in the Chemokine Cxcl12/Sdf1 in the Bone Mesenchymal Stem/Progenitor Cells. *J Bone Miner Res*. 2018;33(4):679-690.
110. Kitaori T, Ito H, Schwarz EM, et al. Stromal cell-derived factor 1/CXCR4 signaling is critical for the recruitment of mesenchymal stem cells to the fracture site during skeletal repair in a mouse model. *Arthritis Rheum*. 2009;60(3):813-823.
111. Ma Q, Jones D, Borghesani PR, et al. Impaired B-lymphopoiesis, myelopoiesis, and derailed cerebellar neuron migration in CXCR4- and SDF-1-deficient mice. *P Natl Acad Sci USA*. 1998;95(16):9448-9453.
112. Guang LG, Boskey AL, Zhu W. Age-related CXC chemokine receptor-4-deficiency impairs osteogenic differentiation potency of mouse bone marrow mesenchymal stromal stem cells. *Int J Biochem Cell Biol*. 2013;45(8):1813-1820.
113. Zhang Y, Depond M, He L, et al. CXCR4/CXCL12 axis counteracts hematopoietic stem cell exhaustion through selective protection against oxidative stress. *Sci Rep*. 2016;6:37827.
114. Jakobsen LP, Borup R, Vestergaard J, et al. Expression analyses of human cleft palate tissue suggest a role for osteopontin and immune related factors in palatal development. *Exp Mol Med*. 2009;41(2):77-85.
115. Zhang S, Che DH, Yang F, et al. Tumor-associated macrophages promote tumor metastasis via the TGF-beta/SOX9 axis in non-small cell lung cancer. *Oncotarget*. 2017;8(59):99801-99815.
116. Huang JQ, Wei FK, Xu XL, et al. SOX9 drives the epithelial-mesenchymal transition in non-small-cell lung cancer through the Wnt/beta-catenin pathway. *J Transl Med*. 2019;17(1):143.
117. Kogata N, Bland P, Tsang M, Oliemuller E, Lowe A, Howard BA. Sox9 regulates cell state and activity of embryonic mouse mammary progenitor cells. *Commun Biol*. 2018;1:228.
118. Li T, Huang H, Shi G, et al. TGF-beta1-SOX9 axis-inducible COL10A1 promotes invasion and metastasis in gastric cancer via epithelial-to-mesenchymal transition. *Cell Death Dis*. 2018;9(9):849.
119. Choi BJ, Park SA, Lee SY, Cha YN, Surh YJ. Hypoxia induces epithelial-mesenchymal transition in colorectal cancer cells through ubiquitin-specific protease 47-mediated stabilization of Snail: A potential role of Sox9. *Sci Rep*. 2017;7(1):15918.
120. Kawai T, Yasuchika K, Ishii T, et al. SOX9 is a novel cancer stem cell marker surrogated by osteopontin in human hepatocellular carcinoma. *Sci Rep*. 2016;6:30489.
121. Huang J, Guo L. Knockdown of SOX9 Inhibits the Proliferation, Invasion, and EMT in Thyroid Cancer Cells. *Oncol Res*. 2017;25(2):167-176.
122. Sakai D, Suzuki T, Osumi N, Wakamatsu Y. Cooperative action of Sox9, Snail2 and PKA signaling in early neural crest development. *Development*. 2006;133(7):1323-1333.
123. Suliman HB, Keenan JE, Piantadosi CA. Mitochondrial quality-control dysregulation in conditional HO-1(-/-) mice. *JCI Insight*. 2017;2(3):e89676.

124. Kreiser D, Nguyen X, Wong R, et al. Heme oxygenase-1 modulates fetal growth in the rat. *Lab Invest.* 2002;82(6):687-692.
125. Cremers NA, Lundvig DM, van Dalen SC, et al. Curcumin-induced heme oxygenase-1 expression prevents H₂O₂-induced cell death in wild type and heme oxygenase-2 knockout adipose-derived mesenchymal stem cells. *Int J Mol Sci.* 2014;15(10):17974-17999.
126. Toyama RP, Xikota JC, Schwarzbald ML, et al. Dose-dependent sickness behavior, abortion and inflammation induced by systemic LPS injection in pregnant mice. *J Matern Fetal Neonatal Med.* 2015;28(4):426-430.
127. Schumacher A, Wafula PO, Teles A, et al. Blockage of heme oxygenase-1 abrogates the protective effect of regulatory T cells on murine pregnancy and promotes the maturation of dendritic cells. *PLoS One.* 2012;7(8):e42301.
128. Cao J, Puri N, Sodhi K, Bellner L, Abraham NG, Kappas A. Apo A1 Mimetic Rescues the Diabetic Phenotype of HO-2 Knockout Mice via an Increase in HO-1 Adiponectin and LKBI Signaling Pathway. *Int J Hypertens.* 2012;2012:628147.
129. Qu Y, Chen J, Benvenisti-Zarom L, Ma X, Regan RF. Effect of targeted deletion of the heme oxygenase-2 gene on hemoglobin toxicity in the striatum. *J Cereb Blood Flow Metab.* 2005;25(11):1466-1475.

Part II

Diminished cytoprotection by inhibition of HO-activity in mice promotes heme-induced placental inflammation and abortion

CHAPTER 4

Heme oxygenase protects against placental vascular inflammation and abortion by the alarmin heme in mice

Suttorp CM, van Rheden REM, van Dijk NWM, Helmich MPAC, Kuijpers-Jagtman AM, Wagener FADTG.

Int J Mol Sci. 2020 Jul 29;21(15):5385.

Abstract

Both infectious as non-infectious inflammation can cause placental dysfunction and pregnancy complications. During the first trimester of human gestation, when palatogenesis takes place, intrauterine hematoma and hemorrhage are common phenomena, causing the release of large amounts of heme, a well-known alarmin. We postulated that exposure of pregnant mice to heme during palatogenesis would initiate oxidative and inflammatory stress, leading to pathological pregnancy, increasing the incidence of palatal clefting and abortion. Both heme oxygenase isoforms (HO-1 and HO-2) break down heme, thereby generating anti-oxidative and -inflammatory products. HO may thus counteract these heme-induced injurious stresses. To test this hypothesis, we administered heme to pregnant CD1 outbred mice at Day E12 by intraperitoneal injection in increasing doses: 30, 75 or 150 $\mu\text{mol/kg}$ body weight (30H, 75H or 150H) in the presence or absence of HO-activity inhibitor SnMP from Day E11. Exposure to heme resulted in a dose-dependent increase in abortion. At 75H half of the fetuses were resorbed, while at 150H all fetuses were aborted. HO-activity protected against heme-induced abortion since inhibition of HO-activity aggravated heme-induced detrimental effects. The fetuses surviving heme administration demonstrated normal palatal fusion. Immunostainings at Day E16 demonstrated higher numbers of ICAM-1 positive blood vessels, macrophages and HO-1 positive cells in placenta after administration of 75H or SnMP + 30H. Summarizing, heme acts as an endogenous “alarmin” during pregnancy in a dose-dependent fashion, while HO-activity protects against heme-induced placental vascular inflammation and abortion.

Keywords: embryology, cleft palate, abortion, placenta, vascular inflammation, heme, heme oxygenase, oxidative stress, inflammatory stress, ICAM-1, macrophage.

Abbreviations

ABC	Avidin-biotin peroxidase complex
ANOVA	Analysis of variance
BCRP	Breast Cancer Resistance Protein
CLP	Cleft lip and palate
CO	Carbon monoxide
DAB	Diaminobenzidine-peroxidase
DPX	Distyrene plasticizer xylene
E0	Gestational/Embryonic day 0
F4/80	EGF-like module-containing mucin-like hormone receptor-like 1
HCl	Hydrochloric acid
HE	Haematoxylin and eosin
HO	Heme oxygenase
Hp	Haptoglobin
Hpx	Hemopexin
ICAM-1	Intercellular adhesion molecule-1
IL-1 β	Interleukine-1 beta
KO	Knockout
KS-test	Kolmogorov-Smirnov test
LPS	Lipopolysaccharide
LRP1	Low density lipoprotein receptor-related protein 1
MAP	Morbidly Adherent Placenta
MES	Midline epithelial seam
NDS	Normal donkey serum
NF- κ B	Nuclear factor kappa B
Nrf2	Nuclear factor (erythroid-derived 2)-like 2
PBSG	Phosphate-buffered saline with glycine
PGE ₂	Prostaglandin E ₂
PIF	Pre-Implantation Factor
SD	Standard deviation
SnMP	Tin mesoporphyrin
TLR-4	Toll-like receptor-4
TNF α	Tumor necrosis factor-alfa
Wt	Wild-type

Introduction

Cleft lip and palate (CLP) is a serious orofacial birth defect affecting approximately 1/750 newborns worldwide with ethnic and geographical variation¹. CLP is associated with various problems related to facial growth, feeding, speech, hearing and psychosocial status². Palatogenesis is a dynamic and complex process and requires elevation, growth and adhesion of both palatal shelves, formation of the midline epithelial seam (MES), disintegration of this MES and arrangement of mesenchymal confluence. Failure of one of these events results in palatal clefting^{3,4}. Both genetic and environmental factors play a role in the etiology of CLP⁵. Environmental factors such as infections, maternal smoking and alcohol use may increase the risk of congenital abnormalities, including CLP^{6,7}. Both infectious and non-infectious placental inflammation can cause pregnancy complications and poor perinatal outcome⁸.

During the first trimester of human gestation, intrauterine hematoma is commonly present^{9,10}, causing the release of large amounts of the alarmin heme^{11,12}. We and others previously demonstrated that this free heme is responsible for a wide variety of inflammatory pathologies, including adverse effects in sickle cell disease, malaria, sepsis and kidney failure¹³⁻¹⁷. Heme was revealed to have the potential of threatening vascular endothelial cells¹⁸, and oxidation of hemoglobin to methemoglobin was shown to lead to the liberation of heme moieties¹⁹, triggering a pro-oxidant and cytotoxic environment in the vasculature^{20,21}. Oxidation of heme to ferryl state also provokes inflammatory response^{22,23}. Free heme administration was found to generate vascular oxidative and inflammatory stress following TLR4 activation, resulting in hampered wound repair, intrauterine fetal growth restriction and fetal abortion^{11,24-27}. Intrauterine hematoma/hemorrhage is associated with an increased risk of early and late pregnancy loss²⁸, although its volume, location, gestational age, duration and the presence of vaginal bleeding determine the pregnancy outcome^{9,29,30}.

To protect against the adverse effects of free heme diverse defense systems are present. Free hemoglobin and heme molecules are first scavenged by haptoglobin (Hp) and hemopexin (Hpx), respectively^{31,32}, whereas the Breast Cancer Resistance Protein (BCRP) may further protect against heme-induced toxicity by exporting heme molecules across the plasma membrane¹⁷. The injurious effects of free heme molecules may also be counteracted by the antioxidant enzyme system heme oxygenase (HO)³³. HO is a key regulator during embryonic development including placentation, spiral artery remodeling and blood pressure control^{25,34,35}. Reduced HO-activity in the human placenta is associated with placental inflammation, including expression of adhesion molecules, influx of inflammatory cells, pre-eclampsia, fetal growth retardation and even abortion^{34,36-38}. HO-1 is the highly inducible isoform, while HO-2 is constitutively expressed³⁹. We previously demonstrated that abrogation of HO-2 expression in mice led to fetal growth restriction and craniofacial anomalies⁴⁰.

By degrading heme, the HO system generates the products free iron/ferritin, carbon monoxide (CO), and biliverdin/bilirubin^{32,34}. These HO effector molecules upregulate vasodilation and anti-apoptotic signaling, inhibit platelet aggregation and reduce leukocyte adhesion and pro-inflammatory cytokine expression³⁸. Heme release following kidney surgery in mice was found to activate the inflammasome in macrophages by inducing the cytokine IL-1 β ⁴¹, while HO-1 inhibited the induction of IL-1 β in acute inflammatory arthritis in mice⁴².

We postulate that exposure of pregnant mice to heme during palatogenesis initiates oxidative and inflammatory stress, leading to pathological pregnancy, increasing the incidence of palatal clefting and abortion. We expect that HO-activity protects against heme-induced pregnancy pathology, while HO-activity inhibitors exacerbate heme-induced inflammatory insults.

Materials and Methods

Mice selection, mating, housing, ethical permission

To obtain fetuses for this study, plugged CD1 outbred mice, 12–17 weeks of age, were purchased from Envigo, Venray, The Netherlands ($n = 31$), and from Charles River, Sulzfeld, Germany ($n = 7$). At the facility of the animal supplier, the female mice were mated with CD1 outbred male mice for 1 day and checked for the presence of a vaginal copulation plug on the next morning, taken as Day 0 of pregnancy (Gestational/Embryonic Day 0, E0)⁴³. The plugged animals were transported to our animal facility and housed under specific pathogen-free housing conditions with 12 h light/dark cycle and ad libitum access to water and powdered rodent chow (Sniff, Soest, The Netherlands). The animals could acclimatize for at least 1 week before the start of the experiment. All mice were randomly assigned to the control or experimental groups by drawing lots. Ethical permission for the study was obtained according to the guidelines of the Board for Animal Experiments of the Radboud University Nijmegen (Ethical permission # RU-DEC 2012-166; date: 20 August 2012).

Heme and/or SnMP administration, sample size, animal welfare monitoring

To investigate palatal clefting, fetuses should be studied beyond the time point palatal fusion takes place. In wt mice the palatal shelves fuse between embryonic Day E14.5 and E15.5, and the capacity to fuse is lost after Day E16⁴⁴. Fetuses of Day E16 were therefore considered suitable for studying palatal clefting.

Plugged CD1 females were subdivided for the heme administration in different doses: 30, 75 or 150 $\mu\text{mol/kg}$ body weight (referred to as heme 30H, 75H and 150H, respectively). Heme was administered via intraperitoneal (i.p.) injection at Day E12, see **Figure 1**.

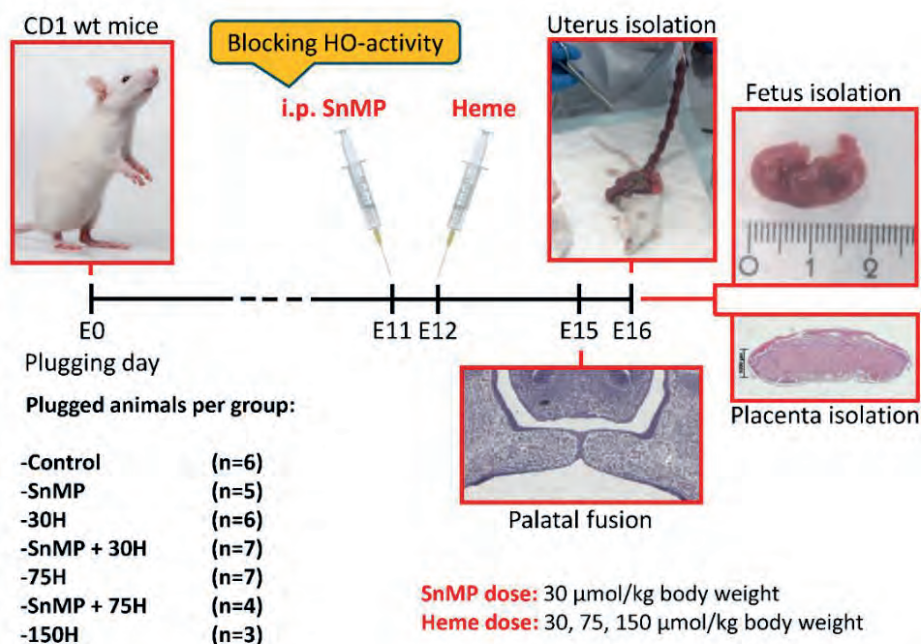


Figure 1. Administration of heme and/or SnMP in plugged mice via intraperitoneal injection. Plugged mice received SnMP (30 $\mu\text{mol/kg}$ body weight) at Day E11 and/or heme in different dose (30, 75 and 150 $\mu\text{mol/kg}$ body weight) at Day E12 by intraperitoneal (i.p.) injection. All plugged mice were killed by CO_2/O_2 inhalation for 10 min at Day E16; the uteri were removed; and the fetuses and placentas were isolated. The first animals that received administration of SnMP + 75H ($n = 4$) or 150H ($n = 3$) demonstrated resorption of all fetuses. Since no fetuses could be obtained, the remaining animals of both groups ($n = 4$) were reassigned to the SnMP + 30H group and 75H group. The plugged animals were eventually divided into 7 groups as follows: control $n = 6$, SnMP $n = 5$, 30H $n = 6$, SnMP + 30H $n = 7$, 75H $n = 7$, SnMP + 75H $n = 4$, 150H $n = 3$. In total, 38 uteri were removed. In 1 mouse from the SnMP group, 2 mice from the 30H group and 2 mice from the SnMP + 30H group, no non-viable/hemorrhagic embryonic implantations or fetuses were found in the uterus, and those animals were regarded as not pregnant. Furthermore, in 2 mice of the 75H group, total abortion had occurred. Finally, from 24 mice (control $n = 6$, SnMP $n = 4$, 30H $n = 4$, SnMP + 30H $n = 5$, 75H $n = 5$) in total, 294 fetuses and placentas were obtained (control $n = 91$, SnMP $n = 56$, 30H $n = 43$, SnMP + 30H $n = 58$, 75H $n = 46$).

Tin mesoporphyrin (SnMP) can bind strongly to the HO-1 and HO-2 enzyme, but cannot be broken down by both isotypes, therefore acting as a competitive inhibitor of HO-activity^{45,46}. To abrogate the HO system prior to heme administration half of the animals of the 30H and 75H groups received SnMP 30 $\mu\text{mol/kg}$ body weight (later referred to as SnMP) via i.p. injection at E11.

In addition, the control group received neither heme nor SnMP, while another group received SnMP only. Heme and SnMP were purchased from Frontier Scientific, Carnforth, UK.

Heme and SnMP were freshly dissolved with Trizma base. The pH was adjusted to pH 7.6–8.0 with HCl. The heme and SnMP solution were filter sterilized before administration.

To detect an effect size of 0.25 (generalized estimation of the reduction in fetal and placental weight in the experimental groups) and a significance level of 0.05 for the 7 groups with power of 0.80, a total sample size of $n = 231$ fetuses for this study was calculated by the one-way ANOVA power analysis *a priori* (G*Power 3.1 software)⁴⁷. This indicated that the mean sample size per group should comprise approximately 33 fetuses.

We estimated that the litter size could range from 14 to 18 pups, suggesting that each group should contain at least 3 pregnant mice. The chance of conception was assumed to be around 70%, indicating that for each group at least 5 mice should be mated.

Animal welfare was monitored daily during the stay at our animal facility, and the degree of discomfort after administration was scored according to the guidelines of the Board for Animal Experiments of the Radboud University Nijmegen.

Adult mouse body weight comparison

At embryonic Days E12 and E15, the plugged mice were weighed. The body weight comparison, the percentage of the weight change between Days E12 and E15, of the pregnant mice, not pregnant mice and the mice that demonstrated total abortion was calculated. The status pregnant, not pregnant or total abortion was confirmed by examination of the uterus.

Fetal loss rate and fetal number calculation

At Day E16, the animals were killed by CO₂/O₂ inhalation for 10 min. All fetuses were isolated from the uterus, see **Figure 2A**. The fetuses were separated from the placentas. For the fetus-carrying mice, the fetal loss rate, the percentage of non-viable and hemorrhagic embryonic implantations to the total number of embryonic implantations (non-viable or hemorrhagic embryonic implantations + fetuses), and the fetal number were calculated.

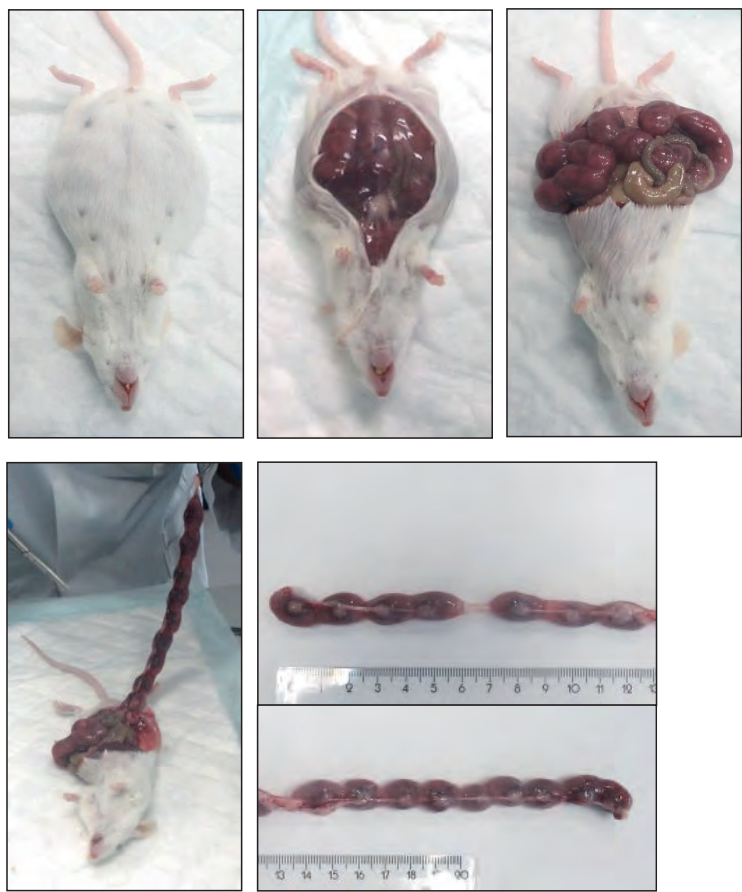
Placental weight and fetal body weight and length

All fetuses and placentas were weighed. The body length of the fetuses was measured on photographs using Fiji Image J 1.51n software (National Institutes of Health, Bethesda, MD, USA), see **Figure 2B**.

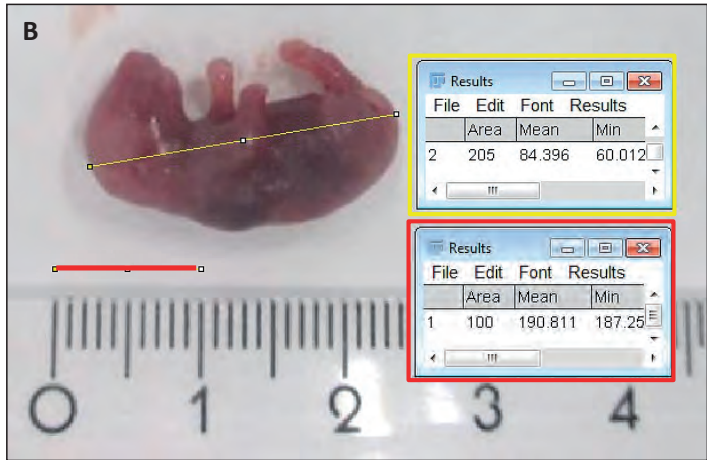
Paraffin embedding and selection cutting of head and placenta samples

The fetuses were decapitated, the head samples and placentas were fixed for 24 h in 4% paraformaldehyde and further processed for routine paraffin embedding. Serial coronal sections of 5- μ m thickness, through the secondary palate in head samples and through the middle part of the placenta, were mounted on Superfrost Plus slides (Menzel-Gläser, Braunschweig, Germany).

A



B



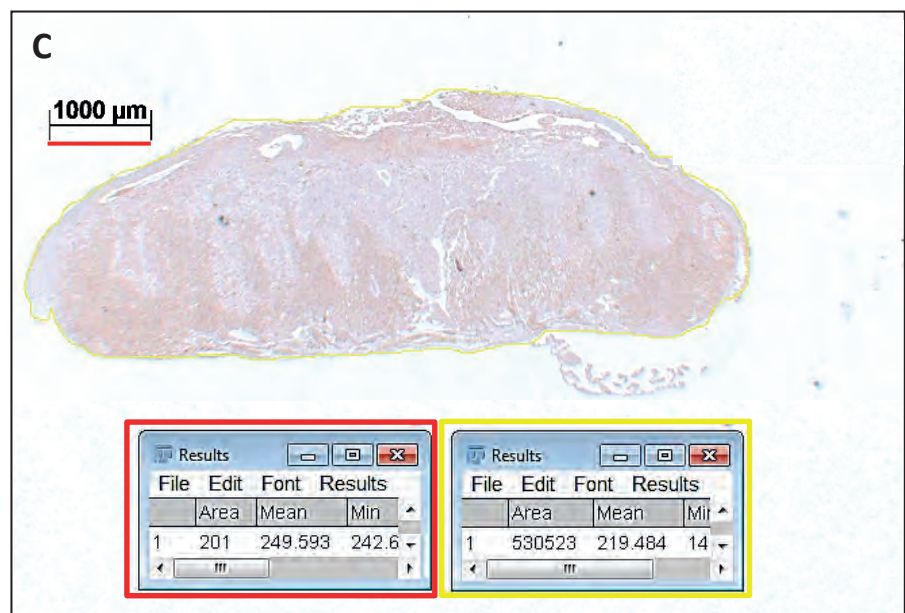


Figure 2. Isolation of fetuses and placentas and measurement of fetal body length and placental section surface area. (A) After sacrifice of the plugged mice at Day E16, the uteri were isolated (centimeter ruler). (B) The fetuses were separated from the placentas, photographed and a scale bar was drawn at the centimeter ruler of 10 mm, and the total number of pixels of the bar was determined (e.g., 30H; 100 pixels). A line depicting the length of the body of the fetus was drawn and the number of pixels was recorded (e.g., 205 pixels). The body length was calculated (e.g., 205/100 = 2.05 cm). (C) Placental sections surface area measurement. Coronal sections through the middle of the placenta (e.g., SnMP and ICAM-1 immunostaining). A scale bar was drawn at the ruler in each photograph of 1000 µm and the total number of pixels of the bar was determined (e.g., 201 pixels). The surface of 1000 µm x 1000 µm (1mm²) included the total number of 40,401 (201 x 201) pixels. The outline of the total placenta was drawn, and the number of pixels was recorded (e.g., 530,523 pixels). Next, the total section surface was calculated (e.g., 530,523/40,401 = 13.1 mm²).

Hematoxylin-Eosin staining of palatal sections and immunohistochemical stainings of placental sections

Selected paraffin embedded palatal and placental sections were deparaffinized using Histosafe (Adamas Instruments B.V., Rhenen, The Netherlands) and rehydrated using ethanol (100-96%). Then, the endogenous peroxidase quenching step with 3% hydrogen peroxide in methanol was performed, followed by further rehydration by ethanol 96% till PBS. The palatal sections were routinely stained with Hematoxylin and Eosin (HE). Antigens were retrieved with citrate buffer at 70°C for 10 min, followed by incubation in 0.015% trypsin in PBS at 35 °C for 5 min. Next, the placental sections were pre-incubated with 10% normal donkey serum (NDS) in phosphate-buffered saline with glycine (PBSG). Primary antibodies (**Table 1**) for cytokine IL-1β, vascular adhesion molecule-1 (ICAM-1), macrophage marker F4/80⁴⁸ and HO-1 were diluted in 2% NDS in PBSG and incubated overnight at 4°C. After washing with PBSG, sections were incubated for 60 min with a biotin-labeled secondary antibody (**Table 2**), as previously

described⁴⁹. Next, the sections were washed with PBSG and treated with avidin-biotin peroxidase complex (ABC) for 45 min in the dark. After extensive washing with PBSG, diaminobenzidine (DAB)-peroxidase staining was performed for 10 min. Finally, the nuclei were counterstained with Hematoxylin for 10 s and sections were rinsed for 10 min in water, dehydrated and embedded in distyrene plasticizer xylene (DPX).

Microscopic photographs of the HE and immunohistochemical stained sections were taken using a Carl Zeiss Imager Z.1 system (Carl Zeiss Microimaging GmbH, Jena, Germany) with AxioVision 4.8 v software (Zeiss, Göttingen, Germany).

The palatal sections were classified into 4 stages of palatogenesis based on the anatomy of the palatal shelves, as previously described by Dudas et al.⁴⁴. Per individual fetus, the presence of palatal fusion was studied on multiple transversal sections.

Table 1. Primary antibodies used for immunohistochemical staining for IL-1 β , ICAM-1, F4/80 and HO-1. Source and used concentrations of the antibodies are described.

First Antibody	Specificity	Concentration ($\mu\text{g/mL}$)	Source
sc-1252	IL-1B	0.2	Santa Cruz Biotechnology, Santa Cruz, CA, USA
CD54	ICAM-1	0.34	Proteintech via Sanbio, Uden, The Netherlands
A3-1 (ab6640)	F4/80	1.0	Abcam Cambridge Biomedical Campus, Cambridge, UK
SPA 895	HO-1	1.0	Stressgen, Victoria, BC, USA

Table 2. Secondary antibodies used for immunohistochemical staining for IL-1 β , ICAM-1, F4/80 and HO-1. Source and used concentrations of the antibodies are described.

Secondary Antibody	Specificity	Concentration ($\mu\text{g/mL}$)	Source
705-065-147	Donkey anti-goat Biotin	2.8	Jackson ImmunoResearch West Grove, PA, USA
711-065-147	Donkey anti-rabbit Biotin	2.0	Jackson ImmunoResearch West Grove, PA, USA
712-065-153	Donkey anti-rat Biotin	4.6	Jackson ImmunoResearch West Grove, PA, USA
711-065-147	Donkey anti-rabbit Biotin	2.0	Jackson ImmunoResearch West Grove, PA, USA

Quantification of IL-1 β , ICAM-1, F4/80 and HO-1 immunoreactivity in placental sections

Because the transversal sections through the middle of the placenta showed a significant variance in size, immunoreactivity was adjusted to surface area. The specific surface area per placental section was measured using Fiji Image J 1.51n software, see

Figure 2C. The number of IL-1 β and ICAM-1 positive blood vessels and the number of F4/80 (macrophages) and HO-1 positive cells within the outline of the placental sections were counted, and the mean number per mm² per group was calculated.

The counting was performed twice, by two observers (C.M.S. and F.A.D.T.G.W.), independently and blinded for the groups. The inter- and intra-examiner reliability was determined

Statistical analysis

The data for fetal loss rate, adult mouse body weight comparison, the number of ICAM-1 positive blood vessels/mm² and macrophages/mm² in placental sections were quantitatively scored and showed a normal distribution as evaluated by the Kolmogorov–Smirnov test (KS-test). The data were analyzed using ANOVA and Tukey's multiple comparison *post hoc* test to compare the differences between the groups.

The data for fetal number, placenta weight, fetal body weight, fetal body length, the number of IL-1 β positive blood vessels/mm² and HO-1 positive cells/mm² in placental sections were quantitatively scored and showed a non-normal distribution as evaluated by the KS-test. The data were analyzed using the non-parametric Kruskal–Wallis ANOVA on ranks test and Dunn's Multiple Comparison *post hoc* test to compare differences between the groups.

To determine the inter- and intra-examiner reliability, the coefficient of determination (R^2) was calculated by the square of the Pearson correlation coefficient, and acceptable scores > 0.80 were obtained for the counting.

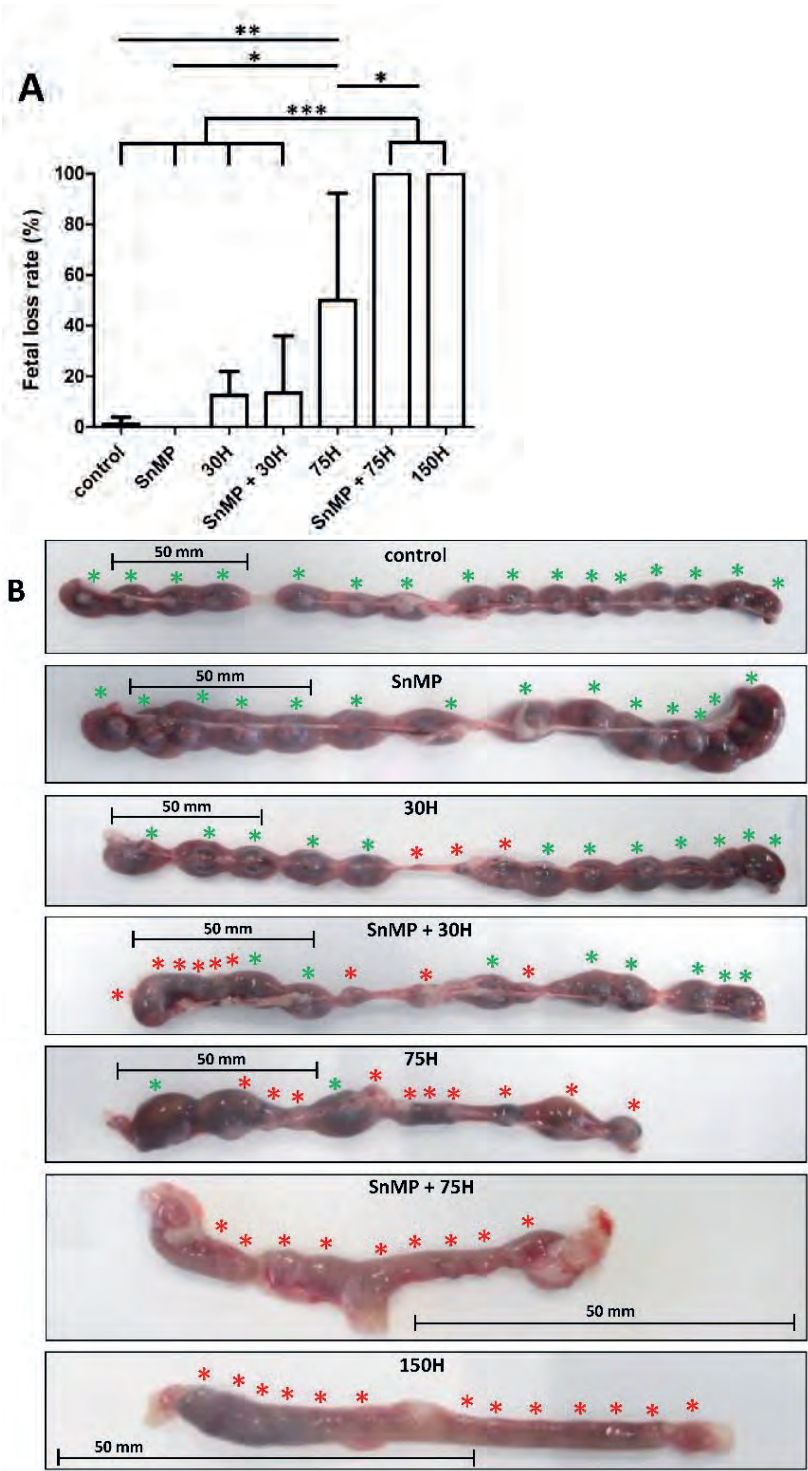
Differences were considered significant if $p < 0.05$. All statistical analyses of the data were performed using GraphPad Prism 5.03 software (GraphPad Software Inc.©, San Diego, CA, USA).

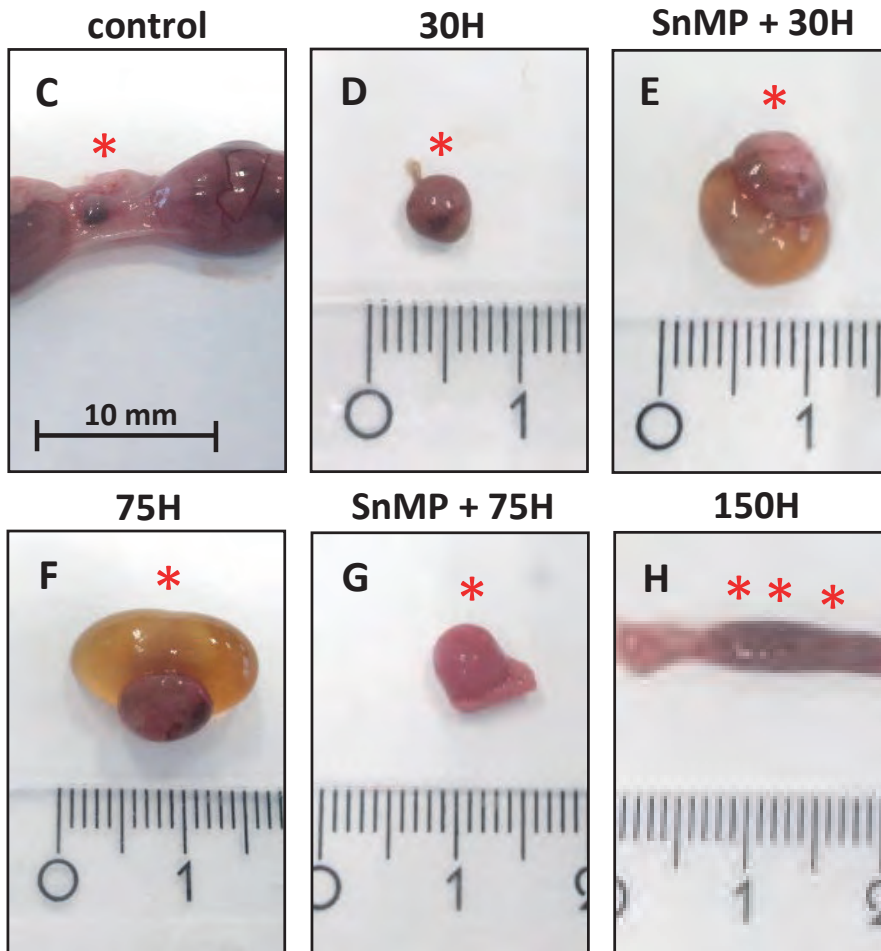
Results

HO-activity protects against heme-induced abortion

We studied the consequences of HO-activity inhibition and the dose-dependent effects of heme administration on fetal development in mice. Higher fetal loss rate was found in the 75H group ($p < 0.01$) compared to the control group where just one fetal resorption in total was found, see **Figure 3**.

In both the 150H group ($p < 0.001$) and SnMP + 75H group ($p < 0.001$), only abortions were observed, which was significantly more compared to the 75H group. In mice receiving SnMP, no abortions were found.





mice determined at E16, compared for the different heme and/or SnMP administrations (control $n = 6$; SnMP $n = 4$; 30H $n = 4$; SnMP + 30H $n = 5$; 75H $n = 7$; SnMP + 75H $n = 4$; 150H $n = 3$). Data are shown as mean \pm SD. * $p < 0.05$, ** $p < 0.01$, *** $p < 0.001$. (B) The isolated uteri were photographed, the green asterisk indicated a fetus, the red asterisk indicated a fetal resorption. A representative uterus per group is shown. (C–G) Isolated fetal resorptions from different groups (centimeter ruler). Fetal resorption showing an amniotic sac that contained an abnormal yellow-brownish pigmentation of the amniotic fluid (E,F), characteristic for the presence of free heme molecules. (H) Part of the uterus containing an amorphous mass because of total abortion (centimeter ruler).

The observed total abortions corresponded with the body weight of the plugged mice between Days E12 and E15, see **Figure 4**. As expected, compared to the non-pregnant mice, the pregnant mice showed an increase in body weight ($p < 0.001$), whereas mice that demonstrated total abortion showed body weight reduction ($p < 0.01$).

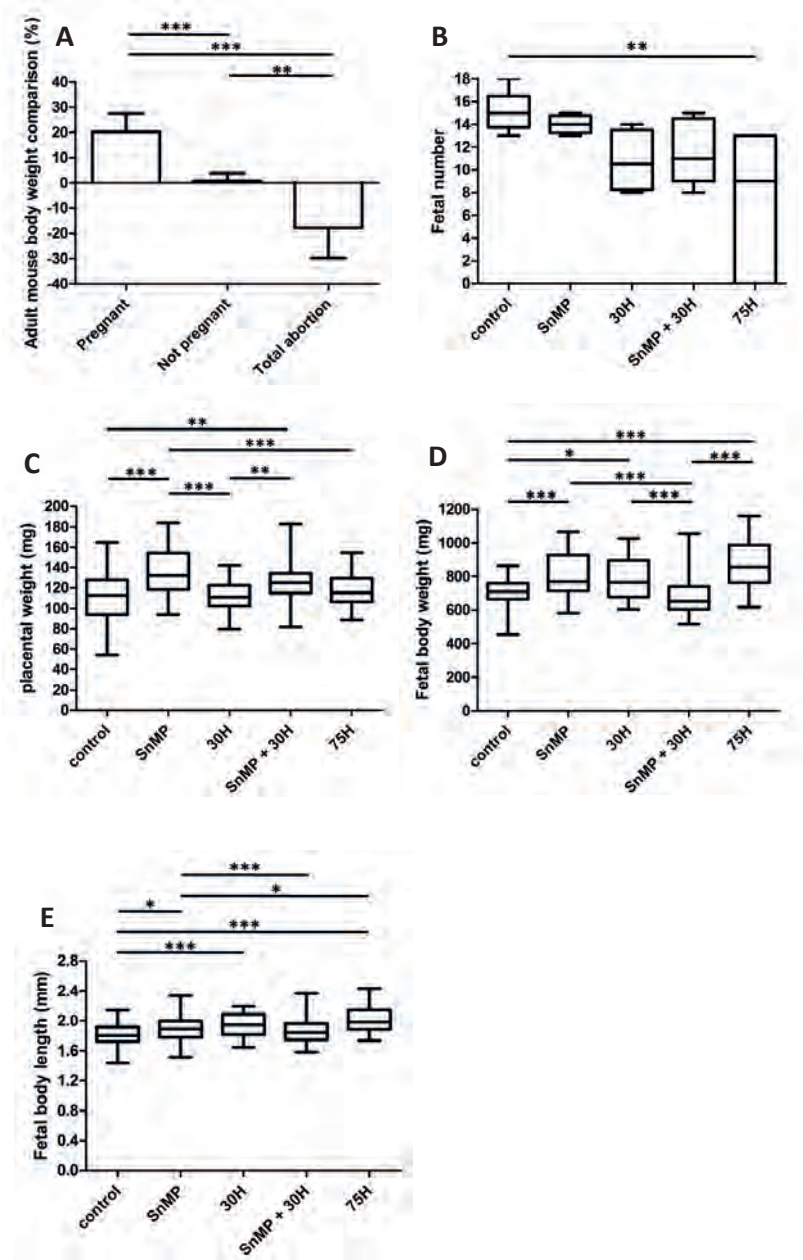


Figure 4. Adult mouse body weight comparison, fetal number, fetal body weight and placental weight affected by HO-activity inhibition and heme administration. (A) Bar chart for the adult mouse body weight comparison, the percentage (%) of the weight change between Days E12 and E15. Unfortunately, the weight at Day E15 was unintentionally not collected from two pregnant mice (75H group) and two mice that demonstrated abortion (SnMP + 75H and 75H groups). Eventually, the body weight comparison of the pregnant mice ($n = 22$; control $n = 6$, SnMP $n = 4$, 30H $n = 4$, SnMP + 30H $n = 5$, 75H $n = 3$), not pregnant mice ($n = 5$; SnMP $n = 1$, 30H $n = 2$, SnMP + 30H $n = 2$) and mice that demonstrated total abortion ($n = 7$; 75H $n = 1$, SnMP + 75H $n = 3$, 150H $n = 3$) was calculated. Data are shown as mean \pm SD. **(B)** Box-and-whisker plot with

10–90 percentiles of quantitative assessment of the fetal number (number of fetuses per pregnant mouse of the different groups). Number of pregnant mice per group; control $n = 6$, SnMP $n = 4$, 30H $n = 4$, SnMP + 30H $n = 5$, 75H $n = 7$. Number of fetuses per group: control $n = 91$, SnMP $n = 56$, 30H $n = 43$, SnMP + 30H $n = 58$, 75H $n = 46$. **(C)** Box-and-whisker plot with 10–90 percentiles of quantitative assessment of the placental weight of the different groups (control $n = 91$, SnMP $n = 56$, 30H $n = 43$, SnMP + 30H $n = 58$, 75H $n = 46$). Box-and-whisker plot with 10–90 percentiles of quantitative assessment of the **(D)** fetal body weight and **(E)** fetal body length of the fetuses of the different groups (control $n = 91$, SnMP $n = 56$, 30H $n = 43$, SnMP + 30H $n = 58$, 75H $n = 46$) were measured. * $p < 0.05$, ** $p < 0.01$, *** $p < 0.001$.

No adult mice died after heme and/or SnMP administration. The treated plugged mice demonstrated normal behavior, and the different experimental groups scored only a low to mild degree of discomfort.

Fewer fetuses per pregnant mouse in the 75H group ($p < 0.01$) were obtained compared to the controls, see **Figure 4B**. In the other experimental groups (30H, SnMP and SnMP + 30H), the fetal number was also lower compared to the controls, but this trend did not reach statistical significance ($p > 0.05$).

Placental weight increase after HO-activity inhibition

Considering that downregulation of HO-1 and HO-2 expression in humans' placenta is associated with placental pathology^{34,36-38}, and placentas from HO-1^{+/-} mice were lighter than those from wt mice⁵⁰, we studied the effect of heme administration and the absence or presence of HO-activity at the mouse placental weight. The placentas were heavier in the SnMP group ($p < 0.001$) compared to the groups without SnMP administration, i.e., control, 30H and 75H groups, see **Figure 4C**. A higher placental weight was found in the SnMP + 30H group ($p < 0.01$) compared to the control and 30H groups.

Fetal body size increase after inhibition of HO-activity and heme administration

Because downregulation of HO-1 expression in human placentas is associated with pregnancy complications and mouse fetuses from HO-1^{+/-} pregnancies were smaller than those from wt pairings⁵⁰, the effect of HO-activity inhibition and/or heme administration on mouse fetal body size was examined. Administration of SnMP increased the fetal body weight ($p < 0.001$) and fetal body length ($p < 0.05$) compared to the controls, see **Figure 4D,E**, respectively. Administration of 75H also significantly increased fetal body weight ($p < 0.001$) and fetal body length ($p < 0.001$) compared to the controls. A representative fetus per group is shown in **Figure 5A**.

Palatal fusion despite inhibition of HO-activity and heme administration

As activation of pro-inflammatory pathways increased the risk of palatal clefting in humans^{6,7,51}, the effects of inhibition of HO-activity and/or heme administration on palatal fusion was studied in mice. The palatal shelves were fused in the fetuses at Day E16, and disintegration of the MES was found in palatal sections from fetuses of both

the control and the different experimental groups: 30H, 75H, SnMP and SnMP + 30H. A representative HE stained palatal section per group is shown in **Figure 5B**. In the surviving fetuses, no effects on palatal fusion were found despite inhibition of HO-activity and/or exposure to heme.

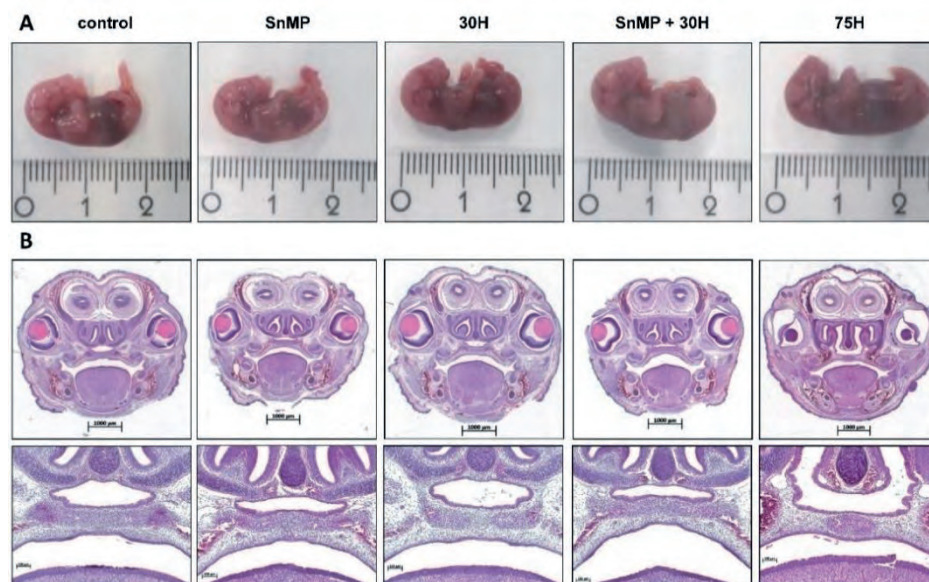
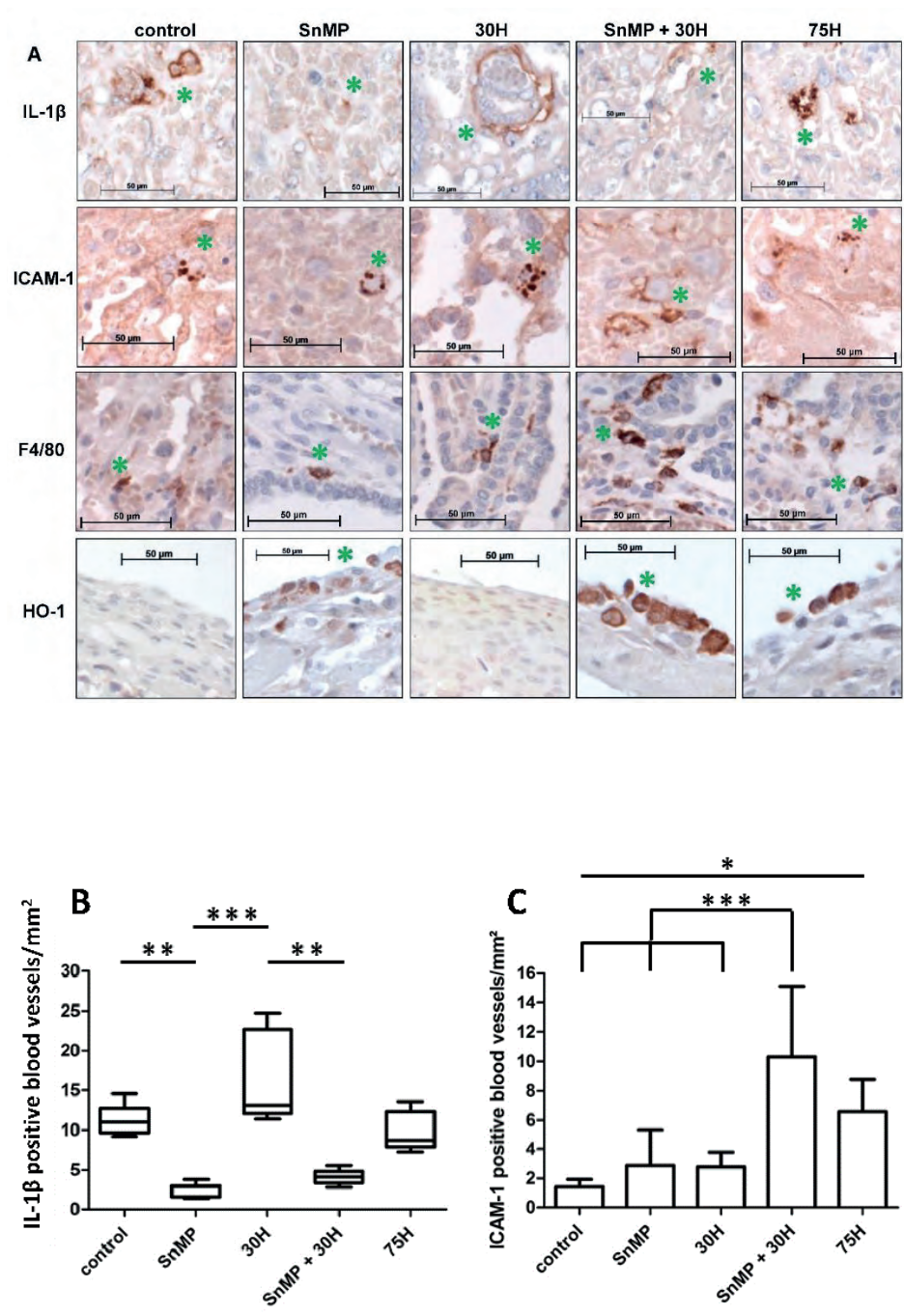


Figure 5. Palatal fusion despite inhibition of HO-activity and heme administration. (A) A representative fetus per group is shown: fetus control, 1.96 cm, 659.5 mg; fetus SnMP, 1.94 cm, 846.3 mg; fetus 30H, 1.95 cm, 832.3 mg; fetus SnMP + 30H, 1.69 cm, 654.1 mg; fetus 75H, 2.43 cm, 1125.9 mg (centimeter ruler). **(B)** The palatal sections were classified into four stages of palatogenesis based on the anatomy of the palatal shelves: elevation, horizontal growth, midline adhesion and fusion. Representative HE staining palatal sections (magnification: x100) of the different groups: control; SnMP; 30H; SnMP + 30H; 75H. Fusion of the shelves of the secondary palate, together with disintegration of the MES, was observed in all fetuses of the control and different experimental groups. A minimum of five transversal sections from at least five head samples per group was assayed.

Inhibition of HO-activity reduces IL-1 β expression in placental blood vessels

Others found that IL-1 β induction is counteracted by HO-1 activity during acute inflammatory arthritis in mice⁴². Here, the effects of exposure to SnMP and/or different heme doses, respectively, five and four days after administration, on IL-1 β expression in mouse placenta were studied.

Lower numbers of IL-1 β positive blood vessels were found after administration of SnMP (median = 2.91/mm²) compared to the control (median = 11.0/mm²; $p < 0.01$) and 30H group (median = 13.1/mm²; $p < 0.001$), see **Figure 6A,B**. Lower numbers of IL-1 β positive blood vessels were also found after administration of SnMP + 30H (median = 4.13/mm²) compared to the 30H group (median = 13.1/mm²; $p < 0.01$).



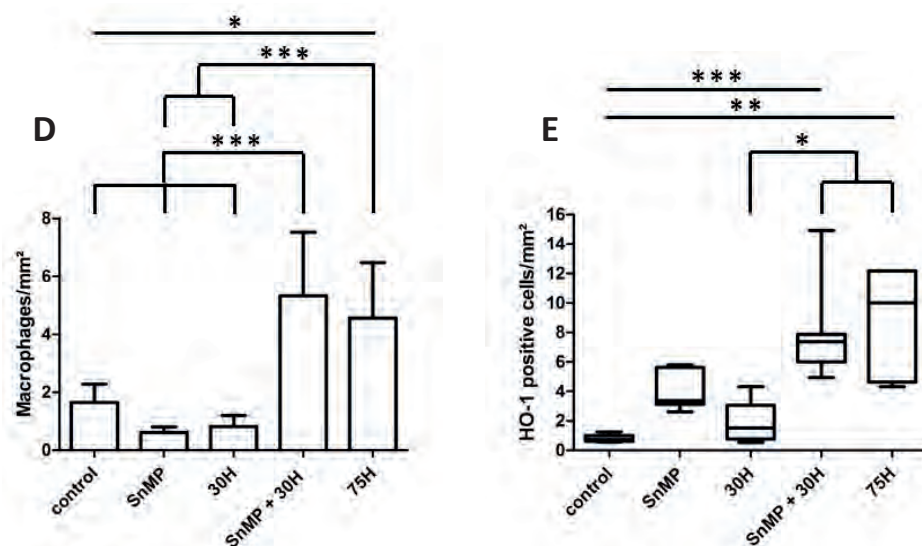


Figure 6. Quantification of IL-1 β , ICAM-1, F4/80 and HO-1 immunoreactivity in placenta. (A) Placental sections stained for immunoreactivity of IL-1 β , ICAM-1, F4/80 and HO-1. Representative IL-1 β , ICAM-1, F4/80 and HO-1 immunostaining in placenta from the control and experimental groups. Green asterisk indicates IL-1 β positive blood vessel, ICAM-1 positive blood vessel, F4/80 positive macrophage and HO-1 positive cell, respectively. (B) Box-and-whisker plot with 10–90 percentiles of quantitative assessment of the IL-1 β positive blood vessels/mm² compared for the different heme and/or SnMP administrations. (C) Bar chart of ICAM-1 positive blood vessels/mm² compared for the different heme and/or SnMP administrations. Data are shown as mean \pm SD. (D) Bar chart of number of macrophages/ mm² compared for the different heme and/or SnMP administrations (control $n = 6$; SnMP $n = 7$; 30H $n = 6$; SnMP + 30H $n = 7$; 75H $n = 5$). Data are shown as mean \pm SD. (E) Box-and-whisker plot with 10–90 percentiles of quantitative assessment of the HO-1 positive cells/mm² compared for the different heme and/or SnMP administrations. Quantification of IL-1 β , ICAM-1, F4/80 and HO-1 immunoreactivity in placenta (Control $n = 6$; SnMP $n = 7$; 30H $n = 6$; SnMP + 30H $n = 7$; 75H $n = 5$). * $p < 0.05$, ** $p < 0.01$, *** $p < 0.001$. A minimum of five sections from a minimum five placentas per group was assayed.

Heme-induced ICAM-1 expression in placental blood vessels is counteracted by HO-activity

Since we and others previously demonstrated that heme can induce adhesion molecule expression in vascular endothelial cells^{26,52,53}, we examined whether heme exposure and/or HO-activity inhibition could alter the expression of ICAM-1 in placenta in mice.

Higher numbers of ICAM-1 positive blood vessels were found after administration of 75H (mean = 6.6/mm²; $p < 0.05$) compared to the controls, see **Figure 6A,C**. In addition, more ICAM-1 positive blood vessels were found after administration of SnMP + 30H (mean = 10.3/mm²; $p < 0.001$) compared to the control (mean = 1.43/mm²), 30H (mean = 2.76/mm²) and SnMP groups (mean = 2.87/mm²).

Placental macrophage recruitment increases after heme administration and decreased HO-activity

Since ICAM-1 expression was increased following exposure to 75H and SnMP + 30H, we assessed whether there was also enhanced influx of macrophages in the activated endothelium. Downregulation of HO-activity in human placenta is associated with inflammatory cell influx^{34,36}. We therefore studied the effects of HO-activity inhibition and heme administration at the placental macrophage influx in mice. Higher numbers of macrophages were found after administration of 75H (mean = 4.6/mm²) compared to the control ($p < 0.05$), 30H ($p < 0.001$) and SnMP groups ($p < 0.001$), see **Figure 6A,D**. Increased macrophage influx was also found after administration of SnMP + 30H (mean = 5.3/mm²; $p < 0.001$) compared to the control (mean = 1.6/mm²), 30H (mean = 0.8/mm²) and SnMP groups (mean = 0.6/mm²).

Placental HO-1 expression increases after heme administration

Since heme, the substrate of the HO system, was found to induce HO-1 expression^{32,34,38}, we investigated whether heme administration resulted in upregulation of placental HO-1 expression. Higher numbers of HO-1 positive cells were found after administration of 75H (median = 10.0/mm²) compared to the control (median = 0.7/mm²; $p < 0.001$) and 30H group (median = 1.5/mm²; $p < 0.05$), see **Figure 6A,E**. Higher numbers of HO-1 positive cells were also found after administration of SnMP + 30H (median = 7.4/mm²) compared to the control ($p < 0.001$) and 30H group ($p < 0.05$). Notably, HO-1 positive cells were predominantly found in the perimetrium, the thin outer epithelial cell layer of the placenta.

Discussion

This study demonstrated that mimicking intrauterine hemorrhage/hematoma by i.p. administration of the endogenous “alarmin” heme, at Day E12 in pregnant mice, causes abortion/resorption in a dose-dependent fashion. No effect on the fusion of the palatal shelves was found in the surviving fetuses. Since we found a fetal loss rate of 50% in the 75H group, we were only able to study palatogenesis at Day E16 in the limited number of surviving fetuses.

Harmful effects of heme exposure have also been found in humans since uterine hematomas are associated with increased risk at intrauterine growth restriction, preterm delivery, and miscarriage⁵⁴⁻⁵⁷. In our study, HO-activity rescued fetuses from heme-induced abortion. Administration of 75H led to fetal loss in half of the fetuses, however, blocking the HO-activity by SnMP prior to 75H administration resulted in total abortion. Blocking of HO-activity by i.p. injection of zinc mesoporphyrin in mice earlier during pregnancy at Days E0 and E3⁵⁸, E4 and E6 was previously found to increase the abortion rate^{36,58}. In mice undergoing abortion, downregulation of both

HO-1 and HO-2 was found in placental tissue compared to normal pregnant mice at Day E14⁵⁹. We previously found fetal growth restriction, severe malformations, and craniofacial anomalies in HO-2 KO fetuses at Day E15⁴⁰. By contrast, upregulation of HO-1 by cobalt-protoporphyrin³⁶, or exposure to carbon monoxide⁶⁰ a product of heme break-down, rescued abortion-prone CBA/J x DBA/2J fetuses from abortion.

Notably, in our study no increased abortion was found after i.p. injection of SnMP at E11 alone. By contrast, the fetal body size was even increased after HO-activity inhibition, suggesting that HO-activity might be more crucial during implantation compared to fetal development at a later stage. Interestingly, others showed that adult HO-2 KO mice were obese, induced by disrupted metabolic homeostasis, caused by insulin resistance and elevated blood pressure⁶¹. Furthermore, in HO-2 KO mice increased brain edema was observed after intracerebral hemorrhage⁶². In rats resuscitated from cardiac arrest, induction of HO-1 by hemin reduced brain edema improved neurologic outcome⁶³. In contrast, SnMP administration reduced intracerebral mass in an intracerebral hemorrhage model in pigs by decreasing both hematoma and edema volumes⁶⁴. Although the literature shows conflicting results, we cannot rule out that edema formation contributed to the fetal body size increase after HO-activity inhibition. However, we show here that HO-activity is also crucial for protecting against the injurious actions of heme at later stages during embryonic development.

Similarly, i.p. injection of another TLR4-ligand, lipopolysaccharide (LPS) increased abortion in rats and mice in a dose-dependent manner^{65,66}. However, administration of different anti-inflammatory drugs protected against LPS-induced abortion. In rats, administration of azithromycin⁶⁷ and, in mice, administration of vitamin D³⁶⁸, berberine⁶⁹, Pre-Implantation Factor (PIF)⁷⁰, curcumin⁷¹, sildenafil⁷² or heparin⁷² protected from LPS-induced abortion. For example, HO-1 expression in mouse placenta demonstrated also a dose- and time-dependent protection following exposure to LPS⁷³. Interestingly, almost all of these protecting agents are also potent HO-1 inducers⁷⁴⁻⁷⁸, suggesting that HO-1 also protects against the injurious effects of other TLR4-ligands besides heme.

In human placental endothelial cells, exposure to LPS was found to induce IL-1 β expression within 24 h *in vitro*^{79,80}. Increased levels of IL-1 β were found in placental endothelial cells following exposure for 24 h to trophoblast debris from preeclamptic placentae *in vitro*⁸¹. In human pregnancies with reduced fetal movement increased placental expression of IL-1 β was observed compared to the controls, although some controls also demonstrated some IL-1 β expression⁸².

Expression of the pro-inflammatory cytokine IL-1 β was observed in blood vessels in the placentas of the controls, as well as in placentas exposed to 30H and 75H. Recent data show that heme exposure triggers the NLRP3 inflammasome pathway, inducing IL-1 β production in human endothelial cells *in vitro*⁸³. Intrauterine infections

are able to trigger the expression of IL-1 β , which stimulates uterine contractions⁸⁴, by elevating PGE₂ levels and myometrial contractility⁸⁵. By contrast, HO-1 was found to inhibit IL-1 β induction during acute inflammatory arthritis in mice⁴², however, we observed that HO-1 inhibition by administration of SnMP decreased placental IL-1 β expression in mice. Unfortunately, a limitation of our study was that the effects of SnMP and heme administration were only evaluated five and four days, respectively, after administration. This means that we were not able to evaluate the expression of IL-1 β shortly after SnMP and/or heme administration, with the risk that this expression has been dampened.

Both administration of 75H and SnMP + 30H increased placental vascular ICAM-1 expression and macrophage influx. However, no increases in ICAM-1 and macrophage influx were found after administration of heme 30, showing that heme-induced ICAM-1 expression is dose-dependent and likely related to scavenging by Hpx or HO-mediated breakdown at lower concentrations. When ICAM-1 expression together with the number of macrophages in placenta was elevated in sound-stressed mice, increased abortion was found⁸⁶. Moreover, decreased abortion was observed following i.p. injection of monoclonal antibodies to ICAM-1 in mice, indicating that ICAM-1 facilitates immunologically-mediated abortion⁸⁷. Increased levels of ICAM-1 were found in placental endothelial cells following exposure to trophoblast debris from preeclamptic placentae *in vitro*⁸¹. In women suffering from Morbidly Adherent Placenta (MAP), an abnormal adherence of the placenta to the myometrium, massive hemorrhage can occur, resulting in severe morbidity and mortality and increased ICAM-1 expression⁸⁸. In addition, in serum⁸⁹⁻⁹² and placenta^{92,93} from preeclampsia patients, increased ICAM-1 expression was found.

Placental inflammation in uncomplicated human gestations was only present in 4% of the cases⁹⁴. Intrauterine infection induces pro-inflammatory cytokines, particularly IL-1 β and TNF α , and influx of macrophages in placenta and uterus, and it may lead to premature birth⁸⁴. In mice, initiated preterm labor by intrauterine infusion of LPS provoked a massive influx of neutrophils in the myometrium⁹⁵. Macrophage influx in placenta and myometrium is associated with placental inflammation and preterm labor in human, mouse, and rat⁹⁶⁻⁹⁸.

Our data show that HO-1 expression in placenta increased after administration of both 75H and SnMP + 30H. HO-1 positive cells were predominantly found in the perimetrium⁹⁹, indicating that besides the vasculature free heme molecules were able to reach the developing fetus through diffusion. In HO-1^{+/-} mice induction of HO-activity in placenta by administration of Pravastatin was shown to improve placental function and fetal survival at E14.5¹⁰⁰. In human pathological pregnancies, low expression of HO-2 stimulated migration of inflammatory cells to the feto-maternal interface, possibly caused by enhanced serum levels of free heme³⁴. We speculate that in our experiment low levels of free heme were scavenged by Hpx³¹, while the heme-Hpx complex binding

to LRP1 would activate cytoprotective signaling by Nrf2¹⁰¹ and upregulation of placental HO-1 expression^{32,102}.

It is likely that in our experiment the sudden exposure to high doses of free heme overwhelmed the scavenger Hpx and the HO system¹⁰³, allowing binding to toll-like receptor 4 (TLR4)⁵³ and activation of nuclear factor kappa B (NF- κ B)¹⁰⁴, driving expression of pro-inflammatory cytokines, such as IL-1 β ¹⁰⁵⁻¹⁰⁷.

The novel hypothetical model (**Figure 7**) shows heme-induced endothelial cell activation¹⁰⁸, as exemplified by the expression of ICAM-1¹⁰⁹, facilitating the recruitment of macrophages into placental tissue^{109,110}, resulting in pathological pregnancy, increasing the risk of abortion. Furthermore, heme-induced inflammation might cause craniofacial abnormalities before resorption of the fetuses would occur. However, our studies could not provide evidence for this statement. Inhibition of HO-activity will increase the heme-induced inflammatory response, albeit HO-activity will attenuate heme-induced inflammation, promoting normal fetal development.

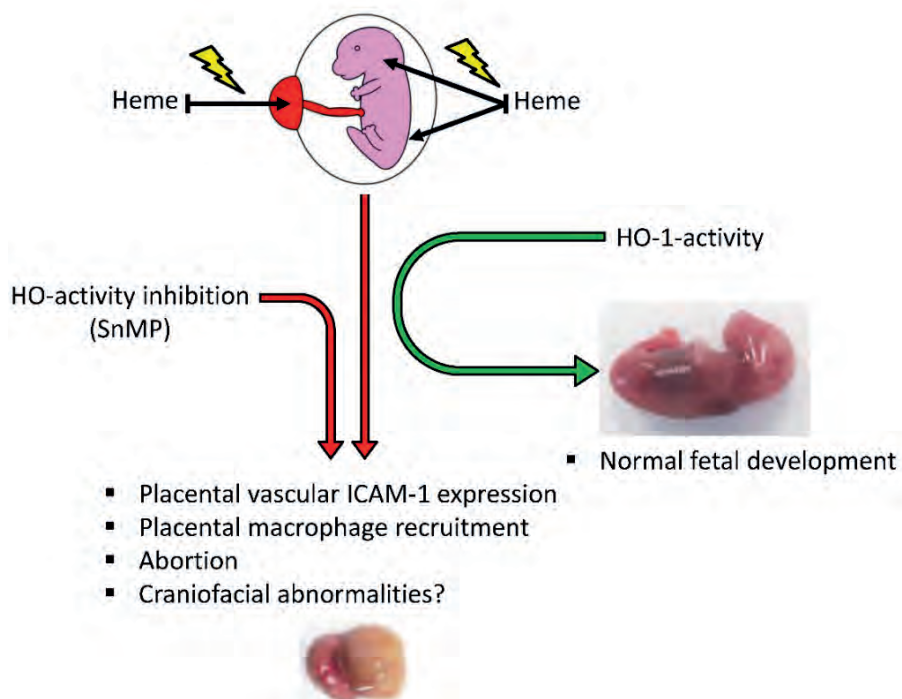


Figure 7. Hypothetical model: Heme oxygenase protects against placental vascular inflammation and abortion by the alarmin heme in mice. This study demonstrated that heme acted as an endogenous “alarmin” during pregnancy in a dose-dependent fashion, while HO-activity protected against heme-induced placental vascular inflammation and abortion. We postulate that heme-induced inflammatory response promoted endothelial cell activation, which upregulated the expression of ICAM-1, facilitating the recruitment of macrophages into placental tissue, resulting in a pathological pregnancy, increasing the risk of abortion and possibly craniofacial abnormalities. Inhibition of HO-activity will increase the heme-induced inflammatory response, albeit HO-activity will attenuate heme-induced inflammation, promoting normal fetal development.

References

1. Mossey PA, Modell B. Epidemiology of Oral Clefts 2012: An International Perspective. *Front Oral Biol.* 2012;16:1-18.
2. Kuijpers-Jagtman A. Cleft Lip and Palate: Role of the Orthodontist in the Interdisciplinary Management Team. *Integrated Clinical Orthodontics.* 2013:153-167.
3. Nakajima A, C FS, Gulka AOD, Hanai JL. TGF-beta Signaling and the Epithelial-Mesenchymal Transition during Palatal Fusion. *Int J Mol Sci.* 2018;19(11).
4. Ito Y, Yeo JY, Chytil A, et al. Conditional inactivation of Tgfb2 in cranial neural crest causes cleft palate and calvaria defects. *Development.* 2003;130(21):5269-5280.
5. Watkins SE, Meyer RE, Strauss RP, Aylsworth AS. Classification, epidemiology, and genetics of orofacial clefts. *Clin Plast Surg.* 2014;41(2):149-163.
6. Brocardo PS, Gil-Mohapel J, Christie BR. The role of oxidative stress in fetal alcohol spectrum disorders. *Brain Res Rev.* 2011;67(1-2):209-225.
7. Spilson SV, Kim HJ, Chung KC. Association between maternal diabetes mellitus and newborn oral cleft. *Ann Plast Surg.* 2001;47(5):477-481.
8. Brien ME, Baker B, Duval C, Gaudreault V, Jones RL, Girard S. Alarmins at the maternal-fetal interface: involvement of inflammation in placental dysfunction and pregnancy complications (1). *Can J Physiol Pharmacol.* 2019;97(3):206-212.
9. Seki H, Kuromaki K, Takeda S, Kinoshita K. Persistent subchorionic hematoma with clinical symptoms until delivery. *Int J Gynaecol Obstet.* 1998;63(2):123-128.
10. Johns J, Hyett J, Jauniaux E. Obstetric outcome after threatened miscarriage with and without a hematoma on ultrasound. *Obstet Gynecol.* 2003;102(3):483-487.
11. Wagener FA, Eggert A, Boerman OC, et al. Heme is a potent inducer of inflammation in mice and is counteracted by heme oxygenase. *Blood.* 2001;98(6):1802-1811.
12. Kassa T, Jana S, Meng F, Alayash AI. Differential heme release from various hemoglobin redox states and the upregulation of cellular heme oxygenase-1. *FEBS Open Bio.* 2016;6(9):876-884.
13. Vendrame F, Olops L, Saad STO, Costa FF, Fertrin KY. Differences in heme and hemopexin content in lipoproteins from patients with sickle cell disease. *J Clin Lipidol.* 2018;12(6):1532-1538.
14. Nagaraj VA, Padmanaban G. Insights on Heme Synthesis in the Malaria Parasite. *Trends Parasitol.* 2017;33(8):583-586.
15. Singh N, Ahmad Z, Baid N, Kumar A. Host heme oxygenase-1: Friend or foe in tackling pathogens? *IUBMB Life.* 2018;70(9):869-880.
16. Bolisetty S, Zarjou A, Agarwal A. Heme Oxygenase 1 as a Therapeutic Target in Acute Kidney Injury. *Am J Kidney Dis.* 2017;69(4):531-545.
17. Wagener FA, Dankers AC, van Summeren F, et al. Heme Oxygenase-1 and breast cancer resistance protein protect against heme-induced toxicity. *Curr Pharm Des.* 2013;19(15):2698-2707.
18. Balla G, Vercellotti GM, Muller-Eberhard U, Eaton J, Jacob HS. Exposure of endothelial cells to free heme potentiates damage mediated by granulocytes and toxic oxygen species. *Lab Invest.* 1991;64(5):648-655.
19. Balla J, Jacob HS, Balla G, Nath K, Eaton JW, Vercellotti GM. Endothelial-cell heme uptake from heme proteins: induction of sensitization and desensitization to oxidant damage. *Proc Natl Acad Sci U S A.* 1993;90(20):9285-9289.
20. Mueller CF, Laude K, McNally JS, Harrison DG. ATVB in focus: redox mechanisms in blood vessels. *Arterioscler Thromb Vasc Biol.* 2005;25(2):274-278.
21. Nagy E, Eaton JW, Jeney V, et al. Red cells, hemoglobin, heme, iron, and atherogenesis. *Arterioscler Thromb Vasc Biol.* 2010;30(7):1347-1353.
22. Silva G, Jeney V, Chora A, Larsen R, Balla J, Soares MP. Oxidized hemoglobin is an endogenous proinflammatory agonist that targets vascular endothelial cells. *J Biol Chem.* 2009;284(43):29582-29595.
23. Posta N, Csoz E, Oros M, et al. Hemoglobin oxidation generates globin-derived peptides in atherosclerotic lesions and intraventricular hemorrhage of the brain, provoking endothelial dysfunction. *Lab Invest.* 2020;100(7):986-1002.
24. Wagener FA, Scharstuhl A, Tyrrell RM, et al. The heme-heme oxygenase system in wound healing; implications for scar formation. *Curr Drug Targets.* 2010;11(12):1571-1585.
25. Zenclussen ML, Casalis PA, El-Mousleh T, et al. Haem oxygenase-1 dictates intrauterine fetal survival in mice via carbon monoxide. *J Pathol.* 2011;225(2):293-304.

26. Wagener FA, Feldman E, de Witte T, Abraham NG. Heme induces the expression of adhesion molecules ICAM-1, VCAM-1, and E selectin in vascular endothelial cells. *Proc Soc Exp Biol Med*. 1997;216(3):456-463.
27. Wagener FA, van Beurden HE, von den Hoff JW, Adema GJ, Figdor CG. The heme-heme oxygenase system: a molecular switch in wound healing. *Blood*. 2003;102(2):521-528.
28. Tuuli MG, Norman SM, Odibo AO, Macones GA, Cahill AG. Perinatal outcomes in women with subchorionic hematoma: a systematic review and meta-analysis. *Obstet Gynecol*. 2011;117(5):1205-1212.
29. Xiang L, Wei Z, Cao Y. Symptoms of an intrauterine hematoma associated with pregnancy complications: a systematic review. *PLoS One*. 2014;9(11):e111676.
30. Nyberg DA, Mack LA, Benedetti TJ, Cyr DR, Schuman WP. Placental abruption and placental hemorrhage: correlation of sonographic findings with fetal outcome. *Radiology*. 1987;164(2):357-361.
31. Ascenzi P, Bocedi A, Visca P, et al. Hemoglobin and heme scavenging. *IUBMB Life*. 2005;57(11):749-759.
32. Wagener FA, Volk HD, Willis D, et al. Different faces of the heme-heme oxygenase system in inflammation. *Pharmacol Rev*. 2003;55(3):551-571.
33. Goriach A, Dimova EY, Petry A, et al. Reactive oxygen species, nutrition, hypoxia and diseases: Problems solved? *Redox Biol*. 2015;6:372-385.
34. Zencclussen AC, Lim E, Knoeller S, et al. Heme oxygenases in pregnancy II: HO-2 is downregulated in human pathologic pregnancies. *Am J Reprod Immunol*. 2003;50(1):66-76.
35. Zencclussen ML, Linzke N, Schumacher A, et al. Heme oxygenase-1 is critically involved in placentation, spiral artery remodeling, and blood pressure regulation during murine pregnancy. *Front Pharmacol*. 2014;5:291.
36. Sollwedel A, Bertoja AZ, Zencclussen ML, et al. Protection from abortion by heme oxygenase-1 up-regulation is associated with increased levels of Bag-1 and neuropilin-1 at the fetal-maternal interface. *J Immunol*. 2005;175(8):4875-4885.
37. Miya M, Okamoto A, Nikaido T, Tachimoto-Kawaguchi R, Tanaka T. Immunohistochemical localization of heme oxygenase-1 and bilirubin/biopyrrin of heme metabolites as antioxidants in human placenta with preeclampsia. *Hypertens Pregnancy*. 2020;39(1):33-42.
38. Grochot-Przeczek A, Dulak J, Jozkowicz A. Haem oxygenase-I: non-canonical roles in physiology and pathology. *Clin Sci*. 2012;122(3-4):93-103.
39. Ewing JF, Maines MD. Regulation and expression of heme oxygenase enzymes in aged-rat brain: Age related depression in HO-1 and HO-2 expression and altered stress-response. *J Neural Transm*. 2006;113(4):439-454.
40. Suttrop CM, Cremers NA, van Rheden R, et al. Chemokine Signaling during Midline Epithelial Seam Disintegration Facilitates Palatal Fusion. *Front Cell Dev Biol*. 2017;5.
41. Li QW, Fu WH, Yao JW, et al. Heme Induces IL-1 beta Secretion Through Activating NLRP3 in Kidney Inflammation. *Cell Biochem Biophys*. 2014;69(3):495-502.
42. Benallaoua M, Francois M, Batteux F, et al. Pharmacologic induction of heme oxygenase 1 reduces acute inflammatory arthritis in mice. *Arthritis Rheum*. 2007;56(8):2585-2594.
43. Behringer R, Gertsenstein M, Nagy KV, Nagy A. Selecting Female Mice in Estrus and Checking Plugs. *Cold Spring Harb Protoc*. 2016;2016(8).
44. Dudas M, Li WY, Kim J, Yang A, Kaartinen V. Palatal fusion - where do the midline cells go? A review on cleft palate, a major human birth defect. *Acta Histochem*. 2007;109(1):1-14.
45. Lutton JD, Jiang S, Drummond GS, Abraham NG, Kappas A. Comparative pharmacology of zinc mesoporphyrin and tin mesoporphyrin: toxic actions of zinc mesoporphyrin on hematopoiesis and progenitor cell mobilization. *Pharmacology*. 1999;58(1):44-50.
46. Stevenson DK, Rodgers PA, Vreman HJ. The use of metalloporphyrins for the chemoprevention of neonatal jaundice. *Am J Dis Child*. 1989;143(3):353-356.
47. Faul F, Erdfelder E, Lang AG, Buchner A. G*Power 3: a flexible statistical power analysis program for the social, behavioral, and biomedical sciences. *Behav Res Methods*. 2007;39(2):175-191.
48. Lin HH, Faunce DE, Stacey M, et al. The macrophage F4/80 receptor is required for the induction of antigen-specific efferent regulatory T cells in peripheral tolerance. *J Exp Med*. 2005;201(10):1615-1625.
49. Tan SD, Xie R, Klein-Nulend J, et al. Orthodontic force stimulates eNOS and iNOS in rat osteocytes. *J Dent Res*. 2009;88(3):255-260.

50. Zhao H, Wong RJ, Kalish FS, Nayak NR, Stevenson DK. Effect of Heme Oxygenase-1 Deficiency on Placental Development. *Placenta*. 2009;30(10):861-868.
51. Mossey PA, Little J, Munger RG, Dixon MJ, Shaw WC. Cleft lip and palate. *Lancet*. 2009;374(9703):1773-1785.
52. Belcher JD, Mahaseth H, Welch TE, Otterbein LE, Hebbel RP, Vercellotti GM. Heme oxygenase-1 is a modulator of inflammation and vaso-occlusion in transgenic sickle mice. *J Clin Invest*. 2006;116(3):808-816.
53. Belcher JD, Chen CS, Nguyen J, et al. Heme triggers TLR4 signaling leading to endothelial cell activation and vaso-occlusion in murine sickle cell disease. *Blood*. 2014;123(3):377-390.
54. Hashem A, Sarsam SD. The Impact of Incidental Ultrasound Finding of Subchorionic and Retroplacental Hematoma in Early Pregnancy. *J Obstet Gyn India*. 2019;69(1):43-49.
55. Ji WQ, Li WD, Mei SS, He P. Intrauterine hematomas in the second and third trimesters associated with adverse pregnancy outcomes: a retrospective study. *J Matern-Fetal Neo M*. 2017;30(18):2151-2155.
56. Ott J, Pecnik P, Promberger R, Pils S, Binder J, Chalubinski KM. Intra- versus retroplacental hematomas: a retrospective case-control study on pregnancy outcomes. *BMC Pregnancy Childbirth*. 2017;17(1):366.
57. MacMullen NJ, Dulski LA, Meagher B. Red alert: perinatal hemorrhage. *MCN Am J Matern Child Nurs*. 2005;30(1):46-51.
58. Schumacher A, Wafula PO, Teles A, et al. Blockage of heme oxygenase-1 abrogates the protective effect of regulatory T cells on murine pregnancy and promotes the maturation of dendritic cells. *PLoS One*. 2012;7(8):e42301.
59. Zenclussen AC, Sollwedel A, Bertoja AZ, et al. Heme oxygenase as a therapeutic target in immunological pregnancy complications. *Int Immunopharmacol*. 2005;5(1):41-51.
60. El-Mousleh T, Casalis PA, Wollenberg I, et al. Exploring the potential of low doses carbon monoxide as therapy in pregnancy complications. *Med Gas Res*. 2012;2(1):4.
61. Cao J, Puri N, Sodhi K, Bellner L, Abraham NG, Kappas A. Apo A1 Mimetic Rescues the Diabetic Phenotype of HO-2 Knockout Mice via an Increase in HO-1 Adiponectin and LKB1 Signaling Pathway. *Int J Hypertens*. 2012;2012:628147.
62. Wang J, Dore S. Heme oxygenase 2 deficiency increases brain swelling and inflammation after intracerebral hemorrhage. *Neuroscience*. 2008;155(4):1133-1141.
63. Zhang B, Wei X, Cui X, Kobayashi T, Li W. Effects of heme oxygenase 1 on brain edema and neurologic outcome after cardiopulmonary resuscitation in rats. *Anesthesiology*. 2008;109(2):260-268.
64. Wagner KR, Hua Y, de Courten-Myers GM, et al. Tin-mesoporphyrin, a potent heme oxygenase inhibitor, for treatment of intracerebral hemorrhage: in vivo and in vitro studies. *Cell Mol Biol (Noisy-le-grand)*. 2000;46(3):597-608.
65. Daguindau E, Gautier T, Chague C, et al. Is It Time to Reconsider the Lipopolysaccharide Paradigm in Acute Graft-Versus-Host Disease? *Front Immunol*. 2017;8:952.
66. Toyama RP, Xikota JC, Schwarzbald ML, et al. Dose-dependent sickness behavior, abortion and inflammation induced by systemic LPS injection in pregnant mice. *J Matern Fetal Neonatal Med*. 2015;28(4):426-430.
67. Er A. Azithromycin prevents pregnancy loss: reducing the level of tumor necrosis factor-alpha and raising the level of interleukin-10 in rats. *Mediators Inflamm*. 2013;2013:928137.
68. Zhou Y, Chen YH, Fu L, et al. Vitamin D3 pretreatment protects against lipopolysaccharide-induced early embryo loss through its anti-inflammatory effects. *American Journal of Reproductive Immunology*. 2017;77(3).
69. Siuki MM, Nasab NF, Barati E, Firizi MN, Jalilvand T, Ahmadabad HN. The protective effect of berberine against lipopolysaccharide-induced abortion by modulation of inflammatory/immune responses. *Immunopharm Immunot*. 2018;40(4):333-337.
70. Di Simone N, Di Nicuolo F, Marana R, et al. Synthetic Preimplantation Factor (PIF) prevents fetal loss by modulating LPS induced inflammatory response. *PLoS One*. 2017;12(7):e0180642.
71. Wang X, Kong N, Zhou C, et al. Effect of Remote Ischemic Preconditioning on Perioperative Cardiac Events in Patients Undergoing Elective Percutaneous Coronary Intervention: A Meta-Analysis of 16 Randomized Trials. *Cardiol Res Pract*. 2017;2017:6907167.

72. Luna RL, Nunes AK, Oliveira AG, et al. Sildenafil (Viagra(R)) blocks inflammatory injury in LPS-induced mouse abortion: A potential prophylactic treatment against acute pregnancy loss? *Placenta*. 2015;36(10):1122-1129.
73. Zhang C, Li XY, Zhao L, Wang H, Xu DX. Lipopolysaccharide (LPS) up-regulates the expression of haem oxygenase-1 in mouse placenta. *Placenta*. 2007;28(8-9):951-957.
74. Wang Z, Zhang H, Sun X, Ren L. The protective role of vitamin D3 in a murine model of asthma via the suppression of TGF-beta/Smad signaling and activation of the Nrf2/HO-1 pathway. *Mol Med Rep*. 2016;14(3):2389-2396.
75. Liang Y, Fan C, Yan X, et al. Berberine ameliorates lipopolysaccharide-induced acute lung injury via the PERK-mediated Nrf2/HO-1 signaling axis. *Phytother Res*. 2019;33(1):130-148.
76. Shi W, Zhang D, Wang L, Sreeharsha N, Ning Y. Curcumin synergistically potentiates the protective effect of sitagliptin against chronic deltamethrin nephrotoxicity in rats: Impact on pro-inflammatory cytokines and Nrf2/Ho-1 pathway. *J Biochem Mol Toxicol*. 2019;33(10):e22386.
77. Jeong JH, Kim HG, Choi OH. Sildenafil Inhibits Advanced Glycation End Products-induced sFlt-1 Release Through Upregulation of Heme Oxygenase-1. *J Menopausal Med*. 2014;20(2):57-68.
78. Yin X, Chen S, Hu Z, et al. [Effect of unfractionated heparin on the expression of heme oxygenase-1 in intestinal mucosa of mice with sepsis]. *Zhonghua Wei Zhong Bing Ji Jiu Yi Xue*. 2016;28(5):423-426.
79. Pontillo A, Girardelli M, Agostinis C, Masat E, Bulla R, Crovella S. Bacterial LPS differently modulates inflammasome gene expression and IL-1beta secretion in trophoblast cells, decidual stromal cells, and decidual endothelial cells. *Reprod Sci*. 2013;20(5):563-566.
80. Duval C, Brien ME, Gaudreault V, et al. Differential effect of LPS and IL-1beta in term placental explants. *Placenta*. 2019;75:9-15.
81. Shen F, Wei J, Snowise S, et al. Trophoblast debris extruded from preeclamptic placentae activates endothelial cells: a mechanism by which the placenta communicates with the maternal endothelium. *Placenta*. 2014;35(10):839-847.
82. Girard S, Heazell AE, Derricott H, et al. Circulating cytokines and alarmins associated with placental inflammation in high-risk pregnancies. *Am J Reprod Immunol*. 2014;72(4):422-434.
83. Erdei J, Toth A, Balogh E, et al. Induction of NLRP3 Inflammasome Activation by Heme in Human Endothelial Cells. *Oxid Med Cell Longev*. 2018;2018.
84. Pollard JK, Mitchell MD. Intrauterine infection and the effects of inflammatory mediators on prostaglandin production by myometrial cells from pregnant women. *Am J Obstet Gynecol*. 1996;174(2):682-686.
85. Oger S, Mehats C, Dallot E, Ferre F, Leroy MJ. Interleukin-1 beta induces phosphodiesterase 4B2 expression in human myometrial cells through a prostaglandin E-2- and cyclic adenosine 3',5'-monophosphate-dependent pathway. *J Clin Endocr Metab*. 2002;87(12):5524-5531.
86. Blois S, Tometten M, Kandil J, et al. Intercellular adhesion molecule-1/LFA-1 cross talk is a proximate mediator capable of disrupting immune integration and tolerance mechanism at the feto-maternal interface in murine pregnancies. *Journal of Immunology*. 2005;174(4):1820-1829.
87. Takeshita T, Satomi M, Akira S, Nakagawa Y, Takahashi H, Araki T. Preventive effect of monoclonal antibodies to intercellular adhesion molecule-1 and leukocyte function-associate antigen-1 on murine spontaneous fetal resorption. *American Journal of Reproductive Immunology*. 2000;43(3):180-185.
88. Korkmazer E, Nizam R, Arslan E, Akkurt O. Relationship between intercellular adhesion molecule-1 and morbidly adherent placenta. *J Perinat Med*. 2019;47(1):45-49.
89. Szarka A, Rigo J, Lazar L, Beko G, Molvarec A. Circulating cytokines, chemokines and adhesion molecules in normal pregnancy and preeclampsia determined by multiplex suspension array. *Bmc Immunol*. 2010;11.
90. Kim SY, Ryu HM, Yang JH, et al. Maternal serum levels of VCAM-1, ICAM-1 and E-selectin in preeclampsia. *J Korean Med Sci*. 2004;19(5):688-692.
91. Docheva N, Romero R, Chaemsaitong P, et al. The profiles of soluble adhesion molecules in the "great obstetrical syndromes". *J Matern-Fetal Neo M*. 2019;32(13):2113-2136.
92. Abe E, Matsubara K, Oka K, Kusanagi Y, Ito M. Cytokine regulation of intercellular adhesion molecule-1 expression on trophoblasts in preeclampsia. *Gynecol Obstet Inves*. 2008;66(1):27-33.
93. Goksu Erol AY, Nazli M, Elis Yildiz S. Significance of platelet endothelial cell adhesion molecule-1 (PECAM-1) and intercellular adhesion molecule-1 (ICAM-1) expressions in preeclamptic placentae. *Endocrine*. 2012;42(1):125-131.

94. Salafia CM, Weigl C, Silberman L. The prevalence and distribution of acute placental inflammation in uncomplicated term pregnancies. *Obstetrics and gynecology*. 1989;73(3 Pt 1):383-389.
95. Shynlova O, Nedd-Roderique T, Li Y, Dorogin A, Lye SJ. Myometrial immune cells contribute to term parturition, preterm labour and post-partum involution in mice. *J Cell Mol Med*. 2013;17(1):90-102.
96. Leong AS, Norman JE, Smith R. Vascular and myometrial changes in the human uterus at term. *Reprod Sci*. 2008;15(1):59-65.
97. Ledingham MA, Thomson AJ, Jordan F, Young A, Crawford M, Norman JE. Cell adhesion molecule expression in the cervix and myometrium during pregnancy and parturition. *Obstet Gynecol*. 2001;97(2):235-242.
98. Hamilton S, Oomomian Y, Stephen G, et al. Macrophages infiltrate the human and rat decidua during term and preterm labor: evidence that decidual inflammation precedes labor. *Biol Reprod*. 2012;86(2):39.
99. Bhartiya D, James K. Very small embryonic-like stem cells (VSELs) in adult mouse uterine perimetrium and myometrium. *J Ovarian Res*. 2017;10(1):29.
100. Tsur A, Kalish F, Burgess J, et al. Pravastatin improves fetal survival in mice with a partial deficiency of heme oxygenase-1. *Placenta*. 2019;75:1-8.
101. Sussan TE, Sudini K, Talbot CC, Jr., et al. Nrf2 regulates gene-environment interactions in an animal model of intrauterine inflammation: Implications for preterm birth and prematurity. *Sci Rep*. 2017;7:40194.
102. Nielsen MJ, Moller HJ, Moestrup SK. Hemoglobin and heme scavenger receptors. *Antioxid Redox Signal*. 2010;12(2):261-273.
103. Frimat M, Boudhabhay I, Roumenina LT. Hemolysis Derived Products Toxicity and Endothelium: Model of the Second Hit. *Toxins (Basel)*. 2019;11(11).
104. Martins R, Knapp S. Heme and hemolysis in innate immunity: adding insult to injury. *Curr Opin Immunol*. 2018;50:14-20.
105. Wang G, Manaenko A, Shao A, et al. Low-density lipoprotein receptor-related protein-1 facilitates heme scavenging after intracerebral hemorrhage in mice. *J Cereb Blood Flow Metab*. 2017;37(4):1299-1310.
106. Hvidberg V, Maniecki MB, Jacobsen C, Hojrup P, Moller HJ, Moestrup SK. Identification of the receptor scavenging hemopexin-heme complexes. *Blood*. 2005;106(7):2572-2579.
107. Lin S, Yin Q, Zhong Q, et al. Heme activates TLR4-mediated inflammatory injury via MyD88/TRIF signaling pathway in intracerebral hemorrhage. *J Neuroinflammation*. 2012;9:46.
108. Wang X, Athayde N, Trudinger B. Endothelial cell expression of adhesion molecules is induced by fetal plasma from pregnancies with umbilical placental vascular disease. *BJOG*. 2002;109(7):770-777.
109. Juliano PB, Blotta MH, Altemani AM. ICAM-1 is overexpressed by villous trophoblasts in placentitis. *Placenta*. 2006;27(6-7):750-757.
110. Belcher JD, Beckman JD, Balla G, Balla J, Vercellotti G. Heme degradation and vascular injury. *Antioxid Redox Signal*. 2010;12(2):233-248.

Part III

Mechanical stress, generated by orthodontic forces in rats or by splinting of excisional wounds in mice, induces the cytoprotective enzyme HO-1

CHAPTER 5

Orthodontic forces induce the cytoprotective enzyme heme oxygenase-1 in rats

Suttorp CM, Xie R, Lundvig DMS, Kuijpers-Jagtman AM, Uijttenboogaart JT, van Rheden REM, Maltha JC, Wagener FADTG.

Front Physiol. 2016 Jul 19;7:283.

Abstract

Orthodontic forces disturb the microenvironment of the periodontal ligament (PDL) and induce craniofacial bone remodeling which is necessary for tooth movement. Unfortunately, orthodontic tooth movement is often hampered by ischemic injury and cell death within the PDL (hyalinization) and root resorption. Large inter-individual differences in hyalinization and root resorption have been observed, and may be explained by differential protection against hyalinization. Heme oxygenase-1 (HO-1) forms an important protective mechanism by breaking down heme into the strong antioxidants biliverdin/bilirubin and the signaling molecule carbon monoxide. These versatile HO-1 products protect against ischemic and inflammatory injury. We postulate that orthodontic forces induce HO-1 expression in the PDL during experimental tooth movement. Twenty-five 6-week-old male Wistar rats were used in this study. The upper three molars at one side were moved mesially using a Nickel-Titanium coil spring, providing a continuous orthodontic force of 10 cN. The contralateral side served as control. After 6, 12, 72, 96, and 120 h groups of rats were killed. On parasagittal sections immunohistochemical staining was performed for analysis of HO-1 expression and quantification of osteoclasts. Orthodontic force induced a significant time-dependent HO-1 expression in mononuclear cells within the PDL at both the apposition- and resorption side. Shortly after placement of the orthodontic appliance HO-1 expression was highly induced in PDL cells but dropped to control levels within 72 h. Some osteoclasts were also HO-1 positive but this induction was independent of time- and mechanical stress. It is tempting to speculate that differential induction of tissue protecting- and osteoclast activating genes in the PDL determine the level of bone resorption and hyalinization and, subsequently, “fast” and “slow” tooth movers during orthodontic treatment.

Keywords: orthodontic tooth movement, alveolar bone remodeling, cytoprotective enzymes, hyalinization, root resorption.

Abbreviations

ABC	Avidin-biotin peroxidase complex
ANOVA	Analysis of variance
AP	Alkaline phosphatase
CD68	Cluster of Differentiation 68
CO	Carbon monoxide
DAB	Diaminobenzidine-peroxidase
ECM	Extracellular matrix
EDTA	Ethylenediaminetetraacetic acid
ED1	Anti-CD68 antibody
HE	Haematoxylin and eosin
IL-1 β	Interleukin-1 beta
KS-test	Kolmogorov-Smirnov test
NBT	Nitro-blue tetrazolium
NDS	Normal donkey serum
Ni-Ti	Nickel-Titanium
PBS	Phosphate-buffered saline
PBSG	Phosphate-buffered saline with glycine
PDL	Periodontal ligament
PFA	Paraformaldehyde
ROS	Reactive oxygen species

Introduction

Although orthodontic tooth movement has been described in multiple studies the exact biological mechanisms are still not elucidated. Large differences in the rate of orthodontic tooth movement are found between individuals in identical experimental settings and are largely independent of the magnitude of the orthodontic force¹⁻³.

The periodontal ligament (PDL) contains a variety of cells, blood vessels, nerves and extracellular matrix (ECM) molecules. Forces applied to a tooth compress the blood vessels at the resorption side, while dilating them at the apposition side leading to inflammation and subsequent remodeling of periodontal tissues. At the resorption side, recruited osteoclasts will degrade the alveolar bone allowing tooth movement⁴⁻⁶, whereas at the apposition side signaling pathways are activated to stimulate precursor cells in the PDL to differentiate into osteoblasts^{7,8}.

Unfortunately, at the resorption side, ischemic injury can result in cell death in a process called hyalinization. At these hyalinized regions of the PDL no living osteoclasts are present to facilitate alveolar bone resorption. The necrotic tissue needs to be removed by macrophages and multinucleated giant cells, and to be replaced by newly formed connective tissue. However, these multinucleated giant cells and macrophages can also initiate root resorption, one of the most important challenges in orthodontics^{9,10}. Orthodontic patients can be classified as “fast” or “slow” tooth movers, indicating variance in response of the PDL to hyalinization formation¹¹.

Protection against inflammatory, mechanical, and ischemic stresses, as present during hyalinization, may determine the efficacy of individual orthodontic tooth movement. Interestingly, it was recently observed that differential levels of the osteoclast activating cytokine IL-1 β also modulate orthodontic tooth movement^{3,12}. “Fast tooth movers” may have decreased levels of hyalinization via higher induction of cytoprotective genes and/or increased levels of osteoclast activating genes. Heme oxygenase-1 (HO-1) is one of the most important examples of cytoprotective genes against ischemia reperfusion injury^{13,14}. Protection against ischemic injury and cell death by HO-1 overexpression is demonstrated for example in liver and heart transplantations¹⁵. HO-1 degrades heme into free iron, carbon monoxide (CO) and biliverdin¹⁶. Biliverdin is then directly converted into bilirubin by biliverdin reductase. CO is a signaling molecule that regulates inflammation, angiogenesis, and apoptotic signaling. Biliverdin and bilirubin are both potent antioxidants, while free iron is scavenged by co-induced ferritin¹⁷. The level of HO-1 induction following a stimulus varies within the human population because of its highly polymorphic promoter¹⁸.

HO-1 is induced by a wide array of stresses¹³. In an *in vitro* study, HO-1 induction by mechanical stress in PDL cells was previously demonstrated¹⁹. In the present study we aim to translate this *in vitro* finding of HO-1 induction in the PDL cells to an *in vivo* experimental setting in rats using orthodontic forces. We postulate that HO-1 will be induced by orthodontic forces and subsequently reduces or prevents

hyalinization formation and root resorption. Protection against those unwanted side effects may ameliorate orthodontic tooth movement.

Materials and Methods

Experimental animals

Twenty-five 6-week-old male Wistar rats were used in this study. The animals were housed under normal laboratory conditions with *ad libitum* access to water and powdered rodent chow (Sniff, Soest, The Netherlands). The animals were allowed to acclimatize for at least 1 week before the start of the experiment. Ethical permission for the study was obtained according to the guidelines of the Board for Animal Experiments of the Radboud University Nijmegen (Reference number: RU-DEC-2006-160).

Force application

The rats were at random divided into 5 groups, with 5 animals per group. A split-mouth design was used to control for individual variances. The three maxillary molars on one randomly chosen side were moved mesially as one unit by means of a coil spring as described previously^{20,21}. The contralateral maxillary molars served as controls. A Nickel-Titanium (Ni-Ti) 10 cN Santalloy® closing coil spring (GAC, New York, NY, USA) was attached to the molar block via incisor anchorage to deliver a constant mesially directed force. An important advantage of this biomechanical design is that a constant low force per molar was applied preventing tipping of the molars. The effect could be estimated as a force of 170 cN per human molar which is within the range used in the clinic. This design has been proven functional and caused tooth movement during an period of 12 weeks²².

After 6, 12, 72, 96, and 120 h of force application, groups of rats were killed and perfused with 4% paraformaldehyde (PFA) in phosphate-buffered saline (PBS). The maxillae were removed, post-fixed for 24 h in 4% PFA, decalcified in 10% ethylenediaminetetraacetic acid (EDTA), and embedded in paraffin.

Haematoxylin-Eosin staining of maxillary parasagittal sections

Serial parasagittal sections (5 µm) mounted on Superfrost Plus slides (Menzel-Gläser, Braunschweig, Germany) were routinely stained with haematoxylin and eosin (HE) for general tissue survey. For immunohistochemical evaluation, sections containing at least the radicular pulp of three roots of the maxillary molars were selected.

Immunohistochemical staining

Immunostaining for HO-1 and protein Cluster of Differentiation 68 (CD68) was done essentially as previously described²³. CD68 is a marker for cells of the macrophage lineage, including monocytes, giant cells and osteoclasts and is recognized by the anti-CD68 (ED1)-antibody²⁴. Cells within the PDL were counted as osteoclasts when they were ED1-positive, multinuclear, and located at the alveolar bone outline.

In brief, tissue sections were deparaffinized and rehydrated, followed by quenching of endogenous peroxidase activity using 3% H₂O₂ in methanol. After post-fixation in 4% paraformaldehyde (PFA), antigen retrieval was performed by heating sections in 10 mM citrate pH 6 at 70°C for 10 min, followed by incubation in 1% trypsin (Difco Laboratories, Detroit, MI) at 37°C for 7 min. Sections were subsequently blocked in 10% normal donkey serum (NDS; Chemicon, Temecula, CA) before overnight incubation at 4°C with primary antibody diluted in 2% NDS. The primary antibodies were polyclonal rabbit anti-HO-1 antibody (1:600; SPA-895, Stressgen, Ann Arbor, MI) and monoclonal mouse anti-CD68 ED1 antibody (1:200; MCA341R, Serotec, Breda, The Netherlands). Then sections were incubated with biotin-conjugated donkey anti-rabbit or anti-mouse secondary antibodies (1:3000 – 1:5000; Jackson Labs, West Grove, PA) for 1 h, followed by 45 min incubation with Vectastain ABC-Elite kit (Vector Laboratories, Burlingame, CA). Immunostaining was visualized by incubating the sections for 10 min with 3'3'-diaminobenzidine tetrahydrochloride (DAB; Sigma, St. Louis, MO). Staining was intensified with 0.5% CuSO₄, and counterstained with haematoxylin. Photographs were taken on a Carl Zeiss Imager Z.1 system (Carl Zeiss Microimaging GmbH, Jena, Germany) under bright field conditions.

Analysis of immunohistochemical data

The PDL region containing the roots of first and second molars was selected for quantitative measurement of HO-1 positive cells. Roots fulfilling the following criteria were included in the study: (1) The root structure is present from the cemento-enamel junction to the apex, (2) the radicular pulp is present in the root structure, (3) no artifacts are present in the PDL structure. Almost all third molars were excluded because the root structure was not present over the whole length of the root in most sections. For standardization, root length was measured from apex to the top of the alveolar crest at the line through the middle of the root by using an ocular graticule (**Figure 1**). This allowed us to quantify the number of HO-1 and ED1 positive cells per mm of root length.

HO-1 positive mononuclear PDL cells and ED1 positive multinuclear osteoclasts were counted along the mesial and distal areas of the PDL in both experimental and control sides by blinded observers. Because the three maxillary molars were moved mesially as one unit, the mesial areas of all roots at the experimental sides were considered resorption sides, whereas the distal areas were considered apposition sides

(Figure 2). To determine the inter-examiner reliability, 10 sections were measured by the two observers and acceptable $R^2 > 0.80$ were obtained for cell counting and root length measurements. For positively stained mononuclear and osteoclast cells, data was presented as the number of positive cells per mm of root length.

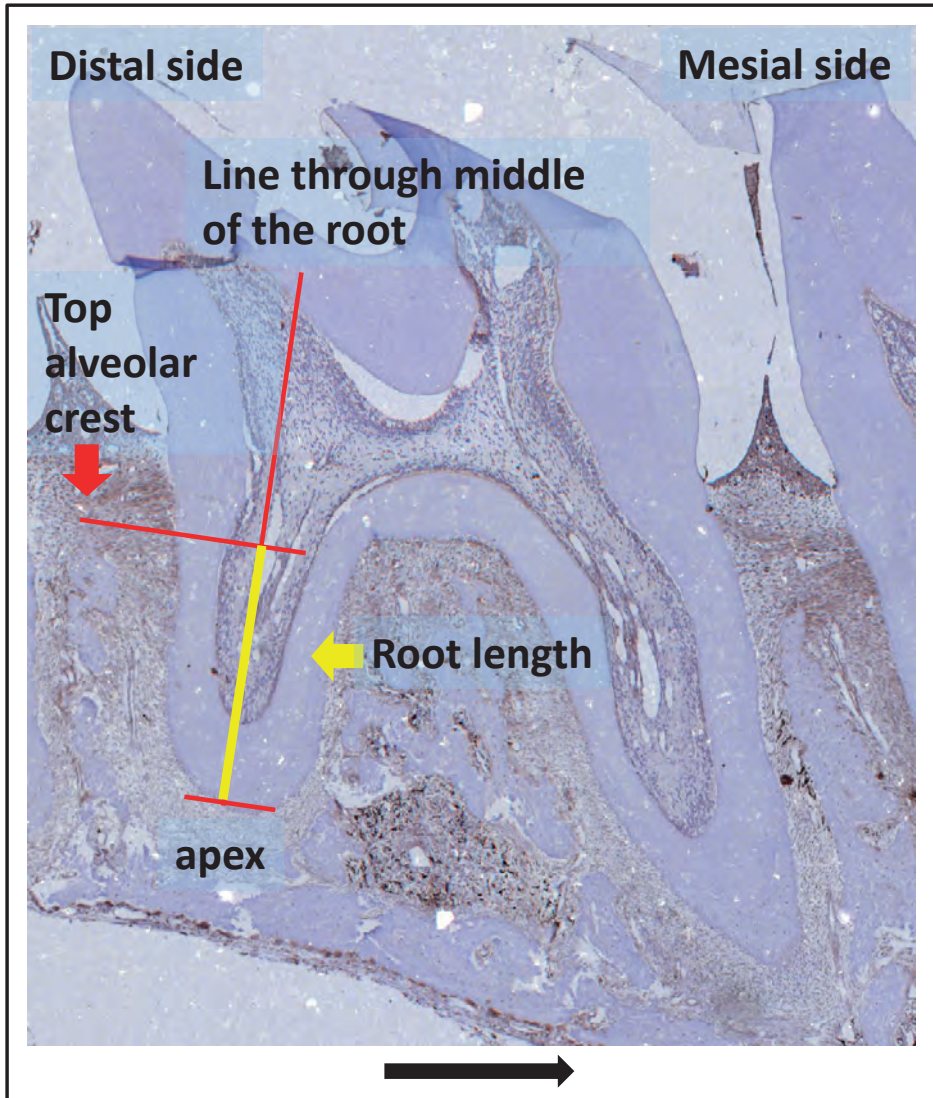


Figure 1: Root length measurement (yellow line) as used for determining the number of cells/mm root explained in detail: root length was measured from apex to the top of the alveolar crest at the line through the middle of the root (HO-1 immunostaining, magnification: x25, experimental group 120 h, black arrow indicated the direction of the tooth movement).

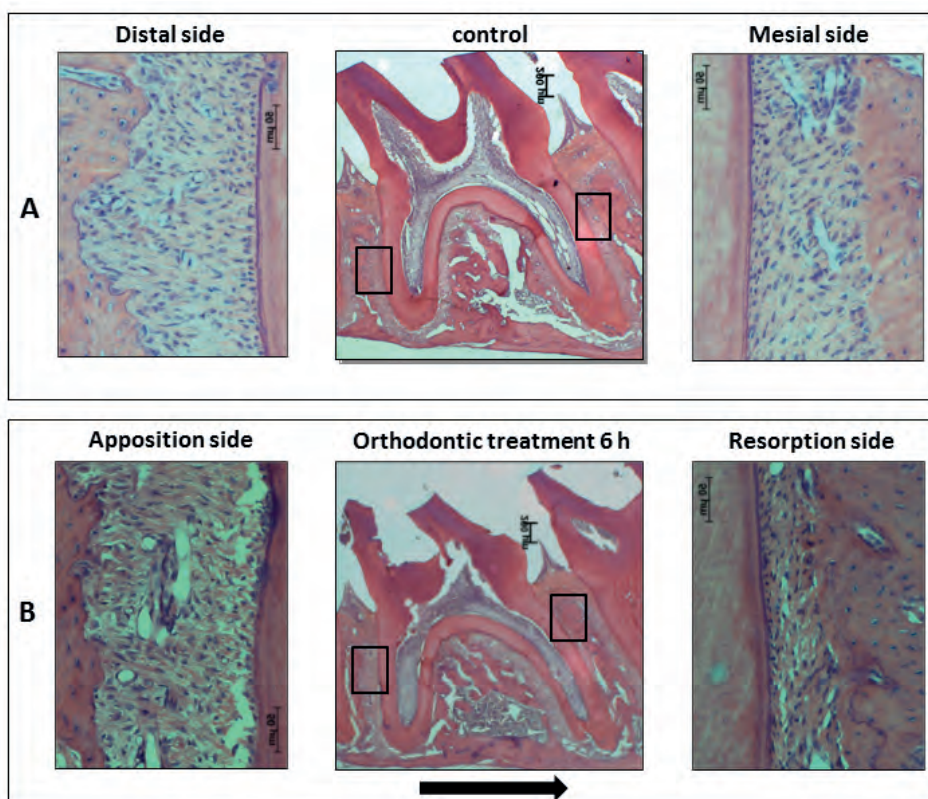


Figure 2. Applied orthodontic force results in changes in morphology of the PDL. (A) No orthodontic force application (HE staining, control molar, picture magnification: x25; distal- and mesial side, picture magnification: x400, control group 6 h). At the distal side irregular alveolar bone outline is present due to resorption by osteoclasts (molar distal drift in rats). At the mesial side a more regular alveolar bone outline is observed. **(B)** After 6 h of orthodontic force application (HE staining, orthodontic treatment 6 h picture magnification: x25, apposition- and resorption side picture magnification: x400) changes in the width of the PDL at both the mesial- and distal side were observed (black arrow indicates the direction of the tooth movement). At the mesial side the width of the PDL was reduced and bloodvessels of the PDL were compressed (resorption side). At the distal side the width of the PDL was increased and bloodvessels of the PDL were stretched (apposition side).

Statistical analysis

The data from HO-1 positive mononuclear cells for control samples showed a normal distribution as measured by the Kolmogorov-Smirnov test (KS-test). No time dependency throughout the experimental period and no side dependency by one-way analysis of variance (ANOVA) was found. Therefore, these data were pooled and used as baseline HO-1 expression in PDL.

The data from both HO-1 positive mononuclear PDL cells for experimental samples and the control and experimental osteoclasts (HO-1 and ED1) showed a non-normal distribution and was analyzed using non-parametric Kruskal-Wallis ANOVA on ranks and Mann-Whitney tests.

The data for the HO-1 positive osteoclasts at the distal area of the control samples was normally distributed. Therefore, ANOVA and Tukey's multiple comparison *post hoc* test were used to analyze the time dependency.

Independent-Samples *T*-test was performed to compare differences between osteoclasts for each marker (HO-1 and ED1) at the distal areas. Differences were assumed to be significant if $p < 0,05$.

Results

Effects of orthodontic force on HO-1 expression in PDL cells

Histological evaluation of HE-stained sections demonstrated that application of mechanical stress significantly reduced the width of the PDL at the resorption side, whereas the width at the apposition site was increased (**Figure 2**). This confirms that the Ni-Ti coil spring appliance produced a mesially-orientated force acting on the PDL and the molar block. Hyalinized regions in the PDL were only observed at the resorption side in the experimental group (**figure 6**), but not in the control group.

First, we investigated the HO-1 expression in parasagittal sections at the control (no force) side. In these sections, HO-1 positive cells were strongly present in the bone marrow and only few HO-1 expressing cells were found in the PDL. The large number of cells expressing high levels of HO-1 in the bone marrow was used as an internal control for the staining procedure. Hardly any HO-1 positive cells were found in sections from pulp tissue, whereas interdental papillae were positive for HO-1 expressing cells (**Figure 3**).

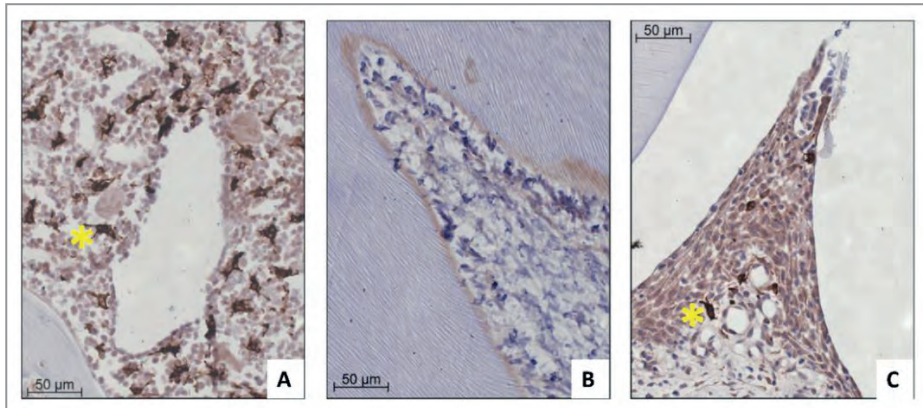


Figure 3: HO-1 expression in bone marrow, pulp tissue and interdental papilla tissue representative for both control and experimental group (HO-1 immunostaining, magnification: x400, yellow asterisk indicates a HO-1 overexpressing cell). **(A)** Large numbers of HO-1 overexpressing cells in bone marrow (control group 120 h). **(B)** Negligible numbers of HO-1 positive cells were present in pulp tissue (experimental group 12 h). **(C)** Few HO-1 positive cells in interdental papilla tissue (control group 120 h).

Next, we compared the effect of orthodontic force on HO-1 expression. We observed no change in the levels of HO-1 staining for the bone marrow, pulp and interdental papilla following mechanical stress at the measured time points. However, we detected a strong increase in the number of HO-1 positive mononuclear cells in the PDL after force application (**Figure 4B**) compared to the contralateral control side (**Figure 4A**). This was especially evident in the vicinity of blood vessels.

To quantify HO-1 protein in PDL tissue during orthodontic tooth movement experimental sections were examined and compared to controls. In general, there were low numbers of cells strongly expressing HO-1 (<10 cells/mm root) observed in the PDL at the control side. At the control side no statistically significant differences were detected between the number of HO-1 positive mononuclear PDL cells at the distal- and mesial side at any of the investigated time points nor between the different time points ($p = 0,110$). These data were therefore pooled, considered as base-line HO-1 expression in PDL (**Figure 4C**, red horizontal line).

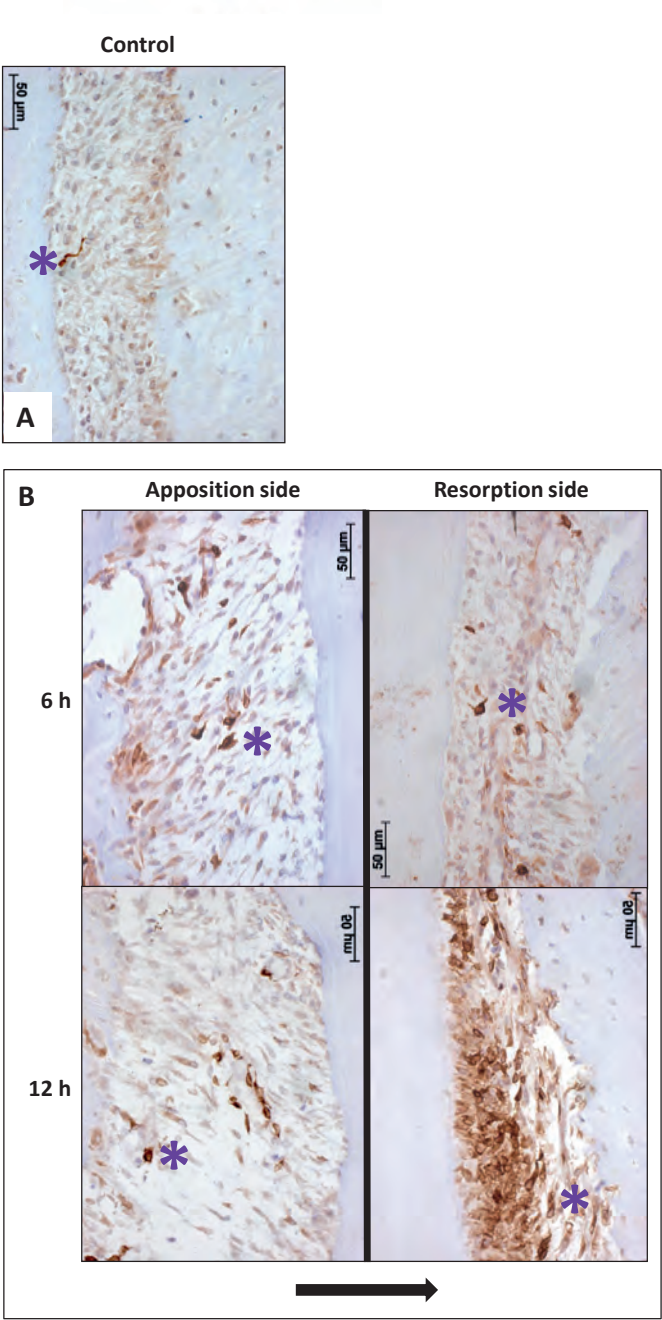
At the experimental side there was a statistically significant time-dependent increase in the number of HO-1 positive cells per mm of root length and the data was therefore separated for the different time points and for both the resorption- and apposition side. Both for the resorption- and apposition side the number of HO-1 positively stained mononuclear PDL cells was significantly increased for the time points 6 and 12 h compared to no force application ($p < 0,001$, **Figure 4C**). Although the number of HO-1 positive stained mononuclear cells was higher at the resorption side after 12 h compared to the apposition side, this did not reach statistical significance ($p = 0.083$).

Summarizing, following orthodontic treatment, the PDL tissue showed a strong increase in the number of HO-1 positive cells at both the apposition- and resorption side compared to the contralateral control side, but returned within 72 h to baseline levels.

HO-1 expression in osteoclasts

When no force was applied, osteoclasts were mainly observed in the bone marrow and in the PDL at the distal side (molar distal drift in rats, **Figure 2**). However, upon mechanical stress, the number of osteoclasts within the PDL decreased at the distal side (apposition side), whereas at the resorption side the osteoclast numbers increased. A portion of the observed osteoclasts were also positively stained for HO-1 (**Figure 5A**). In control sections, HO-1 positively stained osteoclasts were observed in both the PDL and the bone marrow. The HO-1 expression levels in osteoclasts were, however, less intense compared to those in the HO-1 positive mononuclear PDL cells and bone marrow cells (**Figures 3-5A**).

In control sections the number of HO-1 and ED1 positive osteoclasts per mm of root length was significantly higher at the distal side compared to the mesial side (**Figure 5B**). The data were therefore separated for both areas.



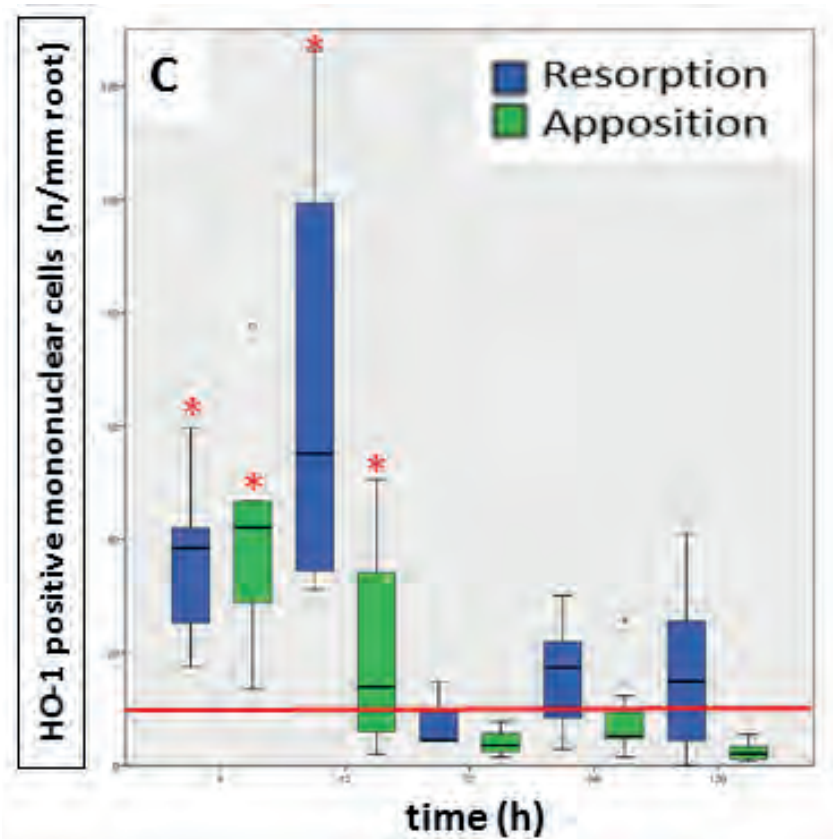


Figure 4: Effects of orthodontic force on HO-1 expression in the PDL. (HO-1 immunostaining, magnification: x400, purple asterisk indicates a HO-1 overexpressing cell, black arrow indicates the direction of the tooth movement). **(A)** Only few strong HO-1 positive cells are observed in PDL tissue in control sections (control group 6 h). **(B)** Many HO-1 overexpressing cells were present in PDL tissue at both the apposition- and resorption side in experimental sections of experimental time 6 and 12 h. This was especially evident in the vicinity of blood vessels. **(C)** Box-plot of mononuclear PDL cells at the experimental sides compared to control. The number of HO-1 positive mononuclear PDL cells is significantly higher at 6 and 12 h of force application compared to the control group (base-line HO-1 expression in PDL, red horizontal line), for both the apposition- and resorption side (Kruskal-Wallis ANOVA on ranks tests, $p < 0.001$). *Significantly different from base-line HO-1 expression in PDL, $p < 0.05$.

When applying the mesially directed force, changes in the numbers of osteoclasts were observed at both sides (**Figure 5B**). After 120 h the numbers of HO-1 positive ($p = 0.349$) and ED1 positive ($p = 0.065$) osteoclasts found at the mesial side (resorption side) were similar to the distal side in control sections, and with a similar HO-1/ED1 ratio. In conclusion, expression of HO-1 in osteoclasts was demonstrated to be independent of time- and mechanical stress.

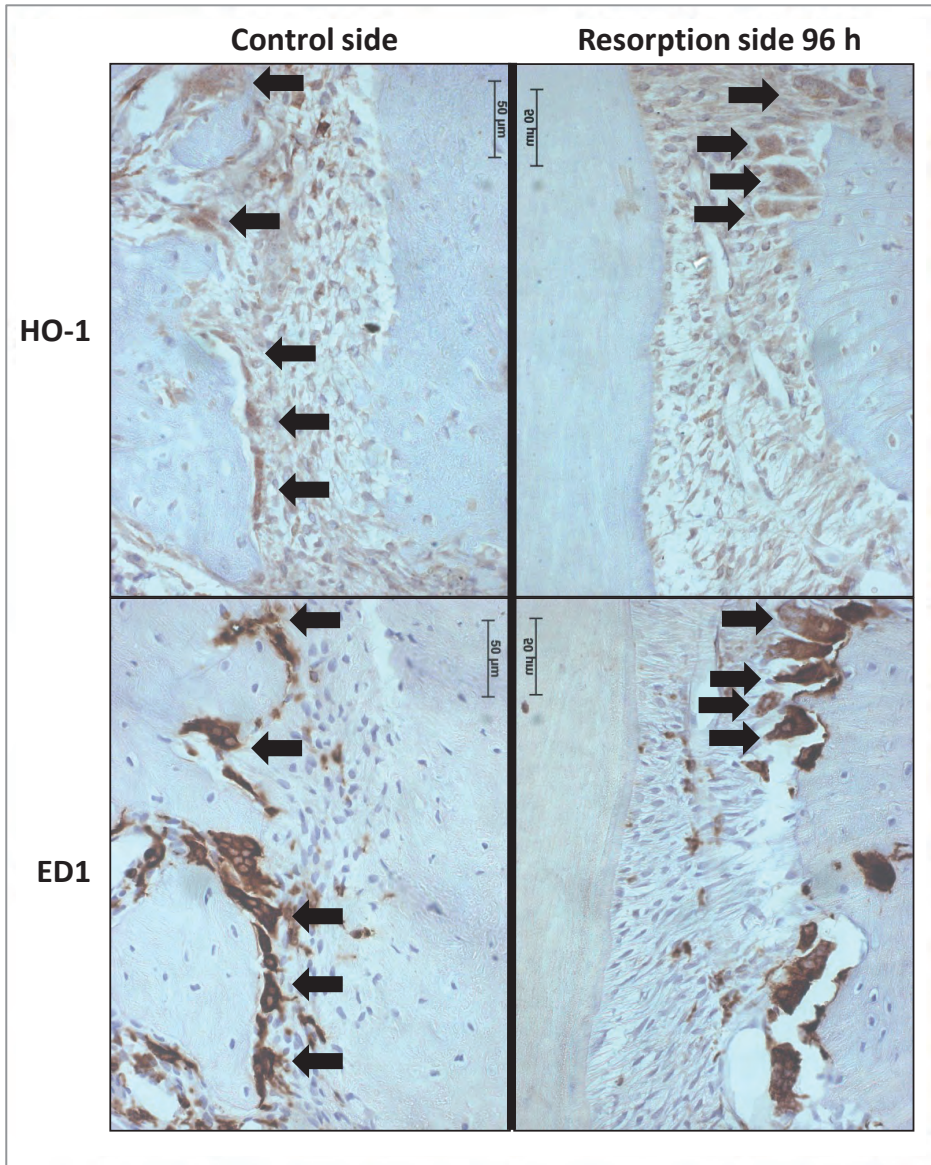


Figure 5A: Effects of orthodontic force on HO-1 and ED1 positive osteoclasts. (A) HO-1 (upper lane) and ED1 (lower lane) positive osteoclasts are found both before [control group, distal side (left panel)] and after [experimental group 96 h, resorption side (right panel)] force application as shown by immunohistochemistry. (magnification: x400, black arrows indicating an HO-1 and ED1 positive osteoclast, cells that were multinuclear and located at the alveolar bone outline were marked as osteoclasts).

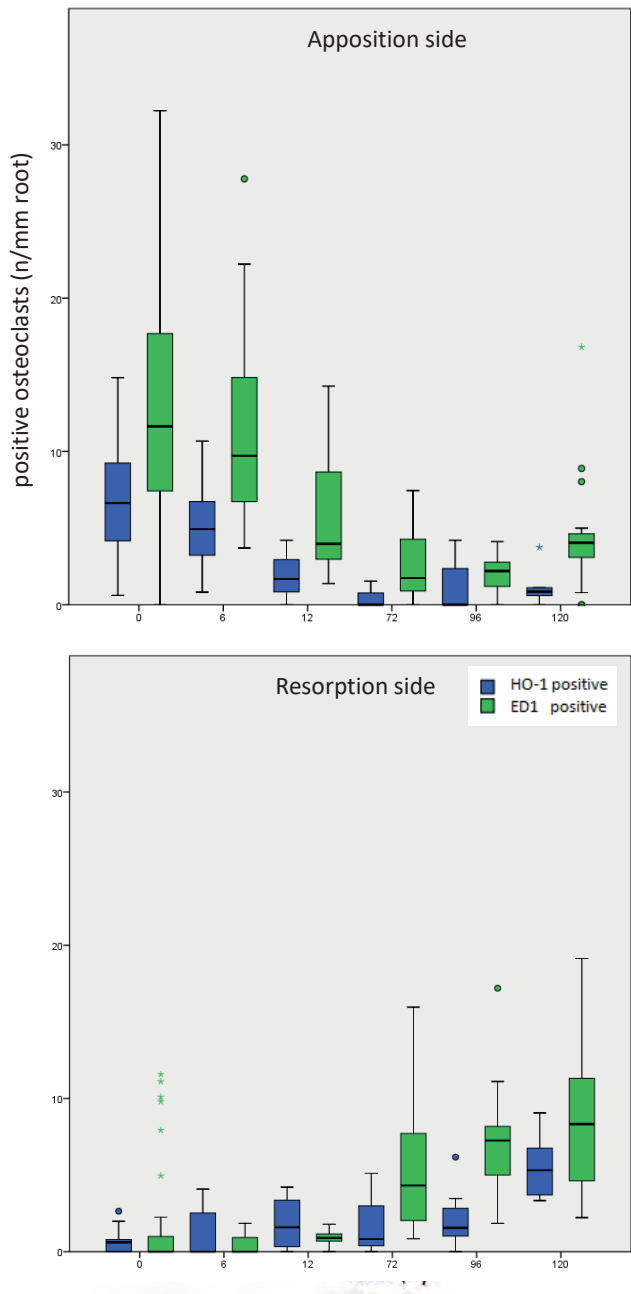


Figure 5B: Effects of orthodontic force on HO-1 and ED1 positive osteoclasts. When no force is present osteoclasts are mainly present at the distal site. Upon mechanical stress, ED1 or HO-1 positive osteoclast numbers decrease at the distal side, what is now called the apposition side (**upper panel**), whereas the number of osteoclasts at the resorption side increase (**lower panel**). HO-1 expression levels in the osteoclasts and the HO-1/ED1 ratio remain similar following mechanical stress (Independent-Samples *T*-tests, $p > 0.05$).

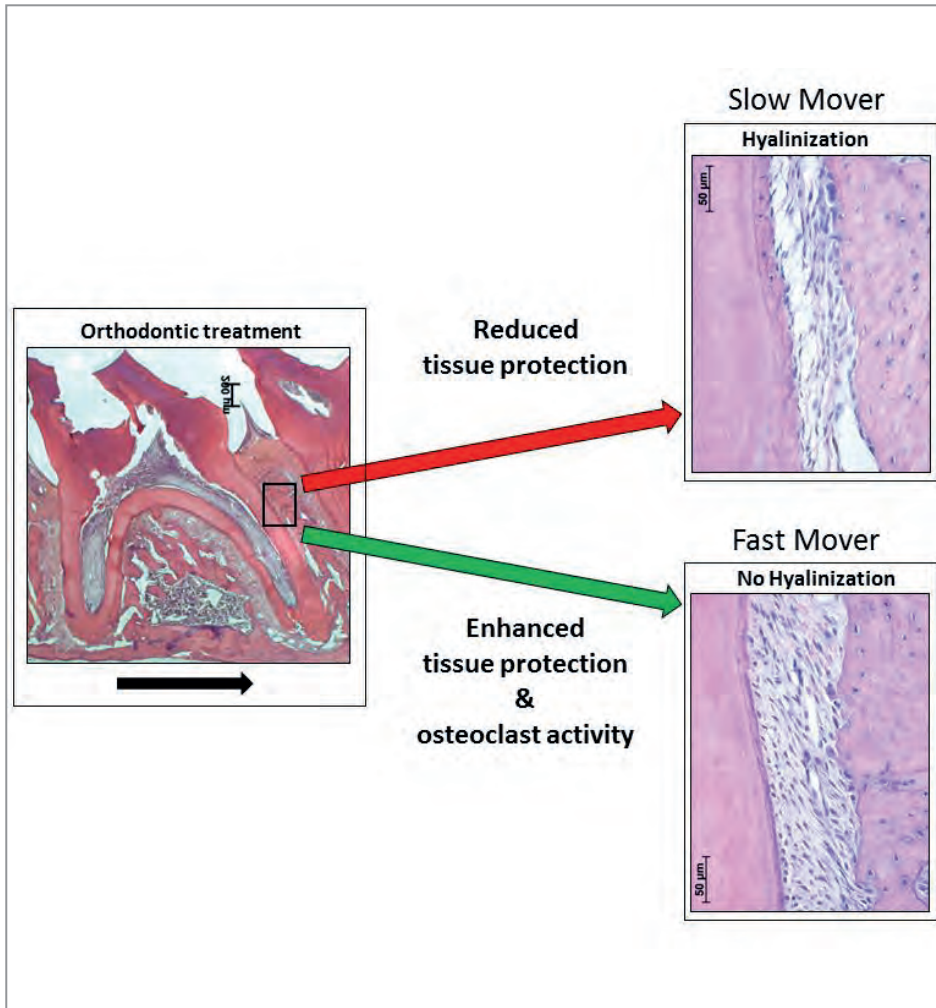


Figure 6: Orthodontic force can result in hyalinization- or no hyalinization formation in the PDL, resulting in “slow” or “fast” tooth movers. In this hypothetical model we postulate that differential expression of tissue protective genes determine, in concert with osteoclast activating genes, the tooth movement. Applied orthodontic force results in mechanical stress within the PDL. This mechanical stress induces expression of HO-1 in PDL cells. Reduced HO-1 expression levels may lead to increased levels of ischemic injury and cell death (hyalinization), resulting in a hampered orthodontic tooth movement rate. Expression of cytoprotective enzymes, as HO-1, likely reduces ischemic injury and cell death. We hypothesize that differential expression of osteoclast activating genes (e.g., IL-1 β) and tissue protecting genes (e.g., HO-1) determines the remodeling of the PDL, or alveolar bone and therefore the orthodontic tooth movement rate. Differences in gene expression levels (e.g., as a result of polymorphisms) levels possibly explain the “slow” and “fast” tooth movers following orthodontic treatment. “Fast” tooth movers have enhanced osteoclastic activity (e.g., high IL-1 β) and protection against hyalinization (e.g., high HO-1), whereas “slow” tooth movers show hyalinization hampering osteoclast activity (black arrow indicates the direction of the tooth movement).

Discussion

We demonstrated here for the first time that applying an orthodontic force strongly induces expression of the cytoprotective enzyme HO-1 in PDL cells at both the resorption- and apposition side in rats. Morphological changes within the PDL because of ischemic stress at the resorption side (compression of blood vessels, hyalinization areas) and mechanical stress at the apposition side (stretched blood vessels and increased PDL width) were observed (**Figure 2**). In general, the control side demonstrated relatively low numbers of HO-1 positive cells. Only bone marrow cells showed constitutively high expression levels of HO-1. Orthodontic force strongly induced HO-1 expression in cells situated closely around blood vessels, suggesting that these cells may be pericytes or infiltrated leukocytes²⁵. A major part of the HO-1 positive PDL cells are fibroblasts, while only a minor part of osteoblasts and cementoblasts are HO-1 positive. In PDL cells HO-1 induction occurred shortly after placing the orthodontic appliance but dropped within 72 h to control values. Thus, although the orthodontic force was applied continuously HO-1 induction within the PDL cells was only temporary. Induction of HO-1 by mechanical stress was previously demonstrated in several *in vivo*²⁶ and *in vitro*¹⁹ experimental settings but not yet during orthodontic tooth movement.

Osteoclasts are bone-specific, indicating the existence of different subsets of osteoclasts at different bone-sites^{27,28}. Induction of HO-1 inhibited osteoclastogenesis *in vitro* and *in vivo* in arthritis models²⁹. It was demonstrated that induction of HO-1 in osteoclast precursors resulted in reduced osteoclast differentiation and subsequently decreased bone resorption. It was also shown that the majority of osteoclasts attached to bone erosions in human joints from patients with rheumatoid arthritis were negative for HO-1²⁹. If these findings of osteoclasts in an arthritic setting could be seen in the oral setting as well, this could have major impact on our understanding of both tooth movement and root resorption. Effects of orthodontic force on HO-1 expression in osteoclasts was therefore studied in more detail.

As demonstrated previously, after application of a mesially-directed force with a Ni-Ti coil spring almost all osteoclasts had disappeared from the distal side within 12 h, while at the mesial side (new resorption side) the number of osteoclasts increased and after 120 h the numbers were similar to the distal side in the control group²⁰. There giant cells are also multinuclear and ED1 positive, we cannot exclude that giant cells entering the PDL and accidentally located at the alveolar bone outline were marked as osteoclasts. However, we remain confident that the large majority of the observed multinuclear, ED1 positive alveolar bone lining cells were osteoclasts.

Both experimental- and control sides demonstrated comparable proportions of HO-1 positive osteoclasts. The proportions of HO-1/ED1 positive cells had not changed significantly, indicating that the basal levels of HO-1 expression in osteoclasts was independent of time and mechanical strain. Thus, mechanical stress did not induce HO-1 expression in osteoclasts. This was also true for the dental pulp cells, interdental

papilla tissue, and bone marrow cells. Since large numbers of HO-1 positive osteoclasts are present in the bone marrow, where normal osteoclast differentiation occurs it is unlikely that osteoclastogenesis is hampered following force induction. In rheumatoid arthritis bone resorption is mainly a pathological process¹⁸, whereas alveolar bone resorption is a normal physiological adaptive process. Functional differences were indeed described between osteoclasts located at long flat bones (craniofacial region) and long bones (axial skeleton) with respect to their acid- and protease secretion during bone degradation^{27,28}.

Reduction or prevention of hyalinized tissue formation is thought to facilitate orthodontic tooth movement and to decrease undermining resorption. It is tempting to speculate that the levels of cytoprotective genes that are activated during orthodontic tooth movement determine whether tooth movement or hyalinization take place. HO-1 has been demonstrated to attenuate inflammation and to prevent tissue injury and apoptosis following ischemic injury^{30,31}. Expression of this cytoprotective HO-1 within the PDL likely generates a protecting environment and subsequently inhibits ischemic injury¹⁰.

In humans the levels of HO-1 induction are largely controlled by a promoter polymorphism, that has been shown to have strong clinical significance^{15,18}. The existence of “slow” and “fast” tooth movers¹¹ could thus possibly be explained by differences in individual expression of HO-1. The HO-1 promoter polymorphism in humans, determining the levels of HO-1 induction, are not present at the equivalent positions in the rat and mouse ho-1 genes³². The influence of gene polymorphism of IL-1 β at the tooth movement rate has been demonstrated previously in orthodontic patients³. Therefore, we hypothesize that remodeling of the PDL and alveolar bone is determined by the sum of the expression of osteoclast activating- and tissue protecting genes in the PDL microenvironment. Differences found in tooth movement rate could be explained by differential expression of these genes (**Figure 6**). Interestingly, HO-1 induction is attenuated at higher age³³, which may further explain the increased levels of root resorption and hyalinization after orthodontic treatment at older age.

Since HO-1 was only shortly induced during the application of the continuous orthodontic force, this suggests that accommodation to the mechanical and ischemic stress takes place. Interestingly, when orthodontic forces are interrupted with inactive periods strongly reduced root resorption has been observed in rats and dogs³⁴. The mechanism of this protection remains unknown. Possibly, renewal of HO-1 induction occurs during intermittent force application, contributing to decreased root resorption and hyalinization formation. Further research to tooth displacement and hyalinization by modulating the HO-1 system is warranted to reveal the exact role of HO-1 during orthodontic tooth movement.

Conclusion

Summarizing, the present study showed that orthodontic forces induced HO-1 expression in the PDL in rats in the mononuclear cell population. Although the force was applied continuously, the HO-1 expression was only temporarily. HO-1 positive osteoclasts are present but this HO-1 expression was shown to be independent of time- and mechanical stress. HO-1 induction may be a novel target for reducing unwanted side effects of orthodontic force application in the future.

References

1. Pilon JJ, Kuijpers-Jagtman AM, Maltha JC. Magnitude of orthodontic forces and rate of bodily tooth movement. An experimental study. *Am J Orthod Dentofacial Orthop.* 1996;110(1):16-23.
2. Van Leeuwen EJ, Kuijpers-Jagtman AM, Von den Hoff JW, Wagener FA, Maltha JC. Rate of orthodontic tooth movement after changing the force magnitude: an experimental study in beagle dogs. *Orthod Craniofac Res.* 2010;13(4):238-245.
3. Iwasaki LR, Gibson CS, Crouch LD, Marx DB, Pandey JP, Nickel JC. Speed of tooth movement is related to stress and IL-1 gene polymorphisms. *Am J Orthod Dentofacial Orthop.* 2006;130(6):698 e691-699.
4. Sanuki R, Shionome C, Kuwabara A, et al. Compressive force induces osteoclast differentiation via prostaglandin E(2) production in MC3T3-E1 cells. *Connect Tissue Res.* 2010;51(2):150-158.
5. Kook SH, Jang YS, Lee JC. Human periodontal ligament fibroblasts stimulate osteoclastogenesis in response to compression force through TNF-alpha-mediated activation of CD4+ T cells. *J Cell Biochem.* 2011;112(10):2891-2901.
6. Krishnan V, Davidovitch Z. On a path to unfolding the biological mechanisms of orthodontic tooth movement. *J Dent Res.* 2009;88(7):597-608.
7. Park KH, Han DI, Rhee YH, Jeong SJ, Kim SH, Park YG. Protein kinase C betaII and delta/theta play critical roles in bone morphogenic protein-4-stimulated osteoblastic differentiation of MC3T3-E1 cells. *Biochem Biophys Res Commun.* 2010;403(1):7-12.
8. Tamura M, Nemoto E, Sato MM, Nakashima A, Shimauchi H. Role of the Wnt signaling pathway in bone and tooth. *Front Biosci (Elite Ed).* 2010;2:1405-1413.
9. Brudvik P, Rygh P. Multi-nucleated cells remove the main hyalinized tissue and start resorption of adjacent root surfaces. *Eur J Orthod.* 1994;16(4):265-273.
10. von Bohl M, Kuijpers-Jagtman AM. Hyalinization during orthodontic tooth movement: a systematic review on tissue reactions. *Eur J Orthod.* 2009;31(1):30-36.
11. van Leeuwen EJ, Maltha JC, Kuijpers-Jagtman AM. Tooth movement with light continuous and discontinuous forces in beagle dogs. *Eur J Oral Sci.* 1999;107(6):468-474.
12. Cao Y, Jansen ID, Sprangers S, et al. IL-1beta differently stimulates proliferation and multinucleation of distinct mouse bone marrow osteoclast precursor subsets. *J Leukoc Biol.* 2016.
13. Wagener FA, Volk HD, Willis D, et al. Different faces of the heme-heme oxygenase system in inflammation. *Pharmacol Rev.* 2003;55(3):551-571.
14. Katori M, Anselmo DM, Busuttill RW, Kupiec-Weglinski JW. A novel strategy against ischemia and reperfusion injury: cytoprotection with heme oxygenase system. *Transpl Immunol.* 2002;9(2-4):227-233.
15. Exner M, Minar E, Wagner O, Schillinger M. The role of heme oxygenase-1 promoter polymorphisms in human disease. *Free Radic Biol Med.* 2004;37(8):1097-1104.
16. Grochot-Przeczek A, Dulak J, Jozkowicz A. Haem oxygenase-1: non-canonical roles in physiology and pathology. *Clin Sci (Lond).* 2012;122(3):93-103.
17. Babusikova E, Jesenak M, Durdik P, Dobrota D, Banovcin P. Exhaled carbon monoxide as a new marker of respiratory diseases in children. *J Physiol Pharmacol.* 2008;59 Suppl 6:9-17.
18. Wagener FA, Toonen EJ, Wigman L, et al. HMOX1 promoter polymorphism modulates the relationship between disease activity and joint damage in rheumatoid arthritis. *Arthritis Rheum.* 2008;58(11):3388-3393.
19. Cho JH, Lee SK, Lee JW, Kim EC. The role of heme oxygenase-1 in mechanical stress- and lipopolysaccharide-induced osteogenic differentiation in human periodontal ligament cells. *Angle Orthod.* 2010;80(4):552-559.
20. Xie R, Kuijpers-Jagtman AM, Maltha JC. Osteoclast differentiation and recruitment during early stages of experimental tooth movement in rats. *Eur J Oral Sci.* 2009;117(1):43-50.
21. Ren Y, Maltha JC, Van 't Hof MA, Kuijpers-Jagtman AM. Age effect on orthodontic tooth movement in rats. *J Dent Res.* 2003;82(1):38-42.
22. Ren Y, Maltha JC, Kuijpers-Jagtman AM. The rat as a model for orthodontic tooth movement--a critical review and a proposed solution. *Eur J Orthod.* 2004;26(5):483-490.
23. Tan SD, Xie R, Klein-Nulend J, et al. Orthodontic force stimulates eNOS and iNOS in rat osteocytes. *J Dent Res.* 2009;88(3):255-260.
24. Sminia T, Dijkstra CD. The origin of osteoclasts: an immunohistochemical study on macrophages and osteoclasts in embryonic rat bone. *Calcif Tissue Int.* 1986;39(4):263-266.

25. Zeng M, Kou X, Yang R, et al. Orthodontic Force Induces Systemic Inflammatory Monocyte Responses. *J Dent Res*. 2015.
26. Rawlinson SC, Zaman G, Mosley JR, Pitsillides AA, Lanyon LE. Heme oxygenase isozymes in bone: induction of HO-1 mRNA following physiological levels of mechanical loading in vivo. *Bone*. 1998;23(5):433-436.
27. Everts V, de Vries TJ, Helfrich MH. Osteoclast heterogeneity: lessons from osteopetrosis and inflammatory conditions. *Biochim Biophys Acta*. 2009;1792(8):757-765.
28. Henriksen K, Bollerslev J, Everts V, Karsdal MA. Osteoclast activity and subtypes as a function of physiology and pathology--implications for future treatments of osteoporosis. *Endocr Rev*. 2011;32(1):31-63.
29. Zwerina J, Tzima S, Hayer S, et al. Heme oxygenase 1 (HO-1) regulates osteoclastogenesis and bone resorption. *FASEB J*. 2005;19(14):2011-2013.
30. Zarjou A, Kim J, Traylor AM, et al. Paracrine effects of mesenchymal stem cells in cisplatin-induced renal injury require heme oxygenase-1. *Am J Physiol Renal Physiol*. 2011;300(1):F254-262.
31. Kumar KJ, Yang HL, Tsai YC, et al. Lucidone protects human skin keratinocytes against free radical-induced oxidative damage and inflammation through the up-regulation of HO-1/Nrf2 antioxidant genes and down-regulation of NF-kappaB signaling pathway. *Food Chem Toxicol*. 2013;59:55-66.
32. Shibahara S, Kitamuro T, Takahashi K. Heme degradation and human disease: diversity is the soul of life. *Antioxid Redox Signal*. 2002;4(4):593-602.
33. Abraham NG, Kappas A. Pharmacological and clinical aspects of heme oxygenase. *Pharmacol Rev*. 2008;60(1):79-127.
34. Kameyama T, Matsumoto Y, Warita H, Soma K. Inactivated periods of constant orthodontic forces related to desirable tooth movement in rats. *J Orthod*. 2003;30(1):31-37; discussion 21-32.

Orthodontic forces induce the cytoprotective enzyme heme oxygenase-1 in rats.

CHAPTER 6

Mechanical stress changes the complex interplay between HO-1, inflammation and fibrosis, during excisional wound repair

Cremers NAJ, **Suttorp CM**, Gerritsen MM, Wong RJ, van Run-van Breda C, van Dam GM, Brouwer KM, Kuijpers-Jagtman AM, Carels CEL, Lundvig DMS, Wagener FADTG

Front Med (Lausanne). 2015 Dec 15;2:86.

Abstract

Mechanical stress following surgery or injury can promote pathological wound healing and fibrosis, and lead to functional loss and esthetic problems. Splinted excisional wounds can be used as model for inducing mechanical stress. The cytoprotective enzyme heme oxygenase-1 (HO-1) is thought to orchestrate the defense against inflammatory and oxidative insults that drive fibrosis. Here, we investigated the activation of the HO-1 system in a splinted and non-splinted full-thickness excisional wound model using HO-1-*luc* transgenic mice. Effects of splinting on wound closure, HO-1 promoter activity, and markers of inflammation and fibrosis were assessed. After seven days, splinted wounds were more than three times larger than non-splinted wounds, demonstrating a delay in wound closure. HO-1 promoter activity rapidly decreased following removal of the (epi)dermis, but was induced in both splinted and non-splinted wounds during skin repair. Splinting induced more HO-1 gene expression in 7-day wounds; however, HO-1 protein expression remained lower in the epidermis, likely due to lower numbers of keratinocytes in the re-epithelialization tissue. Higher numbers of F4/80-positive macrophages, α SMA-positive myofibroblasts, and increased levels of the inflammatory genes IL-1 β , TNF- α , and COX-2 were present in 7-day splinted wounds. Surprisingly, mRNA expression of newly-formed collagen (type III) was lower in 7-day wounds after splinting; whereas, VEGF and MMP-9 were increased. In summary, these data demonstrate that splinting delays cutaneous wound closure and HO-1 protein induction. The pro-inflammatory environment following splinting, may facilitate higher myofibroblast numbers and increases the risk of fibrosis and scar formation. Therefore, inducing HO-1 activity against mechanical stress-induced inflammation and fibrosis may be an interesting strategy to prevent negative effects of surgery on growth and function in patients with orofacial clefts or in patients with burns.

Keywords: cleft palate, burns, mechanical stress, wound healing, heme oxygenase-1, inflammation, fibrosis.

Abbreviations

ABC	Avidin-biotin-peroxidase complex
ANOVA	Analysis of variance
α -SMA	Alpha smooth muscle actin
AU	Arbitrary units
CL/P	Cleft lip with or without cleft palate
CO	Carbon monoxide
COX-2	Cyclooxygenase-2
CXCL1	Chemokine (C-X-C) ligand 1
DAB	Diaminobenzidine-peroxidase
DPX	Distyrene plasticizer xylene
ECM	Extracellular matrix
F4/80	EGF-like module-containing mucin-like hormone receptor-like 1
HO	Heme oxygenase
ICAM-1	Intercellular adhesion molecule-1
IL-1 β	Interleukin-1 beta
MCP-1	Monocyte chemotactic protein-1
MMP-9	Matrix metalloproteinase-9
NDS	Normal donkey serum
PBSG	Phosphate buffered saline with glycin
ROI	Regions of interest
TNF- α	Tumor necrosis factor-alpha
VEGF	Vascular endothelial growth factor

Introduction

Cleft lip with or without cleft palate (CL/P) is a developmental craniofacial disorder that is characterized by an opening in the upper lip and/ or palate and alveolar bone¹. Patients with CL/P need multiple surgeries that inevitably result in scar formation (**Figure 1A**)^{2,3}. In particular, scars on the palate may disrupt normal midfacial growth and impair dento-alveolar development^{4,5}. Also, patients with severe burns can exhibit excessive scar formation (**Figure 1B**)⁶. Scarring can be exaggerated by mechanical tension, such as during growth of the child and during wound repair⁷. Overall, pathological wound healing following mechanical stress can result in hypertrophic scars, and subsequently lead to functional, psychosocial, and esthetical problems for patients^{8,9}.

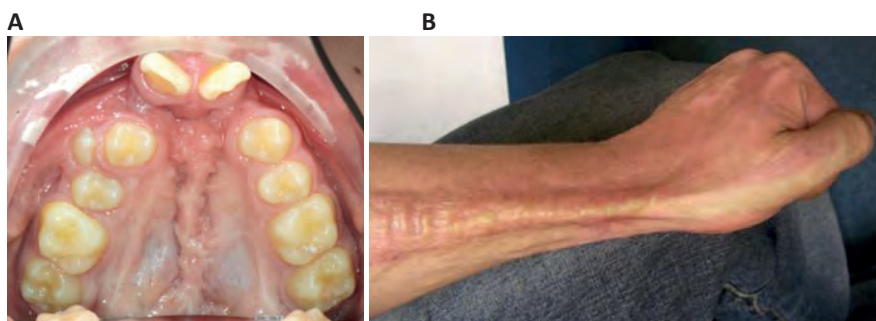


Figure 1. Mechanical stress may promote excessive scar formation following injury. (A) An intra-oral photo of the maxillary arch of a patient of our clinic with an operated complete bilateral cleft lip and palate is shown. Mechanical stress-induced scar formation impairs development of the upper jaw and the dentition. **(B)** Also, burns can result in excessive scar formation leading to cosmetic and functional problems as exemplified by scar formation near the wrist.

Mechanical load, together with cytokine expression and the composition of the extracellular matrix (ECM), promotes the differentiation of fibroblasts into myofibroblasts¹⁰⁻¹². During wound repair, myofibroblasts play a key role in the deposition of ECM and in wound contraction, thereby reducing wound size and preventing invasion by pathogens^{10,12}. When a wound closes, myofibroblasts normally disappear by apoptosis. However, during pathologic wound healing, extended presence of myofibroblasts may result in excessive wound contracture and ECM deposition, leading to excessive scar formation and functional problems^{5,13}. Mechanical stress during wound repair can trigger a continued expression of the myofibroblast marker alpha smooth muscle actin (α -SMA), and a prolonged survival of myofibroblasts^{5,14-17}. Prolonged inflammatory and oxidative stress may also increase myofibroblast survival¹⁸. A better understanding of the effects of mechanical stress during the wound healing process is warranted to develop novel adjuvant therapies.

Rodents, in contrast to humans, possess a subcutaneous muscle layer (*m. panniculus carnosus*), which can cause wound contraction¹⁹. In these animals, the use of splinting can induce static mechanical stress to healing wounds^{5,14,20}, interfere with

this muscle contraction, and thus better simulate human wound healing that is mainly dependent on granulation and re-epithelialization of tissues¹⁹. The effects of static mechanical stress on the different phases of wound healing, caused by splinting, remains to be unraveled. In addition, the involvement of cytoprotective mechanisms needs further exploration. Activation of the cytoprotective heme oxygenase (HO) system has shown protective effects in both inflammatory and fibrotic models^{6,18,21}.

Heme oxygenase is an enzyme that catabolizes heme, yielding the gasotransmitter carbon monoxide (CO), free iron, which is scavenged by co-induced ferritin, and biliverdin that is rapidly converted into the antioxidant bilirubin by biliverdin reductase²². The HO system possesses antioxidative, anti-inflammatory, anti-fibrotic, and anti-apoptotic properties^{18,23}, and can influence cell proliferation, differentiation, and migration. When these processes are disrupted, wound repair may be hampered²⁴. There are two isoforms of HO, the inducible HO-1 and the constitutively expressed HO-2. It has been shown that HO-1 is rapidly induced in wounded tissues^{25,26}. Decreased HO-1 or HO-2 expression and enzyme activity in mice results in slower cutaneous wound closure; whereas induction of HO-1 expression or administration of the HO effector molecule bilirubin attenuates the inflammatory response and accelerates wound healing in HO-1-deficient mice²⁷⁻²⁹.

In this study, we investigated the expression of HO-1 during wound repair in both non-splinted and splinted wounds using transgenic HO-1-*luc* mice. Because mechanical stress has been shown to induce HO-1 expression in different experimental settings in a time- and force-dependent manner³⁰⁻³², we therefore postulated that mechanical stress by splinting would induce HO-1 expression during wound healing. In addition, we investigated the effects of mechanical stress on markers of inflammation, ECM remodeling, and fibrosis.

Materials and Methods

Animals

The Committee for Animal Experiments of Radboud University Nijmegen approved all procedures involving mice (RU-DEC 2010-248). Twelve mice (strain: HO-1-*luc* FVB/ N-Tg background), 4 to 5 months of age and weighing 30 ± 5 g, were provided with food and water *ad libitum*. Mice were maintained on a 12 h light/dark cycle and specific pathogen-free housing conditions at the Central Animal Facility Nijmegen. More details on the housing conditions have been previously described³³. Mice were originally derived from Xenogen Corporation (Alameda, CA, USA) and generated as previously described³⁴.

The mice were euthanized with a standard CO₂/O₂ protocol seven days after wounding, after which control skin, and wounded skin were isolated. Half of the tissue

was fixed for 24h in 4% paraformaldehyde and then embedded in paraffin following regular histosafe procedures and the other half was snap-frozen in liquid nitrogen and stored at -80°C until isolation of mRNA.

Excisional non-splinted and splinted wound model

Splinted ($n = 6$) and non-splinted ($n = 6$) full-thickness excisional wounds 4 mm in diameter were created on the dorsum of the mice after shaving as previously described³⁵. In brief, excisional wounds were created using a sterile disposable 4-mm skin biopsy punch (Kai Medical, Seki City, Japan) on the dorsum to either side of the midline, and halfway between the shoulders and pelvis. Circular silicone splints of 6-mm inner- and 12-mm outer-diameter made from silicone sheets (3M, Saint Paul, Minnesota, USA) were glued to the skin around the wound. Mice receiving splinted excisional wounds were wrapped with semi-permeable dressing (Petflex; Andover, Salisbury, MA, USA) around their torso, to cover the wound. One mouse in the splinted group died due to pulmonary failure as a result of respiratory obstruction by the bandage during the recovery from anaesthesia.

Photographs of the wounds were taken immediately after wounding and then 1h and 1, 3, 5 and 7 days thereafter with a reference placed perpendicular next to the wounds for wound size normalization. The area of the wounds was blindly measured in triplicates using ImageJ (NIH) v1.44p software.

HO-1 promoter activity measurements

Heme oxygenase-1 promoter activity was determined at baseline, immediately after wounding and 1h and 1, 3, and 7 days thereafter in the HO-1-*luc*-Tg mice by *in vivo* bioluminescence imaging using the IVIS Lumina system (Caliper Life Sciences, Hopkinton, MA, USA) as previously described³⁶. Images were quantified using Living Image 3.0 software (Caliper Life Sciences) by selecting regions of interest (ROI). The amount of emitted photons per second (total flux) per ROI was measured, and then calculated as fold change from baseline levels.

Immunohistochemical staining

Immunohistochemical staining for HO-1, macrophages (F4/80), and myofibroblasts (α -SMA) were performed on paraffin sections of the wounds as previously described³⁵. In short, paraffin-embedded tissues were cut into 5- μ m sections, which were then de-paraffinized, quenched for endogenous peroxidase activity with 3% H₂O₂ in methanol for 20 min, and rehydrated. Sections were post-fixed with 4% formalin, and washed with PBS containing 0.075 μ g/ mL glycine (PBSG). Antigens were retrieved with citrate buffer (0.01 M, pH 6.0) at 70°C for 10 min, followed by incubation in 0.075 g/mL trypsin in PBS at 37°C for 7 min. Next, the sections were pre-incubated with 10% normal donkey serum (NDS) in PBSG. First antibodies (HO-1 from Stressgen #SPA-895 1:600 dilution, α -

SMA from Sigma-Aldrich #A2547 1:600 dilution, and F4/80 from AbD Serotec #MCA497R 1:200 dilution) were diluted in 2% NDS in PBSG and incubated overnight at 4°C. After washing with PBSG, sections were incubated for 60 min with a biotin-labeled secondary antibody against host species (1:5000 dilution). Next, the sections were washed with PBSG and treated with avidin-biotin-peroxidase complex (ABC) for 45 min in the dark. After extensive washing with PBSG, diaminobenzidine-peroxidase (DAB) staining was performed for 10 min. After rinsing with water, staining was intensified with Cu₂SO₄ in 0.9% NaCl and rinsed with water again. Finally, the nuclei were stained with hematoxylin for 10 s and sections were rinsed for 10 min in water, dehydrated and embedded in distyrene plasticizer xylene (DPX).

Immunoreactivity was evaluated by blindly scoring the wounds. For the HO-1 staining, we scored both the epidermal and dermal region of the wounds separately, since there were two different positively stained populations. A single section per wound was semi-quantitatively scored, by two assessors independently of each other, as previously described according to the following scale: 0 (minimal), 1 (mild), 2 (moderate), and 3 (marked)³⁵.

RNA isolation and quantitative-RT-PCR

Non-wounded control skin and wounds were pulverized in TRIzol (Invitrogen) using a micro-dismembrator (Sartorius BBI Systems GmbH, Melsungen, Germany) and RNA was further extracted as previously described³⁷. Quantitative-RealTime-PCR was performed. mRNA expression levels were calculated as minus delta delta Ct (-ΔΔCt) values, normalized to the reference gene GAPDH, and corrected for non-wounded control skin. Fold change were calculated by $2^{\Delta(-\Delta Ct)}$. The sequences of the mouse-specific primers are shown in **Table 1**.

Table 1. Mouse primers.

Marker	Gene name	Forward primer (5'-3')	Reverse primer (5'-3')
Reference gene	GAPDH	GGCAAATTCACGGCACA	GTTAGTGGGGTCTCGCTCCTG
Inflammation	IL-1β	TGCAGCTGGAGAGTGTGG	TCCACTTTGCTCTTGACTTCTATC
	TNF-α	CTCTTCTCATTCTGCTTG	GGGAACCTTCTCATCCCTTGG
	COX-2	CCAGCACTTCACCCATCAGTT	ACCCAGGTCTCGCTTATGA
	MCP-1	ACTGAAGCCAGCTCTCTTCTC	TTCTTCTTGGGGTCAGCACAGAC
Cytoprotection	HO-1	CAACATTGAGCTGTTTGAGG	TGGTCTTTGTGTTCTCTGTC
	HO-2	AAGGAAGGGACCAAGGAAG	AGTGGTGGCCAGCTTAAATAG
Angiogenesis	VEGF	GGAGATCCTTCAGGAGCACTT	GGCGATTAGCAGCAGATATAAGAA
Fibrosis	α-SMA (acta2)	CAGGCATGGATGGCATCAATCAC	ACTCTAGCTGTGAAGTCAGTGTCTG
	MMP-9	TGCCCATTTTCAGCAGCAGAC	GTGCAGGCCGAATAGGAGC
	Collagen 3a1	ATCCCATTTGGAGAATGTTG	AAGCACAGGAGCAGGTGTAG
Keratinocytes	Krt-6	GACGACCTACGCAACACC	AGGTTGGCACACTGCTTC

Statistics

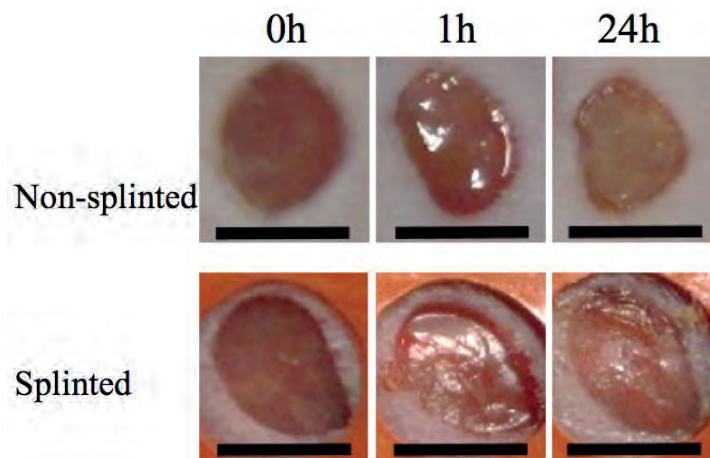
Data were analyzed using GraphPad Prism 5.01 software (San Diego, CA, US). No outliers were detected using the Grubbs' test. Data was analyzed by a paired *t*-test for comparisons of two groups and a one- or two-way analysis of variance (ANOVA) for the comparison of multiple groups with a *post-hoc* Bonferroni correction for multiple comparisons. The non-parametrical one-tailed Mann-Whitney *U*-test was used to compare the arbitrary scored immunohistological sections. Results were considered significant different when $p < 0.05$ (* $p < 0.05$, ** $p < 0.01$, *** $p < 0.001$).

Results

Static mechanical stress induced by splinting delays excisional wound closure

Because mechanical stress can lead to excessive scar formation (**Figure 1A,B**), we used both splinted and non-splinted excisional wound healing to assess the effects of static mechanical stress on wound closure. Wound sizes of non-splinted and splinted wounds were monitored over time and representative photos are shown in **Figure 2A**. After quantification of the wound area the wound closure time in relation to $t = 0$ h was displayed (**Figure 2B**). All wounds closed gradually, but there were differences in wound closure between splinted and non-splinted wounds. After 3 days, significant differences between the groups were found. Non-splinted wounds were already closed for 45%; whereas, splinted wounds had only closed by 10%. After 7 days, closure of non-splinted wounds was 75% of the wound area, while that for splinted wounds was only 23%. This corresponds to a 3.3 times faster wound closure rate when no mechanical stress was applied. This demonstrates that splinting effectively delays wound closure.

A



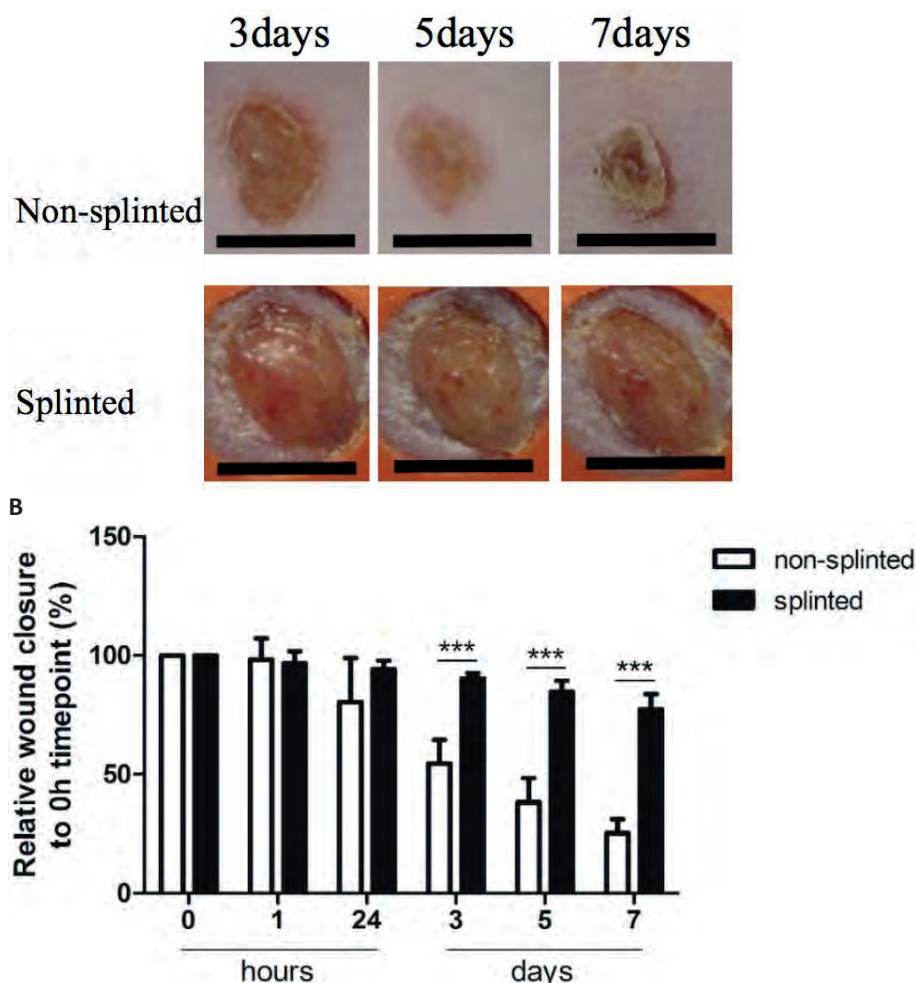


Figure 2: Splinted and non-splinted excisional wound closure over time. (A) Representative pictures of non-splinted and splinted wounds immediately following injury, and 1 h, and 1, 3, 5 and 7 days after wounding (black bars = 4 mm). **(B)** Quantification of closure of non-splinted ($n = 6$) and splinted ($n = 5$) wounds over time (0-7 days). Each mouse had two wounds. Time point 0 h was used as 100%. Data represent mean \pm SD. * is significantly different between non-splinted and splinted wounds (***) $p < 0.001$.

The HO system is affected by mechanical stress during excisional wound healing

Heme oxygenase-1 is a critical regulator and expressed in distinct cell types during the different phases of wound repair. To investigate the role of HO-1 following mechanical stress (splinting) during excisional wound healing, we used HO-1-*luc* mice to monitor HO-1 promoter activity (**Figure 3A**). HO-1 promoter activity was already present in the kidneys in non-injured HO-1-*luc* mice. In the wound area, HO-1 promoter activity was evident especially at days 3 and 7 after splinting.

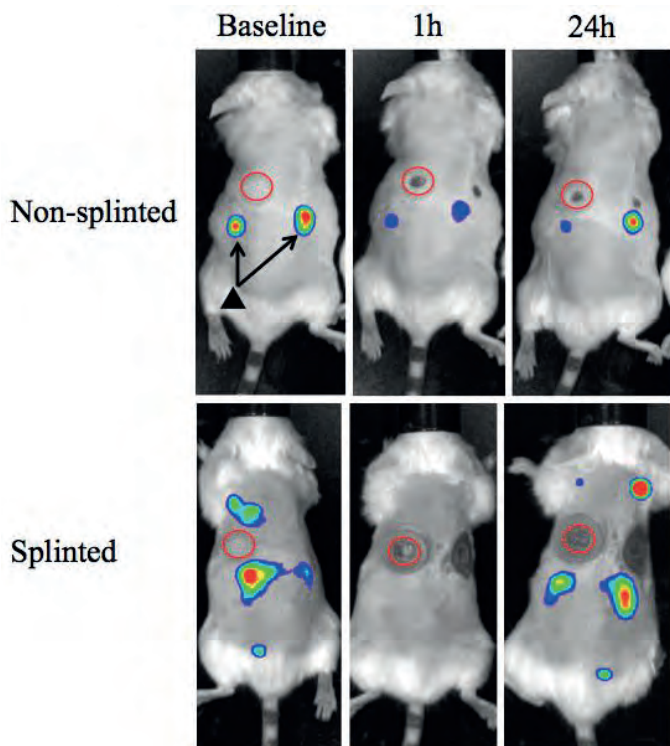
Surprisingly, we found that following wounding, there was an initial significant decrease in HO-1 promoter activity after 1 h in both splinted as well as non-splinted

wounds (**Figure 3B**). This decrease of HO-1 promoter activity returned to basal levels at day 1 and further increased at days 3-7, independent of splinting. Three days following wounding, the splinted wounds showed a significant increase of HO-1 promoter activity compared to basal levels.

To further elucidate the role of splinting on HO-1 expression during wound repair, we measured both HO-1 mRNA and protein expression in day-7 wounds. Using RT-PCR, HO-1 mRNA expression was assessed in the wounds and corrected for expression in non-wounded control skin (**Figure 4A**). Here, we found significantly higher (2.6 times) HO-1 mRNA expression in splinted wounds compared to non-splinted wounds. As expected, the constitutively-expressed HO-2 levels were not significantly different after induction of mechanical stress.

Immunohistochemical staining demonstrated that HO-1 levels were severely affected by wounding when compared to non-wounded skin. The number of HO-1-positive cells 7 days after wounding was increased in the dermal region of the wounds; also, more HO-1-positive cells were present in the epidermal region when compared to non-wounded skin.

A



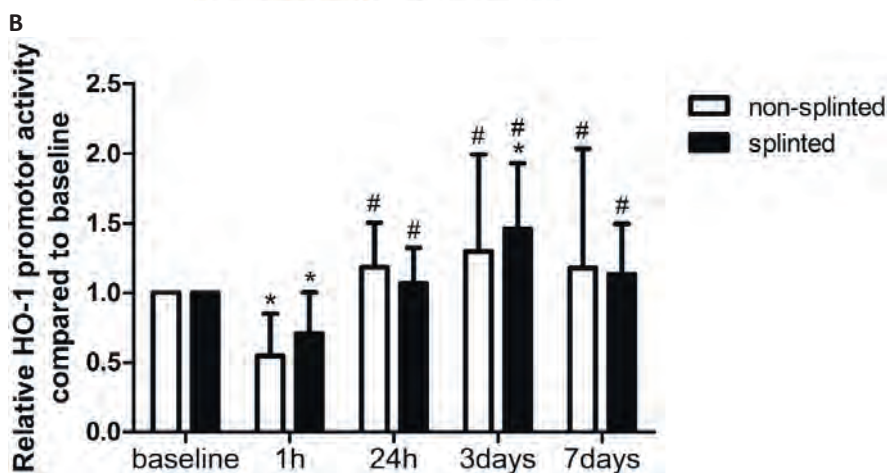
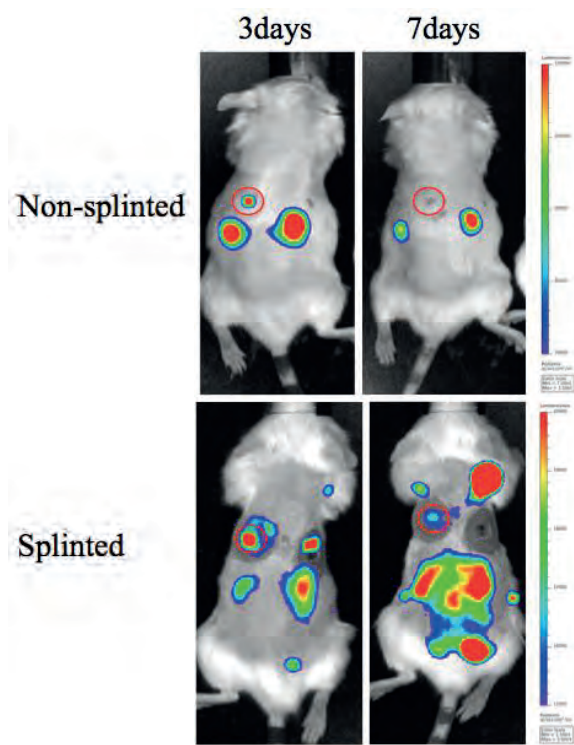
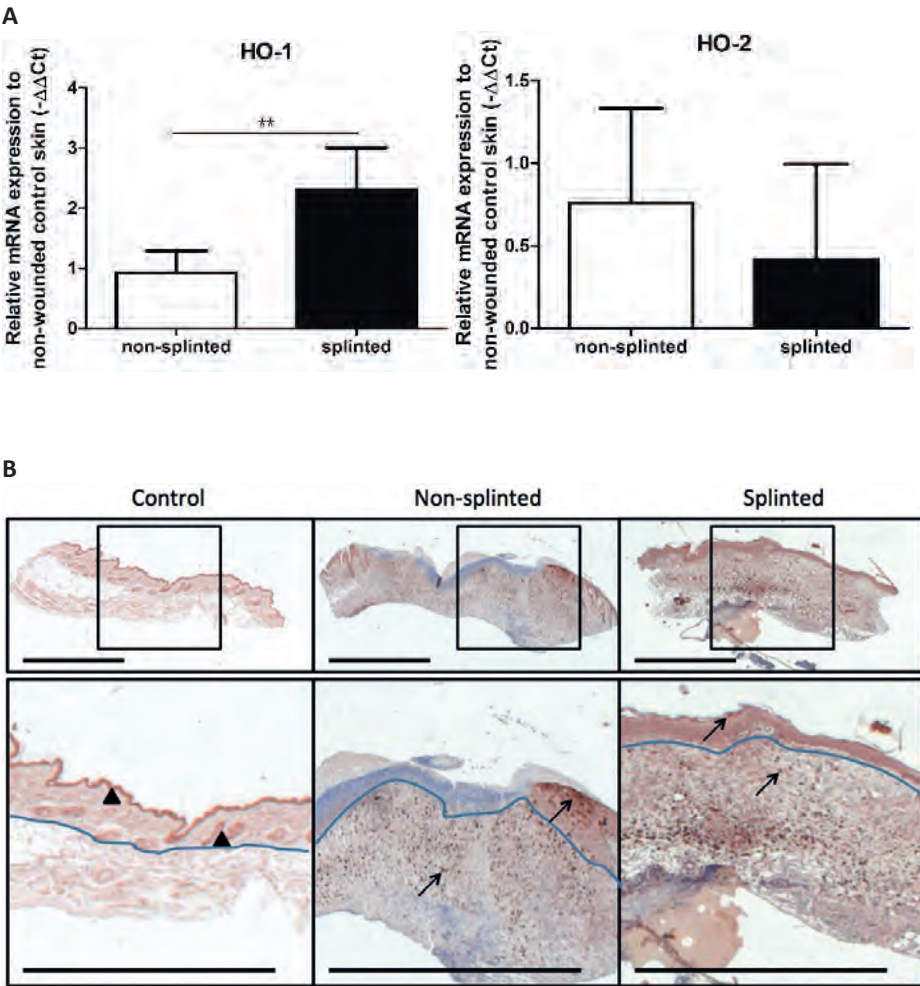


Figure 3: HO-1 promoter activity in splinted and non-splinted wounds. (A) Representative images of HO-1 promoter activity of non-splinted and splinted wounds over time using the IVIS system to measure *in vivo* bioluminescence in HO-1-*luc* mice. The rainbow colored bar at the right side indicates the amount of luciferase signal represented in each group with a high signal in red and low signal in blue. The red circles surround the wounds in the mice and indicate the measured region of interest (ROI). Note: black triangle (▲) with black arrows shows that there is basal HO-1 promoter activity around the kidneys. **(B)** Quantification of HO-1 promoter activity during non-splinted ($n = 6$) and splinted ($n = 5$) wound healing. Each mouse had two wounds. Data represent mean \pm SD. * is significantly different within the non-splinted or splinted group when compared to the baseline at the start of the experiment ($*p < 0.05$). # is significantly different within the non-splinted or splinted group when compared to 1 h after wounding ($\#p < 0.05$).

Heme oxygenase-1 protein was particularly evident in the epithelial cells at the leading edge of the wound in the epidermis and in recruited inflammatory leukocytes in the dermis (**Figure 4B**). Since we observed two different populations of HO-1-positive cells depending on their region, the wounds were scored for the level of HO-1 protein expression in both the epidermal and dermal regions, which were compared between the different treatment groups (**Figure 4C**).

Importantly, non-splinted wounds showed significantly higher HO-1 protein expression in the epidermal region compared to splinted wounds. In the dermal region, HO-1 was slightly higher after mechanical stress compared to the non-splinted wounds; however, this did not reach statistical significance ($p=0.21$). Variation in HO-1 protein expression was found between animals, but was independent of the wound model.



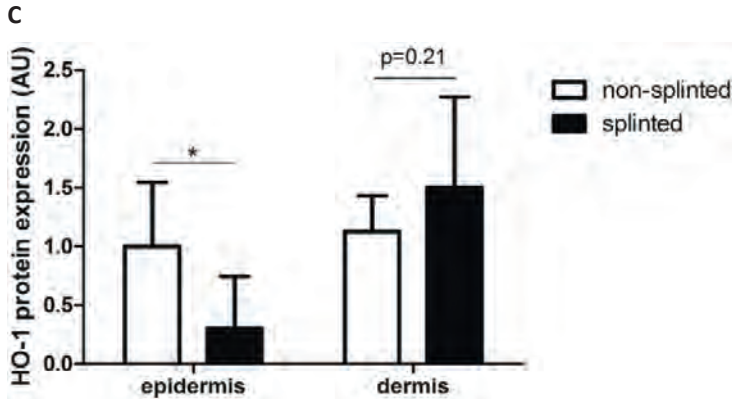


Figure 4: HO expression in wounds. (A) HO-1 and HO-2 mRNA expression levels in non-splinted and splinted wounds were determined in 7-day wounds and compared to control unwounded skin. Data represent mean \pm SD. * is significantly different between non-splinted and splinted wounds (** $p < 0.01$). (B) HO-1 protein expression in control and non-splinted and splinted wounds after 7 days of healing. Region above the marked blue line is the epidermis and underneath the line is the dermal layer (bars = 1 mm). Note: black triangle (\blacktriangle) in the non-wounded control skin shows HO-1-positive keratinocytes at the front of the epithelial layer, and HO-1 positive hair follicles. Black arrows (\rightarrow) shows HO-1-positive cells in the epidermis and dermis of non-splinted and splinted wounds. (C) Quantification of scored HO-1 protein staining in epidermis and dermis of the wounds after 7 days in arbitrary units (AU). Data represent mean \pm SD. * is significantly different between non-splinted and splinted wounds (* $p < 0.05$).

Thus, wounding initially decreased HO-1 promoter activity in the wound, after which HO-1 levels were restored and further induced by recruitment of inflammatory cells and keratinocytes. Surprisingly, although splinted wounds delay HO-1 expression, as shown by an increased HO-1 promoter activity and HO-1 mRNA expression, HO-1 protein expression was, in contrast to in the dermis, lower in the epidermis when compared to non-splinted wounds.

Interplay between HO-1 and inflammation in non-splinted and splinted wound healing

Since there was a clear delay in wound closure and HO-1 protein expression in splinted wounds, we investigated whether this delay correlated with altered levels of inflammatory gene expression. Because HO-1 has anti-inflammatory and antioxidative properties, we expected that the delayed HO-activity in the skin would result in increased levels of inflammation. Therefore, we quantitated the number of F4/80-positive macrophages using immunohistochemical staining in sections of non-splinted and splinted wounds (**Figure 5A**).

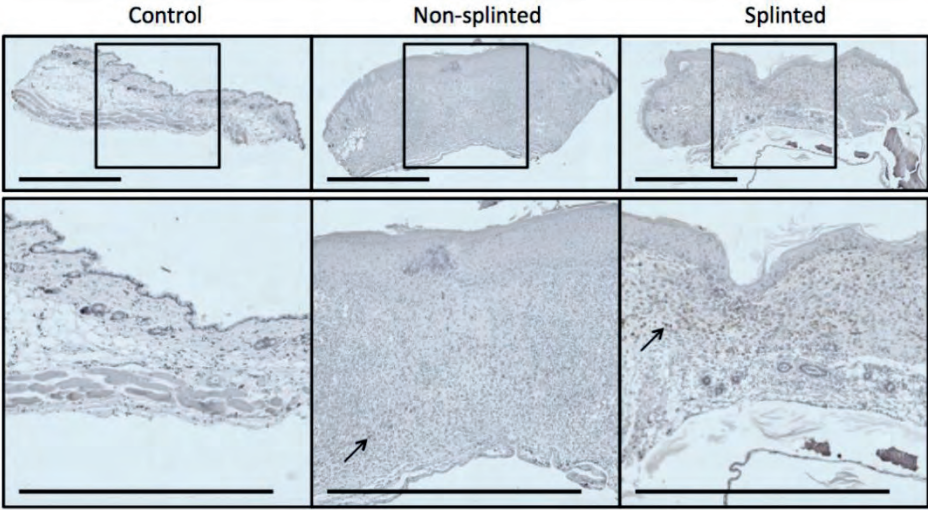
We found that there were indeed significantly more macrophages present in 7-day splinted wounds compared to non-splinted wounds (**Figure 5B**). Next, we investigated whether mRNA expression of monocyte chemotactic protein (MCP-1), the main chemokine to attract monocytes/ macrophages, was altered by mechanical stress.

We observed that MCP-1 was elevated 1.8 fold in splinted wounds compared to non-splinted wounds, however, this difference did not reach statistical significance ($p=0.10$).

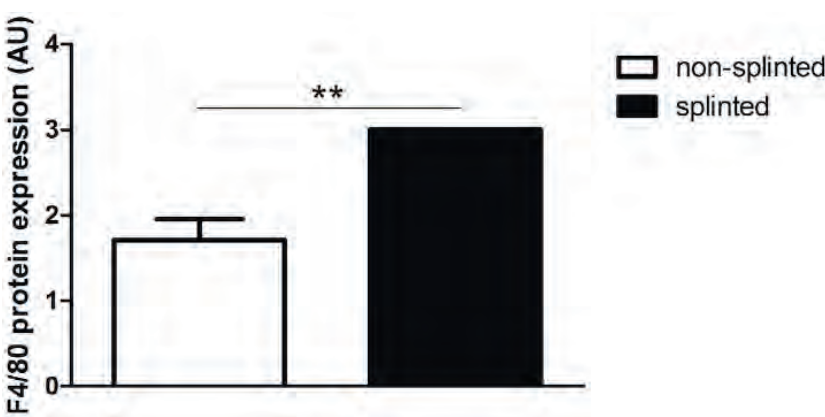
Finally, when we examined the gene expression of several other inflammatory markers, we found that mRNA expression levels of the pro-inflammatory cytokines IL-1 β , TNF- α , and COX-2 in splinted wounds were significantly higher when compared to non-splinted wounds (36.9-, 24.4-, 8.8-fold, respectively) (**Figure 5C**).

In summary, we showed that delayed wound closure and reduced HO-1 protein expression following mechanical stress was clearly associated with elevated levels of macrophages and several other inflammatory genes.

A



B



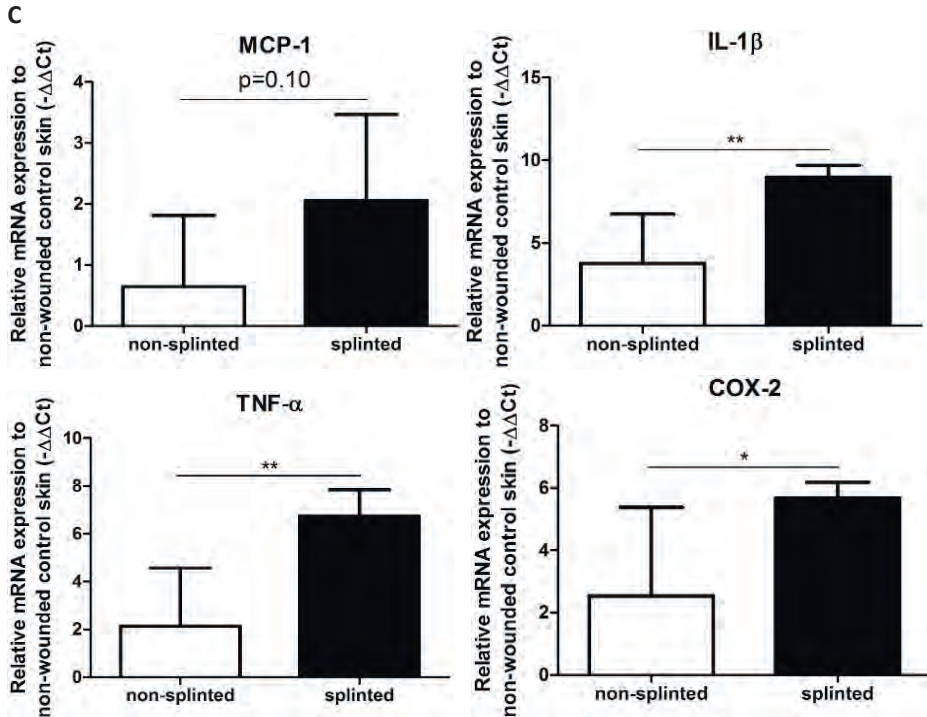


Figure 5: Effects of splinting on markers of inflammation. (A) Immunohistological staining of macrophages (F4/80) in control skin and non-splinted and splinted 7-day wounds (bars = 1 mm). Black arrow (→) shows F4/80-positive macrophages in non-splinted and splinted wounds. (B) Quantification of scored F4/80 protein staining of the wounds after 7 days in arbitrary units (AU). Data represent mean ± SD. * is significantly different between non-splinted and splinted wounds (** $p < 0.01$). (C) mRNA expression levels of inflammatory markers in 7-day non-splinted and splinted wounds normalized to levels in control unwounded skin (MCP-1, IL-1β, TNF-α, and COX-2). Data represent mean ± SD. * is significantly different between non-splinted and splinted wounds (* $p < 0.05$, ** $p < 0.01$).

Effects of mechanical stress on remodeling and fibrotic genes

Because increased levels of inflammation by mechanical stress during wound repair may also affect markers of fibrosis, we investigated the effects of splinting on markers of ECM remodeling and fibrosis.

During wound healing, fibroblasts can transform into myofibroblasts. These myofibroblasts cause wound contraction and produce ECM. Normally, these myofibroblasts go into apoptosis after wound repair has finished. When these myofibroblasts fail to become apoptotic, ECM production continues, and pathologic wound healing with excessive scarring follows. The presence of myofibroblasts is dependent on the phase of wound healing. To investigate the role of splinting on myofibroblasts, we stained 7-day wound sections with the myofibroblast marker α-SMA. In non-wounded skin, α-SMA staining was already evident in the muscles of the vascular wall and the arrector pili muscles of the hair follicles (**Figure 6A**). Following injury, myofibroblasts were present both in non-splinted as well as splinted wounds.

However, quantification of arbitrarily scored α -SMA-positive myofibroblasts showed significantly increased levels in splinted wounds when compared to non-splinted wounds (**Figure 6B**).

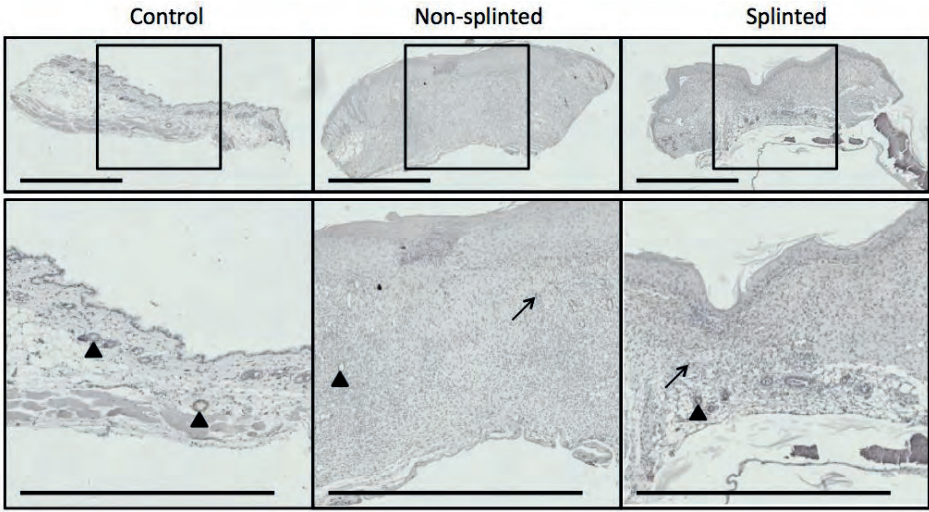
Next, we measured mRNA expression levels of genes involved in remodeling and fibrosis (**Figure 6C**). Vascular endothelial growth factor (VEGF) is an important regulator of angiogenesis, and was 2.9 times higher in splinted wounds compared to non-splinted wounds. Also matrix metalloproteinase (MMP)-9, an important enzyme that helps remodel the provisional ECM following wounding, was increased (four-fold).

Surprisingly, collagen type 3 gene expression, which is produced by (myo)fibroblasts, and forms the major collagen type expressed in granulation tissue, was almost three times lower in splinted wounds compared to non-splinted wounds ($p=0.0544$).

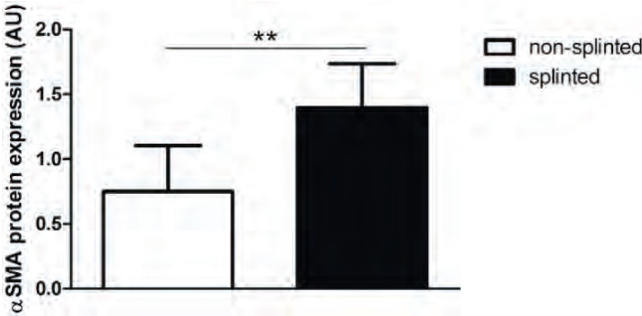
Interestingly, we found significantly more (5.8-fold) gene expression of keratinocyte marker krt-6 in non-splinted wounds compared to splinted wounds.

Thus, there were more myofibroblasts and higher expression of VEGF and MMP-9 in day-7 wounds following mechanical stress.

A



B



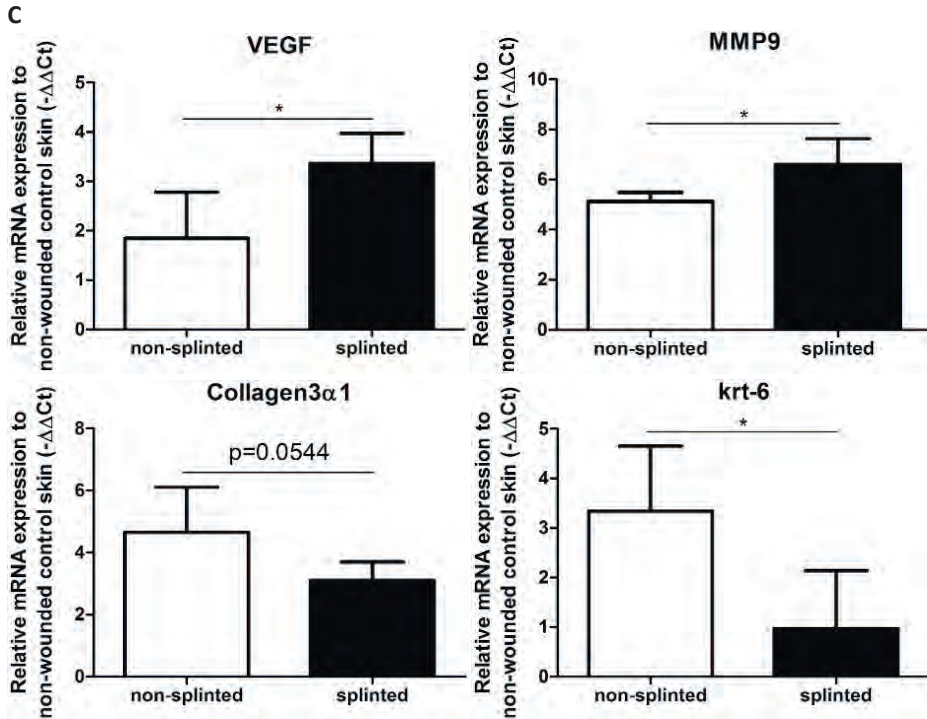


Figure 6: Effects of splinting on markers of fibrosis. (A) Immunohistological staining of α -SMA-positive myofibroblasts in control skin and non-splinted and splinted 7-day wounds (bars = 1 mm). Note: black triangle (\blacktriangle) in the non-wounded control skin shows α -SMA-positive muscles in the vascular wall and the arrector pili muscles of the hair follicles. Black arrow (\rightarrow) shows α -SMA-positive myofibroblasts. (B) Quantification of scored α -SMA protein staining of wounds after 7 days in arbitrary units (AU). Data represent mean \pm SD. * is significantly different between non-splinted and splinted wounds (** $p < 0.01$). (C) mRNA expression levels of VEGF, MMP-9, collagen type 3, and krt-6 in 7-day non-splinted and splinted wounds normalized to levels in control unwounded skin. Data represent mean \pm SD. * is significantly different between non-splinted and splinted wounds (* $p < 0.05$).

Discussion

We found that splinting effectively delayed wound closure. Interestingly, HO-1 promoter activity initially decreased upon wounding, but was followed by induction of HO-1 mRNA and protein. However, HO-1 protein expression was delayed in the splinted wounds. Since HO activity attenuates inflammatory and oxidative stress and is thought to reduce fibrosis, we postulated that the splinting-mediated delay in HO-1 protein expression could result in a reduced defense against inflammatory and fibrotic processes. Indeed, more F4/80-positive macrophages, α -SMA-positive myofibroblasts, and pro-inflammatory cytokines were present in splinted wounds at day 7 when compared to non-splinted wounds. Normally, the wound healing cascade is characterized by three distinct phases: inflammation, proliferation and remodeling^{9,38,39}. This suggests that mechanical stress causes delayed wound closure, a

prolongation of the inflammatory phase, and an altered remodeling phase, and may promote fibrosis.

Mechanical stress and HO-1

We found that mechanical stress by splinting delays wound closure 3.3 times in comparison to non-splinted wounds after 7 days. This was likely largely mediated by inhibiting the contraction of the subcutaneous muscle layer in mice; however, it may also be caused by interfering with other processes involved in wound healing, such as inflammation, proliferation or remodeling.

Previously, it was shown that *in vitro* administration of mechanical stress with a Flex-cell strain unit induces HO-1 mRNA and protein expression in periodontal ligament cells in a time- and force-dependent manner³⁰. HO-1 mRNA levels are also upregulated *in vitro* after mechanical stress in human aortic endothelial cells⁴⁰ and human dental pulp cells⁴¹. Aortic smooth muscle cells also respond to mechanical stress, and induce HO-1 expression in a time-dependent response to laminar shear stress³². In an *in vivo* model with inflammatory, oxidative and mechanical stress, HO-1 mRNA was induced after 6 and 12 h as a result of unilateral urethral obstruction³¹. We therefore postulated that splinting would induce HO-1 as a protective response.

We have shown that within the first hour of wounding, HO-1 promoter activity at the place of the wound decreases. This may be related to the removal of the HO-1-positive skin layer. This suggests that there is basal HO-1 promoter activity present in normal skin, which we previously validated in the epithelium of the skin⁶. More precisely, keratinocytes in the hyperproliferative epithelium express high levels of HO-1 as normal physiology^{25,26}. After the initial decrease in HO-1 promoter activity in both groups, HO-1 promoter activity significantly increased within one day, which may be due to the attraction of HO-1-positive macrophages during the inflammatory phase, and the influx of HO-1-positive epithelial cells during the re-epithelialization of the wounds^{22,26,42}. This rapid HO-1 induction is in line with a previous study in mouse excisional wounds, showing increased HO-1 mRNA and protein at day 1 after wounding²⁴. Additionally, the constitutively-expressed HO-2 was also not affected by wounding in this previous study, which was similar to our current results. We found that effects on HO-1 promoter activity were independent of the wound model, since both splinted and non-splinted wounds showed similar activity. However, at day 3, there was only a significant increase in the splinted model compared to the baseline level. Increased HO-1 expression was also found for both models in 7-day wounds at the mRNA level when compared to non-wounded skin. This increase was significantly higher after mechanical stress.

On the protein level, we saw contradictory results with significantly more HO-1 protein staining in the epidermis of non-splinted wounds and a slight, non-statistically significant, increase of HO-1 protein in the dermis in splinted wounds after 7 days. Thus,

although HO-1 induction was shown in diverse models of mechanical stress, we found only HO-1 promoter activation and HO-1 mRNA induction. HO-1 protein expression was, in fact, reduced by the static mechanical stress of the splint in the epidermal region.

When comparing protein levels in the epidermis, HO-1-positive cells were clustered in re-epithelialized tissue underneath the wound crust and were likely newly-formed keratinocytes^{25,26}. It is likely that the highly increased keratinocyte gene expression in non-splinted wounds account for the observed increase in HO-1 protein expression.

In the dermis, HO-1-positive cells in inflamed tissues were individually spread, and based on their location and morphology, appeared to be macrophages^{25,42}. We and others demonstrated previously that HO-1-positive macrophages can be recruited during the wound repair process^{6,25,26}.

It is, however, striking that splinted wounds exhibited similar levels of HO-1-positive cells in the dermis when compared to non-splinted wounds, while there were higher levels of F4/80-positive macrophages in splinted wounds.

Mechanical stress by splinting enhances inflammation; the role of HO-1

Macrophages promote strong inflammatory responses through secretion of cytokines, such as IL-1 β and TNF- α ⁴³. It is thought that during the wound repair process, first pro-inflammatory M1 macrophages enter the wound site to clear cellular debris and destroy invading pathogens. Besides pro-inflammatory M1 macrophages, there are other macrophage subsets, including the anti-inflammatory M2 macrophages and the Mhem, Mox, and M4 macrophages⁴⁴⁻⁴⁶. To enter the proliferation phase, resolution of inflammation is necessary. Under the right conditions, M1 macrophages may therefore skew into other anti-inflammatory macrophage subsets^{45,46}. The presence of large numbers of macrophages in the splinted wounds and the increased levels of pro-inflammatory mediators IL-1 β , TNF- α and COX-2 suggests that in the splinted wounds there were mainly M1 macrophages present. Prolonged inflammation and high levels of oxidative stress may result in excessive deposition of ECM, leading to fibrosis and excessive/hypertrophic scarring^{18,47}. Cytokines that mediate inflammation, such as IL-1 β and TNF- α , are involved in mechanical stretch-induced inflammation. For example, *in vitro* administration of mechanical stress induces both IL-1 β and COX-2 in fibroblast-like synoviocyte cells⁴⁸, epithelial cells⁴⁹, chondrocytes⁵⁰, and cardiac muscle cells⁵¹ in a time- and force-dependent manner. This increased expression of inflammatory markers corresponded to our findings. Moreover, we found a trend in MCP-1 mRNA induction ($p=0.10$) after mechanical stress, matching the enhanced protein staining for macrophages after mechanical stress.

Heme oxygenase-1-positive macrophages are thought to protect the wound environment against oxidative stress^{25,52}. Following injury, the HO substrate heme is

abundantly released at the edges of the wound site and can stimulate recruitment of leukocytes^{6,25,53}. In contrast, HO activity inhibits leukocyte recruitment via down-regulation of vascular adhesion molecules⁶. Moreover, HO-1 activity inhibits production of various pro-inflammatory cytokines, including IL-1 β and TNF- α ^{54,55}. In 7-day wounds, the inflammation levels were high in both non-splinted and splinted wounds, but however were much higher after mechanical stress in the splinted wounds.

The expression of HO-1 may facilitate resolution of inflammatory and oxidative stress at the wound site. When mechanical stress delays HO-1 protein expression, this may also delay resolution of inflammation, and lead to fibrogenesis.

Mechanical stress results in more fibrosis by a prolonged survival of myofibroblasts; the relation between inflammation, remodeling and HO-1

Mechanical stress, which is present in CL/P patients following palatal surgery and in patients with wounds in the vicinity of joints, increases the risk of excessive scar formation. In our splinting model, we demonstrated the increased presence of pro-inflammatory and pro-fibrotic cells and markers, suggesting that mechanical stress interferes with resolution of inflammation, which may ultimately lead to hampered wound repair and excessive scar formation. Application of mechanical loading to healing wounds in mice can cause hypertrophic scarring, through decreased apoptosis of myofibroblasts⁵⁶. It is tempting to speculate that the delayed HO-1 protein expression in the splinted model contributes to the delay in resolution of inflammation and allows the pro-inflammatory environment and the myofibroblast survival that we observed in the wound area at day 7.

When myofibroblasts fail to go into apoptosis, this leads to continuation of contraction and production of ECM, and ultimately to fibrosis^{5,13,17,18}. We found an increased presence of myofibroblasts after splinting, suggesting that either more myofibroblasts are formed upon mechanical stress, less myofibroblasts die, or splinting causes a delay in the myofibroblast formation when compared to non-splinted wounds. This corresponds to other reports, which showed that mechanical tension induces myofibroblast differentiation in wound granulation tissue in 6-day splinted wounds compared to non-splinted wounds^{14,20}. These processes may be fine-tuned by HO-1 and its effector molecules as is shown *in vitro* by regulating the apoptosis of fibroblasts^{18,57}.

Pathological cutaneous wound healing resulting in excessive scarring and fibrosis is the consequence of an imbalance between ECM synthesis by myofibroblasts and degradation and remodeling by MMPs¹³. We found that remodeling marker MMP-9 was increased after mechanical stress, which was also observed by other groups⁵⁸⁻⁶⁰. VEGF is an important promoter of angiogenesis and therefore microvessel density might be increased by mechanical tension. Chemokine and cytokine processing by MMPs affects the progression of inflammatory responses and leukocyte migration⁶¹. For example, MMP-9 can inactivate/degrade CXCL1, CXCL4, CXCL9, and CXCL10,

resulting in anti-inflammatory effects^{62,63}. Increased MMP-9 may be indicative of inflammation and poor wound healing⁶⁴. The interplay between VEGF and HO-1 is complex and it was demonstrated that they can both inhibit or induce each other⁶⁵⁻⁶⁸. Induction of HO-1 in a rat excisional wound model enhanced wound healing by increased cellular proliferation and collagen synthesis²⁸. HO-1 induction also reduced the inflammatory response by inhibition of pro-inflammatory molecules TNF- α , and ICAM-1 and an induction of the anti-inflammatory cytokine IL-10²⁸.

In summary, mechanical stress leads to delayed wound closure, increased inflammation, and altered remodeling during the wound healing process. Since more myofibroblasts are present after splinting, mechanical stress may result in more scar formation. This was associated with a delayed anti-inflammatory and anti-fibrotic HO-1 protein expression in splinted wounds compared to non-splinted wounds. Since HO-1 attacks multiple targets that play an important role during fibrogenesis, pharmacologic induction of HO-1 may facilitate resolution of inflammation and attenuate fibrosis.

Conclusion

We demonstrated that splinting significantly delays wound closure and potentiates the influx of pro-inflammatory leukocytes and myofibroblasts in day-7 wounds, which may promote fibrosis. The cytoprotective HO-1 gene is increased upon wounding, but HO-1 protein was lower in the epidermis after mechanical stress, probably as a result of the increased number of HO-1-positive keratinocytes in the re-epithelialization tissue of non-splinted wounds. Therefore, targeted pharmacologic induction of cytoprotective mechanisms, including HO-1, as preventive therapy against mechanical stress-induced inflammation and fibrosis must be considered.

References

1. Bartzela TN, Carels CE, Bronkhorst EM, Ronning E, Rizell S, Kuijpers-Jagtman AM. Tooth agenesis patterns in bilateral cleft lip and palate. *Eur J Oral Sci.* 2010;118(1):47-52.
2. Nolle PJ, Katsaros C, Van't Hof MA, Kuijpers-Jagtman AM. Treatment outcome in unilateral cleft lip and palate evaluated with the GOSLON yardstick: a meta-analysis of 1236 patients. *Plast Reconstr Surg.* 2005;116(5):1255-1262.
3. Biggs LC, Goudy SL, Dunnwald M. Palatogenesis and cutaneous repair: A two-headed coin. *Dev Dyn.* 2015;244(3):289-310.
4. Li J, Johnson CA, Smith AA, et al. Disrupting the intrinsic growth potential of a suture contributes to midfacial hypoplasia. *Bone.* 2014;81:186-195.
5. Brouwer KM, Lundvig DM, Middelkoop E, Wagener FA, Von den Hoff JW. Mechanical cues in orofacial tissue engineering and regenerative medicine. *Wound Repair Regen.* 2015;23(3):302-311.
6. Wagener FA, van Beurden HE, von den Hoff JW, Adema GJ, Figdor CG. The heme-heme oxygenase system: a molecular switch in wound healing. *Blood.* 2003;102(2):521-528.
7. van Beurden HE, Von den Hoff JW, Torensma R, Maltha JC, Kuijpers-Jagtman AM. Myofibroblasts in palatal wound healing: prospects for the reduction of wound contraction after cleft palate repair. *J Dent Res.* 2005;84(10):871-880.
8. Erming SA, Martin P, Tomic-Canic M. Wound repair and regeneration: mechanisms, signaling, and translation. *Sci Transl Med.* 2014;6(265):265sr266.
9. Gurtner GC, Werner S, Barrandon Y, Longaker MT. Wound repair and regeneration. *Nature.* 2008;453(7193):314-321.
10. Hinz B, Gabbiani G. Mechanisms of force generation and transmission by myofibroblasts. *Curr Opin Biotechnol.* 2003;14(5):538-546.
11. Eckes B, Zweers MC, Zhang ZG, et al. Mechanical tension and integrin alpha 2 beta 1 regulate fibroblast functions. *J Invest Dermatol Symp Proc.* 2006;11(1):66-72.
12. Desmouliere A, Chaponnier C, Gabbiani G. Tissue repair, contraction, and the myofibroblast. *Wound Repair Regen.* 2005;13(1):7-12.
13. Micallef L, Vedrenne N, Billet F, Coulomb B, Darby IA, Desmouliere A. The myofibroblast, multiple origins for major roles in normal and pathological tissue repair. *Fibrogenesis Tissue Repair.* 2012;5(Suppl 1):S5.
14. Hinz B, Mastrangelo D, Iselin CE, Chaponnier C, Gabbiani G. Mechanical tension controls granulation tissue contractile activity and myofibroblast differentiation. *Am J Pathol.* 2001;159(3):1009-1020.
15. van der Veer WM, Bloemen MC, Ulrich MM, et al. Potential cellular and molecular causes of hypertrophic scar formation. *Burns.* 2009;35(1):15-29.
16. Darby IA, Laverdet B, Bonte F, Desmouliere A. Fibroblasts and myofibroblasts in wound healing. *Clin Cosmet Invest Dermatol.* 2014;7:301-311.
17. Van De Water L, Varney S, Tomasek JJ. Mechanoregulation of the Myofibroblast in Wound Contraction, Scarring, and Fibrosis: Opportunities for New Therapeutic Intervention. *Adv Wound Care (New Rochelle).* 2013;2(4):122-141.
18. Lundvig DM, Immenschuh S, Wagener FA. Heme oxygenase, inflammation, and fibrosis: the good, the bad, and the ugly? *Front Pharmacol.* 2012;3:81.
19. Galiano RD, Michaels Jt, Dobrynsky M, Levine JP, Gurtner GC. Quantitative and reproducible murine model of excisional wound healing. *Wound Repair Regen.* 2004;12(4):485-492.
20. Tomasek JJ, Gabbiani G, Hinz B, Chaponnier C, Brown RA. Myofibroblasts and mechano-regulation of connective tissue remodelling. *Nat Rev Mol Cell Biol.* 2002;3(5):349-363.
21. Gozzelino R, Jeney V, Soares MP. Mechanisms of cell protection by heme oxygenase-1. *Annu Rev Pharmacol Toxicol.* 2010;50:323-354.
22. Wagener FA, Volk HD, Willis D, et al. Different faces of the heme-heme oxygenase system in inflammation. *Pharmacol Rev.* 2003;55(3):551-571.
23. Wagener FA, Dankers AC, van Summeren F, et al. Heme Oxygenase-1 and breast cancer resistance protein protect against heme-induced toxicity. *Curr Pharm Des.* 2013;19(15):2698-2707.
24. Schafer M, Werner S. Oxidative stress in normal and impaired wound repair. *Pharmacol Res.* 2008;58(2):165-171.
25. Hanselmann C, Mauch C, Werner S. Haem oxygenase-1: a novel player in cutaneous wound repair and psoriasis? *Biochem J.* 2001;353(Pt 3):459-466.

26. Kampfer H, Kolb N, Manderscheid M, Wetzler C, Pfeilschifter J, Frank S. Macrophage-derived heme-oxygenase-1: expression, regulation, and possible functions in skin repair. *Mol Med*. 2001;7(7):488-498.
27. Grochot-Przeczek A, Lach R, Mis J, et al. Heme oxygenase-1 accelerates cutaneous wound healing in mice. *PLoS One*. 2009;4(6):e5803.
28. Ahanger AA, Prawez S, Leo MD, et al. Pro-healing potential of hemin: an inducer of heme oxygenase-1. *Eur J Pharmacol*. 2010;645(1-3):165-170.
29. Wagener FA, Scharstuhl A, Tyrrell RM, et al. The heme-heme oxygenase system in wound healing; implications for scar formation. *Curr Drug Targets*. 2010;11(12):1571-1585.
30. Cho JH, Lee SK, Lee JW, Kim EC. The role of heme oxygenase-1 in mechanical stress- and lipopolysaccharide-induced osteogenic differentiation in human periodontal ligament cells. *Angle Orthod*. 2010;80(4):552-559.
31. Carlsen I, Nilsson L, Frokiaer J, Norregaard R. Changes in phosphorylated heat-shock protein 27 in response to acute ureteral obstruction in rats. *Acta Physiol (Oxf)*. 2013;209(2):167-178.
32. Wagner CT, Durante W, Christodoulides N, Hellums JD, Schafer AL. Hemodynamic forces induce the expression of heme oxygenase in cultured vascular smooth muscle cells. *J Clin Invest*. 1997;100(3):589-596.
33. Wever KE, Wagener FA, Frielink C, et al. Diannexin protects against renal ischemia reperfusion injury and targets phosphatidylserines in ischemic tissue. *PLoS One*. 2011;6(8):e24276.
34. Su H, van Dam GM, Buis CI, et al. Spatiotemporal expression of heme oxygenase-1 detected by in vivo bioluminescence after hepatic ischemia in HO-1/Luc mice. *Liver Transpl*. 2006;12(11):1634-1639.
35. Lundvig DM, Scharstuhl A, Cremers NA, et al. Delayed cutaneous wound closure in HO-2 deficient mice despite normal HO-1 expression. *J Cell Mol Med*. 2014;18(12):2488-2498.
36. van den Brand BT, Vermeij EA, Waterborg CE, et al. Intravenous delivery of HIV-based lentiviral vectors preferentially transduces F4/80+ and Ly-6C+ cells in spleen, important target cells in autoimmune arthritis. *PLoS One*. 2013;8(2):e55356.
37. Cremers NA, Lundvig DM, van Dalen SC, et al. Curcumin-induced heme oxygenase-1 expression prevents H2O2-induced cell death in wild type and heme oxygenase-2 knockout adipose-derived mesenchymal stem cells. *Int J Mol Sci*. 2014;15(10):17974-17999.
38. Baum CL, Arpey CJ. Normal cutaneous wound healing: clinical correlation with cellular and molecular events. *Dermatol Surg*. 2005;31(6):674-686; discussion 686.
39. Singer AJ, Clark RA. Cutaneous wound healing. *N Engl J Med*. 1999;341(10):738-746.
40. Liu XM, Peyton KJ, Durante W. Physiological cyclic strain promotes endothelial cell survival via the induction of heme oxygenase-1. *Am J Physiol Heart Circ Physiol*. 2013;304(12):H1634-1643.
41. Lee SK, Lee CY, Kook YA, Lee SK, Kim EC. Mechanical stress promotes odontoblastic differentiation via the heme oxygenase-1 pathway in human dental pulp cell line. *Life Sci*. 2010;86(3-4):107-114.
42. Schurmann C, Seitz O, Klein C, et al. Tight spatial and temporal control in dynamic basal to distal migration of epithelial inflammatory responses and infiltration of cytoprotective macrophages determine healing skin flap transplants in mice. *Ann Surg*. 2009;249(3):519-534.
43. Rees P, Greaves N, Bayat A. Chemokines in wound healing and as potential therapeutic targets for reducing cutaneous scarring. *Advances in wound care*. 2015:1-17.
44. Hull TD, Agarwal A, George JF. The mononuclear phagocyte system in homeostasis and disease: a role for heme oxygenase-1. *Antioxid Redox Signal*. 2014;20(11):1770-1788.
45. Chistiakov DA, Bobryshev YV, Orekhov AN. Changes in transcriptome of macrophages in atherosclerosis. *J Cell Mol Med*. 2015;19(6):1163-1173.
46. Medbury HJ, Williams H, Fletcher JP. Clinical significance of macrophage phenotypes in cardiovascular disease. *Clin Transl Med*. 2014;3(1):63.
47. Sidgwick GP, Bayat A. Extracellular matrix molecules implicated in hypertrophic and keloid scarring. *J Eur Acad Dermatol Venerol*. 2012;26(2):141-152.
48. Takao M, Okinaga T, Ariyoshi W, et al. Role of heme oxygenase-1 in inflammatory response induced by mechanical stretch in synovial cells. *Inflamm Res*. 2011;60(9):861-867.
49. Toshinaga A, Hosokawa R, Okinaga T, Masaki C. Inflammatory response in epithelial cells induced by mechanical stress is suppressed by hyaluronic acid. *The Japanese Society of Inflammation and Regeneration* 2010 30(2):120-117.
50. Huang J, Ballou LR, Hasty KA. Cyclic equibiaxial tensile strain induces both anabolic and catabolic responses in articular chondrocytes. *Gene*. 2007;404(1-2):101-109.

51. Vandenburgh HH, Shansky J, Solerssi R, Chromiak J. Mechanical stimulation of skeletal muscle increases prostaglandin F₂ alpha production, cyclooxygenase activity, and cell growth by a pertussis toxin sensitive mechanism. *J Cell Physiol.* 1995;163(2):285-294.
52. Ishii T, Itoh K, Sato H, Bannai S. Oxidative stress-inducible proteins in macrophages. *Free Radic Res.* 1999;31(4):351-355.
53. auf dem Keller U, Kumin A, Braun S, Werner S. Reactive oxygen species and their detoxification in healing skin wounds. *J Invest Dermatol Symp Proc.* 2006;11(1):106-111.
54. Morse D, Pischke SE, Zhou Z, et al. Suppression of inflammatory cytokine production by carbon monoxide involves the JNK pathway and AP-1. *J Biol Chem.* 2003;278(39):36993-36998.
55. Lee TS, Tsai HL, Chau LY. Induction of heme oxygenase-1 expression in murine macrophages is essential for the anti-inflammatory effect of low dose 15-deoxy-Delta 12,14-prostaglandin J₂. *J Biol Chem.* 2003;278(21):19325-19330.
56. Aarabi S, Bhatt KA, Shi Y, et al. Mechanical load initiates hypertrophic scar formation through decreased cellular apoptosis. *FASEB J.* 2007;21(12):3250-3261.
57. Scharstuhl A, Mutsaers HA, Pennings SW, Szarek WA, Russel FG, Wagener FA. Curcumin-induced fibroblast apoptosis and in vitro wound contraction are regulated by antioxidants and heme oxygenase: implications for scar formation. *J Cell Mol Med.* 2009;13(4):712-725.
58. Beckmann R, Houben A, Tohidnezhad M, et al. Mechanical forces induce changes in VEGF and VEGFR-1/sFlt-1 expression in human chondrocytes. *Int J Mol Sci.* 2014;15(9):15456-15474.
59. Kawata T, Kohno S, Kaku M, et al. Expression of vascular endothelial growth factor on neovascularization during experimental tooth movement by magnets. *Biomedical Research-India.* 2011;22(2):249-254.
60. Huang D, Liu Y, Huang Y, et al. Mechanical compression upregulates MMP9 through SMAD3 but not SMAD2 modulation in hypertrophic scar fibroblasts. *Connect Tissue Res.* 2014;55(5-6):391-396.
61. Van Lint P, Libert C. Chemokine and cytokine processing by matrix metalloproteinases and its effect on leukocyte migration and inflammation. *J Leukoc Biol.* 2007;82(6):1375-1381.
62. Van den Steen PE, Proost P, Wuyts A, Van Damme J, Opdenakker G. Neutrophil gelatinase B potentiates interleukin-8 tenfold by aminoterminal processing, whereas it degrades CTAP-III, PF-4, and GRO-alpha and leaves RANTES and MCP-2 intact. *Blood.* 2000;96(8):2673-2681.
63. Van den Steen PE, Husson SJ, Proost P, Van Damme J, Opdenakker G. Carboxyterminal cleavage of the chemokines MIG and IP-10 by gelatinase B and neutrophil collagenase. *Biochem Biophys Res Commun.* 2003;310(3):889-896.
64. Liu Y, Min D, Bolton T, et al. Increased matrix metalloproteinase-9 predicts poor wound healing in diabetic foot ulcers. *Diabetes Care.* 2009;32(1):117-119.
65. Bussolati B, Ahmed A, Pemberton H, et al. Bifunctional role for VEGF-induced heme oxygenase-1 in vivo: induction of angiogenesis and inhibition of leukocytic infiltration. *Blood.* 2004;103(3):761-766.
66. Jozkowicz A, Huk I, Nigisch A, Weigel G, Weidinger F, Dulak J. Effect of prostaglandin-J(2) on VEGF synthesis depends on the induction of heme oxygenase-1. *Antioxid Redox Signal.* 2002;4(4):577-585.
67. Chao HM, Chuang MJ, Liu JH, et al. Baicalein protects against retinal ischemia by antioxidation, antiapoptosis, downregulation of HIF-1alpha, VEGF, and MMP-9 and upregulation of HO-1. *J Ocul Pharmacol Ther.* 2013;29(6):539-549.
68. Jayasooriya RG, Park SR, Choi YH, Hyun JW, Chang WY, Kim GY. Camptothecin suppresses expression of matrix metalloproteinase-9 and vascular endothelial growth factor in DU145 cells through PI3K/Akt-mediated inhibition of NF-kappaB activity and Nrf2-dependent induction of HO-1 expression. *Environ Toxicol Pharmacol.* 2015;39(3):1189-1198.

Part IV

Umbilical cord blood stem cells and molecular targets in tissue engineering may promote muscle and skin regeneration following surgical CLP repair

CHAPTER 7

Tissue engineering strategies combining molecular targets against inflammation and fibrosis, and umbilical cord blood stem cells to improve hampered muscle and skin regeneration following cleft repair

Schreurs M, **Suttorp CM**, Mutsaers HAM, Kuijpers-Jagtman AM, Von den Hoff JW, Ongkosuwito EM, Carvajal Monroy PL, Wagener FADTG.

Med Res Rev. 2020 Jan;40(1):9-26.

Abbreviations

CL	Cleft lip
CL(P)	Cleft lip and/or palate
CLP	Cleft lip and palate
CNCCs	Cranial neural crest cells
CPM	Cranial paraxial mesoderm
ECM	Extracellular matrix
FDA	Food and Drug Administration
FGF	Fibroblast growth factor
bFGF	basic Fibroblast growth factor
HGF	Hepatocyte growth factor
HO	Heme oxygenase
IFN γ	Interferon- γ
IGF-1	Insulin-like growth factor 1
IGF-2	Insulin-like growth factor 2
IL-1 β	Interleukin-1 beta
IL-6	Interleukin-6
MCP-1	Monocyte chemoattractant protein-1
MIP-2	Macrophage Inflammatory protein 2
MMPs	Matrix metalloproteinases
MSC	Mesenchymal stem/stromal cells
MyHC	Multinucleated myosin heavy chain
MyoD	Myoblast determination protein 1
Pax7	Paired box transcription factor
PDGF	Platelet-derived growth factor
PIC	Polyisocyanopeptide
SCs	Satellite cells
α -SMA	Alpha smooth muscle actin
TGF- β 1	Transforming growth factor beta 1
TIMPS	Tissue inhibitors of matrix metalloproteinases
TNF- α	Tumor necrosis factor alpha
UCMSC	Umbilical cord mesenchymal stem cells
hUCMSC	Human umbilical cord blood mesenchymal stem cells
VEGF	Vascular endothelial growth factor

Contents

Abstract

1. Introduction
2. Facial and lip myogenesis
3. Muscle anatomy in the normal and cleft lip
4. Cleft surgery can result in fibrosis and scar formation
5. Stem cells repair wounds and facilitate skin and muscle regeneration
6. Regenerative medicine to attenuate scarring and muscle fibrosis
7. Umbilical cord: from waste material to source of therapeutic stem cells
8. Clinical challenges for scaffold-based cord blood stem cells with anti-fibrotic/
anti- inflammatory factors
9. Conclusions

References

Abstract

Cleft lip with or without cleft palate is a congenital deformity that occurs in about 1 of 700 newborns, affecting the dentition, bone, skin, muscles and mucosa in the orofacial region. A cleft can give rise to problems with maxillofacial growth, dental development, speech, and eating, and can also cause hearing impairment. Surgical repair of the lip may lead to impaired regeneration of muscle and skin, fibrosis, and scar formation. This may result in hampered facial growth and dental development affecting oral function and lip and nose esthetics. Therefore, secondary surgery to correct the scar is often indicated. We will discuss the molecular and cellular pathways involved in facial and lip myogenesis, muscle anatomy in the normal and cleft lip, and complications following surgery. The aim of this review is to outline a novel molecular and cellular strategy to improve musculature and skin regeneration and to reduce scar formation following cleft repair. Orofacial clefting can be diagnosed in the fetus through prenatal ultrasound screening and allows planning for the harvesting of umbilical cord blood stem cells upon birth. Tissue engineering techniques using these cord blood stem cells and molecular targeting of inflammation and fibrosis during surgery may promote tissue regeneration. We expect that this novel strategy improves both muscle and skin regeneration, resulting in better function and esthetics after cleft repair.

Keywords: cleft lip and palate, oral surgery, scarring, tissue engineering, umbilical cord blood stem cells.

1. Introduction

Cleft lip with (CLP) or without cleft palate (CL) occurs in about 1 to 700 newborns with ethnic and geographical variation and is one of the most common facial congenital anomalies¹⁻³. A cleft lip only (CL) is present in about 0.6 per 1000 live births⁴. CL(P) is either uni- or bilateral (**Figure 1**) and can occur isolated or as part of a syndrome⁵.



Figure 1. (A): Unoperated orofacial clefting in mild to severe form, left to right: unilateral subepithelial cleft lip, unilateral cleft lip and palate, bilateral cleft lip alveolus. (B): Lip closure with an optimal, normal and suboptimal esthetic outcome. (B) left: unilateral cleft lip with well-aligned vermilion border, normal lip length, and normal shape of nostrils. (B) middle: unilateral cleft lip and palate with deficient lateral vermilion and white roll malalignment. (B) right: bilateral cleft lip and palate after surgical closing with vermilion notching, short upper lip, and high rising nostrils. (C): Left: unoperated cleft lip and palate with cleft in the alveolar ridge and anterior displacement of the premaxilla. (C) middle: cleft palate with excessive scarring, and fistula following surgery. (C) right: adult patient in profile with a hypoplastic maxilla due to scarring after cleft lip and palate closure that resulted to a class III skeletal jaw relation.

Since only 30% of children born with CLP have a genetic syndrome, a combination of genetic and environmental factors is thought to play a role in the etiology of orofacial clefting^{6,7}. These environmental risk factors include smoking⁸, alcohol consumption⁹, phenytoin exposure¹⁰, diabetes¹¹, and maternal¹² and paternal age¹³. Other factors such as folate supplementation, zinc and daily multivitamin intake, can reduce the risk of CL(P)¹⁴.

There is a large variation in the severity of cleft lip, ranging from mild subepithelial to complete bilateral clefting (**Figure 1**). The more severe the cleft lip, the more the shape and size of the alveolar process are affected. The cleft in the alveolar process can range from a small dimple in the arch in combination with a minor cleft of the lip to a total cleft of the alveolar ridge and anterior displacement of the premaxilla¹⁴

(Figure 1), Clefts of the primary or secondary palate differ in embryonic origin and underlying fusion or differentiation defects. Fusion defects of the primary palate lead to complete clefting of the lip either or not combined with a complete or incomplete clefting of the alveolus. Differentiation defects of the primary palate give rise to incomplete, submucous or hypoplastic cleft lip and/or alveolus. Fusion defects of the secondary palate lead to complete or incomplete hard palate clefts that may be combined with a cleft in the soft palate and/or uvula. Differentiation defects of the secondary palate give rise to a combination of submucous, hypoplastic hard and soft palate defects¹⁵⁻¹⁷.

If the cleft is not surgically corrected, patients are more prone to hearing problems due to otitis media with effusion¹⁸, and have difficulties with speech, feeding, and abnormal dental development due to loss of lip pressure. In addition, they may encounter social isolation. Clefts can cause serious psychological problems including low self-esteem and acceptance by peers^{19,20}.

Scarring following surgical correction of the cleft lip can have a major effect on subsequent anterior-posterior and vertical growth of the maxilla, as well as on the position of the maxillary incisors²¹. Excessive pressure of the repaired upper lip leads to palatal inclination of the upper front teeth and an increased overbite but decreased overjet²². When the patient grows older a reversed overjet often develops due to growth restriction of the maxilla, especially in CLP cases. Several factors contribute to suboptimal lip muscle repair including the skills and experience of the surgeon²³, type and extension of the cleft²⁴, genetic factors²⁵, muscle fiber type distribution, and impaired muscle regeneration^{26,27}. In this review, we therefore present a novel tissue engineering strategy that aims to prevent scarring and subsequent functional problems following cleft surgery by promoting muscle and skin regeneration.

2. Facial and lip myogenesis

Orofacial development involves the migration, proliferation, differentiation, and apoptosis of mesenchymal and epithelial cells²⁸. From the 4th week of gestation cranial neural crest cells (CNCCs) migrate from the dorsal part of the neural tube to form the human face. Next, these CNCCs differentiate into the mesenchymal cells that form structures such as cartilage and bone. The cranial paraxial mesoderm (CPM) provides the precursors for the cranial muscles. Both CNCCs and CPM form the templates for the adult craniofacial structures in the branchial arches²⁹. In the 5th week of gestation, the CNCCs form the frontonasal prominence, the bilateral maxillary prominences and the bilateral mandibular prominences. In the 6th and 7th week the medial nasal prominences grow and fuse with each other to form an intermaxillary segment. This intermaxillary segment will later fuse with the maxillary prominences and form the upper lip. Any disruption in these well-orchestrated processes can lead to a cleft in lip, alveolus and/or palate^{28,30-32}.

The muscles of the upper lip are all derived from the mesoderm of the 2nd pharyngeal arch and are partly determine facial expression^{33,34} (**Figure 2**). Mesenchymal condensations that form the individual upper lip muscles emerge sequentially, starting from the 6th week of gestation in humans³⁵. During development of the facial muscles, these mesenchymal condensations differentiate and move to their definitive location where they mature³⁴. In summary, the main muscles of the upper lip originate from mesenchymal condensations in the pharyngeal arches.

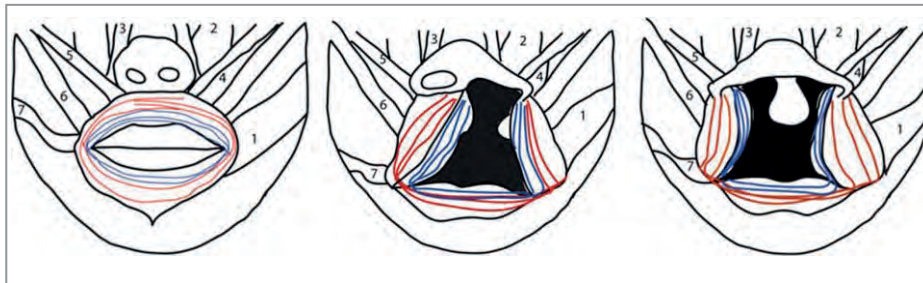


Figure 2. Left: Muscle complex involved in the function of the upper lip: seven pairs of facial and lip muscles connected to the circular orbicularis oris muscle (red: superficial fibers, blue; deep fibers); buccinator (1), levator labii superioris (2), levator labii superioris alaeque nasi (3), levator anguli oris (4), zygomaticus minor (5), zygomaticus major (6), and the risorius muscle (7). Middle: unilateral cleft lip with abnormal orientation and insertion of the orbicularis oris muscle, superficial muscle fibers (red) and deep muscle fibers (blue) are deficient. Right: bilateral cleft lip with abnormal orientation and insertion of the orbicularis oris muscle.

3. Muscle anatomy in the normal and cleft lip

The upper lip muscles comprise the orbicularis oris and seven pairs of other facial and lip muscles. The facial muscles are divided into a superficial (extrinsic) layer and a deep (intrinsic) layer, which work either synergistically or antagonistically in the coordination of lip movements³⁵. The orbicularis oris muscle is the primary muscle of the lip and therefore the most important muscle in cleft lip surgery¹⁴. Facial expressions and lip movements during speaking are supported by the superficial part of the orbicularis oris, while mastication is mediated by the deep layer. The superficial muscle fibers end up in the philtrum ridge on one side, whereas the deep layers cross the midline to insert on the opposite side. The philtrum dimple originates from a reduced attachment of muscles to the surface³⁶ (**Figure 2**).

The orbicularis oris muscle together with the deep buccinator muscles compress the lips and cheeks against the teeth. The buccinator originates at the mandible to attach to the modiolus of the upper and lower lips. The superficial muscles of the lip, the levator labii superioris, the levator labii superioris alaeque nasi and the zygomaticus minor originate in the orbicularis oris and move the upper lip upwards and sideways. The zygomaticus major muscle flanks the upper lip on both sides and raises the lip³⁷. The levator anguli oris is a deep muscle elevating the corners of the lips. All

muscle fibers of these muscles originate and insert into the skin and the mucous membrane (**Figure 2**).

The orbicularis oris muscle contains both slow and fast fibers. The slow fibers are more resistant against fatigue and have a low activation threshold, whereas the fast fibers are more prone to fatigue and have a high activation threshold³⁸. Both the superficial and deep orbicularis oris muscle are predominantly composed of fast fibers, but there is a slight difference in fiber type composition between the superficial (98% fast) and deep muscle layers pars peripheralis (95% fast) and pars marginalis (91% fast). This indicates that these muscles should be reconstructed separately during surgery³⁸.

In a cleft lip, all facial muscle fibers lack their insertions in the midline and therefore have an abnormal orientation on one or both sides (uni/bilateral cleft, respectively) (**Figure 2**). The orbicularis oris normally functions as a sphincter but, in a cleft lip, it pulls the two portions of the lip laterally leading to an imbalance between lip and tongue pressure. When a cleft lip is not surgically corrected at a young age, the anterior teeth will often become malpositioned³⁹.

The superficial fibers of the orbicularis oris muscle are oriented parallel to the cleft, medial towards the columella and lateral to the alar base. The fibers at the medial side are deficient. The superficial fibers are more disorganized with increasing severity of the cleft. By contrast, the orientation of the deep layer of the orbicularis oris remains unchanged. This muscle runs perpendicular to the cleft and ends at the edges of the cleft^{40,41} (**Figure 2**).

In cleft lip, an increased amount of fast muscle fibers is present⁴², which has also been demonstrated in the musculus levator veli palatini of the cleft soft palate⁴³. In vitro studies have shown that satellite cells (SCs) from fast muscle fibers proliferate less than those from slow muscle fibers⁴⁴. This, together with the reduced capillary supply and disorganization of the muscle fibers may compromise muscle regeneration in a cleft lip after surgical repair⁴⁵.

Summarizing, in CL(P) the orientation, insertion and composition of the muscles of the lip are abnormal, which hampers muscle regeneration after surgery, affecting the oral function and dental development.

4. Cleft surgery can result in fibrosis and scar formation.

The two main techniques in unilateral cleft lip surgery are the triangular flap technique (Tennison-Randall) and the rotation advancement technique (Millard), which have similar outcomes^{46,47}. Common bilateral cleft lip techniques include the Millard technique, the Manchester technique and the Tennison technique⁴⁸. Cleft lip is often accompanied by a cleft palate and cleft alveolus¹⁷, and is treated at different time points after birth depending on the treatment protocol^{49 24}.

Surgery of the lip usually takes place in the first year after birth, often in conjunction with the repair of the nose and the soft palate⁵⁰. The hard palate is closed

as late as possible, taking into account the speech development of the patient and the potential negative effects on facial growth. There is a large variation in the timing of surgical treatments between CLP surgical centers⁵¹. However, the outcome is often suboptimal, depending on the severity of the original defect and the displacement of the cleft maxilla⁵². Dehiscence of the lip or the palate shortly after surgery or scar formation with subsequent hampered growth of the maxilla are found⁵³. Revision surgery is therefore required in 33% of the CLP patients compared to 12% of the patients with an intact secondary palate⁵⁴.

Normally, wound healing of skin and muscle is characterized by four successive and overlapping phases: hemostasis, inflammation, proliferation and remodeling^{55,56}. Disruption of blood vessels because of cleft surgery causes bleeding. Next, a blood clot containing fibrin will form by platelet aggregation. During hemostasis, platelets release cytokines and growth factors that attract inflammatory cells like granulocytes and macrophages⁵⁷. These inflammatory cells remove apoptotic cells, debris and invading bacteria. Released cytokines and growth factors then stimulate keratinocyte and fibroblast proliferation, and angiogenesis to promote tissue regeneration. This proliferative phase consists of epithelial proliferation, the formation of granulation tissue and epithelialization. These processes are regulated by fibroblasts and endothelial cells⁵⁵. Fibroblasts produce collagen, glycosaminoglycans and proteoglycans, the major components of the extracellular matrix (ECM)⁵⁸. Mechanical strain, transforming growth factor beta 1 (TGF- β 1) and the ECM molecule ED-A fibronectin induce the differentiation of fibroblasts into myofibroblasts⁵⁹. Myofibroblasts contract the granulation tissue and deposit large amounts of ECM molecules. Subsequently, matrix metalloproteinases (MMPs) and tissue inhibitors of matrix metalloproteinases (TIMPS) control the remodeling process⁶⁰. During remodeling cross-linking and reorientation of collagen fibers occurs, while the number of capillaries regresses returning the vascular density to normal. The immature type III collagen is modified to mature type I collagen⁶¹. At the end of this phase, the myofibroblasts die by apoptosis leaving a rather acellular scar. However, multiple molecular and mechanical factors can affect wound healing after CL(P) surgery and promote fibrosis and scar formation resulting in major functional and aesthetic problems⁶²⁻⁶⁴.

In normal skin, ECM deposition and degradation are balanced. An accumulation of collagen type I and III fibers and other ECM proteins after injury results in a disorganized fiber structure and hypertrophic scar formation^{65,66}. Wound tension or mechanical stress is another causative factor for scar formation^{67,68}. The skin of the human face is maximally extensible perpendicular to relaxed skin tension lines, implying that tension is minimized when surgical incisions are created along these lines⁶⁷. Prolonged inflammation and oxidative stress block the remodeling phase and promotes excessive fibrosis and scarring⁶⁹⁻⁷¹. Therefore, stringent control of oxidative and

inflammatory factors is important for the outcome of wound repair in skin and muscle. Several factors including the cytokines interleukin-1 beta (IL-1 β), interleukin-6 (IL-6), tumor necrosis factor alpha (TNF- α), TGF- β 1, monocyte chemoattractant protein-1 (MCP1) and heme can induce fibrosis and scarring. These factors promote inflammatory cell adhesion, migration/proliferation of leukocytes and fibroblasts, and dysregulation of ECM remodeling^{60,72,73}. Thus, to prevent excessive scarring, we need to limit the inflammatory and fibrotic processes and promote regeneration.

5. Stem cells repair wounds and facilitate skin and muscle regeneration

Stem cells facilitate maintenance and repair processes in skin and muscle by replenishing lost tissue and by creating a regenerative micro-environment. Stem cells have a prolonged self-renewal capacity and can differentiate into various cell types, making them ideal for use in regenerative medicine. Stem cells are required at the site of injury to allow the regeneration of dermal, epidermal⁷⁴ and muscle tissue⁷⁵.

Moreover, they promote scarless wound healing by generating a regenerative microenvironment via the secretion of protective factors that can inhibit myofibroblasts in a paracrine fashion⁷⁶⁻⁸¹.

Following skin wounding, epidermal stem cells in the basal layer are activated, proliferate and migrate to the site of injury where they contribute to regeneration⁸². Muscle repair following injury is facilitated by satellite cells (SCs). SCs are muscle stem cells originating from the CPM that are responsible for postnatal muscle growth, maintenance, and repair^{83,84}. They express the paired box transcription factor 7 (Pax7) and are located between the sarcolemma and basal lamina surrounding a single muscle fiber. After the injury, SCs become activated and migrate to the site of injury, proliferate, and differentiate into myoD-positive myoblasts that fuse to form new multinucleated myosin heavy chain (MyHC)-positive myofibers or repair damaged myofibers^{83,85,86} (**Figure 3**). A small portion of these SCs stay quiescent to allow future regeneration cycles. Signaling molecules like insulin-like growth factor 1 and 2 (IGF-1, IGF-2), platelet-derived growth factor (PDGF), fibroblast growth factor (FGF) and hepatocyte growth factor (HGF) derived from recruited macrophages, injured myofibers and disrupted ECM regulate this process^{85,87}. HGF induces the activation of quiescent SCs⁸⁷. IGF-1 and 2 enhance myogenic proliferation and differentiation, and promote cell survival. PDGF regulates the proliferation and differentiation of myoblasts and supports angiogenesis. FGF is upregulated during muscle regeneration, but its exact role is unclear.

Muscle-specific transcription factors like Pax7, myogenic factor 5, myoblast determination protein 1 (MyoD), myogenin and finally structural proteins like MyHC are sequentially expressed⁸⁸ (**Figure 3**).

Most of the studies on muscle regeneration have been performed on skeletal muscles of limb and trunk. During embryonic development the limb and trunk muscles

are derived from the somites whereas lip muscles are derived from the CPM in the branchial arches³³. Head muscles also contain less SCs than limb muscles⁴⁴ and injuries regenerate slower^{89,90}. In addition, Pax7 and myogenic regulatory factor 4 levels in limb muscles are lower than in head muscles. SCs from the masseter muscle proliferate more and differentiate later than those from limb muscles⁴⁴. SCs from different branchiomic muscles, however, behave in a similar way. The lower regenerative capacity of branchiomic muscles compared to limb muscle may impair muscle healing after cleft surgery⁹⁰. The reduced blood supply and aberrant muscle orientation in a cleft lip may further impair the regeneration process⁴¹. Thus, stem cells could provide a solution for skin repair, but also for muscle repair.

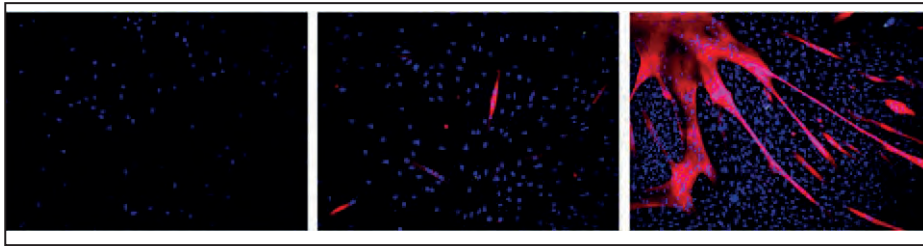


Figure 3: Immunofluorescence staining of muscle fiber formation from masseter satellite cells (SCs): **Left:** after 3 days of culture, DAPI (blue) stains nuclei, Pax 7 (red), **Middle:** after 7 days of culture, DAPI (blue), MyHC (red). **Right:** after 10 days of culture DAPI (blue), MyHC (red). Magnification $\times 400$. DAPI, 4',6-diamidino-2-phenylindole; MyHC, myosin heavy chain; Pax 7, paired box transcription factor 7.

6. Regenerative medicine to attenuate scarring and muscle fibrosis

To overcome the functional and esthetic problems related to scarring after cleft lip surgery, we present a novel tissue engineering strategy. This involves a combination of umbilical cord blood stem cells with regenerative capacity together with anti-inflammatory and antifibrotic molecules.

In comparison to adults, fetuses display less scarring following wound healing⁹¹. Fetal wounds differ in several ways from adult wounds, including a reduced inflammatory response. They also have higher expression levels of MMPs compared to their inhibitors, the TIMPs⁹¹. Further, PDGF disappears more rapidly from fetal wounds, that also show lower FGF levels and increased TGF- β 3 levels. In addition, the level of TGF- β 1/2 is lower⁹², the biomechanical strain is lower and the ECM is enriched in hyaluronic acid and type III collagen⁹³.

Tissue regeneration is often hampered by the occurrence of fibrosis. TGF- β 1 is a pro-inflammatory factor that recruits macrophages and other inflammatory cells to the wound site, thus contributing to fibrosis and excessive scarring⁹⁴. In muscles, TGF- β 1 stimulates the synthesis of collagen and other ECM components, and promotes myofibroblast formation and fibrosis⁹⁵. Myostatin, also a member of the TGF- β family inhibits muscle regeneration by reducing the proliferation of stem cells and

myoblasts⁹⁶. The inhibition of myostatin and TGF- β may enhance muscle regeneration⁹⁷. The proteoglycan decorin has a stimulatory effect on autophagy and inflammation, and an inhibitory effect on angiogenesis by inhibiting both TGF- β 1 and myostatin. This protein can be used to prevent fibrosis and enhance muscle regeneration⁹⁸. Decorin also upregulates myogenic genes and promotes skeletal muscle regeneration after injury⁹⁹. Losartan, an angiotensin II receptor antagonist, neutralizes the effect of TGF- β 1, reduces fibrosis and has already been used clinically in therapy for myocardial fibrosis^{100,101}.

Oxidative stress and inflammation can be counteracted by the induction of heme oxygenase (HO) by metalloporphyrins¹⁰². The enzyme HO degrades free heme generating carbon monoxide, ferrous iron/ferritin and biliverdin/bilirubin, which can be used to reduce inflammation. HO-1 deficient humans and mice demonstrate chronic inflammatory stress^{103,104}. HO-1 has pro-angiogenic effects via regulating vascular endothelial growth factor (VEGF) synthesis^{105,106}. HO-2 deficient mice have elevated levels of pro-inflammatory chemokines including keratinocyte chemoattractant, macrophage inflammatory protein 2 (MIP-2), and MCP-1. These mice show delayed wound healing and an exaggerated inflammatory response after corneal epithelial wounding^{107,108}.

Alternatively, systemic administration of anti-inflammatory therapeutics during surgery may attenuate scarring. These include neuropeptide α -melanocyte stimulating hormone¹⁰⁹, fibroblast growth factor 9 (FGF9)¹¹⁰, WNT 3A¹¹¹, interleukin 10 (IL-10)¹¹², interleukin 6 (IL-6)¹¹³, anti-VEGF antibody¹¹⁴, TGF- β 3¹¹⁴ and CXC chemokine receptor type 4 antagonists¹¹⁵. IL-10 downregulates pro-inflammatory cytokines IL-6 and IL-8 and may thus attenuate scar formation¹¹².

TGF- β 1 is the main target in antifibrotic therapies that include the administration of fibroblast growth factor basic (bFGF), insulin growth factor 1 (IGF-1), losartan, suramin, decorin, relaxin, interferon- γ (IFN γ) and angiotensin II receptor blockers. Antagonists of the IL-1 receptor (anakinra; Food and Drug Administration (FDA) approved) reduces TGF- β 1 expression and could be used for the reduction of scar formation¹¹⁶.

Over the years, various drugs have been developed that target profibrotic signaling pathways such as TGF- β and PDGF, to reduce the progression of fibrosis. Still, hardly any drugs are available for the treatment of organ fibrosis. Currently, there are only two FDA approved drugs that are used for the treatment of idiopathic pulmonary fibrosis, namely pirfenidone and nintedanib¹¹⁷.

Pirfenidone, that is pyridine(5-methyl-1-phenyl-2-(1H)-pyridone), is an oral agent that can elicit anti-inflammatory, antioxidative and antiproliferative effects¹¹⁸. Even though, the exact mechanism of action is still not fully understood, the antifibrotic effect of pirfenidone has been demonstrated in several organs, for example lung, liver and kidney¹¹⁸. In human liver cells, it has been shown that it attenuates TGF- β -induced

mRNA expression of α -SMA and type I collagen¹¹⁹. Also in human precision-cut liver slices a reduction in the gene expression of type I collagen was observed following treatment with pirfenidone¹²⁰.

Nintedanib, formerly known as BIBF 1120, is an intracellular triple angiokine inhibitor targeting the VEGF, FGF, and PDGF receptors¹²¹. Nintedanib competitively binds to the adenosine triphosphate binding pocket of these receptors inhibiting their activation and thereby inhibiting the fibrotic process. In addition, nintedanib has also been demonstrated to inhibit members of the proto-oncogene tyrosine-protein kinase (Src)-family (Src, Lyn, and Lck), which are activated in various types of cancer and belong to the non-receptor tyrosine kinases¹²².

Galunisertib, LY2157299, is an oral small molecule inhibitor of the TGF- β receptor I kinase that specifically inhibits SMAD2 phosphorylation¹²³. Using human precision-cut liver slices, it has been demonstrated that galunisertib attenuates SMAD2 phosphorylation in healthy and cirrhotic liver tissue and reduces the expression of several collagen subtypes (collagen types I, III, IV, V and VI). In addition, it reduces the expression of numerous genes associated with collagen maturation and homeostasis¹²⁴. Interestingly, there is also evidence suggesting that galunisertib can inhibit TGF- β signaling in human oral keratinocytes¹²⁵.

Overall, there are three distinct routes to target profibrotic signaling: **(A)** inhibiting transcription or translation of pro-fibrotic factors, **(B)** blocking interleukin receptor binding and activation, and **(C)** interfering with down-stream signaling events. Since the fibrotic process is highly similar in all organs, therapeutic targets identified in, for instance, the liver might also be used to reduce scar formation following cleft surgery. The three drugs described above have proven antifibrotic efficacy and are therefore ideal candidates for further study in the context of cleft repair.

7. Umbilical cord: from waste material to source of therapeutic stem cells

Adult stem cells like mesenchymal stem/stromal cells (MSC) can be found throughout the body. Mesenchymal stem cells are currently widely used for regenerative medicine purposes. They may stimulate the regeneration of the injured skin and muscle following surgical lip closure by replenishing the required cells and by providing a microenvironment that attenuates scarring and fibrosis¹²⁶. MSCs can differentiate into several types of cells including endothelial cells, myocytes, keratinocytes, and fibroblasts¹²⁷⁻¹²⁹. Moreover, stem cells produce several anti-inflammatory and antifibrotic mediators, and secrete factors that create a regenerative microenvironment¹³⁰⁻¹³³. Cord blood stem cells embedded in a scaffold secrete for example MMP-9, mediating collagen degradation in uterine scars, which improves the regeneration of the endometrium, myometrium and blood vessels¹³⁴. Administered cord blood stem cells also promote the recruitment of endogenous stem cells^{135,136}.

The isolation of MSCs from bone marrow or adipose tissue from the the baby is rather invasive and can cause complications such as infection, bleeding, and chronic pain¹³⁷. Moreover, it is expensive to harvest them and to expand them by controlled cell culture¹³⁸. Therefore, there is a need for alternative sources of MSCs. Human umbilical cord blood cells are obtained by a simple, safe, and painless procedure upon birth. Mesenchymal stem cells can be easily isolated from cord blood and preserved for later¹³⁹. Since prenatal ultrasound screening allows early detection of a cleft in the 11th to 13th week of gestation^{140,141}, the preservation of umbilical cord (blood) upon birth can be planned in an early stage and should be considered as a new strategy to optimize cleft surgery (**Figure 4**). Cord blood can be collected from the umbilical vein or from the placenta. Only the mononuclear fraction which contains the stem cells is needed for preservation. In addition, stem cells can be harvested simultaneously from the umbilical cord tissue itself. The umbilical cord mesenchymal stem cells (UCMSC) can be taken from the amniotic membrane, the cord lining, Wharton's jelly, and the perivascular region of the umbilical cord¹⁴². The umbilical cord blood and tissue contain a heterogeneous mixture of stem and progenitor cells at different stages of differentiation¹³⁸. It is an attractive source of stem cells because it is considered biowaste accompanying the delivery of a baby. We propose here that these UCMSCS could be used during CL(P) surgeries to facilitate skin and muscle tissue regeneration (**Figure 4**).

The successful use of human umbilical cord blood and tissue mesenchymal stem cells (hUCMSC) has been shown for other fields in a variety of in vitro, animal and human studies. It has been demonstrated that umbilical cord blood cells can differentiate into epithelial cells¹⁴³, osteoblasts and adipocytes¹⁴⁴, and also have a myogenic potential. In a study on Duchenne Muscular Dystrophy, myoblasts from Duchenne and Becker muscular dystrophy patients were isolated from the biceps, co-cultured with hUCMSCS obtained from healthy babies and analyzed by immunofluorescence microscopy. After 15 days of culturing, dystrophin-positive myofibers were present demonstrating the differentiation of hUCMSCS into muscle cells in vitro¹⁴⁵. In another in vitro study, hUCMSCS – derived mononuclear cells gave rise to fibroblast-like cells expressing mesenchymal antigens. When these cells were cultured under promyogenic conditions they expressed myogenic markers like MyoD, MyoG, and MyHC¹⁴⁶. This indicates that hUCMSCS can differentiate into myogenic stem cells in vitro, which could possibly facilitate regeneration of the orbicularis oris muscle after cleft lip surgery.

In vivo, the healing of deep burn wounds in adult Wistar rats was improved with intravenously injected cord blood stem cells compared to controls. The hUCMSCS migrated into the wound and decreased the quantity of inflammatory cells, while neovascularization was increased compared to the control groups¹⁴⁷. A biomimetic scaffold with hUCMSCS and fibrin showed an improved full-thickness skin wound repair

without scar formation in rats compared to controls without scaffold or with a scaffold without hUCMSC¹⁴⁸. Similarly, hUCMSCS in combination with a collagen-fibrin double layer membrane and a single layer collagen membrane resulted in accelerated wound repair in mice when compared to mice treated without hUCMSC¹⁴⁹.

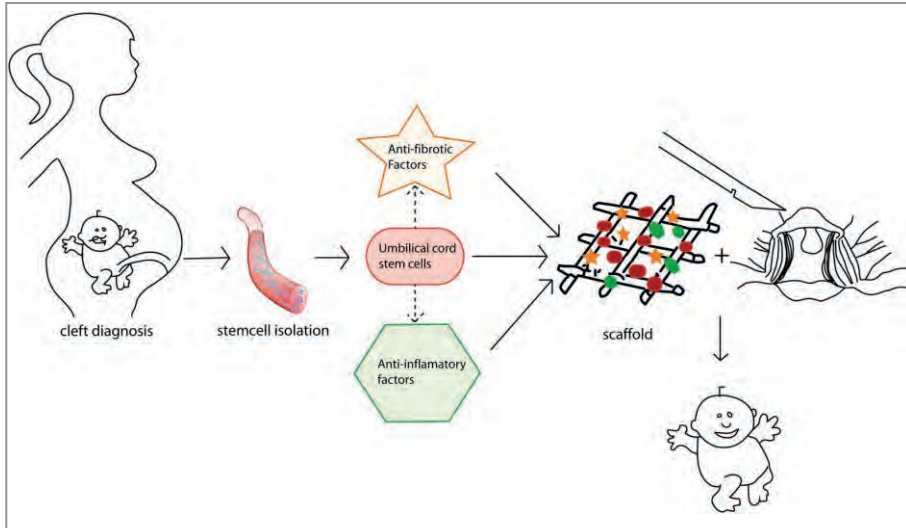


Figure 4: Following detection of a cleft lip and/or palate (CL/P) using prenatal ultrasound screening, cord blood stem cells are isolated upon birth. These stem cells express antifibrotic factors and anti-inflammatory factors and can be used in tissue engineering strategies in combination with factors targeting inflammation and fibrosis (e.g. anakinra, pirfenidone and nintedanib) within a scaffold during cleft surgery to promote skin and muscle regeneration and function and to inhibit scar formation.

The application of hUCMSCS within a small intestinal submucosa-derived ECM scaffold to a full thickness excisional wound in mice also enhanced wound repair and angiogenesis at the wound site. An increase in angiogenic growth factors like HGF, VEGF and angiopoietin was observed¹⁵⁰. Wharton's jelly mesenchymal stem cells also upregulated genes involved in re-epithelialization, neovascularization, fibroblast proliferation, and migration in an excisional full thickness murine wound model¹⁵¹. All these in vivo animal studies support the use of umbilical cord stem cells as a novel wound repair strategy.

In patients with Crohn's Disease the intravenous infusion of allogeneic hUCMSCS improved disease conditions with only mild side effects like fever and respiratory tract infection¹⁵². In atopic dermatitis, a chronic and relapsing skin disease involving pruritus, xerosis and eczematous lesions, infusion of hUCMSCS was effective without side effects¹⁵⁰. Moreover, also allogeneic hUCMSCS have been successfully used in multiple sclerosis patients improving the patients' symptoms without serious adverse effects¹⁵³.

Besides effectiveness, the question should also be answered whether it is safe to use hUCMSCs. In children with cerebral palsy (motor disorder in childhood)

autologous hUCMSCS improved whole brain connectivity and motor function¹⁵⁴. Similar studies found that infusion of autologous cord blood cells in children with autism spectrum disorder improved behavior and was safe^{155,156}. A 6-year follow-up study also demonstrated the long-term safety profile of hUCMSCS infusion for drug-resistant systemic lupus erythematosus patients. The treatment reduced the disease activity significantly¹⁵⁷. This confirms that the use of hUCMSCS is thus safe and no tumor-related effects occur¹⁵⁷. A study with allogeneic hUCMSCS in an osteoarthritic patient showed regeneration of cartilage without adverse effects up to 7 years of follow up¹⁵⁸. Allogenic cord blood stem cell transplantation was also successfully used in babies with severe combined immunodeficiency syndrome and led to a reconstitution of hematopoietic cells^{159,160}. No long-term graft versus host disease was observed.

Summarizing, the umbilical cord tissue and umbilical cord blood is an easily accessible source of MSC for the regeneration of skin and muscle tissue. These stem cells can differentiate into the required cell types and secrete regenerative factors^{143,145,146}. hUCMSCS are safe for use in children and adults¹⁵⁴⁻¹⁵⁷, while no immunogenic rejection was observed after allogeneic transplantation^{152,153}. The low immunogenicity of hUCMSCS would also allow the use of hUCMSCS from a central cord blood stem cell bank when autologous stem cells are not available. We therefore postulate that cord blood stem cells can be used as a novel adjuvant strategy in cleft surgery to prevent fibrosis and scarring to improve the outcome of the surgery. This will eventually lead to a better quality of life for patients with CL(P).

8. Clinical challenges for scaffold-based cord blood stem cells with anti-fibrotic/anti-inflammatory factors

Direct injection of cord blood stem cells into a wound site is not always effective¹³⁴. In muscle tissue, isolated stem cells can be applied to the site of injury to improve regeneration¹⁶¹. However, the success rate after isolation and injection of stem cells has been low. Stem cells seem to lose their migratory and regenerative potential and often die¹⁶².

Thus, stem cell therapy is complicated by the limited number of cells surviving after administration at the wound site. This is due to the harsh conditions within the wound microenvironment characterized by a wealth of pro-oxidative and pro-inflammatory mediators, and only limited blood flow¹⁶³⁻¹⁶⁵. Stem cells inducing anti-apoptotic, anti-inflammatory, and anti-oxidative genes can better withstand these insults and have better chance of surviving¹⁶³.

Cytoprotective genes include enzyme systems such as HO-1, glutathione S-transferase, dismutases, catalases, and peroxidases. HO-1 induction improves stem cell survival and improves the outcome of stem cell therapy^{163,166,167}. In contrast, abrogation of HO-activity decreases the efficacy of stem cell therapy^{168,169}. Preconditioning strategies in which cytoprotective pathways (e.g. via nrf2 activation) are activated in

cord blood stem cells could, therefore, promote their survival and achieve a better outcome of cleft surgery^{170,171}. Alternatively, the administration of antioxidants (vitamins A, C, and E, glutathione/NAC, mannose-specific lectins, and bilirubin) could protect stem cells from dying¹⁷²⁻¹⁷⁵.

Anti-inflammatory and antifibrotic factors, and stem cells can be applied in a scaffold. Scaffolds are used as an artificial ECM, which supports cell attachment, proliferation and differentiation of cells^{176,177}. The scaffold guides the newly formed tissue and allows ingrowth of blood vessels and nerves crucial for cell survival. Different types of scaffolds are available prepared from a wide range of biomaterials. Skin and muscle scaffolds can be of natural origin such as fibrin, alginate or collagen, or can be synthetic such as polypropylene, polyesters, polyurethanes and polyisocyanopeptide (PIC) hydrogel^{178,179}. They can be produced with a variety of methods, such as 3D printing and electro-spinning. Synthetic biomaterials can be degradable or nondegradable. The advantages of synthetic biomaterials are their low immunogenicity and reproducible quality, while they can be custom made with the required mechanical properties and shape¹⁸⁰. Scaffolds can be seeded with cord blood stem cells together with the anti-inflammatory and anti-fibrotic factors to create a regenerative microenvironment that facilitates tissue regeneration and prevents scar formation. Tissue engineering/regenerative medicine scaffolds require the appropriate physical and cellular signals to promote tissue regeneration¹⁸¹. The sum of the biochemical signals and biophysical cues from the microenvironment dictate the fate of stem cells¹⁸². The sum of pro- and anti-inflammatory and fibrotic factors, the shape of scaffolds, stiffness of the matrix, nanotopography and the presence of biofunctional groups as RGD-sequences discriminates between scarring and regeneration of tissue¹⁸³. Mechanical cues may be applied in tissue engineering by adjusting the type, stiffness and architecture of the scaffolds facilitating the differentiation of cord blood stem cells into either skin or muscle tissue⁶⁸.

9. Conclusions

The functional and esthetical outcome of cleft palate repair is often hampered by fibrosis and scarring. In this review, we discuss novel tissue engineering strategies to promote muscle and skin regeneration, while preventing scarring. Umbilical cord blood stem cells are a promising, safe, and non-invasive source of stem cells that can be combined in a scaffold together with anti-inflammatory and antifibrotic molecules. Overexpression of cytoprotective molecules in these stem cells by preconditioning before applying them to the wound area may not only increase stem cell survival but also further contribute to a regenerating microenvironment. We expect that this novel strategy improves both muscle and skin regeneration after cleft repair resulting in a better functional and esthetic outcome.

References

1. Gundlach KK, Maus C. Epidemiological studies on the frequency of clefts in Europe and world-wide. *J Craniomaxillofac Surg*. 2006;34 Suppl 2:1-2.
2. Mossey PA, Little J, Munger RG, Dixon MJ, Shaw WC. Cleft lip and palate. *Lancet*. 2009;374(9703):1773-1785.
3. Tanaka SA, Mahabir RC, Jupiter DC, Menezes JM. Updating the epidemiology of cleft lip with or without cleft palate. *Plast Reconstr Surg*. 2012;129(3):511e-518e.
4. Harville EW, Wilcox AJ, Lie RT, Vindenes H, Åbyholm F. Cleft Lip and Palate versus Cleft Lip Only: Are They Distinct Defects? *American Journal of Epidemiology*. 2005;162(5):448-453.
5. Venkatesh R. Syndromes and anomalies associated with cleft. *Indian Journal of Plastic Surgery : Official Publication of the Association of Plastic Surgeons of India*. 2009;42(Suppl):S51-S55.
6. Drew SJ. Clefting syndromes. *Atlas Oral Maxillofac Surg Clin North Am*. 2014;22(2):175-181.
7. Watkins SE, Meyer RE, Strauss RP, Aylsworth AS. Classification, epidemiology, and genetics of orofacial clefts. *Clin Plast Surg*. 2014;41(2):149-163.
8. Shi M, Wehby GL, Murray JC. Review on Genetic Variants and Maternal Smoking in the Etiology of Oral Clefts and Other Birth Defects. *Birth defects research Part C, Embryo today : reviews*. 2008;84(1):16-29.
9. DeRoo LA, Wilcox AJ, Drevon CA, Lie RT. First-Trimester Maternal Alcohol Consumption and the Risk of Infant Oral Clefts in Norway: A Population-based Case-Control Study. *American Journal of Epidemiology*. 2008;168(6):638-646.
10. Webster WS, Howe AM, Abela D, Oakes DJ. The relationship between cleft lip, maxillary hypoplasia, hypoxia and phenytoin. *Curr Pharm Des*. 2006;12(12):1431-1448.
11. Correa A, Gilboa SM, Besser LM, et al. Diabetes mellitus and birth defects. *American journal of obstetrics and gynecology*. 2008;199(3):237.e231-237.e239.
12. Bille C, Skytthe A, Vach W, et al. Parent's age and the risk of oral clefts. *Epidemiology*. 2005;16(3):311-316.
13. Herkrath AP, Herkrath FJ, Rebelo MA, Vettore MV. Parental age as a risk factor for non-syndromic oral clefts: a meta-analysis. *J Dent*. 2012;40(1):3-14.
14. Shkoukani MA, Chen M, Vong A. Cleft Lip – A Comprehensive Review. *Frontiers in Pediatrics*. 2013;1:53.
15. Vermeij-Keers C, Rozendaal AM, Luijsterburg AJM, et al. Subphenotyping and Classification of Cleft Lip and Alveolus in Adult Unoperated Patients: A New Embryological Approach. *Cleft Palate Craniofac J*. 2018;55(9):1267-1276.
16. Dixon MJ, Marazita ML, Beaty TH, Murray JC. Cleft lip and palate: understanding genetic and environmental influences. *Nature reviews Genetics*. 2011;12(3):167-178.
17. Asllanaj B, Kragt L, Voshol I, et al. Dentition Patterns in Different Unilateral Cleft Lip Subphenotypes. *J Dent Res*. 2017;96(13):1482-1489.
18. Flynn T, Moller C, Jonsson R, Lohmander A. The high prevalence of otitis media with effusion in children with cleft lip and palate as compared to children without clefts. *Int J Pediatr Otorhinolaryngol*. 2009;73(10):1441-1446.
19. Sinko K, Jagsch R, Precht V, Watzinger F, Hollmann K, Baumann A. Evaluation of esthetic, functional, and quality-of-life outcome in adult cleft lip and palate patients. *Cleft Palate Craniofac J*. 2005;42(4):355-361.
20. Raud Westberg L, Hoglund Santamarta L, Karlsson J, Nyberg J, Neovius E, Lohmander A. Speech outcome in young children born with unilateral cleft lip and palate treated with one- or two-stage palatal repair and the impact of early intervention. *Logoped Phoniatr Vocol*. 2017;1-9.
21. Shi B, Losee JE. The impact of cleft lip and palate repair on maxillofacial growth. *Int J Oral Sci*. 2015;7(1):14-17.
22. Liao YF, Mars M. Long-term effects of clefts on craniofacial morphology in patients with unilateral cleft lip and palate. *Cleft Palate Craniofac J*. 2005;42(6):601-609.
23. Shaw W, Semb G. The Scandcleft randomised trials of primary surgery for unilateral cleft lip and palate: 11. What next? *J Plast Surg Hand Surg*. 2017;51(1):88-93.
24. Farronato G, Kairyte L, Giannini L, Galbiati G, Maspero C. How various surgical protocols of the unilateral cleft lip and palate influence the facial growth and possible orthodontic problems? Which is the best timing of lip, palate and alveolus repair? literature review. *Stomatologija*. 2014;16(2):53-60.

25. Biggs LC, Naridze RL, DeMali KA, et al. Interferon regulatory factor 6 regulates keratinocyte migration. *Journal of Cell Science*. 2014;127(13):2840-2848.
26. Lazzeri D, Viacava P, Pollina LE, et al. Dystrophic-like alterations characterize orbicularis oris and palatopharyngeal muscles in patients affected by cleft lip and palate. *Cleft Palate Craniofac J*. 2008;45(6):587-591.
27. Krey KF, Dannhauer KH, Hemprich A, et al. Cytophotometrical and immunohistochemical analysis of soft palate muscles of children with isolated cleft palate and combined cleft lip and palate. *Exp Toxicol Pathol*. 2002;54(1):69-75.
28. Rahimov F, Jugessur A, Murray JC. Genetics of Nonsyndromic Orofacial Clefts. *The Cleft palate-craniofacial journal : official publication of the American Cleft Palate-Craniofacial Association*. 2012;49(1):73-91.
29. Rinon A, Lazar S, Marshall H, et al. Cranial neural crest cells regulate head muscle patterning and differentiation during vertebrate embryogenesis. *Development*. 2007;134(17):3065-3075.
30. Jugessur A, Murray JC. Orofacial clefting: recent insights into a complex trait. *Current opinion in genetics & development*. 2005;15(3):270-278.
31. Jiang R, Bush JO, Lidral AC. Development of the Upper Lip: Morphogenetic and Molecular Mechanisms. *Developmental dynamics : an official publication of the American Association of Anatomists*. 2006;235(5):1152-1166.
32. Leslie EJ, Marazita ML. Genetics of cleft lip and cleft palate. *Am J Med Genet C Semin Med Genet*. 2013;163c(4):246-258.
33. Graham A, Okabe M, Quinlan R. The role of the endoderm in the development and evolution of the pharyngeal arches. *Journal of Anatomy*. 2005;207(5):479-487.
34. Tzahor E. Heart and craniofacial muscle development: A new developmental theme of distinct myogenic fields. *Developmental Biology*. 2009;327(2):273-279.
35. Gasser RF. The development of the facial muscles in man. *American Journal of Anatomy*. 1967;120(2):357-375.
36. Rogers CR, Meara JG, Mulliken JB. The philtrum in cleft lip: review of anatomy and techniques for construction. *J Craniofac Surg*. 2014;25(1):9-13.
37. Grabb WC, Rosenstein SW, Bzoch KR. *Cleft lip and palate; surgical, dental, and speech aspects*. Little, Brown; 1971.
38. Dong C, Zheng S. Immunohistochemical analysis of orbicularis oris muscle fiber distribution at the philtrum in healthy infants. *Int J Pediatr Otorhinolaryngol*. 2015;79(12):2208-2212.
39. Spauwen PH, Hardjowasito W, Boersma J, Latief BS. Dental cast study of adult patients with untreated unilateral cleft lip or cleft lip and palate in indonesia compared with surgically treated patients in The Netherlands. *The Cleft palate-craniofacial journal : official publication of the American Cleft Palate-Craniofacial Association*. 1993;30(3):313-319.
40. Gundlach KK, Pfeifer G. The arrangement of muscle fibres in cleft lips. *J Maxillofac Surg*. 1979;7(2):109-116.
41. Wijayaweera CJ, Amaratunga NA, Angunawela P. Arrangement of the orbicularis oris muscle in different types of cleft lips. *J Craniofac Surg*. 2000;11(3):232-235.
42. Wijayaweera CJ, de S Amaratunga A, Angunawela P. Histopathology of Cleft Lip Muscle: an Enzyme Histochemical and Electron Microscopic Study. *Asian Journal of Oral and Maxillofacial Surgery*. 2002;14(4):219-225.
43. Lindman R, Paulin G, Stal PS. Morphological characterization of the levator veli palatini muscle in children born with cleft palates. *Cleft Palate Craniofac J*. 2001;38(5):438-448.
44. Ono Y, Boldrin L, Knopp P, Morgan JE, Zammit PS. Muscle satellite cells are a functionally heterogeneous population in both somite-derived and branchiomeric muscles. *Dev Biol*. 2010;337(1):29-41.
45. Schendel SA, Pearl RM, De'Armond SJ. Pathophysiology of cleft lip muscle. *Plast Reconstr Surg*. 1989;83(5):777-784.
46. Heycock MH. A field guide to cleft-lip repair. *Br J Surg*. 1971;58(8):567-570.
47. Adetayo AM, James O, Adeyemo WL, Ogunlewe MO, Butali A. Unilateral cleft lip repair: a comparison of treatment outcome with two surgical techniques using quantitative (anthropometry) assessment. *Journal of the Korean Association of Oral and Maxillofacial Surgeons*. 2018;44(1):3-11.

48. Adeyemo WL, James O, Adeyemi MO, et al. An evaluation of surgical outcome of bilateral cleft lip surgery using a modified Millard's (Fork Flap) technique. *African journal of paediatric surgery* : *AJPS*. 2013;10(4):307-310.
49. Semb G, Enemark H, Friede H, et al. A Scandcleft randomised trials of primary surgery for unilateral cleft lip and palate: 1. Planning and management. *J Plast Surg Hand Surg*. 2017;51(1):2-13.
50. Hammoudeh JA, Imahiyerobo TA, Liang F, et al. Early Cleft Lip Repair Revisited: A Safe and Effective Approach Utilizing a Multidisciplinary Protocol. *Plastic and reconstructive surgery Global open*. 2017;5(6):e1340-e1340.
51. Holland S, Gabbay JS, Heller JB, et al. Delayed Closure of the Hard Palate Leads to Speech Problems and Deleterious Maxillary Growth. *Plastic and Reconstructive Surgery*. 2007;119(4):1302-1310.
52. Bonanthaya K, Rao DD, Shetty P, Uguru C. Correlation of vermilion symmetry to alveolar cleft defect in unilateral cleft lip repair. *Int J Oral Maxillofac Surg*. 2016;45(6):688-691.
53. Li Y, Shi B, Song QG, Zuo H, Zheng Q. Effects of lip repair on maxillary growth and facial soft tissue development in patients with a complete unilateral cleft of lip, alveolus and palate. *J Craniomaxillofac Surg*. 2006;34(6):355-361.
54. Mulliken JB, Wu JK, Padwa BL. Repair of bilateral cleft lip: review, revisions, and reflections. *J Craniofac Surg*. 2003;14(5):609-620.
55. Xue M, Jackson CJ. Extracellular Matrix Reorganization During Wound Healing and Its Impact on Abnormal Scarring. *Adv Wound Care (New Rochelle)*. 2015;4(3):119-136.
56. Wagener FA, Scharstuhl A, Tyrrell RM, et al. The heme-heme oxygenase system in wound healing; implications for scar formation. *Curr Drug Targets*. 2010;11(12):1571-1585.
57. Satish L, Kathju S. Cellular and Molecular Characteristics of Scarless versus Fibrotic Wound Healing. *Dermatol Res Pract*. 2010;2010:790234.
58. Mendonca RJ, Coutinho-Netto J. Cellular aspects of wound healing. *An Bras Dermatol*. 2009;84(3):257-262.
59. Darby IA, Laverdet B, Bonté F, Desmoulière A. Fibroblasts and myofibroblasts in wound healing. *Clinical, cosmetic and investigational dermatology*. 2014;7:301-311.
60. Gabbiani G. The myofibroblast in wound healing and fibrocontractive diseases. *J Pathol*. 2003;200(4):500-503.
61. Gauglitz GG, Korting HC, Pavicic T, Ruzicka T, Jeschke MG. Hypertrophic scarring and keloids: pathomechanisms and current and emerging treatment strategies. *Mol Med*. 2011;17(1-2):113-125.
62. Lian N, Li T. Growth factor pathways in hypertrophic scars: Molecular pathogenesis and therapeutic implications. *Biomed Pharmacother*. 2016;84:42-50.
63. Guo S, DiPietro LA. Factors Affecting Wound Healing. *Journal of Dental Research*. 2010;89(3):219-229.
64. Lundvig DM, Immenschuh S, Wagener FA. Heme oxygenase, inflammation, and fibrosis: the good, the bad, and the ugly? *Front Pharmacol*. 2012;3:81.
65. Grieb G, Steffens G, Pallua N, Bernhagen J, Bucala R. Circulating fibrocytes--biology and mechanisms in wound healing and scar formation. *Int Rev Cell Mol Biol*. 2011;291:1-19.
66. Volk SW, Wang Y, Mauldin EA, Liechty KW, Adams SL. Diminished type III collagen promotes myofibroblast differentiation and increases scar deposition in cutaneous wound healing. *Cells Tissues Organs*. 2011;194(1):25-37.
67. Son D, Harijan A. Overview of Surgical Scar Prevention and Management. *Journal of Korean Medical Science*. 2014;29(6):751-757.
68. Brouwer KM, Lundvig DM, Middelkoop E, Wagener FA, Von den Hoff JW. Mechanical cues in orofacial tissue engineering and regenerative medicine. *Wound Repair Regen*. 2015;23(3):302-311.
69. Levy BD, Clish CB, Schmidt B, Gronert K, Serhan CN. Lipid mediator class switching during acute inflammation: signals in resolution. *Nat Immunol*. 2001;2(7):612-619.
70. Mack M. Inflammation and fibrosis. *Matrix Biol*. 2018;68-69:106-121.
71. O'Reilly S. Toll Like Receptors in systemic sclerosis: An emerging target. *Immunol Lett*. 2018;195:2-8.
72. van der Veer WM, Bloemen MC, Ulrich MM, et al. Potential cellular and molecular causes of hypertrophic scar formation. *Burns*. 2009;35(1):15-29.
73. Jeney V, Balla J, Yachie A, et al. Pro-oxidant and cytotoxic effects of circulating heme. *Blood*. 2002;100(3):879-887.

74. Chen D, Hao H, Tong C, et al. Transdifferentiation of Umbilical Cord-Derived Mesenchymal Stem Cells Into Epidermal-Like Cells by the Mimicking Skin Microenvironment. *Int J Low Extrem Wounds*. 2015;14(2):136-145.
75. Bana N, Sanooghi D, Soleimani M, et al. A Comparative Study to Evaluate Myogenic Differentiation Potential of Human Chorion versus Umbilical Cord Blood-derived Mesenchymal Stem Cells. *Tissue and Cell*. 2017;49(4):495-502.
76. Li M, Luan F, Zhao Y, et al. Mesenchymal stem cell-conditioned medium accelerates wound healing with fewer scars. *Int Wound J*. 2017;14(1):64-73.
77. Mortier L, Delesalle F, Formstecher P, Polakowska R. Human umbilical cord blood cells form epidermis in the skin equivalent model. *Exp Dermatol*. 2010;19(10):929-930.
78. Maarse W, Pistorius LR, Van Eeten WK, et al. Prenatal ultrasound screening for orofacial clefts. *Ultrasound Obstet Gynecol*. 2011;38(4):434-439.
79. Lim IJ, Phan TT. Epithelial and mesenchymal stem cells from the umbilical cord lining membrane. *Cell Transplant*. 2014;23(4-5):497-503.
80. Zhang CP, Fu XB. Therapeutic potential of stem cells in skin repair and regeneration. *Chin J Traumatol*. 2008;11(4):209-221.
81. Kanji S, Das H. Advances of Stem Cell Therapeutics in Cutaneous Wound Healing and Regeneration. *Mediators Inflamm*. 2017;2017:5217967.
82. Fuchs E. Epithelial Skin Biology: Three Decades of Developmental Biology, a Hundred Questions Answered and a Thousand New Ones to Address. *Curr Top Dev Biol*. 2016;116:357-374.
83. Carvajal Monroy PL, Grefte S, Kuipers-Jagtman AM, et al. A rat model for muscle regeneration in the soft palate. *PLoS One*. 2013;8(3):e59193.
84. Carvajal Monroy PL, Yablonska-Reuveni Z, Grefte S, Kuipers-Jagtman AM, Wagener FA, Von den Hoff JW. Isolation and Characterization of Satellite Cells from Rat Head Branchiomeric Muscles. *J Vis Exp*. 2015(101):e52802.
85. Ciciliot S, Schiaffino S. Regeneration of mammalian skeletal muscle. Basic mechanisms and clinical implications. *Curr Pharm Des*. 2010;16(8):906-914.
86. Carvajal Monroy PL, Grefte S, Kuipers-Jagtman AM, Von den Hoff JW, Wagener FA. Neonatal Satellite Cells Form Small Myotubes In Vitro. *J Dent Res*. 2017;96(3):331-338.
87. Ten Broek RW, Grefte S, Von den Hoff JW. Regulatory factors and cell populations involved in skeletal muscle regeneration. *J Cell Physiol*. 2010;224(1):7-16.
88. Karalaki M, Fili S, Philippou A, Koutsilieris M. Muscle regeneration: cellular and molecular events. *In Vivo*. 2009;23(5):779-796.
89. Pavlath GK, Thaloer D, Rando TA, Cheong M, English AW, Zheng B. Heterogeneity among muscle precursor cells in adult skeletal muscles with differing regenerative capacities. *Dev Dyn*. 1998;212(4):495-508.
90. Carvajal Monroy PL, Grefte S, Kuipers-Jagtman AM, Von den Hoff JW, Wagener FADTG. Neonatal Satellite Cells Form Small Myotubes In Vitro. *Journal of Dental Research*. 2016;96(3):331-338.
91. Dang CM, Beanes SR, Lee H, Zhang X, Soo C, Ting K. Scarless fetal wounds are associated with an increased matrix metalloproteinase-to-tissue-derived inhibitor of metalloproteinase ratio. *Plast Reconstr Surg*. 2003;111(7):2273-2285.
92. Walraven M, Gouverneur M, Middelkoop E, Beelen RH, Ulrich MM. Altered TGF-beta signaling in fetal fibroblasts: what is known about the underlying mechanisms? *Wound Repair Regen*. 2014;22(1):3-13.
93. Wang P-H, Huang B-S, Horng H-C, Yeh C-C, Chen Y-J. Wound healing. *Journal of the Chinese Medical Association*. 2017.
94. Penn JW, Grobelaar AO, Rolfe KJ. The role of the TGF-beta family in wound healing, burns and scarring: a review. *Int J Burns Trauma*. 2012;2(1):18-28.
95. Border WA, Noble NA. Transforming growth factor beta in tissue fibrosis. *N Engl J Med*. 1994;331(19):1286-1292.
96. Zhu J, Li Y, Shen W, et al. Relationships between transforming growth factor-beta1, myostatin, and decorin: implications for skeletal muscle fibrosis. *J Biol Chem*. 2007;282(35):25852-25863.
97. Wagner KR. Muscle regeneration through myostatin inhibition. *Curr Opin Rheumatol*. 2005;17(6):720-724.
98. Kishioka Y, Thomas M, Wakamatsu J, et al. Decorin enhances the proliferation and differentiation of myogenic cells through suppressing myostatin activity. *J Cell Physiol*. 2008;215(3):856-867.

99. Li Y, Li J, Zhu J, et al. Decorin gene transfer promotes muscle cell differentiation and muscle regeneration. *Mol Ther.* 2007;15(9):1616-1622.
100. Bedair HS, Karthikeyan T, Quintero A, Li Y, Huard J. Angiotensin II receptor blockade administered after injury improves muscle regeneration and decreases fibrosis in normal skeletal muscle. *Am J Sports Med.* 2008;36(8):1548-1554.
101. Shibasaki Y, Nishiue T, Masaki H, et al. Impact of the angiotensin II receptor antagonist, losartan, on myocardial fibrosis in patients with end-stage renal disease: assessment by ultrasonic integrated backscatter and biochemical markers. *Hypertens Res.* 2005;28(10):787-795.
102. Shan Y, Pepe J, Lu TH, Elbirt KK, Lambrecht RW, Bonkovsky HL. Induction of the heme oxygenase-1 gene by metalloporphyrins. *Arch Biochem Biophys.* 2000;380(2):219-227.
103. Yachie A, Niida Y, Wada T, et al. Oxidative stress causes enhanced endothelial cell injury in human heme oxygenase-1 deficiency. *J Clin Invest.* 1999;103(1):129-135.
104. Kapturczak MH, Wasserfall C, Brusko T, et al. Heme oxygenase-1 modulates early inflammatory responses: evidence from the heme oxygenase-1-deficient mouse. *Am J Pathol.* 2004;165(3):1045-1053.
105. Bussolati B, Ahmed A, Pemberton H, et al. Bifunctional role for VEGF-induced heme oxygenase-1 in vivo: induction of angiogenesis and inhibition of leukocytic infiltration. *Blood.* 2004;103(3):761-766.
106. Bussolati B, Mason JC. Dual role of VEGF-induced heme-oxygenase-1 in angiogenesis. *Antioxid Redox Signal.* 2006;8(7-8):1153-1163.
107. Seta F, Bellner L, Rezzani R, et al. Heme oxygenase-2 is a critical determinant for execution of an acute inflammatory and reparative response. *Am J Pathol.* 2006;169(5):1612-1623.
108. Bellner L, Wolstein J, Patil KA, Dunn MW, Laniado-Schwartzman M. Biliverdin Rescues the HO-2 Null Mouse Phenotype of Unresolved Chronic Inflammation Following Corneal Epithelial Injury. *Invest Ophthalmol Vis Sci.* 2011;52(6):3246-3253.
109. de Souza KS, Cantaruti TA, Azevedo GM, Jr., et al. Improved cutaneous wound healing after intraperitoneal injection of alpha-melanocyte-stimulating hormone. *Exp Dermatol.* 2015;24(3):198-203.
110. Gay D, Kwon O, Zhang Z, et al. Fgf9 from dermal gammadelta T cells induces hair follicle neogenesis after wounding. *Nat Med.* 2013;19(7):916-923.
111. Whyte JL, Smith AA, Liu B, et al. Augmenting Endogenous Wnt Signaling Improves Skin Wound Healing. *PLoS ONE.* 2013;8(10):e76883.
112. King A, Balaji S, Le LD, Crombleholme TM, Keswani SG. Regenerative Wound Healing: The Role of Interleukin-10. *Advances in Wound Care.* 2014;3(4):315-323.
113. Gallucci RM, Sugawara T, Yucesoy B, et al. Interleukin-6 treatment augments cutaneous wound healing in immunosuppressed mice. *J Interferon Cytokine Res.* 2001;21(8):603-609.
114. Moore AL, Marshall CD, Barnes LA, Murphy MP, Ransom RC, Longaker MT. Scarless wound healing: Transitioning from fetal research to regenerative healing. *Wiley Interdiscip Rev Dev Biol.* 2018;7(2).
115. Ding J, Ma Z, Liu H, et al. The therapeutic potential of a C-X-C chemokine receptor type 4 (CXCR-4) antagonist on hypertrophic scarring in vivo. *Wound Repair Regen.* 2014;22(5):622-630.
116. Yan C, Gao N, Sun H, et al. Targeting Imbalance between IL-1beta and IL-1 Receptor Antagonist Ameliorates Delayed Epithelium Wound Healing in Diabetic Mouse Corneas. *Am J Pathol.* 2016;186(6):1466-1480.
117. Raghu G, Selman M. Nintedanib and Pirfenidone. New Antifibrotic Treatments Indicated for Idiopathic Pulmonary Fibrosis Offer Hopes and Raises Questions. *American Journal of Respiratory and Critical Care Medicine.* 2015;191(3):252-254.
118. Macias-Barragan J, Sandoval-Rodriguez A, Navarro-Partida J, Armendariz-Borunda J. The multifaceted role of pirfenidone and its novel targets. *Fibrogenesis Tissue Repair.* 2010;3:16.
119. Zhao XY, Zeng X, Li XM, Wang TL, Wang BE. Pirfenidone inhibits carbon tetrachloride- and albumin complex-induced liver fibrosis in rodents by preventing activation of hepatic stellate cells. *Clin Exp Pharmacol Physiol.* 2009;36(10):963-968.
120. Westra IM, Mutsaers HA, Luangmonkong T, et al. Human precision-cut liver slices as a model to test antifibrotic drugs in the early onset of liver fibrosis. *Toxicol In Vitro.* 2016;35:77-85.
121. Wuyts WA, Kolb M, Stowasser S, Stansen W, Huggins JT, Raghu G. First Data on Efficacy and Safety of Nintedanib in Patients with Idiopathic Pulmonary Fibrosis and Forced Vital Capacity of $\leq 50\%$ of Predicted Value. *Lung.* 2016;194(5):739-743.

122. Hilberg F, Roth GJ, Krssak M, et al. BIBF 1120: triple angiokinase inhibitor with sustained receptor blockade and good antitumor efficacy. *Cancer Res.* 2008;68(12):4774-4782.
123. Herberitz S, Sawyer JS, Stauber AJ, et al. Clinical development of galunisertib (LY2157299 monohydrate), a small molecule inhibitor of transforming growth factor-beta signaling pathway. *Drug Des Devel Ther.* 2015;9:4479-4499.
124. Luangmonkong T, Suriguga S, Bigaeva E, et al. Evaluating the antifibrotic potency of galunisertib in a human ex vivo model of liver fibrosis. *Br J Pharmacol.* 2017;174(18):3107-3117.
125. Wang W, Xiong H, Hu Z, et al. Experimental study on TGF-beta1-mediated CD147 expression in oral submucous fibrosis. *Oral Dis.* 2018;24(6):993-1000.
126. Doi H, Kitajima Y, Luo L, et al. Potency of umbilical cord blood- and Wharton's jelly-derived mesenchymal stem cells for scarless wound healing. *Sci Rep.* 2016;6:18844.
127. Sasaki M, Abe R, Fujita Y, Ando S, Inokuma D, Shimizu H. Mesenchymal stem cells are recruited into wounded skin and contribute to wound repair by transdifferentiation into multiple skin cell type. *J Immunol.* 2008;180(4):2581-2587.
128. Nunes VA, Cavaçana N, Canovas M, Strauss BE, Zatz M. Stem cells from umbilical cord blood differentiate into myotubes and express dystrophin in vitro only after exposure to in vivo muscle environment. *Biol Cell.* 2007;99(4):185-196.
129. Brzoska E, Grabowska I, Hoser G, et al. Participation of stem cells from human cord blood in skeletal muscle regeneration of SCID mice. *Exp Hematol.* 2006;34(9):1262-1270.
130. Caplan AI, Sorrell JM. The MSC curtain that stops the immune system. *Immunol Lett.* 2015;168(2):136-139.
131. Liao Y, Ivanova L, Zhu H, et al. Cord Blood-Derived Stem Cells Suppress Fibrosis and May Prevent Malignant Progression in Recessive Dystrophic Epidermolysis Bullosa. *Stem Cells.* 2018;36(12):1839-1850.
132. Moroncini G, Paolini C, Orlando F, et al. Mesenchymal stromal cells from human umbilical cord prevent the development of lung fibrosis in immunocompetent mice. *PLoS One.* 2018;13(6):e0196048.
133. Liu B, Ding F, Hu D, et al. Human umbilical cord mesenchymal stem cell conditioned medium attenuates renal fibrosis by reducing inflammation and epithelial-to-mesenchymal transition via the TLR4/NF-kappaB signaling pathway in vivo and in vitro. *Stem Cell Res Ther.* 2018;9(1):7.
134. Xu L, Ding L, Wang L, et al. Umbilical cord-derived mesenchymal stem cells on scaffolds facilitate collagen degradation via upregulation of MMP-9 in rat uterine scars. *Stem Cell Res Ther.* 2017;8(1):84.
135. Shin L, Peterson DA. Human mesenchymal stem cell grafts enhance normal and impaired wound healing by recruiting existing endogenous tissue stem/progenitor cells. *Stem Cells Transl Med.* 2013;2(1):33-42.
136. Kim J, Lee JH, Yeo SM, Chung HM, Chae JI. Stem cell recruitment factors secreted from cord blood-derived stem cells that are not secreted from mature endothelial cells enhance wound healing. *In Vitro Cell Dev Biol Anim.* 2014;50(2):146-154.
137. Dandoy CE, Ardura MI, Papanicolaou GA, Auletta JJ. Bacterial bloodstream infections in the allogeneic hematopoietic cell transplant patient: new considerations for a persistent nemesis. *Bone Marrow Transplant.* 2017;52(8):1091-1106.
138. Harris DT. Stem Cell Banking for Regenerative and Personalized Medicine. *Biomedicines.* 2014;2(1):50-79.
139. El Omar R, Beroud J, Stoltz JF, Menu P, Velot E, Decot V. Umbilical cord mesenchymal stem cells: the new gold standard for mesenchymal stem cell-based therapies? *Tissue Eng Part B Rev.* 2014;20(5):523-544.
140. Maarse W, Berge SJ, Pistorius L, et al. Diagnostic accuracy of transabdominal ultrasound in detecting prenatal cleft lip and palate: a systematic review. *Ultrasound Obstet Gynecol.* 2010;35(4):495-502.
141. Sepulveda W, Wong AE, Martinez-Ten P, Perez-Pedregosa J. Retronasal triangle: a sonographic landmark for the screening of cleft palate in the first trimester. *Ultrasound Obstet Gynecol.* 2010;35(1):7-13.
142. Araujo AB, Salton GD, Furlan JM, et al. Comparison of human mesenchymal stromal cells from four neonatal tissues: Amniotic membrane, chorionic membrane, placental decidua and umbilical cord. *Cytotherapy.* 2017;19(5):577-585.

143. Kamolz LP, Kolbus A, Wick N, et al. Cultured human epithelium: human umbilical cord blood stem cells differentiate into keratinocytes under in vitro conditions. *Burns*. 2006;32(1):16-19.
144. Shi S, Jia S, Liu J, Chen G. Accelerated regeneration of skin injury by co-transplantation of mesenchymal stem cells from Wharton's jelly of the human umbilical cord mixed with microparticles. *Cell Biochem Biophys*. 2015;71(2):951-956.
145. Jazedje T, Secco M, Vieira NM, et al. Stem cells from umbilical cord blood do have myogenic potential, with and without differentiation induction in vitro. *Journal of Translational Medicine*. 2009;7:6-6.
146. Gang EJ, Jeong JA, Hong SH, et al. Skeletal myogenic differentiation of mesenchymal stem cells isolated from human umbilical cord blood. *Stem Cells*. 2004;22(4):617-624.
147. Liu L, Yu Y, Hou Y, et al. Human umbilical cord mesenchymal stem cells transplantation promotes cutaneous wound healing of severe burned rats. *PLoS One*. 2014;9(2):e88348.
148. Montanucci P, di Pasquali C, Ferri I, et al. Human Umbilical Cord Wharton Jelly-Derived Adult Mesenchymal Stem Cells, in Biohybrid Scaffolds, for Experimental Skin Regeneration. *Stem Cells International*. 2017;2017:1472642.
149. Nan W, Liu R, Chen H, et al. Umbilical Cord Mesenchymal Stem Cells Combined With a Collagenfibrin Double-layered Membrane Accelerates Wound Healing. *Wounds*. 2015;27(5):134-140.
150. Kim HS, Lee JH, Roh KH, Jun HJ, Kang KS, Kim TY. Clinical Trial of Human Umbilical Cord Blood-Derived Stem Cells for the Treatment of Moderate-to-Severe Atopic Dermatitis: Phase I/IIa Studies. *Stem Cells*. 2017;35(1):248-255.
151. Arno AI, Amini-Nik S, Blit PH, et al. Human Wharton's jelly mesenchymal stem cells promote skin wound healing through paracrine signaling. *Stem Cell Research & Therapy*. 2014;5(1):28.
152. Zhang J, Lv S, Liu X, Song B, Shi L. Umbilical Cord Mesenchymal Stem Cell Treatment for Crohn's Disease: A Randomized Controlled Clinical Trial. *Gut Liver*. 2018;12(1):73-78.
153. Meng M, Liu Y, Wang W, et al. Umbilical cord mesenchymal stem cell transplantation in the treatment of multiple sclerosis. *American Journal of Translational Research*. 2018;10(1):212-223.
154. Sun JM, Song AW, Case LE, et al. Effect of Autologous Cord Blood Infusion on Motor Function and Brain Connectivity in Young Children with Cerebral Palsy: A Randomized, Placebo-Controlled Trial. *Stem Cells Transl Med*. 2017;6(12):2071-2078.
155. Chez M, Lepage C, Parise C, Dang-Chu A, Hankins A, Carroll M. Safety and Observations from a Placebo-Controlled, Crossover Study to Assess Use of Autologous Umbilical Cord Blood Stem Cells to Improve Symptoms in Children with Autism. *Stem Cells Transl Med*. 2018;7(4):333-341.
156. Dawson G, Sun JM, Davlantis KS, et al. Autologous Cord Blood Infusions Are Safe and Feasible in Young Children with Autism Spectrum Disorder: Results of a Single-Center Phase I Open-Label Trial. *Stem Cells Transl Med*. 2017;6(5):1332-1339.
157. Wang D, Niu L, Feng X, et al. Long-term safety of umbilical cord mesenchymal stem cells transplantation for systemic lupus erythematosus: a 6-year follow-up study. *Clin Exp Med*. 2017;17(3):333-340.
158. Park YB, Ha CW, Lee CH, Yoon YC, Park YG. Cartilage Regeneration in Osteoarthritic Patients by a Composite of Allogeneic Umbilical Cord Blood-Derived Mesenchymal Stem Cells and Hyaluronate Hydrogel: Results from a Clinical Trial for Safety and Proof-of-Concept with 7 Years of Extended Follow-Up. *Stem Cells Transl Med*. 2017;6(2):613-621.
159. Schonberger S, Ott H, Gudowius S, et al. Saving the red baby: successful allogeneic cord blood transplantation in Omenn syndrome. *Clin Immunol*. 2009;130(3):259-263.
160. Fagioli F, Biasin E, Berger M, et al. Successful unrelated cord blood transplantation in two children with severe combined immunodeficiency syndrome. *Bone Marrow Transplant*. 2003;31(2):133-136.
161. Arutyunyan I, Fatkhudinov T, Elchaninov A, et al. Umbilical cord-derived mesenchymal stromal/stem cells enhance recovery of surgically induced skeletal muscle ischemia in a rat model. *Histol Histopathol*. 2018:18057.
162. Fan Y, Maley M, Beilharz M, Grounds M. Rapid death of injected myoblasts in myoblast transfer therapy. *Muscle Nerve*. 1996;19(7):853-860.
163. Cremers NA, Lundvig DM, van Dalen SC, et al. Curcumin-induced heme oxygenase-1 expression prevents H₂O₂-induced cell death in wild type and heme oxygenase-2 knockout adipose-derived mesenchymal stem cells. *Int J Mol Sci*. 2014;15(10):17974-17999.

164. Mohammadzadeh M, Halabian R, Gharehbaghian A, et al. Nrf-2 overexpression in mesenchymal stem cells reduces oxidative stress-induced apoptosis and cytotoxicity. *Cell Stress Chaperones*. 2012;17(5):553-565.
165. Cerqueira MT, Pirraco RP, Marques AP. Stem Cells in Skin Wound Healing: Are We There Yet? *Adv Wound Care (New Rochelle)*. 2016;5(4):164-175.
166. Hou C, Shen L, Huang Q, et al. The effect of heme oxygenase-1 complexed with collagen on MSC performance in the treatment of diabetic ischemic ulcer. *Biomaterials*. 2013;34(1):112-120.
167. Tang YL, Tang Y, Zhang YC, Qian K, Shen L, Phillips MI. Improved graft mesenchymal stem cell survival in ischemic heart with a hypoxia-regulated heme oxygenase-1 vector. *J Am Coll Cardiol*. 2005;46(7):1339-1350.
168. Lin CY, Peng CY, Huang TT, et al. Exacerbation of oxidative stress-induced cell death and differentiation in induced pluripotent stem cells lacking heme oxygenase-1. *Stem Cells Dev*. 2012;21(10):1675-1687.
169. Hamed-Asl P, Halabian R, Bahmani P, et al. Adenovirus-mediated expression of the HO-1 protein within MSCs decreased cytotoxicity and inhibited apoptosis induced by oxidative stresses. *Cell Stress Chaperones*. 2012;17(2):181-190.
170. Vijayan V, Wagener F, Immenschuh S. The macrophage heme-heme oxygenase-1 system and its role in inflammation. *Biochem Pharmacol*. 2018;153:159-167.
171. Wagener FA, Immenschuh S. Editorial: Molecular Mechanisms Protecting against Tissue Injury. *Front Pharmacol*. 2016;7:272.
172. Zeng W, Xiao J, Zheng G, et al. Antioxidant treatment enhances human mesenchymal stem cell anti-stress ability and therapeutic efficacy in an acute liver failure model. *Sci Rep*. 2015;5:11100.
173. Hinge AS, Limaye LS, Suroliya A, Kale VP. In vitro protection of umbilical cord blood-derived primitive hematopoietic stem progenitor cell pool by mannose-specific lectins via antioxidant mechanisms. *Transfusion*. 2010;50(8):1815-1826.
174. Drowley L, Okada M, Beckman S, et al. Cellular antioxidant levels influence muscle stem cell therapy. *Mol Ther*. 2010;18(10):1865-1873.
175. Yin X, Mayr M, Xiao Q, Wang W, Xu Q. Proteomic analysis reveals higher demand for antioxidant protection in embryonic stem cell-derived smooth muscle cells. *Proteomics*. 2006;6(24):6437-6446.
176. Chaudhari AA, Vig K, Baganizi DR, et al. Future Prospects for Scaffolding Methods and Biomaterials in Skin Tissue Engineering: A Review. *Int J Mol Sci*. 2016;17(12).
177. Roger M, Fullard N, Costello L, et al. Bioengineering the microanatomy of human skin. *J Anat*. 2019;234(4):438-455.
178. Op 't Veld RC, van den Boomen OI, Lundvig DMS, et al. Thermosensitive biomimetic polyisocyanopeptide hydrogels may facilitate wound repair. *Biomaterials*. 2018;181:392-401.
179. Von den Hoff JW, Carvajal Monroy PL, Ongkosuwito EM, van Kuppevelt TH, Daamen WF. Muscle fibrosis in the soft palate: Delivery of cells, growth factors and anti-fibrotics. *Adv Drug Deliv Rev*. 2018.
180. Jammalamadaka U, Tappa K. Recent Advances in Biomaterials for 3D Printing and Tissue Engineering. *J Funct Biomater*. 2018;9(1).
181. Howard D, Buttery LD, Shakesheff KM, Roberts SJ. Tissue engineering: strategies, stem cells and scaffolds. *J Anat*. 2008;213(1):66-72.
182. Kumar VS, Rao NK, Mohan KR, et al. Minimizing complications associated with coronal approach by application of various modifications in surgical technique for treating facial trauma: A prospective study. *Natl J Maxillofac Surg*. 2016;7(1):21-28.
183. Liu K, Mihaila SM, Rowan A, Oosterwijk E, Kouwer P. Synthetic extracellular matrices with nonlinear elasticity regulate cellular organization. *Biomacromolecules*. 2019.

Part V

General discussion and Summary

CHAPTER 8

General discussion and future perspectives

Overview

Synopsis of the problem

Section 1. Diminished cytoprotection in HO-2 deficient mice hampers fetal growth and development

1.1 The differences between HO-1 and HO-2

1.2 Reduced HO-2 activity is related to complications in human and murine pregnancies

Section 2. Diminished cytoprotection by inhibition of HO-activity in mice aggravates heme-induced abortion and placental inflammation

2.1 Decreased HO-activity from E11 in mice is not causing congenital malformation or abortion

2.2 HO-activity rescues mouse fetuses from heme-induced abortion

2.3 Defense mechanisms against free heme molecules

2.4 HO-1 induction as a potential therapeutic strategy to prevent abortion

2.5 HO-activity inhibition in mice increases the placental weight

2.6 HO-activity rescues mouse fetuses from heme-induced placental inflammation

2.7 ICAM-1 expression and macrophage influx mediate placental inflammation and pathological pregnancy

2.8 HO-1 induction polarizes macrophages to the anti-inflammatory M2 phenotype

2.9 The role of placental HO-activity in pregnancy pathology

Section 3. Cytoprotective mechanisms and signaling pathways facilitate palatogenesis in mice

3.1 Palatal fusion in mice despite HO-2 abrogation, inhibition of HO-activity and/ or heme administration

3.2 Mechanisms of MES disintegration during palatal fusion

3.3 CXCL11-CXCR3 signaling is associated with macrophage recruitment during MES disintegration in mice

3.4 CXCL11-CXCR3 signaling is associated with epithelial cell migration during MES disintegration in mice

3.5 Does HO-1 induction in recruited palatal macrophages compensate for the absence of HO-2 in mice?

3.6 CXCL12-CXCR4 signaling is associated with palatal osteogenesis in mice

Section 4. Mechanical stress induces the cytoprotective enzyme HO-1 within the PDL in rats and in the dermis of splinted wounds in mice

4.1 Orthodontic forces induce the cytoprotective enzyme HO-1 within the PDL in rats

4.2 Splinting of excisional wounds in mice induces the cytoprotective enzyme HO-1 in the dermis

Section 5. Umbilical cord blood stem cells and HO-1 induction in tissue engineering may promote muscle and skin regeneration following surgical CLP repair

5.1 MSCs in tissue remodeling

5.2 HO-1 is a promising target to improve MSC therapy in wound repair

Section 6. Clinical relevance for CLP patients and future perspectives

6.1 The potential of cytoprotective mechanisms in prevention of pregnancy pathology

6.2 The potential of cytoprotective mechanisms and signaling pathways in palatogenesis and wound healing

6.3 Palatogenesis and potential parallels with wound healing

6.4 Future treatment concepts at the CLP clinic

6.5 Shaping the face; cytoprotective mechanisms, signaling pathways, and cleft repair

Abbreviations

ADSCs	Adipose tissue-derived stem cells
ALP	Alkaline phosphatase
ALS	Amyotrophic lateral sclerosis
Apaf1	Apoptotic protease activating factor 1
Bmp2	Bone Morphogenetic Protein 2
BVR	Biliverdin reductase
CO	Carbon monoxide
CoPP	Cobalt protoporphyrin
CLP	Cleft lip and palate
CNCCs	Cranial neural crest cells
CXCL11	Chemokine (C-X-C) ligand 11
CXCL12	Chemokine (C-X-C) ligand 12
CXCR3	Chemokine (C-X-C) receptor 3
CXCR4	Chemokine (C-X-C) receptor 4
E0	Embryonic day 0
EMT	Epithelial-to-mesenchymal transformation
ERK2	Extracellular signal-regulated kinase 2
FVB	Friend leukemia virus B
G-CSF	Granulocyte colony-stimulating factor
GM-CSF	Granulocyte-macrophage colony-stimulating factor
Hb	Hemoglobin
HGF	Hepatocyte growth factor
HMOX1	Heme Oxygenase 1 gene
HMOX2	Heme Oxygenase 2 gene
HO	Heme oxygenase
HO-1	Heme oxygenase-1
HO-2	Heme oxygenase-2
H ₂ O ₂	Hydrogen peroxide
HPX	Hemopexin
ICAM-1	Intercellular Adhesion Molecule 1
IL-6	Interleukin-6
IL-1 β	Interleukine-1 beta
iNOS	inducible nitric oxide synthase
I.p.	Intraperitoneal
kDa	kilo Dalton
LDB1	LIM domain binding protein 1
LPS	Lipopolysaccharide
MEE	Medial edge epithelium
MES	Midline epithelial seam

MS	Multiple sclerosis
MSCs	Mesenchymal stem cells
NK cells	Natural killer cells
Nrf2	Nuclear factor erythroid 2-related factor 2
Pax3	Paired box 3
Pbx1	Pre-B-cell leukemia transcription factor 1
RANKL	Receptor activator of nuclear factor kappa-B ligand
Rbfox2	RNA Binding Fox-1 Homolog 2
ROS	Reactive oxygen species
SnMP	Tin mesoporphyrin
SnPP	Tin protoporphyrin
Sox9	SRY-Box Transcription Factor 9
Tcof1	Treacher Collins Syndrome Protein 1
tln1	Talin 1
TNF- α	Tumor necrosis factor-alfa
Ugt1	UDP-glucuronosyltransferase 1A1
VEGF	Vascular endothelial growth factor
Wt	Wild-type
ZnPPIX	Zinc protoporphyrin-9

Synopsis of the problem

The craniofacial malformation CLP belongs to the most common congenital birth defect of the craniofacial region¹. Patients with CLP often have to undergo surgical treatment from early childhood until adulthood². Exposure of healing wounds to oxidative and inflammatory stress, together with mechanical stress promote excessive scar formation^{3,4}. Moreover, residual scars following surgical lip repair are commonly observed, and about half of the CLP patients are not satisfied with their aesthetic outcome and ask for additional upper lip and nose corrections^{5,6}.

Interestingly, similar biological processes that are important during palatogenesis and CLP formation during embryonic development are also crucial during wound repair⁷. These processes include mesenchymal-epithelial cross-talk, chemokine signaling, mesenchymal and epithelial cell proliferation, differentiation and apoptosis. The cytoprotective HO enzyme system, having both anti-oxidative and anti-inflammatory effects, is important during both embryonic development⁸⁻¹¹, and wound repair^{12,13}. We aimed at better understanding the role of cytoprotective mechanisms and signaling pathways in the process of palatogenesis and wound healing. We postulated that inhibiting cytoprotective pathways impairs, whereas inducing cytoprotective pathways promotes palatogenesis and wound repair.

Section 1. Diminished cytoprotection in HO-2 deficient mice hampers fetal growth and development

1.1 The differences between HO-1 and HO-2

Heme molecules are essential for life, having roles in diverse biological processes as cellular differentiation and apoptosis, and they also serve as a cofactor for numerous proteins, such as hemoglobin and cytochromes^{14,15}. Unbound cellular heme is highly reactive and can generate damaging ROS, such as H₂O₂, via the Fenton reaction¹⁶⁻¹⁸. As discussed earlier in this thesis, heme can be broken down by the enzyme system HO into biliverdin, Fe²⁺ and CO^{19,20}. Biliverdin is next converted into bilirubin by biliverdin reductase (BVR). Besides the protection against high unbound heme levels, the heme break-down products biliverdin/bilirubin, CO and co-induced ferritin possess antioxidant, anti-inflammatory, and anti-apoptotic properties, regulating tissue-specific growth and survival of cells as well²¹⁻²⁵. In all vertebrate species the two isoforms of the heme-degrading HO enzyme system, namely HMOX1 and HMOX2^{16,26}, share only 50% similarity in their amino acid sequences^{27,28}. However, both isoforms contain a “heme binding area”, consisting of a similar 24 amino acid sequence, facilitating the catabolism of heme^{29,30}. Although both isoforms catalyze heme degradation, those two proteins have been shown to possess different functions³¹. The HO-1 protein has a molecular mass of 32 kDa and was first purified from the microsomal fraction of porcine spleen³², and rat liver³³. HO proteins are anchored into the endoplasmic reticulum and can migrate to the nucleus^{32,34,35}. HO-1 can be induced in response to a variety of external stimuli³⁶. It is rapidly induced by a wide array of physical and chemical stresses including heat shock, glucose or iron starvation, heme, cytokines, lipopolysaccharide (LPS), growth factors, oxidative stress, free radicals, H₂O₂, hypoxia and CO^{31,36}. In contrast to the inducible HO-1 isoform, the HO-2 isoform is mainly constitutively expressed³⁶. The HO-2 protein has a molecular mass of 36 kDa and is particularly highly expressed in the testis and brain^{37,38}.

1.2 Reduced HO-2 activity is related to complications in human and murine pregnancies

In **Chapter 2**, we first investigated the effects of reduced cytoprotection by the absence of HO-2 expression on embryonic growth and development, and palatogenesis, using wt and HO-2 KO mice (**Research question 1**).

Fetal abortions were found in both wt and HO-2 KO mice. Within the group of in total 23 HO-2 KO fetuses we only found one minor, and one severe congenital malformation. The other HO-2 KO fetuses demonstrated normal morphology, but those fetuses demonstrated significant growth restriction. We showed in the offspring of HO-2 KO mice a one-day growth delay at E15 compared to the offspring of E15 wt mice.

One HO-2 KO fetus of E16 had a severe malformed head and body and demonstrated a very reduced weight. No malformations or craniofacial anomalies were found in the wt fetuses. We showed that HO-2 abrogation is associated with growth restriction and congenital malformations (**Figure 1**). Most fetuses developed normally in the absence of HO-2, possibly due the fact that the isozyme HO-1 was taking over some of HO-2 functioning.

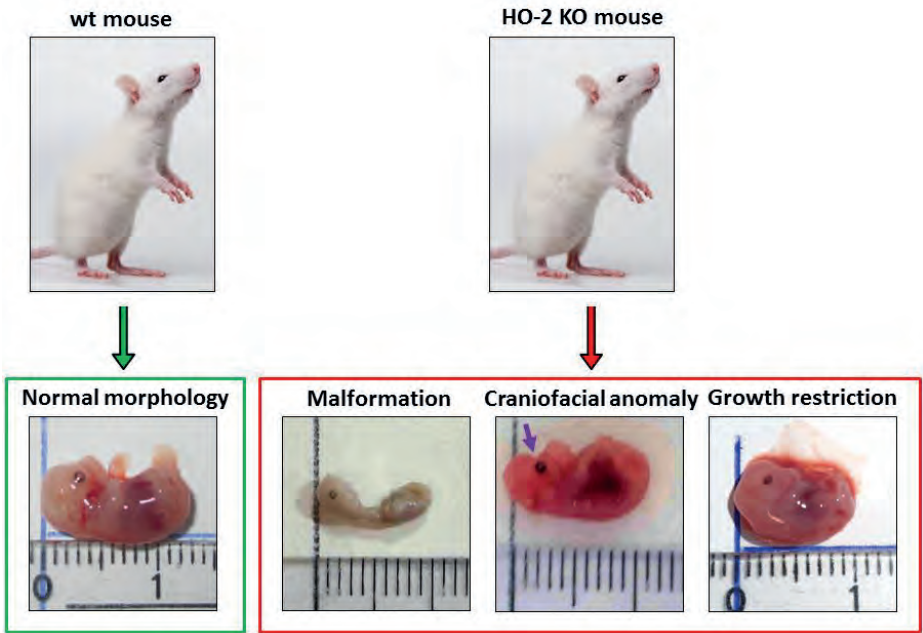


Figure 1: HO-2 abrogation increased the risk of congenital malformations in mice. No malformations or craniofacial anomalies were found in the wt fetuses. Abrogation of the HO-2 gene may cause malformations, craniofacial anomalies (purple arrow) and growth restriction. However, most HO-2 KO fetuses demonstrated no congenital malformations.

The number of experimental studies on the role of HO-2 expression in fetal development is only limited. In pregnant rats HO-2 mRNA levels in the uterus were detected during pregnancy, but peaked at E16³⁹. Decreased HO-2 protein expression at the fetomaternal interface of abortion-prone DBA/2-mated CBA/J mice at E14 was found⁴⁰. Additionally, lower placental HO-2 mRNA levels at E13 were measured in CBA/J mice exposed to ultrasound stress during early gestation, and after i.p. injection of recombinant murine IL-12, leading to placental necrosis and foetal rejection⁴¹.

In humans, several studies assessed the expression of HO-2 in placentas of healthy and pathological pregnancies. In the myometrium a 15-fold increase of HO-2 expression was found in pregnant women versus non-pregnant⁴². HO-2 expression has been localized throughout the human placenta, indicating a potential role in placental development and function⁴³. In human placenta, HO-2 mRNA levels were higher than

the HO-1 mRNA levels⁴⁴. Reduced endothelial HO-2 expression has been observed in human pregnancies complicated by preeclampsia and fetal growth restriction compared with control third-trimester pregnancies⁹. Furthermore, placentas from smokers demonstrated increased HO-2 expression compared to nonsmokers⁴⁵. Inhibited invasion of cultured human trophoblast following administration of HO-2 antibodies or HO inhibitor protoporphyrin-9 *in vitro* has been observed⁴⁶. These studies thus showed that reduced placental HO-2 expression is related to pregnancy complications as preeclampsia, abortion, and fetal growth restriction.

Section 2. Diminished cytoprotection by inhibition of HO-activity in mice aggravates heme-induced abortion and placental inflammation

2.1 Decreased HO-activity from E11 in mice is not causing congenital malformation or abortion

In **Chapters 3 and 4**, we further investigated the effect of reduced cytoprotection on embryonic growth and development, by inhibiting the activity of both HO-1 and HO-2 isozymes from day E11 using SnMP (**Research question 2**).

Interestingly, in the pregnant CD1 mice no increase in the abortion rate nor malformations following SnMP administration were found compared to the controls. Surprisingly, SnMP administration even significantly increased the fetal body size measured at E16. We thus showed that blocking of HO-activity in the period between day E11 and E16 did not increase the risk of congenital malformations in the absence of stressors (**Figure 2**).

Also, the timing of inhibition of HO-activity during pregnancy seems therefore important. When HO-activity is already reduced following fertilization, as in HO-2 KO mice, it may have larger disturbing effects on the oocyte implantation and embryonic development. By targeting HO-activity at E11, it was possible to exclude the effects on implantation, and to focus especially on craniofacial development.

The relation between HO-1 deficiency and embryonic development has not been studied extensively. In wt mice, HO-1 is overexpressed in the ovaries whilst HO-1-deficient mice show deficient ovulation⁴⁷. HO-1 KO mice demonstrated a very low birth rate in the offspring, mainly due to intrauterine abortions⁴⁸. HO-1^{+/-} mice also demonstrated a significantly lower birth rate compared to wt mice⁴⁹. Both HO-1 KO and HO-1^{+/-} mice exhibit a prolonged time for blastocyst attachment versus wt mice⁵⁰. Furthermore, HO-1 KO and HO-1^{+/-} mice implantations demonstrated intrauterine growth restriction^{51,52}. In HO-1 KO mice, lacking HO expression from E0, more than 80% of their fetuses die *in utero*⁵⁰. We considered HO-1 KO mice therefore not suitable for our experiments because of their very low birth rate.

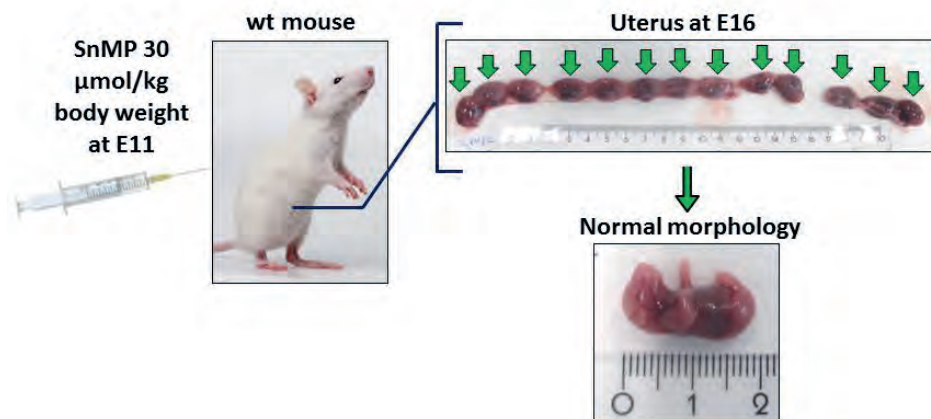


Figure 2: Absence of HO-activity from E11 did not result in increased risk of congenital malformations or abortion. HO-activity was inhibited by administration of SnMP 30 $\mu\text{mol/kg}$ body weight by i.p. injection at E11. The uterus contained viable fetuses (green arrow). No congenital malformations were observed following SnMP administration at E16. SnMP administration even increased the fetal body size measured at E16

A microsatellite polymorphism of the HO-1 gene, leading to lower levels of HO-1 expression, is associated with idiopathic recurrent miscarriage in humans⁵³. It has been hypothesized that low HO-1 levels could possibly lead to elevated concentrations of free heme⁵⁴.

Administration of SnMP (30 $\mu\text{mol/kg}$) to pregnant mice at E12.5 in Friend leukemia virus B (FVB) inbred mice did not result in fetal loss at E14.5⁵⁵. Another study demonstrated that blocking HO-activity with zinc protoporphyrin (ZnPPiX) (40 mg/kg), injected at days E0, E3 and E6, increased the abortion rate from 0% to 33% in CBA/J \times BALB/c mouse fetuses at E14⁵⁶. Furthermore, they demonstrated that this ZnPPiX treatment boosted the abortion rate from 22% to 50% in abortion-prone CBA/J \times DBA/2J fetuses at E14⁵⁶. Others found that in abortion-prone CBA/J \times DBA/2J fetuses, inhibition of HO-activity by ZnPPiX (40 mg/kg) at day E4 increased HO-1 expression in giant cells, and HO-2 expression in giant cells, spongiotrophoblasts and labyrinthic cells in placenta E14, and increased the abortion rate at day E14⁵⁴. HO induction in these cells was considered as a feedback mechanism due to inhibition of HO-activity⁵⁴.

Interestingly, pharmacological blocking of HO-activity by SnMP administration has been successfully used for decades to prevent neonatal hyperbilirubinemia in humans⁵⁷⁻⁵⁹. In newborn mice, after intragastric injections of heme in dose 30 $\mu\text{mol/kg}$ at day 1, the increased HO-activity returned to control levels in the liver following

ZnPPIX (30 $\mu\text{mol/kg}$) at day 4⁶⁰. In *Ugt1*^{-/-} mice bilirubin-induced neonatal lethality at E20, caused by deletion of UDP-glucuronosyltransferase 1A1 (*Ugt1*), was rescued by HO-activity inhibition (ZnPPIX 100 $\mu\text{mol/kg}$) at day 2 through 7, 9, 11 and 13⁶¹. In rats, through measurements of hepatic and splenic serum bilirubin levels blocking of HO-1, obtained by i.p. injection of ZnPPIX (40 $\mu\text{mol/kg}$), lasted for less than 1 week⁶². We did not find an increased abortion rate following blocking of HO-activity from day E11. Others found that blocking HO-activity at day E0, E4, E3 and E6 resulted in increased abortion rate⁵⁶.

Our findings demonstrate that HO-activity, in the absence of stressors, seems more crucial during implantation compared to fetal development at a later stage. Moreover, the lack of fetal abortion or congenital malformations following HO-activity inhibition from E11 may be related to the absence of inflammatory or oxidative stressors.

The importance of having a firefighter squad is especially noted in the presence but not the absence of a pyromaniac. In analogy to this: in the absence of injurious stressors the significance of cytoprotective enzyme systems may be underestimated. Therefore, we next analyzed the role of cytoprotective mechanisms in the presence or absence of alarmins.

2.2 HO-activity rescues mouse fetuses from heme-induced abortion

In **Chapter 4**, we studied the effect of dose-dependent exposure to oxidative and inflammatory stress, generated by administration of the alarmin heme at E12 (30, 75 or 150 $\mu\text{mol/kg}$).

Moreover, the effects of heme (30 and 75 $\mu\text{mol/kg}$) combined with the inhibition of HO-activity at fetal development was investigated. The activity of both isozymes of the HO system, HO-1 and HO-2, activity was blocked from E11 by SnMP (30 $\mu\text{mol/kg}$) (**Research question 2**).

Our results showed that i.p. injection of heme 30 $\mu\text{mol/kg}$ or SnMP, or the combination of heme 30 $\mu\text{mol/kg}$ with SnMP did not increase the risk of abortion. Apparently, application of low levels of heme to the mother, in the presence or absence of HO-activity, did not lead to oxidative and inflammatory stress levels provoking abortion. Cytoprotective mechanisms can thus handle this amount of heme.

On the other hand, oxidative and inflammatory stress levels generated by administration of heme 75 $\mu\text{mol/kg}$ certainly affected fetal development since half of the fetuses at E16 were resorbed (**Figure 3**). Administration of heme 150 $\mu\text{mol/kg}$ resulted in complete fetal abortion.

Moreover, administration of heme 75 $\mu\text{mol/kg}$ following HO-activity inhibition resulted in complete fetal abortion at E16, indicating that high oxidative and inflammatory stress levels completely disturbed fetal development. Under higher stress levels, HO-activity seems to be crucial for fetal survival (**Figure 3**).

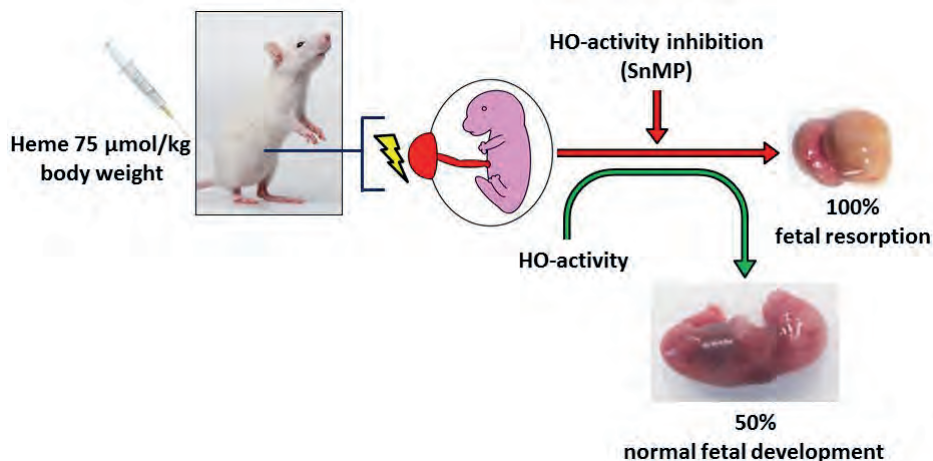


Figure 3: HO-activity rescued mouse fetuses from heme-induced abortion. Administration of heme 75 μmol/kg body weight by i.p. injection in pregnant mice at E12 following inhibition of HO-activity at E11 by SnMP administration resulted in complete fetal abortion. Administration of heme 75 μmol/kg body weight resulted in abortion in half of the fetuses.

2.3 Defense mechanisms against free heme molecules

Harmful effects of heme exposure have also been found in humans since uterine hematomas are associated with increased risk of intrauterine growth restriction, preterm delivery, and miscarriage⁶³⁻⁶⁶. Intrauterine hemorrhage and hematoma is associated with an increased risk of early and late pregnancy loss⁶⁷. The volume, location, gestational age, duration of hemorrhage and hematoma and the presence of vaginal bleeding determine the ultimate pregnancy outcome⁶⁸⁻⁷⁰. During hemorrhage, erythrocyte rupture leads to hemoglobin release into the circulation⁷¹. After release into plasma free hemoglobin can be captured by the acute-phase protein haptoglobin⁷². However, in the extracellular space, unbound hemoglobin undergoes different oxidation stages resulting in the release of free heme molecules⁷³. To protect against the adverse effects of free heme, free heme molecules are scavenged by hemopexin (HPX)⁷³, an acute-phase plasma glycoprotein, mainly produced by the liver and released into plasma^{74,75}. One molecule of HPX binds to one molecule of heme⁷⁶. To obtain circulating free heme molecules the amount of administered free heme must exceed the amount of HPX, otherwise all free heme will be bound (**Figure 4**). The heme molecules, unbound or bound by HPX, are then available for degradation by the HO-system. In wt mice, circulating levels of hemopexin are very high (0.5–1.2 g/L), thus providing considerable protection against free heme⁷⁵. After heme administration (3.5 μmol/kg and 17.5 μmol/kg) no depletion of plasma levels of HPX was found in wt mice⁷⁷. However, injection of 35 μmol/kg of heme in wt mice resulted in almost complete depletion of HPX in the plasma 6 h after injection⁷⁷. Heme administered in dose 35 μmol/kg or 70 μmol/kg by injection into the tail vein in 8 to 12 weeks old wt mice caused a strong reduction of plasma HPX level in wild-type mice 6 hours after injection⁷⁸. In

another study, heme injected in the tail vein in C57BL/6J mice in dose 50 and 120 $\mu\text{mol/kg}$ body weight resulted in cardiac and plasma IL-6 expression⁷⁹. Importantly, in these studies, heme was injected only in not pregnant mice, and its effect at fetal development was not studied. It was shown that administration of heme in dose 35 $\mu\text{mol/kg}$ depleted HPX, and higher doses, 50 and 120 $\mu\text{mol/kg}$, provoked an inflammatory response, demonstrated by cardiac IL-6 expression⁷⁹. These data indicate that heme administration up to 35 $\mu\text{mol/kg}$ gets almost fully scavenged by HPX, and only heme in higher dose exceeds the HPX levels, leading to circulating free heme molecules in mice.

Our study demonstrated that mimicking intrauterine hemorrhage/hematoma by administration of heme at day E12 in pregnant mice, causes fetal abortion in a dose-dependent fashion. No experiments were previously performed to study the effects of heme administration in different doses in pregnant mice to study the embryonic development in the second trimester. Therefore, we were not able to compare our results of heme administration at fetal abortion with other studies.

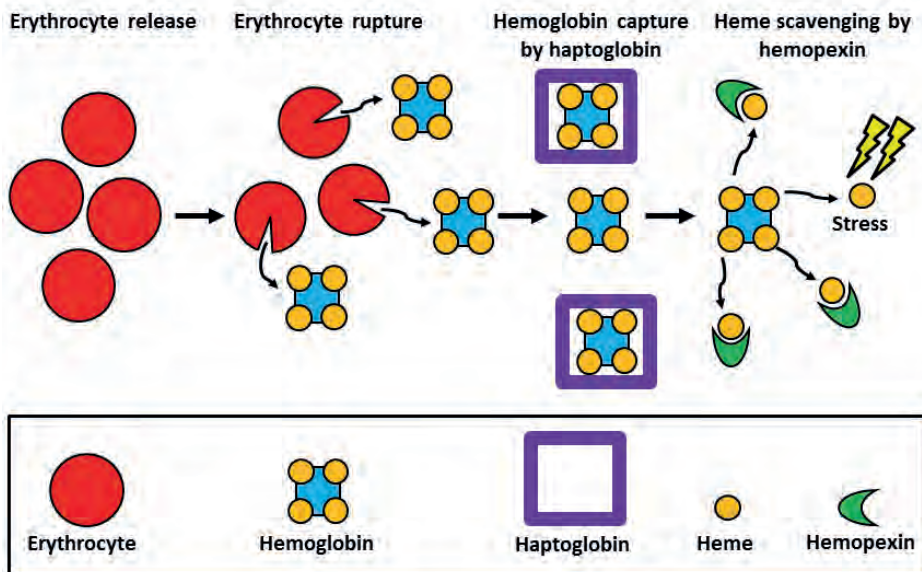


Figure 4: Erythrocyte breakdown can lead to stress inducing free heme release despite hemoglobin and heme scavenging. Following hemorrhage, erythrocyte rupture leads to the release of free hemoglobin. Free hemoglobin can be captured by haptoglobin, but oxidation of unbound hemoglobin molecules can lead to free heme molecule release. Free heme molecules can be scavenged by hemopexin (HPX). Heme molecules, unbound or bound by HPX, can be broken down by the HO system. When not all free heme is broken down these circulating molecules generate oxidative and inflammatory stress. The amount of oxidative and inflammatory stress strongly depends on the dose of free heme molecules.

2.4 HO-1 induction as a potential therapeutic strategy to prevent abortion

Another explanation for the fact that administration of heme 30 $\mu\text{mol/kg}$ did not disturb fetal development is that low heme and iron levels may have induced HO-1 with beneficiary effects at fetal development. The relation between hemoglobin levels and fetal survival has been studied in humans and mice. During pregnancy the need for iron increases substantially in the mother and her fetus⁸⁰. Anemia is characterized by reduced hemoglobin (Hb) ($\text{Hb} < 10 \text{ g/dl}$), the iron-bearing protein in red blood cells⁸⁰. Anemia is associated with increased risk of low birth weight in humans ($< 2500 \text{ g}$)⁸⁰. Chinese mothers supplemented with iron-folic acid demonstrated lower neonatal mortality compared to mothers supplemented with only folic acid⁸¹. Furthermore, Nepalese mothers supplemented with iron-folic acid showed lower neonatal and perinatal mortality compared with mothers who received micronutrients only⁸². Pregnant mice receiving an iron-deficient diet demonstrated a higher abortion rate, but also a reduced fetal growth⁸³. Evaluation of data from several cohort studies indicates a U-shaped association between hemoglobin levels and adverse perinatal outcomes⁸⁴. Seemingly, too low as well as too high hemoglobin, heme or iron levels can thus harm fetal development in humans.

Induction of HO-1 could be a therapeutic strategy against inflammatory and oxidative insults. Curcumin is generally known as a spice used in the Indian kitchen^{85,86}. In renal proximal tubule cells curcumin induces HO-1 *in vitro*⁸⁷. Curcumin induced HO-1 expression in human skin fibroblasts *in vitro*⁸⁸. Curcumin was found to decrease H_2O_2 -induced apoptosis in H9c2 cardiomyoblasts by upregulation of HO-1 *in vitro*⁸⁹. Curcumin has anti-inflammatory, anti-oxidant, antitoxicant, neuroprotective, immunomodulatory, anti-apoptotic, anti-angiogenic, antihypertensive, and antidiabetic properties⁹⁰. Curcumin stimulates expression of nuclear factor erythroid 2-related factor 2 (Nrf2) and increases HO-1 expression in a concentration- and time-dependent manner⁹¹. However, curcumin is extensively bio-transformed into its water-soluble metabolites, glucuronides, and sulfates, making that only a small portion of substance is absorbed and bioavailable⁹².

Administration to developing chicken fetuses of “sunset yellow” and “tartrazine”, two food coloring agents, resulted in embryotoxicity and morphological malformations in feather, head, and limbs, and resulted in reduced weight and length. However, administration of curcumin by injection *in ovo* reversed these adverse effects⁹³. Curcumin (10 $\mu\text{mol/L}$) reduces also high glucose-induced neural tube defects formation in E8.5 mouse fetuses by blocking cellular stress and caspase activation, suggesting that curcumin supplements could reduce the negative effects of diabetes⁹⁴. Curcumin has demonstrated beneficial effects, as amyloid β -binding, tau inhibition, metal chelation, neurogenesis, synaptogenesis, and antioxidant and anti-inflammatory effects on brain health⁹⁵. Notably, curcumin inhibited the expression of pro-inflammatory factors and macrophage infiltration in placenta, and ameliorated LPS-

induced adverse pregnancy outcomes in mice by inhibiting inflammation⁹⁶. Furthermore, administration of curcumin of 100 mg/kg through abdominal cavity injection in mice reduced LPS-induced placental inflammation⁹⁷. Curcumin administration thus inhibits placental inflammatory stress, promoting the healthy pregnancy outcome in mice. HO induction, possibly by curcumin administration, may could be a therapeutic strategy to prevent fetal abortion. It is tempting to speculate that the presence of HO-activity inhibitors would abrogate the curcumin-induced protection against birth defects by high glucose, diabetes, or food coloring agents.

By contrast, in other experiments harmful effects of curcumin on embryo development in the early stages of pregnancy were observed. Curcumin 10–40 μM in drinking water for 4 days significantly reduced oocyte maturation, fertilization, and embryonic development *in vitro*⁹⁸. They also found that consumption of drinking water containing 40 μM curcumin led to decreased oocyte maturation in mice *in vivo*⁹⁸. Curcumin disturbed embryonic development in the early stages of pregnancy in zebrafish⁹⁹. After incubation in medium containing with curcumin in dose 6, 12 or 24 μM for 24 hours, only mouse blastocysts treated with 24 μM curcumin displayed increased apoptosis and decreased total cell number *in vitro*¹⁰⁰. They further showed that treatment with 24 μM curcumin was associated with decreased implantation rate and increased resorption of post-implantation embryos in mouse uterus *in vivo*¹⁰⁰. On the contrary, others found no affected reproduction after administration of low, medium, and high dose curcumin mixed in the experimental diet of pregnant rats¹⁰¹. Thus, curcumin not only has beneficiary effects, but can also disturb fetal development. More research should be performed on the dose-response relation before curcumin can be used as a safe therapy in humans.

As mentioned earlier, blocking HO-activity by SnMP followed by heme (75 $\mu\text{mol/kg}$) administration in our study resulted in abortion of all fetuses. However, administration of 75 $\mu\text{mol/kg}$ heme led to fetal loss in half of the fetuses, showing that HO-activity rescues from heme-induced abortion (**Figure 3**). Interestingly, other studies found that administration low dose (50 ppm) exposure to CO, a product of heme degradation by HO-activity, during gestation day E3–E8 rescued from growth restriction and fetal abortion in HO-1 KO mice mothers⁵⁰. In *Hmox1*^{+/-} mice application of CO prevented intrauterine growth restriction by improving spiral arteries remodeling, and normalization of the blood pressure⁵¹. The design of our experiment in **Chapter 4** was successful in demonstrating the dose-dependent relation in pregnant mice between heme administration and the occurrence of fetal abortion. Notably, the cytoprotective HO-system thus rescued mouse fetuses from heme-induced abortion.

2.5 HO-activity inhibition in mice increases the placental weight

In **Chapter 2** we showed that HO-2 abrogation in mice caused fetal growth restriction. But, in **Chapter 3 and 4** blocking of isozymes HO-1 and HO-2 from day E11 increased

the fetal weight in mice (**Research question 2**). In **Chapter 4** administration of heme 75 $\mu\text{mol/kg}$ at day E12 in pregnant mice also increased the fetal weight. Depending on the dose free heme can thus have beneficiary effects at fetal growth in mice, possibly by strong HO-1 induction. Interestingly, in **Chapter 4** blocking of isozymes HO-1 and HO-2 from day E11 by SnMP increased the fetal and placental weight in mice (**Figure 5**).

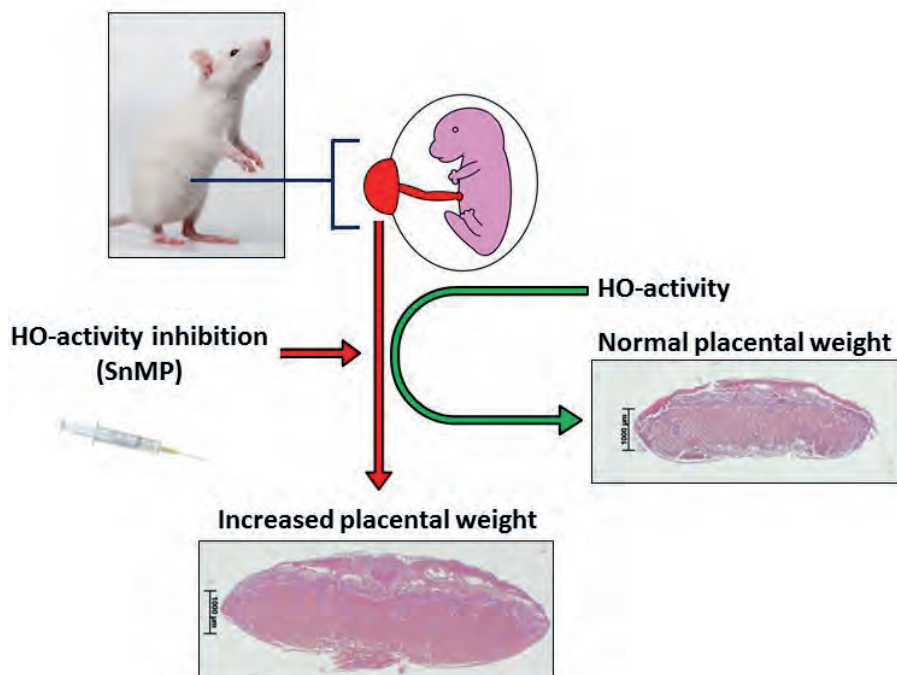


Figure 5: HO-activity inhibition increased the placental weight. Representative HE stained coronal sections through the middle part of the placenta of the control and SnMP group are shown. The placentas at E16 were heavier following administration of SnMP by i.p. injection at E11.

Although to a lesser extent, increased placental weight was also found after administration of the combination heme 30 $\mu\text{mol/kg}$ with SnMP. In the aborted fetuses the placenta was also resorbed. Therefore, we were only able to examine placentas of the viable fetuses.

2.6 HO-activity rescues mouse fetuses from heme-induced placental inflammation

We studied fetal development in relation to placental function (**Chapter 4**). By performing immunostainings, we searched for markers of inflammation within the placenta following administration of heme 30 and 75 $\mu\text{mol/kg}$, and SnMP, and the combination heme 30 $\mu\text{mol/kg}$ with SnMP. We showed that administration of heme 30 $\mu\text{mol/kg}$ did not increase the expression levels of adhesion molecule ICAM-1 or the influx of macrophages and HO-1 positive cells in placenta. However, administration of

heme 30 $\mu\text{mol/kg}$ body weight with SnMP increased the expression levels of adhesion molecule ICAM-1, together with increased numbers of macrophages and HO-1 positive cells in placenta. Our findings indicated that HO-activity rescued mouse fetuses from heme-induced placental inflammation (**Figure 6**). Administration of heme 75 $\mu\text{mol/kg}$ by i.p. injection increased the expression levels of vascular ICAM-1, together with increased numbers of macrophages and HO-1 positive cells in placenta. These findings indicate an influx of macrophages is triggered by heme-induced oxidative and inflammatory stress. Our experiments thus demonstrated a dose-dependent effect of heme administration on placental inflammation.

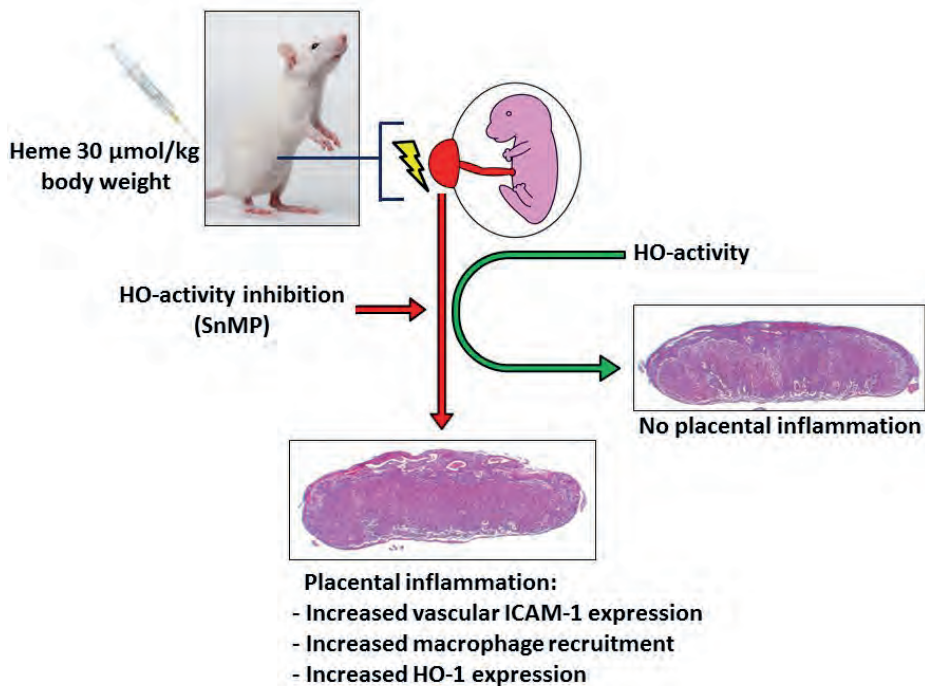


Figure 6: HO-activity rescued mouse fetuses from placental inflammation following administration of heme 30 $\mu\text{mol/kg}$ body weight. Administration of heme 30 $\mu\text{mol/kg}$ body weight in pregnant mice by i.p. injection at E12 following inhibition of HO-activity by SnMP administration by i.p. injection at E11 resulted in placental inflammation, characterized by increased ICAM-1 expression and increased macrophage recruitment. Following heme 30 $\mu\text{mol/kg}$ body weight administration HO-1 expression was upregulated, but HO-activity was directly inhibited by SnMP. Administration of heme 30 $\mu\text{mol/kg}$ body weight in the presence of HO-activity was not found to result in placental inflammation.

2.7 ICAM-1 expression and macrophage influx mediate placental inflammation and pathological pregnancy

Placental inflammation in uncomplicated human gestations is only observed in 4% of the cases¹⁰². Increased ICAM-1 expression has been detected in placenta from preeclampsia patients^{103,104}. Preeclampsia, characterized by new-onset hypertension

and proteinuria, can rapidly progress to serious complications, as death of both mother and fetus¹⁰⁵. The incidence of preeclampsia ranges from 3-7%¹⁰⁶. Preeclampsia causes approximately 14% of all pregnancy-related maternal deaths, and 15% of premature births worldwide¹⁰⁷. In spontaneous human abortion, occurring within the first 12 weeks of the pregnancy, increased influx of pro-inflammatory M1 macrophages in the decidual stroma of placenta has been observed^{108,109}. In women suffering from morbidly adherent placenta, an abnormal adherence of the placenta to the myometrium, massive hemorrhage can occur causing severe morbidity and mortality¹¹⁰. Furthermore, in morbidly adherent placenta increased ICAM-1 expression has been found¹¹⁰. Increased ICAM-1 expression levels in maternal serum and amniotic fluid at 16 weeks' gestation is an early marker of intrauterine growth restriction¹¹¹. ICAM-1 expression in amniotic has been found to be a marker of preeclampsia¹¹¹. Raised serum levels of ICAM-1 were detected in preeclamptic patients¹¹². The relation between abortion and placental ICAM-1 expression has been demonstrated in different experimental studies in mice. In sound-stressed mice elevated ICAM-1 expression and macrophage numbers in placenta were causing increased risk of abortion¹¹³. Placental endothelial cells exposed to trophoblast debris from preeclamptic placentae showed increased ICAM-1 expression *in vitro*¹¹⁴. Interestingly, i.p. injection of monoclonal antibodies against ICAM-1 in mice decreased the abortion rate, corroborating that ICAM-1 actively promotes immunologically mediated abortion¹¹⁵.

Macrophages play essential roles in fetal tolerance, trophoblast invasion, and tissue and vascular remodeling¹¹⁶. Decidual macrophages appear to display homeostatic and tolerogenic properties in healthy pregnancies¹¹⁷. Macrophages are functionally subdivided into classically activated (M1) and alternatively activated (M2) subtypes based on their cytokine expression patterns¹¹⁸. However, there is a growing list of variations within or between the M1 and M2 macrophage subsets (e.g., M0, M1a, M1b, M1c, M2a, M2b, M2c, M2d, M3, M4, M5, Mha, and Mox) that have been worked out extensively in mice, but not yet in humans¹¹⁹. M1 macrophages have a pro-inflammatory phenotype with pathogen-killing abilities¹²⁰. M1 macrophages are involved in inflammatory responses by producing chemokines, as CXCL1, CXCL2, CXCL3, CXCL5, CXCL8, CXCL9, CXCL10 and pro-inflammatory cytokines, as TNF- α , IL-1, IL-6, IL-12¹²¹. Pathogenic LPS and tissue damage-induced interferon gamma (IFN- γ) and tumor necrosis factor- α (TNF- α) induce pro-inflammatory M1 macrophages¹²². Large numbers of M1 macrophages were observed in the decidua of placentas of spontaneous abortions¹²³. In pregnancies complicated by preeclampsia increased number of M1 macrophages were associated with poor placental development¹²⁴.

Monocytes from women with preeclampsia are polarized to the M1 macrophage phenotype, producing higher levels of pro-inflammatory cytokines¹²⁴. Hypoxic conditions, oxidative stress, and inflammation induce necrosis of trophoblasts¹²⁵. Macrophage-mediated apoptosis of extravillous trophoblasts has been

associated with preeclampsia¹²⁶. In pregnancy-induced hypertension elevated numbers of M1 macrophages in placenta were found¹²⁷. Furthermore, pregnancy-induced hypertension showed higher concentrations of TNF- α and IL-1 β , and expressed lower concentrations of IL-4, IL-10, and IL-13¹²⁷. M2 macrophages promote cell proliferation and tissue repair¹²⁰. Furthermore, M2 macrophages display an immunosuppressive phenotype¹²⁸. M2 macrophages produce anti-inflammatory cytokines, such as IL-10¹²¹. Once the placenta is developed, an M2 phenotype predominates, which prevents fetal rejection throughout the pregnancy¹¹⁶. During normal pregnancy, most of the decidual macrophages are characterized by an immunosuppressive phenotype with M2 polarization, supporting the notion that M2 macrophages play a major role in fetomaternal immune tolerance¹²⁹. The number of M2 macrophages was decreased in the decidua of preeclamptic women¹³⁰. In pregnancy-induced hypertension low numbers of M2 macrophages were found¹²⁷. Since circulating monocytes specifically infiltrate the placental decidua at the onset of pregnancy and develop into either macrophages or dendritic cells, the composition of peripheral blood monocytes may affect the development of decidual immune effectors¹³¹. Correcting the M1/M2 balance is a potential treatment that may be relevant in other states of hyperinflammation, such as complications of pregnancy¹³².

In our study administration of heme 30 $\mu\text{mol/kg}$ body weight with SnMP, and heme 75 $\mu\text{mol/kg}$ body weight in mice resulted in increased numbers of macrophages in the placenta (**Chapter 4**). Also in humans increased numbers of macrophages were detected in placentas of infants with growth restriction¹³³. Our unpublished data demonstrated increased numbers of inducible nitric oxide synthase (iNOS) positive cells in placenta following administration of heme 30 $\mu\text{mol/kg}$ body weight with SnMP, and heme 75 $\mu\text{mol/kg}$ body weight in mice. Notably, increased placental expression of iNOS is associated with inflammation and apoptosis in preeclampsia in mice¹³⁴, and iNOS expression in placental macrophages is linked to the M1 phenotype¹³⁵. Since we linked an influx of macrophages in the placenta with raised ICAM-1 levels and increased risk of fetal abortion, it is likely that most macrophages within the placenta following administration of SnMP + heme 30 $\mu\text{mol/kg}$ body weight and heme 75 $\mu\text{mol/kg}$ body weight belong to the M1 phenotype.

2.8 HO-1 induction polarizes macrophages to the anti-inflammatory M2 phenotype

Notably, several studies showed that HO-1-activity promotes the polarization of macrophages to the M2 phenotype. HO-1-overexpressing macrophages showed anti-inflammatory and cytoprotective abilities, indicating that HO-1 expression polarizes macrophages to the M2 phenotype¹³⁶. Administration of heme (15mg/kg) by i.p. injection in rat enhanced the anti-inflammatory macrophage M2 phenotype and suppressed the pro-inflammatory macrophage M1 phenotype in the liver and was associated with enhanced HO-1 expression¹³⁷. In Zucker diabetic fatty rats, i.p. injection

of heme (30 mg/kg) increased the HO-activity, which reduced the pro-inflammatory macrophage M1 phenotype, and enhanced the anti-inflammatory macrophage M2 phenotype in the heart¹³⁸. In diabetic mice increased numbers of macrophages were measured in stomach, and loss of HO-1 positive M2 macrophages was observed¹³⁹. Heme-hemopexin complexes were found to revert heme-induced pro-inflammatory activation of macrophages in a mouse model of sickle cell disease¹⁴⁰. Furthermore, low-density lipoprotein receptor-related protein 1 (LRP-1) activation in isolated macrophages from wild-type C57/Bl6 mice was found to promote the development of an anti-inflammatory M2 functional phenotype *in vitro*¹⁴¹. HO-1 induction was found to drive the phenotypic shift to M2 macrophages¹⁴². Induction of HO-1, possibly via activation of the LRP1 receptor by heme-hemopexin complexes, can thus generate an anti-inflammatory environment by shifting macrophages from the M1 to M2 phenotype, and heme administration in low dose has the potential to be a novel anti-inflammatory therapeutic strategy.

2.9 The role of placental HO-activity in pregnancy pathology

In **Chapter 4**, fetuses that survived administration of heme 75 $\mu\text{mol/kg}$ at day E12 demonstrated an increased fetal weight at E16 (**Research question 2**). However, HO-1 deficiency is associated with growth restriction in mice and humans¹⁴³⁻¹⁴⁵. HO-1 was found to promote placental vascular proliferation and cell growth¹⁴⁶. Increased HO-activity improves placental function, perhaps through the vasodilator effects of CO and the angiogenic effects of HO-1^{143,147}. By Ahmed et al., 2000 it is suggested that CO, one of the products of heme degradation by HO, induce placental blood vessel relaxation to generate cytoprotection¹⁴⁶. They also showed that heme reduced vascular tension by 61% in U46619-precontracted placental arteries in term placental villous explants *in vitro*¹⁴⁶. Furthermore, preincubation of placental vessels with HO inhibitor tin protoporphyrin IX (SnPP) prevented against heme-induced fall in tension in placental vessels *ex vivo*¹⁴⁶. In rats, increased HO-1 expression, obtained by i.p. injection of hHO-1 adenovirus at day E15, was found to improve placental function, possibly by the vasodilator effects of CO and the vasoproliferative effects of HO-1, and resulted in increased pup size at day 1 of life¹⁴³. They further showed that inhibition of HO-activity in rats by i.p. injection of zinc deuteroporphyrin IX 2,4 bis glycol at day E16 resulted in a significant decrease in pup size at day 1 of life¹⁴³. In pregnancy, a woman's total HO-activity level is increased compared with that of a non-pregnant woman⁵⁵. In the myometrium, both HO-1 and HO-2 were increased 15-fold in pregnant women versus nonpregnant⁴². Transcript levels of HO-1 are still highest in the placenta compared with other organs¹⁴⁷. HO-1 and HO-2 are spatially and temporally localized throughout the placenta and gestation, indicating its potential role in placenta functionality, proper placenta development and maintenance of healthy pregnancy^{43,148}. Using the rat and mouse as placental models, researchers have shown that HO-1 levels are largely

elevated at the time of placental vascular development¹⁴⁹. HO-1 and HO-2 expression was increased in placentas from smokers when compared to non-smokers⁴⁵. Exposure of pregnant mice to CO, administered in a sealed chamber throughout gestation, increased the uterine artery blood flow, possibly generated by HO-mediated vasodilation through CO¹⁵⁰. The administration of cobalt protoporphyrin (CoPP), an inducer of HO-1, reduces the mean arterial pressure in a rat model of placental ischemia¹⁵¹. HO-1 induction by CoPP at day E14 significantly decreased mean arterial pressure in inflammatory cytokine TNF- α -infused pregnant rats¹⁵². Pregnant mice exposed for 24 hours to sound, consisting of a 70-dB tone lasting 1-second long that was repeated 4 times per minute, on day E12.5 and E14.5 demonstrated reduced placental HO-1 expression levels at E16.5¹⁵³. CO 125 ppm administered in a sealed chamber in the period E3-E8 led to higher fetal and placental weights and avoided fetal death at E14¹⁵⁴. They further showed that CO administration further suppressed placental apoptosis and regulated placental angiogenesis¹⁵⁴. CO promoted vasodilatation and angiogenesis decreased the expression of inflammatory cytokines and suppressed apoptosis, stimulating placental function, leading to higher fetal and placental weights.

It is tempting to speculate that heme administration in higher levels than HPX can be degraded by the HO-system when sufficient HO enzymes are available, generating CO, promoting placental vasodilatation, angiogenesis, and fetal development. It is likely that in our experiment (**Chapter 4**) HO-1 induction within the placenta rescued mouse fetuses from heme-induced abortion and promoted fetal development.

Evidently, ICAM-1-mediated macrophage influx during placental inflammation is related to increased risk of fetal growth restriction and fetal abortion. We conclude that our study design was successful in demonstrating a direct relation between increased ICAM-1 expression, macrophage influx and fetal growth restriction following heme exposure in a dose-dependent manner in mice (**Chapter 4**).

We further showed that the absence of HO-activity is lethal in mouse fetuses when exposed to heme 75 μ mol/kg administration (**Figure 7**). In other studies it was already found that HO-activity was crucial for oocyte implantation⁵⁰, angiogenesis¹⁵⁵, and now also showed to protect against inflammatory insults¹⁵⁶. This supports that the HO-system is instrumental for facilitating reproduction. HO-derived CO release promotes placental vasodilatation and angiogenesis and suppresses placental inflammatory cytokine expression and apoptosis. In addition, CO and HO-1 overexpression may skew placental macrophages from the inflammatory M1 to the anti-inflammatory M2 phenotype.

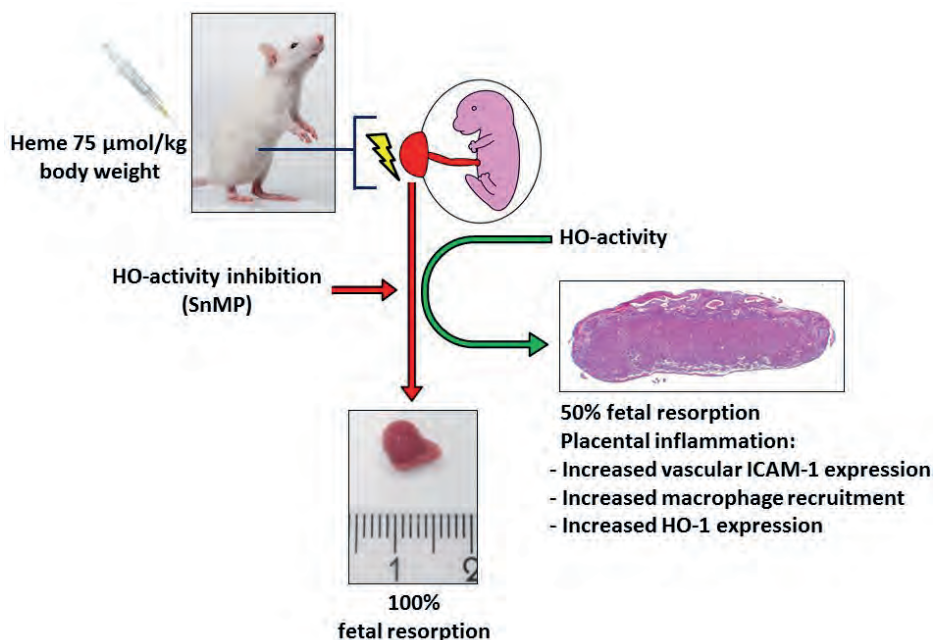


Figure 7: HO-activity rescued mouse fetuses from fetal resorption following administration of heme 75 $\mu\text{mol/kg}$ body weight. Administration of heme 75 $\mu\text{mol/kg}$ body weight in pregnant mice at E12 following inhibition of HO-activity at E11 by SnMP administration resulted in resorption of all fetuses and placentae. Administration of heme 75 $\mu\text{mol/kg}$ body weight was found to result in resorption of half of the fetuses and caused placental inflammation.

Section 3. Cytoprotective mechanisms and signaling pathways facilitate palatogenesis in mice

3.1 Palatal fusion in mice despite HO-2 abrogation, inhibition of HO-activity and/ or heme administration

The relation between environmental factors, pathological pregnancies and CLP formation has only been limited investigated in animal experimental studies. Interestingly, transgenic CL/Fr mice showed 15% to 40% spontaneously CLP development in the offspring, while exposure of the pregnant mouse mother to hypoxia from E10-E11 increased the incidence of CLP up to 81%¹⁵⁷. In A/J mice, having a spontaneous incidence of clefting of about 7%, exposure to hypoxia from E10-E11 doubled the incidence of CLP in the offspring¹⁵⁸. Since environmental factors as smoking¹⁵⁹, alcohol consumption¹⁶⁰, diabetes¹⁶¹, infections^{162,163}, folate acid deficiency^{162,163}, zinc deficiency^{162,163}, contact to teratogens^{162,163}, and bleeding episodes during pregnancy¹⁶⁴ are associated with increased risk for CLP, we postulated that exposure of the pregnant mother to oxidative and inflammatory stress is able to disturb the process of palatogenesis.

In **Chapter 2**, we demonstrated that reduced cytoprotection by HO-2 abrogation in HO-2 KO mice resulted in craniofacial dysmorphology in one fetus (**Research question 1**). Notably, most HO-2 KO fetuses did not show any congenital malformations. However, no difference in palatal adhesion, MES disintegration and palatal fusion was observed between the sections from wt and HO-2 KO fetuses at E15 (**Figure 8**). In **Chapter 3**, we found no difference in fetal development nor palatal fusion at E16 following reduced cytoprotection from E11, obtained by inhibiting both HO isozymes from day E11 by SnMP administration, compared to the controls (**Research question 2**). In **Chapter 4**, we found no differences in the fusion of the palatal shelves at E16 following administration of heme in dose 30 and 75 $\mu\text{mol/kg}$ body weight, and heme in dose 30 $\mu\text{mol/kg}$ body weight in the absence of HO-activity (**Research question 2**). Since all fetuses were resorbed after administration of heme 150 $\mu\text{mol/kg}$ body weight, and heme 75 $\mu\text{mol/kg}$ body weight in combination with SnMP, we were not able to study palatogenesis in these groups. It is speculating whether additional stressors could lead to hampered palatal fusion, or disturb placental function, leading to disrupted fetal development, or resulting in fetal resorption. It would be interesting to study effects of heme and/or SnMP administration on palatal fusion in mice that demonstrate spontaneous development, as the CLP CL/Fr mice¹⁵⁷ and A/J mice¹⁵⁸.

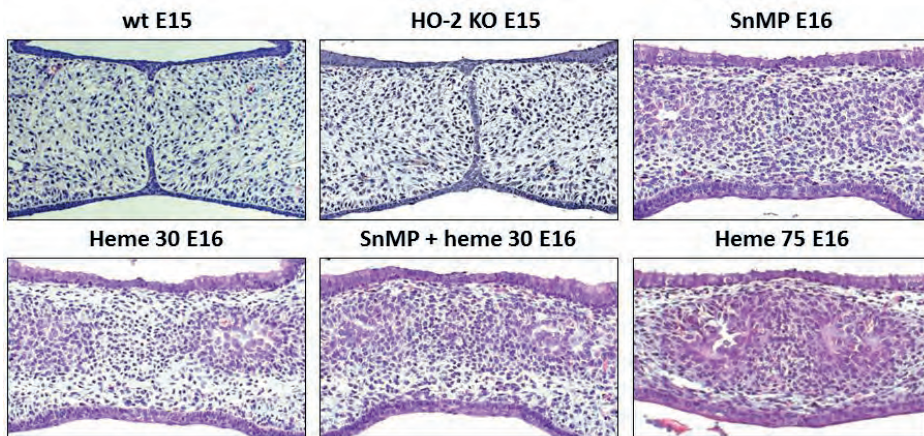


Figure 8: Palatal fusion despite HO-2 abrogation, inhibition of HO-activity and/ or heme administration. Representative HE stained coronal sections through the middle part of the secondary palate in mice per group are shown. Absence of HO-2 expression in HO-2 KO mice did not affect MES disintegration or palatal fusion at E15. HO-activity inhibition by administration of SnMP at E11 and/ or administration of heme 30 $\mu\text{mol/kg}$ body weight did not lead to disturbed palatal fusion at E16. The fetuses that survived administration of heme 75 $\mu\text{mol/kg}$ body weight did not demonstrate palatal fusion disruption.

3.2 Mechanisms of MES disintegration during palatal fusion

The main hypotheses underlying midline epithelial seam (MES) disintegration involve epithelial cell migration to the oral^{165,166}, or nasal epithelium^{166,167}, epithelial-to-mesenchymal transformation (EMT)¹⁶⁸, epithelial cell apoptosis¹⁶⁹, or a combination of

these events¹⁷⁰. In our study we detected for the first time Sox9 expression in the disintegrating MES during palatal fusion in mice¹⁷¹. Since Sox9 signaling was essential in the EMT mechanism of different cell types¹⁷²⁻¹⁷⁹, we postulate that Sox9 expression is involved in MES disintegration by EMT.

In addition, within the disintegrating MES we found multiple apoptotic DNA fragments, using DNA Fragment End Labeling (FragEL™), in wt and HO-2 KO fetuses at E15. Cleavage of nuclear DNA by cellular endonucleases is regarded as a characteristic of apoptosis¹⁸⁰. Multiple studies found that apoptotic cell death occurs within the medial edge epithelium (MEE) and the disintegrating MES, suggesting that the process of apoptosis is essential for palatal fusion. The external epithelial surface of the tips of the palatal shelves, MEE, is composed of an outer layer of flat periderm cells and an inner layer of basal cuboidal cells on a basement membrane^{181,182}. Periderm cells undergo apoptosis at shelf-shelf contact, facilitating palatal shelf adhesion¹⁸¹. Also others detected apoptosis in the palatal shelves of chicken, by using TUNEL staining, showing that apoptosis only occurred in the periderm of the MEE¹⁸³. Following palatal shelf adhesion, the MES must further disintegrate to allow mesenchymal confluence, necessary for palatal fusion^{184,185}. In multiple studies epithelial cell apoptosis has been observed within the disintegrating MES¹⁸⁶. Within the fusing palatal shelves of ICR mouse fetuses (Japan SLC, Shizuoka, Japan) apoptotic cell death was identified in the disintegrating MES, and in the oral and nasal epithelial triangles by labeling of DNA fragmentation using TUNEL staining¹⁸⁷. By labeling of the cells of the MEE with a retroviral vector carrying the *lacZ* gene, it was found that almost all cells of the MES underwent cell death and very few labeled cells were found in the mesenchyme compartment of cultured mouse palatal shelves *in vitro*¹⁸⁸. In palates from mouse fetuses of E16.5 stained with acridine orange, an indicator of cell death, apoptosis was detected within the disintegrating MES *in vivo*¹⁸⁹. They also showed that isolated cultured mouse palates exposed to pan-caspase inhibitor z-VAD did not fuse *in vitro*¹⁸⁹, which supports that caspase-induced apoptosis is required for palatal shelf fusion. Isolated E13.5 palatal shelves of wt mouse fetuses cultured for 4 days with blocking FasL antibody or z-VAD for 4 days resulted in lack of fusion of the palatal shelves, indicating that the FasL-Fas-caspase extrinsic apoptosis pathway is essential for palatal fusion¹⁹⁰. Furthermore, exposure to citral, an inhibitor of retinol dehydrogenase, reduced apoptosis within the MES, and resulted in non-fusion of cultured palate shelves *in vitro*¹⁸⁹. However, administration of retinoic acid (100 mg/kg) by i.p. injection at pregnant female mice at E14 resulted in increased cell death of the MEE, causing failed adhesion of the cultured palatal shelves *in vitro*¹⁸⁹. The findings of these studies indicate that apoptotic cell death is required for MES disintegration to allow palatal fusion.

On the contrary, others found that apoptotic cell death is not crucial in the process of palatal fusion. An argument against cell death as the major mechanism for

MES disintegration is that extensive cell death of the MES cells would weaken the fusion site, leading to non-fusion of the palatal shelves¹⁶⁹. Palatal shelves cultured at E13.5 of *Apaf1* knockout mice, deficient in caspase 3 activation, demonstrated complete palatal fusion without DNA fragmentation-mediated programmed cell death, indicating that apoptotic cell death is not essential for palate fusion *in vivo*¹⁶⁷. In cultured isolated palatal shelves of ICR mouse fetuses at E13 prevention of cell death, obtained by inhibition of caspases-1 and -3 by aurintricarboxylic acid, did not hamper palatal fusion¹⁹¹. They showed that in the absence of apoptotic cell death the MEE of opposing palatal shelves still adhere, and MES disintegration occurs, indicating that apoptosis is not necessary in mouse palatal fusion *in vitro*¹⁹¹. Notably, elevated oxidative stress levels, obtained by exposure to homocysteine (100 μ M), did not affect fusion of cultured murine palates *in vitro*¹⁹². In cultured human embryonic palatal mesenchymal cells folate deficiency elevated homocysteine levels and homocysteine-induced oxidative stress, resulting in dose-dependent apoptosis *in vitro*¹⁹². Moreover, others found that teratogenic effects of folate deficiency, obtained by treatment with the antifolate drug methotrexate, did not affect the fusion of cultured rabbit palatal shelves *in vitro*¹⁹³.

3.3 CXCL11-CXCR3 signaling is associated with macrophage recruitment during MES disintegration in mice

In **Chapter 2**, we demonstrated that multiple apoptotic DNA fragments were phagocytized by recruited CXCR3-positive F4/80-positive macrophages in the palatal shelves of wt and HO-2 KO mice. We also detected increased expression of chemokine CXCL11 within the MES (**Research question 3**). Based on our findings, CXCL11-CXCR3 signaling likely recruits CXCR3-positive macrophages to clean up the remnants of the disintegrating MES, further supporting that apoptotic cell death is involved in the process of MES disintegration.

Others also observed that F4/80-positive macrophages in fusing palatal shelves of mouse fetuses were detected near TUNEL stained DNA fragmentations¹⁹⁴. In fusing palatal shelves of rats, macrophages were observed near the epithelial cells of the disintegrating MES¹⁹⁵. Others found macrophages with phagocytosed remnants in their cells near the disintegrating MES in fusing palatal shelves of rats at E17¹⁹⁶. Moreover, in human fusing palates obtained by legal abortion macrophages were observed near the disintegrating MES¹⁹⁷. However, others found only few macrophages near the disintegrating MES of the human palate¹⁹⁸.

Only few studies demonstrated that CXCL11-CXCR3 chemokine-chemokine receptor signaling is involved in the recruitment of macrophages. In zebrafish, treatment with the CXCR3 antagonist NBI74330 attenuated the recruitment of macrophages to the site of infection¹⁹⁹. CXCL11-CXCR3 signaling made zebrafish more resistant to mycobacterial infection and macrophages were more motile²⁰⁰. In *M.*

tuberculosis-infected CXCR3 KO mice, decreased numbers of macrophages were observed in isolated tissue²⁰¹. Blocking of CXCR3 signaling by the CXCR3 antagonist TAK suppressed the infiltration of macrophages to a kidney graft in rats²⁰². Since CXCL11-CXCR3 signaling is involved in macrophage recruitment we hypothesized that CXCL11-CXCR3 signaling in the fusing palatal shelves recruits macrophages to clear the MES.

3.4 CXCL11-CXCR3 signaling is associated with epithelial cell migration during MES disintegration in mice

However, another hypothesis is that disappearance of the MES can be explained by epithelial cell migration to the oral^{165,166}, and/or nasal epithelium^{166,167}. Several studies have shown that CXCL11-CXCR3 signaling promotes epithelial cell migration. In CXCR3 KO mice impaired wound healing was observed with thick keratinized scar formation²⁰³. Cultured human primary epidermal keratinocytes were found to express receptor CXCR3²⁰⁴. In cultured human neonatal foreskin keratinocytes CXCL11 expression was observed²⁰⁵, and CXCL11 and CXCR3 expression were found to promote motility of cultured human neonatal foreskin epidermal keratinocytes *in vitro*²⁰⁶. Expression of CXCR3 on cultured keratinocytes isolated from human skin promoted re-epithelization in a wound-healing model *in vitro*²⁰⁷. In human keratinocyte HaCaT cells exposure to recombinant human parathyroid hormone inhibited CXCL11 expression, leading to inhibited cell proliferation²⁰⁸. Since expression of chemokine receptor CXCR3 and its ligand chemokine CXCL11 were both expressed within the MES, CXCL11-CXCR3 autocrine signaling may control migration of epithelial cells during MES disintegration. Besides the hypothesis that the MES disintegrates by apoptotic cell death, the increased CXCL11 and CXCR3 expression we found within the MES could also indicate that epithelial cell migration contributes to MES disintegration. Based on our findings we cannot rule out that CXCL11-CXCR3 signaling is involved in both macrophage recruitment to phagocytose the apoptotic remnants of the MES, and migration of epithelial cells of the MES.

3.5 Does HO-1 induction in recruited palatal macrophages compensate for the absence of HO-2 in mice?

In **Chapter 2**, we further showed that some macrophages express HO-1, and significantly more HO-1-positive cells were present in the palatal mesenchyme of HO-2 KO fetuses compared to wt fetuses, in which HO-1-positive cells were scarce.

We suggested that the higher HO-1 expression during embryonic development is a compensating mechanism for HO-2 deletion in recruited macrophages in the fusing palatal shelves. Others previously found that HO-2 KO macrophages showed hampered phagocytosis in a mouse corneal epithelial debridement model²⁰⁹. However, we demonstrated that the oral HO-2 KO macrophages were still able to phagocytose

apoptotic DNA fragments, possibly facilitated by HO-1 overexpression. We did not observe HO-1 expression within the disintegrating MES at E15.

HO-1 expression in macrophages appears to play an important role for the clearance of hemoglobin-haptoglobin and heme-hemopexin complexes²¹⁰. Hemoglobin-haptoglobin complexes are taken up by macrophages via a CD163-mediated receptor endocytosis-dependent mechanism²¹¹⁻²¹³. Heme-hemopexin complexes are taken up via LRP1 (Figure 9)²¹⁴.

HO-1 induction in HO-2 KO macrophages within the fusing palate

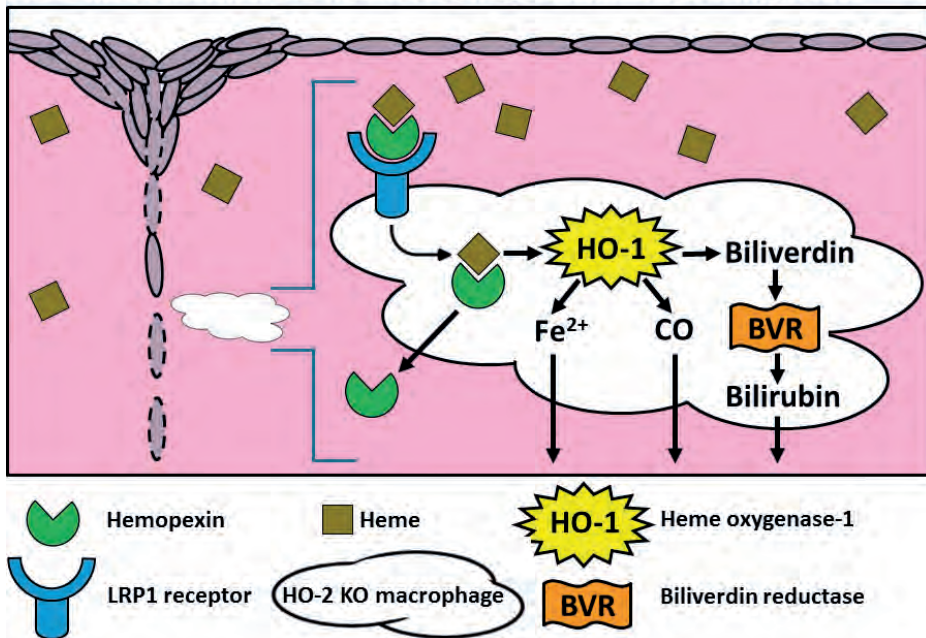


Figure 9: Hypothetical model: HO-1 induction is compensating for HO-2 deletion in macrophages. Within the fusing palatal shelves of HO-2 KO fetuses heme is scavenged by hemopexin (HPX) and endocytosed via LRP1 receptor by macrophages, and enzymatically degraded via HO-1 into free iron (Fe²⁺), and the protective molecules carbon monoxide (CO) and biliverdin. Intracellular Fe²⁺ promotes induction of the iron scavenger ferritin, leading to a net decrease in free iron and overall decrease in oxidant status. Biliverdin reductase (BVR) converts biliverdin into the antioxidant bilirubin. The products of heme degradation, generated by HO-1 and BVR, have anti-inflammatory properties and promote the anti-inflammatory macrophage M2 phenotype. This figure is not at anatomical scale.

Following cellular uptake by macrophages HPX-heme complexes are degraded by lysosomes²¹⁴. Hemopexin is not degraded after its uptake²¹⁵. Inside the macrophage the heme molecules are enzymatically degraded via HO-activity into the protective molecule CO, and Fe²⁺ and biliverdin²¹⁰. Biliverdin is swiftly converted into bilirubin via biliverdin reductase, which is a potent antioxidant molecule. The increase in intracellular Fe²⁺ promotes induction of the iron scavenger ferritin, leading to a net decrease in free iron and overall decrease in oxidant status^{216,217}. Notably, increased

expression of haptoglobin and HPX in liver and kidney was not sufficient to protect HO-1 KO mice against heme-induced toxicity²¹⁸. Heme scavenging by HPX reverts pro-inflammatory activation of macrophages by this molecule in a murine sickle cell disease model⁷⁴. Hemoglobin-haptoglobin complexes have been shown to induce an anti-inflammatory phenotype in macrophages²¹¹. Heme-mediated induction of HO-1 in macrophages provides beneficial effects in an experimental mouse model of pancreatitis²¹⁹. Heme-protein complexes may thus activate anti-inflammatory responses by inducing HO-activity²²⁰. In accordance with our results, it is tempting to speculate that in the HO-2 KO fetuses elevated levels of free heme got scavenged by HPX and endocytosed by macrophages, inducing HO-1 expression, promoting the anti-inflammatory macrophage M2 phenotype. Heme-induced HO-1 activity may improve the phagocytic ability of macrophages⁷³, which could promote the clearance of the disintegrating MES.

3.6 CXCL12-CXCR4 signaling is associated with palatal osteogenesis in mice

In the process of the orofacial region development, CNCCs migrate from the lateral ridges of the neural plate to the first branchial arch and act as stem cells to form the cartilage and bones of the maxilla, mandible, zygoma and the mastication muscles²²¹⁻²²⁵. Several studies demonstrated that defects in CNCC migration and proliferation can cause craniofacial malformations, including cleft palate. In Treacher Collins Syndrome Protein 1 (*Tcof1*) heterozygous mutant E7.5–E10.5 mouse fetuses deficient migration of CNCCs was observed, resulting in severe craniofacial malformations²²⁶. CXCL12-CXCR4 signaling is essential in the recruitment, localization, maintenance, development, and differentiation of progenitor stem cells of the musculoskeletal system²²⁷. Genetic knockout experiments revealed the vital role of CXCL12-CXCR4 signaling in fetal development. Mice deficient for CXCR4 die perinatally and display defects in the hematopoietic and nervous systems²²⁸. Mice lacking CXCL12 or CXCR4 demonstrated defective vascular development and die in utero²²⁹. Furthermore, mice lacking CXCL12 were found to have cardiac ventricular septal defect and die perinatally²³⁰.

In **Chapter 3**, we provided evidence that chemokine CXCL12, the ligand of receptor CXCR4, was overexpressed by the epithelial cells of the MES (**Research question 4**). However, we did not observe CXCR4 overexpression within the disintegrating MES. Only a few Sox9-CXCR4 double-positive stained cells were found near the remnants of the MES at E15 in both wt and HO-2 KO fetuses, suggesting that most CNCCs within the palatal shelves are already differentiated into other mesenchymal cell types before palatal fusion. We further found clusters of Sox9 expressing cells surrounding CXCR4-positive cells in the ALP-positive osteogenic centers in the central and lateral region of the palatal shelves at E15 and E16 in wt mice. In these osteogenic centers overexpression of chemokine CXCL12, the ligand of receptor

CXCR4, was observed. Since our results showed that Sox9 and CXCR4 do almost not have overlapping expression, we suggested that Sox9-positive cells are osteoblast progenitors, acting as stem cells, maintaining the osteoblast pool to drive osteogenesis. Both CXCL12 and CXCR4 would later be expressed by the mature osteoblasts. We hypothesized that chemokine CXCL12 by the MES possibly acts to activate osteoblasts progenitors to facilitate palatal bone formation (Figure 10).

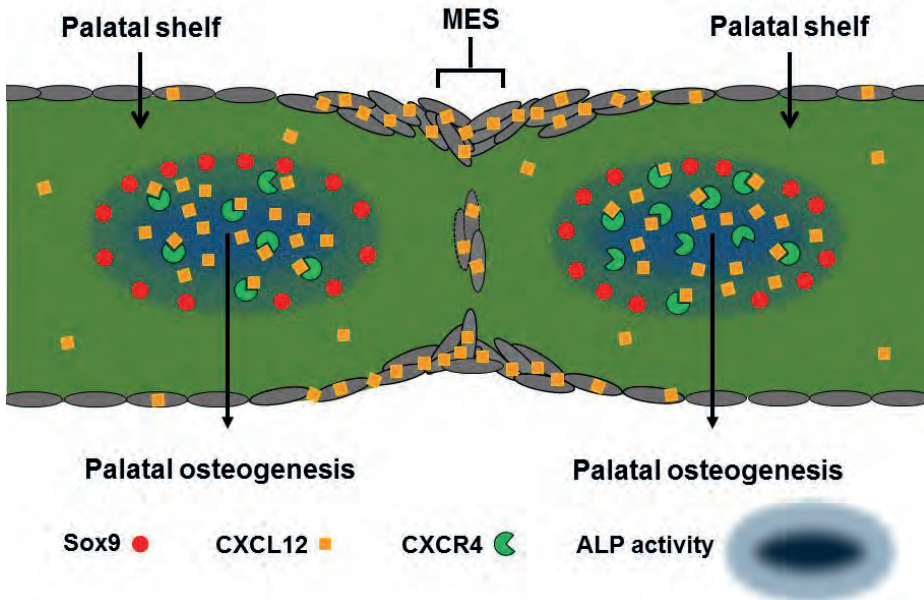


Figure 10: Hypothetical model: CXCL12-CXCR4 chemokine-receptor signaling is associated with palatal osteogenesis. We hypothesized that the CXCL12-CXCR4 interplay facilitates osteogenesis by promoting osteoblast maturation during palatal fusion in mice. Sox9 positive cells near the osteogenic centers were regarded as osteoblast progenitors.

Disturbed osteogenesis in fusing palatal shelves is associated with palatal clefting. Hh-Smo signaling negatively regulates Wnt/BMP pathways by upregulating antagonists, resulting in defective osteogenesis and cleft palate in mice²³¹. Splicing factor RNA Binding Fox-1 Homolog 2 (*Rbfox2*) is expressed in CNCCs, and deletion of *Rbfox2* in CNCCs leads to cleft palate and defects in craniofacial bone development²³². Persistent expression of Pax3 in CNCCs was found to disrupt bone morphogenetic protein (BMP)-induced osteogenesis, leading to ocular defects, malformation of the sphenoid bone, cleft palate and perinatal lethality in mice²³³. Notably, palatal clefting can also occur secondary by underdevelopment of the mandible, leading to failure of the tongue to descend, impeding the elevation of the palatal shelves, causing secondary palatal clefting. Conditional deletion of extracellular signal-regulated kinase 2 (ERK2) exhibited in *Wnt1-Cre;Erk2^{fl/fl}* mice mandibular micrognathia caused by osteogenic differentiation defects in CNCCs, leading to malpositioning of the tongue and thereby to cleft palate²³⁴. Bmp2 deletion in CNCCs using floxed Bmp2 and Wnt1-Cre alleles in

mouse fetuses of E14.5 demonstrated deficient mandibular size due to proliferation and differentiation defects, leading to posterior tongue displacement, blocking the adhesion of the palatal shelves, mimicking the Pierre Robin sequence in humans²³⁵.

Following chemotactic transmigration, immature MSCs must undergo osteogenic differentiation into osteoblasts for bone formation, and CXCL12 is important in this process²²⁷. Blocking of the CXCL12-CXCR4 signal axis in CXCR4^{flox/flox} homozygous mice impaired bone nodule mineralization, caused by inhibited BMP2-induced osteogenic differentiation of osteoblast progenitors²³⁶. Deletion of CXCL12 or CXCR4 in osteoprogenitor cells in mice shows decreased bone formation *in vivo*²³⁷. Furthermore, adding CXCL12 to cultured murine MSCs enhanced the BMP2-induced ALP-activity *in vitro*²³⁶. Administration of CXCL12 to osteogenic medium significantly increased expression of ALP in MSCs *in vitro*²³⁸. Local administration of AMD3100, a CXCL12-CXCR4 antagonist, inhibited new bone formation during bone regeneration in a rat distraction osteogenesis model²³⁹. Bone marrow-derived MSCs were found to express receptor CXCR4 together with its ligand chemokine CXCL12 and can thus act in an autocrine loop²⁴⁰. We earlier demonstrated CXCL11 expression within the disintegrating MES²⁴¹, suggesting that chemokine signaling is involved in the process of palatal fusion. Based on our data (**Chapter 3**) and others, we hypothesized that CXCL12 would be expressed within the disintegrating MES and palatal mesenchyme to activate and recruit osteoblasts progenitors to facilitate palatal bone formation. Simultaneous expression of CXCL12 and CXCR4 by the osteogenic centers possibly indicates that CXCL12-CXCR4 signaling might promote osteoblast maturation via an autocrine loop.

Section 4. Mechanical stress induces the cytoprotective enzyme HO-1 within the PDL in rats and in the dermis of splinted wounds in mice

4.1 Orthodontic forces induce the cytoprotective enzyme HO-1 within the PDL in rats

CLP patients demonstrate a higher prevalence of dental anomalies, including variations in tooth size, shape, number, structure and formation, and eruption timing compared to the general population^{242,243}. Studies have demonstrated that both genetics and the surgical repair of the palate influence the occurrence of dental anomalies in CLP patients²⁴⁴. Thereby, scarring following surgical cleft repair can interfere with the development of the dentition^{245,246}. Patients with CLP often require complex long-term orthodontic treatment in order to achieve a good facial appearance, with an esthetic, functional and stable occlusion²⁴⁷.

In **Chapter 4**, we studied expression of HO-1 in the mononuclear cells and osteoclasts within the PDL 6, 12, 72, 96, and 120 hours after orthodontic force application in rats (**Research question 5**). On immunohistochemical stained parasagittal

sections significant higher numbers of HO-1 positive mononuclear cells within the PDL at both the resorption- and apposition side were found 6 and 12 hours after orthodontic force application. However, HO-1 expression within the PDL dropped to control levels within 72 hours. Some osteoclasts were also HO-1 positive, but this induction was shown to be independent of time- and mechanical stress. We were the first to demonstrate that orthodontic force application strongly induces HO-1 expression in PDL cells *in vivo* (Figure 11).

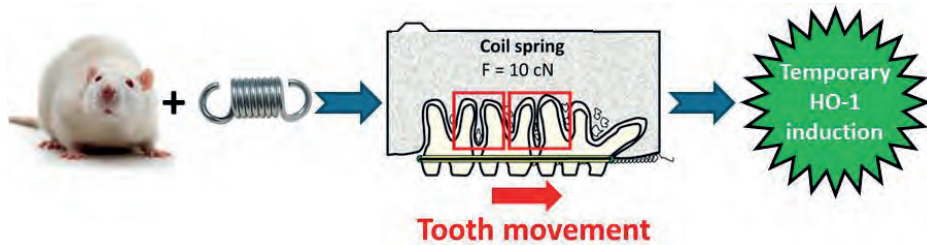


Figure 11: Orthodontic force application to the three maxillary molars in rats. By a Nickel-Titanium (Ni-Ti) 10 cN Santalloy® closing coil spring (GAC, New York, NY, USA) the block of three maxillary molars were moved mesially as one unit by a constant force via incisor anchorage. A constant low force per molar was applied to prevent tipping of the molars. Although the applied force was constant, the induction of HO-1 in mononuclear cells of the PDL was temporary since control expression levels of HO-1 in the PDL were found after 72 hours.

Several earlier studies have shown that inflammatory stress can induce HO-1 expression in PDL cells *in vitro*. LPS and nicotine increased the protein expression of HO-1 in human PDL cells²⁴⁸. In immortalized human PDL cells, treatment with LPS plus a combination of TNF α and IL-1 β increased HO-1 expression *in vitro*²⁴⁹. Notably, suppression of HO-1 expression in transiently transfected human PDL cells with HO-1 small interfering RNA (siRNA) before presentation of nicotine and LPS attenuated the expression of inflammatory and osteoclastogenic cytokines *in vitro*²⁵⁰. In cultured immortalized human PDL cells exposure to substance P, a neuropeptide that mediates bone metabolism, upregulated HO-1 expression²⁵¹ and induced osteogenic differentiation *in vitro*²⁵².

The link between mechanical stress and HO-1 expression in PDL cells had only been studied *in vitro*. In cultured human immortalized PDL cells enhanced HO-1 expression was observed following subsection of intermittent uniaxial mechanical strain *in vitro*²⁵³. Importantly, we showed in our orthodontic force model that HO-1 expression was only temporarily, because the numbers of HO-1 positive mononuclear cells in the PDL returned to control levels within 72 hours, while the constant orthodontic force was still applied. Interestingly, when orthodontic forces are interrupted with inactive periods strongly reduced root resorption has been observed in rats and dogs²⁵⁴. Possibly, renewal of HO-1 induction occurs during intermittent force application, contributing to decreased root resorption and hyalinization formation. We state that more *in vitro* and *in vivo* experiments are required to reveal the relation between mechanical stress, hyalinization, root resorption and HO-1 expression by the PDL.

In **Chapter 4**, we found within the PDL that both HO-1 positive and HO-1 negative osteoclasts were present at both the experimental- and control sides. Others found in an arthritis model in mice that induction of HO-1 in osteoclast precursors resulted in reduced osteoclast differentiation²⁵⁵. They also observed that most osteoclasts attaching to bone erosions in human joints from patients with rheumatoid arthritis were negative for HO-1²⁵⁵. It would be interesting to investigate if all osteoclasts within the PDL are active, and whether HO-1 expression may keep osteoclasts temporary inactive. These inactive osteoclasts can then later become active to replace osteoclasts which are at the end of their lifespan. HO-1 expression within the PDL following orthodontic force application has only been studied to a limited extend. More research is needed to develop better insight into the relation between HO-1 expression by osteoclasts and orthodontic tooth movement. Treatment with magnolol, an inducer of HO-1 expression, inhibited osteoclast differentiation of RAW 264.7 macrophages *in vitro*²⁵⁶. Treatment with heme strongly inhibited RANKL-induced osteoclastogenesis in cultured wild-type macrophages *in vitro*. However, heme administration was ineffective in inhibition of osteoclastogenesis in HO-1^{+/-} cells, suggesting that CO and/or bilirubin potentially inhibit RANKL-induced osteoclastogenesis²⁵⁷.

4.2 Splinting of excisional wounds in mice induces the cytoprotective enzyme HO-1 in the dermis

In **Chapter 5**, we described that splinting of excisional wounds in mice causes static mechanical stress (**Research question 5**). In mice, splinting inhibits wound contraction by the *musculus panniculus carnosus*²⁵⁸, while in humans, the *musculus panniculus carnosus* is considered of no functional significance²⁵⁹. In mice, splinting better simulates human wound healing that is mainly dependent on granulation and re-epithelialization of tissues²⁶⁰. Recently, inhibition of Engrailed-1 (En1) mediated mechanical signaling in skin wound of adult mice, by administration of chemical verteporfin, resulted in healing without scarring²⁶¹. Mechanical stress is also present in the healing palate of CLP patients following surgical palatal cleft closure. As reviewed in the general introduction, mechanical stress promotes scar formation^{245,262}, contributing to development of iatrogenic transverse narrowing of the maxilla²⁶³ and midfacial growth deficiency^{7,264}. In splinted wounds of day 7, we observed higher numbers of macrophages, myofibroblasts, increased levels of inflammatory genes, and more HO-1 gene expression within the dermis. Our findings indicate that mechanical stress by splinting promotes a pro-inflammatory microenvironment, increasing the risk of excessive scar formation. Notably, we found less HO-1 expression within the epidermis of the splinted wounds compared to the non-splinted wounds.

In non-splinted wounds from diabetic rats, treatment with 10% hemin ointment for 21 days upregulated HO-1, VEGF and ICAM-1 expression²⁶⁵, and promoted

wound repair²⁶⁵. Others found that administration of the HO-effector molecules CO and bilirubin enhanced excisional wound repair in rats²⁶⁶⁻²⁶⁸. Inhibition of HO-activity by tin protoporphyrin-IX resulted in retardation of wound closure in wild-type mice¹³. It was further shown that wound healing in HO-1 KO mice was delayed by complete suppression of re-epithelialisation¹³. Stimulation of keratinocyte proliferation acts via the HO-1/CO pathway *in vitro*²⁶⁹. Inhibition of HO-activity using SnMP injected intradermally in rats resulted in heme-induced influx of leukocytes in the wound area²⁷⁰. In HO-2 KO mice delayed cutaneous wound closure was observed compared to wt controls²⁷¹. Biliverdin application, 1 hour before and twice a day after epithelial injury, rescued HO-2 KO mice from chronic inflammation by accelerated wound closure and reduction of inflammatory cells and inflammatory proteins²⁷². Induction of HO-1 could thus be a novel strategy to reduce inflammation following mechanical stress after surgical cleft palate closure.

Section 5. Umbilical cord blood stem cells and HO-1 induction in tissue engineering may promote muscle and skin regeneration following surgical CLP repair

5.1 MSCs in tissue remodeling

A novel therapeutic approach is the administration of stem cells to create an anti-inflammatory environment. Mesenchymal stem cells (MSCs) can promote wound repair²⁷³⁻²⁷⁷ and regeneration due to attenuation of inflammation^{278,279}. MSCs are able to reduce inflammation by release of immunosuppressive and anti-inflammatory factors, such as TGF- β 1²⁸⁰, Interleukin 4 (IL-4)²⁸¹, and indoleamine 2,3-dioxygenase²⁸². MSCs have been shown to increase anti-inflammatory molecules interleukin 10 (IL-10) and interleukin-1 receptor antagonist (IL1-RA)²⁸³. Cultured human MSCs were found to suppress the proliferation of natural killer (NK) cells *in vitro*²⁸⁴. MSCs reduced the expression of CD83 in dendritic cells *in vitro*, indicating that dendritic cells skewed to a more immature status, likely limiting of antigen uptake, reducing the likelihood of graft rejection²⁸⁵. Cultured human MSCs were found to suppress the proliferation of T-cells *in vitro*, indicating that co-infusion of MSCs can decrease the incidence of graft-versus-host reactions, forming the basis for new strategies in clinical transplantation²⁸⁶.

In scratch assays, by leave a scratch in a confluent monolayer of cultured L929 fibroblasts and HaCaT keratinocytes of approximately 0.4–0.5 mm in width with a sterile pipette tip, administration of MSC-conditioned medium enhanced closure of the cell free area due to accelerated cell migration *in vitro*²⁸⁷. Oral ulcers induced by topical application of formocresol in the oral cavity of dogs demonstrated accelerated healing following submucosal injection of autologous MSCs²⁸⁸. Subcutaneous injection of MSC-conditioned medium increased the number of macrophages and endothelial progenitor

cells in splinted excisional wounds in mice²⁸⁹. MSCs have been shown to constitutively produce growth factors, as vascular endothelial growth factor (VEGF), hepatocyte growth factor (HGF), granulocyte colony-stimulating factor (G-CSF), granulocyte-macrophage colony stimulating factor (GM-CSF), resulting in improved wound healing²⁹⁰. Injected MSCs were able to alleviate cutaneous tissue fibrosis following subcutaneous injections of bleomycin and enhance tissue remodeling in mice²⁹¹. Administration of MSCs decreased the number of α -smooth muscle actin positive myofibroblasts and stimulated the formation of collagen in a basket-weave organization²⁹¹. Injection of adipose-derived stem cells (ADSCs) into the superficial wound bed of full thickness circular excisional wounds of Yorkshire pigs exhibited thicker granulating neodermis, and greater wound contraction²⁹². Injection of ADSCs improved wound healing in a streptozotocin-induced diabetic swine model²⁹³. Epidermal injury was found to recruit stem cells from the hair follicle bulge into the epidermis in mice²⁹⁴. Subcutaneous injection of MSCs promoted cutaneous wound repair by promoting keratinocyte migration in an excisional wound splinting model in mice²⁹⁵. Injection of ADSCs accelerated wound healing of splinted excisional wounds in immunodeficient diabetic mice²⁹⁶. Summarizing, MSC administration may be a novel strategy to improve wound repair and tissue remodeling after surgical cleft repair.

Administration of MSCs forms a promising treatment to improve wound repair and to prevent scarring in wounds²⁹⁷⁻²⁹⁹. Since administration of conditioned media derived from MSCs can already improve wound repair, it is assumed that also paracrine factors are able to generate protective effects^{274,300,301}. Unfortunately, administered MSCs were found to die soon upon administration, and are hardly incorporated into the injured tissue^{302,303}. Only less than 1% of systemically administered MSCs may persist at the injury site after 7 days^{299,304}. The access of MSCs to the wound site may be hampered by damaged blood vessels and by disorganized tissue³⁰². Furthermore, the limited MSCs survival can be explained by the hostile wound environment containing inflammatory and oxidative mediators^{302,303}.

Improving the survival of MSCs at the place of injury may further enhance the protective effects, as these cells can continue to produce paracrine factors to promote wound healing (**Research question 6**).

5.2 HO-1 is a promising target to improve MSC therapy in wound repair

Induction of HO-1 could be such a therapy to increase the survival of MSCs following application. Curcumin-induced HO-1 expression rescued ADSCs from H₂O₂-mediated cell death *in vitro*³⁰⁵. Curcumin protected against H₂O₂-mediated damage in lung MSCs by increased HO-1 expression *in vitro*³⁰⁶. Pretreatment of human cardiac stem cells with HO-1 inducer Cobalt protoporphyrin (CoPP) protected against H₂O₂-induced oxidative stress *in vitro*³⁰⁷. Interestingly, conditioned medium of HO-1 positive MSCs rescued from kidney injury, whereas conditioned medium of HO-1 KO MSCs was

ineffective³⁰⁰. MSCs transduction with adenovirus-hHO-1 increased expression of HO-1, and suppressed apoptosis following exposure to hypoxia *in vitro*³⁰⁸. Induction of HO-1 by CoPP promoted the proliferation of human umbilical vein endothelial cells *in vitro*³⁰⁹. Rat renal tubular epithelial cells treated with H₂O₂ increased HO-1 expression and showed less apoptosis following MSCs administration *in vitro*³¹⁰. HO-1-overexpressing MSCs showed resistance to cell apoptosis following H₂O₂-induced oxidative stress *in vitro*³¹¹. Bone marrow-derived MSCs were found to increase the expression of HO-1 and reduced liver inflammation following LPS-induced acute liver failure in rats by reduced inflammation and apoptosis³¹². Rabbits treated with ADSCs transduced with HO-1 (HO-1-ADSCs) showed cardiac function improvement following experimental myocardial infarction³¹³. HO-1 induction thus promotes proliferation and cell survival of MSCs and protect MSCs against oxidative stress and oxidative stress-induced apoptosis. By enhancing cell survival, induction of HO-1 could possibly be a strategy to improve the outcome of MSC therapy in the treatment of pathological wound repair following CLP surgery.

MSCs can be found throughout the body and are widely used for regenerative medicine purposes. They may stimulate the regeneration of the injured skin and muscle tissues following surgical lip and palate closure by reloading the required cells and by providing a more regenerative microenvironment that attenuates scarring and fibrosis³¹⁴. However, the isolation of MSCs from bone marrow or adipose tissue from the baby can cause complications such as infection, bleeding, and chronic pain³¹⁵. Moreover, it is expensive to harvest them and to expand them by controlled cell culture³¹⁶. Human umbilical cord blood cells are obtained by a simple, safe, and painless procedure following birth. MSCs can be easily isolated from cord blood and preserved for later treatment³¹⁷. The umbilical cord is an attractive source of stem cells because it is considered biowaste accompanying the delivery of a baby. We propose that these umbilical cord MSCs can be used to facilitate skin and muscle tissue regeneration following surgical cleft repair (**Figure 12**).

Transplantation of MSCs in patients with multiple sclerosis (MS), amyotrophic lateral sclerosis (ALS)³¹⁸, and in patients with acute myocardial infarction³¹⁹ has been proven a relatively safe procedure. Treatment of patients with acute myocardial infarction with MSCs isolated from Wharton Jelly is regarded as a safe therapy³¹⁹. However, intravenous infusion of ADSCs may result in thrombus formation around the cells through a coagulation mechanism, which can also cause pulmonary embolism due to the accumulation of cells in the lung region³²⁰. Thromboembolism was confirmed by other studies using umbilical cord MSCs, showing the procoagulant properties after injection in peripheral veins³²¹. More long-term studies and observations regarding the safety of MSC injection are required³²². Human umbilical cord MSCs produce significantly higher amounts of VEGF and basic fibroblast growth factor (bFGF) compared to fibroblasts³²³. Injection of conditioned medium of human umbilical cord

MSCs promoted wound repair and increased neovascularization in full-thickness excisional wounds of streptozotocin-induced diabetic mice³⁰¹. In adult Wistar rats intravenously injected cord blood stem cells improved healing of deep burn wounds³²⁴. Applied umbilical cord MSCs were found to differentiate into keratinocytes in full-thickness skin defect wounds, which promoted cutaneous wound healing³²⁵. In streptozotocin-induced diabetic mice subcutaneous injection of umbilical cord MSCs improved cutaneous wound healing³²⁶. However, others found no significant wound healing improvement of full-thickness skin wounds following injection of umbilical cord MSCs in nude mice³¹⁴. Importantly, for the use of MSCs as a therapy MSCs banking and cell products manufacturing and corresponding quality control system procedures must be applied for assuring the safety and efficiency of the final cell products³²⁷.

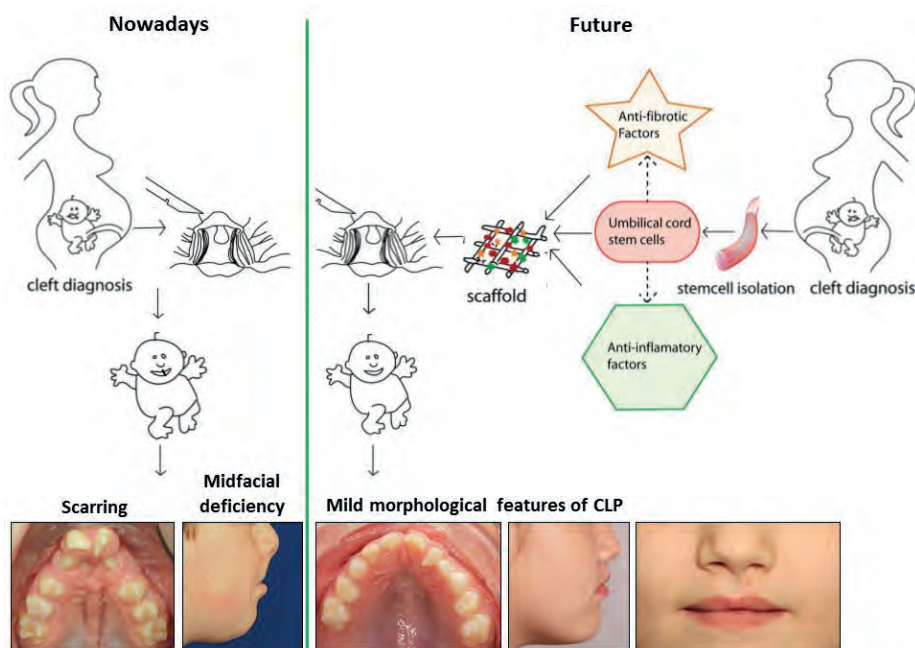


Figure 12: Future tissue engineering using MSCs following surgical CLP shifting the treatment outcome to mild morphological features of CLP. Nowadays, pathological wound healing following palatal cleft surgery can lead to excessive scar tissue formation, contributing to inhibition of the growth of the maxilla, together with posterior constriction of the upper dental arch. Following detection of a CLP using prenatal ultrasound screening, umbilical cord MSCs are isolated upon birth. Stem cells express antifibrotic and anti-inflammatory factors. These stem cells can be used in future tissue engineering strategies in combination with factors targeting inflammation (e.g. HO-1) and fibrosis (e.g. anakinra, pirfenidone and nintedanib)³²⁸ within a scaffold during CLP surgery to promote skin and muscle regeneration and function and to inhibit scar formation. Less scar formation could lead to better soft tissue esthetics and less growth inhibition of the maxilla, and may shift the treatment outcome of CLP surgery to mild morphological features of CLP.

Administration of HO-1 expressing umbilical cord-derived MSCs alleviated D-galactose induced hepatic disorders in rats *in vivo*³²⁹. H₂O₂-stimulated human umbilical

cord MSCs showed increased expression of HO-1, and attenuated inflammation following Tetramethylpyrazine treatment *in vitro*³³⁰. Although, the number of studies on the effects of HO-1 expression in umbilical cord-derived MSCs is limited. More research is needed to elucidate the role of HO-1 expression in cell survival of umbilical cord-derived MSCs. Stem cells in combination with factors targeting inflammation and fibrosis within a scaffold can be used in future tissue engineering strategies during CLP surgery to promote skin and muscle regeneration and function and to inhibit scar formation. Less scar formation could lead to better soft tissue esthetics and less growth inhibition of the maxilla and may shift the treatment outcome of CLP surgery to mild morphological features of CLP.

Section 6. Clinical relevance for CLP patients and future perspectives

6.1 The potential of cytoprotective mechanisms in prevention of pregnancy pathology

Having presented these pre-clinical data, we will address their possible clinical implications. We were successful in mimicking intrauterine hemorrhage/hematoma by i.p. administration of heme at day E12 in pregnant mice, causing fetal abortion in a dose-dependent fashion. Moreover, we showed that HO-activity rescue fetuses from abortion following heme exposure, since inhibition of HO-activity aggravated the effects of heme 75 $\mu\text{mol/kg}$ body weight administration³³¹.

We showed that heme administration increased the expression levels of adhesion molecule ICAM-1, resulting in increased influx of macrophages and HO-1 positive cells in placenta in a dose-dependent manner, which was further increased following inhibition of HO-activity³³¹.

In contrast to animal studies using specific strains, patients have their unique immune system, and the large differences in genetics and different exposure to environment factors between patients make it difficult to translate data from animal experiments directly to the clinic. Since a microsatellite polymorphism of the HO-1 gene in pregnant mothers, leading to low levels of HO-1 induction, is associated with idiopathic recurrent miscarriage⁵³, we hypothesize that safe HO-1 induction during the first trimester could possibly be a novel therapy to protect against elevated concentrations of inflammatory stressors, such as LPS and free heme.

Furthermore, since uterine hematomas are associated with increased risk of intrauterine growth restriction, preterm delivery and miscarriage⁶³⁻⁶⁶, we suggest that HO-1 induction might protect against free heme release following intrauterine hemorrhage and may reduce the risk of fetal abortion when this happens. The number of experimental studies done on the relation between heme exposure, HO-activity and placental and fetal development is scarce. Despite the positive effects of HO-1 induction

we found on placental and fetal development during heme-induced pathological pregnancies in mice (**Chapter 4**), it is uncertain if HO-1 induction is an effective and safe therapy to protect against oxidative and inflammatory stress-induced fetal abortion in humans.

6.2 The potential of cytoprotective mechanisms and signaling pathways in palatogenesis and wound healing

Similar to previous studies, where CXCL11 recruited CXCR3-positive macrophages, the increased expression of CXCL11 in the disintegrating MES was associated to recruit macrophages to phagocytose apoptotic cells from the MES²⁴¹. Our findings (**Chapter 2**) support the hypothesis that the MES disintegrates by epithelial cell apoptosis, although we cannot rule out that CXCL11-CXCR3 signaling also promotes epithelial cell migration^{203,204,206-208}.

Since expression of chemokine receptor CXCR3 and its ligand chemokine CXCL11 were both expressed within the MES, CXCL11-CXCR3 autocrine signaling might control migration and apoptosis of epithelial cells during its disintegration. This finding thus supports the hypothesis that the MES disintegrates by epithelial cell migration. Although our study provided novel information, the current knowledge is still too limited to develop novel therapies to promote the process of palatal fusion in human.

In **Chapter 3**, we proposed that CXCL12-CXCR4 signaling facilitates palatal osteogenesis¹⁷¹. However, the number of studies on CXCL12-CXCR4 signaling and palatal osteogenesis is scarce. Since defective osteogenesis within the palate was found to cause cleft palate in mice²³¹, we suggest that CXCL12-CXCR4 regulates palatal osteogenesis, essential in the process of palatogenesis. Because of the current limited insights, we expect that clinical therapies that regulate chemokine signaling to promote palatal osteogenesis will however not be soon available.

Despite we showed that abrogation of HO-2 gene can result in fetal malformations (**Chapter 2**), we did not find hampered MES disintegration or palatal expression of CXCL11 or CXCR3 following absence of HO-2 expression²⁴¹. Furthermore, pharmacologically inhibition of HO-activity by administration of SnMP at E11 did not affect palatal fusion nor did it alter the expression of CXCL12 or CXCR4 within the palate¹⁷¹. The potential of HO-1 induction and chemokine-receptor signaling within the fusing palatal shelves should further be studied.

Several *in vivo* experiments improved wound repair using MSCs administration in mice^{295,296}, dogs²⁸⁸, and pigs^{292,293}. MSCs were found to enhance wound healing by secretion of various paracrine factors²⁹⁰. MSCs may stimulate the regeneration of the injured skin and muscle tissue following surgical CLP repair³¹⁴. However, administered MSCs were found to die soon upon administration, and are only limited incorporated into the injured tissue^{302,303}. Induction of HO-1 in MSCs has been found to promote proliferation and suppressed apoptosis, and could improve survival of MSCs within the

hostile environment within the wound³⁰². We expect that administration of MSCs is a promising therapy to improve wound healing following surgical CLP repair, and induction of cytoprotective pathways as HO-1 may further improve MSC cell survival after application. Improved wound healing could lead to less scar formation, and possibly could cause less growth inhibition of the maxilla in patients with CLP, resulting in a better shape of the face.

6.3 Palatogenesis and potential parallels with wound healing

Similarities in molecular and cellular signaling are reported in embryonic development and cutaneous wound repair³³². Notably, the regenerative processes in palatal fusion and wound repair show familiar cellular signaling pathways and gene regulatory networks⁷. Since CXCL11-CXCR3 signaling was found to promote keratinocyte migration²⁰⁶ and macrophage recruitment in zebrafish¹⁹⁹, and our data showed CXCL11 and CXCR3 expression within the disintegrating MES (**Chapter 2**), we state that CXCL11-CXCR3 autocrine signaling regulates remodeling of the epithelial tissues in both processes.

In addition, we related CXCL12 and CXCR4 within the osteogenic centers within the palatal shelves with palatal bone formation (**Chapter 3**), and CXCL12-CXCR4 signaling was found to recruit hematopoietic stem cells and mesenchymal stem cells to the wound area in mice^{333,334}, we propose that CXCL12-CXCR4 signaling may be an import regulator of different biological processes during palatogenesis and cutaneous wound healing. Finally, we showed HO-1 expression within macrophages near the disintegrating MES (**Chapter 2**), and HO-1 induction in the dermis during excisional wound following splinting (**Chapter 6**).

Since HO-1 expression in macrophages promotes formation of the anti-inflammatory M2-like phenotype¹⁴², and HO-1 stimulates wound closure by upregulating anti-inflammatory, antioxidant, and angiogenesis activities in diabetic rats²⁶⁵, it is suggesting that HO-activity is important in the breakdown of heme in the wound healing process.

Because HO-1-overexpressing MSCs showed resistance to cell apoptosis³¹¹ (**Chapter 7**), it is hypothesized that HO-1 induction in stem cells may also promote regenerative processes during cutaneous wound healing.

We conclude that CXCL11-CXCR3 and CXCL12-CXCR4 signaling, and HO-1 induction in macrophages and stem cells are potential targets for future therapies in preventing CLP formation and excessive scarring following wound repair (**Figure 13**). However, more fundamental research on the processes of palatogenesis and wound healing is first necessary.

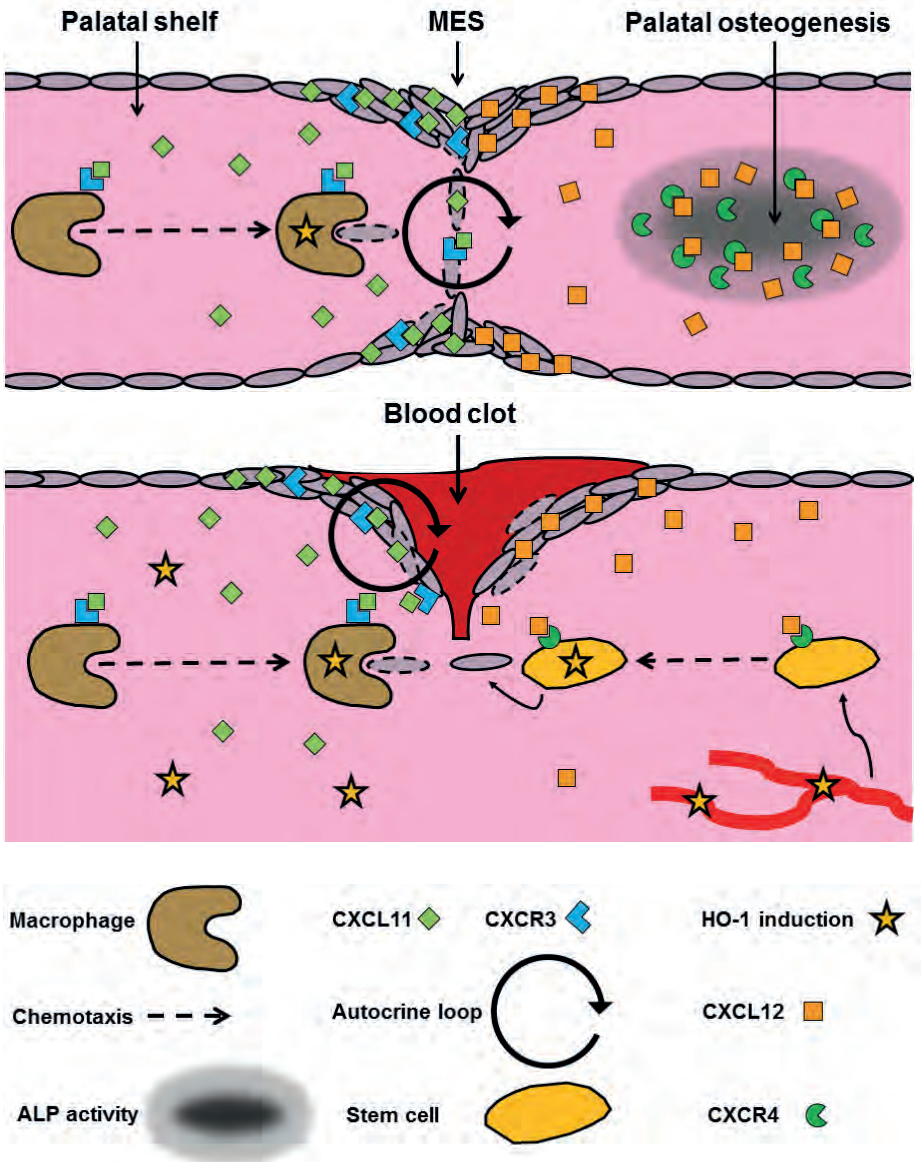


Figure 13: Hypothetical model: Palatogenesis and potential parallels with wound healing. Similarities in molecular and cellular signaling are reported in embryonic development and cutaneous wound in the process of palatal fusion (**upper panel**) and cutaneous wound repair (**lower panel**). CXCL11-CXCR3 autocrine signaling is associated with epithelial tissue remodeling. CXCL11-CXCR3 signaling is related to macrophage recruitment in both palatal fusion and wound healing. CXCL12-CXCR4 signaling is involved in different biological mechanisms in palatogenesis and wound repair. HO-1 expression promotes macrophage function and stem cell survival, indicating that HO-1 induction could both facilitate palatal fusion and cutaneous wound healing.

6.4 Future treatment concepts in the CLP clinic

Prevention of CLP remains the ultimate goal of research by identifying the etiology and risk factors³³⁵. Previous trials investigated the role of maternal multivitamins and folic acid supplementation in the prevention of congenital anomalies^{336,337}. Folic acid supplementation during pregnancy has been found to reduce the risk of neural tube defects in newborns²³². Women in intermediate and high-risk categories for neural tube defects who wish to become pregnant are advised to take a higher dose³³⁸. Notably, women who take folic acid supplements early in their pregnancy can substantially reduce their baby's chances of being born with CLP³³⁹. Nutrition guidelines for pregnant woman and woman planning to become pregnant recommend multivitamin supplementation (containing vitamin A, B6 and C) before and during pregnancy to reduce the risk of CLP^{335,340,341}. On the other hand, evidence from animal studies shows a clear increase in the risk of cleft palate related to excess vitamin A³⁴². It is possible that in the future, when the etiology of CLP is better understood, the cleft team will further extend their recommendations of maternal supplementation in early pregnancy with antioxidative and anti-inflammatory drugs, especially for women from families with a predisposition for CLP and women with diabetes who want to become pregnant. Differential protection against heme, by induction of hemopexin/haptoglobin or HO-1, may determine the outcome of hemorrhage-mediated pregnancy complications. However, more research is needed to determine if maternal supplementation of HO-1 inducers, as curcumin, early in pregnancy would be a safe and effective therapy to reduce the risk of CLP in humans.

As discussed in the introduction of this thesis, scarring following surgical cleft palate repair can contribute to transverse narrowing of the maxilla²⁶³ and hampered maxillary growth, leading to midfacial deficiency²⁷⁰. These effects can lead to more complicated orthodontic treatment, and the need for orthognathic surgery, making the CLP treatment more extensive. In the near future, regenerative medicine using MSCs application could improve the wound healing process following surgical cleft repair. The umbilical cord blood and tissue forms an attractive source of stem cells because it is considered biowaste. Since prenatal ultrasound screening allows early detection of CLP in the 11th to 13th week of gestation the preservation of umbilical cord upon birth can be planned. Application of umbilical cord-derived MSCs following cleft surgery could form a new strategy to optimize wound repair and regeneration with less scarring. In addition, induction of HO-1 before administration in the wound area, or HO-1 induction in MSCs before application could possibly improve the wound microenvironment and the survival of MSCs, respectively. Besides, addition of chemokines could promote the influx of progenitor cells to the wound site. After prenatal ultrasound diagnosis of CLP, the cleft team should organize the harvesting of the umbilical cord upon birth.

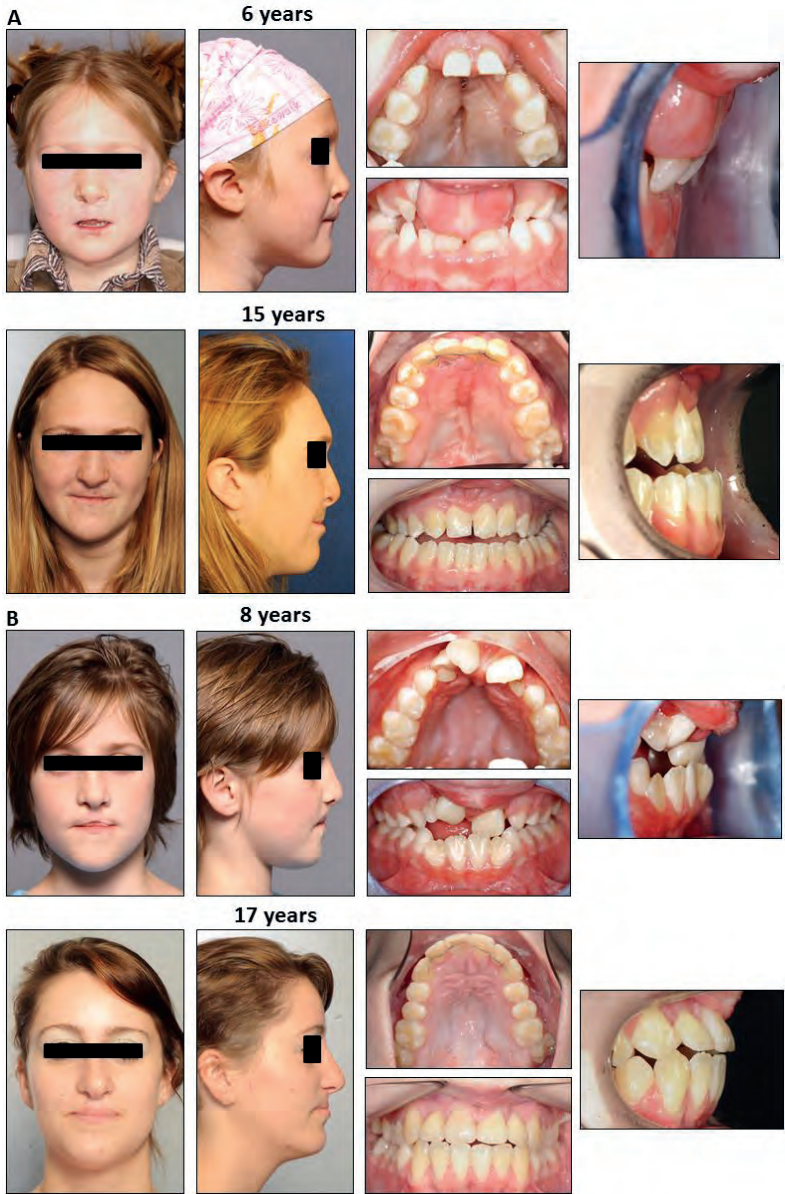


Figure 14: Future tissue engineering following surgical CLP may shift the treatment outcome to mild features of CLP. (A) Following bilateral CLP repair scarring of the lip and palatal mucosa was developed. Moderate maxillary hypoplasia led to compromised facial esthetics with a suboptimal occlusion and dental frontal relationship. The patient regarded the treatment outcome as unfavorable and requested facial esthetic improvement. Surgical maxillary advancement has been planned in adulthood. **(B)** Mild scarring of the lip and palate and a minor maxillary hypoplasia following bilateral CLP repair has been observed, together with fair facial esthetics and acceptable occlusion and dental frontal relationship. The patient considered the treatment outcome as favorable, and there was no demand for further facial esthetic improvement. Future tissue engineering, possibly using umbilical cord-derived MSCs in combination with factors targeting inflammation and fibrosis, could reduce scar formation following CLP surgery, and may shift the treatment outcome to mild features of CLP.

Less scarring after surgical cleft palate closure may lead to less impediment of the maxillary growth and development, reducing the need for large orthodontic and orthognathic surgical corrections. Less need for considerable corrections might lead to less invasive treatment protocols, reducing the psycho-social burden of the patient and the family. Furthermore, less scarring could cause less speech impediment, and could possibly result in better functional and esthetic treatment outcomes (**Figure 14**).

6.5 Shaping the face; cytoprotective mechanisms, signaling pathways, and cleft repair

In the introduction of this thesis we already discussed that the mechanisms of CLP formation are not fully understood, but it is accepted that genetic predisposition and environmental factors play a role³⁴³. Environmental factors as diabetes¹⁶¹, infections^{162,163}, smoking¹⁵⁹, alcohol consumption¹⁶⁰, anti-epileptic drugs³⁴⁴, and bleeding episodes during pregnancy¹⁶⁴ are associated with increased risk of CLP. Interestingly, all these factors are also associated with oxidative and inflammatory stress³⁴⁵⁻³⁴⁷. Because of its involvement in the etiology of congenital malformations³⁴⁸, we suggested that high oxidative and inflammatory stress levels may contribute to CLP formation.

Based on our research, we suggest that cytoprotective mechanisms, as the HO enzyme system, could be a potential target in preventing against pregnancy pathology and the development of congenital malformations, as CLP. More insight in the role of oxidative and inflammatory stress at fetal development could create more insights in the complex etiology of CLP.

In patients with CLP an important factor for craniofacial growth forms the iatrogenic effect of surgical interventions³⁴⁹, which can lead to development of structural distortions of the face³⁵⁰. Prolonged inflammation and elevated levels of ROS can result in hampered wound repair and can cause excessive scarring^{351,352}. Chronic inflammation can lead to deposition of excessive collagen type III fibers and ECM proteins within the wound area, fueling the process of hypertrophic scarring³⁵²⁻³⁵⁵. Hypertrophic scar formation impairs soft tissue form, function, or movement³⁵². Scarring following cleft lip repair can cause transverse narrowing of the maxilla²⁶³, and posterior inclination of the upper incisors³⁵⁰. Besides maxillary dental arch constriction³⁵⁶, scarring following surgical cleft palate closure is mainly responsible for sagittal growth inhibition of the maxilla³⁵⁷, leading to midfacial growth deficiency²⁷⁰. Cytoprotective mechanisms could also protect against excessive scarring following surgical CLP repair, leading to reduced maxillary dental arch collapse and less maxillary growth inhibition. Nevertheless, we should not close our eyes for the “surgeon effect”. The experience and skills of the surgeon will remain a decisive factor in the final outcome of cleft surgery.

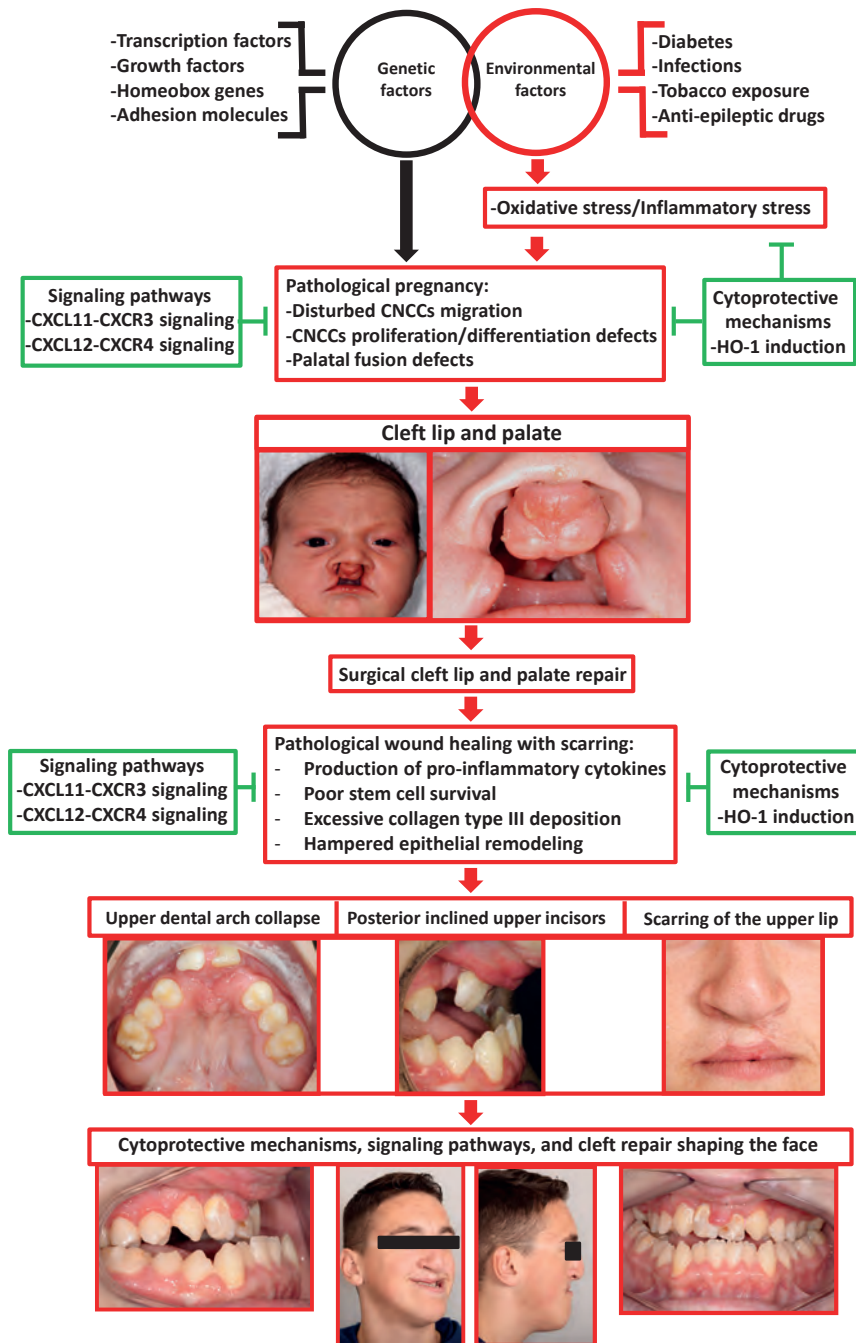


Figure 15: Shaping the face; cytoprotective mechanisms, signaling pathways, and cleft repair. Cytoprotective mechanisms and (inter)cellular signaling pathways are potential targets in prevention of CLP formation, or scar formation following surgical CLP repair. Modulation of cytoprotective mechanisms and cellular signaling pathways could improve wound repair with less scar formation, and may reduce the disturbance of the maxillary dental arch development and the maxillary growth. Cytoprotective mechanisms, signaling pathways and cleft repair all contribute to the final shape of the face.

CXCL12-CXCR4 chemokine-chemokine receptor signaling is regarded as an important cell signaling pathway in guiding the migrating CNCCs to the branchial arches to enable embryonic facial development^{223,333,358-360}. Furthermore, CXCL12-CXCR4 signaling has been found to promote osteogenesis³⁶¹. Based on our data we associated CXCL12 and CXCR4 expression within the fusing palatal shelves with palatal osteogenesis (**Chapter 3**), and CXCL11 and CXCR3 expression within MES with palatal fusion (**Chapter 2**). Since CXCL11-CXCR3 signaling was found to promote keratinocyte migration into the wound area²⁰⁶, and CXCL12-CXCR4 signaling was found to recruit hematopoietic stem cells and mesenchymal stem cells to the wound area^{333,334}, we propose that cellular signaling pathways may could contribute to embryonic craniofacial development, including palatogenesis, and may improve wound repair following surgical CLP repair.

In conclusion, cytoprotective mechanisms and signaling pathways are interesting potential targets in reducing the risk of CLP formation, or reducing scar formation following surgical CLP repair. Less scar formation could lead to less disturbance of the maxillary dental arch and may cause less midfacial deficiency (**Figure 15**). However, more research into the role of cytoprotective mechanisms and cellular signaling pathways is needed in patients with CLP.

References

1. Calzolari E, Bianchi F, Rubini M, Ritvanen A, Neville AJ, Group EW. Epidemiology of cleft palate in Europe: implications for genetic research. *Cleft Palate Craniofac J*. 2004;41(3):244-249.
2. Shaw WC, Semb G, Nelson P, et al. The Eurocleft project 1996-2000: overview. *J Craniomaxillofac Surg*. 2001;29(3):131-140; discussion 141-132.
3. Stuppia L, Capogreco M, Marzo G, et al. Genetics of syndromic and nonsyndromic cleft lip and palate. *J Craniofac Surg*. 2011;22(5):1722-1726.
4. van Beurden HE, Von den Hoff JW, Torensma R, Maltha JC, Kuijpers-Jagtman AM. Myofibroblasts in palatal wound healing: prospects for the reduction of wound contraction after cleft palate repair. *J Dent Res*. 2005;84(10):871-880.
5. Sinko K, Jagsch R, Prechtel V, Watzinger F, Hollmann K, Baumann A. Evaluation of esthetic, functional, and quality-of-life outcome in adult cleft lip and palate patients. *Cleft Palate Craniofac J*. 2005;42(4):355-361.
6. Marcusson A, Paulin G, Ostrup L. Facial appearance in adults who had cleft lip and palate treated in childhood. *Scand J Plast Reconstr Surg Hand Surg*. 2002;36(1):16-23.
7. Biggs LC, Goudy SL, Dunnwald M. Palatogenesis and cutaneous repair: A two-headed coin. *Dev Dyn*. 2015;244(3):289-310.
8. Zenclussen AC, Lim E, Knoeller S, et al. Heme oxygenases in pregnancy II: HO-2 is downregulated in human pathologic pregnancies. *Am J Reprod Immunol*. 2003;50(1):66-76.
9. Barber A, Robson SC, Myatt L, Bulmer JN, Lyall F. Heme oxygenase expression in human placenta and placental bed: reduced expression of placenta endothelial HO-2 in preeclampsia and fetal growth restriction. *FASEB J*. 2001;15(7):1158-1168.
10. Lyall F, Barber A, Myatt L, Bulmer JN, Robson SC. Hemeoxygenase expression in human placenta and placental bed implies a role in regulation of trophoblast invasion and placental function. *FASEB J*. 2000;14(1):208-219.
11. Yoshiki N, Kubota T, Aso T. Expression and localization of heme oxygenase in human placental villi. *Biochem Biophys Res Commun*. 2000;276(3):1136-1142.
12. Hanselmann C, Mauch C, Werner S. Haem oxygenase-1: a novel player in cutaneous wound repair and psoriasis? *Biochem J*. 2001;353(Pt 3):459-466.
13. Grochot-Przeczek A, Lach R, Mis J, et al. Heme oxygenase-1 accelerates cutaneous wound healing in mice. *PLoS One*. 2009;4(6):e5803.
14. Larsen R, Gouveia Z, Soares MP, Gozzelino R. Heme cytotoxicity and the pathogenesis of immune-mediated inflammatory diseases. *Front Pharmacol*. 2012;3:77.
15. Sawicki KT, Chang HC, Ardehali H. Role of heme in cardiovascular physiology and disease. *J Am Heart Assoc*. 2015;4(1):e001138.
16. Tenhunen R, Marver HS, Schmid R. Microsomal heme oxygenase. Characterization of the enzyme. *J Biol Chem*. 1969;244(23):6388-6394.
17. Rifkind JM, Mohanty JG, Nagababu E. The pathophysiology of extracellular hemoglobin associated with enhanced oxidative reactions. *Front Physiol*. 2014;5:500.
18. Winterbourn CC. Toxicity of iron and hydrogen peroxide: the Fenton reaction. *Toxicol Lett*. 1995;82-83:969-974.
19. Gozzelino R, Jeney V, Soares MP. Mechanisms of cell protection by heme oxygenase-1. *Annu Rev Pharmacol Toxicol*. 2010;50:323-354.
20. Grochot-Przeczek A, Dulak J, Jozkowicz A. Haem oxygenase-1: non-canonical roles in physiology and pathology. *Clin Sci (Lond)*. 2012;122(3):93-103.
21. Li C, Lonn ME, Xu X, et al. Sustained expression of heme oxygenase-1 alters iron homeostasis in nonerythroid cells. *Free Radic Biol Med*. 2012;53(2):366-374.
22. Li Volti G, Wang J, Tragano F, Kappas A, Abraham NG. Differential effect of heme oxygenase-1 in endothelial and smooth muscle cell cycle progression. *Biochemical and biophysical research communications*. 2002;296(5):1077-1082.
23. Yet SF, Layne MD, Liu X, et al. Absence of heme oxygenase-1 exacerbates atherosclerotic lesion formation and vascular remodeling. *FASEB J*. 2003;17(12):1759-1761.
24. Yet SF, Tian R, Layne MD, et al. Cardiac-specific expression of heme oxygenase-1 protects against ischemia and reperfusion injury in transgenic mice. *Circ Res*. 2001;89(2):168-173.
25. Collinson EJ, Wimmer-Kleikamp S, Gerega SK, et al. The yeast homolog of heme oxygenase-1 affords cellular antioxidant protection via the transcriptional regulation of known antioxidant genes. *J Biol Chem*. 2011;286(3):2205-2214.

26. Abraham NG, Kappas A. Pharmacological and clinical aspects of heme oxygenase. *Pharmacol Rev.* 2008;60(1):79-127.
27. Cruse I, Maines MD. Evidence suggesting that the two forms of heme oxygenase are products of different genes. *J Biol Chem.* 1988;263(7):3348-3353.
28. Maines MD, Trakshel GM, Kuty RK. Characterization of two constitutive forms of rat liver microsomal heme oxygenase. Only one molecular species of the enzyme is inducible. *J Biol Chem.* 1986;261(1):411-419.
29. Maines MD. The heme oxygenase system: a regulator of second messenger gases. *Annu Rev Pharmacol Toxicol.* 1997;37:517-554.
30. Maines MD, Gibbs PE. 30 some years of heme oxygenase: from a "molecular wrecking ball" to a "mesmerizing" trigger of cellular events. *Biochem Biophys Res Commun.* 2005;338(1):568-577.
31. Maines MD, Panahian N. The heme oxygenase system and cellular defense mechanisms. Do HO-1 and HO-2 have different functions? *Adv Exp Med Biol.* 2001;502:249-272.
32. Yoshida T, Kikuchi G. Purification and properties of heme oxygenase from pig spleen microsomes. *J Biol Chem.* 1978;253(12):4224-4229.
33. Yoshida T, Kikuchi G. Purification and properties of heme oxygenase from rat liver microsomes. *J Biol Chem.* 1979;254(11):4487-4491.
34. Shibahara S, Muller R, Taguchi H, Yoshida T. Cloning and expression of cDNA for rat heme oxygenase. *Proc Natl Acad Sci U S A.* 1985;82(23):7865-7869.
35. Kim HP, Wang X, Galbati F, Ryter SW, Choi AM. Caveolae compartmentalization of heme oxygenase-1 in endothelial cells. *FASEB J.* 2004;18(10):1080-1089.
36. Ryter SW, Alam J, Choi AM. Heme oxygenase-1/carbon monoxide: from basic science to therapeutic applications. *Physiol Rev.* 2006;86(2):583-650.
37. Sun Y, Rotenberg MO, Maines MD. Developmental expression of heme oxygenase isozymes in rat brain. Two HO-2 mRNAs are detected. *J Biol Chem.* 1990;265(14):8212-8217.
38. Trakshel GM, Kuty RK, Maines MD. Purification and characterization of the major constitutive form of testicular heme oxygenase. The noninducible isoform. *J Biol Chem.* 1986;261(24):11131-11137.
39. Kreiser D, Kelly DK, Seidman DS, Stevenson DK, Baum M, Dennery PA. Gestational pattern of heme oxygenase expression in the rat. *Pediatr Res.* 2003;54(2):172-178.
40. Zenclussen AC, Sollwedel A, Bertoja AZ, et al. Heme oxygenase as a therapeutic target in immunological pregnancy complications. *Int Immunopharmacol.* 2005;5(1):41-51.
41. Zenclussen AC, Joachim R, Hagen E, Peiser C, Klapp BF, Arck PC. Heme oxygenase is downregulated in stress-triggered and interleukin-12-mediated murine abortion. *Scand J Immunol.* 2002;55(6):560-569.
42. Acevedo CH, Ahmed A. Hemeoxygenase-1 inhibits human myometrial contractility via carbon monoxide and is upregulated by progesterone during pregnancy. *J Clin Invest.* 1998;101(5):949-955.
43. Venditti CC, Smith GN. Involvement of the heme oxygenase system in the development of preeclampsia and as a possible therapeutic target. *Womens Health (Lond).* 2014;10(6):623-643.
44. McLean M, Bowman M, Clifton V, Smith R, Grossman AB. Expression of the heme oxygenase-carbon monoxide signalling system in human placenta. *J Clin Endocrinol Metab.* 2000;85(6):2345-2349.
45. Sidle EH, Casselman R, Smith GN. Effect of cigarette smoke on placental antioxidant enzyme expression. *Am J Physiol Regul Integr Comp Physiol.* 2007;293(2):R754-758.
46. McCaig D, Lyall F. Inhibitors of heme oxygenase reduce invasion of human primary cytotrophoblast cells in vitro. *Placenta.* 2009;30(6):536-538.
47. Zenclussen ML, Jensen F, Rebelo S, El-Mousleh T, Casalis PA, Zenclussen AC. Heme oxygenase-1 expression in the ovary dictates a proper oocyte ovulation, fertilization, and corpora lutea maintenance. *Am J Reprod Immunol.* 2012;67(5):376-382.
48. Zhao H, Wong RJ, Kalish FS, Nayak NR, Stevenson DK. Effect of Heme Oxygenase-1 Deficiency on Placental Development. *Placenta.* 2009;30(10):861-868.
49. Tsur A, Kalish F, Burgess J, et al. Pravastatin improves fetal survival in mice with a partial deficiency of heme oxygenase-1. *Placenta.* 2019;75:1-8.
50. Zenclussen ML, Casalis PA, El-Mousleh T, et al. Haem oxygenase-1 dictates intrauterine fetal survival in mice via carbon monoxide. *J Pathol.* 2011;225(2):293-304.

51. Linzke N, Schumacher A, Woidacki K, Croy BA, Zenclussen AC. Carbon monoxide promotes proliferation of uterine natural killer cells and remodeling of spiral arteries in pregnant hypertensive heme oxygenase-1 mutant mice. *Hypertension*. 2014;63(3):580-588.
52. Zhao H, Azuma J, Kalish F, Wong RJ, Stevenson DK. Maternal heme oxygenase 1 regulates placental vasculature development via angiogenic factors in mice. *Biol Reprod*. 2011;85(5):1005-1012.
53. Denschlag D, Marculescu R, Unfried G, et al. The size of a microsatellite polymorphism of the haem oxygenase 1 gene is associated with idiopathic recurrent miscarriage. *Mol Hum Reprod*. 2004;10(3):211-214.
54. Sollwedel A, Bertoja AZ, Zenclussen ML, et al. Protection from abortion by heme oxygenase-1 up-regulation is associated with increased levels of Bag-1 and neuropilin-1 at the fetal-maternal interface. *J Immunol*. 2005;175(8):4875-4885.
55. Zhao H, Wong RJ, Doyle TC, et al. Regulation of maternal and fetal hemodynamics by heme oxygenase in mice. *Biol Reprod*. 2008;78(4):744-751.
56. Schumacher A, Wafula PO, Teles A, et al. Blockage of heme oxygenase-1 abrogates the protective effect of regulatory T cells on murine pregnancy and promotes the maturation of dendritic cells. *PLoS One*. 2012;7(8):e42301.
57. Reddy P, Najundaswamy S, Mehta R, Petrova A, Hegyi T. Tin-mesoporphyrin in the treatment of severe hyperbilirubinemia in a very-low-birth-weight infant. *J Perinatol*. 2003;23(6):507-508.
58. Valaes T, Petmezaki S, Henschke C, Drummond GS, Kappas A. Control of jaundice in preterm newborns by an inhibitor of bilirubin production: studies with tin-mesoporphyrin. *Pediatrics*. 1994;93(1):1-11.
59. Kappas A, Drummond GS, Henschke C, Valaes T. Direct comparison of Sn-mesoporphyrin, an inhibitor of bilirubin production, and phototherapy in controlling hyperbilirubinemia in term and near-term newborns. *Pediatrics*. 1995;95(4):468-474.
60. Fujioka K, Kalish F, Wong RJ, Stevenson DK. Inhibition of heme oxygenase activity using a microparticle formulation of zinc protoporphyrin in an acute hemolytic newborn mouse model. *Pediatr Res*. 2016;79(2):251-257.
61. Fujiwara R, Mitsugi R, Uemura A, Itoh T, Tukey RH. Severe Neonatal Hyperbilirubinemia in Crigler-Najjar Syndrome Model Mice Can Be Reversed With Zinc Protoporphyrin. *Hepatal Commun*. 2017;1(8):792-802.
62. Rodgers PA, Seidman DS, Wei PL, Dennery PA, Stevenson DK. Duration of action and tissue distribution of zinc protoporphyrin in neonatal rats. *Pediatr Res*. 1996;39(6):1041-1049.
63. Hashem A, Sarsam SD. The Impact of Incidental Ultrasound Finding of Subchorionic and Retroplacental Hematoma in Early Pregnancy. *J Obstet Gynaecol India*. 2019;69(1):43-49.
64. Ji W, Li W, Mei S, He P. Intrauterine hematomas in the second and third trimesters associated with adverse pregnancy outcomes: a retrospective study. *J Matern Fetal Neonatal Med*. 2017;30(18):2151-2155.
65. Ott J, Pecnik P, Promberger R, Pils S, Binder J, Chalubinski KM. Intra- versus retroplacental hematomas: a retrospective case-control study on pregnancy outcomes. *BMC Pregnancy Childbirth*. 2017;17(1):366.
66. MacMullen NJ, Dulski LA, Meagher B. Red alert: perinatal hemorrhage. *MCN Am J Matern Child Nurs*. 2005;30(1):46-51.
67. Tuuli MG, Norman SM, Odibo AO, Macones GA, Cahill AG. Perinatal outcomes in women with subchorionic hematoma: a systematic review and meta-analysis. *Obstet Gynecol*. 2011;117(5):1205-1212.
68. Seki H, Kuromaki K, Takeda S, Kinoshita K. Persistent subchorionic hematoma with clinical symptoms until delivery. *Int J Gynaecol Obstet*. 1998;63(2):123-128.
69. Xiang L, Wei Z, Cao Y. Symptoms of an intrauterine hematoma associated with pregnancy complications: a systematic review. *PLoS One*. 2014;9(11):e111676.
70. Nyberg DA, Mack LA, Benedetti TJ, Cyr DR, Schuman WP. Placental abruption and placental hemorrhage: correlation of sonographic findings with fetal outcome. *Radiology*. 1987;164(2):357-361.
71. Roumenina LT, Rayes J, Lacroix-Desmazes S, Dimitrov JD. Heme: Modulator of Plasma Systems in Hemolytic Diseases. *Trends Mol Med*. 2016;22(3):200-213.

72. Shim BS, Lee TH, Kang YS. Immunological and biochemical investigations of human serum haptoglobin: composition of haptoglobin-haemoglobin intermediate, haemoglobin-binding sites and presence of additional alleles for beta-chain. *Nature*. 1965;207(5003):1264-1267.
73. Wagener FA, Volk HD, Willis D, et al. Different faces of the heme-heme oxygenase system in inflammation. *Pharmacol Rev*. 2003;55(3):551-571.
74. Tolosano E, Fagoonee S, Morello N, Vinchi F, Fiorito V. Heme scavenging and the other facets of hemopexin. *Antioxid Redox Signal*. 2010;12(2):305-320.
75. Tolosano E, Altruda F. Hemopexin: structure, function, and regulation. *DNA Cell Biol*. 2002;21(4):297-306.
76. Drabkin DL. Heme binding and transport--a spectrophotometric study of plasma glycoglobulin hemochromogens. *Proc Natl Acad Sci U S A*. 1971;68(3):609-613.
77. Sparkenbaugh EM, Chantrathammachart P, Wang S, et al. Excess of heme induces tissue factor-dependent activation of coagulation in mice. *Haematologica*. 2015;100(3):308-314.
78. Vinchi F, Gastaldi S, Silengo L, Altruda F, Tolosano E. Hemopexin prevents endothelial damage and liver congestion in a mouse model of heme overload. *Am J Pathol*. 2008;173(1):289-299.
79. Gbotosho OT, Kapetanaki MG, Ghosh S, Villanueva FS, Ofori-Acquah SF, Kato GJ. Heme Induces IL-6 and Cardiac Hypertrophy Genes Transcripts in Sick Cell Mice. *Front Immunol*. 2020;11:1910.
80. Sekhavat L, Davar R, Hosseini-dezoki S. Relationship between maternal hemoglobin concentration and neonatal birth weight. *Hematology*. 2011;16(6):373-376.
81. Zeng L, Dibley MJ, Cheng Y, et al. Impact of micronutrient supplementation during pregnancy on birth weight, duration of gestation, and perinatal mortality in rural western China: double blind cluster randomised controlled trial. *BMJ*. 2008;337:a2001.
82. Christian P, Osrin D, Manandhar DS, Khatri SK, de LCAM, West KP, Jr. Antenatal micronutrient supplements in Nepal. *Lancet*. 2005;366(9487):711-712.
83. Hubbard AC, Bandyopadhyay S, Wojczyk BS, Spitalnik SL, Hod EA, Prestia KA. Effect of dietary iron on fetal growth in pregnant mice. *Comp Med*. 2013;63(2):127-135.
84. Seeho SKM, Morris JM. Intravenous iron use in pregnancy: Ironing out the issues and evidence. *Aust Nz J Obstet Gyn*. 2018;58(2):145-147.
85. Hatcher H, Planalp R, Cho J, Torti FM, Torti SV. Curcumin: from ancient medicine to current clinical trials. *Cell Mol Life Sci*. 2008;65(11):1631-1652.
86. Epstein J, Sanderson IR, Macdonald TT. Curcumin as a therapeutic agent: the evidence from in vitro, animal and human studies. *Br J Nutr*. 2010;103(11):1545-1557.
87. Hill-Kapturczak N, Thamilselvan V, Liu F, Nick HS, Agarwal A. Mechanism of heme oxygenase-1 gene induction by curcumin in human renal proximal tubule cells. *Am J Physiol Renal Physiol*. 2001;281(5):F851-859.
88. Lima CF, Pereira-Wilson C, Rattan SI. Curcumin induces heme oxygenase-1 in normal human skin fibroblasts through redox signaling: relevance for anti-aging intervention. *Mol Nutr Food Res*. 2011;55(3):430-442.
89. Yang XB, Jiang H, Shi Y. Upregulation of heme oxygenase-1 expression by curcumin conferring protection from hydrogen peroxide-induced apoptosis in H9c2 cardiomyoblasts. *Cell Biosci*. 2017;7.
90. Filardi T, Vari R, Ferretti E, Zicari A, Morano S, Santangelo C. Curcumin: Could This Compound Be Useful in Pregnancy and Pregnancy-Related Complications? *Nutrients*. 2020;12(10).
91. Balogun E, Hoque M, Gong P, et al. Curcumin activates the haem oxygenase-1 gene via regulation of Nrf2 and the antioxidant-responsive element. *Biochem J*. 2003;371(Pt 3):887-895.
92. Vazquez-Fresno R, Rosana ARR, Sajed T, Onokome-Okome T, Wishart NA, Wishart DS. Herbs and Spices- Biomarkers of Intake Based on Human Intervention Studies - A Systematic Review. *Genes Nutr*. 2019;14:18.
93. El-Borm HT, Badawy GM, El-Nabi SH, El-Sherif WA, Atallah MN. The ameliorative effect of curcumin extract on the morphological and skeletal abnormalities induced by sunset yellow and tartrazine in the developing chick embryo *Gallus domesticus*. *Heliyon*. 2020;6(1):e03305.
94. Wu Y, Wang F, Reece EA, Yang P. Curcumin ameliorates high glucose-induced neural tube defects by suppressing cellular stress and apoptosis. *Am J Obstet Gynecol*. 2015;212(6):802 e801-808.
95. Salehi B, Calina D, Docea AO, et al. Curcumin's Nanomedicine Formulations for Therapeutic Application in Neurological Diseases. *J Clin Med*. 2020;9(2).

96. Zhou J, Miao H, Li X, Hu Y, Sun H, Hou Y. Curcumin inhibits placental inflammation to ameliorate LPS-induced adverse pregnancy outcomes in mice via upregulation of phosphorylated Akt. *Inflamm Res*. 2017;66(2):177-185.
97. Guo YZ, He P, Feng AM. Effect of curcumin on expressions of NF-kappa Bp65, TNF-alpha and IL-8 in placental tissue of premature birth of infected mice. *Asian Pac J Trop Med*. 2017;10(2):168-171.
98. Chen CC, Chan WH. Injurious effects of curcumin on maturation of mouse oocytes, fertilization and fetal development via apoptosis. *Int J Mol Sci*. 2012;13(4):4655-4672.
99. Alafiatayo AA, Lai KS, Syahida A, Mahmood M, Shaharuddin NA. Phytochemical Evaluation, Embryotoxicity, and Teratogenic Effects of Curcuma longa Extract on Zebrafish (Danio rerio). *Evid Based Complement Alternat Med*. 2019;2019:3807207.
100. Chen CC, Hsieh MS, Hsuw YD, Huang FJ, Chan WH. Hazardous effects of curcumin on mouse embryonic development through a mitochondria-dependent apoptotic signaling pathway. *Int J Mol Sci*. 2010;11(8):2839-2855.
101. Ganiger S, Malleshappa HN, Krishnappa H, Rajashekhar G, Ramakrishna Rao V, Sullivan F. A two generation reproductive toxicity study with curcumin, turmeric yellow, in Wistar rats. *Food Chem Toxicol*. 2007;45(1):64-69.
102. Salafia CM, Weigl C, Silberman L. The prevalence and distribution of acute placental inflammation in uncomplicated term pregnancies. *Obstet Gynecol*. 1989;73(3 Pt 1):383-389.
103. Abe E, Matsubara K, Oka K, Kusanagi Y, Ito M. Cytokine regulation of intercellular adhesion molecule-1 expression on trophoblasts in preeclampsia. *Gynecol Obstet Invest*. 2008;66(1):27-33.
104. Erol AYG, Nazli M, Yildiz SE. Significance of platelet endothelial cell adhesion molecule-1 (PECAM-1) and intercellular adhesion molecule-1 (ICAM-1) expressions in preeclamptic placentae. *Endocrine*. 2012;42(1):125-131.
105. Rana S, Lemoine E, Granger JP, Karumanchi SA. Preeclampsia: Pathophysiology, Challenges, and Perspectives. *Circ Res*. 2019;124(7):1094-1112.
106. Al-Jameil N, Aziz Khan F, Fareed Khan M, Tabassum H. A brief overview of preeclampsia. *J Clin Med Res*. 2014;6(1):1-7.
107. Fan X, Rai A, Kambham N, et al. Endometrial VEGF induces placental sFLT1 and leads to pregnancy complications. *J Clin Invest*. 2014;124(11):4941-4952.
108. Guenther S, Vrekoussis T, Heublein S, et al. Decidual Macrophages Are Significantly Increased in Spontaneous Miscarriages and Over-Express FasL: A Potential Role for Macrophages in Trophoblast Apoptosis. *Int J Mol Sci*. 2012;13(7):9069-9080.
109. Lambropoulou M, Tamiolakis D, Venizelos J, et al. Imbalance of mononuclear cell infiltrates in the placental tissue from foetuses after spontaneous abortion versus therapeutic termination from 8th to 12th weeks of gestational age. *Clin Exp Med*. 2006;6(4):171-176.
110. Korkmazer E, Nizam R, Arslan E, Akkurt O. Relationship between intercellular adhesion molecule-1 and morbidly adherent placenta. *J Perinat Med*. 2019;47(1):45-49.
111. Baviera G, D'Anna R, Corrado F, Ruello A, Buemi M, Jasonni VM. ICAM-1 in maternal serum and amniotic fluid as an early marker of preeclampsia and IUGR. *J Reprod Med*. 2002;47(3):191-193.
112. Szarka A, Rigo J, Jr., Lazar L, Beko G, Molvarec A. Circulating cytokines, chemokines and adhesion molecules in normal pregnancy and preeclampsia determined by multiplex suspension array. *BMC Immunol*. 2010;11:59.
113. Blois S, Tometten M, Kandil J, et al. Intercellular adhesion molecule-1/LFA-1 cross talk is a proximate mediator capable of disrupting immune integration and tolerance mechanism at the fetomaternal interface in murine pregnancies. *J Immunol*. 2005;174(4):1820-1829.
114. Shen F, Wei J, Snowise S, et al. Trophoblast debris extruded from preeclamptic placentae activates endothelial cells: a mechanism by which the placenta communicates with the maternal endothelium. *Placenta*. 2014;35(10):839-847.
115. Takeshita T, Satomi M, Akira S, Nakagawa Y, Takahashi H, Araki T. Preventive effect of monoclonal antibodies to intercellular adhesion molecule-1 and leukocyte function-associate antigen-1 on murine spontaneous fetal resorption. *Am J Reprod Immunol*. 2000;43(3):180-185.
116. Nagamatsu T, Schust DJ. The contribution of macrophages to normal and pathological pregnancies. *Am J Reprod Immunol*. 2010;63(6):460-471.
117. Ambarus CA, Krausz S, van Eijk M, et al. Systematic validation of specific phenotypic markers for in vitro polarized human macrophages. *J Immunol Methods*. 2012;375(1-2):196-206.

118. Gordon S. Alternative activation of macrophages. *Nat Rev Immunol*. 2003;3(1):23-35.
119. Williams KC, Kim WK. Editorial: Identification of in vivo markers for human polarized macrophages: a need that's finally met. *J Leukoc Biol*. 2015;98(4):449-450.
120. Italiani P, Boraschi D. From Monocytes to M1/M2 Macrophages: Phenotypical vs. Functional Differentiation. *Front Immunol*. 2014;5:514.
121. Lu CH, Lai CY, Yeh DW, et al. Involvement of M1 Macrophage Polarization in Endosomal Toll-Like Receptors Activated Psoriatic Inflammation. *Mediators Inflamm*. 2018;2018:3523642.
122. Martinez FO, Sica A, Mantovani A, Locati M. Macrophage activation and polarization. *Front Biosci*. 2008;13:453-461.
123. Tsao FY, Wu MY, Chang YL, Wu CT, Ho HN. M1 macrophages decrease in the deciduae from normal pregnancies but not from spontaneous abortions or unexplained recurrent spontaneous abortions. *J Formos Med Assoc*. 2018;117(3):204-211.
124. Medeiros LT, Peracoli JC, Bannwart-Castro CF, et al. Monocytes from pregnant women with pre-eclampsia are polarized to a M1 phenotype. *Am J Reprod Immunol*. 2014;72(1):5-13.
125. Huppertz B, Kingdom J, Caniggia I, et al. Hypoxia favours necrotic versus apoptotic shedding of placental syncytiotrophoblast into the maternal circulation. *Placenta*. 2003;24(2-3):181-190.
126. Hutter S, Heublein S, Knabl J, et al. Macrophages: Are They Involved in Endometriosis, Abortion and Preeclampsia and How? *J Nippon Med Sch*. 2013;80(2):97-103.
127. Li Y, Xie Z, Wang Y, Hu H. Macrophage M1/M2 polarization in patients with pregnancy-induced hypertension. *Can J Physiol Pharmacol*. 2018;96(9):922-928.
128. Heikkinen J, Mottonen M, Komi J, Alanen A, Lassila O. Phenotypic characterization of human decidual macrophages. *Clin Exp Immunol*. 2003;131(3):498-505.
129. Gustafsson C, Mjosberg J, Matussek A, et al. Gene expression profiling of human decidual macrophages: evidence for immunosuppressive phenotype. *PLoS One*. 2008;3(4):e2078.
130. Schonkeren D, van der Hoorn ML, Khedoe P, et al. Differential distribution and phenotype of decidual macrophages in preeclampsic versus control pregnancies. *Am J Pathol*. 2011;178(2):709-717.
131. Svensson J, Jenmalm MC, Matussek A, Geffers R, Berg G, Ernerudh J. Macrophages at the Fetal-Maternal Interface Express Markers of Alternative Activation and Are Induced by M-CSF and IL-10. *Journal of Immunology*. 2011;187(7):3671-3682.
132. Svensson-Arvelund J, Ernerudh J. The Role of Macrophages in Promoting and Maintaining Homeostasis at the Fetal-Maternal Interface. *Am J Reprod Immunol*. 2015;74(2):100-109.
133. Sharps MC, Baker BC, Guevara T, et al. Increased placental macrophages and a pro-inflammatory profile in placentas and maternal serum in infants with a decreased growth rate in the third trimester of pregnancy. *Am J Reprod Immunol*. 2020;84(3):e13267.
134. Mao L, Zhou Q, Zhou S, Wilbur RR, Li X. Roles of apolipoprotein E (ApoE) and inducible nitric oxide synthase (iNOS) in inflammation and apoptosis in preeclampsia pathogenesis and progression. *PLoS One*. 2013;8(3):e58168.
135. Brown MB, von Chamier M, Allam AB, Reyes L. M1/M2 macrophage polarity in normal and complicated pregnancy. *Front Immunol*. 2014;5:606.
136. Weis N, Weigert A, von Knethen A, Brune B. Heme oxygenase-1 contributes to an alternative macrophage activation profile induced by apoptotic cell supernatants. *Mol Biol Cell*. 2009;20(5):1280-1288.
137. Ndisang JF, Mishra M. The heme oxygenase system selectively suppresses the proinflammatory macrophage m1 phenotype and potentiates insulin signaling in spontaneously hypertensive rats. *Am J Hypertens*. 2013;26(9):1123-1131.
138. Jadhav A, Tiwari S, Lee P, Ndisang JF. The heme oxygenase system selectively enhances the anti-inflammatory macrophage-M2 phenotype, reduces pericardial adiposity, and ameliorated cardiac injury in diabetic cardiomyopathy in Zucker diabetic fatty rats. *J Pharmacol Exp Ther*. 2013;345(2):239-249.
139. Choi KM, Kashyap PC, Dutta N, et al. CD206-Positive M2 Macrophages That Express Heme Oxygenase-1 Protect Against Diabetic Gastroparesis in Mice. *Gastroenterology*. 2010;138(7):2399-U2261.
140. Vinchi F, Costa da Silva M, Ingoglia G, et al. Hemopexin therapy reverts heme-induced proinflammatory phenotypic switching of macrophages in a mouse model of sickle cell disease. *Blood*. 2016;127(4):473-486.

141. May P, Bock HH, Nofer JR. Low density receptor-related protein 1 (LRP1) promotes anti-inflammatory phenotype in murine macrophages. *Cell Tissue Res*. 2013;354(3):887-889.
142. Naito Y, Takagi T, Higashimura Y. Heme oxygenase-1 and anti-inflammatory M2 macrophages. *Arch Biochem Biophys*. 2014;564:83-88.
143. Kreiser D, Nguyen X, Wong R, et al. Heme oxygenase-1 modulates fetal growth in the rat. *Lab Invest*. 2002;82(6):687-692.
144. Yachie A, Niida Y, Wada T, et al. Oxidative stress causes enhanced endothelial cell injury in human heme oxygenase-1 deficiency. *J Clin Invest*. 1999;103(1):129-135.
145. Poss KD, Tonegawa S. Heme oxygenase 1 is required for mammalian iron reutilization. *Proc Natl Acad Sci U S A*. 1997;94(20):10919-10924.
146. Ahmed A, Rahman M, Zhang X, et al. Induction of placental heme oxygenase-1 is protective against TNFalpha-induced cytotoxicity and promotes vessel relaxation. *Mol Med*. 2000;6(5):391-409.
147. McLaughlin BE, Hutchinson JM, Graham CH, et al. Heme oxygenase activity in term human placenta. *Placenta*. 2000;21(8):870-873.
148. Ihara N, Akagi R, Ejiri K, Kudo T, Furuyama K, Fujita H. Developmental changes of gene expression in heme metabolic enzymes in rat placenta. *FEBS Lett*. 1998;439(1-2):163-167.
149. Watanabe S, Akagi R, Mori M, Tsuchiya T, Sassa S. Marked developmental changes in heme oxygenase-1 (HO-1) expression in the mouse placenta: correlation between HO-1 expression and placental development. *Placenta*. 2004;25(5):387-395.
150. Venditti CC, Casselman R, Murphy MSQ, Adamson SL, Sled JG, Smith GN. Chronic carbon monoxide inhalation during pregnancy augments uterine artery blood flow and uteroplacental vascular growth in mice. *Am J Physiol-Reg I*. 2013;305(8):R939-R948.
151. George EM, Cockrell K, Aranay M, Csongradi E, Stec DE, Granger JP. Induction of heme oxygenase 1 attenuates placental ischemia-induced hypertension. *Hypertension*. 2011;57(5):941-948.
152. George EM, Stout JM, Stec DE, Granger JP. Heme oxygenase induction attenuates TNF-alpha-induced hypertension in pregnant rodents. *Front Pharmacol*. 2015;6:165.
153. Solano ME, Kowal MK, O'Rourke GE, et al. Progesterone and HMOX-1 promote fetal growth by CD8+ T cell modulation. *J Clin Invest*. 2015;125(4):1726-1738.
154. El-Mousleh T, Casalis PA, Wollenberg I, et al. Exploring the potential of low doses carbon monoxide as therapy in pregnancy complications. *Med Gas Res*. 2012;2(1):4.
155. Bussolati B, Mason JC. Dual role of VEGF-induced heme-oxygenase-1 in angiogenesis. *Antioxid Redox Signal*. 2006;8(7-8):1153-1163.
156. Exner M, Minar E, Wagner O, Schillinger M. The role of heme oxygenase-1 promoter polymorphisms in human disease. *Free Radic Biol Med*. 2004;37(8):1097-1104.
157. Millicovsky G, Johnston MC. Hyperoxia and hypoxia in pregnancy: simple experimental manipulation alters the incidence of cleft lip and palate in CL/Fr mice. *Proc Natl Acad Sci U S A*. 1981;78(9):5722-5723.
158. Bailey LJ, Johnston MC, Billet J. Effects of carbon monoxide and hypoxia on cleft lip in A/J mice. *Cleft Palate Craniofac J*. 1995;32(1):14-19.
159. Shi M, Wehby GL, Murray JC. Review on genetic variants and maternal smoking in the etiology of oral clefts and other birth defects. *Birth Defects Res C Embryo Today*. 2008;84(1):16-29.
160. DeRoo LA, Wilcox AJ, Drevon CA, Lie RT. First-trimester maternal alcohol consumption and the risk of infant oral clefts in Norway: a population-based case-control study. *Am J Epidemiol*. 2008;168(6):638-646.
161. Correa A, Gilboa SM, Besser LM, et al. Diabetes mellitus and birth defects. *Am J Obstet Gynecol*. 2008;199(3):237 e231-239.
162. Wyszynski DF, Beaty TH. Review of the role of potential teratogens in the origin of human nonsyndromic oral clefts. *Teratology*. 1996;53(5):309-317.
163. Mitchell LE, Murray JC, O'Brien S, Christensen K. Retinoic acid receptor alpha gene variants, multivitamin use, and liver intake as risk factors for oral clefts: a population-based case-control study in Denmark, 1991-1994. *Am J Epidemiol*. 2003;158(1):69-76.
164. Silva H, Arruda TTS, Souza KSC, et al. Risk factors and comorbidities in Brazilian patients with orofacial clefts. *Braz Oral Res*. 2018;32:e24.
165. Logan SM, Benson MD. Medial epithelial seam cell migration during palatal fusion. *J Cell Physiol*. 2020;235(2):1417-1424.

166. Aoyama G, Kurosaka H, Oka A, et al. Observation of Dynamic Cellular Migration of the Medial Edge Epithelium of the Palatal Shelf in vitro. *Front Physiol.* 2019;10:698.
167. Jin JZ, Ding J. Analysis of cell migration, transdifferentiation and apoptosis during mouse secondary palate fusion. *Development.* 2006;133(17):3341-3347.
168. Nakajima A, C FS, Gulka AOD, Hanai JI. TGF-beta Signaling and the Epithelial-Mesenchymal Transition during Palatal Fusion. *Int J Mol Sci.* 2018;19(11).
169. Lan Y, Xu J, Jiang R. Cellular and Molecular Mechanisms of Palatogenesis. *Curr Top Dev Biol.* 2015;115:59-84.
170. Iseki S. Disintegration of the medial epithelial seam: is cell death important in palatogenesis? *Dev Growth Differ.* 2011;53(2):259-268.
171. Verheijen N, Suttorp CM, van Rheden REM, et al. CXCL12-CXCR4 Interplay Facilitates Palatal Osteogenesis in Mice. *Front Cell Dev Biol.* 2020;8:771.
172. Zhang S, Che D, Yang F, et al. Tumor-associated macrophages promote tumor metastasis via the TGF-beta/SOX9 axis in non-small cell lung cancer. *Oncotarget.* 2017;8(59):99801-99815.
173. Huang JQ, Wei FK, Xu XL, et al. SOX9 drives the epithelial-mesenchymal transition in non-small-cell lung cancer through the Wnt/beta-catenin pathway. *J Transl Med.* 2019;17(1):143.
174. Kogata N, Bland P, Tsang M, Oliemuller E, Lowe A, Howard BA. Sox9 regulates cell state and activity of embryonic mouse mammary progenitor cells. *Commun Biol.* 2018;1.
175. Li T, Huang H, Shi G, et al. TGF-beta1-SOX9 axis-inducible COL10A1 promotes invasion and metastasis in gastric cancer via epithelial-to-mesenchymal transition. *Cell Death Dis.* 2018;9(9):849.
176. Choi BJ, Park SA, Lee SY, Cha YN, Surh YJ. Hypoxia induces epithelial-mesenchymal transition in colorectal cancer cells through ubiquitin-specific protease 47-mediated stabilization of Snail: A potential role of Sox9. *Sci Rep.* 2017;7(1):15918.
177. Kawai T, Yasuchika K, Ishii T, et al. SOX9 is a novel cancer stem cell marker surrogated by osteopontin in human hepatocellular carcinoma. *Sci Rep-Uk.* 2016;6.
178. Huang J, Guo L. Knockdown of SOX9 Inhibits the Proliferation, Invasion, and EMT in Thyroid Cancer Cells. *Oncol Res.* 2017;25(2):167-176.
179. Sakai D, Suzuki T, Osumi N, Wakamatsu Y. Cooperative action of Sox9, Snail2 and PKA signaling in early neural crest development. *Development.* 2006;133(7):1323-1333.
180. Siemieniuch MJ. Apoptotic changes in the epithelium germinativum of the cat (*Felis catus* s. domestica, L. 1758) at different ages and breeding seasons. *Reprod Domest Anim.* 2008;43(4):473-476.
181. Fitchett JE, Hay ED. Medial edge epithelium transforms to mesenchyme after embryonic palatal shelves fuse. *Dev Biol.* 1989;131(2):455-474.
182. Shapiro BL, Sweney L. Electron microscopic and histochemical examination of oral epithelial-mesenchymal interaction (programmed cell death). *J Dent Res.* 1969;48(5):652-660.
183. Sun D, Baur S, Hay ED. Epithelial-mesenchymal transformation is the mechanism for fusion of the craniofacial primordia involved in morphogenesis of the chicken lip. *Dev Biol.* 2000;228(2):337-349.
184. Dudas M, Li WY, Kim J, Yang A, Kaartinen V. Palatal fusion - where do the midline cells go? A review on cleft palate, a major human birth defect. *Acta Histochem.* 2007;109(1):1-14.
185. He F, Xiong W, Wang Y, et al. Epithelial Wnt/beta-catenin signaling regulates palatal shelf fusion through regulation of Tgfbeta3 expression. *Dev Biol.* 2011;350(2):511-519.
186. Kim S, Lewis AE, Singh V, Ma X, Adelstein R, Bush JO. Convergence and extrusion are required for normal fusion of the mammalian secondary palate. *PLoS Biol.* 2015;13(4):e1002122.
187. Mori C, Nakamura N, Okamoto Y, Osawa M, Shiota K. Cytochemical identification of programmed cell death in the fusing fetal mouse palate by specific labelling of DNA fragmentation. *Anat Embryol (Berl).* 1994;190(1):21-28.
188. Cuervo R, Covarrubias L. Death is the major fate of medial edge epithelial cells and the cause of basal lamina degradation during palatogenesis. *Development.* 2004;131(1):15-24.
189. Cuervo R, Valencia C, Chandraratna RA, Covarrubias L. Programmed cell death is required for palate shelf fusion and is regulated by retinoic acid. *Dev Biol.* 2002;245(1):145-156.
190. Huang X, Yokota T, Iwata J, Chai Y. Tgf-beta-mediated FasL-Fas-Caspase pathway is crucial during palatogenesis. *J Dent Res.* 2011;90(8):981-987.
191. Takahara S, Takigawa T, Shiota K. Programmed cell death is not a necessary prerequisite for fusion of the fetal mouse palate. *Int J Dev Biol.* 2004;48(1):39-46.

192. Knott L, Hartridge T, Brown NL, Mansell JP, Sandy JR. Homocysteine oxidation and apoptosis: a potential cause of cleft palate. *In Vitro Cell Dev Biol Anim.* 2003;39(1-2):98-105.
193. DePaola DP, Mandella RD. Folate deficiency and in vitro palatogenesis II: Effects of methotrexate on rabbit palate fusion, folate pools, and dihydrofolate reductase activity. *J Craniofac Genet Dev Biol.* 1984;4(4):321-327.
194. Martinez-Alvarez C, Tudela C, Perez-Miguelsanz J, O'Kane S, Puerta J, Ferguson MW. Medial edge epithelial cell fate during palatal fusion. *Dev Biol.* 2000;220(2):343-357.
195. Nanda R, Kelly WM. Ultrastructural Study of Palatal Fusion in Rat Embryos. *Journal of Dental Research.* 1973;52:111-8.
196. Hughes LV, Furstman L, Bernick S. Prenatal development of the rat palate. *Journal of dental research.* 1967;46(2):373-379.
197. Matthiessen M, Andersen H. Disintegration of the junctional epithelium of human fetal hard palate. *Z Anat Entwicklungsgesch.* 1972;137(2):153-169.
198. Luke DA. Development of the secondary palate in man. *Acta Anat (Basel).* 1976;94(4):596-608.
199. Torraca V, Cui C, Boland R, et al. The CXCR3-CXCL11 signaling axis mediates macrophage recruitment and dissemination of mycobacterial infection. *Dis Model Mech.* 2015;8(3):253-269.
200. Sommer F, Torraca V, Kamel SM, Lombardi A, Meijer AH. Frontline Science: Antagonism between regular and atypical Cxcr3 receptors regulates macrophage migration during infection and injury in zebrafish. *J Leukocyte Biol.* 2020;107(2):185-203.
201. Chakravarty SD, Xu J, Lu B, Gerard C, Flynn J, Chan J. The chemokine receptor CXCR3 attenuates the control of chronic Mycobacterium tuberculosis infection in BALB/c mice. *J Immunol.* 2007;178(3):1723-1735.
202. Kakuta Y, Okumi M, Miyagawa S, et al. Blocking of CCR5 and CXCR3 suppresses the infiltration of macrophages in acute renal allograft rejection. *Transplantation.* 2012;93(1):24-31.
203. Yates CC, Krishna P, Whaley D, Bodnar R, Turner T, Wells A. Lack of CXC chemokine receptor 3 signaling leads to hypertrophic and hypercellular scarring. *Am J Pathol.* 2010;176(4):1743-1755.
204. Bunemann E, Hoff NP, Buhren BA, et al. Chemokine ligand-receptor interactions critically regulate cutaneous wound healing. *Eur J Med Res.* 2018;23(1):4.
205. Kanda N, Watanabe S. Prolactin enhances interferon-gamma-induced production of CXC ligand 9 (CXCL9), CXCL10, and CXCL11 in human keratinocytes. *Endocrinology.* 2007;148(5):2317-2325.
206. Satish L, Blair HC, Glading A, Wells A. Interferon-inducible protein 9 (CXCL11)-induced cell motility in keratinocytes requires calcium flux-dependent activation of mu-calpain. *Mol Cell Biol.* 2005;25(5):1922-1941.
207. Kroeze KL, Boink MA, Sampat-Sardjoeppersad SC, Waaijman T, Scheper RJ, Gibbs S. Autocrine regulation of re-epithelialization after wounding by chemokine receptors CCR1, CCR10, CXCR1, CXCR2, and CXCR3. *J Invest Dermatol.* 2012;132(1):216-225.
208. Bu X, Bi X, Wang W, Shi Y, Hou Q, Gu J. Effects of recombinant human parathyroid hormone (1-34) on cell proliferation, chemokine expression and the Hedgehog pathway in keratinocytes. *Mol Med Rep.* 2018;17(4):5589-5594.
209. Bellner L, Marrazzo G, van Rooijen N, Dunn MW, Abraham NG, Schwartzman ML. Heme oxygenase-2 deletion impairs macrophage function: implication in wound healing. *FASEB J.* 2015;29(1):105-115.
210. Hull TD, Agarwal A, George JF. The mononuclear phagocyte system in homeostasis and disease: a role for heme oxygenase-1. *Antioxid Redox Signal.* 2014;20(11):1770-1788.
211. Schaer CA, Schoedon G, Imhof A, Kurrer MO, Schaer DJ. Constitutive endocytosis of CD163 mediates hemoglobin-heme uptake and determines the noninflammatory and protective transcriptional response of macrophages to hemoglobin. *Circ Res.* 2006;99(9):943-950.
212. Schaer DJ, Buehler PW, Alayash AI, Belcher JD, Vercellotti GM. Hemolysis and free hemoglobin revisited: exploring hemoglobin and heme scavengers as a novel class of therapeutic proteins. *Blood.* 2013;121(8):1276-1284.
213. Kristiansen M, Graversen JH, Jacobsen C, et al. Identification of the haemoglobin scavenger receptor. *Nature.* 2001;409(6817):198-201.
214. Hvidberg V, Maniecki MB, Jacobsen C, Hojrup P, Moller HJ, Moestrup SK. Identification of the receptor scavenging hemopexin-heme complexes. *Blood.* 2005;106(7):2572-2579.
215. Smith A, McCulloh RJ. Hemopexin and haptoglobin: allies against heme toxicity from hemoglobin not contenders. *Front Physiol.* 2015;6:187.

216. Eisenstein RS, Garcia-Mayol D, Pettingell W, Munro HN. Regulation of ferritin and heme oxygenase synthesis in rat fibroblasts by different forms of iron. *Proc Natl Acad Sci U S A*. 1991;88(3):688-692.
217. George EM, Warrington JP, Spradley FT, Palei AC, Granger JP. The heme oxygenases: important regulators of pregnancy and preeclampsia. *Am J Physiol Regul Integr Comp Physiol*. 2014;307(7):R769-777.
218. Kovtunovych G, Eckhaus MA, Ghosh MC, Ollivierre-Wilson H, Rouault TA. Dysfunction of the heme recycling system in heme oxygenase 1-deficient mice: effects on macrophage viability and tissue iron distribution. *Blood*. 2010;116(26):6054-6062.
219. Nakamichi I, Habtezion A, Zhong B, Contag CH, Butcher EC, Omary MB. Hemin-activated macrophages home to the pancreas and protect from acute pancreatitis via heme oxygenase-1 induction. *J Clin Invest*. 2005;115(11):3007-3014.
220. Vijayan V, Wagener F, Immenschuh S. The macrophage heme-heme oxygenase-1 system and its role in inflammation. *Biochem Pharmacol*. 2018;153:159-167.
221. Hammal Z, Cohn JF, Wallace ER, et al. Facial Expressiveness in Infants With and Without Craniofacial Microsomia: Preliminary Findings. *Cleft Palate Craniofac J*. 2018;55(5):711-720.
222. Lee YH, Saint-Jeannet JP. Sox9 function in craniofacial development and disease. *Genesis*. 2011;49(4):200-208.
223. Trainor PA. Specification and patterning of neural crest cells during craniofacial development. *Brain Behav Evol*. 2005;66(4):266-280.
224. Nie X. Sox9 mRNA expression in the developing palate and craniofacial muscles and skeletons. *Acta Odontol Scand*. 2006;64(2):97-103.
225. Casale J, Giwa AO. Embryology, Branchial Arches. In: *StatPearls*. Treasure Island (FL)2021.
226. Dixon J, Jones NC, Sandell LL, et al. Tcof1/Treacle is required for neural crest cell formation and proliferation deficiencies that cause craniofacial abnormalities. *Proc Natl Acad Sci U S A*. 2006;103(36):13403-13408.
227. Gilbert W, Bragg R, Elmanshi AM, et al. Stromal cell-derived factor-1 (CXCL12) and its role in bone and muscle biology. *Cytokine*. 2019;123:154783.
228. Ma Q, Jones D, Borghesani PR, et al. Impaired B-lymphopoiesis, myelopoiesis, and derailed cerebellar neuron migration in CXCR4- and SDF-1-deficient mice. *Proc Natl Acad Sci U S A*. 1998;95(16):9448-9453.
229. Tachibana K, Hirota S, Iizasa H, et al. The chemokine receptor CXCR4 is essential for vascularization of the gastrointestinal tract. *Nature*. 1998;393(6685):591-594.
230. Nagasawa T, Hirota S, Tachibana K, et al. Defects of B-cell lymphopoiesis and bone-marrow myelopoiesis in mice lacking the CXC chemokine PBSF/SDF-1. *Nature*. 1996;382(6592):635-638.
231. Hammond NL, Brookes KJ, Dixon MJ. Ectopic Hedgehog Signaling Causes Cleft Palate and Defective Osteogenesis. *J Dent Res*. 2018;97(13):1485-1493.
232. Cibi DM, Mia MM, Guna Shekeran S, et al. Neural crest-specific deletion of Rbfox2 in mice leads to craniofacial abnormalities including cleft palate. *Elife*. 2019;8.
233. Wu M, Li J, Engleka KA, et al. Persistent expression of Pax3 in the neural crest causes cleft palate and defective osteogenesis in mice. *J Clin Invest*. 2008;118(6):2076-2087.
234. Parada C, Han D, Grimaldi A, et al. Disruption of the ERK/MAPK pathway in neural crest cells as a potential cause of Pierre Robin sequence. *Development*. 2015;142(21):3734-3745.
235. Chen Y, Wang Z, Chen Y, Zhang Y. Conditional deletion of Bmp2 in cranial neural crest cells recapitulates Pierre Robin sequence in mice. *Cell Tissue Res*. 2019;376(2):199-210.
236. Hosogane N, Huang Z, Rawlins BA, et al. Stromal derived factor-1 regulates bone morphogenetic protein 2-induced osteogenic differentiation of primary mesenchymal stem cells. *Int J Biochem Cell Biol*. 2010;42(7):1132-1141.
237. Tzeng YS, Chung NC, Chen YR, Huang HY, Chuang WP, Lai DM. Imbalanced Osteogenesis and Adipogenesis in Mice Deficient in the Chemokine Cxcl12/Sdf1 in the Bone Mesenchymal Stem/Progenitor Cells. *J Bone Miner Res*. 2018;33(4):679-690.
238. Ito H. Chemokines in mesenchymal stem cell therapy for bone repair: a novel concept of recruiting mesenchymal stem cells and the possible cell sources. *Mod Rheumatol*. 2011;21(2):113-121.
239. Xu J, Chen Y, Liu Y, et al. Effect of SDF-1/Cxcr4 Signaling Antagonist AMD3100 on Bone Mineralization in Distraction Osteogenesis. *Calcif Tissue Int*. 2017;100(6):641-652.

240. Sordi V, Malosio ML, Marchesi F, et al. Bone marrow mesenchymal stem cells express a restricted set of functionally active chemokine receptors capable of promoting migration to pancreatic islets. *Blood*. 2005;106(2):419-427.
241. Suttrop CM, Cremers NA, van Rheden R, et al. Chemokine Signaling during Midline Epithelial Seam Disintegration Facilitates Palatal Fusion. *Front Cell Dev Biol*. 2017;5:94.
242. Lourenco Ribeiro L, Teixeira Das Neves L, Costa B, Ribeiro Gomide M. Dental anomalies of the permanent lateral incisors and prevalence of hypodontia outside the cleft area in complete unilateral cleft lip and palate. *Cleft Palate Craniofac J*. 2003;40(2):172-175.
243. Tortora C, Meazzini MC, Garattini G, Brusati R. Prevalence of abnormalities in dental structure, position, and eruption pattern in a population of unilateral and bilateral cleft lip and palate patients. *Cleft Palate Craniofac J*. 2008;45(2):154-162.
244. Akcam MO, Evirgen S, Uslu O, Memikoglu UT. Dental anomalies in individuals with cleft lip and/or palate. *Eur J Orthod*. 2010;32(2):207-213.
245. Brouwer KM, Lundvig DM, Middelkoop E, Wagener FA, Von den Hoff JW. Mechanical cues in orofacial tissue engineering and regenerative medicine. *Wound Repair Regen*. 2015;23(3):302-311.
246. Li J, Johnson CA, Smith AA, et al. Disrupting the intrinsic growth potential of a suture contributes to midfacial hypoplasia. *Bone*. 2015;81:186-195.
247. Shetye P. Orthodontic management of patients with cleft lip and palate. *APOS Trends in Orthodontics*. 2016;6:281.
248. Pi SH, Jeong GS, Oh HW, et al. Heme oxygenase-1 mediates nicotine- and lipopolysaccharide-induced expression of cyclooxygenase-2 and inducible nitric oxide synthase in human periodontal ligament cells. *J Periodontol Res*. 2010;45(2):177-183.
249. Kim YS, Pi SH, Lee YM, Lee SI, Kim EC. The anti-inflammatory role of heme oxygenase-1 in lipopolysaccharide and cytokine-stimulated inducible nitric oxide synthase and nitric oxide production in human periodontal ligament cells. *J Periodontol*. 2009;80(12):2045-2055.
250. Song L, Li J, Yuan X, et al. Carbon monoxide-releasing molecule suppresses inflammatory and osteoclastogenic cytokines in nicotine- and lipopolysaccharide-stimulated human periodontal ligament cells via the heme oxygenase-1 pathway. *Int J Mol Med*. 2017;40(5):1591-1601.
251. Lee HJ, Jeong GS, Pi SH, et al. Heme oxygenase-1 protects human periodontal ligament cells against substance P-induced RANKL expression. *J Periodontol Res*. 2010;45(3):367-374.
252. Kook YA, Lee SK, Son DH, et al. Effects of substance P on osteoblastic differentiation and heme oxygenase-1 in human periodontal ligament cells. *Cell Biol Int*. 2009;33(3):424-428.
253. Cho JH, Lee SK, Lee JW, Kim EC. The role of heme oxygenase-1 in mechanical stress- and lipopolysaccharide-induced osteogenic differentiation in human periodontal ligament cells. *Angle Orthod*. 2010;80(4):552-559.
254. Kameyama T, Matsumoto Y, Warita H, Soma K. Inactivated periods of constant orthodontic forces related to desirable tooth movement in rats. *J Orthod*. 2003;30(1):31-37; discussion 21-32.
255. Zwerina J, Tzima S, Hayer S, et al. Heme oxygenase 1 (HO-1) regulates osteoclastogenesis and bone resorption. *Faseb Journal*. 2005;19(12):2011-+.
256. Lu SH, Chen TH, Chou TC. Magnolol Inhibits RANKL-induced osteoclast differentiation of raw 264.7 macrophages through heme oxygenase-1-dependent inhibition of NFATc1 expression. *J Nat Prod*. 2015;78(1):61-68.
257. Bak SU, Kim S, Hwang HJ, et al. Heme oxygenase-1 (HO-1)/carbon monoxide (CO) axis suppresses RANKL-induced osteoclastic differentiation by inhibiting redox-sensitive NF-kappa B activation. *Bmb Rep*. 2017;50(2):103-108.
258. Davidson JM, Yu F, Opalenik SR. Splinting Strategies to Overcome Confounding Wound Contraction in Experimental Animal Models. *Adv Wound Care (New Rochelle)*. 2013;2(4):142-148.
259. Naldaiz-Gastesi N, Bahri OA, Lopez de Munain A, McCullagh KJA, Izeta A. The panniculus carnosus muscle: an evolutionary enigma at the intersection of distinct research fields. *J Anat*. 2018.
260. Galiano RD, Michaels Jt, Dobryansky M, Levine JP, Gurtner GC. Quantitative and reproducible murine model of excisional wound healing. *Wound Repair Regen*. 2004;12(4):485-492.
261. Mascharak S, desJardins-Park HE, Davitt MF, et al. Preventing Engrailed-1 activation in fibroblasts yields wound regeneration without scarring. *Science*. 2021;372(6540).

262. Son D, Harijan A. Overview of surgical scar prevention and management. *J Korean Med Sci*. 2014;29(6):751-757.
263. Rousseau P, Metzger M, Frucht S, Schupp W, Hempel M, Otten J-E. Effect of lip closure on early maxillary growth in patients with cleft lip and palate. *JAMA Facial Plast Surg*. 2013;15(5):369-373.
264. Nollet PJ, Katsaros C, Van't Hof MA, Kuijpers-Jagtman AM. Treatment outcome in unilateral cleft lip and palate evaluated with the GOSLON yardstick: a meta-analysis of 1236 patients. *Plast Reconstr Surg*. 2005;116(5):1255-1262.
265. Chen QY, Wang GG, Li W, Jiang YX, Lu XH, Zhou PP. Heme Oxygenase-1 Promotes Delayed Wound Healing in Diabetic Rats. *J Diabetes Res*. 2016;2016:9726503.
266. Ahanger AA, Prawez S, Kumar D, et al. Wound healing activity of carbon monoxide liberated from CO-releasing molecule (CO-RM). *Naunyn Schmiedebergs Arch Pharmacol*. 2011;384(1):93-102.
267. Ram M, Singh V, Kumawat S, Kant V, Tandan SK, Kumar D. Bilirubin modulated cytokines, growth factors and angiogenesis to improve cutaneous wound healing process in diabetic rats. *Int Immunopharmacol*. 2016;30:137-149.
268. Ahanger AA, Leo MD, Gopal A, Kant V, Tandan SK, Kumar D. Pro-healing effects of bilirubin in open excision wound model in rats. *Int Wound J*. 2016;13(3):398-402.
269. Clark JE, Green CJ, Motterlini R. Involvement of the heme oxygenase-carbon monoxide pathway in keratinocyte proliferation. *Biochem Biophys Res Commun*. 1997;241(2):215-220.
270. Wagener FA, van Beurden HE, von den Hoff JW, Adema GJ, Figdor CG. The heme-heme oxygenase system: a molecular switch in wound healing. *Blood*. 2003;102(2):521-528.
271. Lundvig DM, Scharstuhl A, Cremers NA, et al. Delayed cutaneous wound closure in HO-2 deficient mice despite normal HO-1 expression. *J Cell Mol Med*. 2014;18(12):2488-2498.
272. Bellner L, Wolstein J, Patil KA, Dunn MW, Laniado-Schwartzman M. Biliverdin Rescues the HO-2 Null Mouse Phenotype of Unresolved Chronic Inflammation Following Corneal Epithelial Injury. *Invest Ophthalmol Vis Sci*. 2011;52(6):3246-3253.
273. Chen D, Hao H, Tong C, et al. Transdifferentiation of Umbilical Cord-Derived Mesenchymal Stem Cells Into Epidermal-Like Cells by the Mimicking Skin Microenvironment. *Int J Low Extrem Wounds*. 2015;14(2):136-145.
274. Li M, Luan F, Zhao Y, et al. Mesenchymal stem cell-conditioned medium accelerates wound healing with fewer scars. *Int Wound J*. 2017;14(1):64-73.
275. Mortier L, Delesalle F, Formstecher P, Polakowska R. Human umbilical cord blood cells form epidermis in the skin equivalent model. *Exp Dermatol*. 2010;19(10):929-930.
276. Zhang CP, Fu XB. Therapeutic potential of stem cells in skin repair and regeneration. *Chin J Traumatol*. 2008;11(4):209-221.
277. Kanji S, Das H. Advances of Stem Cell Therapeutics in Cutaneous Wound Healing and Regeneration. *Mediators Inflamm*. 2017;2017:5217967.
278. Semedo P, Palasio CG, Oliveira CD, et al. Early modulation of inflammation by mesenchymal stem cell after acute kidney injury. *Int Immunopharmacol*. 2009;9(6):677-682.
279. Weiss ARR, Dahlke MH. Immunomodulation by Mesenchymal Stem Cells (MSCs): Mechanisms of Action of Living, Apoptotic, and Dead MSCs. *Front Immunol*. 2019;10:1191.
280. de Araujo Farias V, Carrillo-Galvez AB, Martin F, Anderson P. TGF-beta and mesenchymal stromal cells in regenerative medicine, autoimmunity and cancer. *Cytokine Growth Factor Rev*. 2018;43:25-37.
281. Lin T, Pajarinen J, Kohno Y, et al. Transplanted interleukin-4--secreting mesenchymal stromal cells show extended survival and increased bone mineral density in the murine femur. *Cytotherapy*. 2018;20(8):1028-1036.
282. Meisel R, Zibert A, Laryea M, Gobel U, Daubener W, Dilloo D. Human bone marrow stromal cells inhibit allogeneic T-cell responses by indoleamine 2,3-dioxygenase-mediated tryptophan degradation. *Blood*. 2004;103(12):4619-4621.
283. Francois S, Mouisseddine M, Allenet-Lepage B, et al. Human mesenchymal stem cells provide protection against radiation-induced liver injury by antioxidative process, vasculature protection, hepatocyte differentiation, and trophic effects. *Biomed Res Int*. 2013;2013:151679.
284. Sotiropoulou PA, Perez SA, Gritzapis AD, Baxevanis CN, Papamichail M. Interactions between human mesenchymal stem cells and natural killer cells. *Stem Cells*. 2006;24(1):74-85.

285. Jiang XX, Zhang Y, Liu B, et al. Human mesenchymal stem cells inhibit differentiation and function of monocyte-derived dendritic cells. *Blood*. 2005;105(10):4120-4126.
286. Tse WT, Pendleton JD, Beyer WM, Egalka MC, Guinan EC. Suppression of allogeneic T-cell proliferation by human marrow stromal cells: implications in transplantation. *Transplantation*. 2003;75(3):389-397.
287. Walter MN, Wright KT, Fuller HR, MacNeil S, Johnson WE. Mesenchymal stem cell-conditioned medium accelerates skin wound healing: an in vitro study of fibroblast and keratinocyte scratch assays. *Exp Cell Res*. 2010;316(7):1271-1281.
288. El-Menoufy H, Aly LA, Aziz MT, et al. The role of bone marrow-derived mesenchymal stem cells in treating formocresol induced oral ulcers in dogs. *J Oral Pathol Med*. 2010;39(4):281-289.
289. Chen L, Tredget EE, Wu PY, Wu Y. Paracrine factors of mesenchymal stem cells recruit macrophages and endothelial lineage cells and enhance wound healing. *PLoS One*. 2008;3(4):e1886.
290. Herdrich BJ, Lind RC, Liechty KW. Multipotent adult progenitor cells: their role in wound healing and the treatment of dermal wounds. *Cytotherapy*. 2008;10(6):543-550.
291. Wu Y, Huang S, Enhe J, et al. Bone marrow-derived mesenchymal stem cell attenuates skin fibrosis development in mice. *Int Wound J*. 2014;11(6):701-710.
292. James I, Bourne D, Silva M, et al. Adipose stem cells enhance excisional wound healing in a porcine model. *J Surg Res*. 2018;229:243-253.
293. Irons RF, Cahill KW, Rattigan DA, et al. Acceleration of diabetic wound healing with adipose-derived stem cells, endothelial-differentiated stem cells, and topical conditioned medium therapy in a swine model. *J Vasc Surg*. 2018;68(6S):115S-125S.
294. Ito M, Liu Y, Yang Z, et al. Stem cells in the hair follicle bulge contribute to wound repair but not to homeostasis of the epidermis. *Nat Med*. 2005;11(12):1351-1354.
295. Huo J, Sun S, Geng Z, et al. Bone Marrow-Derived Mesenchymal Stem Cells Promoted Cutaneous Wound Healing by Regulating Keratinocyte Migration via beta2-Adrenergic Receptor Signaling. *Mol Pharm*. 2018;15(7):2513-2527.
296. Kinoshita K, Kuno S, Ishimine H, et al. Therapeutic Potential of Adipose-Derived SSEA-3-Positive Muse Cells for Treating Diabetic Skin Ulcers. *Stem Cells Transl Med*. 2015;4(2):146-155.
297. Butler KL, Goverman J, Ma H, et al. Stem cells and burns: review and therapeutic implications. *J Burn Care Res*. 2010;31(6):874-881.
298. Bertozzi N, Simonacci F, Grieco MP, Grignaffini E, Raposio E. The biological and clinical basis for the use of adipose-derived stem cells in the field of wound healing. *Ann Med Surg (Lond)*. 2017;20:41-48.
299. Chen FM, Wu LA, Zhang M, Zhang R, Sun HH. Homing of endogenous stem/progenitor cells for in situ tissue regeneration: Promises, strategies, and translational perspectives. *Biomaterials*. 2011;32(12):3189-3209.
300. Zarjou A, Kim J, Traylor AM, et al. Paracrine effects of mesenchymal stem cells in cisplatin-induced renal injury require heme oxygenase-1. *Am J Physiol Renal Physiol*. 2011;300(1):F254-262.
301. Kim JY, Song SH, Kim KL, et al. Human cord blood-derived endothelial progenitor cells and their conditioned media exhibit therapeutic equivalence for diabetic wound healing. *Cell Transplant*. 2010;19(12):1635-1644.
302. Isakson M, de Blacam C, Whelan D, McArdle A, Clover AJ. Mesenchymal Stem Cells and Cutaneous Wound Healing: Current Evidence and Future Potential. *Stem Cells Int*. 2015;2015:831095.
303. Cerqueira MT, Pirraco RP, Marques AP. Stem Cells in Skin Wound Healing: Are We There Yet? *Adv Wound Care (New Rochelle)*. 2016;5(4):164-175.
304. Parekkadan B, Milwid JM. Mesenchymal stem cells as therapeutics. *Annu Rev Biomed Eng*. 2010;12:87-117.
305. Cremers NA, Lundvig DM, van Dalen SC, et al. Curcumin-induced heme oxygenase-1 expression prevents H2O2-induced cell death in wild type and heme oxygenase-2 knockout adipose-derived mesenchymal stem cells. *Int J Mol Sci*. 2014;15(10):17974-17999.
306. Ke S, Zhang Y, Lan Z, Li S, Zhu W, Liu L. Curcumin protects murine lung mesenchymal stem cells from H2O2 by modulating the Akt/Nrf2/HO-1 pathway. *J Int Med Res*. 2020;48(4):300060520910665.

307. Cai C, Teng L, Vu D, et al. The heme oxygenase 1 inducer (CoPP) protects human cardiac stem cells against apoptosis through activation of the extracellular signal-regulated kinase (ERK)/NRF2 signaling pathway and cytokine release. *J Biol Chem*. 2012;287(40):33720-33732.
308. Zeng B, Ren XF, Lin GS, et al. Paracrine action of HO-1-modified mesenchymal stem cells mediates cardiac protection and functional improvement. *Cell Biology International*. 2008;32(10):1256-1264.
309. Hou C, Shen L, Huang Q, et al. The effect of heme oxygenase-1 complexed with collagen on MSC performance in the treatment of diabetic ischemic ulcer. *Biomaterials*. 2013;34(1):112-120.
310. Liu H, McTaggart SJ, Johnson DW, Gobe GC. Original article anti-oxidant pathways are stimulated by mesenchymal stromal cells in renal repair after ischemic injury. *Cytotherapy*. 2012;14(2):162-172.
311. Tsubokawa T, Yagi K, Nakanishi C, et al. Impact of anti-apoptotic and anti-oxidative effects of bone marrow mesenchymal stem cells with transient overexpression of heme oxygenase-1 on myocardial ischemia. *Am J Physiol Heart Circ Physiol*. 2010;298(5):H1320-1329.
312. Zhang ZH, Zhu W, Ren HZ, et al. Mesenchymal stem cells increase expression of heme oxygenase-1 leading to anti-inflammatory activity in treatment of acute liver failure. *Stem Cell Res Ther*. 2017;8(1):70.
313. Yang JJ, Yang X, Liu ZQ, et al. Transplantation of adipose tissue-derived stem cells overexpressing heme oxygenase-1 improves functions and remodeling of infarcted myocardium in rabbits. *Tohoku J Exp Med*. 2012;226(3):231-241.
314. Doi H, Kitajima Y, Luo L, et al. Potency of umbilical cord blood- and Wharton's jelly-derived mesenchymal stem cells for scarless wound healing. *Sci Rep*. 2016;6:18844.
315. Dandoy CE, Ardura MI, Papanicolaou GA, Auletta JJ. Bacterial bloodstream infections in the allogeneic hematopoietic cell transplant patient: new considerations for a persistent nemesis. *Bone Marrow Transplant*. 2017;52(8):1091-1106.
316. Harris DT. Stem Cell Banking for Regenerative and Personalized Medicine. *Biomedicines*. 2014;2(1):50-79.
317. El Omar R, Beroud J, Stoltz JF, Menu P, Velot E, Decot V. Umbilical cord mesenchymal stem cells: the new gold standard for mesenchymal stem cell-based therapies? *Tissue Eng Part B Rev*. 2014;20(5):523-544.
318. Karussis D, Karageorgiou C, Vaknin-Dembinsky A, et al. Safety and immunological effects of mesenchymal stem cell transplantation in patients with multiple sclerosis and amyotrophic lateral sclerosis. *Arch Neurol*. 2010;67(10):1187-1194.
319. Musialek P, Mazurek A, Jarocho D, et al. Myocardial regeneration strategy using Wharton's jelly mesenchymal stem cells as an off-the-shelf 'unlimited' therapeutic agent: results from the Acute Myocardial Infarction First-in-Man Study. *Postepy Kardiol Interwencyjne*. 2015;11(2):100-107.
320. Tatsumi K, Ohashi K, Matsubara Y, et al. Tissue factor triggers procoagulation in transplanted mesenchymal stem cells leading to thromboembolism. *Biochem Biophys Res Commun*. 2013;431(2):203-209.
321. Wu Z, Zhang S, Zhou L, et al. Thromboembolism Induced by Umbilical Cord Mesenchymal Stem Cell Infusion: A Report of Two Cases and Literature Review. *Transplant Proc*. 2017;49(7):1656-1658.
322. Musial-Wysocka A, Kot M, Majka M. The Pros and Cons of Mesenchymal Stem Cell-Based Therapies. *Cell Transplant*. 2019;28(7):801-812.
323. You HJ, Namgoong S, Han SK, Jeong SH, Dhong ES, Kim WK. Wound-healing potential of human umbilical cord blood-derived mesenchymal stromal cells in vitro--a pilot study. *Cytotherapy*. 2015;17(11):1506-1513.
324. Liu L, Yu Y, Hou Y, et al. Human umbilical cord mesenchymal stem cells transplantation promotes cutaneous wound healing of severe burned rats. *PLoS One*. 2014;9(2):e88348.
325. Luo G, Cheng W, He W, et al. Promotion of cutaneous wound healing by local application of mesenchymal stem cells derived from human umbilical cord blood. *Wound Repair Regen*. 2010;18(5):506-513.
326. Zhang S, Chen L, Zhang G, Zhang B. Umbilical cord-matrix stem cells induce the functional restoration of vascular endothelial cells and enhance skin wound healing in diabetic mice via the polarized macrophages. *Stem Cell Res Ther*. 2020;11(1):39.
327. Wang Y, Han ZB, Song YP, Han ZC. Safety of mesenchymal stem cells for clinical application. *Stem Cells Int*. 2012;2012:652034.

328. Schreurs M, Suttorp CM, Mutsaers HAM, et al. Tissue engineering strategies combining molecular targets against inflammation and fibrosis, and umbilical cord blood stem cells to improve hampered muscle and skin regeneration following cleft repair. *Med Res Rev.* 2020;40(1):9-26.
329. Yan W, Li D, Chen T, Tian G, Zhou P, Ju X. Umbilical Cord MSCs Reverse D-Galactose-Induced Hepatic Mitochondrial Dysfunction via Activation of Nrf2/HO-1 Pathway. *Biol Pharm Bull.* 2017;40(8):1174-1182.
330. Zhang LS, Wang XF, Lu XY, et al. Tetramethylpyrazine enhanced the therapeutic effects of human umbilical cord mesenchymal stem cells in experimental autoimmune encephalomyelitis mice through Nrf2/HO-1 signaling pathway. *Stem Cell Research & Therapy.* 2020;11(1).
331. Suttorp CM, van Rheden REM, van Dijk NWM, Helmich M, Kuijpers-Jagtman AM, Wagener F. Heme Oxygenase Protects against Placental Vascular Inflammation and Abortion by the Alarmin Heme in Mice. *Int J Mol Sci.* 2020;21(15).
332. Martin P, Parkhurst SM. Parallels between tissue repair and embryo morphogenesis. *Development.* 2004;131(13):3021-3034.
333. Rezzoug F, Seelan RS, Bhattacharjee V, Greene RM, Pisano MM. Chemokine-mediated migration of mesencephalic neural crest cells. *Cytokine.* 2011;56(3):760-768.
334. Tang T, Jiang H, Yu Y, et al. A new method of wound treatment: targeted therapy of skin wounds with reactive oxygen species-responsive nanoparticles containing SDF-1alpha. *International journal of nanomedicine.* 2015;10:6571-6585.
335. Oginni FO, Adenekan AT. Prevention of oro-facial clefts in developing world. *Ann Maxillofac Surg.* 2012;2(2):163-169.
336. Wilson RD, Genetics C, Wilson RD, et al. Pre-conception Folic Acid and Multivitamin Supplementation for the Primary and Secondary Prevention of Neural Tube Defects and Other Folic Acid-Sensitive Congenital Anomalies. *J Obstet Gynaecol Can.* 2015;37(6):534-552.
337. Czeizel AE, Bartfai Z, Banhidy F. Primary prevention of neural-tube defects and some other congenital abnormalities by folic acid and multivitamins: history, missed opportunity and tasks. *Ther Adv Drug Saf.* 2011;2(4):173-188.
338. Ryan-Harshman M, Aldoori W. Folic acid and prevention of neural tube defects. *Can Fam Physician.* 2008;54(1):36-38.
339. Wilcox AJ, Lie RT, Solvoll K, et al. Folic acid supplements and risk of facial clefts: national population based case-control study. *BMJ.* 2007;334(7591):464.
340. Shkoukani MA, Chen M, Vong A. Cleft lip - a comprehensive review. *Front Pediatr.* 2013;1:53.
341. Briggs RM. Vitamin supplementation as a possible factor in the incidence of cleft lip/palate deformities in humans. *Clinics in plastic surgery.* 1976;3(4):647-652.
342. Kochhar DM, Johnson EM. Morphological and Autoradiographic Studies of Cleft Palate Induced in Rat Embryos by Maternal Hypervitaminosis A. *J Embryol Exp Morph.* 1965;14:223-&.
343. Chung MK, Lao TT, Ting YH, Leung TY, Lau TK, Wong TW. Environmental factors in the first trimester and risk of oral-facial clefts in the offspring. *Reprod Sci.* 2013;20(7):797-803.
344. Webster WS, Howe AM, Abela D, Oakes DJ. The relationship between cleft lip, maxillary hypoplasia, hypoxia and phenytoin. *Curr Pharm Des.* 2006;12(12):1431-1448.
345. Chen X, Scholl TO. Oxidative stress: changes in pregnancy and with gestational diabetes mellitus. *Curr Diab Rep.* 2005;5(4):282-288.
346. Albano E. Alcohol, oxidative stress and free radical damage. *Proc Nutr Soc.* 2006;65(3):278-290.
347. Kamceva G, Arsova-Sarafinovska Z, Ruskovska T, Zdravkovska M, Kamceva-Panova L, Stikova E. Cigarette Smoking and Oxidative Stress in Patients with Coronary Artery Disease. *Open Access Maced J Med Sci.* 2016;4(4):636-640.
348. Sakai D, Trainor PA. Face off against ROS: Tcof1/Treacle safeguards neuroepithelial cells and progenitor neural crest cells from oxidative stress during craniofacial development. *Dev Growth Differ.* 2016;58(7):577-585.
349. Meazzini MC, Donati V, Garattini G, Brusati R. Maxillary growth impairment in cleft lip and palate patients: a simplified approach in the search for a cause. *J Craniofac Surg.* 2008;19(5):1302-1307.
350. Segna E, Khonsari RH, Meazzini MC, Battista VMA, Picard A, Autelitano L. Maxillary shape at the end of puberty in operated unilateral cleft lip and palate: A geometric morphometric assessment using computer tomography. *J Stomatol Oral Maxillofac Surg.* 2020;121(1):9-13.
351. van der Veer WM, Bloemen MC, Ulrich MM, et al. Potential cellular and molecular causes of hypertrophic scar formation. *Burns.* 2009;35(1):15-29.

352. Papathanasiou E, Trotman CA, Scott AR, Van Dyke TE. Current and Emerging Treatments for Postsurgical Cleft Lip Scarring: Effectiveness and Mechanisms. *J Dent Res*. 2017;96(12):1370-1377.
353. Grieb G, Steffens G, Pallua N, Bernhagen J, Bucala R. Circulating fibrocytes--biology and mechanisms in wound healing and scar formation. *Int Rev Cell Mol Biol*. 2011;291:1-19.
354. Volk SW, Wang Y, Mauldin EA, Liechty KW, Adams SL. Diminished type III collagen promotes myofibroblast differentiation and increases scar deposition in cutaneous wound healing. *Cells Tissues Organs*. 2011;194(1):25-37.
355. Marshall CD, Hu MS, Leavitt T, Barnes LA, Lorenz HP, Longaker MT. Cutaneous Scarring: Basic Science, Current Treatments, and Future Directions. *Adv Wound Care (New Rochelle)*. 2018;7(2):29-45.
356. Ishikawa H, Nakamura S, Misaki K, Kudoh M, Fukuda H, Yoshida S. Scar tissue distribution on palates and its relation to maxillary dental arch form. *Cleft Palate Craniofac J*. 1998;35(4):313-319.
357. Ross RB. Treatment variables affecting facial growth in complete unilateral cleft lip and palate. *Cleft Palate J*. 1987;24(1):5-77.
358. Guo Y, Hangoc G, Bian H, Pelus LM, Broxmeyer HE. SDF-1/CXCL12 enhances survival and chemotaxis of murine embryonic stem cells and production of primitive and definitive hematopoietic progenitor cells. *Stem Cells*. 2005;23(9):1324-1332.
359. Kulesa PM, Bailey CM, Kasemeier-Kulesa JC, McLennan R. Cranial neural crest migration: new rules for an old road. *Dev Biol*. 2010;344(2):543-554.
360. Theveneau E, Marchant L, Kuriyama S, et al. Collective chemotaxis requires contact-dependent cell polarity. *Dev Cell*. 2010;19(1):39-53.
361. Liu C, Weng Y, Yuan T, et al. CXCL12/CXCR4 signal axis plays an important role in mediating bone morphogenetic protein 9-induced osteogenic differentiation of mesenchymal stem cells. *Int J Med Sci*. 2013;10(9):1181-1192.

CHAPTER 9

Summary

Chapter 1 introduces the topic of cleft lip and palate, its etiology, incidence, classification, treatment strategies and iatrogenic effects following cleft surgery. The process of wound repair and scarring in relation to oxidative, inflammatory and mechanical stresses is discussed. The close similarity between biological processes involved in palatogenesis and wound repair is reviewed. Furthermore, the putative decisive roles of the cytoprotective heme oxygenase (HO) enzyme system and chemokine-chemokine-receptor signaling in embryonic development of the orofacial region and wound healing are discussed. We postulated that the balance between oxidative and inflammatory stresses and cytoprotective mechanisms influences the outcome of fetal development, palatal fusion, wound repair, the level of scar formation, and therefore determines the final shape of the face in patients with cleft lip and palate (CLP). We therefore split this thesis into five parts:

Part I: Diminished cytoprotection in HO-2 deficient mice hampers fetal growth, without affecting chemokine signaling during palatal fusion or palatal osteogenesis.

Part II: Diminished cytoprotection by inhibition of HO-activity in mice promotes heme-induced placental inflammation and fetal abortion.

Part III: Mechanical stress, generated by orthodontic forces in rats or by splinting of excisional wounds in mice, induces the cytoprotective enzyme HO-1.

Part IV: Umbilical cord blood stem cells and molecular targets in tissue engineering may promote muscle and skin regeneration following surgical CLP repair.

Part V: General discussion and Summary.

Part I consists of two studies investigating the potential role of chemokine-chemokine-receptor signaling during palatogenesis in relation to diminished cytoprotection by genetic and pharmacological targeting of HO.

In **Chapter 2**, the disappearance of the midline epithelial seam (MES), a crucial process during palatal fusion and CLP formation, was investigated. During palatogenesis several processes are similar to wound repair processes, including mesenchymal-epithelial transformation (EMT), chemokine signaling, cell proliferation, differentiation and apoptosis. Therefore, we postulated that chemokine CXCL11, its receptor CXCR3, and HO are not only important factors during wound repair, but also play a decisive role during palatogenesis. The contribution of HO-2 in this process was studied using heme oxygenase-2 deficient (HO-2 knockout; HO-2 KO) mice and wild type (wt) mice. HO-2 KO mice embryos at embryonic day E15-16 suffered from fetal growth restriction and craniofacial abnormalities but had no disturbed palatal fusion. In both wt and HO-2 KO mice fetuses, CXCR3-positive macrophages were observed near the CXCL11 expressing

MES, and contained multiple apoptotic DNA fragments, supporting the hypothesis that the MES disintegrates by epithelial apoptosis. Since macrophages located near the MES were HO-1 positive, and more HO-1 positive cells were present in palates of HO-2 KO mice fetuses, HO-1 induction forms probably a compensatory mechanism to handle oxidative stressors. HO and CXCL11-CXCR3 signaling are thus both involved in embryogenesis and palatal fusion.

In **Chapter 3**, we studied the association between palatal osteogenesis, an essential process during palatal fusion, and chemokine-chemokine-receptor signaling. In the process of osteogenesis Sox9 promotes osteogenic differentiation and stimulates CXCL12-CXCR4 chemokine-chemokine-receptor signaling. This facilitates elevation of alkaline phosphatase (ALP)-activity in osteoblasts to initiate bone mineralization. Disturbed migration of cranial neural crest cells (CNCCs) by excess oxidative and inflammatory stress is associated with increased risk of CLP. The cytoprotective HO enzymes are powerful guardians harnessing against injurious oxidative and inflammatory stressors and enhancing osteogenic ALP-activity. By contrast, abrogation of HO-1 or HO-2 expression promotes pregnancy pathologies. We therefore postulated that Sox9, CXCR4, and HO-1 are expressed in the ALP-activity positive osteogenic regions within the CNCCs-derived palatal mesenchyme. To investigate these hypotheses, we studied expression of Sox9, CXCL12, CXCR4, and HO-1 in relation to palatal osteogenesis between embryonic day E15 and E16 using (immuno)histochemical stainings of coronal palatal sections from wt mice fetuses. In addition, the effects of abrogated HO-2 expression in HO-2 KO mice fetuses, and inhibited HO-1 and HO-2 activity by administrating HO-enzyme activity inhibitor SnMP at E11 in wt mice fetuses were investigated at E15 or E16 following palatal fusion. Overexpression of Sox9, CXCL12, CXCR4, and HO-1 was detected in ALP-positive osteogenic regions within the palatal mesenchyme. Overexpression of Sox9 and CXCL12 was also detected within the disintegrating MES. Neither palatal fusion nor MES disintegration seemed affected by either HO-2 abrogation or inhibition of HO-1 and HO-2 activity. Sox9-positive progenitors seem important to maintain the CXCR4-positive osteoblast pool and drive osteogenesis. Sox9 expression may facilitate MES disintegration and palatal fusion by promoting EMT. Our findings further suggest that CXCL12 expression by the MES and the palatal mesenchyme may promote osteogenic differentiation to create osteogenic centers.

Part II contains one study examining the effects of diminished cytoprotection by pharmacological inhibition of HO-activity during palatal fusion, heme-induced placental inflammation, and fetal abortion in mice.

In **Chapter 4**, we studied the dose-dependent effects of exposure to heme during palatal fusion, placental and fetal development in relation to diminished cytoprotection

by pharmacological inhibition of HO-activity in mice. Both infectious and non-infectious inflammation can cause placental dysfunction and pregnancy complications. During the first trimester of human gestation, when palatogenesis takes place, intrauterine hematoma and hemorrhage are common phenomena, causing the release of large amounts of heme, a well-known endogenous damage-associated molecule, recognized as an “alarmin”. We hypothesized that exposure of pregnant mice to heme during palatogenesis would initiate oxidative and inflammatory stress, leading to pathological pregnancy, increasing the incidence of palatal clefting and abortion. Both HO isoforms (HO-1 and HO-2) break down heme, thereby generating anti-oxidative and inflammatory products. HO may thus counteract heme-induced injurious stresses. To test this hypothesis, we administered heme (H) to pregnant CD1 outbred mice at embryonic day E12 by intraperitoneal injection in increasing doses: 30, 75 or 150 $\mu\text{mol/kg}$ body weight (30H, 75H or 150H) in the presence or absence of HO-activity inhibitor SnMP at embryonic day E11. Exposure to heme resulted in a dose-dependent increase in abortion. At 75H half of the fetuses were resorbed, while at 150H all fetuses were aborted. HO-activity protected against heme-induced abortion since inhibition of HO-activity aggravated heme-induced detrimental effects. The fetuses surviving heme administration demonstrated normal palatal fusion. In placenta, immunostainings at embryonic day E16 demonstrated higher numbers of ICAM-1 positive blood vessels, F4/80-positive macrophages and HO-1 positive cells after administration of 75H or SnMP + 30H. Summarizing, heme acts as an “alarmin” during pregnancy in a dose-dependent fashion, while HO-activity protects against heme-induced placental vascular inflammation and abortion.

Part III consists of two studies exploring the relation between mechanical stress, generated by orthodontic forces in rats, or by splinting of excisional wounds in mice, and the induction of the cytoprotective enzyme HO-1.

In **Chapter 5**, the time-dependent expression of the cytoprotective enzyme HO-1 within the PDL following application of continuous orthodontic forces in rats was examined. Orthodontic forces disturb the microenvironment of the periodontal ligament (PDL) and induce alveolar bone remodeling which is necessary for tooth movement. Orthodontic tooth movement is hampered by ischemic injury and cell death within the PDL (hyalinization), caused by reduced capillary blood flow, which is associated with hampered tooth movement and initiation of root resorption. Large inter-individual differences in hyalinization and root resorption have been observed between orthodontic patients and may be explained by differential protection against hyalinization or heme release. HO-1 forms an important protective mechanism by breaking down heme into the strong antioxidants biliverdin/bilirubin and the signaling molecule carbon monoxide. These versatile HO-1 products protect against ischemic and

inflammatory injury. We postulate that orthodontic forces induce HO-1 expression in the PDL during experimental tooth movement. Twenty-five 6-week-old male Wistar rats were used in this study. The upper three molars at one side were moved mesially using a Nickel-Titanium coil spring, providing a continuous orthodontic force of 10 cN. The contralateral side served as control. After 6, 12, 72, 96, and 120 h groups of rats were killed. On parasagittal sections immunohistochemical staining was performed for analysis of HO-1 expression and quantification of osteoclasts. Orthodontic force generated a significant time-dependent HO-1 induction in mononuclear cells within the PDL at both the apposition- and resorption side. Shortly after placement of the orthodontic appliance HO-1 expression was highly induced in PDL cells, but dropped to control levels within 72 h. Some osteoclasts were also HO-1 positive but this induction was shown to be independent of time- and mechanical stress. Based on our findings we propose that differential induction of tissue protecting- and osteoclast activating genes in the PDL determine the level of bone resorption and hyalinization and, subsequently, “fast” and “slow” tooth movers during orthodontic treatment.

In **Chapter 6**, since CLP patients after cleft surgery experience mechanical stress during wound repair from myofibroblasts and the growing head, static mechanical stress was induced in a mouse model to simulate the increased injurious environment. Mechanical stress during wound repair was applied using a splinted excisional wound model. HO-1 is thought to orchestrate the defense against inflammatory and oxidative insults that drive fibrosis. Therefore, we investigated the activation of the HO-system in splinted and non-splinted excisional wound models using HO-1 luciferase (luc) transgenic mice. These mice co-express luciferase when HO-1 gets induced, which can be seen and measured *in vivo* by administration of the substrate luciferin, which results in the release of photons. After seven days, splinting had delayed cutaneous wound closure and HO-1 protein expression, whereas the number of F4/80-positive macrophages, α SMA-positive myofibroblasts, and pro-inflammatory signals IL-1 β , TNF- α , and COX-2 were increased after application of mechanical stress. The pro-inflammatory environment following splinting may explain the higher myofibroblast numbers and increased risk of fibrosis and scar formation when compared to non-splinted wounds. Induction of HO-1 may be a strategy to prevent against mechanical stress-induced inflammation in wound repair after cleft surgery.

Part IV contained a narrative review on the potential of using umbilical cord blood stem cells in combination with molecular targets to improve tissue engineering to promote muscle and skin repair following cleft surgery.

In **Chapter 7**, we reviewed the literature to outline a novel molecular and cellular strategy to improve musculature and skin regeneration, and to reduce scar formation following cleft repair. Cleft lip with or without cleft palate is a congenital deformity,

affecting the dentition, bone, skin, muscles and mucosa in the orofacial region. Surgical repair of the cleft lip may lead to impaired regeneration of muscle and skin, fibrosis, and scar formation. This may result in hampered facial growth and dental development affecting oral function and lip and nose esthetics. We discussed the molecular and cellular pathways involved in facial and lip myogenesis, muscle anatomy in the normal and cleft lip, and complications following cleft lip surgery. Orofacial clefting can be diagnosed in the fetus through prenatal ultrasound screening and allows planning for the harvesting of umbilical cord blood stem cells upon birth. Tissue engineering techniques using these umbilical cord blood stem cells and molecular targeting of inflammation and fibrosis during surgery may promote tissue regeneration. We expect that this novel strategy improves both muscle and skin regeneration, resulting in better function and esthetics after cleft repair.

In **Part V** the most important results of the thesis and their clinical relevance are summarized and discussed, and future perspectives for therapeutic approaches are suggested.

The induction of cytoprotective pathways, such as HO-1, by pharmacological therapy may harness inflammatory and oxidative insults. Therefore, these strategies may prevent pathological pregnancies and could possibly improve tissue engineering with the use of umbilical stem cells to improve the outcome following surgical cleft repair. However, more mechanistic and translational research is necessary before it can be used in the clinic.

In conclusion, decreased activity of protective pathways can hamper embryonic development and wound repair, whereas induction of protective signaling cascades, with a focus on pathways that mediate the resolution of oxidative and inflammatory stress, may provide a regenerative microenvironment that prevents CLP formation and improves wound repair.

CHAPTER 10

Summary in Dutch

Hoofdstuk 1 introduceert het onderwerp schisis, de etiologie, incidentie, classificatie, behandelstrategieën, en de iatrogene effecten als gevolg van schisis-chirurgie. Het proces van wondgenezing en littekenvorming in relatie tot oxidatieve, inflammatoire en mechanische stress wordt bediscussieerd. Er is een sterke overeenkomst tussen de biologische processen die zijn betrokken bij de vorming van het palatum en bij wondgenezing. De rol van het celbeschermende haem oxygenase (HO) enzymesysteem en chemokine-chemokine-receptor signalering gedurende de embryonale ontwikkeling van het orofaciale gebied en wondgenezing wordt bediscussieerd. Wij postuleerden dat de balans tussen oxidatieve en inflammatoire stress en celbeschermende mechanismen de uitkomst van de foetale ontwikkeling, het palatinale fusieproces en het ontstaan van schisis, de wondgenezing, de mate van littekenvorming beïnvloedt, en daarmee de uiteindelijke vorm van het gezicht bepaalt. Dit proefschrift is opgesplitst in vijf delen:

Deel I: Verminderde celbescherming in HO-2 deficiënte muizen remt de foetale groei, zonder daarbij de fusie van het palatum of de palatinale botvorming te beïnvloeden.

Deel II: Verminderde celbescherming verkregen door remming van de HO-activiteit in muizen bevordert de ontwikkeling van haem-geïnduceerde ontsteking van de placenta en van abortus van de foetus.

Deel III: Mechanische stress, gegenereerd door orthodontische krachten in ratten, of door het spalken van excisionele wonden in muizen, activeert het celbeschermende mechanisme HO-1.

Deel IV: Stamcellen van de navelstreng en moleculaire elementen in de wetenschap van weefselontwikkeling kunnen mogelijk het herstel van spieren en huid bevorderen na schisischirurgie.

Deel V: Algemene discussie en samenvatting.

Deel I bestaat uit twee studies die de potentiële rol van chemokine-chemokine-receptor signalering bestuderen tijdens de palatogenese in relatie tot verminderde celbescherming door het genetisch en farmacologisch attaqueren van HO.

In **Hoofdstuk 2** werd de fusie van de epitheliale naad (midline epithelial seam; MES) in het midden van het palatum nader onderzocht. Dit is een cruciaal proces tijdens de fusie van beide palatumhelften. Wanneer dit fout gaat heeft dit een palatoschisis tot gevolg. Tijdens de palatogenese zijn verschillende ontwikkelingsprocessen vergelijkbaar met wondgenezingsprocessen, waaronder mesenchymale-epitheliale transformatie (EMT), chemokine signalering en proliferatie, differentiatie en apoptose van cellen. Daarom veronderstelden we dat chemokine CXCL11, zijn receptor CXCR3 en het celbeschermende HO niet alleen belangrijk zijn tijdens wondgenezing, maar ook

een beslissende rol spelen bij het samenvoegen van de MES. De rol van HO-2 in dit proces werd bestudeerd met behulp van haem oxygenase-2 deficiënte (HO-2 knockout; HO-2 KO) muizen en wild type (wt) muizen. HO-2 KO muizenfoetussen op dag 15-16 van de embryonale ontwikkeling (E15-E16) leden aan foetale groeibeperking en craniofaciale afwijkingen, maar hadden geen verstoorde palatale fusie. In zowel wt- als HO-2 KO muizenfoetussen werden er CXCR3-positieve macrofagen waargenomen in de buurt van de tot CXCL11 expressie brengende MES. Deze palatale macrofagen bleken meerdere apoptotische DNA-fragmenten te bevatten. Dit ondersteunt de theorie dat de MES desintegreert door apoptose van het epitheel. Aangezien macrofagen dicht bij de MES HO-1-positief waren en er meer HO-1-positieve cellen aanwezig zijn in het palatum van HO-2 KO-muizenfoetussen, dient HO-1 inductie mogelijk als een compensatiemechanisme om oxidatieve stress te neutraliseren. HO- en CXCL11/CXCR3-signalering zijn dus beiden betrokken bij de embryogenese en de fusie van het palatum.

In **Hoofdstuk 3** werd het verband tussen het proces van palatale botvorming, wat een essentieel onderdeel is van de fusie van het palatum, en chemokine-chemokine-receptor signalering bestudeerd. Tijdens het botvormingsproces bevordert Sox9 de differentiatie van voorlopercellen naar botvormende cellen. Bovendien stimuleert het de CXCL12-CXCR4 chemokine-chemokine-receptor signalering, wat de alkaline phosphatase (ALP)-activiteit in osteoblasten verhoogt ter initiëring van de botmineralisatie. Verstoorde migratie van craniale neurale lijstcellen door overmatige oxidatieve en inflammatoire stress is geassocieerd met een verhoogde kans op schisis. De HO enzymen zijn krachtige celbeschermers die de oxidatieve en inflammatoire stress in toom houden, en de botvormende ALP-activiteit verhogen. Uitschakeling van de HO-1 of HO-2 expressie daarentegen bevordert het ontstaan van zwangerschapspathologie. Daarom postuleerden wij dat Sox9, CXCR4, en HO-1 tot expressie zouden komen in de botvormende regio's die positief zijn voor ALP-activiteit binnen het palatale mesenchym. Om deze hypothesen te onderzoeken hebben wij (immuno)histochemische kleuringen uitgevoerd op coronale palatinale coupes van wt muizen foetussen tussen embryonale dag 15 en 16, en de expressie van Sox9, CXCL12, CXCR4, en HO-1 bestudeerd in relatie tot de palatinale botvorming. Het effect van de uitschakeling van HO-2 expressie in HO-2 KO muizen foetussen en de remming van HO-1 en HO-2 activiteit werd onderzocht. Overexpressie van Sox9 en CXCL12 binnen de uiteenvallende MES werd aangetoond. Fusie van het palatum, noch het uiteenvallen van de MES leken te zijn beïnvloed door de afwezigheid van HO-2 of remming van HO-activiteit. Sox9-positieve voorlopercellen lijken belangrijk voor het behoud van de groep CXCR4-positieve osteoblasten ter stimulering van de botvorming. Sox9 expressie faciliteert mogelijk het uiteenvallen van de MES en de fusie van het palatum door het bevorderen van mesenchymale-epitheliale transformatie. Onze bevindingen suggereren verder dat expressie van CXCL12 door de MES en het palatinale mesenchym

mogelijk de differentiatie van voorlopercellen in botvormende cellen bevordert en botvormende centra vormt.

Deel II bestaat uit één studie die het effect van verminderde celbescherming door farmacologische remming van HO-activiteit op de fusie van het palatum, haem-geïnduceerde ontsteking van de placenta, en foetale abortus in muizen bestudeert.

In **Hoofdstuk 4** werd het dosis-afhankelijke effect van de blootstelling aan haem op de fusie van het palatum, de ontwikkeling van de placenta en de foetus in relatie tot verminderde celbescherming, door farmacologische remming van de HO-activiteit, in muizen bestudeerd. Zowel infectieuze als non-infectieuze ontsteking kan het functioneren van de placenta verstoren en leiden tot zwangerschapscomplicaties. Gedurende het eerste trimester van de zwangerschap bij mensen, wanneer de vorming van het palatum plaatsvindt, zijn bloedingen en hematomen in de baarmoeder vaak voorkomende fenomenen, veroorzaakt door het vrijkomen van grote hoeveelheden haem, een welbekende endogeen met schade-geassocieerd molecuul, erkend als een “alarmsignaal”. Wij stelden dat blootstelling van zwangere muizen aan haem gedurende de vorming van het palatum mogelijk oxidatieve en inflammatoire stress initieert, wat kan leiden tot een pathologische zwangerschap, hetgeen het risico op schisis en het ontstaan van abortus verhoogt. Beide isovormen van HO (HO-1 en HO-2) breken haem af en genereren daarbij anti-oxidatieve en -inflammatoire producten. HO gaat mogelijk deze door haem geïnduceerde schadelijke signalering tegen. Om deze hypothese te toetsen hebben wij haem toegediend aan zwangere CD1 niet-inteelt muizen op E12 door middel van intraperitoneale injectie in toenemende doses: 30, 75, of 150 µmol/kg lichaamsgewicht (30H, 75H, of 150H) in de aan- of afwezigheid van de HO-activiteitsremmer SnMP vanaf E11. Blootstelling aan haem leidde tot een dosis-afhankelijke toename in abortus. Bij 75H waren de helft van de foetussen geresorbeerd, terwijl bij 150H alle foetussen waren geresorbeerd. HO-activiteit beschermt tegen haem-geïnduceerde abortus want remming van de HO-activiteit verergerde de haem-geïnduceerde schadelijke effecten. De foetussen die de toediening van haem overleefden lieten een normale fusie van het palatum zien. Immunokleuringen van de placenta op E16 toonden een verhoogde aantal ICAM-1 positieve bloedvaten, F4/80 - positieve macrofagen en HO-1 positieve cellen na toediening van 75H of SnMP + 30H. Samenvattend, haem acteert als een “alarmsignaal” tijdens de zwangerschap op een dosis-afhankelijke manier, terwijl HO-activiteit beschermt tegen haem-geïnduceerde vasculaire ontsteking in de placenta en het optreden van abortus.

Deel III bestaat uit twee studies die de relatie tussen mechanische stress, gegenereerd door orthodontische krachten in ratten, of door het spalken van excisionele wonden in muizen, en de inductie van het celbeschermende enzym HO-1 bestudeert.

In **Hoofdstuk 5** werd de tijdsafhankelijke expressie van het celbeschermende enzym HO-1 in het parodontaal ligament in ratten bestudeerd na het aanbrengen van een continue orthodontische kracht. Een orthodontische kracht verstoort de micro omgeving van het parodontale ligament en induceert remodelering van het alveolaire bot, wat noodzakelijk is voor orthodontische tandverplaatsing. Orthodontische tandverplaatsing gaat gepaard met ischemische schade en celdood in het parodontale ligament (hyalinisatie), veroorzaakt door een verminderde capillaire bloedstroom, hetgeen weer geassocieerd is met een vertraagde tandverplaatsing en de initiatie van wortelresorptie. Grote verschillen tussen individuen in de mate van hyalinisatie en wortelresorptie zijn waargenomen en kunnen worden verklaard door een verschil in bescherming tegen de vorming van hyalinisatie en het vrijgekomen haem. HO-1 vormt een belangrijk beschermingsmechanisme door het omzetten van haem in de sterke anti-oxidanten biliverdine/bilirubine en het signaalmolecuul koolstofmonoxide. Deze veelzijdige producten van HO-1 beschermen tegen ischemische en inflammatoire schade. Wij postuleren dat orthodontische krachten expressie van HO-1 induceren in het parodontaal ligament tijdens de experimentele tandverplaatsing. Vijfentwintig 6 weken oude Wistar ratten werden voor deze studie gebruikt. In de bovenkaak werden drie molaren aan één zijde naar mesiaal verplaatst door gebruik te maken van een Nickel-Titanium veer die een continue orthodontische kracht van 10 cN genereert. De contralaterale kant diende als de controle. Na 6, 12, 72, 96, en 120 uur werden de ratten gedood. Op parasagittale doorsneden werden immunohistochemisch kleuringen uitgevoerd ter analyse van de HO-1 expressie en de osteoclasten werden gekwantificeerd. Orthodontische krachten induceerden een significante tijdsafhankelijke expressie van HO-1 in mononucleaire cellen in het parodontale ligament, zowel aan de appositie- als aan de resorptie zijde. Kort na plaatsing van de orthodontische apparatuur werd HO-1 expressie sterk geïnduceerd in de cellen van het parodontale ligament, maar deze expressie daalde tot het niveau van de controles binnen 72 uur. Verscheidene osteoclasten waren positief voor HO-1, maar deze inductie bleek onafhankelijk van tijd en mechanische stress. Op basis van onze bevindingen speculeerden wij dat verschil in inductie van weefsel beschermende en osteoclast activerende genen in het parodontale ligament het niveau van botafbraak en hyalinisatie bepalen, en daarmee het fenomeen van de “snelle” en “langzame” tandverplaatsers gedurende de orthodontische behandeling zouden kunnen verklaren.

In **Hoofdstuk 6** werd een statische mechanische stress geïnduceerd met behulp van een spalk als model voor de postoperatieve situatie in patiënten met schisis. Op deze manier werden de verhoogde schadelijke omgevingsfactoren en de effecten van verminderde beschermende processen tijdens wondgenezing gesimuleerd. Deze mechanische stress werd toegebracht met behulp van een spalk in een excisioneel wondmodel. HO-1 speelt een rol bij de verdediging tegen inflammatoire en oxidatieve

insulten die op hun beurt fibrose en littekens veroorzaken. Daarom onderzochten we de activering van het HO-1 systeem in gespalkte en niet-gespalkte excisionele wonden met behulp van HO-1 luciferase (luc) transgene muizen. Deze muizen brengen luciferase tot co-expressie wanneer HO-1 wordt geactiveerd. Dit kan in vivo worden gemeten door het substraat luciferine toe te dienen dat leidt tot het vrijkomen van fotonen. Na zeven dagen heeft het spalken van de wonden de wondsluiting en HO-1 eiwit inductie vertraagd, terwijl het aantal F4/80-positieve macrofagen, α SMA-positieve myofibroblasten en de pro-inflammatoire signalen IL-1 β , TNF α en COX-2 verhoogd waren na blootstelling aan mechanische stress. De pro-inflammatoire omgeving die ontstaat ten gevolge van het spalken kan het toegenomen aantal myofibroblasten en het verhoogde risico op fibrose en littekens verklaren. Inductie van HO-1 zou een mogelijke strategie kunnen zijn ter voorkoming van door mechanische stress geïnduceerde ontsteking gedurende de wondgenezing na schisis-chirurgie.

Deel IV bestaat uit één review over het potentieel van het gebruik van stamcellen uit de bloed van de navelstreng in combinatie met moleculaire aangrijpingspunten ter verbetering van de regeneratie van de spieren en huid na schisis-chirurgie.

In **Hoofdstuk 7** hebben wij de literatuur besproken die de vernieuwende moleculaire en cellulaire strategieën ter verbetering van spier- en huid regeneratie beschrijft, hetgeen mogelijk de vorming van littekenweefsel na schisis chirurgie zou kunnen verminderen. De gespleten lip met of zonder een gespleten gehemelte is een aangeboren afwijking die de ontwikkeling van het gebit, bot, huid, spieren en mucosa in het orofaciale gebied beïnvloedt. Chirurgisch herstel van de schisis kan mogelijk leiden tot verminderde regeneratie van de spieren en huid, en het vormen van fibrose en littekenweefsel. Dit alles kan resulteren in remming van de gelaatsgroei en verstoring van de gebitsontwikkeling, hetgeen een effect kan hebben op de orale functies, alsmede de esthetiek van de lip en de neus negatief kan beïnvloeden. Wij bediscussieerden de moleculaire en cellulaire paden die betrokken zijn bij de myogenese in het gelaat en de lip, de spier anatomie van een normale en gespleten lip, en de complicaties na lip chirurgie. Een orofaciale schisis kan prenataal worden gediagnosticeerd middels echo-onderzoek, hetgeen het vooraf inplannen van het oogsten van bloedstamcellen uit de navelstreng mogelijk maakt. Weefselontwikkeling met gebruik van deze bloedstamcellen uit de navelstreng, samen met het molecuulair aanpakken van het ontstekingsproces en de littekenvorming als gevolg van de chirurgie, kunnen mogelijk het weefselherstel bevorderen. Wij verwachten dat deze nieuwe strategie het herstel van spieren en huid verbetert, hetgeen tot een betere functie en esthetiek na schisis chirurgie zou moeten leiden.

In **Deel V** werden de belangrijkste resultaten van dit proefschrift en de klinische relevantie besproken en samengevat, en enkele toekomstige perspectieven van therapeutische benaderingen werden aanbevolen.

De inductie van celbeschermende paden, zoals HO-1, door farmacologische therapie kan mogelijk inflammatoire en oxidatieve dreiging beheersen. Deze strategieën kunnen mogelijk pathologische zwangerschappen voorkomen en kunnen wellicht weefselontwikkeling verder bevorderen door gebruik te maken van stamcellen uit de navelstreng ter verbetering van de behandelresultaten van schisis chirurgie. Meer fundamenteel onderzoek is echter noodzakelijk voordat onze data kan worden vertaald naar een therapie dat kan worden ingezet in de kliniek.

Wij concludeerden dat verminderde activiteit van celbescherming de embryonale ontwikkeling en wondgenezing kan verstoren, terwijl het induceren van beschermende signaal mechanismen, met name de paden die de oxidatieve en inflammatoire stress temperen, mogelijk een herstellende micro omgeving bewerkstelligt. Dit zou het ontstaan van schisis kunnen voorkomen en de wondgenezing mogelijk kunnen bevorderen.

Acknowledgements

In 2010, I decided to leave my dental office in a small village called Bodegraven, located in the west of Holland, after having worked as a general dentist for 5 years. The prospect of having to work for the coming 4 decades between the same 4 walls made me decide to search for new opportunities. That's why I applied for the orthodontic postgraduate program at the Radboud university medical center in Nijmegen in 2010. Besides my wish to become an orthodontist, I felt the need to increase my scientific skills. Furthermore, I also wanted to meet new colleagues to exchange views about dental science. I was fortunate to start my orthodontic education in April 2011, and in 2015 I successfully finished the postgraduate program. I enjoyed my four years with my nice classmates and my colleagues at our lab. I then continued my research, and finally completed my thesis in 2021, I made my first step into the right direction as an academic worker. In the coming years I would like to contribute further to the postgraduate orthodontic program and the dental education program at the Radboud university medical center. Importantly, my PhD thesis could not have been finished without the help of others, and therefore I want to thank many people.

First of all my warm gratitude goes to my co-promotor dr. Frank Wagener, my dad in biology, not to be confused with my biological dad! You supported me almost weekly already since the starts of my orthodontic education in 2011, meaning that we have had at least 500 meetings up to now! Your expertise of the HO system was the key in our research. Your scientific education and patience strongly supported me during my long way as a PhD student. Without your help this thesis would never had been completed. Your endless kindness makes you the most exceptional person at the work floor in the department. I hope that our successful cooperation will continue and will bring forward many more studies on the function and therapeutic potential of the HO system.

Secondly, I would like to thank Professor Anne-Marie Kuijpers-Jagtman for allowing me to perform this research project under her supervision. Thank you very much for your sharp insights and scientific experience that lifted the quality of our articles to a higher level.

Dear Dr. Jan Schols and Dr. Edwin Ongkosuwito of the Section of Orthodontics and Craniofacial Biology of the dental department, thank you for giving me the time and support for my research. I intend to contribute to many research projects of the dental department in the coming years.

Dear Niels Cremers and Dries Desmedt, thank you for being my paranymphs. Niels, our scientific discussions on the HO system, on wound healing and pregnancy pathology

were very useful for this thesis. I hope that we can further join our efforts in new studies in the future. Unfortunately, you left Nijmegen in 2017 to move to Belgium. Otherwise, we could have had more running training through the forests of Nijmegen.

Dries, thank you for our great time during our orthodontic education with your great sense of humor, and for bringing me in contact with Dina, my wife and mother of our one-year-old daughter Belle.

Special thanks to Nanne Verheijen for our joint work at the lab, including the many hours behind the Zeiss microscope. We completed our complex article well on time, which was I think, a nice achievement. I wish you, your husband and your baby girl Aafke all the best.

Many thanks to Michaël Schreurs, Rick Mutsaers, Hans Von den Hoff, Edwin Ongkosuwito and Paola Carvajal Monroy for our cooperation in writing the review of this thesis. We published this review in a high ranked medical journal, which was a great experience.

Many thanks to Vincent Cuijpers for explaining me to work with the Zeiss microscope, and for the interesting discussions on themes in as well as outside the scientific field.

Dear Dr. Jaap Maltha, thank you for your time for explaining me the basics of statistics in animal experimental studies, so that I was able to do most of the statistical analyses in this thesis myself.

I would like to express my appreciation to the people at the Orthodontics and Craniofacial Biology lab, René van Rheden, Pia Helmich, Natasha van Dijk, Sven van Kempen, Bas Pennings and Marjon Bloemen for their work on the many (immuno)histochemical stainings for this thesis.

Dear researchers Ditte, Aysel, Liesbeth, Roel, Paola, Doris and Christian, Jyoti and Sophie thank you for your chats and for your help in the lab.

For my experiments in this thesis I had to use laboratory animals. I would like to thank the central animal laboratory, especially the SPF unit, dear Jeroen thanks for your help with these experiments.

Dr. Mette Kuijpers, Dr. Vanessa Heinz-Sternemann, and Drs. Veronique Borstlap-Engels, thank you for taking the time to explain the treatment protocols of CLP patients, and to teach me many practical tricks that improved my clinical skills.

I would like to extend my gratitude to dr. Wilbert Boelens who has been my mentor during my PhD program. Thank you for the meetings to evaluate my planning and progress.

A word of thanks to my supervisors during my orthodontic training: Jan Schols, Ricardo Ophof, Rosemie Kiekens, Katja van Oort-Bongaarts, René Noverraz, Barbara Oosterkamp, Anne-Marie Renkema and Hero Breuning. Thank you for your time and effort to teach me the practical skills necessary for being an orthodontist.

Dear classmates year 2011-2015: Dries, Olivier, Christian, Eveline, Aaltje, Eva and Michelle thank you for those great 4 years. Besides all educational moments, I look back with joy to the congresses we have visited abroad and all the fun we had. Olivier, thank you for sharing our desk for four years, and for our good cooperation in the CBCT course that we have been organizing since 2015.

Many thanks to the clinical assistants Wilma and Maaïke for helping me with the treatment of patients during my orthodontic training, and later in the CLP clinic of our department. You both bring a good atmosphere to the clinic where there is room for a joke now and then.

Thanks to the administrator and secretaries of the Section of Orthodontics and Craniofacial Biology, Jacqueline, Marieke, Karin and Tineke for your kind help.

Dear Joey and Thao, thanks for the nice time we had together working in the dental clinic Van Dedem in Hoorn where I worked for 5 years part-time as an orthodontist. Unfortunately, I was no longer able to combine my part-time work outside the university and my part-time academic career, which made me decide to quit my work in Hoorn. Also, the long rides to Hoorn (almost 2 hours back and forth) appeared to be very unpractical, especially since my wife and I are fortunate to raise a little child. Thanks a lot for giving me the time and tools to develop my practical skills in your clinic. I hope that we will still meet each other regularly despite the geographical distance between us.

Warm thanks to my parents Chris and Anja, and my little great brother Wilbert and his partner Ilse and their children Elisa and Elin for taking the time to listen to my talks on my research. I enjoyed our many visits to the center of Nijmegen together for lunches and dinners. I hope that we are soon able to spend more free time in Nijmegen as well as in the west and south of Holland.

Special thanks to my special grandmother who passed away last year at the age of 93 years. I hold on to the beautiful memories of the many trips we had together with my brother back in the good old days.

At last, thanks to my beloved wife Dina. Through my classmate Dries and his wife Anne-Marie we first met in Nijmegen in September of 2012. Since then we were a couple and married in 2015. Thank you for your love. In 2019 we were very fortunate to get our beautiful baby girl Belle. I hope we will get more free time in the weekends now, so we can enjoy together the nice time of raising a little child. Thanks to my sweet little daughter Belle who usually makes me feel 10 years younger, but also sometimes 10 years older. I'm looking forward to the trips we can undertake soon at "Friday daddy day".

Curriculum Vitae

Maarten Suttorp was born in Gouda, the Netherlands on Friday 13th of November 1981. In 2000, he graduated from high school at “St. Antoniuscollege” (Atheneum) in Gouda. He enlisted for dental training but was rejected on random selection and started to study biomedical sciences at the University of Amsterdam and earned his first year in July 2001. In September 2001 he was able to start his undergraduate dental education at the Faculties of Dentistry at the University of Amsterdam (Academisch Centrum Tandheelkunde Amsterdam; ACTA). In June 2006 he graduated as a dentist. After having worked as a general dentist for 5 years in the villages Reeuwijk and Bodegraven, located close to Gouda, he searched for new opportunities to further develop his practical and scientific skills, and got more interested in orthodontics. In April 2011 he started the postgraduate program in orthodontics at the Radboud University in Nijmegen. He finished his orthodontic specialist education and became registered as an orthodontist in April 2015. Soon after he started a small part-time practice within a dental clinic of two friends and former dental classmates from ACTA in Hoorn. Since April 2016, Maarten started to work-part time at the section of Orthodontics and Craniofacial Biology at the Department of Dentistry of the Radboud university medical center in Nijmegen on the research of this thesis. Besides his research, Maarten is currently supervising the orthodontic residents in the clinic and treats patients in the CLP clinic as an acting orthodontist. Furthermore, he is teaching orthodontics in the undergraduate dental curriculum. He intends to continue his efforts to develop more insights into the potential therapeutic role of the HO system.



List of publications

In this thesis

Cremers NA, **Suttorp CM**, Gerritsen MM, Wong RJ, van Run-van Breda C, van Dam GM, Brouwer KM, Kuijpers-Jagtman AM, Carels CE, Lundvig DM, Wagener FA. Mechanical stress changes the complex interplay between HO-1, inflammation and fibrosis, during excisional wound repair. *Front Med (Lausanne)*. 2015 Dec 15;2:86.

Suttorp CM, Xie R, Lundvig DM, Kuijpers-Jagtman AM, Uijttenboogaart JT, Van Rheden R, Maltha JC, Wagener FA. Orthodontic forces induce the cytoprotective enzyme heme oxygenase-1 in rats. *Front Physiol*. 2016 Jul 19;7:283.

Suttorp CM, Cremers NA, van Rheden R, Regan RF, Helmich P, van Kempen S, Kuijpers-Jagtman AM, Wagener FADTG. Chemokine signaling during midline epithelial seam disintegration facilitates palatal fusion. *Front Cell Dev Biol*. 2017 Oct 30;5:94.

Schreurs M, **Suttorp CM**, Mutsaers HAM, Kuijpers-Jagtman AM, Von den Hoff JW, Ongkosuwito EM, Carvajal Monroy PL, Wagener FADTG. Tissue engineering strategies combining molecular targets against inflammation and fibrosis, and umbilical cord blood stem cells to improve hampered muscle and skin regeneration following cleft repair. *Med Res Rev*. 2020 Jan;40(1):9-26.

Suttorp CM, van Rheden REM, van Dijk NWM, Helmich MPAC, Kuijpers-Jagtman AM, Wagener FADTG. Heme oxygenase protects against placental vascular inflammation and abortion by the alarmin heme in mice. *Int J Mol Sci*. 2020 Jul 29;21(15):5385.

Verheijen N, **Suttorp CM**, van Rheden REM, Regan RF, Helmich MPAC, Kuijpers-Jagtman AM, Wagener FADTG. CXCL12-CXCR4 Interplay facilitates palatal osteogenesis in mice. *Front Cell Dev Biol*. 2020 Aug 21;8:771.

Other publications

van Dijk PG, **Suttorp CM**, van der Waal I. Een vergrote tong [Macroglossia]. *Ned Tijdschr Tandheelkd*. 2006 Apr;113(4):146-7.

Suttorp CM, van Dijk PG, de Cleen MJ, Koch AE, van der Waal I. Resorptie van 2 bovenincisieën bij een 14-jarige jongen [Resorption of two upper incisors in a 14-year-old boy]. *Ned Tijdschr Tandheelkd*. 2006 Jun;113(6):241-2.

Darroudi AM, Kuijpers-Jagtman AM, Ongkosuwito EM, **Suttorp CM**, Bronkhorst EM, Breuning KH. Accuracy of a computed tomography scanning procedure to manufacture digital models. *Am J Orthod Dentofacial Orthop*. 2017 May;151(5):995-1003.

Suttorp CM, Desmedt DJS, Maal TJJ, Breuning KH. Facial improvement after mandibular midline distraction and surgically assisted rapid maxillary expansion. *Am J Orthod Dentofacial Orthop*. 2017 Oct;152(4):523-542.

Maltha JC, Kuijpers-Jagtman AM, **Suttorp CM**, Noerhadi NA, Kuijpers M, Ongkosuwito EM. Größenordnung der Kraft und Geschwindigkeit der kieferorthopädischen Zahnbewegung: Erkenntnisse aus Studien an Hunden [Force magnitude and rate of orthodontic tooth movement: What we learned from dog studies]. *Informationen aus Orthodontie & Kieferorthopädie*. 2017;49:91 – 97.

Suttorp CM, Camardella LT, Desmedt DJ, Baan F, Maal TJ, Breuning KH. Recurrence of the anterior open bite after orthognathic surgery: 3D Analysis of Dental, Soft Tissue, Skeletal and Airway Changes in Unravelling the Aetiology of Relapse. 2018. *Oral Health Case Reports*, vol. 4, iss. 2, (2018) pp. 148-159.

Scholtes E, **Suttorp CM**, Loomans BA, Van Elsas P, Schols JG. Combined orthodontic, surgical, and restorative approach to treat a complicated crown-root fracture in a maxillary central incisor. *Am J Orthod Dentofacial Orthop*. 2018 Oct;154(4):570-582.

PHD PORTFOLIO

Name PhD candidate: C.M. Suttorp Department: Orthodontics and Craniofacial Biology Graduate School: Radboudumc, RIMLS		PhD period: 06-04-2016 – 01-01-2020 Promotor: Prof.dr. A.M. Kuijpers-Jagtman Co-promotor: Dr F.A.D.T.G. Wagener	
	Year(s)	ECTS	
TRAINING ACTIVITIES			
a) Courses & Workshops			
- Experiments on animals Act course article 9, Utrecht	2011		7
- Erasmus course A10 Research methodology and biostatistics	2011		5
- Critical Appraisal Course	2011		2
- Introduction day Radboudumc	2016		0.5
- Graduate School specific introductory course	2016		1
- Course Epic	2018		0.5
b) Seminars & lectures			
- Orthodontics Research forum	2017, -18, -19		0.5
- Dentistry PhD seminars	2017, -18, -19		1
c) Symposia & congresses			
- NVOS congress Utrecht	2016		0.25
- Congress EOS Stockholm 2016	2016		2
- Congress EOS Montreux 2017	2017		2
- NVOS congress Vianen	2017		0.25
- Booy foundation Congress Amsterdam	2018		0.5
- Congress EOS Edinburgh 2018^	2018		2
- NVvO congress 2018 Amsterdam	2018		1
- NVvO Congress Soestduinen	2019		0.5
- Congress EOS Nice 2019^	2019		2
- NVvO congress Maastricht	2019		1
d) Other			
- Staff meeting department of Orthodontics and Craniofacial Biology	2016, -17, -18, -19		4
TEACHING ACTIVITIES			
e) Lecturing			
- Poster presentation EOS Stockholm 2016^	2016		0.25
- CBCT applicatiecursus PAOT Nijmegen^	2016, -17, -18, -19		8
- Profiel kind en ontwikkeling klinische orthodontie^	2017, -18, -19		6
- Oral lecture Orthodontics Research forum^	2018, -19		0.25
- Poster presentation EOS Edinburgh 2018^	2018		0.25
- Blok groei orthodontie colleges^	2018		1.5
- Oral lecture EOS Nice 2019^	2019		0.25
f) Supervision of internships / other			
- Supervision of bachelor students:	2016, -17		3
- Supervision of master students:	2017, -18		3
- Supervision of master student:	2017, -18		3
- Supervision of AIOS orthodontics:	2017, -18, -19		3
- Clinical supervision AIOS orthodontic clinic	2017, -18, -19		70
- Patient treatment clinic Cleft Lip and Palate	2018		12
- Treatment plan session AIOS group	2017, -18, -19		22
TOTAL			165.5

[^]Indicate oral or poster presentation

Research data management

Findability:

The data described in this thesis are stored at the Research Network disc of the department of Dentistry, Radboud university medical center in Nijmegen, the Netherlands.

Accessibility:

Data and protocols can be obtained on request from the department of Dentistry, Radboud university medical center in Nijmegen, the Netherlands. Dr. F.A.D.T.G. Wagener has access to the data, and can be reached at frank.wagener@radboudumc.nl

Interoperability:

The data are documented in Dutch and English according to the FAIR principles.

Reusability:

The data described in this thesis are documented to be reused for further research and analysis.

“Niets is mensen te gek, behalve non-conformisme”

Rypke Zeilmaker, Dutch science journalist, 2013

